A Whole Mantle Attenuation Tomography based on the ISC Amplitude Data Analysis

by

Hiroaki NEGISHI

A thesis submitted in partial fulfillment of the requirements for the degree of Doctor of Philosophy (geophysics)

in Kyoto University

February, 1999

Abstract

A whole mantle P-wave attenuation structure was obtained by using the amplitude data reported by the International Seismological Center (ISC). Since the ISC amplitudes are measured for short-period body waves, they are likely to be affected strongly by site effects and the other factors. Therefore I analyzed amplitude fluctuations of the data before the inversion process.

The amplitudes from 3,445 events (m_b < 7.0) for 718 ISC stations in the world were analyzed from the ISC CD-ROMs. To eliminate various complicating effects, I have included only events that had at least 15 amplitudes at periods of 0.5 to 3.0 seconds and epicentral distances between 28 and 89 degrees. Data associated with travel paths that bottom in the lowermost mantle (>2700 km depth) are excluded to avoid the diffraction effect of the D" layer. Hypocenter parameters were obtained from the database improved by Engdahl *et al.* [1998], and source mechanism are taken from Harvard and USGS moment tensor solutions. Average station terms and azimuth-independent station terms and first and second azimuth-dependent station terms were calculated for relative log-scaled amplitude and relative travel time residuals. The average terms and the azimuth-independent terms for amplitudes of stations in the central part of old continents, such as Eurasia and North America, are generally large, while small for stations around the Pacific Ocean and the southern Europe. These station anomalies seem to have a only weak correlation with the type of crustal structure. The first azimuthal terms have more complex distributions and do not show an obvious global tendency. The second-azimuthal terms are distributed systematically in an E-W direction in the western Pacific Ocean, in a N-S direction in North America, and mixed directions in Europe. The travel time residuals show the results that are similar to Dziewonski and Anderson [1983]. The second azimuthal terms show a relation to the S-wave polarization anisotropy.

The whole mantle three-dimensional structure of P-wave attenuation was then obtained by applying a tomographic method to the amplitude data of the ISC Bulletin. A grid

modeling tomographic method was developed and applied to the data. The simultaneous inversion technique determined source amplitudes and a one-dimensional attenuation structure down to 2,700 km depth, then three-dimensional perturbations from the 1-D model were obtained. The attenuation in the upper mantle is stronger than that in the lower mantle. Such tendency is also seen in the various standard Earth models obtained from free-oscillation analyses. The long-wavelength lateral variations in attenuation show similar patterns to previous P-wave velocity studies. A major high attenuation zone appears to be located in the central Pacific in the middle to lower mantle, while there is low-attenuation spreading beneath the Eurasia continental shield in the upper to middle mantle. There exists some remarkably high attenuation zones through the upper and lower mantle. Hotspots are located around these regions, therefore, the high attenuation may be due to upwelling flow.

This study presents the first model of whole mantle attenuation heterogeneity for short-period body waves. This new information will contribute valuable information for investigations about geothermal and geodynamical features of the Earth.

Acknowledgments

I am very grateful to Prof. Masataka Ando for his supports and encouragement throughout my graduate course at the Research Center for Earthquake Prediction, Disaster Prevention Research Institute, Kyoto University. I also thank Prof. Kazuro Hirahara of Nagoya University for instilling in me the great interest in the structure of the Earth's interior, and giving me advice and helpful comments during this study. I wish to express my sincere appreciation to Drs. Takuo Shibutani and Manabu Hashimoto for their valuable advice and generous help in many aspects in my doctor course. I also thank Prof. Brian L.N. Kennett of the Australian National University and Satoshi Kaneshima of Tokyo Institute of Technology for their valuable comments and discussions. Thanks are also due to Drs. Yasuyuki Nakamura, Anshu Jin, Fumiaki Takeuchi, and Atsuki Kubo for their valuable comments, help and showing their scientific interests. I am very grateful to Prof. James J. Mori for critical reading of manuscript. The author express his thanks to Prof. E. Robert Engdahl of the United States Geological Survey for providing the improved hypocenter and reprocessing arrival time data base. Chapter 2 of this thesis is led by my graduate study under Prof. Tamao Sato in Hirosaki University. I deeply thank him for giving me the chance to delve into the investigations and follow the interests of seismology.

The author has been supported by Research Fellowships of the Japan Society for the Promotion of Science for Young Scientists. Part of this work was supported by Grant-in-Aid for JSPS Fellows (No. 9504).

Finally, the author is grateful to all the staff members who are reading seismological data and keeping careful observations at all of the ISC stations.

Note

This thesis is based on the following papers:

Amplitude and travel time fluctuations for the ISC stations, submitted to Journal of Geophysical Research, by Hiroaki Negishi

A whole mantle attenuation tomography based on the ISC amplitude analysis, to be submitted to Geophysical Journal International, by Hiroaki Negishi

Amplitude and arrival time fluctuations of teleseismic P waves observed in northern part of Tohoku region, Japan, Journal of Seismological Society of Japan, **46**, 297 - 308, 1993, by Hiroaki Negishi and Tamao Sato.

The three-dimensional attenuation structure beneath the Philippine archipelago based on seismic intensity data inversion, Earth and Planetary Science Letters, **151**, 1 - 11, 1997, by Glenda M. Besana, Hiroaki Negishi and Masataka Ando.

The 1995 Kobe earthquake: Seismic image of the source zone and its implications for the rupture nucleation, Journal of Geophysical Research, **103**, 9967 - 9986, 1998, by Dapeng Zhao and Hiroaki Negishi.

Table of Contents

		page
Abstract		2
Acknowledgments		4
Note		5
Chapter 1.	General Introduction	9
Figures		13
Chapter 2.	Amplitude and travel time fluctuations for P waves at teleseismic distances	16
2.1	Introduction	17
2.2	Dataset and other settings	18
2.2.1	ISC Bulletin	18
2.2.2	P phase amplitude data	19
2.2.3	Earth model of velocity structure	20
2.2.4	Hypocentral parameters	21
2.2.5	Source mechanisms and geometrical spreading	22
2.3	Relative log-scaled amplitude analysis	23
2.4	Results of amplitude analysis	25
2.5	Travel time data analysis	27
2.6	Discussion	29

2.6.1 Correlation between amplitude and travel time 29

2.6.2 Crustal structure and amplitude 30

Figures 32

Chapter 3. A whole mantle P wave attenuation structure obtained from ISC amplitude data 65

3.1 Introduction 66

3.2 Methodology of grid model attenuation tomography 67

3.2.1 Basic theory of attenuation tomography 67

3.2.2 Grid modeling formulation 68

3.2.3 Smoothness constraint 72

3.2.4 LSQR inversion algorithm 74

3.2.5 Resolution 75

3.3 One-dimensional attenuation structure and setting for tomographic inversion 77

3.3.1 Setting of data and modeling space 77

3.3.2 Results of one-dimensional inversion 79

3.3.3 Setting and conducting the tomographic inversion 80

3.3.4 Checkerboard resolution test 81

3.4 Tomographic result 82

3.5 Discussion 86

Tables 89

Figures 91

Chapter 4. General Conclusion 170

Bibliography 173

Appendix A. Azimuthal variation of log-amplitude anomaly and

relative travel time residuals. 183

A-1 Azimuthal variation of log-amplitude 184

A-2 Azimuthal variation of travel time 206

Appendix B. Amplitude and travel time station corrections for ISC stations. 228

B-1 Amplitude station corrections 229

B-2 Travel time station corrections 234

Appendix C. The whole-mantle P-wave attenuation structure : QPB3DV2 240

Chapter 1. General Introduction

Studying of the Earth's deep interior is one of the basic problems in Earth and planetary sciences. The seismic and volcanic activity of the planetary Earth is mainly due to the dynamics of the mantle and core. Seismological data have provided us with much information about the internal structure of the Earth, and have brought great help to understanding the Earth's dynamics, thermal structure, and origin. Particularly, arrival time data of various seismic phases are most important and useful information. Hypocenter distributions which are determined by many arrival times have cleared the images of subducted plates, active faults and thermal boundaries in the crust and mantle. In the 1930's, a spherically symmetric Earth model was constructed by Jeffreys and Bullen [1940] by analyzing arrival times of the world-wide data. This new information shed light onto the Earth. After the discovery of plate tectonics, there was considerable interest in the large-scale heterogeneity of the mantle. Many studies have been carried out to map the global variations of the upper mantle structure by using surface wave analysis, because surface waves can sample the entire globe rather uniformly in spite of a non-uniform distribution of earthquakes and seismic stations [Inoue, 1993].

Many heterogeneous images have been obtained for the Earth's interior by using travel time analysis, starting from the pioneering studies of Aki and Lee [1976] and Aki *et al.* [1977]. Their method has been improved and applied to local and regional studies (*e.g.*, Hirahara *et al.* [1989], Thurber [1983], Zhao *et al.* [1992], Negishi [1996], Zhao *et al.* [1996], Zhao and Negishi [1998]). Arrival times of short-period body waves can be used for not only regional studies but also global studies. Particularly, teleseismic P-phases enable study of the deeper parts of the Earth because of clear phase and ray bottoming depths, while surface waves have much less information about the lower mantle. Cleary and Hales [1966] first analyzed the travel times of teleseismic P-phases to calculate a world-wide distribution of station anomalies, and they found earlier arrivals of P phases in shield and the Western Pacific areas and later arrivals in the active tectonic regions. In 1980's, some investigators tried to image the whole mantle elastic structure. Dziewonski [1984] inverted 500,000 teleseismic P arrivals from 5,000 shallow events to obtain a model of lower mantle heterogeneity (Fig. 1.1). The upper mantle heterogeneity was assumed to be incorporated in adjustments of hypocenter and

azimuth-dependent station corrections obtained by Dziewonski and Anderson [1983]. Negishi and Sato [1993] applied this method to the amplitude and arrival time data observed in northern part of Tohoku region, Japan. I use the same method in Chapter 2 of this thesis. Inoue *et al.* [1990] inverted over 2,000,000 arrivals of P-waves to obtain a three-dimensional P-wave velocity structure for the whole mantle of the Earth. This was the first study which delineated the entire mantle structure with reliability mapping (Fig. 1.2). With improvements of computer algorithms and developments in computer power, investigators have applied tomographic techniques to huge data sets of arrival times and constructed not only P-wave velocity but also S-wave velocity and bulk sound structure of the Earth (*e.g.,* Pulliam *et al.* [1993], van der Hilst *et al.* [1997], Kennett *et al.* [1998]). We can say that we already have a general image of the "elastic Earth".

On the other hand, do we have a general image of the "anelastic Earth" as well ?

Anelasticity of the Earth reflects the thermal state and the other physical properties more sensitively than elasticity. The attenuation of seismic waves is one of the parameters that represents the Earth's anelasticity. The attenuation of seismic waves, which can be specified by the quality factor Q, has an important bearing on the physical state of the Earth's deep interior, such as the temperature, the degree of partial melting, and so forth. Hence, extensive investigations of variations of attenuation are particularly important for better understanding of the dynamics of the Earth's interior. The attenuation structure of the Earth has been studied by using mainly long-period seismic data, free oscillation of the Earth and long-period surface waves. In the 1960's and 1970's, some depth-dependent Q models were established on the basis of such long-period data (*e.g.*, MM8 by Anderson *et al.* [1965], Model G by Teng [1968], SL8 by Anderson and Hart [1978]). Dziewonski and Anderson [1981] analyzed a large data set of body waves, surface waves and free oscillations of the Earth, and obtained the radial model of velocity, Q, density, and the other physical parameters. This model, Preliminary Reference Earth Model (PREM), is still used by many geoscientists. This attenuation model was recently improved by Montagner and Kennett [1996] with a more recent velocity structure, and they established a new standard Earth model, named AK135. Tomographic studies of global attenuation heterogeneity have also

been done using long-period surface waves and free oscillations of the Earth (*e.g.*, Suda *et al.* [1991], Durek *et al.* [1993], Romanowicz [1995]). These investigations, however, resolved only the upper mantle. The whole mantle image of attenuation heterogeneity is not yet clear.

Recently I took notice of the amplitude data reported in the Bulletin of the International Seismological Center. The International Seismological Center (ISC) have compiled vast amounts of P-, S- and some later phase data from 1964 to the present. Many investigators have used the data to obtain regional to global scale heterogeneous structures of the Earth. The compiled data include not only arrival time but also amplitude of the first-arrival phase in order to determine magnitude, m_b. These data, however, have seldom been used for structural investigations because seismologists have considered the amplitude values unreliable, because of contamination by uncertainty factors (*e.g.*, site effects due to local geology, ground noise, picking error). However, I thought that the structural information can be resolved from the data by applying appropriate corrections. Statistical characteristics of short-period amplitudes of P-waves have been analyzed by several investigators (Stewart [1981], Nakanishi and Motoya [1990], Negishi and Sato [1993]). They found that the teleseismic amplitude data of short-period P-waves include not only site effects, such as local geology, but also the effects of lateral heterogeneity in the crust and the upper mantle.

In this thesis, I applied a tomographic approach to obtain a whole mantle attenuation structure, using the ISC amplitude data. In Chapter 2, I analyzed the fluctuations of the ISC amplitude based on the statistical method of Negishi and Sato [1993], and defined station corrections of amplitude, "relative log-scaled amplitude anomaly". This parameter corresponds to the travel time station corrections defined by Dziewonski and Anderson [1983]. In Chapter 3, a whole mantle P-wave attenuation structure was obtained by using the ISC amplitude data, with application of the amplitude station corrections obtained in the previous chapter. A grid model attenuation tomographic method, which is one of an approach for representing the three-dimensional attenuation heterogeneity, was adopted. This model is clearly very preliminary and the details of the patterns will likely change as our ability to gain resolution increases in the future. But this is the first model which delineates the whole mantle attenuation structure including the lower mantle.

Figure Captions

Fig. 1.1 Maps of the P-wave velocity heterogeneity at six different depths in the lower mantle. Black and white patterns indicate faster and slower anomalies than the average velocity at each depth, respectively. The indicated rage is ±1 % for the depth of 670 km, and ±0.5 % for the other depths (after Dziewonski [1984]).

Fig. 1.2 P-wave velocity heterogeneity in the whole mantle. Slowness perturbations from the averages at each depth are shown. Fast and slow anomalies are indicated by cross and circles, respectively. The size of the symbols is proportional to the square root of the perturbation (after Inoue *et al.* [1990]).

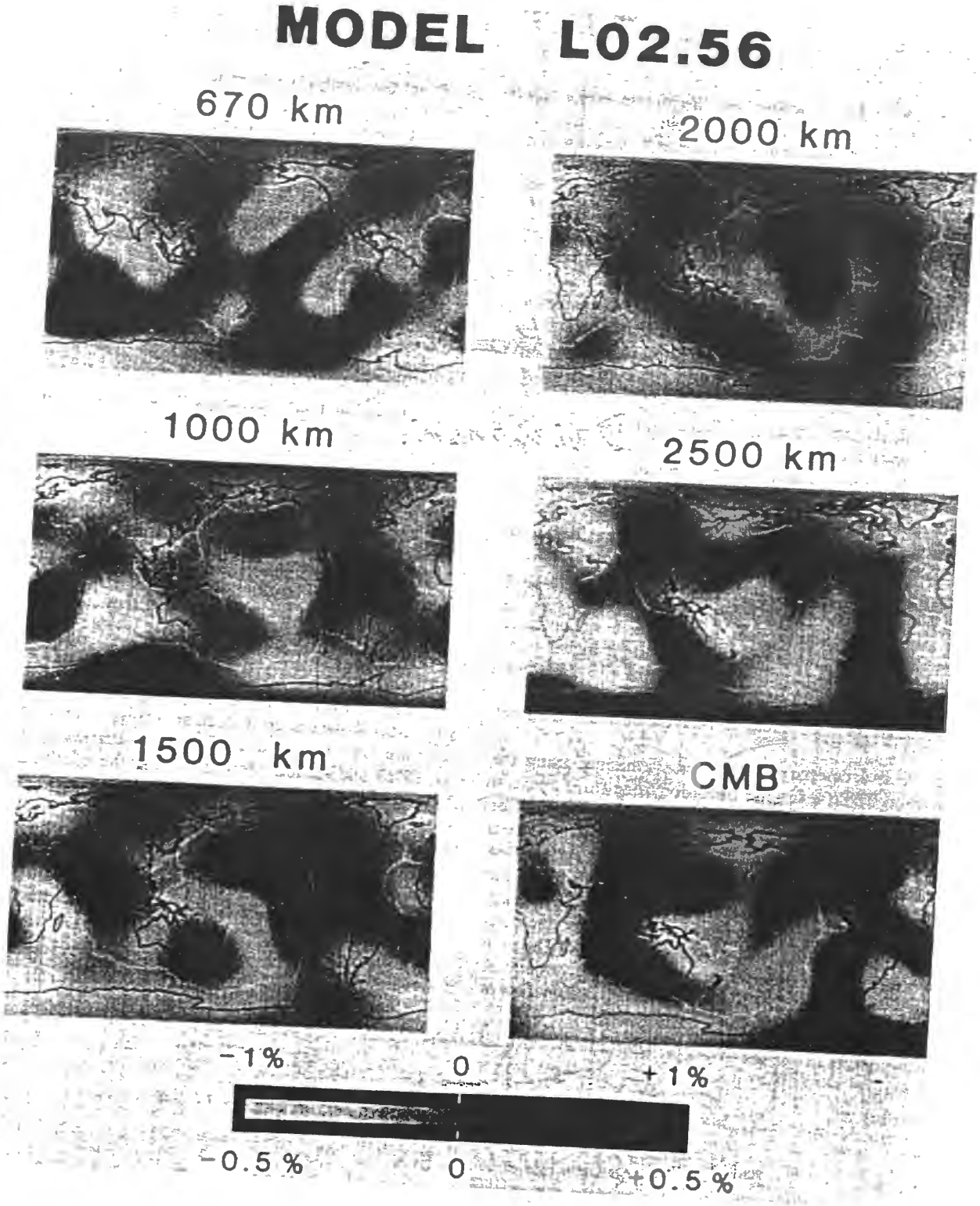
MODEL L02.56
670 km
2000 km
1000 km
2500 km
1500 km
CMB
-1%
0
+1%
-0.5%
0
+0.5%

Figure 1.1

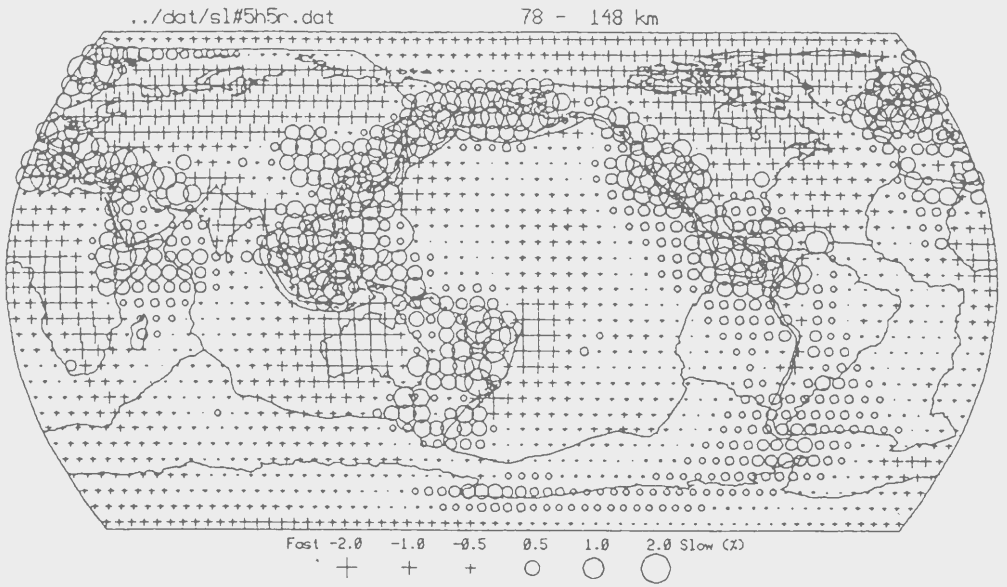
../dat/sl#5h5r.dat
78 - 148 km
Fast -2.0 -1.0 -0.5 0.5 1.0 2.0 Slow (X)

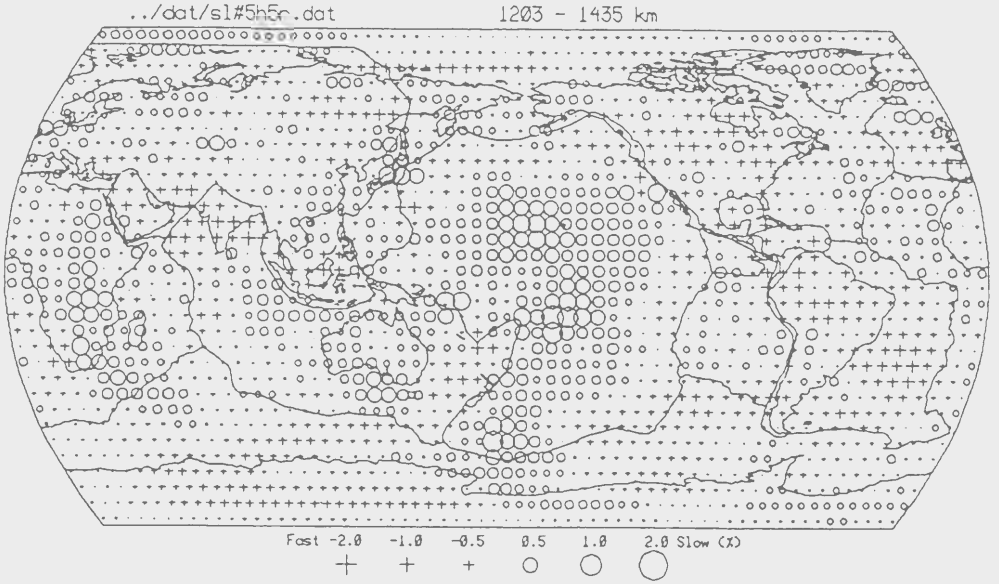
../dat/sl#5h5r.dat
1203 - 1435 km
Fast -2.0 -1.0 -0.5 0.5 1.0 2.0 Slow (X)

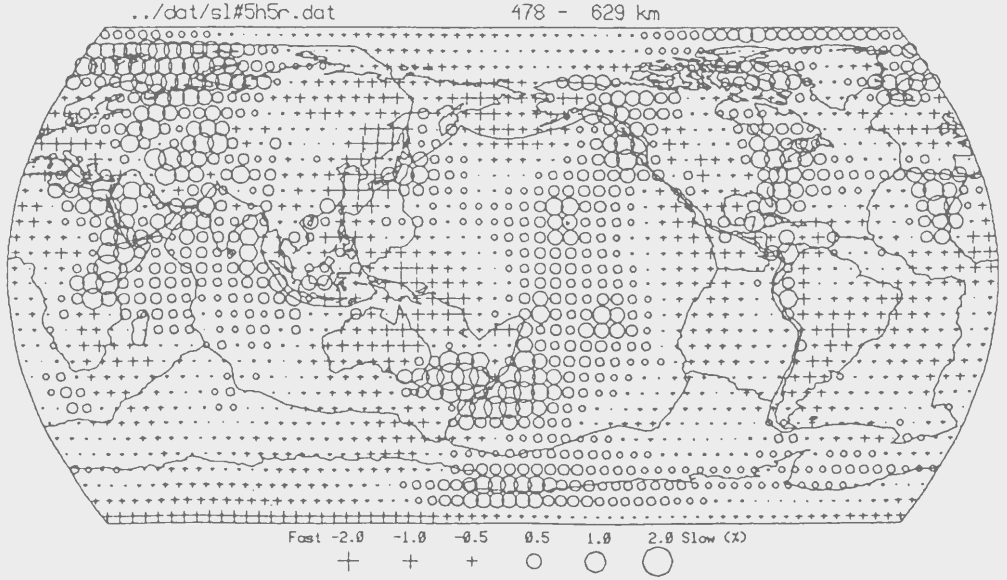
../dat/sl#5h5r.dat
478 - 629 km
Fast -2.0 -1.0 -0.5 0.5 1.0 2.0 Slow (X)

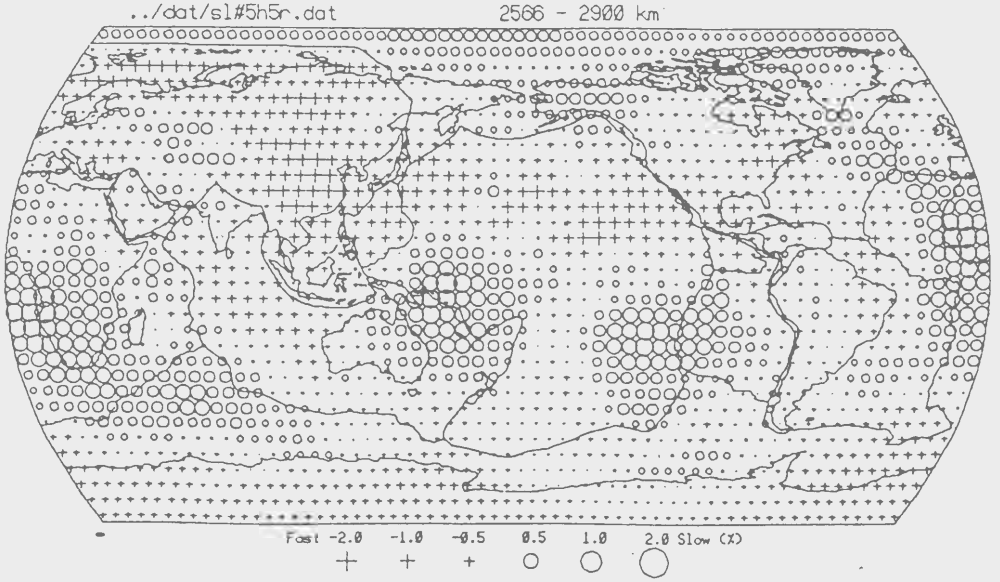
../dat/sl#5h5r.dat
2566 - 2900 km
Fast -2.0 -1.0 -0.5 0.5 1.0 2.0 Slow (X)

Figure 1.2

Chapter 2.

Amplitude and travel time fluctuations for P waves at teleseismic distances

2.1 Introduction

The arrival time data of the International Seismological Center Bulletin (ISCB) have been used for various seismological investigations of the Earth's deep interior. Dziewonski and Anderson [1981] used a very large set of the data for the years 1964 to 1975 to obtain a travel time curve which, together with other subsets of data, was used to derive the Preliminary Reference Earth Model (PREM). Recently some heterogeneous whole mantle images have been derived by applying tomographic methods to more than two million and even more arrival times of the ISCB. These models shed light on the study of mantle dynamics and understanding the Earth's global tectonics, such as slab penetration into the lower mantle (*e.g.*, Fukao *et al.* [1992], Kennett *et al.* [1998]).

On the other hand, amplitude and period data around the first arrival phase have also been reported in the same bulletin in order to determine magnitude, m_b. These data, however, have rarely been used in any structural studies because even the fundamental nature of the ISC short-period amplitudes is not well known and seismologists have considered amplitude values unreliable for analysis, because of contamination by uncertainty factors at each site, such as local geology, ground noise, and picking error. However, this means that the ISC amplitude data may become usable by applying suitable correction for the characteristic values of various site effects. Since amplitudes are sensitive to partial derivatives of velocity and to anelasticity, more detailed structures may be resolved by combining amplitudes with the travel time data (Thomson and Gubbins [1982]). For example, Haddon and Husebye [1978] used amplitude data to investigate the velocity heterogeneity beneath the Norwegian Seismic Array (NORSAR) in conjunction with the travel times.

Dziewonski and Anderson [1983] investigated the fluctuations of P wave travel times of the ISCB and obtained station residuals, including azimuthal effects, for 994 seismic stations. They found that the azimuthally station corrections exhibit general consistency over broad geographic areas. It is expected that a significant part of the effect of velocity anomalies in the upper mantle can be accommodated by the static and azimuthal dependent station

corrections. They applied these station corrections to the tomographic study (Dziewonski [1984]) and succeeded in deriving three-dimensional model of lateral variations of the P-wave velocity in the lower mantle. Such azimuthal station corrections can provide great help toward understanding the Earth's heterogeneity.

From the above view point, I tried to clarify the fundamental characteristics of the ISC amplitude and travel time data. First, relative log-scaled amplitude anomalies were obtained by statistical analysis. The azimuthally dependent station corrections were also estimated by using the new data base which includes events relocated with the AK135 model (Kennett *et al.* [1995]), generalized by Engdahl *et al.* [1998]. Correlation between relative log-scaled amplitude anomalies and relative travel time residuals are then discussed for each station to conclude whether the amplitude is more affected by the heterogeneity of velocity (focusing or defocusing) or the attenuation.

2.2 Dataset and other settings

2.2.1 ISC Bulletin

The ISC has been compiling data reported from a large number of seismograph stations all over the world. The ISC Bulletin has long been utilized by seismologists as an invaluable data source for studying world seismicity and structure of the Earth's interior. All the arrival time data and hypocenter locations reported from local agencies are compiled by the ISC and re-determined from the first P-wave arrivals using the Jeffreys-Bullen travel time tables (Jeffreys and Bullen [1940]) and the Earth's ellipticity correction suggested by Gutenberg and Richter [1933]. The database contains numerous kinds of earthquake information, such as hypocentral parameters, processed data of various seismic phases, and disaster information. These data are published as printed and machine-readable bulletins with a typical delay of two years. Figure 2.1 shows an example of the printed book page. Adherence to this rather

conservative manner of processing has resulted in the uniformity and reliability of the database. The detailed procedure of the analysis by the ISC is given in Adams *et al.* [1982].

2.2.2 P phase amplitude data

The ISC Bulletin have reported unified magnitudes, m_b, following the procedure outlined by Gutenberg and Richter [1956] for P waves of period shorter than 3 seconds. These amplitudes and periods are measured on short-period vertical instruments. If Q denotes the depth-distance factor, A the amplitude in nanometers and T the period in seconds for the i-th station, then for N observations

$$m_b = \frac{1}{N}\sum_{i=1}^{N}\left[Q(\Delta_i, h) + log10\left(\frac{A_i}{T_i}\right)\right] - 3 \qquad (2.2.1)$$

In this equation, $Q(\Delta_i, h)$ includes structural effects of the Earth's interior, so it is possible that the fluctuations of m_b are related to variations in attenuation along the ray path. Stewart [1981] tried to delineate P-wave attenuation anomalies in the lower mantle under the North Atlantic by assuming that body-wave magnitude residuals are due to structure near the bottoming-points of the rays.

The ISC Bulletin have been issued from 1964 in the form of bulletin books and CD-ROMs, but the data prior to 1983 cannot be used for the present investigation since only the log10(Amplitude/Period) value had been reported. Most of the ISC data are for small events with relatively few reports by individual stations and such events have to be omitted, because they do not provide enough statistical information. I excluded the events greater than magnitude 7, since the effects of source directivity and complexity of the source process could not be ignored for body wave amplitudes in such larger event (Mikumo [1969]). I included events that had at least 15 amplitude data with periods between 0.5 and 3.0 seconds at epicentral distances of 28° and 89°. In this range of epicentral distance, the first arrival phase is direct-P and no other phases are included in the 3 second time window after the P-phase in the AK135 velocity model (Kennett *et al.* [1995]) which I used here. Figures 2.2 (a) and (b) show the WKBJ synthetic record section as a function of epicentral distance and their

amplitudes, respectively. The P-wave amplitudes decay gradually with distance, but being to grow in amplitude at farther than about 90 degree. This is due to the diffraction effect in the lowermost mantle layer, called the D" layer. Therefore, the data associated with rays bottoming in the lower mantle (>2,700 km depth) are excluded to eliminate diffraction effect for the D" layer. To avoid contamination from depth phases, event shallower than 10 km were omitted. Using the constraints stated above, 155,778 amplitudes data, observed at 718 stations from 3,445 events, remained for use in the present study. Figures 2.3 and 2.4 show the epicentral distribution of the events and locations of the stations, respectively.

2.2.3 Earth model of velocity structure

Following the pioneering study of Jeffreys and Bullen [1940], investigators produced radial velocity models using a wide variety of different techniques and different data (*e.g.*, Herrin *et al.* [1968], Dziewonski and Anderson [1981], Kennett and Engdahl [1991]). The locations provided by the ISC are determined using the Jeffreys and Bullen [1940] travel time tables. It has been recognized for many years that there was a baseline problem with the tables, because events with independently determined locations show origin-time errors of the order of 2 seconds. A major effort to improve P-wave travel time tables was made in 1968 (Herrin *et al.* [1968]), but the absence of S-phase arrival times limited the usefulness of this set of tables. An initiative by the International Association of Seismology and Physics of the Earth's Interior (IASPEI) to improve earthquake locations led to the construction of the IASP91 model (Kennett and Engdahl [1991]) and the SP6 model (Morelli and Dziewonski [1993]). From these models, travel times can be calculated for the full range of seismic phases; the main phases have been tabulated (Kennett [1991]) and the same material is available in computational form. The P-wave travel times for these two models are in very close agreement to distances of 80 degrees, and both models indicate an average offset of 1.7 seconds from the Jeffreys and Bullen tables, which is likely to be manifest in the ISC event parameters. Recently, Kennett *et al.* [1995] refined the IASP91 model by relocating events using the IASP91 model, depth phases and re-associating phase picks. The new preferred model, AK135 (shown in Fig. 2.5), gives a significantly better fit to a broad range of phases

than that is provided by the IASP91 and SP6 models (Kennett *et al.* [1995]). I used this AK135 model for calculating geometrical spreading and ray tracing in this study.

2.2.4 Hypocentral parameters

The ISC uses a standard least-squares procedure based on Jeffreys' method of uniform reduction (Jeffreys [1932, 1939], Adams *et al.* [1982]) to obtain hypocenters. The location parameters are determined by using only first-arriving P-wave travel times, which for most events do not include P-wave arrivals corresponding to upgoing ray paths. The distribution of earthquakes is highly heterogeneous on a global scale, and most earthquakes occur in or near subduction zones where lateral variations in seismic velocities of 4 to 8% are not uncommon (Engdahl *et al.* [1998]). Seismological stations are also heterogeneous, mostly located in continental areas and on some islands in oceanic region. Such biased distribution of events and stations lead to large shifts of hypocenter and origin time. Hence, many ISC hypocenters are poorly constrained. It is well known that such mislocation of hypocenters masks structural signals. For example, Davies [1992] showed that mislocation contributes up to 35 % to the travel-time variance signal at teleseismic distances for earthquakes.

Recently Engdahl *et al.* [1998] relocated nearly 100,000 events that occurred during the period from 1964 to 1995 and are well-constrained teleseismically by arrival-time data reported to the ISC and to the USGS-NEIC (National Earthquake Information Center). Their data set of relocated hypocenters, named EHB, is calculated by using not only the P phases but some other phases, S, PKiKP, PKPdf and the teleseismic depth phases pP, pwP, and sP. These source parameters were determined by the new standard model AK135 (Kennett *et al.* [1995]) and ellipticity corrections (Kennett and Gudmundsson [1996]). Figure 2.6 shows an example of the EHB epicenter relocation vectors relative to the ISC epicenters (Engdahl *et al.* [1998]). The largest difference is over 30 km, which corresponds to a travel-time difference of about 4 seconds. This difference cannot be ignored for velocity and attenuation analysis. These hypocentral parameters were used in this study.

2.2.5 Source mechanisms and geometrical spreading

Focal mechanism solutions are also needed to remove the effects of radiation pattern. A double-couple mechanism was assumed here. Figure 2.7 shows the definition of the fault-orientation parameters and the definition of ray propagation directions. We can obtain the radiation pattern from a double-couple point source for P-waves, R, as

$$\begin{aligned} R = & \cos\lambda \sin\delta \sin^2 i_\xi \sin 2(\phi - \phi_s) - \cos\lambda \cos\delta \sin 2i_\xi \cos(\phi - \phi_s) \\ & + \sin\lambda \sin 2\delta \left\{ \cos^2 i_\xi - \sin^2 i_\xi \sin^2(\phi - \phi_s) \right\} \\ & + \sin\lambda \cos 2\delta \sin 2i_\xi \sin(\phi - \phi_s) \end{aligned} \tag{2.2.2}$$

where (ϕ_s, λ, δ) are fault orientation parameters (strike, dip, rake) and (i_ξ, ϕ) are angular ray coordinates (emergence angle from down, azimuth from North), respectively (Aki and Richards [1980]). Figure 2.8 shows the radiation pattern from a point source double couple (Kennett [1983]). The observed amplitude should be divided by this factor to correct for the radiation pattern. The data that emerges near nodal planes (sin theta < 0.1) are excluded. I used the USGS-NEIC and Harvard centroid moment tensor solutions for correction of the radiation pattern for all of events used in this study.

The body wave amplitude from a point source is proportional to the inverse of the hypocentral distance in a homogeneous non-attenuate (Q=∞) media. In a laterally-homogeneous spherical Earth, the geometrical spreading for a seismic wave amplitude can be expressed by (*e.g.*, Aki and Richards [1980])

$$G = \frac{1}{R_0} \sqrt{\frac{\rho_0 V_0}{\rho_s V_s} \frac{\sin\theta}{\sin\Delta \cos i_0} \frac{d\theta}{d\Delta}} \tag{2.2.3}$$

where R_0 is the radius of the Earth, ρ_0 and V_0 the density and the velocity at the surface, ρ_s and V_s the density and the velocity at the source, Δ the angular epicentral distance, θ the emergence angle measured from vertical, and i_0 the incident angle measure from vertical, as shown in Figure 2.9. I applied these corrections to the observed amplitude data by using the AK135 velocity and density model.

2.3 Relative log-scaled amplitude analysis

Body-wave amplitudes from a teleseismic event are controlled by various effects, such as source magnitude, geometrical spreading, structural effects, and source mechanism. Therefore, these effects have to be corrected before carrying out statistical analyses of amplitudes from a large number of teleseismic events. The amplitude that is recorded at the j-th station from the i-th event in a certain frequency range can be expressed by the following equation;

$$A_{ij} = M_i \cdot R_{ij} \cdot G_{ij} \cdot X_{ij} \cdot C_j \tag{2.3.1}$$

where A_{ij} is the amplitude observed at the j-th station from the i-th event, M_i is the source amplitude of i-th event, R_{ij} is the effect of radiation pattern, G_{ij} is the geometrical spreading and attenuation effects in spherical homogeneous structure, X_{ij} indicates the effects of the lateral heterogeneity of velocity and attenuation in the mantle, and C_j is the site effect at the j-th station. When we already know (or suppose) the spherical structure, hypocenter locations, and source mechanisms for all events, the equation for the average of the common-logarithm of (2.3.1) for each event is,

$$\frac{1}{N_i}\sum_j \left(log\, A_{ij}\right) = \frac{1}{N_i}\left[\sum_j \left(log\, C_j\right) + \sum_j \left(log\, X_{ij}\right)\right] + log\, M_i \tag{2.3.2}$$

where N_i indicates the number of data for i-th event. We should assume one-dimensional structures for both velocity and attenuation to estimate G_{ij}. Figure 2.10 (a) shows the WKBJ synthetic seismograms for vertical components at the surface from a 10 km deep source, displayed with a reduction slowness of 7.0 seconds per degree. The amplitude variations of the figure (a) is shown in Figure 2.10 (b). The seismograms were calculated using a non-attenuating AK135 model (left), and an attenuation-included model (Montagner and Kennett [1996]) (right). The amplitudes are normalized by the maximum trace in each figure. The absolute values of each amplitude are much different, but the amplitude variation shows same

pattern between non-attenuated seismograms and attenuated traces. This indicates that the 1-D attenuation effect can be excluded if we analyze relative amplitude variations for each event, so only the 1-D velocity structure is used for estimating G_{ij}. Substitution of (2.3.2) from the logarithm of (2.3.1) becomes,

$$R(\log A)_{ij} = R(\log C)_j + R(\log X)_{ij} \tag{2.3.3}$$

where

$$\begin{aligned} R(\log A)_{ij} &= \log A_{ij} - \frac{1}{N_i}\sum_j \left(\log A_{ij}\right) \\ R(\log C)_j &= \log C_j - \frac{1}{N_i}\sum_j \left(\log C_j\right) \\ R(\log X)_{ij} &= \log X_{ij} - \frac{1}{N_i}\sum_j \left(\log X_{ij}\right) \end{aligned} \tag{2.3.4}$$

Here we call $R(\log A)_{ij}$ the "Relative log-scaled amplitude anomaly (hereinafter referred to as log-amplitude anomaly)" (Negishi and Sato [1993]). We can obtain the lateral heterogeneity term X_{ij} directly when C_j is already known. The estimation of the site effect is, however, so difficult that usually we do not know them. But if we suppose that

$$\sum_j \left(\log C_j\right) = 0 \tag{2.3.5}$$

and the following relation is satisfied for each station,

$$\sum_i \left\{R(\log X)_{ij}\right\} = 0 \tag{2.3.6}$$

the site effect term can be written as

$$\log C_j = \frac{1}{K_j}\sum_i \left\{R(\log A)_{ij}\right\} \tag{2.3.7}$$

where K_j is the number of the event recorded at the j-th station. Therefore, we can obtain the site effect term by averaging the log-amplitude anomaly for each station. Figure 2.11 shows examples of histogram of relative log-amplitude anomalies (left-side of the equation (2.3.3)) at each station. The amplitude data have a lognormal distribution, the same tendency as

observed by Ringdal [1976, 1977]. This indicates that the log-amplitude fluctuation can be expressed by the combination of the station bias, $R(\log C)_j$, and the lognormal-distributed components, that include the effects of heterogeneous structure and random noise. So the assumption of equations (2.3.5) and (2.3.6) are appropriate here.

2.4 Results of amplitude analysis

Figure 2.12 shows the spatial distribution of the site effect terms (right-hand side of the equation (2.3.7)). Open circles and diamonds indicate larger and smaller amplitudes, respectively. The sizes of the symbols are proportional to the anomaly according to the indicated scale. The site effect terms show an obvious geographical variation as can be seen in the figure. The amplitudes are systematically large for stations in the central and southern part of the Eurasia continent, such as China, India and Russia, while stations with small amplitude are concentrated in the Circum-Pacific belt, such as western North America, East- and Southeast-Asia, and Australia. These patterns seems to reflect the differences of the crust and the uppermost mantle structure beneath old continental shield and tectonically-active zones. On the other hand, amplitudes are medium scale for most of the stations in central North America, and a mixture of larger and smaller amplitudes are observed in Europe.

I applied the azimuthal dependency approach (Cleary and Hales [1966], Dziewonski and Anderson [1983]) to the log-amplitude anomalies. Because the azimuthal distribution of events with respect to the station tends to be uneven, azimuthal fluctuations of amplitude anomalies were obtained by the following procedure. The full azimuth range is divided into 18 windows, 20 degree wide. An average of log-amplitude anomalies is calculated if there are at least three data in each given window. These averages are treated with equal weight to reduce the bias due to unequal distribution of events (Dziewonski and Anderson [1983]). Then, the

least squares approach is used to determine azimuthal fluctuations of the amplitude anomaly for each station in the equation,

$$R(\log A)_{ij} = A_0 + A_1 \cos\left(\theta_{ij} - \theta_1\right) + A_2 \cos 2\left(\theta_{ij} - \theta_2\right) \qquad (2.4.1)$$

where A_0, A_1 and A_2 are the azimuth-independent term, first azimuthal dependent term, and second azimuthal dependent term, respectively. θ_{ij} is the azimuth viewed from the j-th station to the i-th event. θ_1 and θ_2 denote the direction of largest amplitude for the first and second azimuthally dependent terms, respectively. We can easily see that the azimuth-independent term (A_0) corresponds to $R(\log C)_j$, and the azimuth-dependent terms (A_1 and A_2) are the same as $R(\log X)_{ij}$ in the equation (2.3.3). A_0 becomes equal to the site effect term, $\log C_j$, when the conditions (2.3.5) and (2.3.6) are satisfied. These five parameters characterize station corrections for the ISC amplitudes for direct-P waves at teleseismic distances including the effects of the crust and the upper mantle. Figure 2.13 is an example of log-amplitude anomalies as a function of azimuth viewed from station to event. The solid curve and horizontal line are the least squares fit to the equation (2.4.1) and the constant term A_0, respectively. The figures of log-amplitude anomalies as a function of azimuth for all station analyzed here are shown in Appendix A. Appendix B lists the resultant five parameters of azimuthal station corrections. The standard deviation before (sd_1) and after (sd_2) the fitting and the variance reduction, which indicates the goodness of fit, are also listed. The variance reduction (vr) is defined as

$$vr = \left[1 - \left(\frac{sd_2}{sd_1}\right)^2\right] \times 100 \qquad (\%) \qquad (2.4.2)$$

Figure 2.14 shows the geographical distribution for the world of the A_0, A_1 and A_2 terms in equation (2.4.1), and Figures 2.15, 2.16 and 2.17 are the expanded views of North America, Europe, and Asia-Oceania, respectively. The sizes of the symbols are proportional to the anomaly according to the indicated scale. The arrow points toward the largest-amplitude direction for A_1, and the bar is parallel to the largest direction for A_2. The azimuth-independent terms show similar pattern as the site effect terms shown in Figure 2.12. This indicates that the assumptions of the equations (2.3.5) and (2.3.6) are satisfied well. The

first-azimuthal terms have more complex distributions and do not show an obvious global tendency. This might be due to local effects around each station because the first azimuthal term reflects major structures in the crust and the upper mantle (Dziewonski and Anderson [1983]). The second-azimuthal terms, on the other hand, can be divided into characteristic regions, showing east-west directions, north-south directions, and complex distributions. The large-amplitude direction aligns in mainly an east-west direction around the western side of the Circum-Pacific zone. However, on the eastern side of the Pacific Ocean, such as the western part of North America, the large direction is parallel to the coast line. This suggests that deeper structure effects the second azimuthal term more than the first azimuthal term.

2.5 Travel time data analysis

The same analysis procedure was applied to the travel time data for comparison with the amplitude fluctuations. The relative travel time residuals were calculated using the AK135 velocity model and the ellipticity correction of Kennett and Gudmundsson [1996]. Then the station corrections for travel time and their azimuthal dependency were obtained by applying equations (2.3.7) and (2.4.1). For travel times, θ_1 and θ_2 denote the direction of latest phase arrival for the first and second azimuth-dependent terms, respectively. Figure 2.18 is an example of travel time anomalies as a function of azimuth viewed from station to event. Figures 2.19 and 2.20 show the spatial distribution of the site effect terms for travel time and the geographical distribution for the world of the terms of equation (2.4.1). Figures 2.21, 2.22 and 2.23 are the same maps as Figures 2.15, 2.16 and 2.17 but for travel time residuals. These results are generally consistent with Dziewonski and Anderson [1983], despite the fact that their data set is completely independent from the data of this study.

The azimuth-independent terms show almost the same pattern as the distribution of the site effect terms for amplitude, except for some faster stations in the Siberia and India

regions and slower stations of Southeast Asia. This systematic distribution of travel time anomalies, the shields are fast and tectonically active regions are slow, was pointed out by Cleary and Hales [1966]. For the first azimuthal term, there is a tendency among the coastal stations for the slow direction to point toward the sea (for example east- and west coasts of North America, southeastern Asia, and South Africa). This is also pointed out by Dziewonski and Anderson [1983]. They suggested that this tendency might be associated with the relative slowness of the downdip propagation of the waves that encounter the thickening crust and possible depression of the upper mantle iso-velocity surfaces. On the other hand, the fast directions point opposite to the direction of the sea in Alaska. This area is characterized by the Pacific plate subducting toward the north beneath the North America plate (Zhao *et al.* [1995]). The larger amplitude (see Figure 2.15) and the faster arrivals from north might be caused by ray-guiding within the subducted high-velocity slab. The most striking feature in Europe is the cluster of the north-direction arrows in the central region. These are pointing away from the Alpine belt.

The second term of relative travel time residuals seems to have clusters of stations that show similar pattern. There is a great deal of regional consistency over a large part of North America. Most stations have NS slower directions in the western part of the United States, Canada and Alaska. In East Asia, in and around China and Japan, the dominant slower direction is E-W or WNW-ESE. The slower directions in these clusters and other stations are roughly consistent with the results of S-wave splitting analysis. It is easy to imagine that these second azimuthal terms correlate with the velocity anisotropy. Figure 2.24 has maps showing the faster split shear wave polarization directions from an ScS study (after Ando [1984]) and from SKS study (after Silver and Chan [1991]). If we assume the origin of the P-wave velocity anisotropy is same as that of the S-wave polarization, the second azimuthal dependency term for travel times should be orthogonal to the fastest direction of S-wave splitting. Comparing the second azimuthal term and shear-wave splitting, good agreements can be seen in some places, e.g. west and east coasts of North America, East Europe, and around China and Japan. For example, the slow directions of the second azimuthal term are roughly parallel with the direction of greatest principal compression in the United States (Zoback and Zoback [1980]). Seismic anisotropy represents dynamics of the Earth's interior,

directly reflecting the instantaneous stress in the mantle (Kaneshima [1991]). Previously, analyses of shear-wave splitting have been the main method to determine the anisotropy. This work shows that an azimuthally dependent analysis of P-waves is also a useful tool to clarify the stress field in the Earth's interior.

2.6 Discussion

2.6.1 Correlation between amplitude and travel time

Lateral fluctuations of travel time residuals reflect lateral variations of velocity structure in the Earth's interior. On the other hand, amplitudes of seismic rays are affected by both velocity heterogeneity and attenuation structure. In general, regional low- and high-velocity anomalies cause focusing or defocusing of rays, in consequence ray amplitudes become larger or smaller, respectively. If larger travel time residuals and larger amplitude are observed at one station, it is possible that the large amplitude is caused by focusing of low-velocity heterogeneity somewhere on the raypath, while early arrival and small amplitude indicate defocusing along the ray path. Therefore the positive correlations indicate that large amplitudes may be caused by focusing with low velocity anomalies. On the other hand, negative correlations between travel times and amplitudes can be caused by not only attenuation effects but also focusing effects by the low-velocity structure, when the low-velocity body exists at deep position and the focus is not near the surface (Haddon and Husebye [1978], Ødegaard and Doornbos [1993]). Ødegaard and Doornbos [1993] investigated the NORSAR (Norwegian Seismic Array) data and found that there is a clear relation between large-amplitude arrivals tend to be late, but late arrivals do not necessarily have large amplitude. Figure 2.25 shows the spatial distribution of correlation coefficients between relative travel time residuals and log-amplitude anomalies at each station. There exist systematic clusters of negative correlation with early arrivals in southern Eurasia (western

China and India) and late arrivals in the southern part of Southeast Asia (Malaysia, Singapore and Indonesia). This suggests that large amplitude observations are due to low attenuation in the crust and the upper mantle in southern Eurasia, while the high attenuation area or the deep low-velocity body may exists just beneath the southeastern Asia region. The other regions seem to have no systematics in general.

2.6.2 Crustal structure and amplitude

Amplitudes of seismic rays are affected by not only velocity and attenuation structure in the mantle but by crustal structure and local geology. I compare the log-amplitude anomalies to a new global model for the Earth's crust named CRUST5.1, presented by Mooney *et al.* [1998]. They constructed a global model which consists of 2,592 tiles on a 5° x 5° scale in which the crust and the uppermost mantle are described by eight layers: ice, water, soft sediment, hard sediment, crystalline upper crust, same type middle crust, same lower crust, and uppermost mantle. All of the tiles are classified into 14 primary crustal types. Figure 2.26 shows the primary crustal types showing P-wave velocities and the global distribution of the crustal types used to construct the model CRUST5.1 (Mooney *et al.* [1998]). The final classification has 139 structure types (84 continental, 26 oceanic, 23 shelf and six unique types for portions of the Red Sea, Black Sea and Caspian Depression) with differences in thickness, density, P- and S-wave velocities for each layer.

Figure 2.27 is a scatter diagram of the site effect term (equation (2.3.7)) for amplitude versus predicted site amplification from CRUST5.1. The predicted amplification factors, $\overset{/}{P}\overset{/}{P}$, were calculated by P-SV scattering matrix assuming vertical incident P-waves as

$$\overset{/}{P}\overset{/}{P} = 2^n \prod_{k=2}^{n} \left(\frac{\rho_k Vp_k}{\rho_{k-1} Vp_{k-1} + \rho_k Vp_k} \right) \tag{2.6.1}$$

where n is the number of layers (from bottom to surface), ρ_k is the density at the k-th layer, and Vp_k is the P-wave velocity at the k-th layer (Aki and Richards [1980]). As shown in Figure 2.27, most of the stations are separated into three ranges of amplification., continental shell ($\overset{/}{P}\overset{/}{P}$ ~ 2 to 3), active tectonic region ($\overset{/}{P}\overset{/}{P}$ ~ 4) and islands ($\overset{/}{P}\overset{/}{P}$ ~ 6 to 7). The site

effect terms have large fluctuations with relation to the predicted site amplification, and there seems to be only a slight positive correlation. Figure 2.28 is a plot of the site effect terms for amplitude versus primary crustal types. There are some differences for each crust type. For example, station amplitudes are relatively small in Phanerozoic and forearc regions, while Platform and late Proterozoic regions have a tendency for larger amplitude observations. It seems that generally the old continents have relatively larger amplitudes, while active tectonic regions have smaller amplitude. Such tendencies can be seen in other teleseismic amplitude studies (*e.g.*, Nakanishi and Motoya [1990], Negishi and Sato [1993]). The fluctuation of the site effect terms for amplitude, however, is so large that it cannot be explained by only the differences of the crustal type. This indicates that the site effect terms for amplitude are affected mainly by local effects, and the elastic structure of the crust and the uppermost mantle hardly affects them. Moreover, it is difficult to explain the fluctuations of site effect terms by the differences of the impedance beneath the seismometers, because the seismic observatory is seldom installed in the sedimentary place. The difference of the site effect term for amplitude may reflects much more local influences, such as local geology and instrumental origin.

Figure Captions

Fig. 2.1 A page of the ISC printed book. The seismic database contains hypocentral parameters, source mechanism, phase-picking data, and disaster information. The main part of this page is about the 1995 Kobe Earthquake.

Fig. 2.2 (a) WKBJ synthetic seismograms plotted as a function of epicentral distance. AK135 velocity model (Kennett *et al.* [1995]) was used. Only the time window around the direct P-phase was calculated. The source depth is 10 km.

(b) Amplitude variations of the figure (a) as a function of epicentral distances. Amplitude value is normalized by the source amplitude.

Fig. 2.3 Map showing locations of 3,445 epicenters that occurred during the period from 1984 to 1995 used in this study. The location parameters of each event were taken from the relocated hypocenters data base named EHB (Engdahl *et al.* [1998]). The events that has more than 15 amplitude data were used. The minimum and maximum body-wave magnitude are 4.4 and 6.9.

Fig. 2.4 Map showing locations of 718 stations used in this study. Totally 155,778 amplitude data observed these stations were used in this study.

Fig. 2.5 AK135 one-dimensional Earth model (Kennett *et al.* [1995]) in the crust and mantle. P-wave velocity (thick solid lien) and density (thin solid line) structure of this model were used for the calculation of geometrical spreading and ray tracing. The effects of one-dimensional attenuation was not included in this study.

Fig. 2.6 EHB epicenter relocation vectors relative to the ISC epicenters (after Engdahl *et al.* [1998]). The largest difference is over 30 km around the subduction region of the southwest Pacific, which corresponds to a arrival time difference of about 4 seconds.

Fig. 2.7 Definition of the fault parameters and ray parameters used to obtain the radiation pattern. 3 fault parameters (strike, dip and rake angles) and 2 ray parameters (azimuth and emergent angle) are used for the source mechanism correction.

Fig. 2.8 Radiation patterns for double-couple point source in a uniform medium. Left: 31 double couple force, mid: radiation pattern for P-waves, right: radiation pattern for S-waves. (after Kennett [1983]).

Fig. 2.9 Geometries and coordinates that using for calculating the geometrical spreading (R_0: the radius of the Earth, ρ_0: the density at the surface, V_0: the velocity at the surface, ρ_s: the density at the hypocenter, V_s: the velocity at the source, Δ: the angular epicentral distance, θ: the emergence angle measured from vertical, i_0: the incident angle measure from vertical).

Fig. 2.10 (a) (left) WKBJ seismograms using a non-attenuating AK135 model. Each trace was normalized by the maximum amplitude for all traces. (right) WKBJ seismograms using a AK135 model with attenuation shown in Fig. 2.5 (Montagner and Kennett [1996]). The difference of the amplitude variation between these figures cannot be seen. This indicates that the 1-D attenuation effect can be excluded if we analyze relative amplitude variations for each event.

(b) Amplitude variations of figures (a) as a function of epicentral distances. The absolute values of each amplitude are much different.

Fig. 2.11 Examples of histogram of the relative log-scaled amplitude residual (referred to as log-amplitude anomaly) for each station (IMA: Indian Mountain, PMR: Paimer, SPA: South Pole, WRA: Warramunga, MAT: Matsushiro, MAI: Maizuru). The log-amplitude anomalies have a log-normal distribution.

Fig. 2.12 Geographical distribution of the average log-amplitude anomalies (site effect terms). The size of the symbols is proportional to the anomaly according to the indicated scale. Circle and diamond indicate larger and smaller amplitude, respectively.

Fig. 2.13 Log-amplitude anomaly fluctuation as a function of back azimuth viewed from station to event. The vertical axis is the common-logarithm of amplitude anomaly. Back azimuth is measured clockwise from North. Solid curve is the least-squares fit of equation (2.4.1). The horizontal line shows the constant term A_0. Vertical thin lines indicate one-sigma standard deviations for each 20 degrees azimuth window. The same figures for all station analyzed here are shown in Appendix A-1.

Fig. 2.14 Geographical distribution of the terms A_0, A_1 and A_2 in equation (2.4.1). The size of the symbols are proportional to the anomaly according to the indicated scale. Circle and diamond indicate larger and smaller amplitude for A_0, respectively. The arrow points toward the largest direction for A_1, and the bar is parallel to the largest direction for A_2. These coefficients are listed in Appendix B-1.

Fig. 2.15 Geographical distribution of the terms A_0, A_1 and A_2 in equation (2.4.1) in North America. Other details are same as Fig. 2.14.

Fig. 2.16 Geographical distribution of the terms A_0, A_1 and A_2 in equation (2.4.1) in Europe. Other details are same as Fig. 2.14.

Fig. 2.17 Geographical distribution of the terms A_0, A_1 and A_2 in equation (2.4.1) in Asia-Oceania. Other details are same as Fig. 2.14.

Fig. 2.18 Relative travel time residual fluctuation as a function of back azimuth viewed from station to event. The vertical axis is the relative travel time residual in second. The same figures for all station analyzed here are shown in Appendix A-2. Other details are same as Fig. 2.13.

Fig. 2.19 Geographical distribution of the relative travel time residuals. Circle and diamond indicate late and early P-wave arrivals for A_0, respectively. The arrow points toward the latest arrival direction for A_1, and the bar is parallel to the latest

direction for A_2. These coefficients are listed in Appendix B-2. Other details are same as Fig. 2.12.

Fig. 2.20 Geographical distribution of the terms A_0, A_1 and A_2 for the relative travel time residuals in equation (2.4.1) for the world. Other details area same as Fig. 2.12.

Fig. 2.21 Geographical distribution of the terms A_0, A_1 and A_2 for the relative travel time residual in North America. Other details area same as Fig. 2.14.

Fig. 2.22 Geographical distribution of the terms A_0, A_1 and A_2 for the relative travel time residual in Europe. Other details area same as Fig. 2.14.

Fig. 2.23 Geographical distribution of the terms A_0, A_1 and A_2 for the relative travel time residual in Asia-Oceania. Other details area same as Fig. 2.14.

Fig. 2.24 (upper) Map showing faster direction of shear wave splitting obtained from ScS (solid lines) study (after Ando [1984]). The length of the lines are proportional to the time difference between the two sprit waves. The dashed lines with a small code show the linear particle motions possibly representing no splitting of shear waves.

(lower) Faster shear wave splitting obtained from SKS analysis (after Silver and Chan [1991]). The bar is parallel to the fastest polarization directions, and the time difference between the split waves is indicated by the size of solid circle.

Fig. 2.25 Geographical distribution of the correlation coefficients between the relative log-amplitude anomaly and the relative travel time residual. Circle indicates positive correlation (larger amplitudes and late arrivals were observed) and diamond indicates negative correlation (large amplitudes and fast arrivals). The size of symbols are proportional to the correlation coefficients.

Fig. 2.26 (upper) Crustal types used to construct the global crustal model CRUST5.1 (after Mooney *et al.* [1998]). Each crustal type has seven crustal layers. The crustal layers are ice, water, soft sediments, hard sediments, and the upper, middle and

lower crystalline crust. Only P-wave velocity is shown here, but the other parameters, such as S-wave velocity and density are also specified.

(lower) Global distributions of CRUST 5.1 types shown in the upper figure. The crustal structure in unmeasured regions has been extrapolated using statistical averages of regions of similar tectonic setting. (after Mooney *et al.* [1998])

Fig. 2.27 Scatter diagram of the site effect term for amplitude station corrections (Averaged log-amplitude anomalies, equation (2.3.7)) versus the predicted site amplifications of CRUST5.1. The predicted amplifications were calculated by P-SV scattering matrix assuming vertical incident P-waves to each crustal structure type. Almost of the plots cam be divided to three ranges of the calculated site amplification, continental shell (~ 2.5), active tectonic region (~ 4) and islands (~ 6 to 7).

Fig. 2.28 (upper) The site effect terms for amplitude versus the primary crustal types of CRUST5.1. Station amplitudes are relatively small in Phanerozoic and forearc regions, while Platform and late Proterozoic regions have a tendency for larger amplitude observations. The fluctuation of the site effect terms for amplitude, however, is so large that it cannot be explained by only the differences of the crustal type.

(lower) P-wave velocity structure of the primary types of CRUST5.1 (after Mooney *et al.* [1998]).

ASAR	Alice Springs Ar.	84.53	221	P	18 54 47.4	(1.2)	−0.9
ASPA	Alice Springs	84.54	221	↑iP	18 54 48.3	(1.3)	0.0
ROB	Roburent	84.55	354	P	18 54 46.6		−1.2
BDI	Bagni Di Lucca	84.56	352	P	18 54 48.1		+0.2
SFI	Santa Sofia	84.58	351	P	18 54 50.2		+2.2
FIN	Finale Ligure	84.61	353	P	18 54 46.3		−1.8
STV	Sta Anna Valdieri	84.63	354	P	18 54 47.0		−1.3
PGD	Poggio Sodo	84.64	351	P	18 54 49.1		+0.8
ENR	Entracque	84.64	354	P	18 54 46.9		−1.4
CRE	Caprese Michel	84.86	351	P	18 54 50.7		+1.3
TOUF	Mont Tourmerait	84.87	354	P	18 54 50.9		+1.4
AUTN	L'Aution	84.87	354	P	18 54 50.9		+1.4
PII	Pisa	84.90	352	P	18 54 49.6		0.0
KER	Bakhtaran	84.93	322	↓iP	18 54 49.2		−0.8
IMI	Imperia	84.93	354	P	18 54 48.7		−1.0
POO	Poona	84.94	293	↑iP	18 54 49.0	(2.0)	−1.4
AURF	Auriere	84.99	354	P	18 54 51.2		+1.1
MVIF	Mont Vial	84.99	354	P	18 54 51.2		+1.1
SBF	Sospel	85.00	354	eP	18 54 50.9		+0.8
REVF	Revere	85.13	354	P	18 54 51.8		+1.0
CALN	Calern	85.15	354	P	18 54 52.1		+1.2
CDR	Cadarache	85.29	355	eP	18 54 51.7		+0.1
ASS	Assisi	85.34	350	P	18 54 52.0		+0.2
FRF	La Forêt Royale	85.36	355	eP	18 54 51.5	(1.5)	−0.4
LRG	Lorgues	85.48	355	eP	18 54 53.2	(1.3)	+0.7
VAY	Valandovo	85.58	343	eP	18 54 54.0		+0.9
LMR	La Mourre	85.59	355	eP	18 54 53.9	(1.6)	+0.8
AQU	l'Aquila	85.96	349	P	18 54 57.1		+2.1
MNS	Montasola	86.01	350	P	18 54 54.4		−0.8
EPF	Esparros	86.10	359	eP	18 54 55.8	(.8)	+0.2
PGF	Pioggiola	86.20	353	eP	18 54 56.7	(1.8)	+0.6
SDI	San Donato	86.55	349	P	18 54 57.6		−0.3
GBA	Gauribidanur Ar.	86.70	288	P	18 54 57.0		−2.2
ORI	Oriolo Calabro	87.82	347	P	18 55 05.9		+1.8
MGR	Morigerati	87.88	347	P	18 55 04.1		−0.2
STKA	Stephens Creek	89.13	211	↑iP	18 55 10.8	(1.2)	+0.3
KOD	Kodaikanal	89.32	285	P	18 55 13		+1.2
BWA	Boorowa	89.49	205	eP	18 55 13.2		+1.0
CAN	Canberra	90.18	204	eP	18 55 16.4		+1.0
SDV	Santo Domingo	95.46	69	eP	18 55 42.5		+2.4
SHRA	Al Sharaya	99.21	322	↓eP	18 55 58.0		+1.1
LITH	Al Lith	99.65	321	↓eP	18 56 02.3		+3.4
BGCA	Bogoin	121.42	337	ePKP	19 01 07.0		−0.7
DBIC	Dimbokro	122.22	5	ePKP	19 01 08.5		−0.7
TIC	Toumodi	122.23	5	PKP	19 01 10.6	(1.1)	+1.4
KIC	Kosan Boka	122.53	5	PKP	19 01 11.2	(.6)	+1.4
ITR	Itaparica	127.59	50	ePKP	19 01 20.7		+1.1
BDFB	Brasilia	128.32	64	PKP	19 01 22.1	(1.1)	+1.2
BAO	Brasilia Array	128.33	64	ePKP	19 01 13.5		−7.4
VNDA	Vanda	128.94	185	PKP	19 01 21.8		+1.2
OPO	Ambohidratompo	130.16	293	PKP	19 01 27.5	(.7)	+3.1
VTY	Vatovaky	130.36	292	PKP	19 01 27.8	(.7)	+3.0
VDA	Vodivohitra	130.69	293	PKP	19 01 28.7		+3.3
ABM	Ambohimiarambe	131.01	292	PKP	19 01 29.5	(.6)	+3.5
PTZ	Petauke	134.92	313	↑iPKP	19 01 36.0		+2.6
PTZ	Petauke				19 01 49.0		
SPA	South Pole	141.05	180	ePKP	19 01 36.0	(1.0)	−6.7
BUL	Bulawayo	141.31	312	PKP	19 01 46.3	(1.7)	+1.4
BFT	Belfast (SA)	145.29	306	↓iPKP	19 01 52.5		+0.9
MAW	Mawson	145.60	217	PKP	19 01 52.3	(1.5)	+1.5
POG	Pongola	145.83	302	↓iPKP	19 01 53.5	(2.3)	+1.0
SLR	Silverton	146.22	308	↓iPKP	19 01 54.5		+1.3
SLR	[.23μm,0s8:1]						
KSR	Koster	147.01	310	↓iPKP	19 01 58.0	(2.1)	+3.5
BFS	Buffelsfontein	147.93	309	↑iPKP	19 02 01.9	(2.3)	+6.0
WIN	Windhoek	148.16	327	ePKP	19 01 55.0	(2.3)	−1.4
BLF	Bloemfontein	150.04	307	↓iPKP	19 02 05.7	(2.6)	+6.4
BOSA	Boshof	150.10	309	↑iPKP	19 02 04.7		+5.3
FRS	Fauresmith	151.00	308	↑iPKP	19 02 06.7	(2.0)	+6.0
HVD	H. Verwoerd Dam	151.61	306	↑iPKP	19 02 50.1		+48.5
GRM	Grahamstown	153.18	301	↓iPKP	19 02 15.0		+11.3
GRM	[96nm,1s0:1]						
POF	Pofadder	153.19	317	↓iPKP	19 02 15.0		+11.1
SYO	Syowa Base	153.88	212	↓ePKP	19 02 12.3		+8.7
CER	Ceres	156.87	313	↓iPKP	19 01 14.0	(2.1)	−54.7

EIDC 16d 18h 42m 23s9, 6°66N×73°19W, h162km, Mb4.3/3
ISC 16d 18h 42m 22s±1s2, 6°78N±°099×73°08W±°092, h161km±14km, n19, σ1s13/16, Mb4.5/4, 3C-4D, Northern Colombia

---

ROM 16d 18h 56m 43s0, 42°8N×13°1E, h5km, Mb2.6
ISC 16d 18h 56m 44s±1s8, 42°8N±°11×13°2E±°18, h5km, n5, σ0s71/5, Central Italy

---

EIDC 16d 18h 59m 46s6, 51°13N×179°05E, h0km, Mb4.6/4
NEIC 16d 18h 59m 50s2, 51°37N×179°13E, h33km, σ1s61, Mb4.6/2, Less reliable solution.
ISC 16d 18h 59m 51s±1s7, 51°4N±°15×179°1E±°13, h41km±15km, n17, σ1s52/16, Mb4.1/4, Rat Islands

---

JMA 16d 19h 03m 03s3±0s6, 43°49N±°04×147°55E±°05, h24km, M3.5, n31, Kuril Islands

---

IGQ 16d 19h 13m 21s1, 1°1S×78°2W, h39km, Mb3.2
ISC 16d 19h 13m 22s±1s3, 1°09S±°069×78°1W±°14, h39km, n10, σ0s60/10, 3C-2D, Ecuador

---

NEIC 16d 19h 20m 23s7, 79°20N×123°76E, h10km, σ0s72, Mb4.5/20, Less reliable solution.
EIDC 16d 19h 20m 23s9, 79°24N×123°31E, h0km, Mb4.4/5
ISC 16d 19h 20m 23s7±0s61, 79°20N±°091×123°9E±°41, h10km, n27, σ0s87/27, Mb4.5/20, 1C, East of Severnaya Zemlya

---

NEIC 16d 19h 21m 32s9, 32°56S×71°67W, h10km, σ0s99, Single network solution.
GUC 16d 19h 21m 33s6, 32°53S×71°68W, h15km
ISC 16d 19h 21m 33s±3s4, 32°6S±°14×71°7W±°26, h10km, n11, σ0s95/11, Near coast of Central Chile

---

NEIC 16d 19h 23m 27s1, 44°77N×6°78E, h5km, σ0s93, ML2.4(GEN).
LDG 16d 19h 23m 27s4, 44°8N×6°4E, h2km, ML2.2
ISC 16d 19h 23m 26s4±0s76, 44°75N±°030×6°69E±°090, h5km, n21, σ0s84/21, France

---

JMA 16d 19h 32m 07s4±0s3, 34°56N±°05×141°01E±°03, h49km
ISC 16d 19h 32m 07s±3s5, 34°5N±°51×141°0E±°28, h49km, n5, σ0s43/5, Off east coast of Honshū

JMA 16d 19h 38m 56s9±0s4, 43°29N±°03×147°28E±°04, h52km, M3.4, n25, Kuril Islands

---

NEIC 16d 19h 43m 47s8, 34°02S×70°04W, h5km, σ0s42, Single network solution.
GUC 16d 19h 43m 48s0, 34°01S×70°07W, h2km
ISC 16d 19h 43m 49s±6s1, 34°0S±°21×70°1W±°39, h7km±15km, n8, σ0s48/8, Chile-Argentina border region

---

JMA 16d 20h 08m 21s3±0s3, 40°01N±°01×143°04E±°03, h0km, M3.0
ISC 16d 20h 08m 19s±2s6, 39°99N±°080×143°0E±°24, h0km, n13, σ0s28/12, Off east coast of Honshū

ISC 16d 20h 17m 05s2±0s89, 43°1N±°11×0°6W±°11, h10km, n6, σ0s37/6, 1D, Pyrenees

---

JMA 16d 20h 22m 09s4±0s2, 36°46N±°01×140°57E±°01, h59km±2km, M2.9
ISC 16d 20h 22m 09s6±0s69, 36°48N±°058×140°6E±°11, h59km, n20, σ0s62/18, Near east coast of Honshū

GUC 16d 20h 45m 12s6, 33°16S×70°29W, h5km
ISC 16d 20h 45m 04s±5s6, 32°7S±°23×70°0W±°34, h5km, n7, σ1s03/7, Mendoza Province, Argentina

---

EIDC 16d 20h 46m 50s3, 34°63N×134°90E, h0km, Mb5.7/15
MOS 16d 20h 46m 51s3, 34°64N×134°99E, h17km, Mb6.8/40, Ms7.2/13
MOS Focal mechanism: C25,D19; NP1:φ=343°,δ47°,λ36°. NP2: φ=227°,δ65°,λ131°. Principal axes: T Plg52°,Azm185°; N Plg36°,Azm27°; P Plg10°,Azm289°. Mo=1.1×10^19Nm (OBN)
JMA 16d 20h 46m 51s8±0s0, 34°59N±°00×135°04E±°00, h16km±2km, M7.2
JMA Felt I=VI J Sumoto, Kôbe, V Toyo'oka, Hikone, Kyôto, IV Nara, Kôchi, Tottori, Tokushima, Okayama, Takamatsu, Maizuru, Himeji, Wakayama, Osaka, Tsu, Tsuruga, Gifu, Fukui, III Oita, Saigô, Hiroshima, Matsuyama, Murotomisaki, Yonago, Matsue, Shiono misaki, Owase, Nagoya, Kanazawa, Iida, Toyama, Wa jima, II Miyazaki, Shimonoseki, Kumamoto, Saga, Uwa jima, Takayama, Karuizawa, Hamamatsu, Shizuoka, Kôfu, Mishima, Nagano, Takada, Yokohama
BJI 16d 20h 46m 52s0, 34°63N×135°02E, h26km, Mb6.1, Ms7.3
NEIC 16d 20h 46m 52s1, 34°58N×135°02E, h22km, σ1s00, Mb6.3/99, Ms6.8/52, Mw6.8(GS), Mw6.9(HRV). Casualties I=XII MM
NEIC MS 6.5 (BRK). Mo=6.3×10^19Nm (PPT). Five thousand five hundred and two people confirmed killed, 36,896 injured and extensive damage I=VII J in the Kobe area and on Awaji-shima. Over 90 percent of the casualties occurred along the southern coast of Honshu between Kobe and Nishinomiya. At least 28 people were killed by a landslide at Nishinomiya. About 310,000 people were evacuated to temporary shelters. Over 200,000 buildings were damaged or destroyed. Numerous fires, gas and water main breaks and power outages occurred in the epicentral area. Felt VII J along a coastal strip extending from Suma Ward, Kobe to Nishinomiya and in the Ichinomiya area on Awaji-shima; V MM at Iwakuni. Also felt IV J on Shikoku. Right-lateral surface faulting was observed for 9 kilometres with horizontal displacement of 1.2 to 1.5 metres in the northern part of Awaji-shima. Liquefaction also occurred in the epicentral area. Depth from broadband displacement seismograms.
NEIC Radiated energy from the P-wave first-motion solution: 8.5±1.6×10^14Nm/8
NEIC Moment tensor solution: s31, scale 10^19Nm; M_{rr}0.09; $M_{\theta\theta}$1.61; $M_{\phi\phi}$−1.70; $M_{r\theta}$−0.39; $M_{r\phi}$−0.33; $M_{\theta\phi}$−0.46. Depth 15km; Principal axes: T 1.74,Plg12°,Azm186°; N 0.09, Plg73°,Azm51°; P −1.84,Plg11°,Azm279°; Best double couple: Mo1.8×10^19Nm; NP1:φ=323°,δ73°,λ0°. NP2:φ=233°, δ90°,λ163°.
NEIC Fault plane solution: P waves. NP1:φ=232°,δ79°,λ153°. NP2:φ=328°,δ64°,λ12°. Principal axes: T Plg27°,Azm187°; P Plg10°,Azm282°. The focal mechanism is well controlled and corresponds to right-lateral strike slip faulting with a moderate reverse component. The preferred fault plane is NP1 and has been identified as the Nojima Fault.
ISC Maximum intensity I=XI MM, maximum peak ground acceleration recorded 833 cm/sec², approximate duration 8–12 sec. (Extract from a report from the Bhabha Atomic Research Centre, Bombay, India).
CSEM 16d 20h 46m 54s2, 34°70N×135°00E, h15km, Mw6.9. Mo=2.9±1.0×10^19Nm. Fault plane solution NP1:φ=318°,δ79°, λ10°. NP2:φ=226°,δ80°,λ169°. Principal Axes: T Plg15°, Azm182°; N Plg75°,Azm5°; P Plg1°,Azm272°.
HRVD 16d 20h 46m 59s4±0s1, 34°78N±°00×134°99E±°01, h20km±.4km, Centroid moment tensor solution. Data used: GSN; LP body waves: s70,c187; Mantle waves: s58, c145; Half duration: 6s6. Moment tensor: Scale 10^19Nm; M_{rr}0.61±.01; $M_{\theta\theta}$1.90±.01; $M_{\phi\phi}$−2.51±.01; $M_{r\theta}$−0.69±.03; $M_{r\phi}$−0.22±.03; $M_{\theta\phi}$−0.57±.01. Principal Axes: T 2.24, Plg22°,Azm186°; N 0.37,Plg67°,Azm22°; P −2.61,Plg6°, Azm278°. Best double couple: Mo2.4×10^19Nm, NP1: φ=324°,δ70°,λ12°. NP2:φ=230°,δ79°,λ160°.
ISC 16d 20h 46m 51s9±0s28, 34°55N±°014×135°04E±°014, h19km±2.2km, (h18km±1.0km:pP−P), n893, σ1s03/827, Mb6.1/168, Ms6.9/72, 67C-108D, Near south coast of Southern Honshū

KOB	Kôbe	0.18	41	P*	20 46 55.6		−1.1
KOB	(I=VI JMA)			S	20 46 59.1		−7
JAJ	Awaji shima	0.24	207	cP*	20 46 57.9		+0.3
OSA	Osaka	0.42	72	dP*	20 47 00.0		−0.4
OSA	(I=IV JMA)			S	20 47 06.1		−5
JKS	Kasai	0.46	339	cP*	20 47 00.0		−1.1
ABU	Abuyama	0.53	55	↓P*	20 47 01	(2.4)	−1.5
JHE	Heguri	0.54	79	dP*	20 47 01.7		−0.9
JWY	Kouya	0.57	126	dP*	20 47 02.9		−0.1
JWM	Minabe	0.75	160	cP*	20 47 07.2		+1.1
JWT	Wachi	0.78	22	cP*	20 47 05.8		−0.9
JAD	Aida	0.82	298	dP*	20 47 06.5		−0.7
MZH2	Maizuru 2	0.89	19	cP*	20 47 07.7		−0.9
JAI	Aioi	0.90	213	cP*	20 47 09.6		+0.9
OKA1	Okayama	0.93	277	P*	20 47 08.8		−0.4
OKA1	(I=IV JMA)			S	20 47 22.3		−1
JJS	Sakaide	0.93	259	dP*	20 47 08.7		−0.6
MAI	Maizuru	0.96	17	P*	20 47 08.1		−1.6
MAI	(I=IV JMA)			S	20 47 20.2		−4
JMT	Mikata	0.98	335	P*	20 47 09.0		−1.0
OWA	Owase	1.07	117	dP*	20 47 11.5		−0.1
TSUJ	Tsu 2	1.15	82	dP*	20 47 12.0		−0.9
JWZ	Kozaga	1.16	151	cPn	20 47 12.7		−0.4
HIK	Hikone	1.22	54	Pn	20 47 13.8		−0.2
HIK	(I=V JMA)			S	20 47 30.7		0
JTG	Taga	1.23	59	dPn	20 47 13.7		−0.3
TSU1	Tsu	1.23	81	dPn	20 47 14.2		+0.1
TSU1	(I=IV JMA)			S	20 47 31.5		+1
TSRJ	Tsuruga	1.25	38	cPn	20 47 14.3		0.0
JMN	Monobe	1.27	230	cPn	20 47 14.9		+0.3
JKR	Kurayoshi	1.30	310	Pn	20 47 14.5		−0.5
TSR	Tsuruga	1.38	37	Pn	20 47 17.6		+1.4
TSR	(I=IV JMA)			S	20 47 34.8		0
MRT2	Murotomisaki 2	1.38	213	Pn	20 47 16.4		+0.1
JJG	Jouge	1.56	274	Pn	20 47 18.6		−0.2
JHS	Saijyo	1.65	286	dPn	20 47 19.6		−0.4
GIF	Gifu	1.65	59	dPn	20 47 20.3		+0.3
GIF	(I=IV JMA)			eS	20 47 39		−2
NAG	Nagoya	1.70	68	dPn	20 47 21.5		+0.7
NAG	(I=III JMA)			eS	20 47 44		+1
FUK	Fukui	1.78	33	dPn	20 47 22.5		+0.5
FUK	(I=IV JMA)			iS	20 47 46.5		+2
JET	Tanbara	1.82	245	Pn	20 47 23.0		+0.4
JNM	Ikuma	1.90	300	Pn	20 47 23.8		+0.1
JKU	Kubokawa	2.06	234	Pn	20 47 25.9		−0.1
JHM	Kurahashi	2.12	259	Pn	20 47 26.7		−0.1
SAI	Saigô	2.15	320	Pn	20 47 27.0		−0.3
JJO	Oda	2.17	287	Pn	20 47 28.0		+0.4
HMM	Hamamatsu	2.22	85	dPn	20 47 28.5		+0.3
HMMJ	Hamamatsu 2	2.23	81	dPn	20 47 28.2		−0.2
TK01	Tokai 1	2.26	110	Pn	20 47 28.5		−0.3
TK02	Tokai 2	2.33	104	Pn	20 47 29.5		−0.3
TK04	Tokai 4	2.35	93	Pn	20 47 30.3		+0.2
JNA	Nagahama	2.35	246	dPn	20 47 30.8		+0.7
KANJ	Kanazawa	2.41	32	dPn	20 47 32.0		+1.0
KANJ	(I=III JMA)			S	20 48 06.5		+6
TKY	Takayama	2.41	48	dPn	20 47 31.1		+0.1
UWA2	Uwa jima 2	2.41	237	Pn	20 47 31.2		+0.2
KAN2	Kanazawa 2	2.42	35	dPn	20 47 31.3		+0.2
TK03	Tokai 3	2.45	98	Pn	20 47 32.0		+0.5
IID	Iida	2.48	67	dPn	20 47 32.2		+0.2
IID	(I=III JMA)			eS	20 48 03		0
IIDJ	Iida	2.53	68	ePn	20 47 33		+0.3
JMD	Masuda	2.60	273	Pn	20 47 34.0		+0.4
SHZ3	Shizuoka 3	2.66	78	dPn	20 47 34.0		−0.5
JKD	Kudamatsu	2.67	260	Pn	20 47 36.3		+1.6
TOY	Toyama	2.78	39	dPn	20 47 36.5		+0.3
SHZ	Shizuoka	2.80	80	dPn	20 47 36.3		−0.3
SHZ	(I=II JMA)			S	20 48 10.5		0
OKY	Okuyama	2.86	75	dPn	20 47 37.2		−0.2
JKI	Kunimi	3.02	253	Pn	20 47 41.2		+1.5
MTMJ	Matsumoto	3.03	47	dPn	20 47 39.9		+0.1
KOF	Kôfu	3.09	68	dPn	20 47 40.9		+0.3
KOF	(I=II JMA)			S	20 48 23.5		+6
JUS	Usuki	3.12	242	eS	20 48 28.3		
NGT	Nagatsuro	3.14	88	dPn	20 47 40.6		−0.8
WAJ	Wa jima	3.21	27	cPn	20 47 42.7		+0.4
WAJ	(I=III JMA)			eS	20 48 29.8		+9
OIT2	Oita 2	3.24	248	Pn	20 47 43.7		+0.9
MIS	Mishima	3.25	79	dPn	20 47 42.6		−0.3
MAT	Matsushiro	3.26	52	dPn	20 47 42.7		−0.3
MAT	Matsushiro			eS	20 48 26		+4
MAJO	Matsushiro	3.26	52	ePn	20 47 42.0		−1.0
MAJO	Matsushiro			eS	20 48 31.1		+9
MJAR	Matsushiro Array	3.26	52	Pn	20 47 43.0		0.0
JTY	Toyota	3.30	266	dPn	20 47 43.7		+0.1
NGN	Nagano	3.32	50	dPn	20 47 44.3		+0.4
KTJJ	Kamata 2	3.33	82	dPn	20 47 43.1		−1.0
KRZ	Karuizawa	3.37	57	eS	20 48 25		
AJI	Ajiro	3.37	81	dPn	20 47 43.6		−1.1
AJI	(I=I JMA)			iS	20 48 25.0		0
JMH	Hososhima	3.50	237	dPn	20 47 48.2		+1.8
NJJJ	Nii jima 2	3.51	91	Pn	20 47 46.6		0.0
CHJJ	Chichibu	3.56	64	dPn	20 47 47.4		+0.1
OSHJ	Oshima	3.57	86	dPn	20 47 47.4		−0.1
OSHJ	Oshima			iS	20 48 30.4		0
CHJ	Chichibu	3.60	65	Pn	20 47 54		+6.1
CHJ	(I=I JMA)			S	20 48 40.2		+9
JFA	Akaike	3.62	258	Pn	20 47 48.0		−0.2
TKD	Takada	3.64	45	Pn	20 47 50.7		+2.2
JNU	Nakatsue	3.75	249	Pn	20 47 50.0		0.0
MAE	Maebashi	3.77	60	Pn	20 47 52		+1.8
JKJ	Kijyo	3.81	234	Pn	20 47 51.1		+0.3
KMG	Kumagaya	3.89	65	Pn	20 47 54.0		+2.0
KMG	(I=I JMA)			eS	20 48 42		+4
YOK	Yokohama	3.89	76	Pn	20 47 55.1		+3.1
TAT	Tateyama	4.00	82	Pn	20 47 53		−0.5
TATJ	Tateyama 2	4.02	82	Pn	20 47 54.7		+0.8
NIIJ	Niigata 2	4.19	49	dPn	20 47 55.9		−0.3
HJJ	Hachijô jima	4.21	109	Pn	20 47 56.0		−0.5
HJJ	Hachijô jima			iS	20 48 48.3		+2
AIK	Aikawa	4.32	36	Pn	20 47 58.9		+0.8
AIK	Aikawa			eS	20 48 54		+5
UNZ	Unzen dake	4.37	247	Pn	20 48 00.6		+1.7
BSO4	Boso 4	4.38	83	Pn	20 47 57.7		−1.3
UTS	Utsunomiya	4.41	62	dPn	20 47 59.3		−0.2
UTS	(I=I JMA)			S	20 48 58.3		+7
JZO	Okuchi	4.43	238	Pn	20 48 00.6		+0.9
JII	Iki	4.47	262	Pn	20 48 00.2		0.0
KAKJ	Kakioka Outpost	4.51	67	dPn	20 47 59.5		−1.3
BSO3	Boso 3	4.51	85	Pn	20 48 00.1		−0.8
JTU	Tsushima	4.66	271	Pn	20 48 01.6		−1.3
NII	Niigata	4.66	43	Pn	20 48 10.9		+7.9
BSO2	Boso 2	4.71	86	Pn	20 48 03.4		−0.3
JFY	Yanaizu	4.73	52	dPn	20 48 04.1		+0.1
NGSJ	Nagasaki 2	4.78	248	Pn	20 48 05.3		+0.7
IZU2	Izuhara 2	4.78	268	Pn	20 48 03.1		−1.6
MIT	Mito	4.79	66	Pn	20 48 04.5		−0.3
MIT	(I=I JMA)			S	20 49 01.7		+1
KAGJ	Kagoshima 2	4.85	227	Pn	20 48 07.3		+1.7
BSO1	Boso 1	4.90	87	Pn	20 48 05.4		−0.9
CHOJ	Chôsi	4.90	75	Pn	20 48 06.6		+0.2
JSU	Suzuyama	4.91	233	Pn	20 48 07.2		+0.8
SHRJ	Shirakawa 2	4.91	58	dPn	20 48 06.2		−0.3
CHO1	Chôsi	4.91	74	Pn	20 48 06		−0.5
JTN	Tanegashima 3	5.18	223	Pn	20 48 11.1		+0.8
JFT	Otama	5.21	54	dPn	20 48 11.1		+0.4
ONAJ	Onahama 2	5.32	60	dPn	20 48 11.8		−0.5
JYS	Shirataka	5.46	46	dPn	20 48 14.5		+0.3
JFK	Kawauchi	5.50	58	dPn	20 48 14.5		−0.3
JYA	Atsumi	5.51	42	Pn	20 48 15.8		+0.8
JMM	Marumori	5.70	53	dPn	20 48 17.7		0.0
JKC	Kuchinoerabu	5.78	226	(S)	20 49 28.9		
JOU	Okura	5.92	48	Pn	20 48 21.3		+0.6
JYK	Kaneyama	6.10	43	Pn	20 48 24.2		+0.9
JIO	Ouri	6.40	51	dPn	20 48 27.8		+0.3
AKIJ	Akita 2	6.58	37	Pn	20 48 31.5		+1.4
JRG	Rokugo	6.59	41	Pn	20 48 31.1		+1.0
JMK	Ichinoseki	6.62	47	dPn	20 48 30.7		+0.1
DFUJ	Ofunato	6.97	48	dPn	20 48 36.1		+0.5
JOM	Ohasama	7.01	44	dPn	20 48 36.4		+0.4
MRKJ	Morioka 2	7.11	43	dPn	20 48 37.7		+0.2
JAH	Hinai	7.17	37	dPn	20 48 38.8		+0.4
SEO	Seoul	7.20	297	ePn	20 48 40		+1.3
JIW	Iwasaki	7.20	32	Pn	20 48 38.8		0.0
MIYJ	Miyako 2	7.38	45	dPn	20 48 41.8		+0.5
JKZ	Kuzumaki	7.38	41	dPn	20 48 41.5		+0.2
JZK	Kikaishima	7.58	216	(S)	20 50 21.5		
JTH	Tanohata	7.65	43	dPn	20 48 45.4		+0.4
JAM	Amami Oshima	7.68	219	cPn	20 48 44.6		−0.9
AOM3	Aomori 3	7.72	35	dPn	20 48 46.5		+0.5
JSI	Shiura	7.75	32	cPn	20 48 47.2		+0.8
HACJ	Hachinohe 2	7.79	40	Pn	20 48 47.9		+0.5
JTM	Tenmabayashi	7.84	36	Pn	20 48 48.7		+1.8
JHY	Hiyama	8.13	28	P	20 48 51.8		0.9
JOR	Okushj	8.26	23	P	20 48 56.0		+2.5
JOT	Ohata	8.30	33	P	20 48 55.0		+0.9
JTK	Tokunoshima	8.53	219	P	20 48 57.4		+0.2
HAK	Hakodate	8.53	30	P	20 49 00		+2.7
HAKJ	Hakodate 2	8.55	30	P	20 48 58.9		+1.3
JYM	Yakumo	8.66	27	P	20 48 59.6		+0.5
JKB	Kayabe	8.71	31	P	20 49 01.1		+1.4
JSH	Shimam	8.97	24	P	20 49 04.6		+1.2
MRR	Muroran	9.04	29	P	20 49 08		+3.7
MRR	Muroran			eS	20 50 59		+12
SUT1	Suttsu	9.17	25	P	20 49 08		+1.1
JNB	Noboribetsu	9.19	29	eS	20 51 03.6		
JMZ	Minamidaito 2	9.31	202	P	20 49 10.2		+2.1
CBIJ	Chichi jima	9.64	139	P	20 49 12.5		−0.3
CBI	Chichi jima	9.65	139	P	20 49 12.5		−0.3
CBI	Chichi jima			S	20 51 02.7		+1
JOW	Kunigami	9.65	219	cP	20 49 10.8		−2.1
JIH	Iheya	9.65	221	P	20 49 12.1		−0.7
JEW	Eniwo	9.67	29	P	20 49 14.9		+1.3
URA	Urakawa	9.72	36	P	20 49 13		−0.7
URA3	Urakawa 3	9.73	36	P	20 49 13.5		−0.4
JBT	Biratori	9.75	33	eS	20 51 17.8		
JEM	Erimo	9.80	38	P	20 49 14.9		0.0
SAP	Sapporo	9.80	28	P	20 49 17		+2.1
JCH	Chûrui	10.35	36	(S)	20 51 23.0		
JFR	Furan	10.41	32	P	20 49 23.2		−0.1
NAH1	Naha	10.46	219	P	20 49 22.5		−1.3
JJT	Tamagu	10.47	219	P	20 49 25.3		+1.3
OBI	Obihiro	10.51	35	P	20 49 25		+0.5
JHR	Hokuryû	10.54	27	P	20 49 26.0		+1.3
RMJ	Rumoi	10.68	27	P	20 49 31		+4.3
JOB	Onbets	10.80	37	P	20 49 26.1		−2.1
ASA	Asahikawa	10.82	30	P	20 49 31		+2.3
JKE	Kume jima 2	10.86	223	dP	20 49 28.3		−1.1
MDJ	Mudanjiang	10.89	339	↓P	20 49 31.2		+1.5
MDJ	[12.4μm,2s7:1]			iS	20 51 32.0		−1
JYG	Yagishiri	11.02	25	P	20 49 34.5		+3.3
JKK	Kamikawa	11.05	31	P	20 49 32.1		+0.3
JAR	Ashorobuto	11.06	35	P	20 49 29.1		−2.1
KUS	Kushiro	11.13	38	P	20 49 30		−3.1
JSS	Shosan	11.16	26	P	20 49 35.7		+2.3
ASAJ	Asahikawa	11.19	29	P	20 49 32.6		−1.3
JMP	Maruseppu	11.42	32	P	20 49 35.4		−1.5
ABJ2	Abashiri 2	11.52	34	P	20 49 35.4		−3.1
SNY	Shenyang	11.57	312	↓iP	20 49 39.0		0.1
SNY	[.24μm,1s8:1]			pP	20 49 46.0		+3

Figure 2.1

(a) WKBJ Seismograms (model AK135)
T - 7.0/degree (sec)

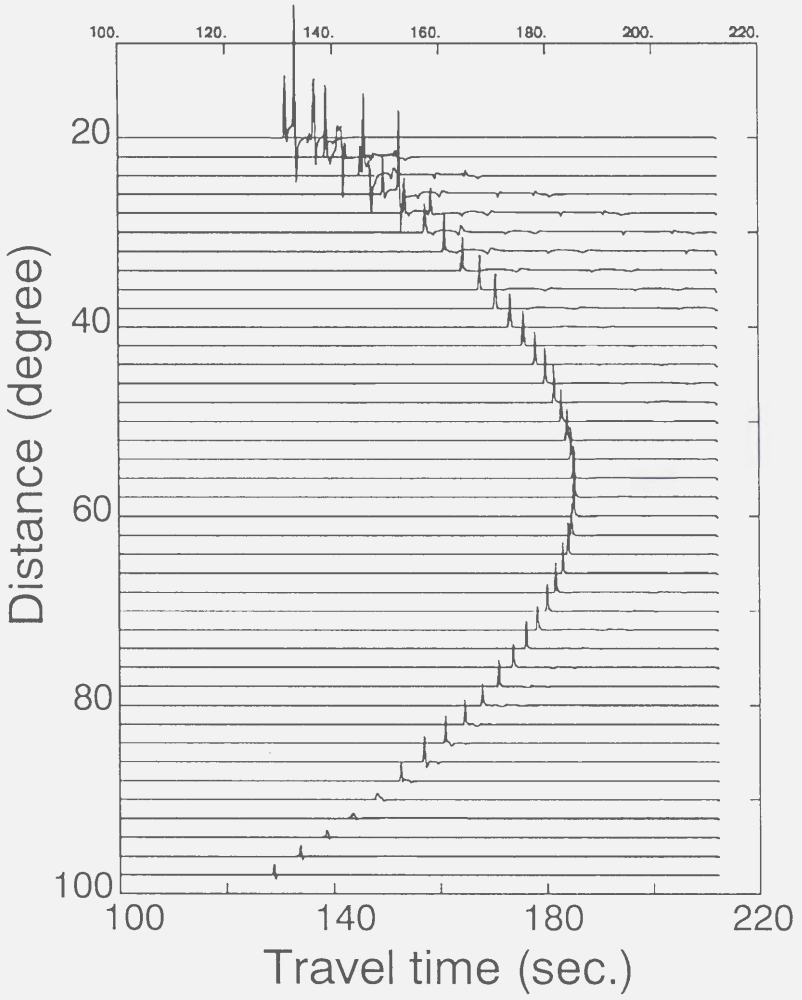

(b) WKBJ Amplitude (model AK135)

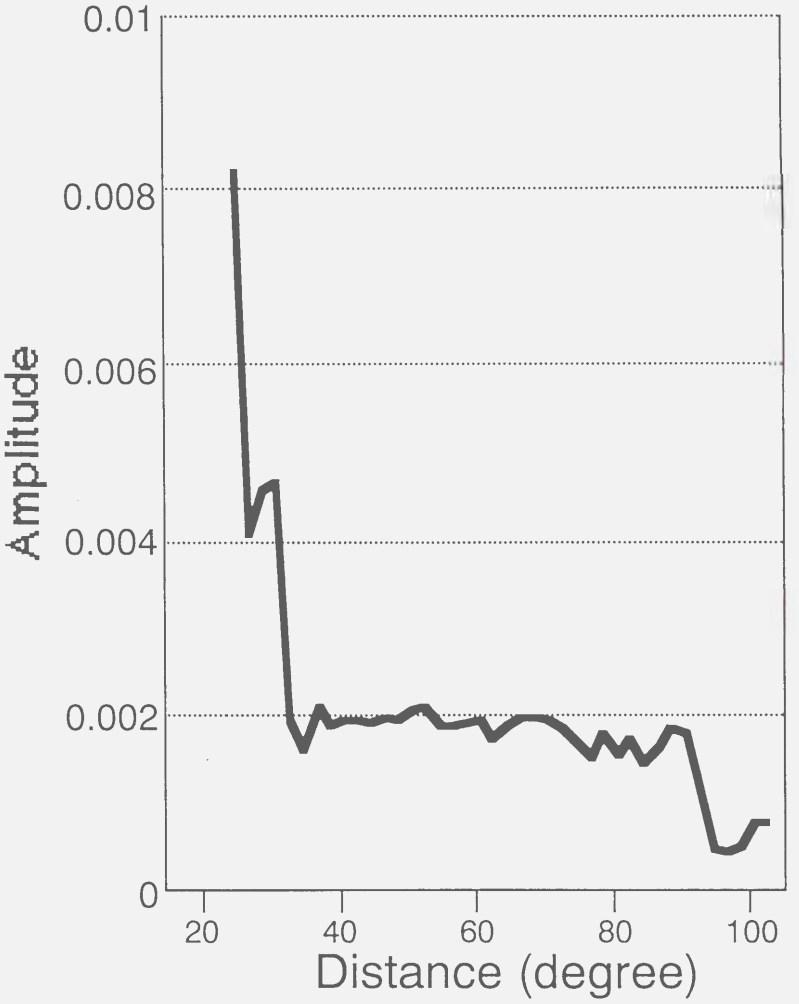

Figure 2.2

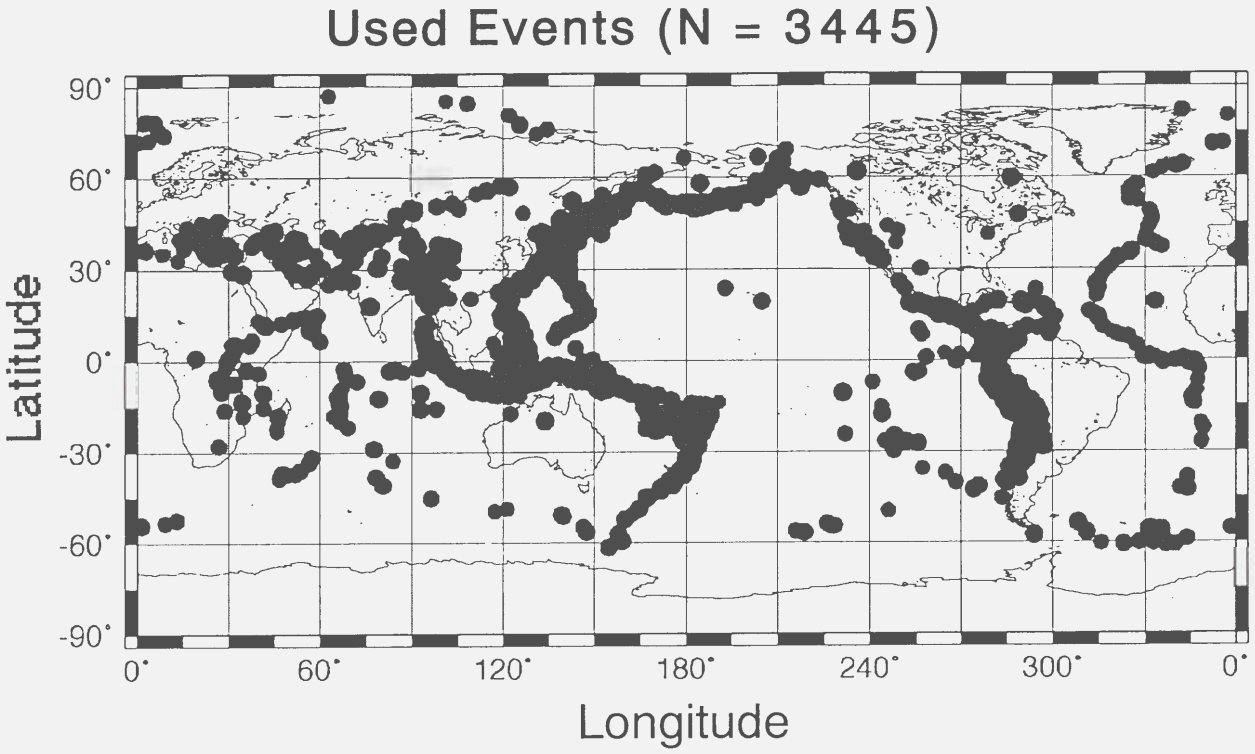
Used Events (N = 3445)
90°
60°
30°
0°
-30°
-60°
-90°
Latitude
0°
60°
120°
180°
240°
300°
0°
Longitude

Figure 2.3

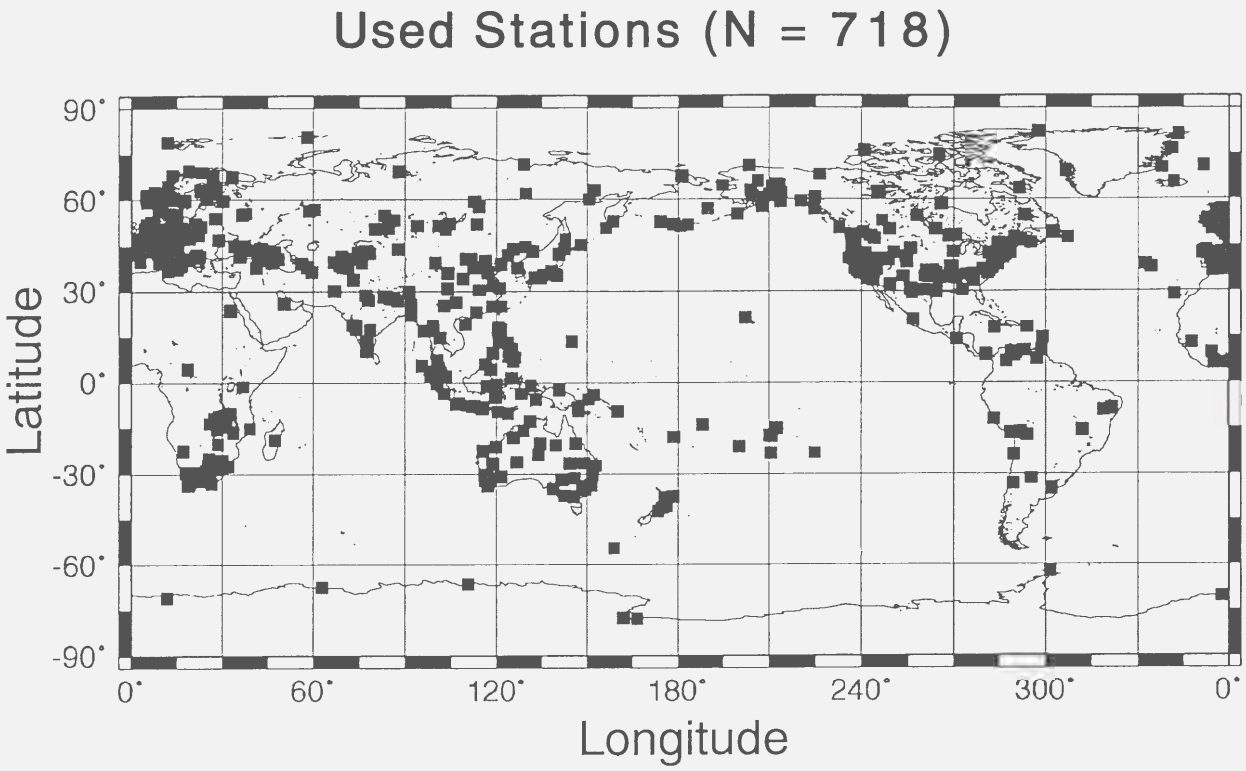
Used Stations (N = 718)
90°
60°
30°
0°
-30°
-60°
-90°
Latitude
0°
60°
120°
180°
240°
300°
0°
Longitude

Figure 2.4

AK135 (Kennett et al., 1995; Montagner and Kennett, 1996)

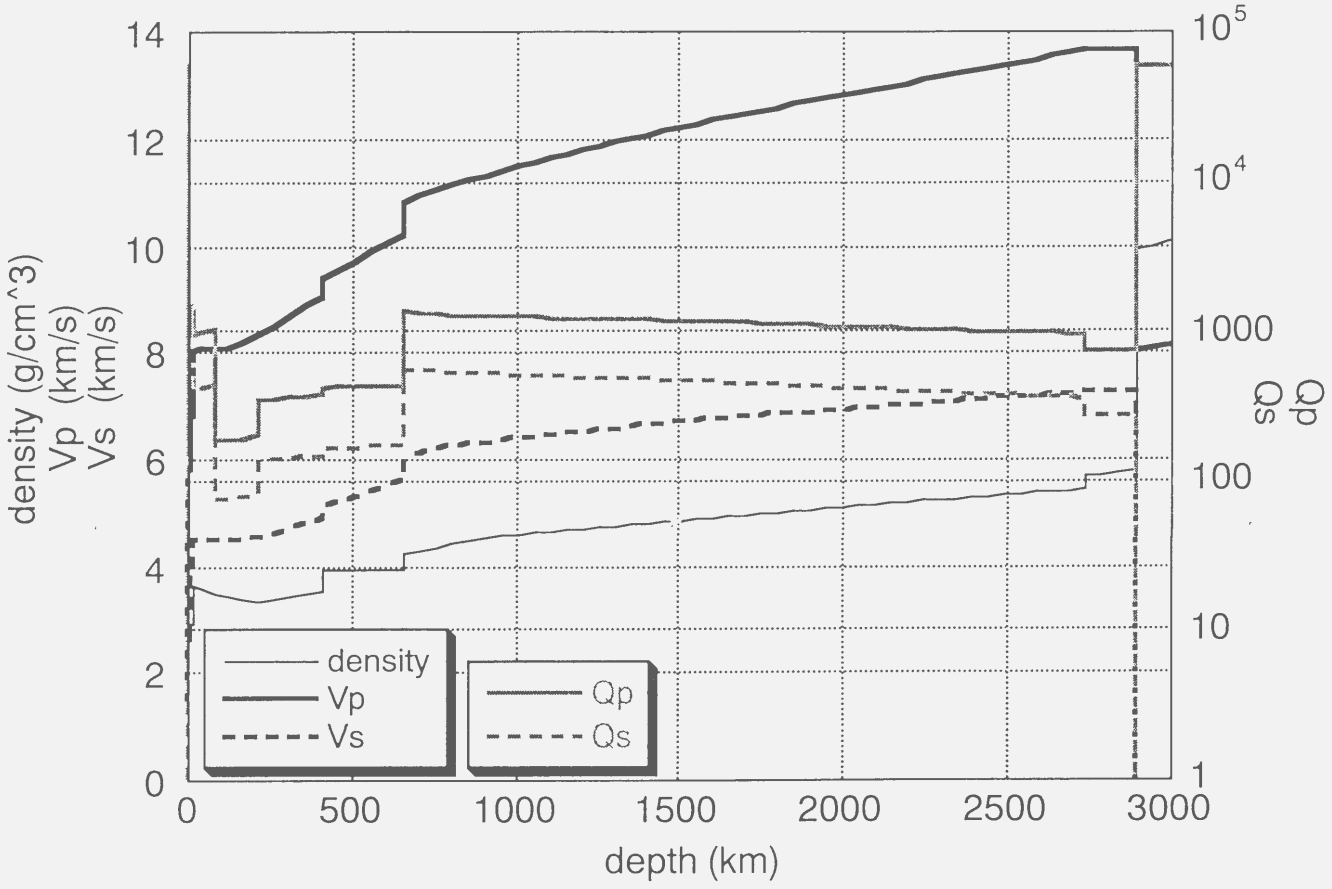

Figure 2.5

(a)

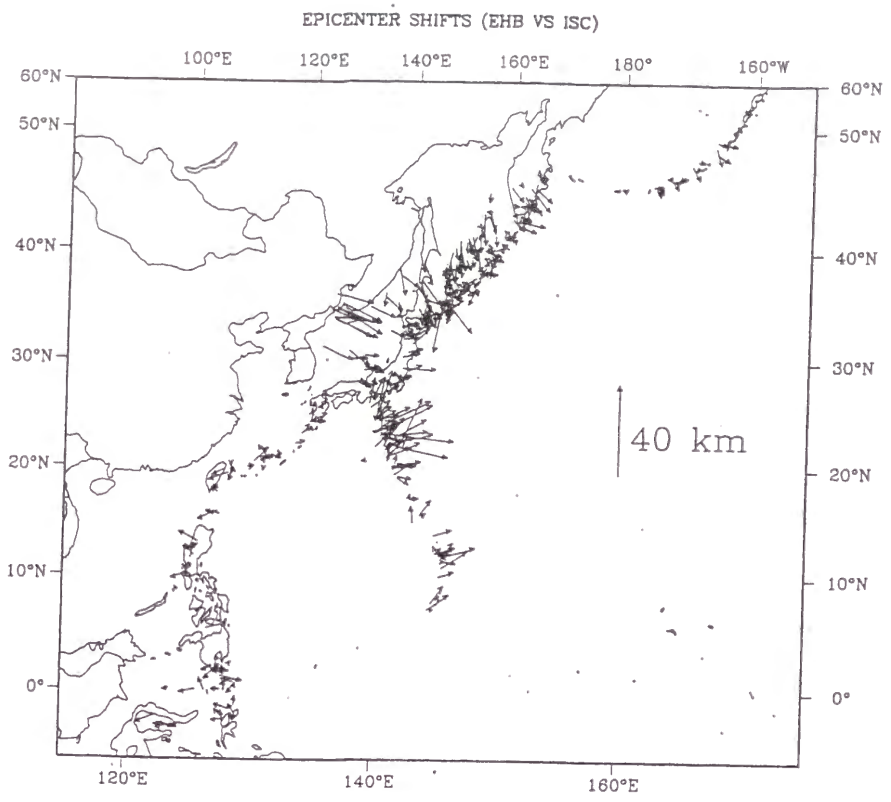
EPICENTER SHIFTS (EHB VS ISC)
100°E
120°E
140°E
160°E
180°
160°W
60°N
50°N
40°N
30°N
20°N
10°N
0°
40 km
120°E
140°E
160°E

(b)

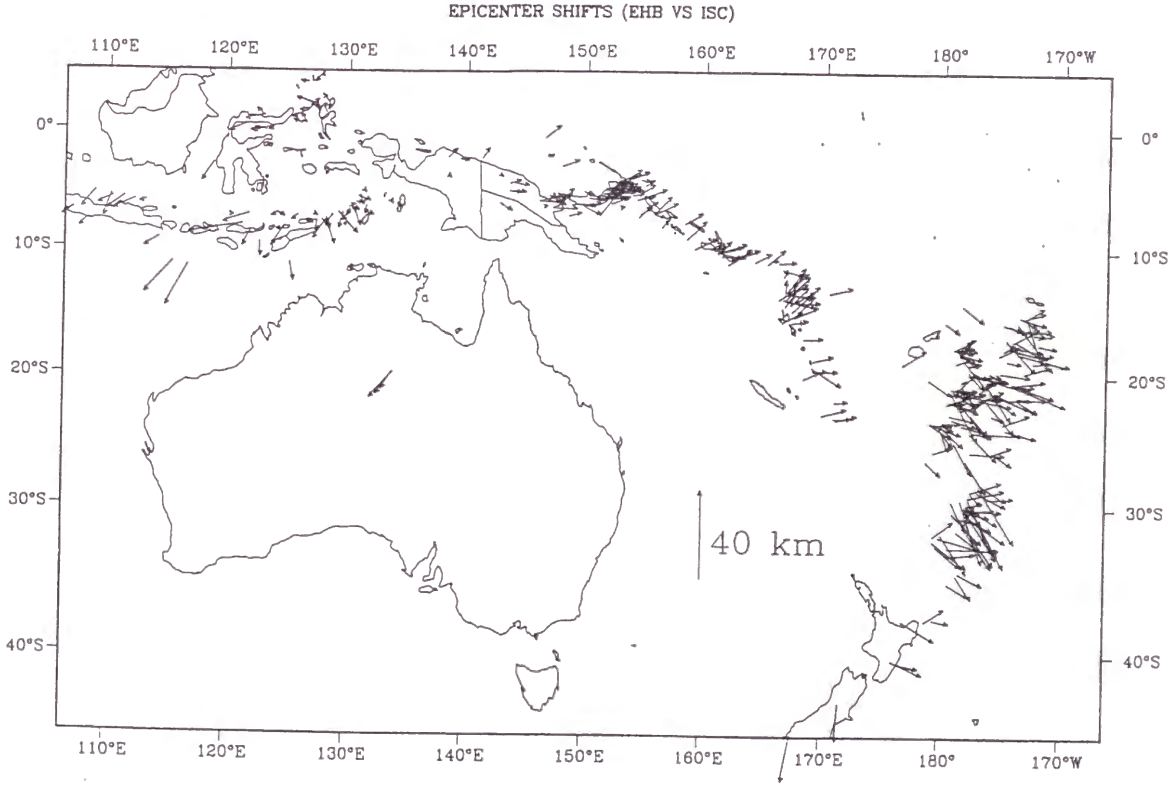
EPICENTER SHIFTS (EHB VS ISC)
110°E
120°E
130°E
140°E
150°E
160°E
170°E
180°
170°W
0°
10°S
20°S
30°S
40°S
40 km

Figure 2.6

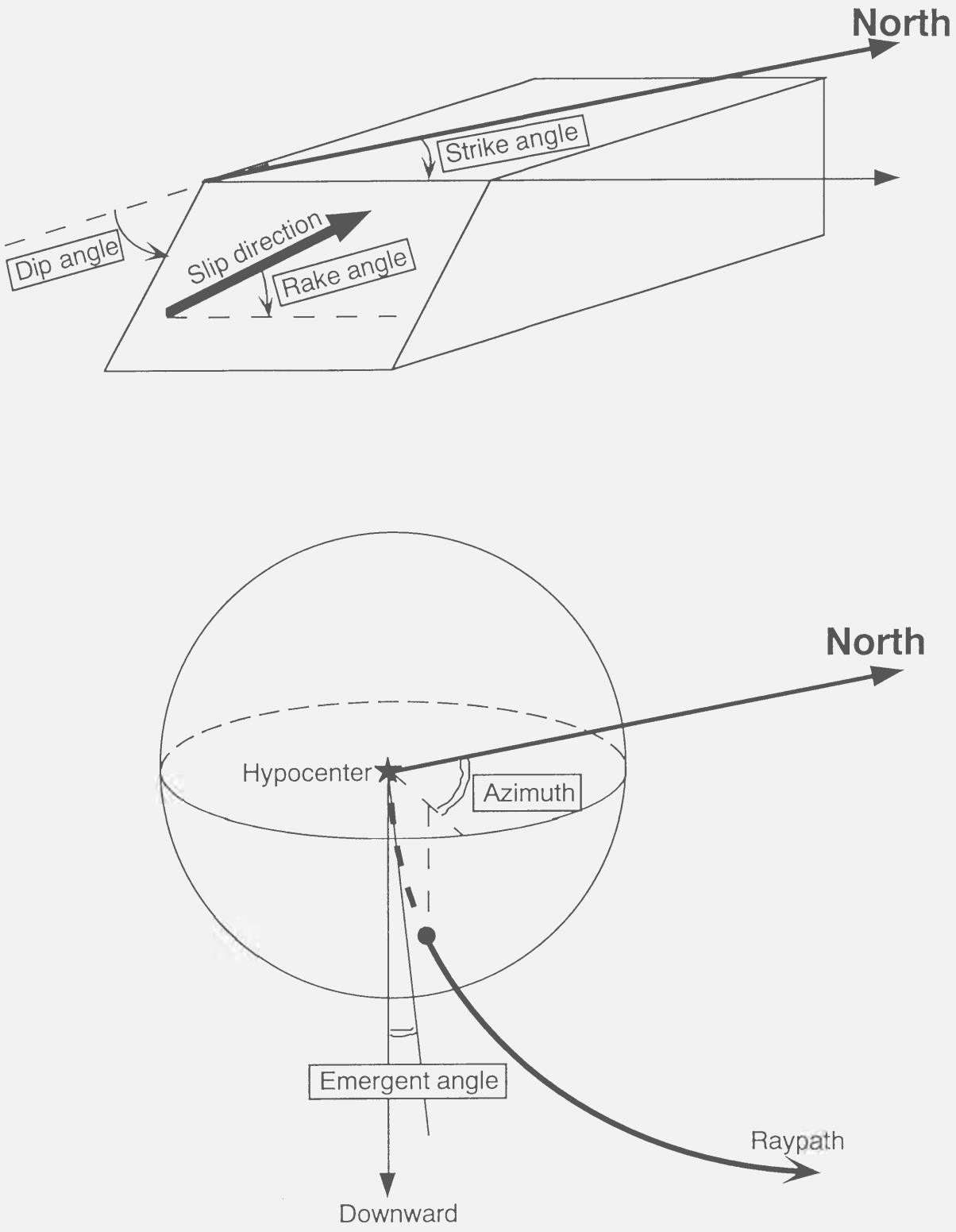
North
Strike angle
Dip angle
Slip direction
Rake angle
North
Hypocenter
Azimuth
Emergent angle
Raypath
Downward

Figure 2.7

d)

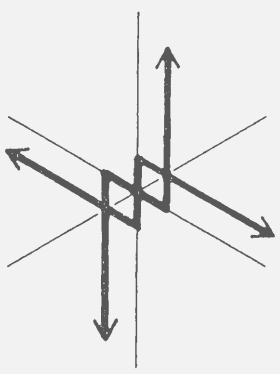

$2\gamma_1\gamma_3$

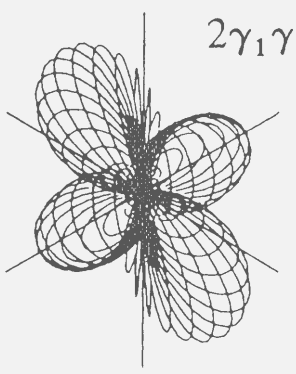

$(\gamma_1^2 + \gamma_3^2 + 4\gamma_3\gamma_1)^{\frac{1}{2}}$

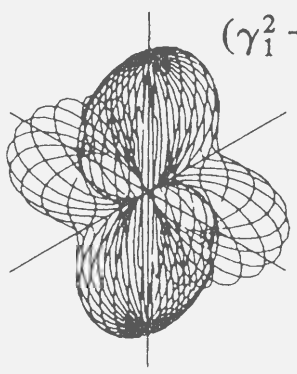

Figure 2.8

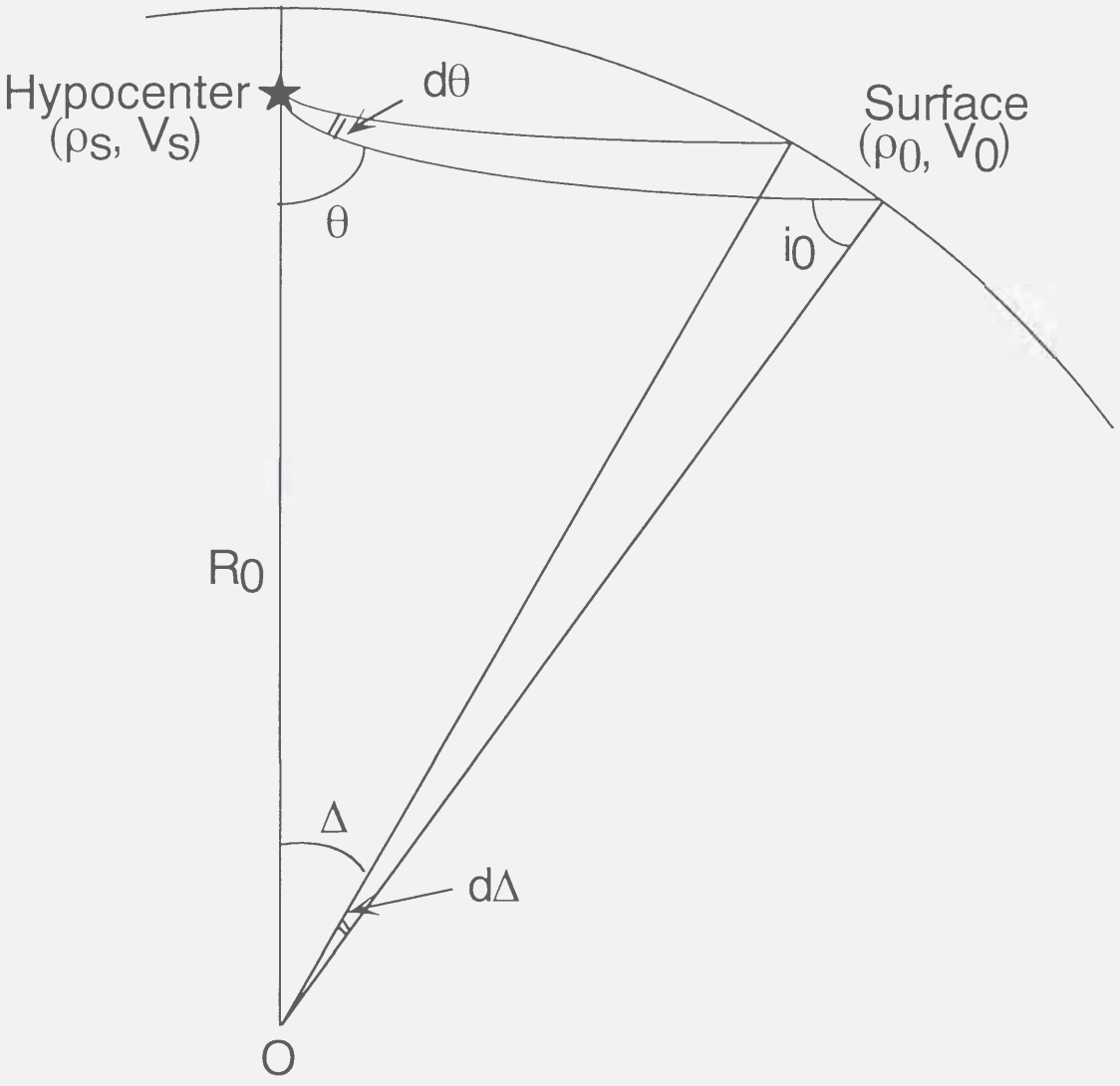

Figure 2.9

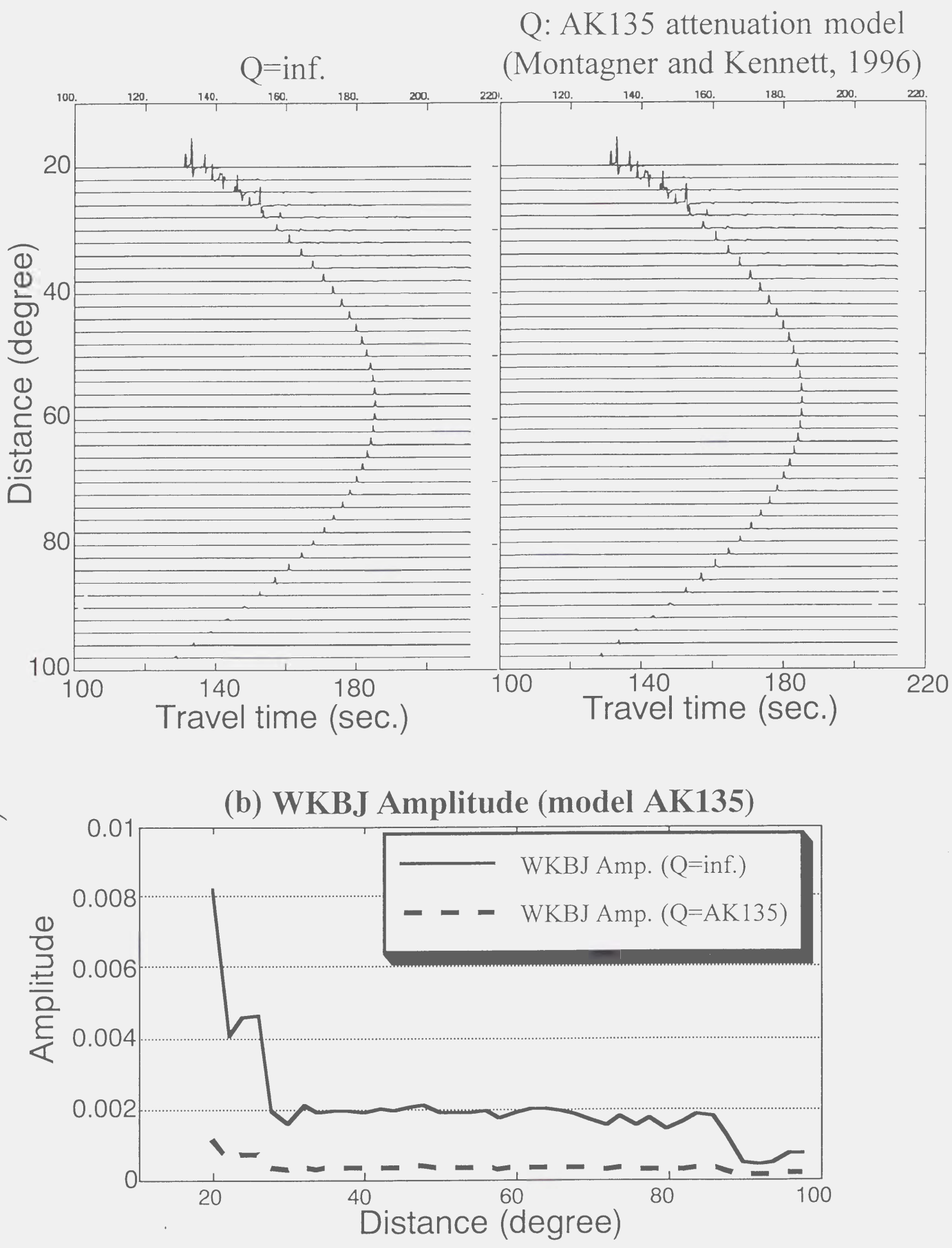
(a) WKBJ Seismograms (model AK135)
T - 7.0/degree (sec)
Q=inf.
Q: AK135 attenuation model
(Montagner and Kennett, 1996)
Distance (degree)
Travel time (sec.)
Travel time (sec.)
(b) WKBJ Amplitude (model AK135)
WKBJ Amp. (Q=inf.)
WKBJ Amp. (Q=AK135)
Amplitude
Distance (degree)

Figure 2.10

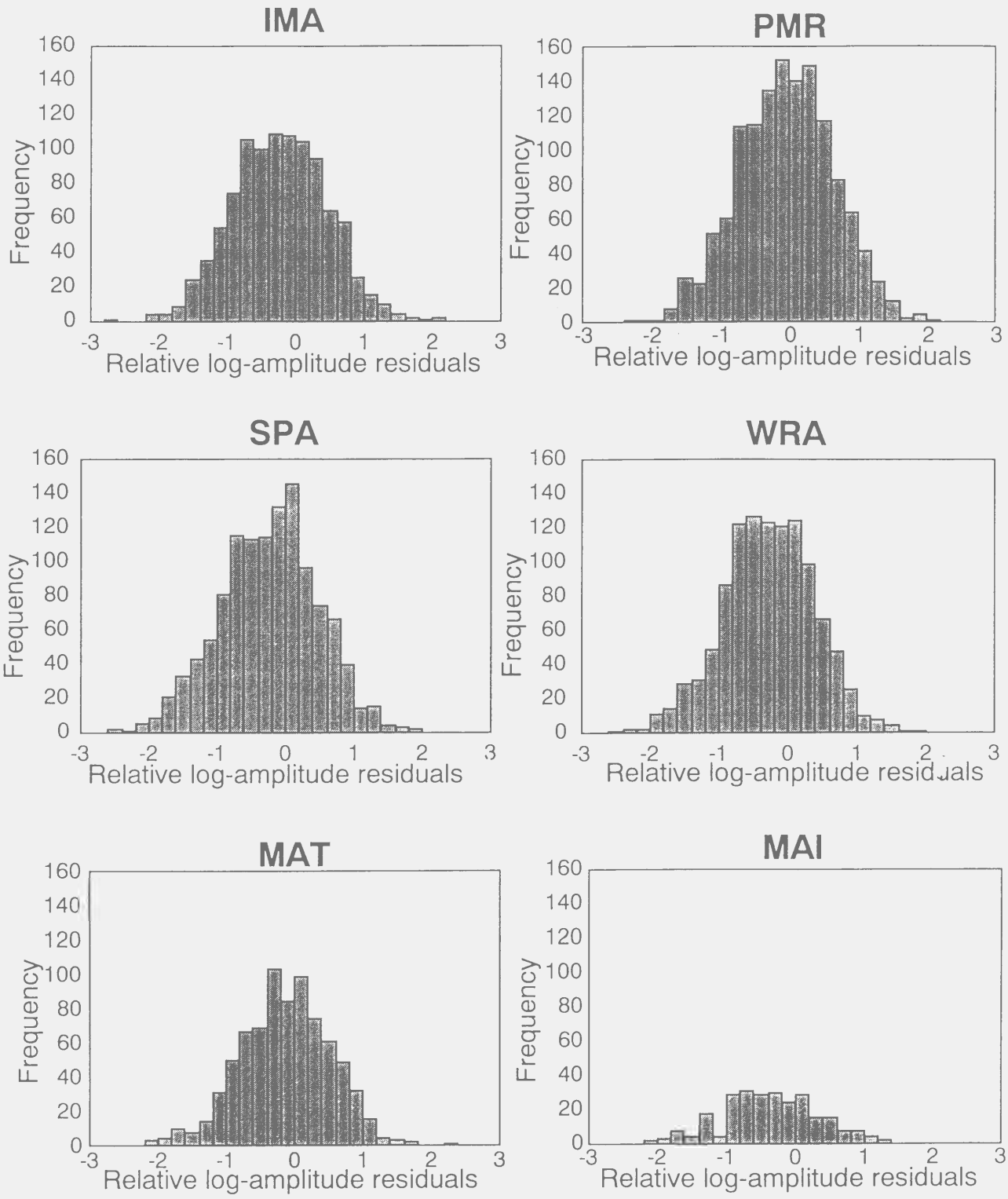
IMA
PMR
SPA
WRA
MAT
MAI
Frequency
Relative log-amplitude residuals
0
20
40
60
80
100
120
140
160
-3
-2
-1
0
1
2
3

Figure 2.11

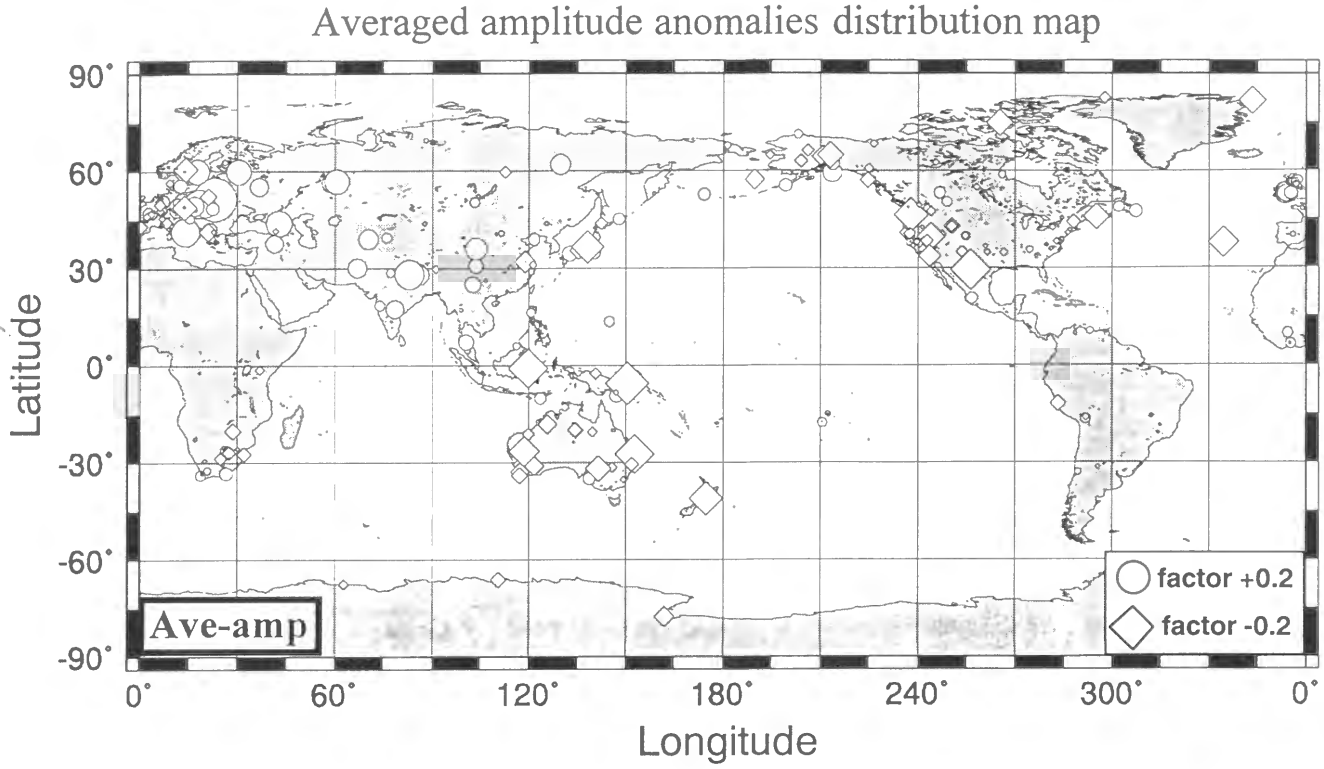
Averaged amplitude anomalies distribution map
90°
60°
30°
0°
-30°
-60°
-90°
Latitude
0°
60°
120°
180°
240°
300°
0°
Longitude
Ave-amp
factor +0.2
factor -0.2

Figure 2.12

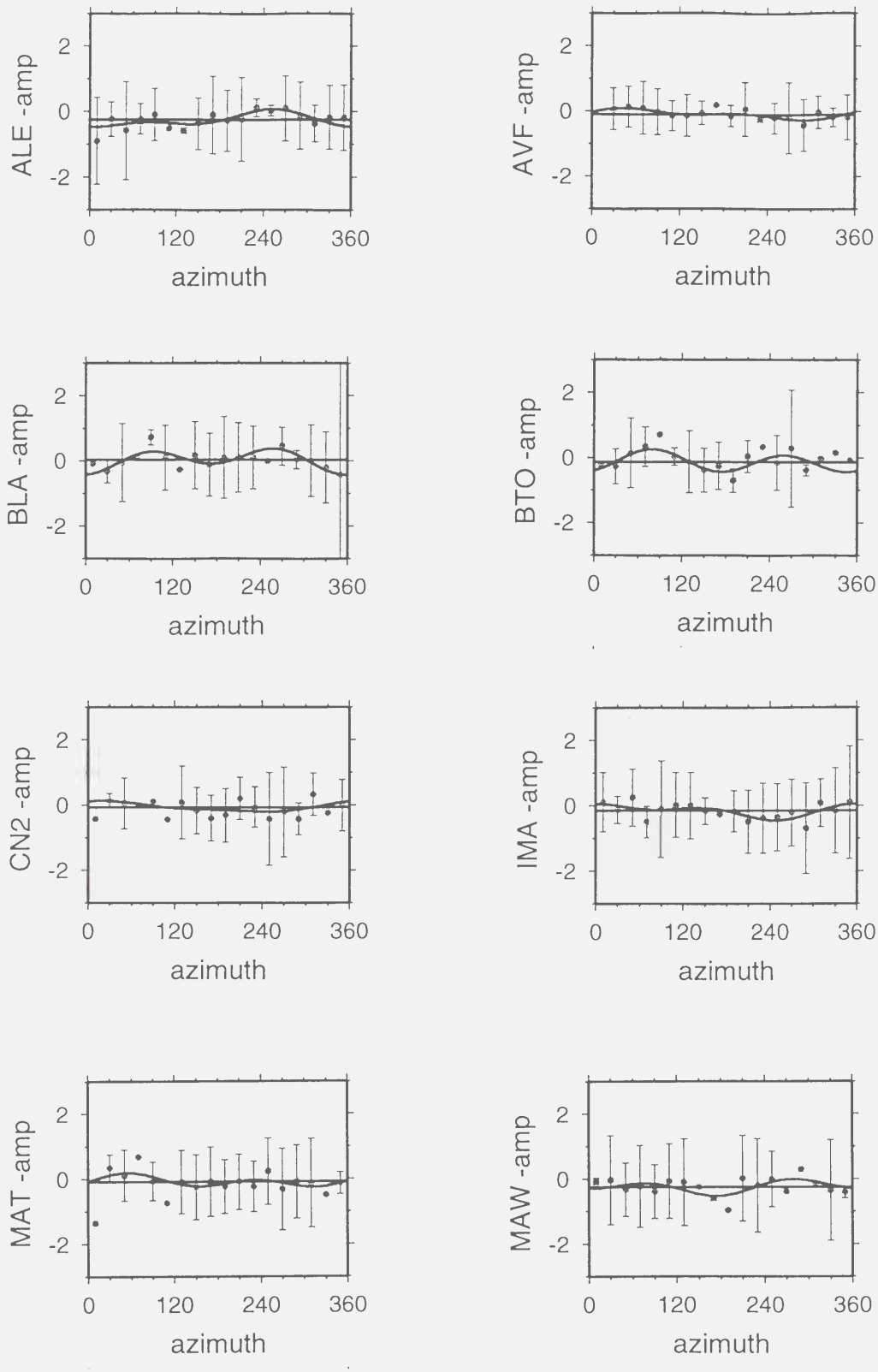
ALE -amp
AVF -amp
BLA -amp
BTO -amp
CN2 -amp
IMA -amp
MAT -amp
MAW -amp
2
0
-2
0
120
240
360
azimuth

Figure 2.13

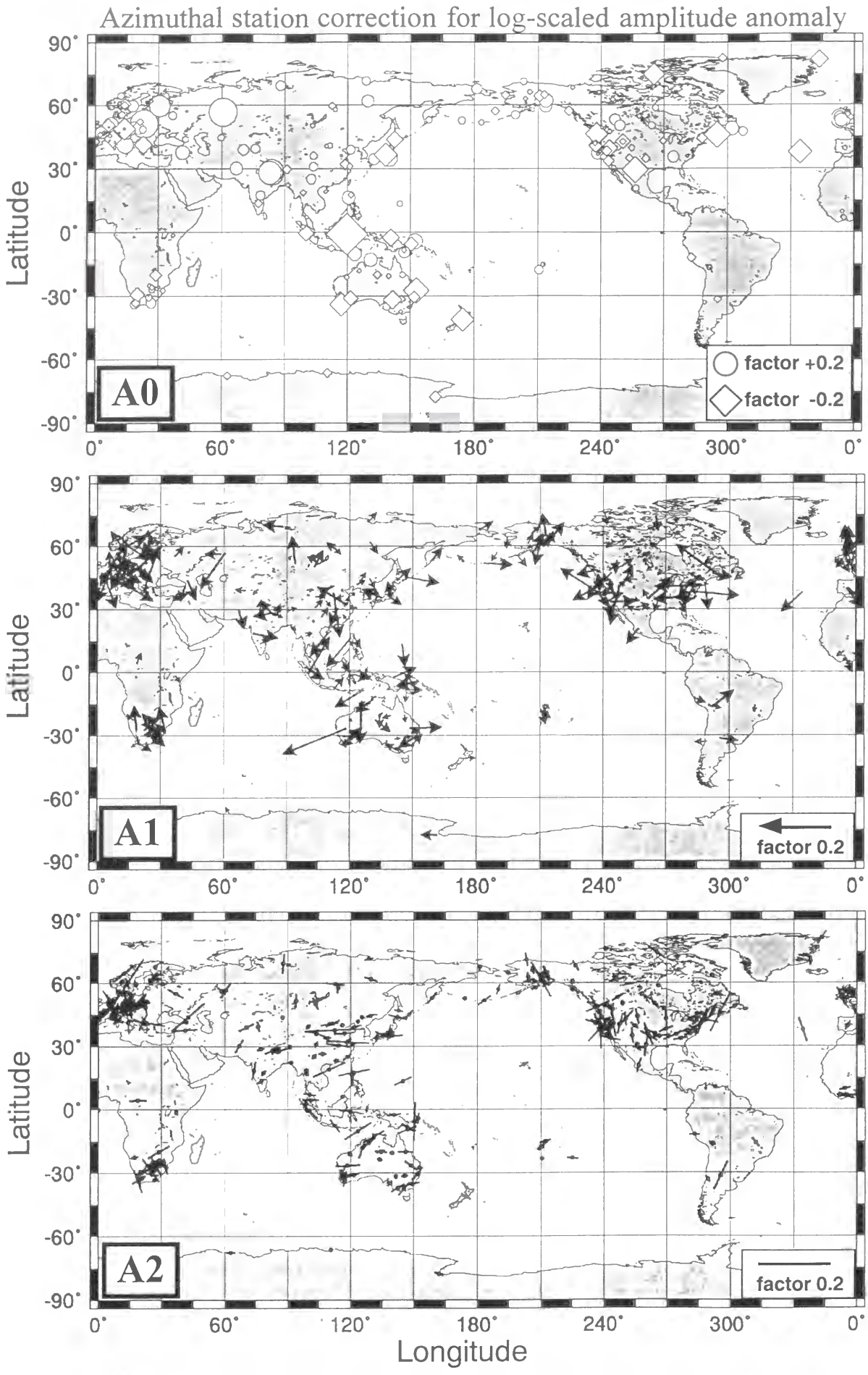
Azimuthal station correction for log-scaled amplitude anomaly
Latitude
Longitude
A0
factor +0.2
factor -0.2
A1
factor 0.2
A2
factor 0.2
90°
60°
30°
0°
-30°
-60°
-90°
0°
60°
120°
180°
240°
300°
0°

Figure 2.14

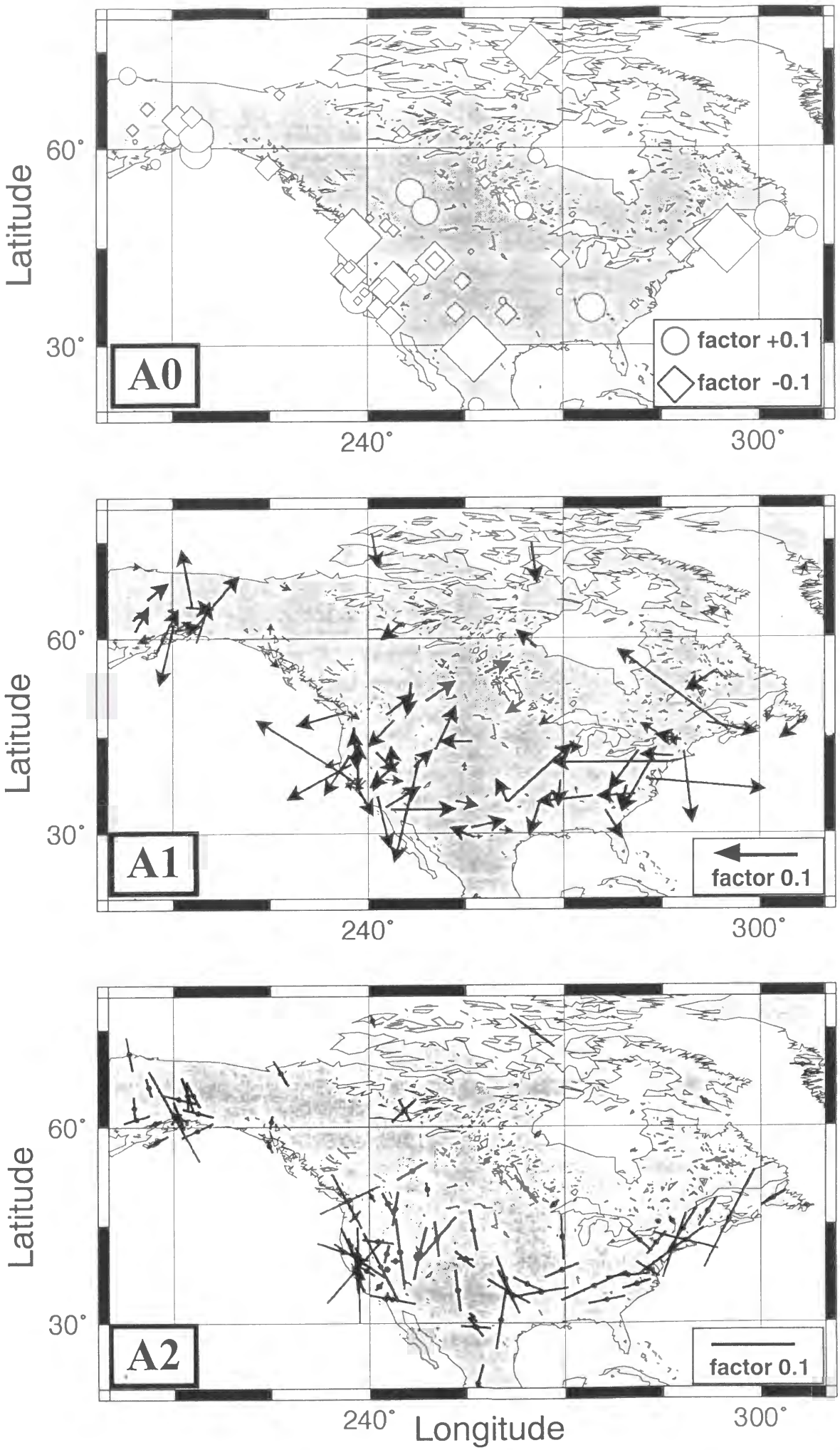
A0
factor +0.1
factor -0.1
A1
factor 0.1
A2
factor 0.1
60°
30°
240°
300°
Latitude
Longitude

Figure 2.15

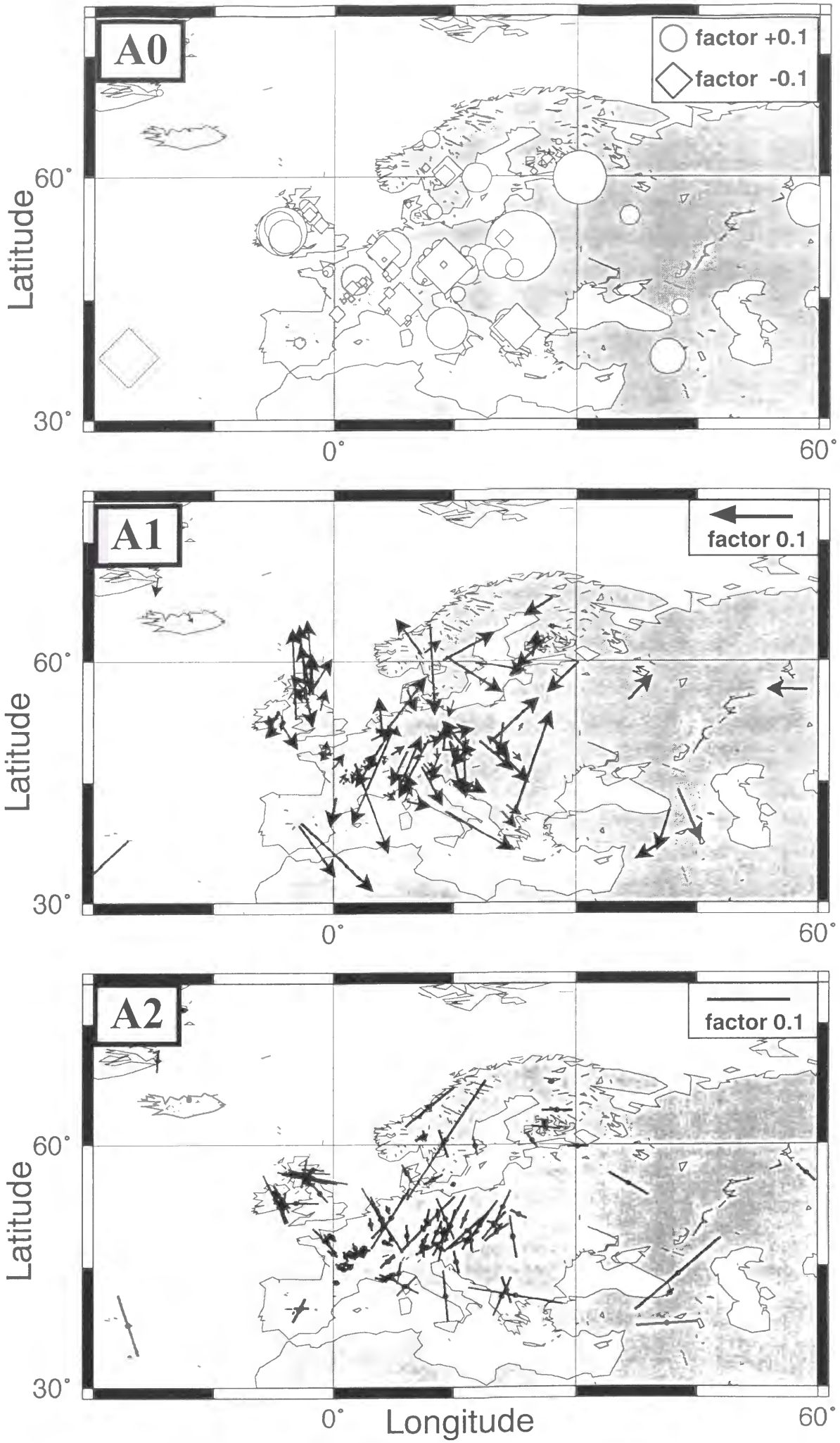
A0
factor +0.1
factor -0.1
A1
factor 0.1
A2
factor 0.1
Latitude
60°
30°
0°
60°
Longitude

Figure 2.16

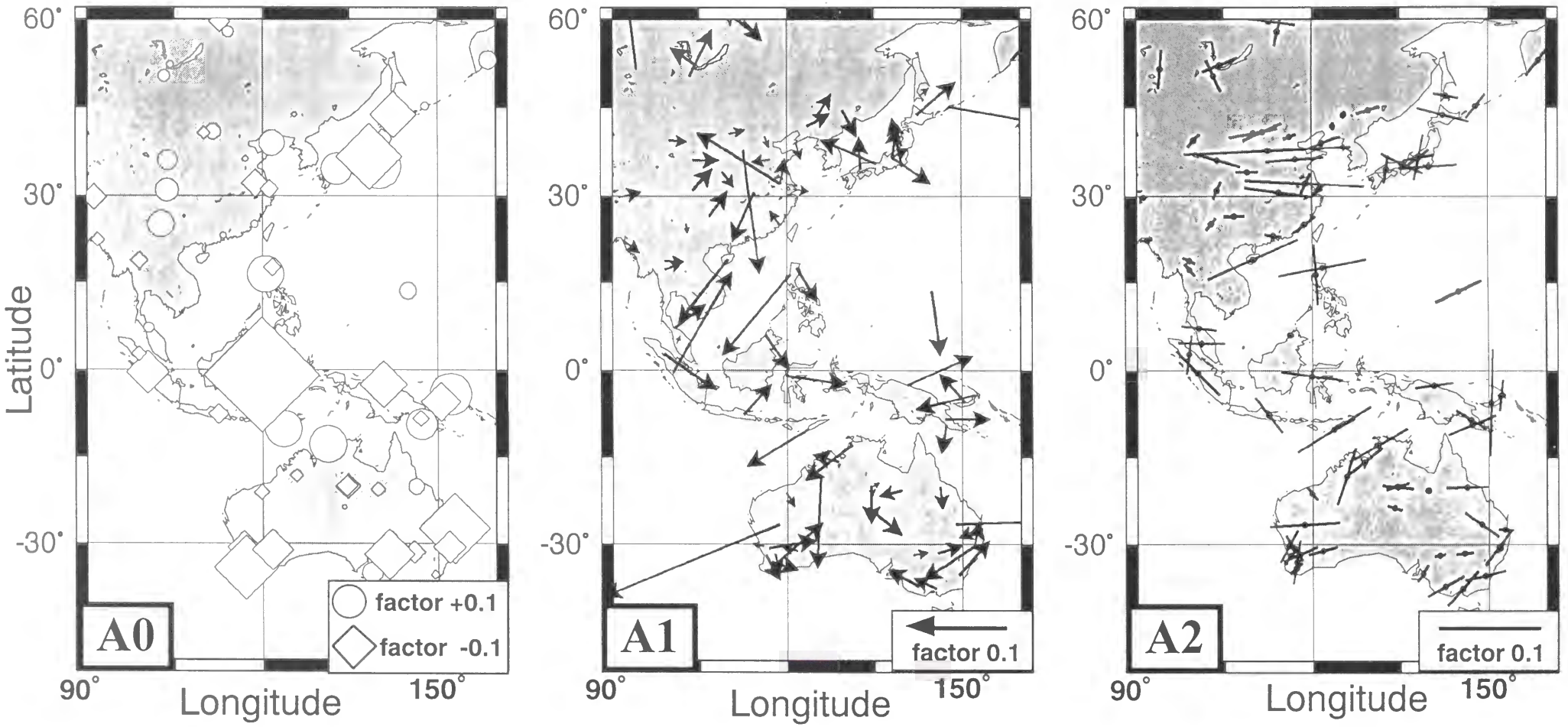
60°
30°
0°
-30°
Latitude
90°
150°
Longitude
A0
factor +0.1
factor -0.1
A1
factor 0.1
A2
factor 0.1

Figure 2.17

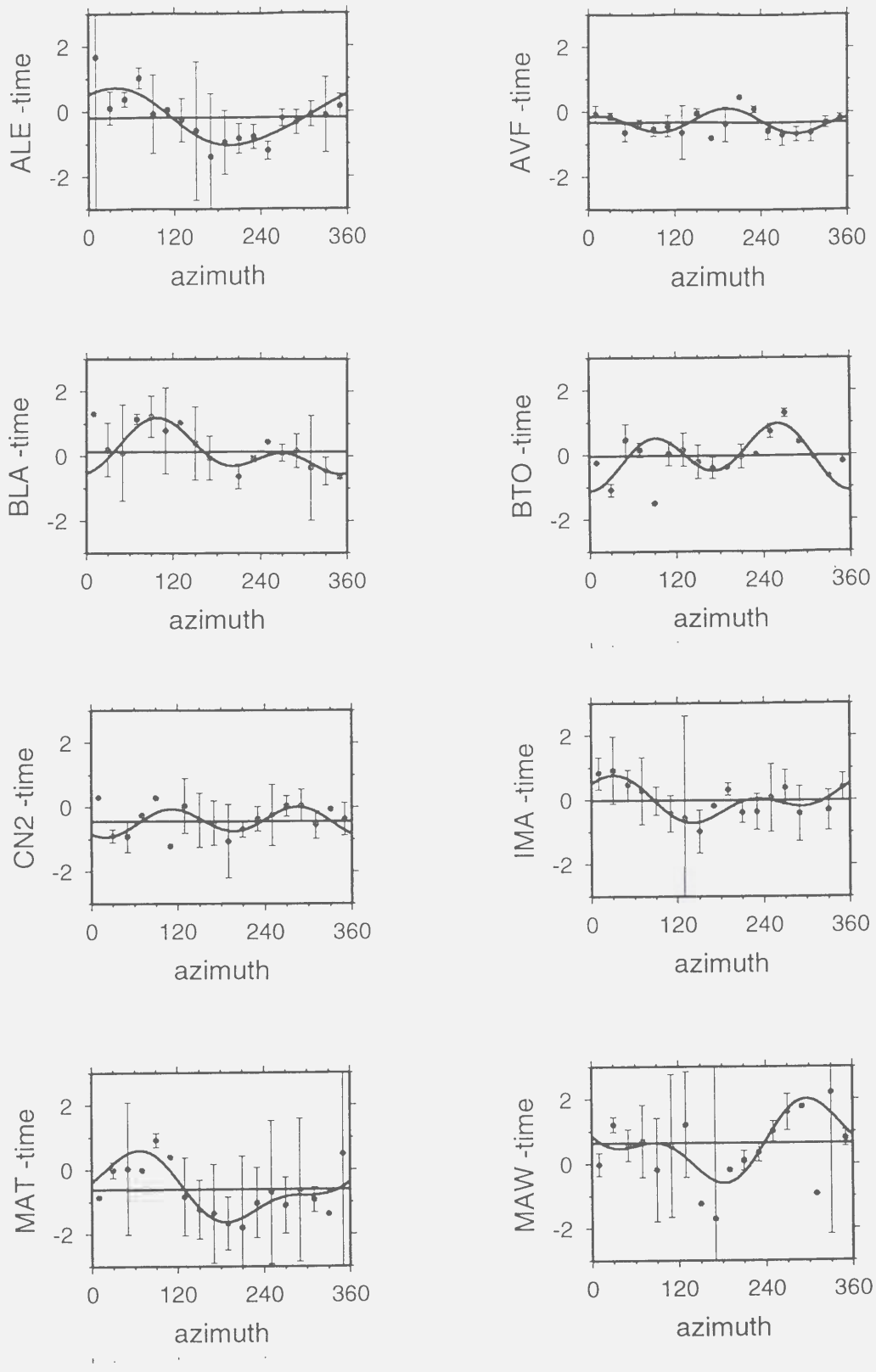
ALE -time
AVF -time
BLA -time
BTO -time
CN2 -time
IMA -time
MAT -time
MAW -time
2
0
-2
0
120
240
360
azimuth

Figure 2.18

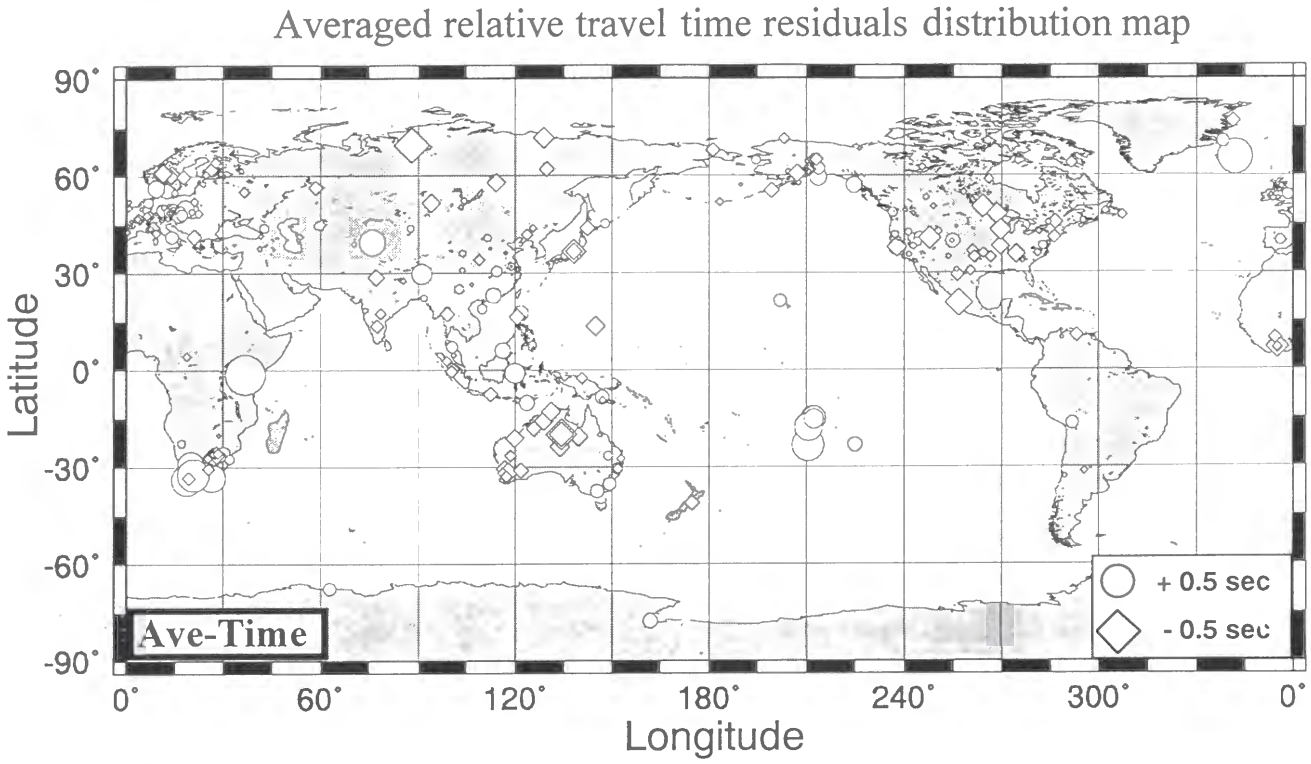
Averaged relative travel time residuals distribution map
90°
60°
30°
0°
-30°
-60°
-90°
Latitude
0°
60°
120°
180°
240°
300°
0°
Longitude
Ave-Time
+ 0.5 sec
- 0.5 sec

Figure 2.19

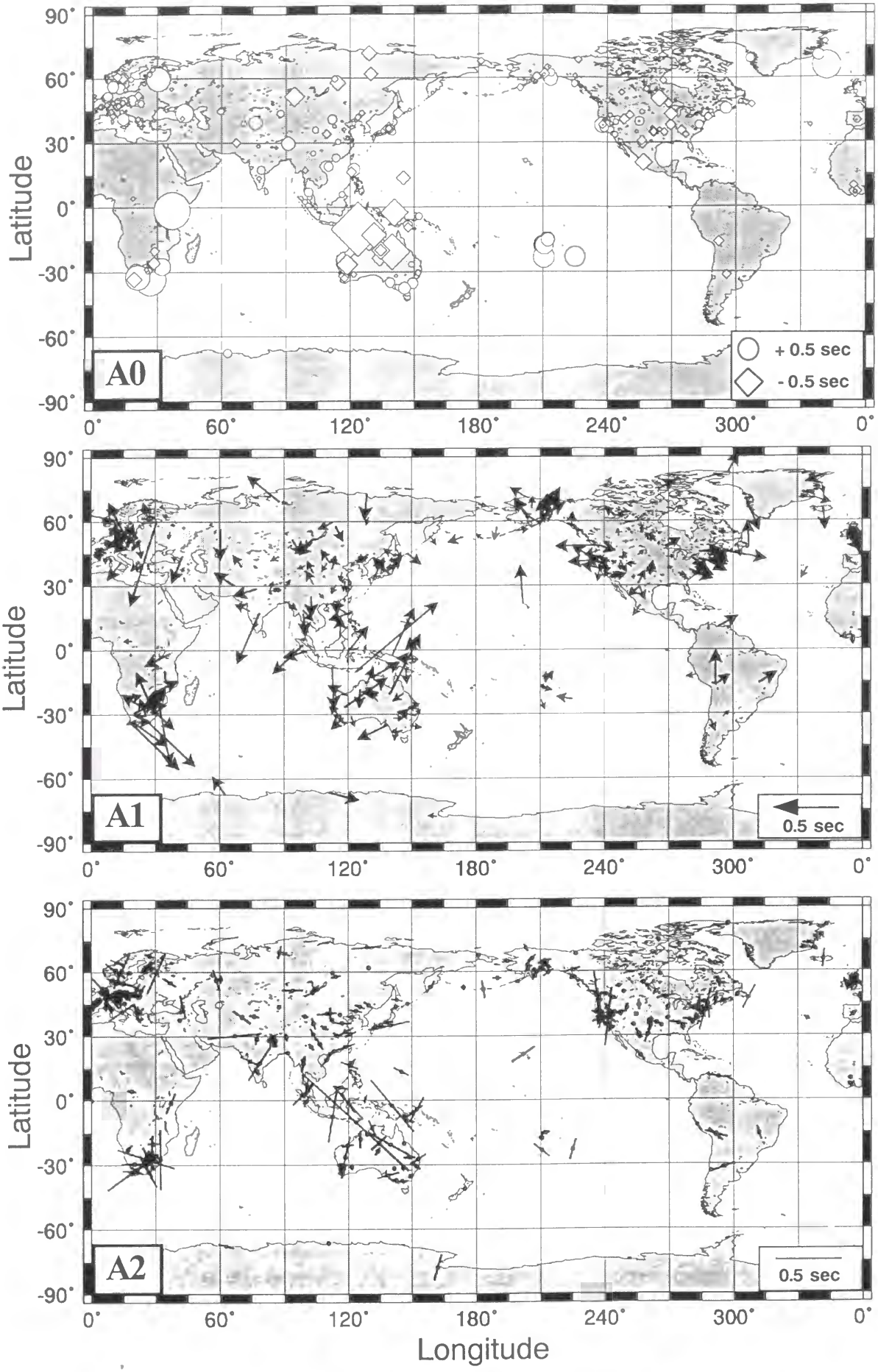
Azimuthal station correction for Relative travel time residuals
A0
+ 0.5 sec
- 0.5 sec
A1
0.5 sec
A2
0.5 sec
Latitude
Longitude
90°
60°
30°
0°
-30°
-60°
-90°
0°
60°
120°
180°
240°
300°
0°

Figure 2.20

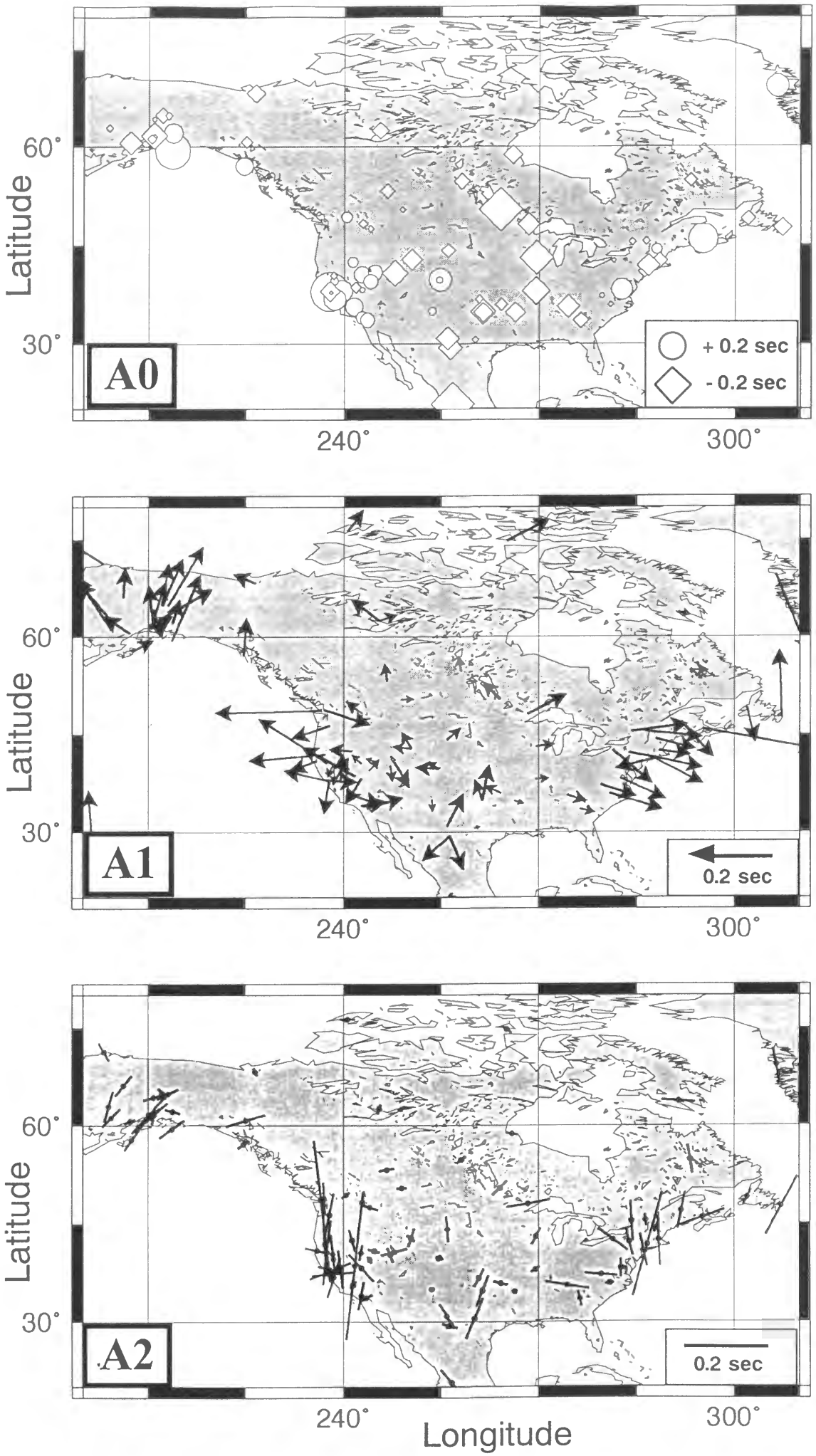
A0
+ 0.2 sec
- 0.2 sec
A1
0.2 sec
A2
0.2 sec
60°
30°
240°
300°
Latitude
Longitude

Figure 2.21

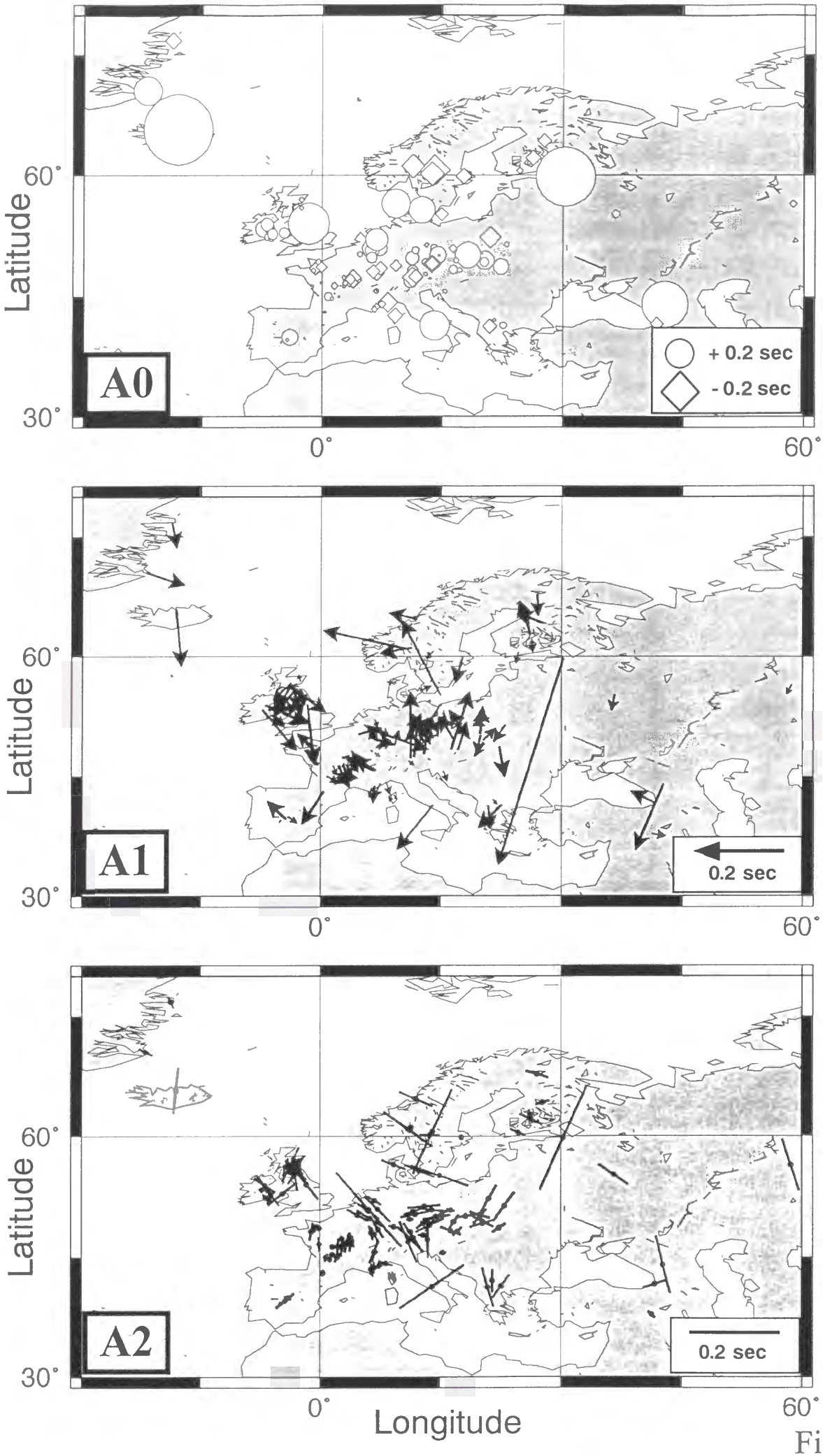
A0
+ 0.2 sec
- 0.2 sec
A1
0.2 sec
A2
0.2 sec
Latitude
Longitude
60°
30°
0°
60°

Figure 2.22

Latitude
-30°
0°
30°
60°
90°
150°
Longitude
A0
+ 0.2 sec
- 0.2 sec
A1
0.2 sec
A2
0.2 sec

Figure 2.23

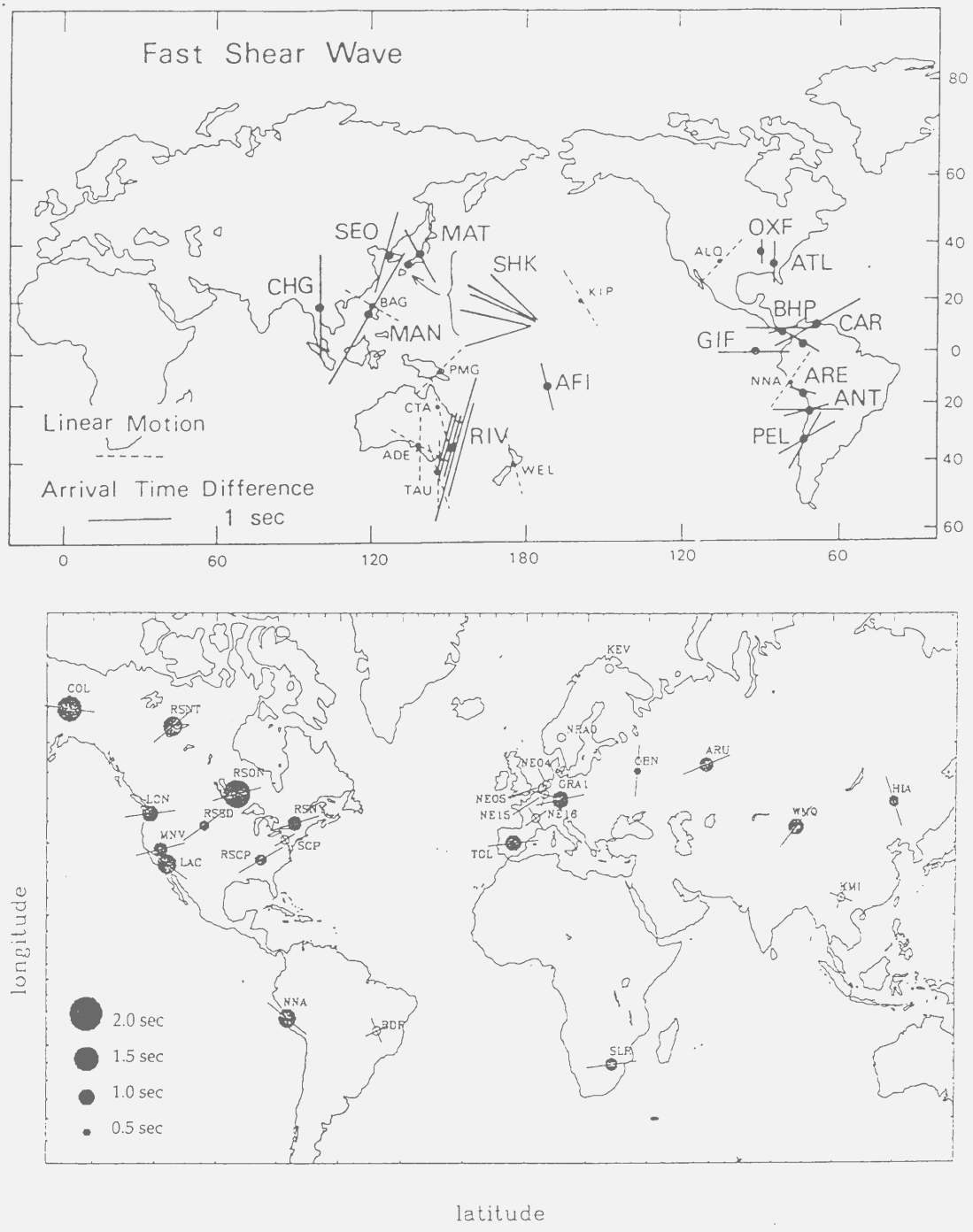
Fast Shear Wave
SEO
MAT
SHK
CHG
BAG
MAN
PMG
AFI
CTA
RIV
ADE
TAU
WEL
KIP
OXF
ALQ
ATL
BHP
CAR
GIF
NNA
ARE
ANT
PEL
Linear Motion
Arrival Time Difference
1 sec
80
60
40
20
0
20
40
60
0
60
120
180
120
60
KEV
COL
RSNT
NRAO
NEO4
GRA1
CEN
ARU
RSON
LON
RSBD
RSNT
NEOS
NE15
NE16
HIA
WNV
LAC
RSCP
SCP
TOL
WWO
IMK
NNA
BDR
SLP
2.0 sec
1.5 sec
1.0 sec
0.5 sec
longitude
latitude

Figure 2.24

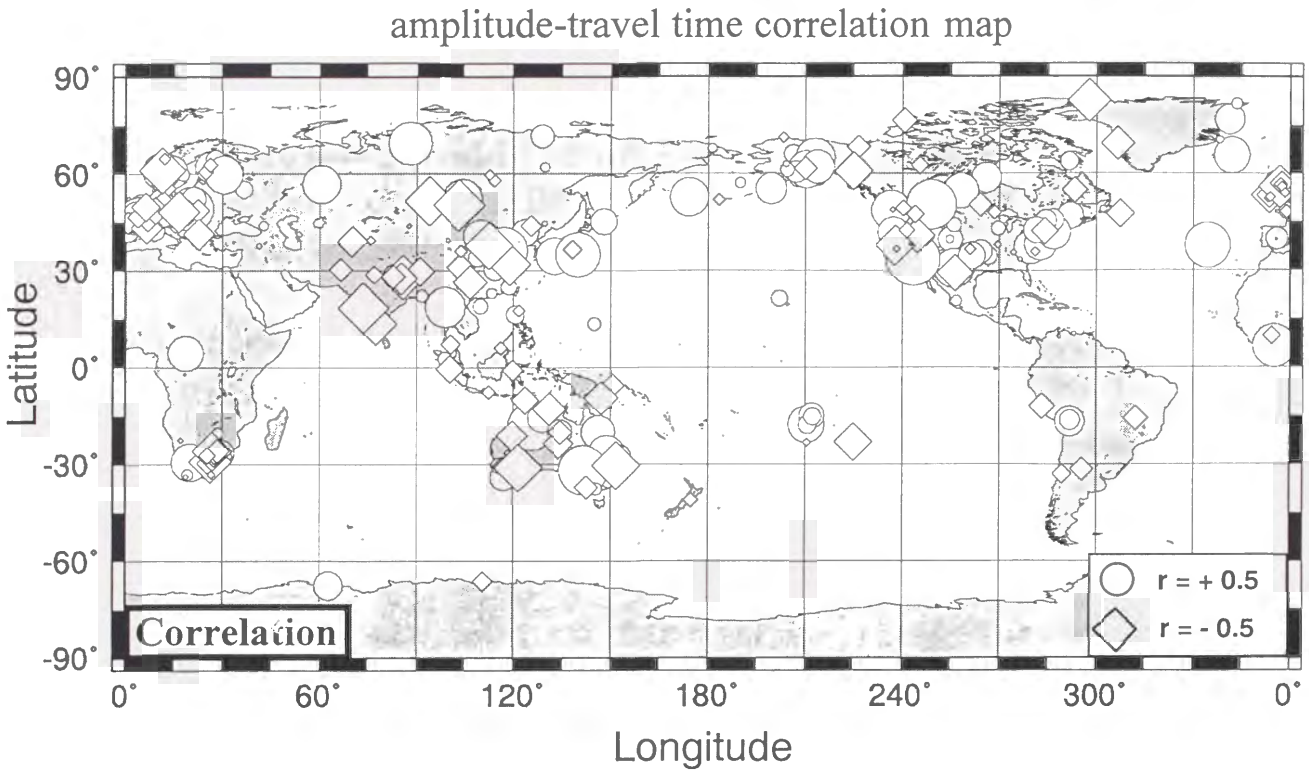
amplitude-travel time correlation map
90°
60°
30°
0°
-30°
-60°
-90°
Latitude
0°
60°
120°
180°
240°
300°
0°
Longitude
Correlation
r = + 0.5
r = - 0.5

Figure 2.25

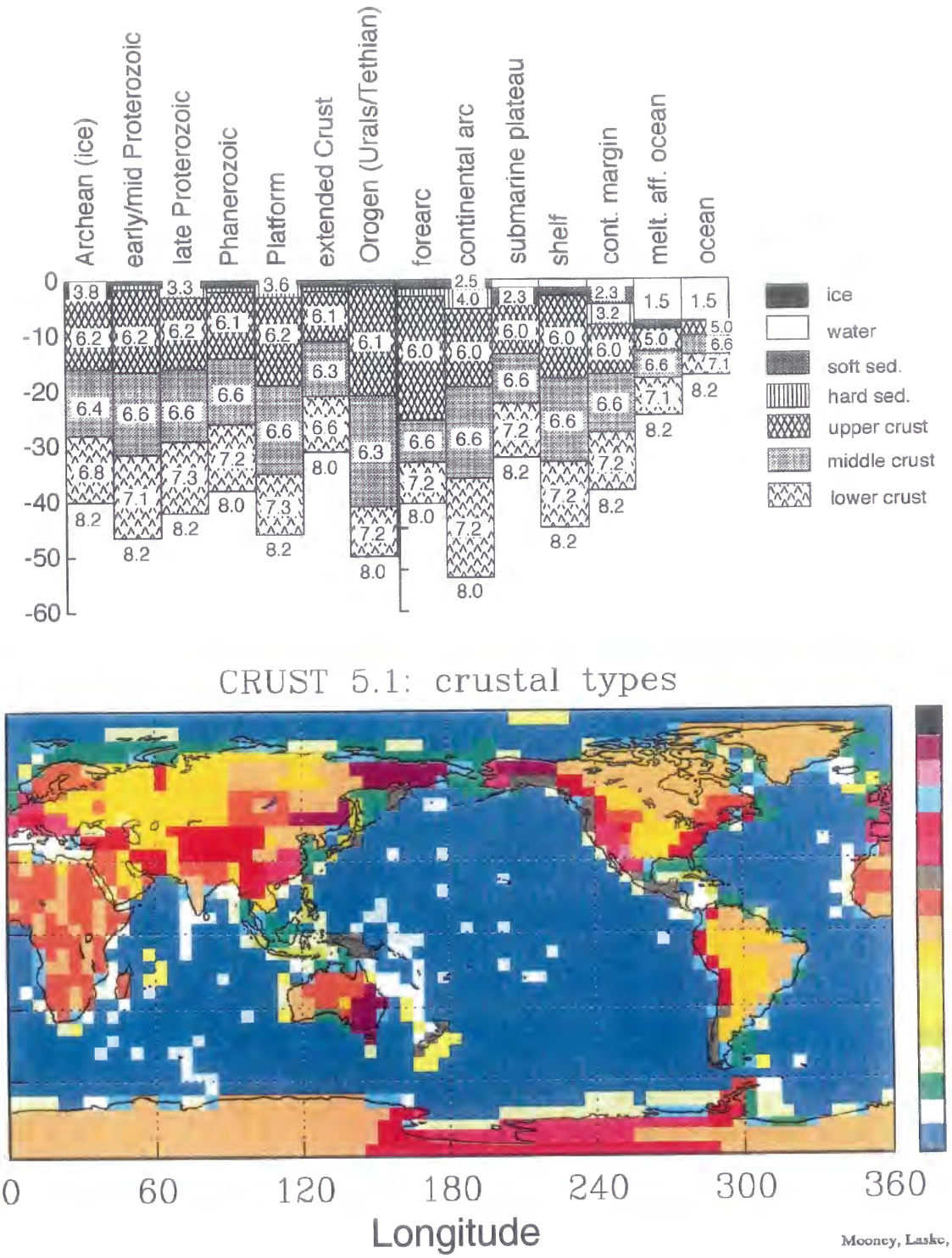
Archean (ice)
early/mid Proterozoic
late Proterozoic
Phanerozoic
Platform
extended Crust
Orogen (Urals/Tethian)
forearc
continental arc
submarine plateau
shelf
cont. margin
melt. aff. ocean
ocean
0
-10
-20
-30
-40
-50
-60
ice
water
soft sed.
hard sed.
upper crust
middle crust
lower crust
CRUST 5.1: crustal types
90
60
30
0
−30
−60
−90
Latitude
0
60
120
180
240
300
360
Longitude
phanerozoic
rifts
transition
orogen
extended crust
cont. arcs
proterozoic
archean
platform
thinned cont
cont. plateaus
island arcs
shelf trans
cont. shelf
melt aff. oc.
oceanic
Mooney, Laske, Masters

Figure 2.26

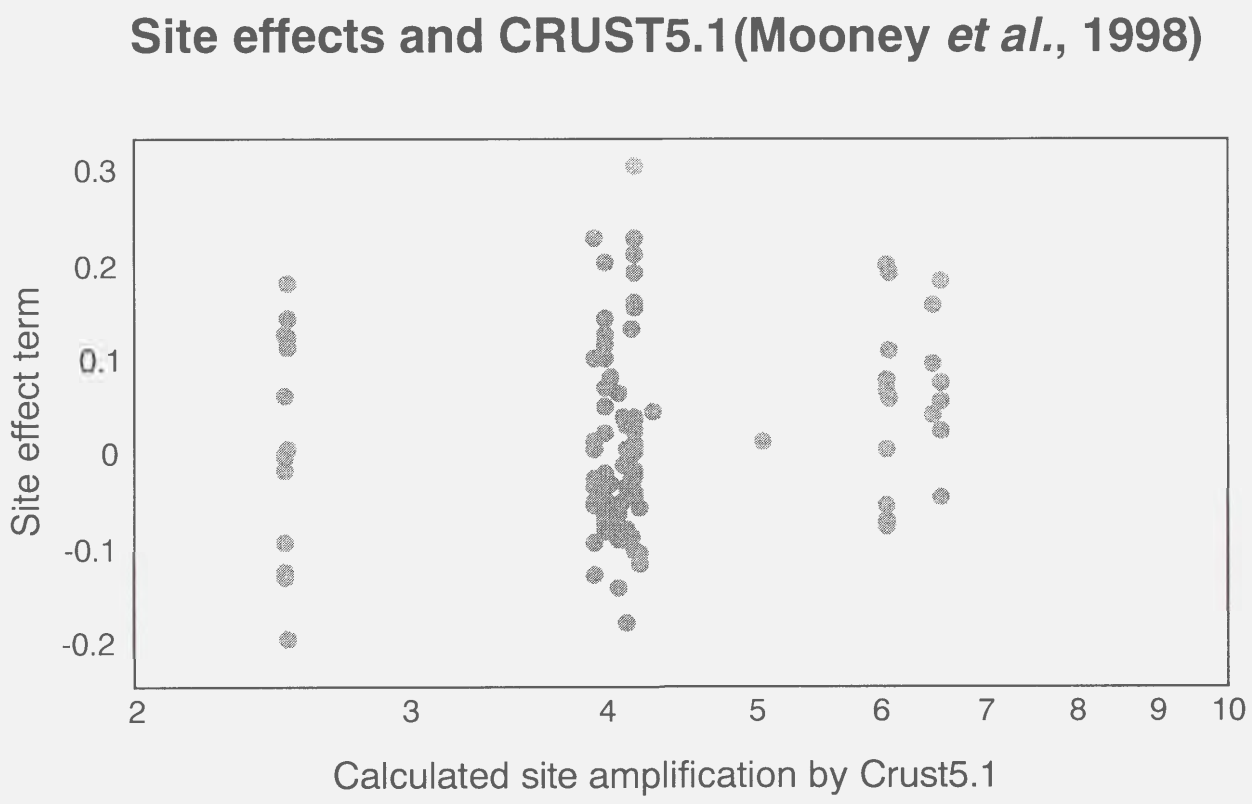
Site effects and CRUST5.1(Mooney *et al.*, 1998)
Site effect term
0.3
0.2
0.1
0
-0.1
-0.2
2
3
4
5
6
7
8
9
10
Calculated site amplification by Crust5.1

Figure 2.27

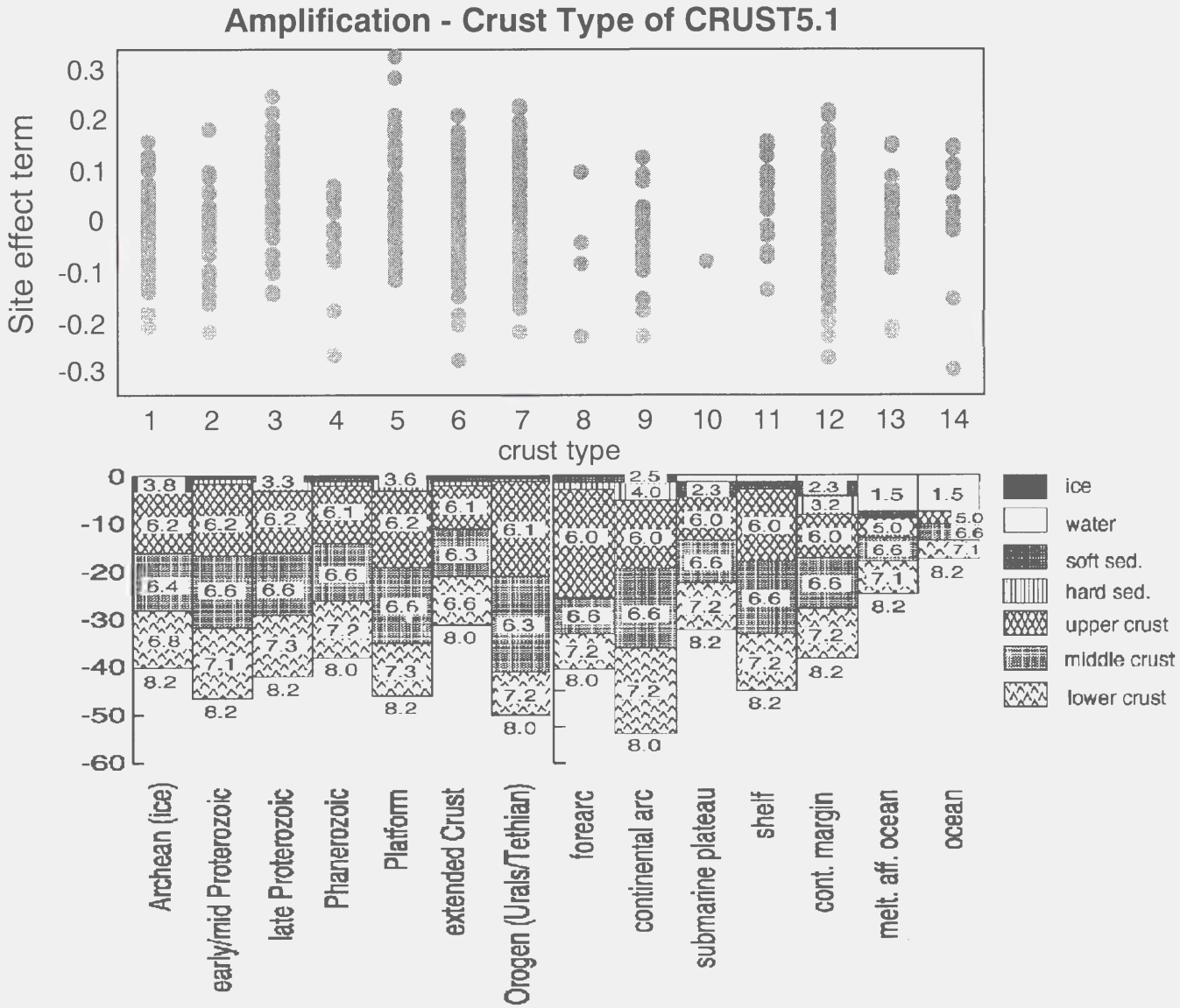
Amplification - Crust Type of CRUST5.1
Site effect term
0.3
0.2
0.1
0
-0.1
-0.2
-0.3
1
2
3
4
5
6
7
8
9
10
11
12
13
14
crust type
0
-10
-20
-30
-40
-50
-60
Archean (ice)
early/mid Proterozoic
late Proterozoic
Phanerozoic
Platform
extended Crust
Orogen (Urals/Tethian)
forearc
continental arc
submarine plateau
shelf
cont. margin
melt. aff. ocean
ocean
ice
water
soft sed.
hard sed.
upper crust
middle crust
lower crust

Figure 2.28

Chapter 3.

A whole mantle P wave attenuation structure obtained from ISC amplitude data

3.1 Introduction

The global three-dimensional anelastic structure of the whole mantle remains poorly resolved compared to the elastic structure, although evidence for large lateral heterogeneity in the mantle attenuation of seismic waves has been abundant since the 1970's.

Many tomographic studies of attenuation have been done for local or regional earthquake data and they have contributed toward understanding the tectonics and dynamics in the crust and the upper mantle (*e.g.*, Ho-Liu *et al.* [1988], Young and Ward [1980], Besana *et al.* [1997]). Investigations on the lateral variation of Q_{ScS}, attenuation factor of multiple bounce ScSn waves, have shown large variations between ocean basins, subduction zones, and back-arc regions (*e.g.*, Sipkin and Jordan [1980], Nakanishi [1979], Flanaghan and Wiens [1990]). Mikami and Hirahara [1981] investigated global variations of attenuative properties in the upper mantle by using WWSSN long-period P-wave records. Their estimate is very rough, but some correlation between the differential attenuation and heat flow were identified. The first investigation of the global heterogeneity of the Earth was done by Romanowicz *et al.* [1987]. They used fundamental spheroidal mode spectra from very long period GEOSCOPE records and obtained a pattern from degree 2 heterogeneity of shear-wave Q in the upper mantle. Subsequently, their method has been applied to various long-period data. Therefore, models in higher degree heterogeneity now exist for the upper mantle (*e.g.*, Suda *et al.* [1991], Durek *et al.* [1993]). At present, QR19 (Romanowicz [1995]) is the best global three-dimensional attenuation model for the upper mantle, with degree 6 heterogeneity for both vertical and horizontal directions. The heterogeneity of this model is consistent with tectonic features in shallower regions, and in deeper parts of the model the pattern shifts and becomes correlated with the hotspot distribution. (Romanowicz [1995]). However, these global models do not match each other very well. Investigations of whole mantle attenuation heterogeneity is still a developing field in seismology.

In this chapter, I applied a tomographic approach to obtain a whole mantle attenuation structure using the ISC amplitude data. The vast amount of ISC amplitude data have seldom

been used for structural investigations. However, I thought that dealing with the data set appropriately could yield valuable structural information. In the previous chapter, I introduced the amplitude station correction. Here I present the P-wave attenuation structure for the whole mantle by applying a tomographic method and station corrections obtained in Chapter 2 to the ISC short-period amplitude data. I divided an inversion process into two subprocess. First a joint inversion for determining source amplitudes and one-dimensional P-wave attenuation structure was applied to the ISC amplitude data corrected in Chapter 2, then I inverted for three-dimensional perturbations from the one-dimensional model. This is due to obtaining a numerically-stable solution of the attenuation structure.

3.2 Methodology of grid model attenuation tomography

3.2.1 Basic theory of attenuation tomography

A teleseismic P-wave amplitude of the i-th event at the j-th station can be expressed by

$$A_{ij}(f) = M_i(f) \cdot R_{ij} \cdot G_{ij} \cdot C_j(f) exp\left(-\pi f t_{ij}^{*}\right) \tag{3.2.1}$$

where $A_{ij}(f)$ denotes the observed amplitude at the frequency f, $M_i(f)$ is the amplitude, R_{ij} is the radiation pattern of the source mechanism, G_{ij} is the geometrical spreading, $C_j(f)$ is the site amplification, and t_{ij}^{*} is the attenuation factor,

$$t^{*} = \int_{raypath} V^{-1} Q^{-1}(f) ds \ . \tag{3.2.2}$$

Since the focal mechanisms are known and the velocity structure and frequency are assumed in this investigation, the logarithm of the corrected equation of (3.2.1) and its discretized form become

$$\begin{aligned} \log A_{ij} &= \log M_i + \log C_j - \pi f \int V^{-1} Q^{-1} ds \\ &= \log M_i + \log C_j - \pi f \sum_k V_k^{-1} Q_k^{-1} \Delta s_k \end{aligned} \tag{3.2.3}$$

where k indicates the position on the raypath and Δs_k is the step length for the ray tracing (Figure 3.1). Here the Q^{-1} value is assumed to be frequency independent in the analyzed frequency range. The principal unknown parameters are M_i, C_j and Q_k^{-1} in this inversion equation. The constructed inversion equation, however, needs more constraints because one degree of freedom still remains in the site effect term. Negishi [1998] investigated the high-resolution attenuation structure in the epicentral area of the 1995 Kobe earthquake using this method and the grid model formulation, which expressed in the next section. He used the criterion that the site effects have a factor more than 2.0 due to the free surface amplification, and succeeded in obtaining fine tomographic images of P and S wave attenuation based on a spectral amplitude analysis. This criterion means that the smallest amplification factor of site effect should be 2.0. The difference between the actual smallest amplification and the assumed amplification (here 2.0) is represented by offsets for all of the source amplitude terms. But I already obtained the relative variation of site amplification factors (site effect terms, equation (2.3.7) in Chapter 2) for each station in the previous chapter, so using the station corrections, site amplification terms of equation (3.2.3) were excluded from the unknown parameters in this study.

3.2.2 Grid modeling formulation

The physical properties of the Earth's mantle varies more in the vertical direction than horizontal direction. So the velocity and attenuation structure in the Earth is usually expressed as a sum of the spherically averaged parameter-depth functions with 3-D perturbations. The spherical harmonic expansion representation has been used in most of the previous studies of the whole mantle velocity or attenuation structure (*e.g.*, Dziewonski [1984], Morelli and Dziewonski [1987], Romanowicz [1995]). This approach has an advantage that fewer parameters can express the global heterogeneous pattern, and the

harmonic model can be compared directly with other geophysical maps, such as gravity and magnetic field. However Inoue *et al.* [1990] pointed out that the capability of representing a distribution by a discrete parameterization model is essentially the same as representing one by harmonics. From the pioneering study of Aki and Lee [1976] and Aki *et al.* [1977], block modeling has been mainly used for local and regional tomographic studies. Recently the block modeling approach has become usable for whole mantle tomography, because of improvements in computer power and development of computational algorithms for solving large and sparse matrix problem. Recent investigations (*e.g.*, Inoue *et al.* [1990], Fukao *et al.* [1992], Kennett *et al.* [1998]) have clarified the whole mantle velocity structure by using fine block models.

On the other hand, Thurber [1983] developed a different approach to the modeling space. The 3-D heterogeneous structure is represented by a 3-D grid of nodes. Parameters (velocity or attenuation) vary continuously in all directions with linear B-spline interpolations among nodes. This representation expresses a smoothly-varying structure anywhere in the modeling space, while in a block configuration parameters change suddenly at block boundary. This is an advantage for three-dimensional ray-tracing, and it is easy to include laterally-varying discontinuities. Zhao *et al.*, [1992] adopted this approach to the Tohoku region in the northern part of Japan, and succeed in clarifying the fine velocity structure of the subducting Pacific plate and the mantle wedge by using pseudo-bending ray tracing (Um and Thurber [1987]) with heterogeneous discontinuities. I modified this grid modeling approach to an attenuation tomography problem.

Figure 3.2 shows schematically the block model and grid model representation. The constant-Q^{-1} block approach treats the Earth as a set of boxes within which the seismic attenuation is constant. In this modeling, the attenuation factor t^* (equation (3.2.2)) becomes

$$t^* = \sum_l \frac{L_l}{V_l} Q_l^{-1} = \sum_l t_l Q_l^{-1} \tag{3.2.4}$$

where V_l, L_l and t_l are the velocity, length of ray-segment, and travel time through the l-th block, respectively. As indicated above, ray tracing and segmentation of rays depend on the configuration of blocks in this approach.

In the grid configuration, the problem has a different form. As shown in Figure 3.2, t^* is represented by the integral along the raypath that is determined independently from the grid node configuration. Q^{-1} on the raypath is interpolated by the Q^{-1} at each grid node surrounding the raypath. The unknown modeling parameter to be solved for is the Q^{-1} at each grid node. The Q^{-1} value at a given point (r, θ, ϕ) is represented by the B-spline interpolation of the peripheral eight nodes, as follows

$$\begin{aligned} Q^{-1}(\phi, \lambda, h) &= \sum_{l=1}^{8} Q_l^{-1} w_l \\ &= \sum_{i=1}^{2}\sum_{j=1}^{2}\sum_{k=1}^{2} Q^{-1}(\phi_i, \lambda_j, h_k)\left\{\left(1-\left|\frac{\phi-\phi_i}{\phi_2-\phi_1}\right|\right)\left(1-\left|\frac{\lambda-\lambda_j}{\lambda_2-\lambda_1}\right|\right)\left(1-\left|\frac{h-h_k}{h_2-h_1}\right|\right)\right\} \end{aligned} \tag{3.2.5}$$

where w_l is the weighting function, ϕ is the latitude, λ is the longitude, h is the depth, and ϕ_i, λ_j, h_k represent the coordinates for the eight grid nodes surrounding the point (ϕ, λ, h). $Q^{-1}(\phi_i, \lambda_j, h_k)$ is the inverse of quality factor at the grid node (see Figure 3.3). The velocity at the position (ϕ, λ, h) is also expressed by the same formulation mentioned above,

$$\begin{aligned} V(\phi, \lambda, h) &= \sum_{l'=1}^{8} V_{l'} u_{l'} \\ &= \sum_{i'=1}^{2}\sum_{j'=1}^{2}\sum_{k'=1}^{2} V(\phi_{i'}, \lambda_{j'}, h_{k'})\left\{\left(1-\left|\frac{\phi-\phi_{i'}}{\phi_2-\phi_1}\right|\right)\left(1-\left|\frac{\lambda-\lambda_{j'}}{\lambda_2-\lambda_1}\right|\right)\left(1-\left|\frac{h-h_{k'}}{h_2-h_1}\right|\right)\right\} \end{aligned} \tag{3.2.6}$$

where $u_{l'}$ is the weighting function for velocity model. Here different configurations of grid arrangement can be used for the velocity and attenuation model. Substituting equations (3.2.5) and (3.2.6) into (3.2.4), t^* becomes

$$\begin{aligned} t^* &= \sum_k V_k^{-1} Q_k^{-1} \Delta s_k \\ &= \sum_{k=1}^{N}\left[V_k^{-1}\sum_{l=1}^{8} Q_l^{-1} w_{lk}\right]\Delta s_k \\ &= \sum_{k=1}^{N}\left[\left(\sum_{l'=1}^{8} V_{l'} u_{l'k}\right)^{-1}\sum_{l=1}^{8} Q_l^{-1} w_{lk}\right]\Delta s_k \end{aligned} \tag{3.2.7}$$

where N is the number of segments of the raypath, and w_{lk} is the interpolation weight for that node. The inversion equation (3.2.3) in the grid modeling formulation then becomes

$$log A_{ij} = log M_i + log C_j - \pi f \sum_{m=1}^{M} \sum_{k=1}^{N_{ij}} \frac{\Delta s_k^{ij}}{V_k^{ij}} \sum_{l=1}^{M} w_{lkm}^{ij} \delta_{lm} Q_l^{-1} \qquad (3.2.8)$$

where A_{ij} is the observed amplitude with corrections for geometrical spreading and source mechanism, M_i is the unknown source amplitude of the i-th event, C_j is the unknown site amplification factor at the j-th station, f is the frequency (assumed to be 1.0 in this study), N_{ij} is the number of segments along the raypath from the i-th source to j-th station, Δs_k^{ij} is the length of the k-th ray-segment, V_k^{ij} is the velocity at the k-th ray-segment, w_{lkm}^{ij} is the interpolation weight at the k-th position on the ray for the l-th grid node, δ_{lm} is the Kronecker delta, and Q_l^{-1} is the unknown parameter of attenuation at the l-th grid node. This inversion equation seems complex but it is linear. The above equation represents one amplitude observation, and I convert it to a matrix equation $\boldsymbol{Gm} = \boldsymbol{d}$, where $\boldsymbol{G}$ is a coefficients matrix, $\boldsymbol{m}$ is an unknown parameter matrix and $\boldsymbol{d}$ is a data matrix, respectively.

The equation (3.2.8) can be solved directly because of its linear form. However such direct solution is often trapped by local minima and sometimes becomes smaller than 0, especially in the problem of the large-scale inversion matrices. Therefore I solve the one-dimensional attenuation structure as a reference model first, and then calculate the perturbations from the reference model to obtain the stable solutions in this study. This approach have been often applied to the local or regional attenuation tomographic studies (*e.g.*, Solomon and Toksöz [1970], Scherbaum [1990], Sanders [1993]). When we know the reference values for each parameter (souece amplitude, site amplification and Q^{-1} model), the inversion equation (3.2.8) can be modified, using the reference attenuation model Q_0^{-1}, to the following form;

$$\Delta log A_{ij} = \Delta log M_i + \Delta log C_j - \pi f \sum_{m=1}^{M} \sum_{k=1}^{N_{ij}} \frac{\Delta s_k^{ij}}{V_k^{ij}} \sum_{l=1}^{M} w_{lkm}^{ij} \delta_{lm} Q_{0l}^{-1} \left(\frac{\Delta Q^{-1}}{Q_0^{-1}} \right)_l \qquad (3.2.9)$$

where $\Delta log A_{ij}$ is the logarithm of the amplitude ratio of the observed amplitude to the calculated amplitude from the reference parameters, $\Delta log M_i$ and $\Delta log C_j$ are the unknown source amplitude and site amplification ratio, respectively (actually $\Delta log C_j$=0 in this study because we already set the site effect term in Chapter 2 as the site amplification). In this

formulation, the Q^{-1} perturbation from the reference model, $\left(\frac{\Delta Q^{-1}}{Q_0^{-1}}\right)_l$, is the unknown parameter to be solved. I used (3.2.9) formulation in this study.

3.2.3 Smoothness constraint

Frequently smoothness is introduced to modeling of an under-constrained problem (*e.g.*, Inoue *et al.* [1990], Lees and Crosson [1989]). In our case, smoothness constraints can be imposed by minimizing a measure of the roughness of the model, where I have chosen the roughness to be the second differential operator in the horizontal plane. This is just the Laplacian operator ∇^2 in vector notation. I augment the system of equations to be solved in the least squares method,

$$\begin{bmatrix} G \\ \alpha D \end{bmatrix} m = \begin{bmatrix} d \\ 0 \end{bmatrix} \tag{3.2.9}$$

where D is the two-dimensional, finite difference Laplacian operator applied over horizontal planes in our model. Solving (3.2.9) by least squares is equivalent to a weighted minimization of the Laplacian operator at each point of the model in horizontal planes. In two dimensions this corresponds to the following equation for the j-th grid:

$$\begin{aligned} & 4\left(j-th\_grid\_parameter\right) - \sum\left(adjacent\_parameter\right) \\ & = 4m_j - \left(m_{j-1} + m_{j+1} + m_{j-n} + m_{j-n}\right) \\ & = 0 \end{aligned} \tag{3.2.10}$$

where n is the number of grids in each latitude. In polar coordinates the element of the roughness matrix D becomes,

$$D_i = \begin{cases} -2\left(1+\dfrac{1}{\sin^2\theta_j}\right) & \{i=j\} \\ \dfrac{1}{\sin^2\theta_j} & \{i=j-1,\ j+1\} \\ 1 & \{i=j-n,\ j+n\} \\ 0 & otherwise \end{cases} \tag{3.2.11}$$

where θ_j is colatitude of the j-th grid. Using the adjustment system, we will minimize the following function

$$|Gm - d|^2 + \alpha^2\left(m^T D^T Dm\right) = |Gm - d|^2 + \alpha^2 \|Dm\|^2 \qquad (3.2.11)$$

where $|\cdot|$ represents the Euclidean norm.

In the equation (3.2.11), the positive parameter α is used to adjust the relative weight of roughness. In the inversion there is a trade-off between α and the misfit reduction. This hyperparameter α is often determined subjectively because we know nothing about it *a priori*. One method to determine the parameter is using ABIC (Akaike's Bayesian Information Criterion) (Akaike [1980]) which has been recently used in some fields of inverse problems. However, the computation of ABIC is almost impossible in such large problems as our tomographic inversion, since it requires trailing procedures including calculation of the Hessian matrix $G^T G$. Moreover, Nishizawa *et al.* [1994] pointed out that the ABIC often leads to wrong results when the number of data is not much larger than the number of unknown parameters, such as in tomography problems. Recently Nishizawa and Noro [1995] and Aoike *et al.* [1998] applied the Extended Information Criterion (EIC) for determining an optimum model in seismic velocity tomography. The EIC is estimated by a numerical simulation based on bootstrap statistics. This method can be used even if the number of unknowns is large, but it needs tens of trial computation of the inversion.

I applied the simplified cross validation approach (Inoue *et al.* [1990]) in this study. The generalized cross validation (*leave-one-out cross-validation*) requires large computational efforts, requiring the number of trial runs equal to the number of data. However, if we have a vast amount of data, the cross validation score can be simplified as follows. First we divide the original data to $\boldsymbol{d}_1$ and $\boldsymbol{d}_2$ by random sampling. Then the inversion process with a trial hyperparameter α is applied to data $\boldsymbol{d}_1$ and we estimate a model $\boldsymbol{m}_{1\alpha}$. This model should predict the remaining data $\boldsymbol{d}_2$, which is independent of the inversion process, if model $\boldsymbol{m}_{1\alpha}$ represents true structure well. So we calculate the synthetic amplitude of the data $\boldsymbol{d}_2$ by using the model $\boldsymbol{m}_{1\alpha}$, and the approximate cross validation score is given as,

$$Sc(\alpha) = \left\| \boldsymbol{d}_2 - \boldsymbol{G}_{2\alpha}\left(\boldsymbol{G}_{1\alpha}^{-1}\boldsymbol{d}_1\right)\right\| = \left\| \boldsymbol{d}_2 - \boldsymbol{G}_{2\alpha}\boldsymbol{m}_{1\alpha}\right\| . \qquad (3.2.12)$$

I found the hyperparameter α that minimizes $Sc(\alpha)$ by a grid search. If data set $\boldsymbol{d}_1$ is taken to be too small, the results tend to depend on the size of $\boldsymbol{d}_1$ and the estimated optimal values become biased. On the other hand, if the size of $\boldsymbol{d}_2$ is too small, the estimated values become unreliable. Figure 3.4 is the results of the cross validation test using three different sizes of $\boldsymbol{d}_1$ and $\boldsymbol{d}_2$, $\boldsymbol{d}_1$: $\boldsymbol{d}_2$ is 2:1, 5:1 and 7:1. These scores are normalized by the score with no smoothness for each test. The three curves show approximately the same minimum position around the hyperparameter 2 or 3. I adopted the value α=2.5 in this study.

3.2.4 LSQR inversion algorithm

Many investigators have adopted the damped least square method (*e.g.*, Aki *et al.* [1977]) or Generalized nonlinear inversion (Tarantora and Valette [1982]) for tomographic analysis. These methods, however, are impracticable in our calculation because of the huge size of the inversion matrices and limitation of computer power. Therefore most of the recent work on large-scale tomography adopt iterative algorithms to solve the equation system, such as the Algebraic Reconstruction Technique (ART) (*e.g.*, Nakanishi [1985], Hirahara [1988]) and the Simultaneous Iterative Reconstruction Technique (SIRT) (Hager and Clayton [1989]). These are mainly based on backprojection techniques. These methods have been used by many investigators, because the calculation process is simple and easy to understand. However, these methods have the undesirable property that they do not converge to the exact least squares solution (Menke [1989]).

To solve the linear equation, I adopted the LSQR method (Paige and Saunders [1982]), which is one kind of conjugate gradient methods. This method is a superior algorithm to solve large and sparse matrix problem, because of its fast convergence and ability to give exact solutions. The LSQR algorithm is briefly described as follows (Nolet [1987]).

$$m_0 = 0$$

$$\alpha_0 = \left|G^t \cdot d\right|, \beta = |d|$$

$$v_0 = \frac{1}{\alpha_0}\left(G^t \cdot d\right), u_0 = \frac{1}{\beta_0} d$$

$$w_0 = v_0$$

$$\rho_0 = \alpha_0, \varphi_0 = \beta_0$$

loop i = 1,n

$$\begin{aligned}
\beta_i &= \left|G \cdot v_{i-1} - \alpha_{i-1} u_{i-1}\right| \\
u_i &= \frac{1}{\beta_i}\left(G \cdot v_{i-1} - \alpha_{i-1} u_{i-1}\right) \\
\alpha_i &= \left|G^t \cdot u_i - \beta_i v_{i-1}\right| \\
v_i &= \frac{1}{\alpha_i}\left(G^t \cdot u_i - \beta_i v_{i-1}\right) \\
m_i &= m_{i-1} + \frac{\rho_{i-1}\varphi_i}{\rho_{i-1}^2 + \beta_i^2} w_{i-1} \\
w_i &= v_i + \frac{\alpha_i \beta_i}{\rho_{i-1}^2 + \beta_i^2} w_{i-1} \\
\rho_i &= \frac{\rho_{i-1}\alpha_i}{\sqrt{\rho_{i-1}{}^2 + \beta_i^2}}, \varphi_i = \frac{\rho_{i-1}\varphi_i}{\sqrt{\rho_{i-1}{}^2 + \beta_i^2}}
\end{aligned} \qquad (3.2.13)$$

end loop

where v_i are the Lanczos vectors (Lanczos [1950]) and n is the number of local iteration, which is the same as the number of unknowns. r_i is the absolute length of the residual vector $Gm - d$, and m_i indicates the solution of i-th local iteration. Figure 3.5 is the simple LSQR program coded in Ratfor (Nolet [1987]). Details of this algorithm are explained by van der Sluis and van der Vorst [1987].

3.2.5 Resolution

In seismological tomographic studies, especially for global problems, hypocenters and stations are not distributed uniformly. Consequently, ray paths sample grids unevenly, and the density of ray sampling has large fluctuations. The solutions are not reliable at grid points that have only a few samples. Moreover, systematic inclinations of ray sampling directions often cause improper results even if the ray sampling is dense. Therefore, it is necessary to investigate not only the solution itself but also the resolution of the results for objective evaluations. For the matrix inversion techniques, such as the damped least squares or generalized inverse method, covariance and resolution matrices ($C_m^{'}$ and R) can be computed with the solution, using the following equations

$$C_m^{'} = \left(G^T G + \alpha^2 D^T D\right)^{-1} \tag{3.2.14}$$

$$R = C_m^{'} G^T G. \tag{3.2.15}$$

There is important difference in these matrices from that in the normal damped least squares. The covariance and resolution matrices $C_m^{'}$ and R are not symmetric because $G^T G$ and $D^T D$ are not commutative.

The actual computation to obtain the inverse matrix of $G^T G + \alpha^2 D^T D$ is, however, impossible due to the huge size of the matrices in our study. Moreover, these computations cannot be made simultaneously with the solution for the iterative back-projection method. Nakanishi and Suetsugu [1986] and Hirahara [1988] produced a new formulation to obtain resolutions for the parameters by an iterative tomographic inversion method. But this method also takes much computation time, and the time for one column of the resolution matrix is the same as the time for one whole solution. So I adopted the synthetic test called the "checkerboard resolution test", as applied in Inoue *et al.* [1990] and Zhao *et al.* [1992].

The procedure for this method is briefly listed as follows. First an attenuation model with a checkerboard pattern in both the horizontal and vertical coordinates is constructed. The checkerboard pattern is expressed as

$$m_{check} = p \sum_k c_k e_k \tag{3.2.16}$$

where p is the perturbation size of the checkerboard pattern, c_k are the coefficients 1 or -1 defining the pattern, and e_k is a unit vector, in which only the k-th grid has the unit value. Then, synthetic data set for the checkerboard structure is produced using the data kernel for the real data set $\boldsymbol{G}$,

$$\boldsymbol{d}_{syn} = \boldsymbol{G}\boldsymbol{m}_{check} \tag{3.2.17}$$

Finally, the synthesized data $\boldsymbol{d}_{syn}$ is backprojected into the Earth to reconstruct the checkerboard pattern. The reconstructed image can be written as

$$\boldsymbol{m}_{back} = p\boldsymbol{R}\sum_k c_k \boldsymbol{e}_k = p\sum_k c_k \hat{\boldsymbol{e}}_k \tag{3.2.18}$$

where $\hat{e}_k$ is not a unit vector but the point spread function at the k-th grid. These coefficients clearly indicate the checkerboard resolution. If non-diagonal elements of the vector $\hat{e}_k$ can be ignored, the ratio $\boldsymbol{m}_{back}$ to $\boldsymbol{m}_{check}$ is the same as the diagonal element vector of the resolution matrix $\boldsymbol{R}$. The obtained structure from the synthetic data set will show a clear checkerboard pattern where the resolution is good. And in the region with poor resolution, the obtained structure becomes a blurred pattern or no pattern.

3.3 One-dimensional attenuation structure and setting for tomographic inversion

3.3.1 Setting of data and modeling space

First a one-dimensional P-wave attenuation structure was calculated. I analyzed the dataset that corrected for radiation pattern of the source mechanism and geometrical spreading of the 1-D velocity structure in Chapter 2. Figures 3.6 and 3.7 show the geographical distribution of stations and events, respectively. Figure 3.8 is the histogram of the bottoming depths of the raypaths. Worse resolution is expected in the uppermantle because body waves

primarily sample the structure near their bottoming depths (Stewart [1981], Tajima and Grand, [1998]) and there are no raypaths with bottoming depth shallower than 700 km. Of course there is no resolution (and no unknown parameters) in the lowermost mantle deeper than 2700 km because no data are sampled there.

We cannot apply observation errors to the inversion because there is no information in the ISC database, so I adopted a robust estimate by applying a weight which is a function of the relative log-amplitude anomaly determined in Chapter 2. The weight w is expressed as the following function of the relative log-amplitude anomaly r,

$$w(r) = \begin{cases} \left[1 - \left(\frac{r}{2.6}\right)^2\right]^2 & ,|r| \le 2.6 \\ 0 & ,|r| > 2.6 \end{cases} \tag{3.3.1}$$

This function is called the Biweight estimation function, which is one kind of M-estimation method (Turkey [1977], Nakagawa and Koyanagi [1982]). The threshold value 2.6 is set to twice the standard deviation of the relative log-scale amplitude anomalies in Figure 2.12 in Chapter 2.

Usually station corrections are not applied to data in velocity tomographic studies except for elevation and telemetry delays. This is because site effects for travel times do not vary rapidly among close stations, and time delays from site effects are smaller than the velocity heterogeneity on a global scale. Such time lags are indicated as low- or high-velocity anomalies at the nearest grid to each station. The site amplification factor, however, has large fluctuations with large values as shown in Chapter 2. Therefore, I applied station corrections to the amplitude data before the inversion. The resultant site effect terms (equation (2.3.7), Figure 2.12 in Chapter 2) was used for the correction terms, and site amplification terms were excluded from the unknown parameters. Finally, 3,461 parameters (16 Q_p^{-1} and 3445 source amplitudes) remained as unknowns.

I set the modeling grid points at 16 different depths; 12, 51, 110, 190, 290, 410, 551, 712, 893, 1095, 1317, 1559, 1821, 2104, 2407 and 2730 km. The grid interval varies with depth, with the interval becoming larger with depth. Figure 3.9 shows the grid configuration

and sampling count at each depth. The step length for the ray tracing, Δs_k in equation (3.2.8), is set to 20 km in this study. A ray samples grid nodes at each step length ,and the step length is smaller than the interval of modeling grid, so the sampling count in grid model tomography is much larger than the hit count in block model tomography. The Q_p^{-1} at any depth in the model is calculated by linearly interpolating the Q_p^{-1} at the upper and lower target depths.

3.3.2 Result of one-dimensional inversion

Figure 3.10 and Table 3.1 show the resultant one-dimensional Q_p^{-1} structure in the mantle. In the computation process, an inequality condition constraint (Menke [1989]) was included in the inversion for obtaining positive Q_p^{-1} values. The AK135 model of Montagner and Kennett [1996], which was obtained from analysis of the Earth's free-oscillations, is also shown for comparison. The general tendency of high-attenuation in the upper mantle and relatively low-attenuation in the lower mantle can be seen, and this pattern is similar to AK135 and other attenuation models (Figure 3.11). Mikami and Hirahara [1981] analyzed a large number of WWSSN long-period P-wave records, and they concluded that the body wave data generally support the SL8 model (Anderson and Hart [1978]), which has low Q (200-280) layers in the upper mantle and increasing Q zones from 350 km to the lower mantle. This is consistent with our results. Q_p^{-1} has a strong frequency dependence between the Earth's free-oscillation periods to the short-period body wave range, with stronger attenuation in the higher frequency (Sato [1991]). Therefore, an offset between my resultant model and AK135 is expected, but such trend is not seen. All of the event occurred in the upper mantle and about 70 % of the rays pass through the lower part of the lower mantle (see Figure 3.8). This means that the separation between source terms and structure terms might be incomplete and it is possible that the bias is absorbed in the source amplitude terms. Figure 3.12 is a lot of the resultant source amplitude versus ISC magnitude. We can see the positive relation between them, despite the fact that no magnitude information was included in the inversion. This indicates that the simultaneous inversion gives fairly reasonable results. But the absolute

values are meaningless because they includes not only magnitude effects but also the bias of the attenuation structure and the offsets of the station amplification corrections.

3.3.3 Settings and conducting the tomographic inversion

The configuration of the three-dimensional grid nodes is shown in Figure 3.13. There are 17 nodes spaced in latitude, 36 in longitude, and 16 in depth. The total number of nodes is 9,794 including nodes on the North- and South-Poles on each layer. The grid interval is 10° for both latitude and longitude, and in the vertical direction the same spacing was used as in the one-dimensional inversion. Smaller thickness intervals are used to model the greater complexity at shallower depths, because we know a priori that the various model parameters (velocity, attenuation, density, etc.) vary more rapidly at shallow depths for both the vertically heterogeneous model and its lateral variations. The deepest grid nodes (2730 km) were used only for interpolating and excluded from the unknowns in this tomographic process.

As expressed in equation (3.2.4), the attenuation factor t^* is proportional to the inverse of (velocity x Q factor). This means there exists a strong trade-off between velocity and Q factor in attenuation tomographic problems. I used the whole-mantle tomographic model of three-dimensional P-wave velocities (Obayashi *et al.* [1997]) for calculating attenuation factors. Figure 3.14 shows the velocity model. These figures are made from the original block data, with the mantle divided into 32 x 64 x 16 (latitude x longitude x radius) blocks. This velocity model is parameterized by 5.625 x 5.625 degree blocks globally and a vertical configuration of layers that is different from the grid configuration used in our attenuation tomography. The grid model tomography, however, can accommodate the interpolation of Q_p^{-1} and Vp from different grid spacings, because the expression of Q_p^{-1} and Vp at optional position is done independently. I used the velocity model in its original configuration. The heterogeneous velocity model was only used for obtaining velocity values in constructing the inversion matrices, while the ray tracing and the calculation of geometrical spreading were performed in the spherical homogeneous model.

3.3.4 Checkerboard resolution test

Prior to inverting the actual data, I examine the checkerboard resolution test. Figure 3.15 shows the horizontal pattern of the initial checkerboard. Two kinds of patterns were tested in order to see the resolutions at different wavelengths, 3 x 3 x 2 grids (upper), and 6 x 6 x 3 grids (lower) in latitude x longitude x depth. Incidentally, a still smaller checkerboard pattern (1 x 1 x 1) cannot be applied to the grid modeling, because parameters are obtained by interpolation of adjacent grids and this procedure would cancel out the contrast. Since the maximum perturbation of the quality factor is approximately 50 to 60 % from the one-dimensional model in the upper mantle (Romanowicz [1995]), I set the test patterns to ±60 % perturbations from the one-dimensional model obtained in the previous section. The synthetic amplitudes are calculated for the ray paths in the actual data set and then they are backprojected into the mantle. The hyperparameter for smoothness constraint is the same value as in the real data inversion.

Figures 3.16 and 3.17 show the reconstructed image of the small (3 x 3 x 2) and large (6 x 6 x 3) patterns, respectively. Figure 3.18 is the map showing distributions of the sampling count. Generally the resolution in the large scale checkerboard is better than in the small scales. The resolutions have a correlation with the fluctuations of sampling count, where regions of dense sampling are well resolved. In the depth rage of 12 - 110 km, the small scale resolution is better at only limited area, around Japan. The large scale resolution is better around the Pacific, Europe, and India. However, the oceans and the northern part of the Eurasia continent are not well resolved. In the depth range of 190 - 410 km, the resolution of both small and large scale patterns are good around the Pacific. In the depth range of 551 - 893 km, the resolution increases, except for the oceans and the high latitude side of the southern hemisphere, mainly due to the large amount of data that have bottoming points around this depth range (Figure 3.8). In the depth range of 1,095 - 1,559 km, the well resolved area moves to the central part of Pacific ocean and the resolution in continental regions decreases for the small scales. The large scale resolution is quite good in this range. In the depth range of 1,821 - 2,407 km, the resolution is good in middle to east Eurasia and the central Pacific ocean. This pattern is almost the same as the distribution of sampling counts.

As shown in these figures, the resolution is extremely poor at the depth of 2,104 km, despite the fact that the sampling is not sparse (Figure 3.18). As shown in the equation (3.2.9), the coefficients for the unknowns of the attenuation structure include the reference value of Q^{-1}, and the reference Q^{-1} at the depth of 2104 km is much smaller than that at the depths of 1,821 and 2,407 km (Fig. 3.10, Table 3.1). This means that the actual weighting of the inversion equation became smaller at the depth of 2,104 km than that at the neighbor depths. Therefore the grid at the neighbor depths absorbed the effects at the depth of 2,104 km, and the range of the perturbations is smaller than that at the other depths. This problem might be solved by introducing some constraints, such as vertical smoothness or weighting factor for each depth. However it increases *a priori* parameters in the inversion and makes the inversion problem more complex. I did not apply any particular operation in the inversion process because the one-dimensional Q_p^{-1} at this depth is reliable.

The polar regions, where the absolute value of latitude is larger than 80°, are not shown because of poor resolution in all depths. This is due to the effect of the smoothness constraint, because the interval of the grid nodes in the longitudinal direction is very narrow in polar regions. This problem was also seen in the other whole mantle tomographic study with block modeling (Inoue *et al.* [1990]).

3.4 Tomographic result

The three-dimensional P-wave attenuation structure, QPB3DV2, was obtained by using the algorithm developed in Section 3.2. Only the nodes sampled by more than 10 rays were solved for in the inversion. The actual computation was performed on a personal computer with Dual Pentium II CPU (400 MHz x 2) with 512MB on-board memory. All the calculations of solutions, cross validation, and checkerboard resolution tests were done on this machine. Since the approximate size of the inversion matrices are over 450 megabytes, the

inversion matrices and the smoothness matrix ($\boldsymbol{G}$, $\boldsymbol{d}$, $\boldsymbol{m}$ and $\boldsymbol{D}$) can be kept in memory. The other data and matrices (e.g., temporary matrix for reordering in LSQR process) were stored on the hard disk. The data access on the hard disk takes about 40 times as that in memory. The computation time for one inversion process is approximately 105 minute.

Figures 3.19 and 3.20 show the resultant Q_p^{-1} perturbations from the one-dimensional model and their standard errors, respectively. Red with large positive values of Q_p^{-1} perturbations and blue shows negative perturbations indicating high and low attenuation, respectively. The color-scale ranges from -60 % (blue) to +60 % (red) and values exceeding these are clipped. The complete table of the attenuation structure is listed in Appendix C. The locations of hotspots according to Richards *et al.* [1988] are also shown in Figure 3.19. The P-wave velocity perturbation obtained by Obayashi *et al.* [1997] is shown in Figure 3.21 for comparison. Vertical cross sections of all information along great circles are also shown in Figures 3.22 to 3.27 (Figure 3.22; Q_p^{-1} perturbations, Figure 3.23; P-wave velocity perturbations obtained by Obayashi *et al.* [1997], Figure 3.24; result of the checkerboard test with 3 x 3 x 2 pattern, Figure 3.25; result of the checkerboard test with 6 x 6 x 3 pattern, Figure 3.26; sampling count, and Figure 3.27; standard error of Q_p^{-1} perturbations). The positions of the cross sections are shown as circles in an inset world map. These maps do not include the D" layer because I did not solve the solution for that region.

There is a high attenuation area in the western part of North America (California to Mexico) in the crust and the uppermost mantle. This high attenuation gradually becomes weak with depth, and it disappears suddenly at the depth of 893 km (cross sections (d), (h)). This anomaly coincides with the distribution of hotspots, such as Yellowstone and Juan de Fuca/Cobb Seamount (Richards *et al.* [1988]). According to the velocity tomography, the back-arc basins in the Circum-Pacific belt exhibits large slow anomalies of about 1.5-2.5 % (Inoue *et al.* [1990]) in the upper mantle. These low velocity anomalies are not consistent with the resultant attenuation pattern. However, the high attenuation anomaly might be a smaller scale feature smeared over a large area, because only large scale patterns were resolved in the checkerboard resolution test. A small region of high attenuation exists in the central part of Europe from the crust to over 800 km depth. At the depth of 190 km, high

attenuation appears around the Black Sea. This anomaly shifts to the east with depth, and disappears beneath the Caspian Sea around the depth of about 1,000 km.

The most remarkable high attenuation anomalies exist around the Southern Pacific (Fiji, Tonga and Polynesia). These attenuated regions have good relation to the distribution of hotspots. The regions around the Tonga and Fiji islands are characterized by high attenuation down to 300 km or deeper (cross sections (a), (d)). This anomaly seems to disappear at about 400 km, but it can be seen again at depths of 1,300 to 1,800 km in the lower mantle. It is possible that the anomaly is too small (or narrow) in the upper part of the lower mantle and it cannot be resolved in this tomography. This anomaly in the upper to lower mantle is also seen in the P-velocity tomography as a low velocity region (Obayashi *et al.* [1997]). The low velocity anomaly spreads to Tasmania and the southern part of New Zealand, while this larger extent of the anomaly does not exist in the attenuation tomography. No characteristic feature is seen in these areas (< -30° in latitude) in the attenuation image, because of the low resolution there. On the other hand, the high attenuation anomaly can be seen through all depths from 51 km to 1,317 km around the Polynesian region. This anomaly shifts to the northwest and combines with the high attenuation region under Tonga and Fiji down to the depth of 1,821 km. It is likely an upwelling which originates in the deeper part of the lower mantle.

The regions around the East Asia show high attenuation in the crust and the uppermost mantle. It shifts to the northern part of China in the upper mantle then spreads out under Southeast Asia at depth greater than 410 km. This anomaly continues down to the deeper part of the lower mantle beneath the Philippines and Papua New Guinea region (cross sections (e) and (f)). A low velocity anomaly is also seen in the velocity tomography (Obayashi *et al.* [1997]) there, but no hotspot is found there.

High attenuation is found in a wide area in the southern Indian Ocean in the upper mantle. This exists at the top of the transition layer and shifts to the Great African Rift Valley in the middle to lower mantle (cross section (d)), although the resolution is poor. A high attenuation anomaly is also seen under the northern Atlantic Ocean at depths of 1,559 to 1,821 km, despite the poor resolution.

Some low attenuation anomalies are found beneath the stable continents. The most remarkable low attenuation anomaly can be confirmed in South Asia in the upper mantle. The clear elongated pattern of low attenuation exists from West Asia to Australia. The shape of the anomaly is consistent with the high velocity pattern in the whole mantle velocity tomography constructed by Kennett *et al.* [1998]. A remarkable region of low attenuation can be seen at depths of 190 to 410 km in the coastal side of the Western Pacific, which may be due in part to the existence of subducting slabs. Such patterns were also found in the P-wave velocity structure of Inoue *et al.* [1990], but their depth for the high velocity region is deeper (478 to 629 km) than our results. However, there is high velocity materials at depths of 120 to 180 km in the S-wave velocity structure of Suetsugu and Nakanishi [1987] , and this fits with our result.

There is a low attenuation anomaly beneath South America and the eastern part of North America in the upper to middle depths of the mantle. Also there exists a remarkable low attenuation body beneath the Eurasia Continent in the lower mantle (cross section (h)). These regions have better resolution and these anomalies are reliable. A low attenuation root is also found beneath central Africa, whose absolute motion with respect to the mantle is very slow (Minster and Jordan [1978]). A low attenuation body beneath the Eurasia continent spreads out at the depth of 2407 km. The shape of this body is, however, the same as the extent of the areas of better resolution, so the reliability of this anomaly is low.

We find a clear low attenuation anomaly beneath Japan and China in the lower mantle, as shown in the cross sections (b), (c) and (f). The resolution of this area is relatively good, so this anomaly is reliable. But no high velocity anomaly can be seen there in the model of Obayashi *et al.* [1997]. There is a low attenuation anomaly along the extension of the subduction zone in the Tonga-Kermadec region in the lower mantle with good resolution. This suggests the existence of slab penetration into the lower mantle (Creager and Jordan [1984]). This anomaly can be seen in P-wave (Inoue *et al.* [1990]) and S-wave velocity structures (Grand [1987]) as high velocity anomalies.

Previous tomographic models of the whole mantle show predominantly degree 2 patterns, with low velocities in the central part of the Pacific Ocean and beneath Africa (*e.g.*,

Masters *et al.* [1982], Inoue *et al.* [1990]). However, a large heterogeneous pattern of degree 2 is not clear in our model. This is due to few data and less resolution around Africa.

3.5 Discussion

There are some reasons why the anelastic stricture of the mantle should be of fundamental interest to geophysics. The most important reason for considering three-dimensional attenuation structures is that it may provide constraints on mantle dynamics that are complementary to those inferred from elastic modeling (Romanowicz [1995]). The absorption of seismic waves is affected by mainly thermal conditions, in other words, heterogeneity of absorption of waves maps the thermal structure in the Earth. The effects of temperature anomalies on attenuation and velocity are different. Figure 3.28 is a sketch of the behavior of attenuation and velocity as a function of temperature (referred from Romanowicz [1995]). The temperature dependence of attenuation follows an Arrhenius exponential law and is therefore much stronger than that of elastic velocity (*e.g.*, Minster and Anderson [1981], Kampfmann and Berckhemer [1985], Jackson *et al.* [1992]). This means that the attenuation structure is more sensitive to temperature variations at higher temperature, while less sensitive at lower temperatures. Therefore, "weak' upwelling currents of elevated temperature relative to the surroundings can be emphasized through the mapping of Q, whereas it is harder to detect the presence of "strong" cold downwelling (such as slabs in the upper mantle) when mapping elastic velocities (Romanowicz [1995]). Also in our results, characteristic high attenuation anomalies were identified clearly, while only large scale low attenuation regions could be found. The velocity structure and the resultant attenuation structure must be interpreted together.

In the present section, I obtained a fine three-dimensional P-wave attenuation structure for the whole mantle. Now I point out a problem due to the effect of the velocity structure.

Amplitudes of seismic body-waves are sensitive to effects in heterogeneity of elastic velocity, which create focusing and defocusing of seismic energy (*e.g.*, Aki and Richards [1980], Resovsky and Ritzwoller [1994]) in addition to anelastic attenuation. For that reason I calculated the amplitude variation due to the whole mantle P-wave velocity structure to estimate the effect of velocity heterogeneity. Here I used the tomographic result of Obayashi et al. [1997]. The density is also set heterogeneous, assuming the density as a linear function of the P-wave velocity. P-wave attenuation structure was set to one-dimension. The amplitude calculation was conducted by using two types of ray tracing, pseudo-bending method on polar coordinate (Koketsu and Sekine [1996]) for kinematic ray tracing and the dynamic ray tracing (Červený [1985], Sekiguchi [1992]). The calculation was carried out as following procedure: 1) Put an event on the actual position, and distribute tentative stations on the surface by 10° x 10° interval. 2) Conduct two-point kinematic ray tracing from the hypocenter to each tentative station. The step length of the path segment was set to 5 km. 3) Calculate the first- and second-partial derivatives of velocity structure, and then conduct dynamic ray tracing. I used the subroutines of Sekiguchi [1992] in the procedure of the dynamic ray tracing. 4) Apply the free-surface correction. The amplitude variation due to the attenuation was also calculated to compare with the velocity effect. In this case the velocity and the density are set to 1-D structures. To eliminate the difference of heterogeneity pattern, I used Obayashi's tomographic pattern as Qp heterogeneity, but the perturbation range was set to ±60 %.

Figures 3.29 shows the ray amplitude variations due to the 3-D P-wave velocity structure for some explosion-type point sources. Only the data with epicentral range between 28° to 89° are shown. Blue circle and red rectangle indicate larger and smaller amplitude than that from 1-D velocity and attenuation structure, respectively. The size of the mark is proportional to the common-logarithm of the amplitude ratio. Figure 3.30 shows the same as Figure 3.29 but obtained from the 3-D attenuation structure. As shown in these figures, amplitude variation due to the Qp heterogeneity is larger and longer wavelength than that due to the Vp structure. The wavelength of amplitude fluctuation is shorter than 20° at the almost area in the 3-D velocity structure, while more global distribution can be seen in the 3-D attenuation structure. There are very large or small amplitudes in some places in the 3-D

velocity structure. These anomalies are caused by the focusing and defocusing effects of velocity structure. However these anomalies appear very irregularly and they should be canceled out by each other with processing a large amount data from various hypocenters. Mentioned above it can be said that the teleseismic amplitude is affected more strongly by the attenuation heterogeneity than the velocity in global scale. This is the opposite tendency to the result of Sekiguchi [1992], who investigated the regional amplitude variation around Kanto-Tokai region, Japan. He calculated the Gaussian-beam amplitude by adopting a 3-D velocity and attenuation structure, and concluded that the effect of the Q structure on the amplitude is small. But in my case, the scalelength of the velocity structure is over 1000 km and its perturbation does not exceed ±3 %. This means that the velocity gradient is very small in horizontally direction, and it is difficult to happen the focusing or defocusing at the wide area. As considering above I did not include the focusing and defocusing effects in the present calculation, because the scale of any heterogeneous velocity model in the whole mantle is much larger than the wavelength of the data used in this study, and present three-dimensional velocity models are not accurate enough to allow for the correction of amplitude data by forward modeling. The consideration of these effects of elastic heterogeneity should be included in the future.

I presented a three-dimensional P-wave attenuation model of the whole mantle, named QPB3DV2. This is the first result of its kind. This model is clearly very preliminary, but I think it will greatly contribute toward understanding the Earth's deep interior and mantle dynamics.

Table Caption

Table 3.1 The spherically symmetric Q_p^{-1} model obtained in this study. The values from AK135 (Montagner and Kennett [1996]) are also shown for comparison.

Depth (km)	Qp^{-1} (x 10^{-3})	s.d. (x 10^{-3})	count	Qp^{-1}(AK135) (x 10^{-3})
12	8.773	2.270	883925	1.146
51	6.023	1.360	1037502	2.274
110	3.472	0.620	1115536	8.681
190	5.093	1.620	1179346	8.186
290	3.752	1.030	1226344	4.566
410	2.134	0.390	1283333	4.566
551	1.372	0.210	1358124	3.793
712	1.042	0.170	1438711	1.210
893	1.708	0.370	1500496	1.262
1095	0.784	0.100	1408180	1.303
1317	0.988	0.240	1383114	1.347
1559	0.802	0.130	1284412	1.395
1821	1.213	0.270	931397	1.456
2104	0.211	0.010	423499	1.540
2407	2.702	0.830	193587	1.635
2731	0.941	0.180	43124	1.737

Table 3.1

Figure Captions

Fig. 3.1 Illustration of discrete raypath. Three-dimensional seismic ray path is divided into N segments of step length Δs. The parameter (velocity and Q^{-1}) of each segment is represented by that at the mid point of each segment.

Fig. 3.2 Comparison of representation of three-dimensional structure by block modeling (left) and grid modeling (right). Raypath is segmented at the block boundaries in block parameterization, while the incremental characteristic length is determined independently in the grid configuration. The attenuation factor (t^*) is represented by the segmented path length, velocity and Q^{-1} at each block in block modeling. On the other hand, t^* is calculated from the velocity and Q^{-1} on the raypath, whose parameters are represented by the B-spline interpolation (w: weighting function) of the peripheral modeling grids. See the text for details.

Fig. 3.3 Representation of velocity and Q^{-1} at optional positions on a raypath. These are obtained by interpolation of values at eight surrounding grid nodes.

Fig. 3.4 Results of the simplified cross-validation test. RMS error of log-amplitudes is shown as a function of the smoothness weight α. The RMS errors are normalized by the value when α=0. The three-curves indicate the results with the different groupings of the data. These curves show approximately the same minimum position around the α as 2 or 3.

Fig. 3.5 Simplified LSQR program from a version of Ratfor (Rational FORTRAN) (after Nolet [1987]). Output variables phibar and r are the absolute and relative lengths of the residual vector $\boldsymbol{Ax} - \boldsymbol{u}$. Vector $\boldsymbol{v}$ and scalars (α, β) correspond to the quantities described by Van der Sluis and Van der Vorst [1987].

Fig. 3.6 Map showing locations of 3,445 epicenters that occurred during the period from 1984 to 1995 used in this study. The location parameters of each event were taken from the relocated hypocenters data base named EHB (Engdahl *et al.*

[1998]). The events that has more than 15 amplitude data were used. The minimum and maximum body-wave magnitude are 4.4 and 6.9.

Fig. 3.7 Map showing locations of 718 stations used in this study. Totally 155,778 amplitude data observed these stations were used in this study.

Fig. 3.8 Histogram of the bottoming depths of all the data. These bottoming depths were calculated by using AK135 velocity model (Kennett *et al.* [1995]). The depth variations are limited between 700 km to 2,700 km because of the limited epicentral distance (28° – 89°).

Fig. 3.9 The one-dimensional distribution of 16 grid nodes and sampling count at each grid depth. The grid interval becomes larger with depth. The number of the sampling count is depend on the step length for the ray tracing: large number of sampling count with shorter step length and small sampling number with longer step length.

Fig. 3.10 The resultant one-dimensional Q^{-1} structure in this study (solid line). Horizontal thin bars represent the standard error at each depth. This model is listed in Table 3.1. The Q^{-1} model of AK135 (Montagner and Kennett [1996]) is also shown for comparison (dashed line).

Fig. 3.11 Various P-wave attenuation models in the mantle obtained by body-wave analysis; MM8 (Anderson *et al.* [1965]), Model G (Teng [1968]), and SL8 (Anderson and Hart [1978]).

Fig. 3.12 Scatter diagram of the resultant source amplitudes versus the ISC body-wave magnitude (m_b).

Fig. 3.13 Horizontal view of the grid configuration for tomographic inversion. The grid interval is set to 10°. There are 17 nodes spaced in latitude, 30 in longitude. Vertical grid configuration is shown in Fig. 3.9. The total number of grid nodes is 9,794 including nodes on the North- and South Poles on each depth.

Fig. 3.14 Three-dimensional P-wave velocity structure of the whole mantle (after Obayashi *et al.* [1997]). Slowness perturbations from the averages at each depth are shown. Red and blue indicate slow and fast P-wave velocity, respectively. Whole the crust and mantle were divided into 32 (latitude) x 64 (longitude) x 16 (depth) blocks. This model was used for the construction of inversion matrices.

Fig. 3.15 Horizontal view of the initial checkerboard pattern for the resolution test. The alternate patterns of ±60% anomalies in Q_p^{-1} extend both horizontally and vertically. Two types of checkerboard size, 3 x 3 x 2 grids (upper) and 6 x 6 x 3 grids (lower) in latitude x longitude x depth, were tested in order to see the resolutions in different wavelengths. Red and blue are correspond to high-attenuation (large Q_p^{-1}) and low-attenuation (small Q_p^{-1}), respectively. The displayed area is 75°S to 75°N in latitude and 0° to 360° (west to east) in longitude.

Fig. 3.16 Resultant images of the resolution test for 3 x 3 x 2 checkerboard pattern. The portion where the resolution is good will show a clear checkerboard pattern, and the pattern becomes blurred where the resolution is poor. The displayed area is 75°S to 75°N in latitude and 0° to 360° (west to east) in longitude. The polar regions are not shown because of poor resolution in all depths (see the text for details).

Fig. 3.17 The same as Fig. 3.16 but for 6 x 6 x 3 checkerboard test.

Fig. 3.18 Horizontal view of the distribution of sampling count. The regions of dense sampling are black.

Fig. 3.19 Q_p^{-1} variation maps for each depth. Red shows large positive values of Q_p^{-1} perturbations and blue shows negative values, indicating high and low attenuation, respectively. The color-scale ranges from -60 % (blue) to +60 % (red) and the values exceeding this range are clipped. The distribution of hotspots according to Richards *et al.*[1988] is also shown as green dots. The displayed area is 75°S to 75°N in latitude and 0° to 360° (west to east) in longitude.

Fig. 3.20 Distributions of the standard error of the attenuation structure. Dark area shows large standard error.

Fig. 3.21 P-wave velocity perturbations of Obayashi *et al.* [1997], but spatially desampled to 10° interval to compare with the attenuation results. Red and blue are correspond to high and low velocity perturbations from the average velocity at each depth, respectively. The displayed area is 75°S to 75°N in latitude and 0° to 360° (west to east) in longitude.

Fig. 3.22 Vertical cross sections of the Q_p^{-1} variation along the great circles, which is indicated by the circle in the map given in the portion of the core. The pole position of the great circle is given at the top left of each figure. Perturbations greater than ±50 % are clipped.

Fig. 3.23 Vertical cross sections of the reduced P-wave velocity perturbation from one-dimensional velocity model (Obayashi *et al.* [1997]). Other details are same as Fig. 3.22.

Fig. 3.24 Vertical cross sections of the result of the checkerboard test for 3 x 3 x 2 pattern along the great circle. The position of the great circle is also given in the figures. Perturbations greater than ±50 % are clipped.

Fig. 3.25 The same as Fig. 3.24 but for 6 x 6 x 3 checkerboard pattern.

Fig. 3.26 Vertical cross sections of the sampling count along the great circle. The regions of dense sampling are indicated by black.

Fig. 3.27 Vertical cross sections of the standard error along the great circle. Dark area shows large standard error.

Fig. 3.28 Comparison of the temperature dependence of velocity and attenuation. Units are arbitrary. The temperature anomalies are referred to an average value neat T=4.5. A) Q_p^{-1} versus temperature. The exponential dependence of Q_p^{-1} on temperature favors hotter than average anomalies, even if colder than average anomalies have

larger amplitude. B) Velocity versus temperature. They have a linear relation, that will emphasize the anomalies that are larger in amplitude, that is, cold anomalies (after Romanowicz, [1995]).

Fig. 3.29 Ray amplitudes of the vertical component of P-waves for an explosion-type point source in the 3-D P-wave velocity structure of Obayashi *et al.* [1997]. Ray amplitudes for frequencies of 1 Hz are shown. Only the position with epicentral range between 28° to 89° are shown. Blue circle and red rectangle indicate larger and smaller amplitude than that from 1-D velocity and attenuation structure, respectively. The size of the mark is proportional to the common-logarithm of the amplitude ratio. The event locations are as follows,

(upper) Ethiopia (1985/05/14 13:25:02.5 10.61°S, 41.38°E, 30.4 km M5.8)

(middle) Bulgaria (1990/05/30 10:40:07.7 45.66°N, 26.65°E, 89.8 km M6.4)

(lower) Kuril (1994/08/02 14:17:54.2 52.25°N, 157.99°E, 150.1 km M5.8)

Fig. 3.30 The same as Fig. 3.29 but obtained from the 3-D attenuation structure. P-wave velocity structure is set to 1-D. Same heterogeneous patter as Fig. 3.29 is used for the Qp heterogeneity, with setting the perturbation range to ±60 %.

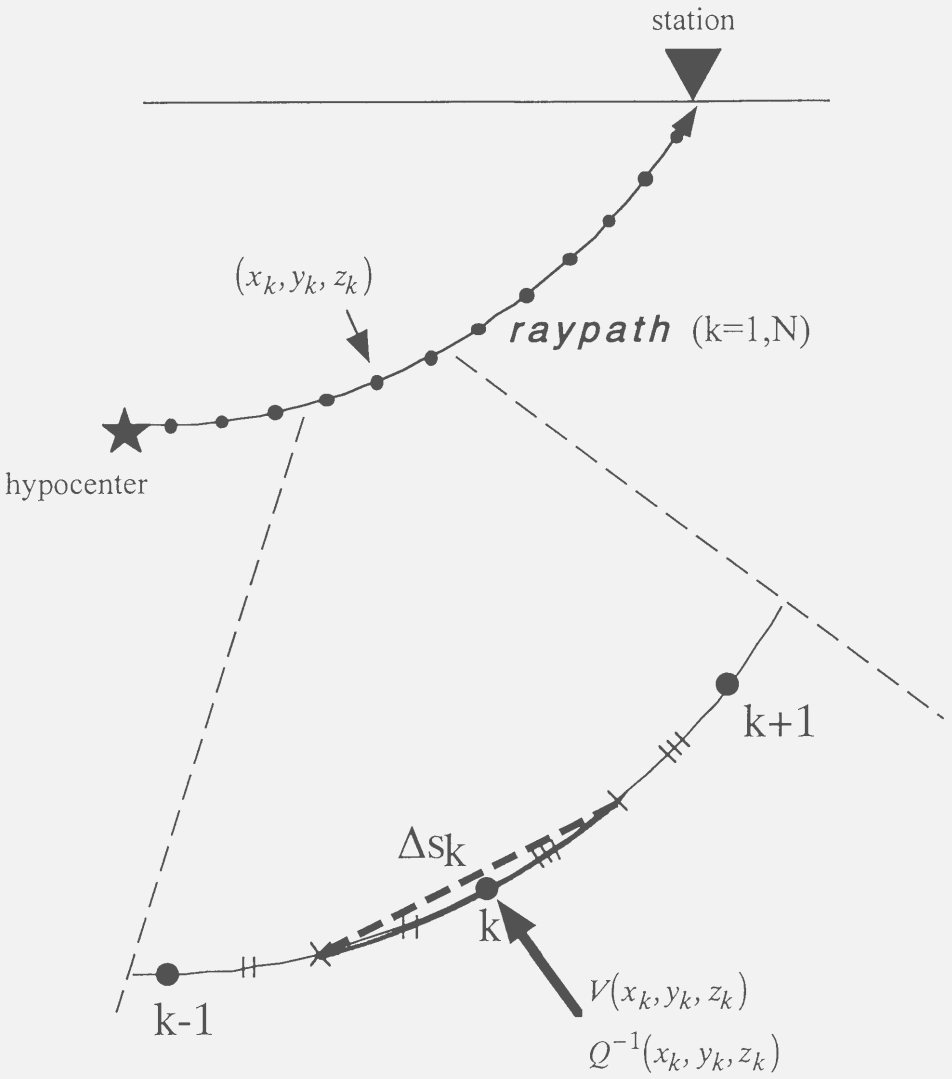
station
(x_k, y_k, z_k)
raypath (k=1,N)
hypocenter
k+1
Δs_k
k
k-1
$V(x_k, y_k, z_k)$
$Q^{-1}(x_k, y_k, z_k)$

Figure 3.1

Block Modeling

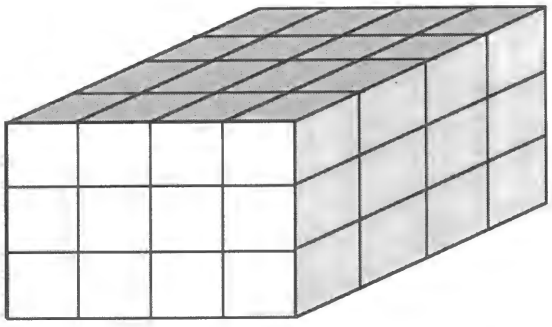

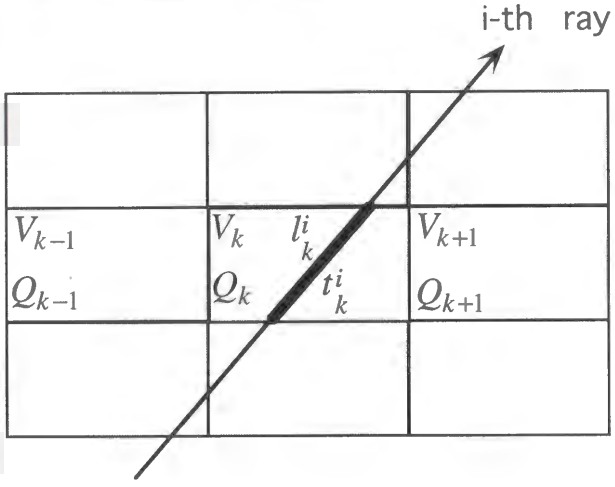

blocks sampled by the ray

$$t^* = \sum_k t_k Q_k^{-1} = \sum_k \frac{l_k}{V_k} Q_k$$

Grid Modeling

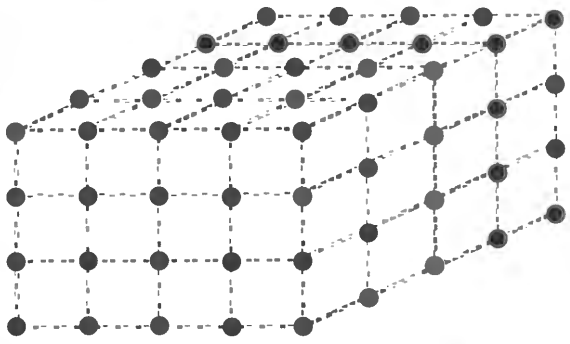

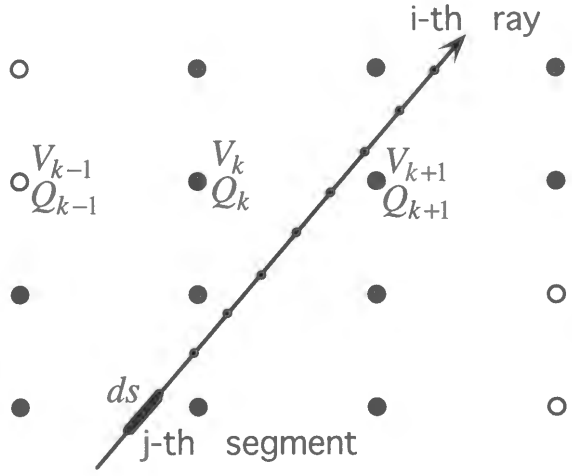

grids sampled by the ray

$$t^* = \sum_j t_j Q_j^{-1} = \sum_j^N \frac{1}{V_j} Q_j^{-1} ds_j$$

$$Q_j^{-1} = \sum_l w_{lk}^j Q_k^{-1}$$

Figure 3.2

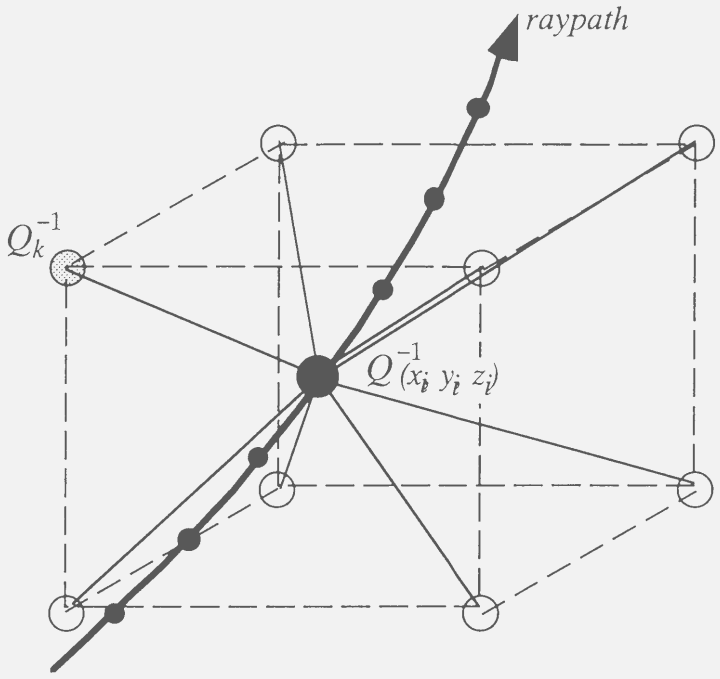

$$Q^{-1}(x_i, y_i, z_i) = \sum_{l=1}^{8} w_{il} Q_l^{-1}$$

Figure 3.3

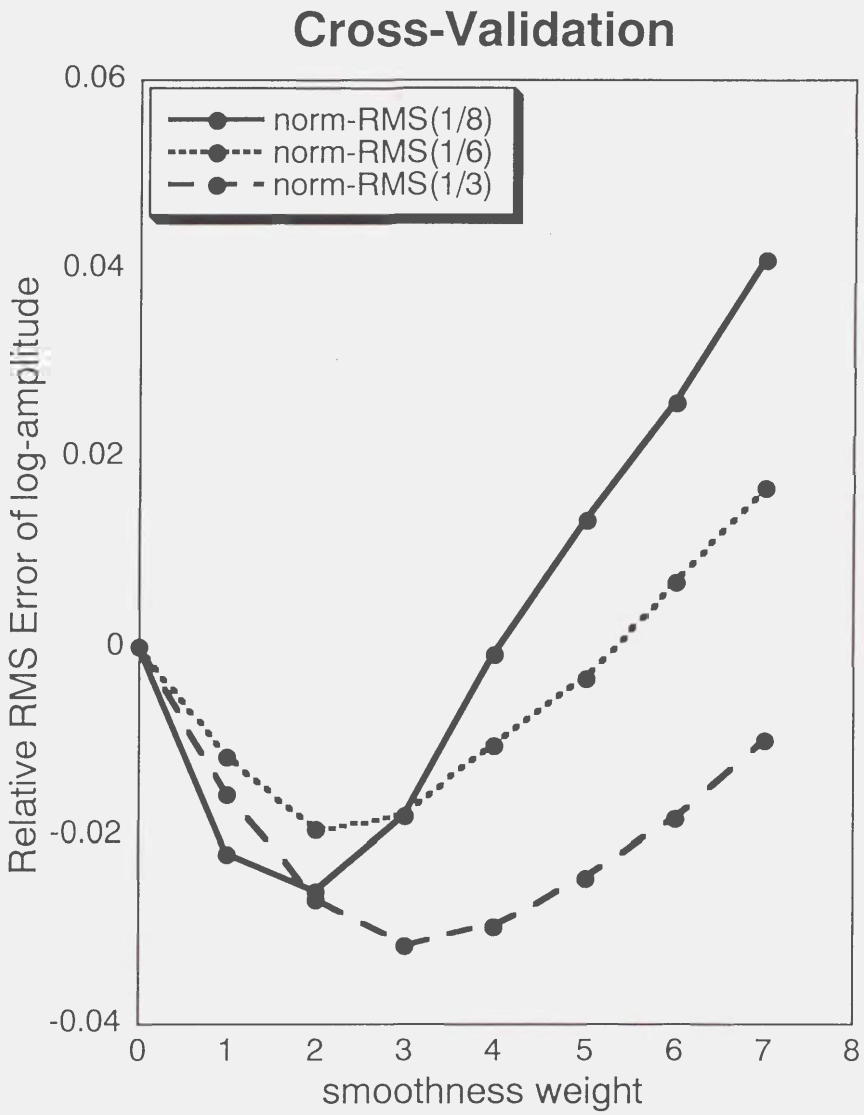
Cross-Validation
norm-RMS(1/8)
norm-RMS(1/6)
norm-RMS(1/3)
Relative RMS Error of log-amplitude
0.06
0.04
0.02
0
-0.02
-0.04
0
1
2
3
4
5
6
7
8
smoothness weight

Figure 3.4

```
subroutine pstomo(m,n,x,u,v,w,itmax)
#
# subroutine to solve the linear tomographic problem Ax=u using the
# lsqr algorithm (C.C.Paige and M.A.Saunders, ACM Trans.Math.Softw.
# 8, 43 - 71 and 195 - 209, 1982).
#
# Input: m is the number of data, n the number of unknowns, u cont-
#    ains the data (is overwritten), itmax is the nr of iterations.
# Output: x is the solution
# Scratch: arrays v(n) and w(n)
# Subroutines: routines avpu and atupv to be supplied by the user.
#    avpu(m,n,u,v) computes u=u+A*v for given input u,v
#    atupv(m,n,u,v) computes v=v+A(transpose)*u for given u,v
#
dimension x(n),u(m),v(n),w(n)
open (9,file='tomo.int',form='unformatted')
do i=1,n { x(i)=0; v(i)=0 }                          # initialize
call normlz(m,u,beta); b1=beta;
call atupv(m,n,u,v); call normlz(n,v,alfa)
rhobar=alfa; phibar=beta; do i=1,n { w(i)=v(i) }
write(6,*) 0,x(1),beta,1
do iter =1,itmax {                          # repeat
   a= - alfa; do i=1,m { u(i)=a*u(i) }              # bidiagonalization
   call avpu(m,n,u,v); call normlz(m,u,beta);
   b= - beta; do i=1,n { v(i)=b*v(i) }
   call atupv(m,n,u,v); call normlz(n,v,alfa)
   rho=sqrt(rhobar*rhobar+beta*beta)                # modified QR
   c=rhobar/rho; s=beta/rho; teta=s*alfa;
   rhobar= - c*alfa; phi=c*phibar; phibar=s*phibar;
   t1=phi/rho; t2= - teta/rho
   do i=1,n { x(i)=t1*w(i)+x(i); w(i)=t2*w(i)+v(i) }  # update
   r=phibar/b1; write(6,*) iter,x(1),phibar,r
   write(9) iter,x,v,alfa,beta,phibar,r             # intermediate output
   }
return; end                                 # return
#
subroutine normlz(n,x,s)                    # normalizes vector x
dimension x(n)
s=0.; do i=1,n { s=s+x(i)**2 }
s=sqrt(s); ss=1./s; do i=1,n { x(i)=x(i)*ss }
return; end
```

Figure 3.5

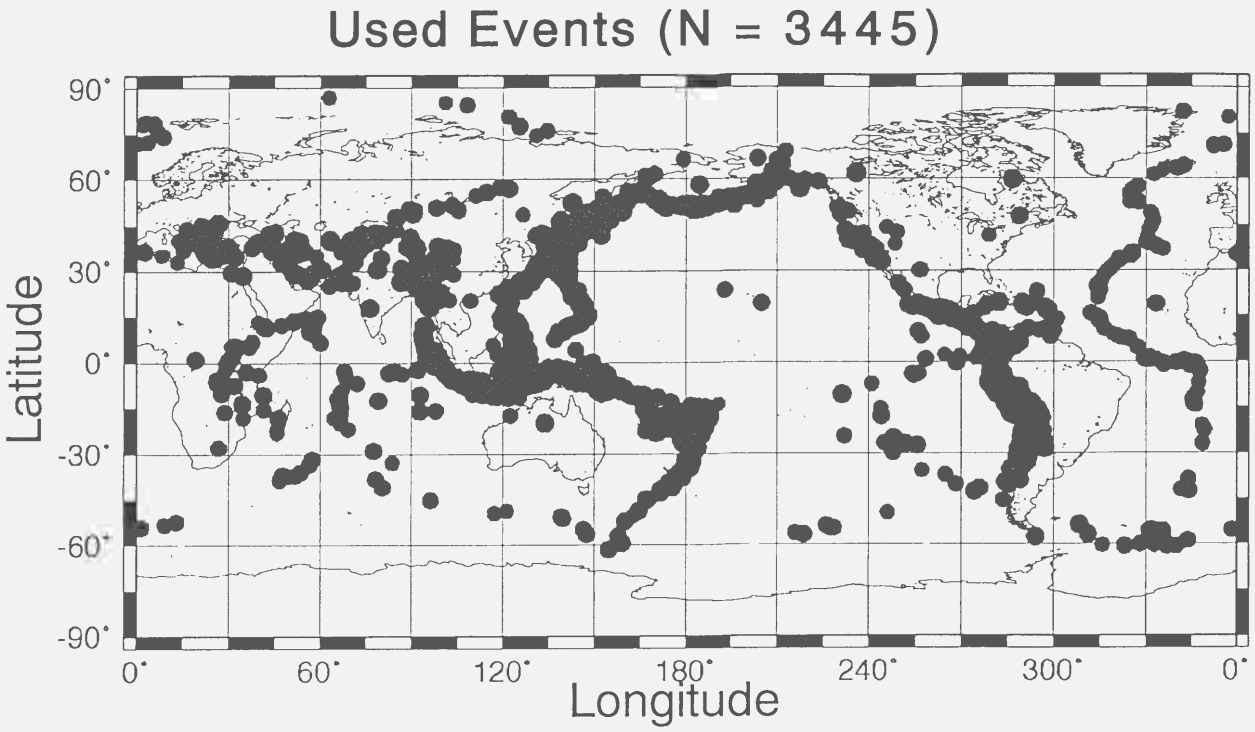
Used Events (N = 3445)
90°
60°
30°
0°
-30°
-60°
-90°
Latitude
0°
60°
120°
180°
240°
300°
0°
Longitude

Figure 3.6

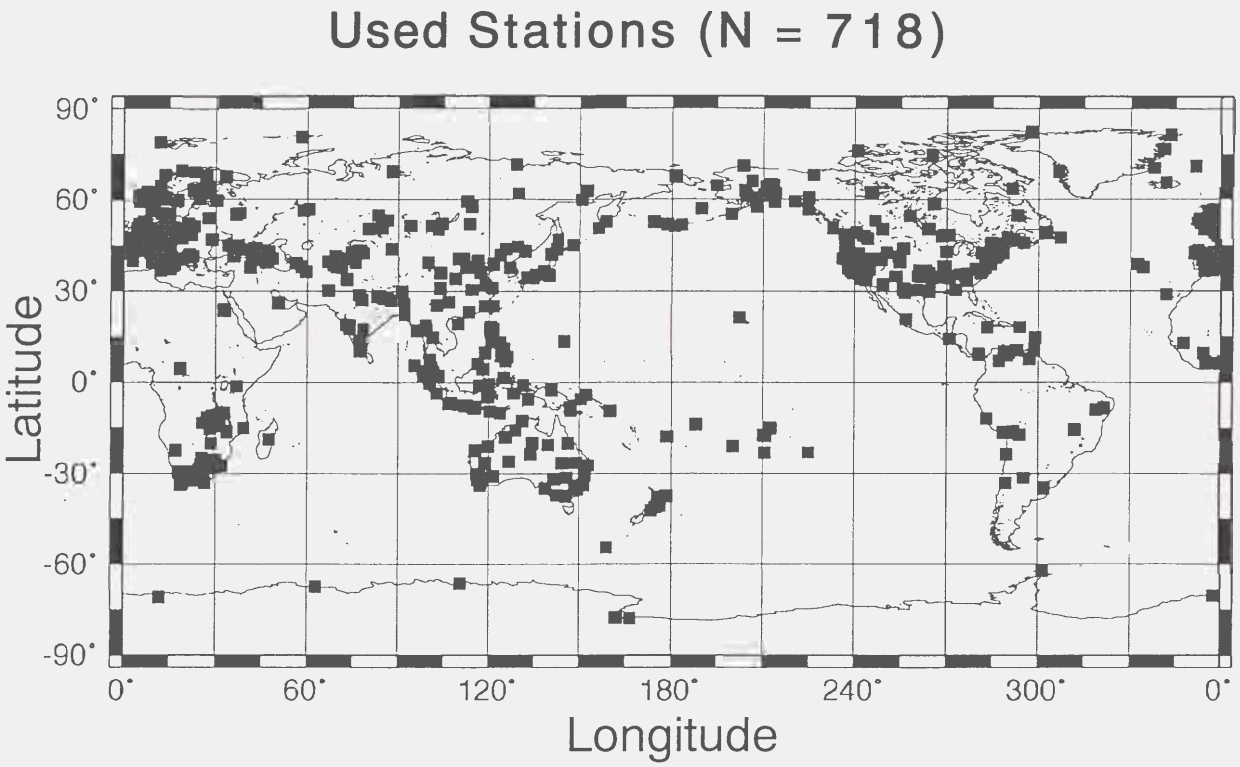
Used Stations (N = 718)
90°
60°
30°
0°
-30°
-60°
-90°
Latitude
0°
60°
120°
180°
240°
300°
0°
Longitude

Figure 3.7

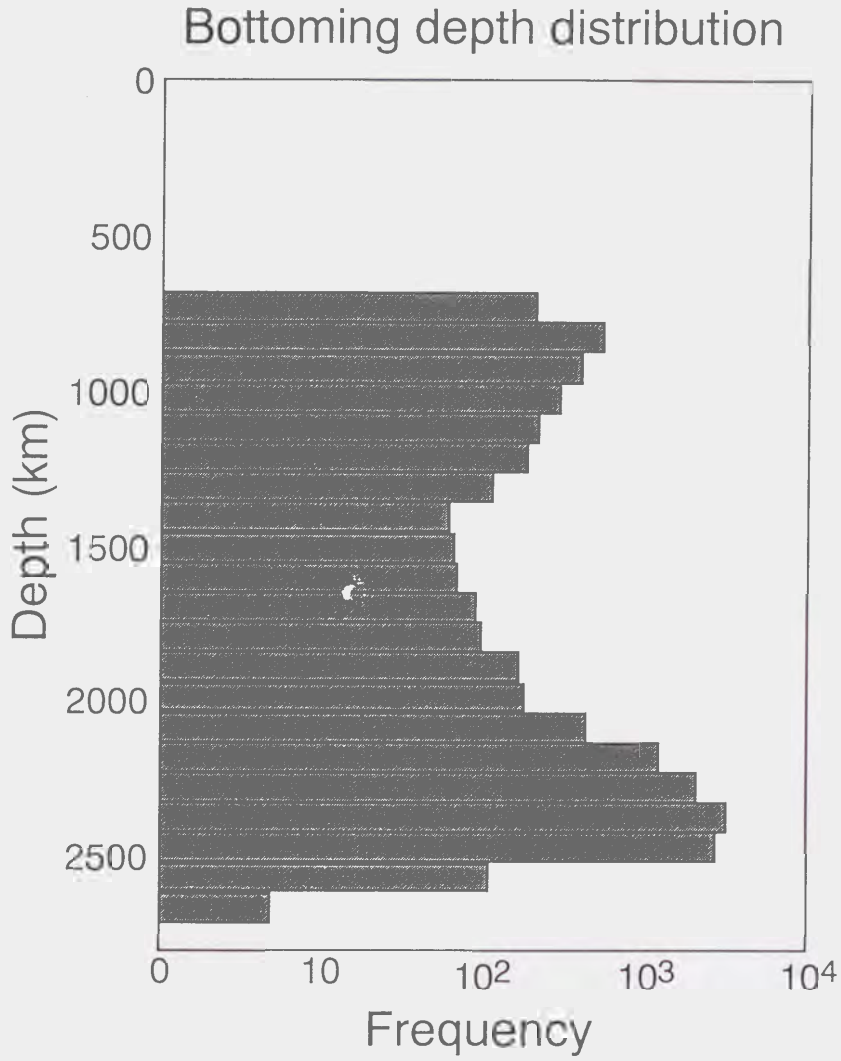
Bottoming depth distribution
0
500
1000
1500
2000
2500
Depth (km)
0
10
10²
10³
10⁴
Frequency

Figure 3.8

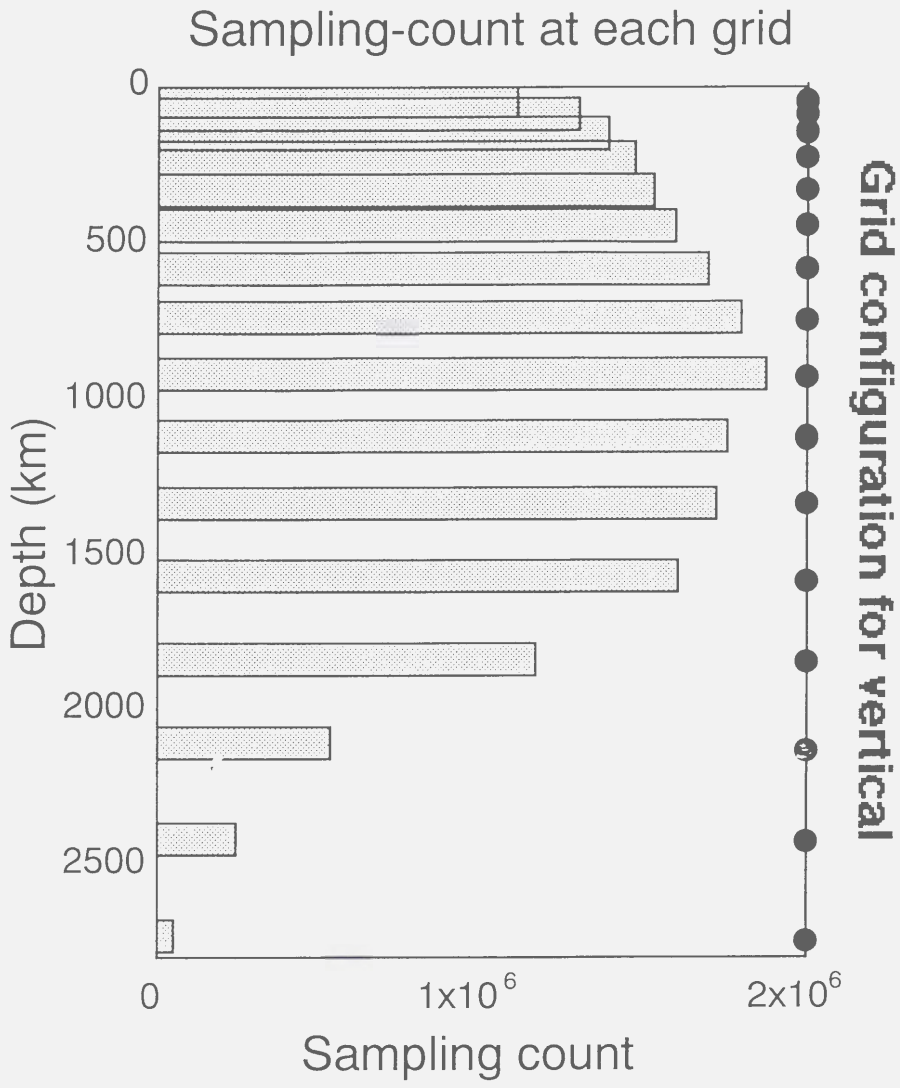
Sampling-count at each grid
0
500
1000
1500
2000
2500
Depth (km)
0
1x10^6
2x10^6
Sampling count
Grid configuration for vertical

Figure 3.9

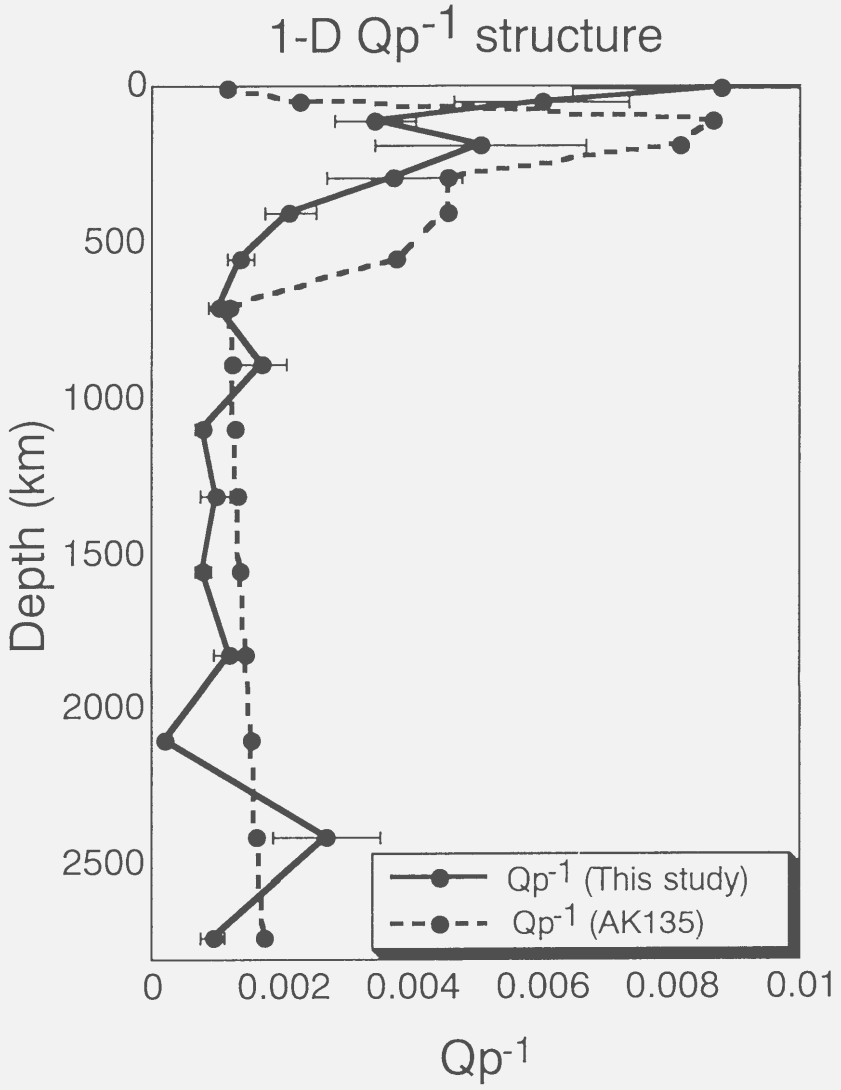
1-D Qp-1 structure
0
500
1000
1500
2000
2500
Depth (km)
Qp-1 (This study)
Qp-1 (AK135)
0
0.002
0.004
0.006
0.008
0.01
Qp-1

Figure 3.10

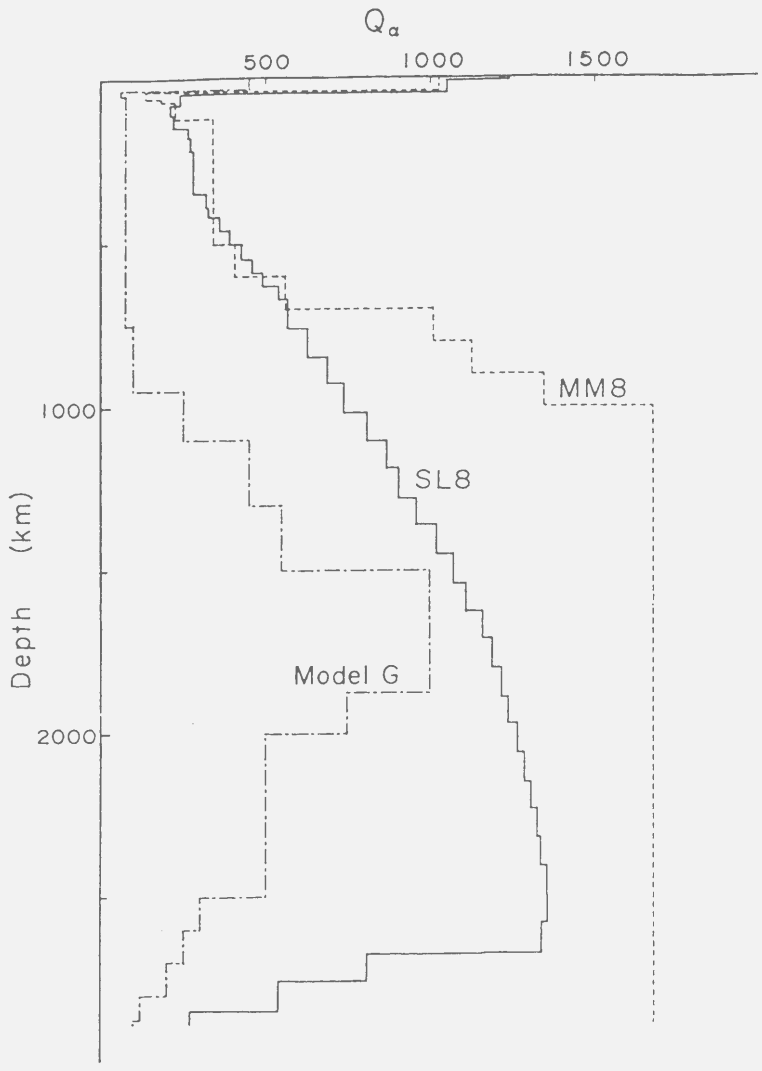

Figure 3.11

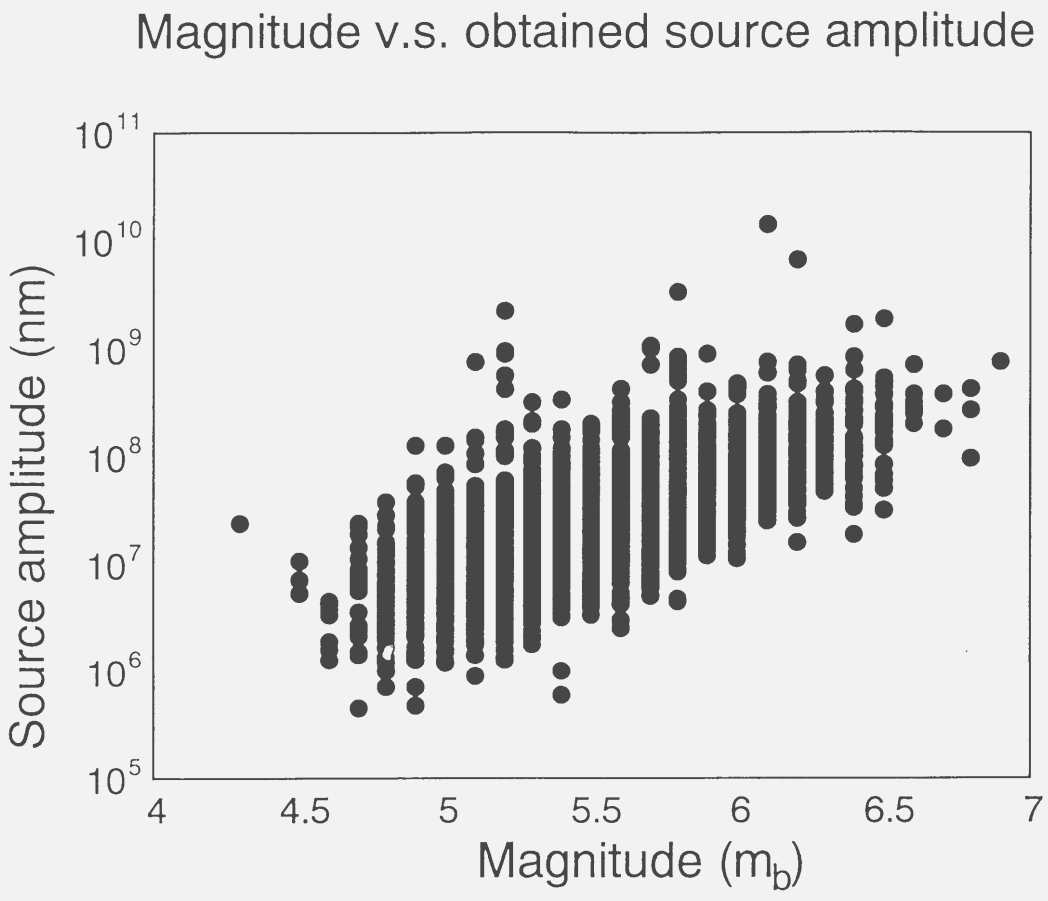
Magnitude v.s. obtained source amplitude
Source amplitude (nm)
10^{11}
10^{10}
10^{9}
10^{8}
10^{7}
10^{6}
10^{5}
4
4.5
5
5.5
6
6.5
7
Magnitude (m_b)

Figure 3.12

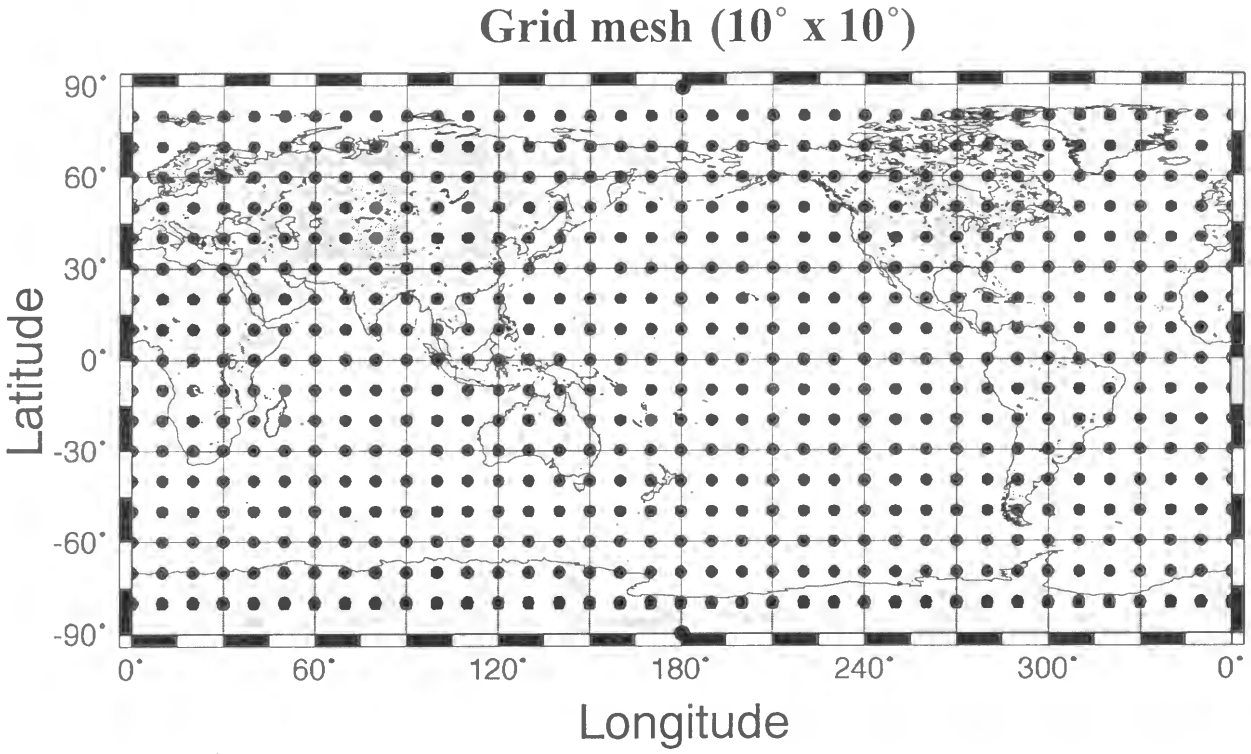
Grid mesh (10° x 10°)
90°
60°
30°
0°
-30°
-60°
-90°
Latitude
0°
60°
120°
180°
240°
300°
0°
Longitude

Figure 3.13

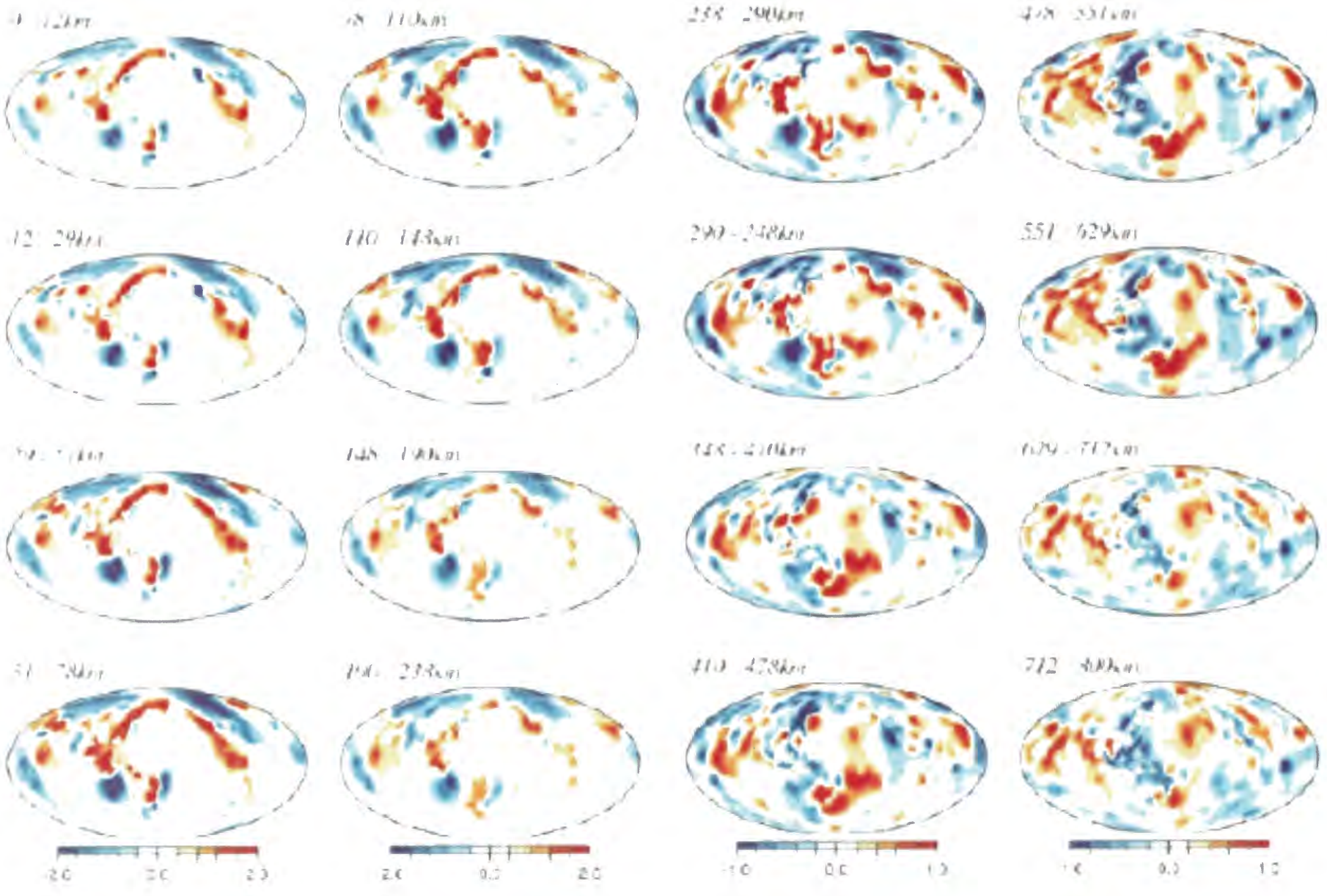

Figure 3.14 (1/2)

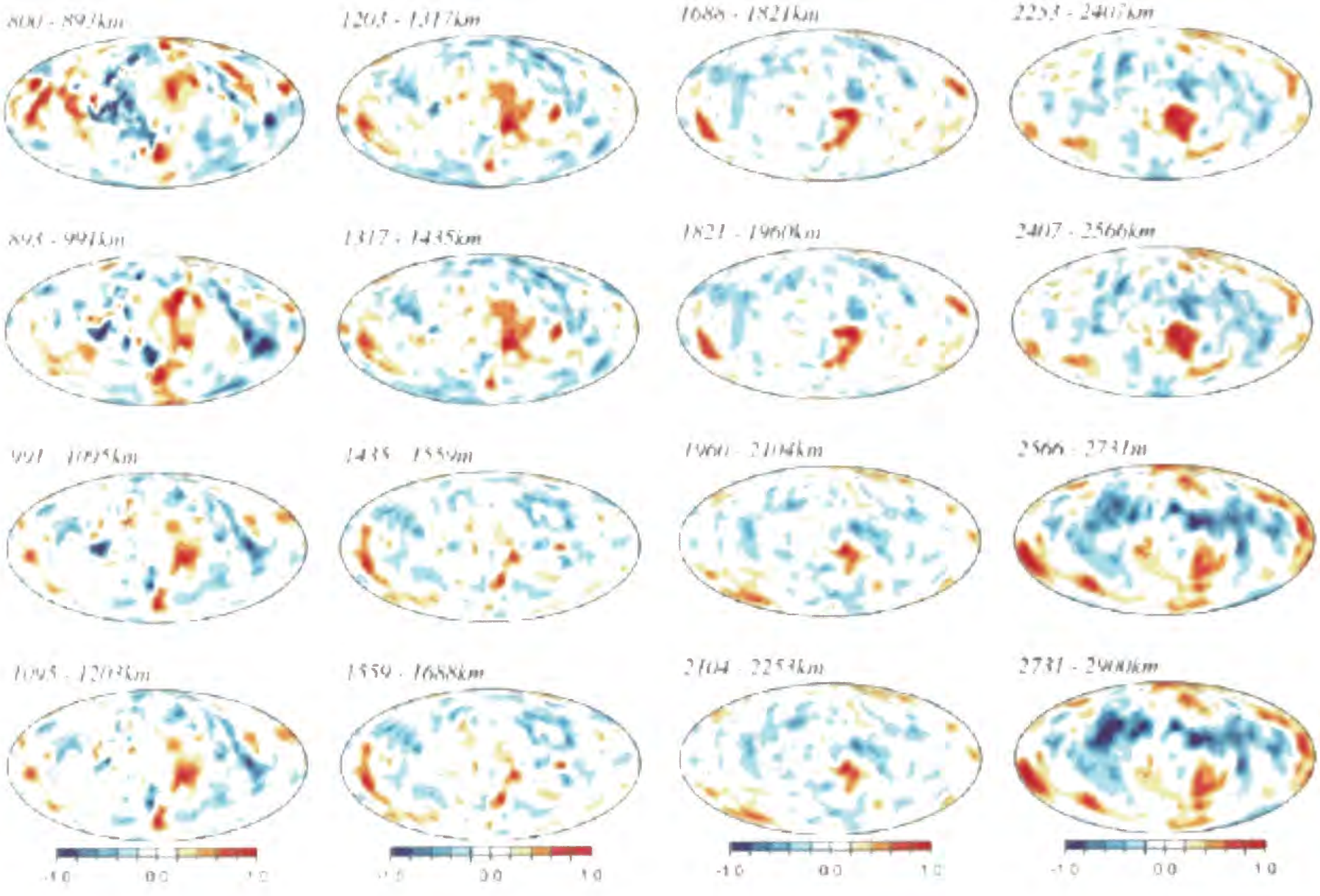

Figure 3.14 (2/2)

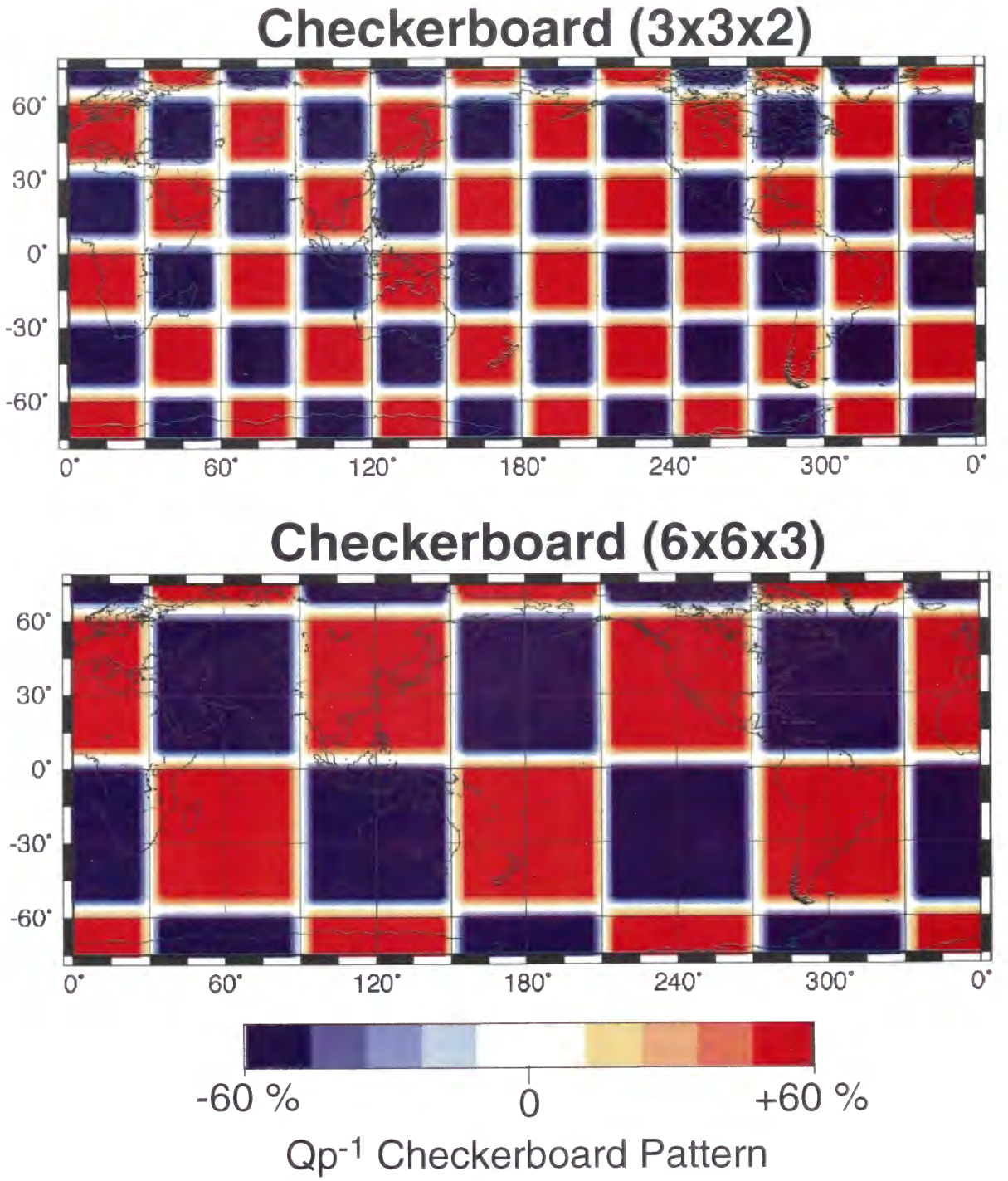
Checkerboard (3x3x2)
60°
30°
0°
-30°
-60°
0°
60°
120°
180°
240°
300°
0°
Checkerboard (6x6x3)
60°
30°
0°
-30°
-60°
0°
60°
120°
180°
240°
300°
0°
-60 %
0
+60 %
Qp-1 Checkerboard Pattern

Figure 3.15

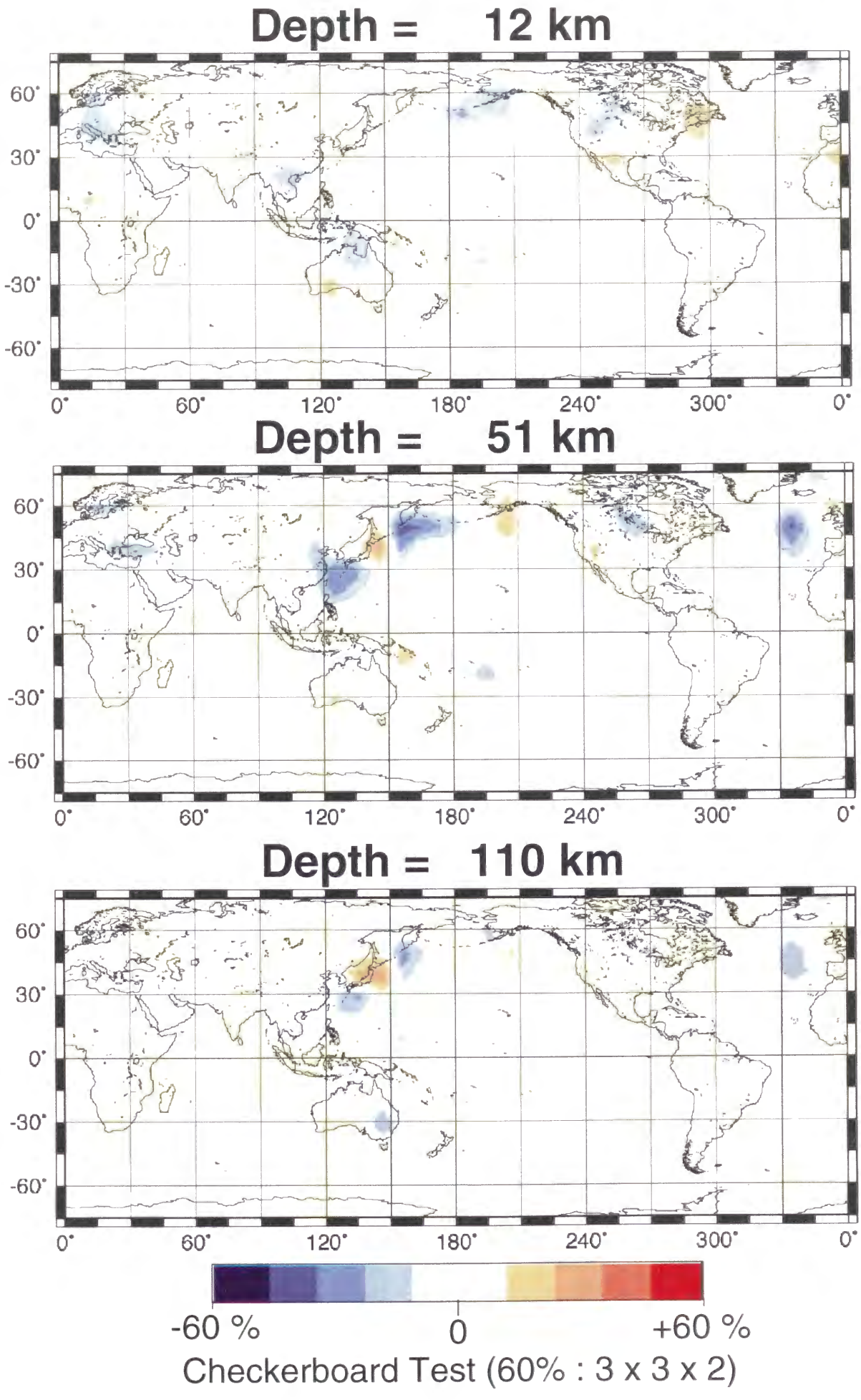

Figure 3.16 (1/5)

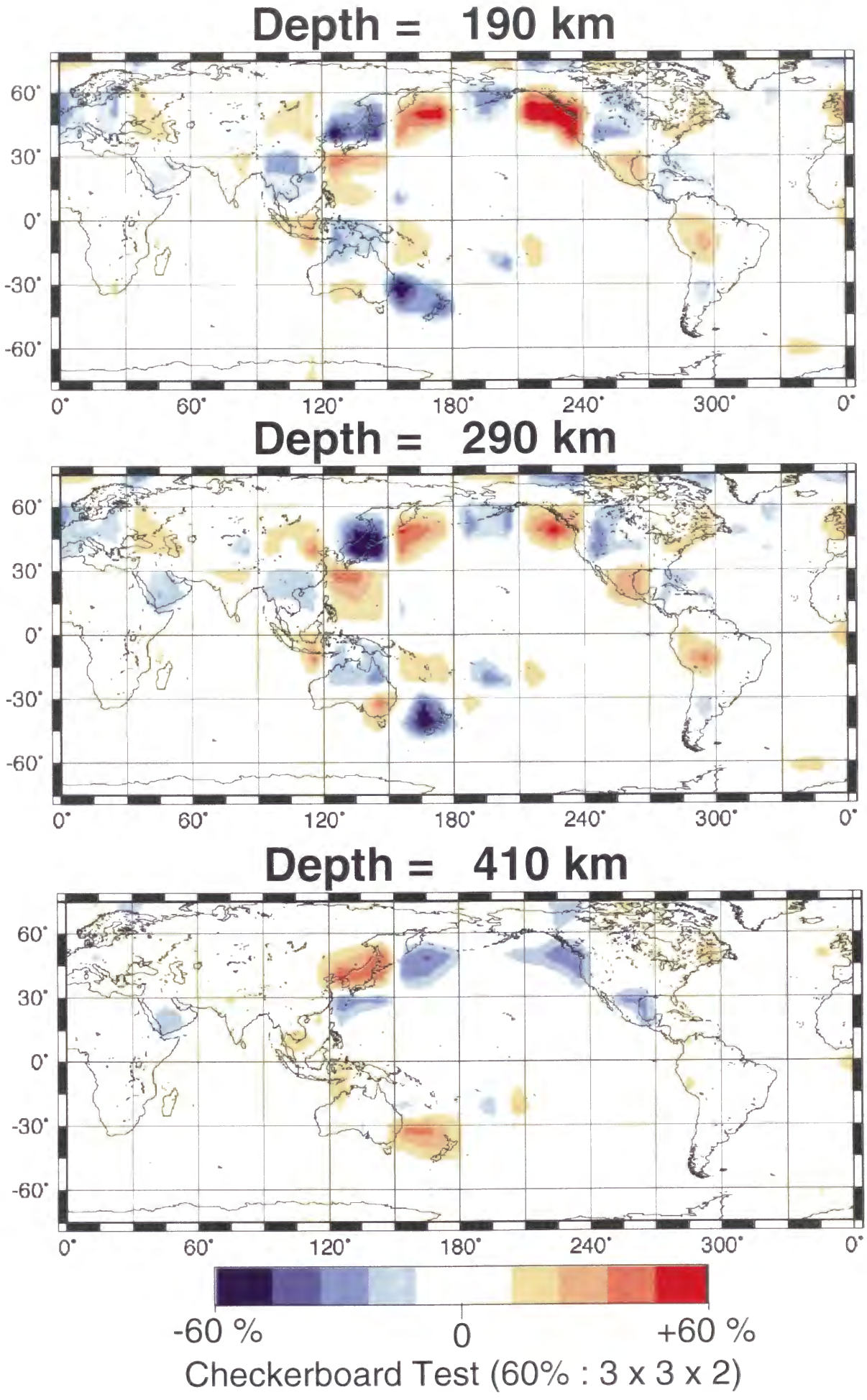

Figure 3.16 (2/5)

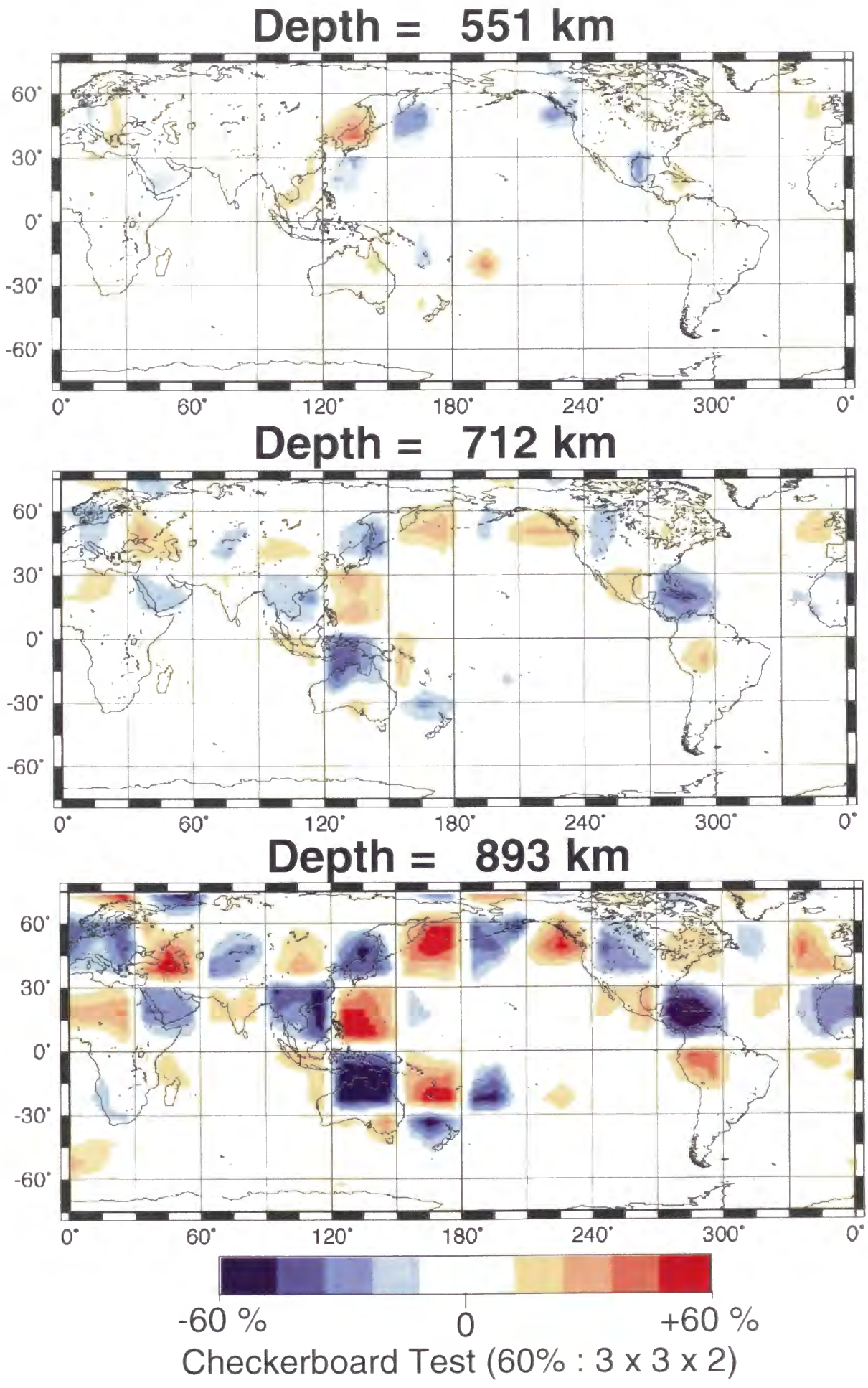

Figure 3.16 (3/5)

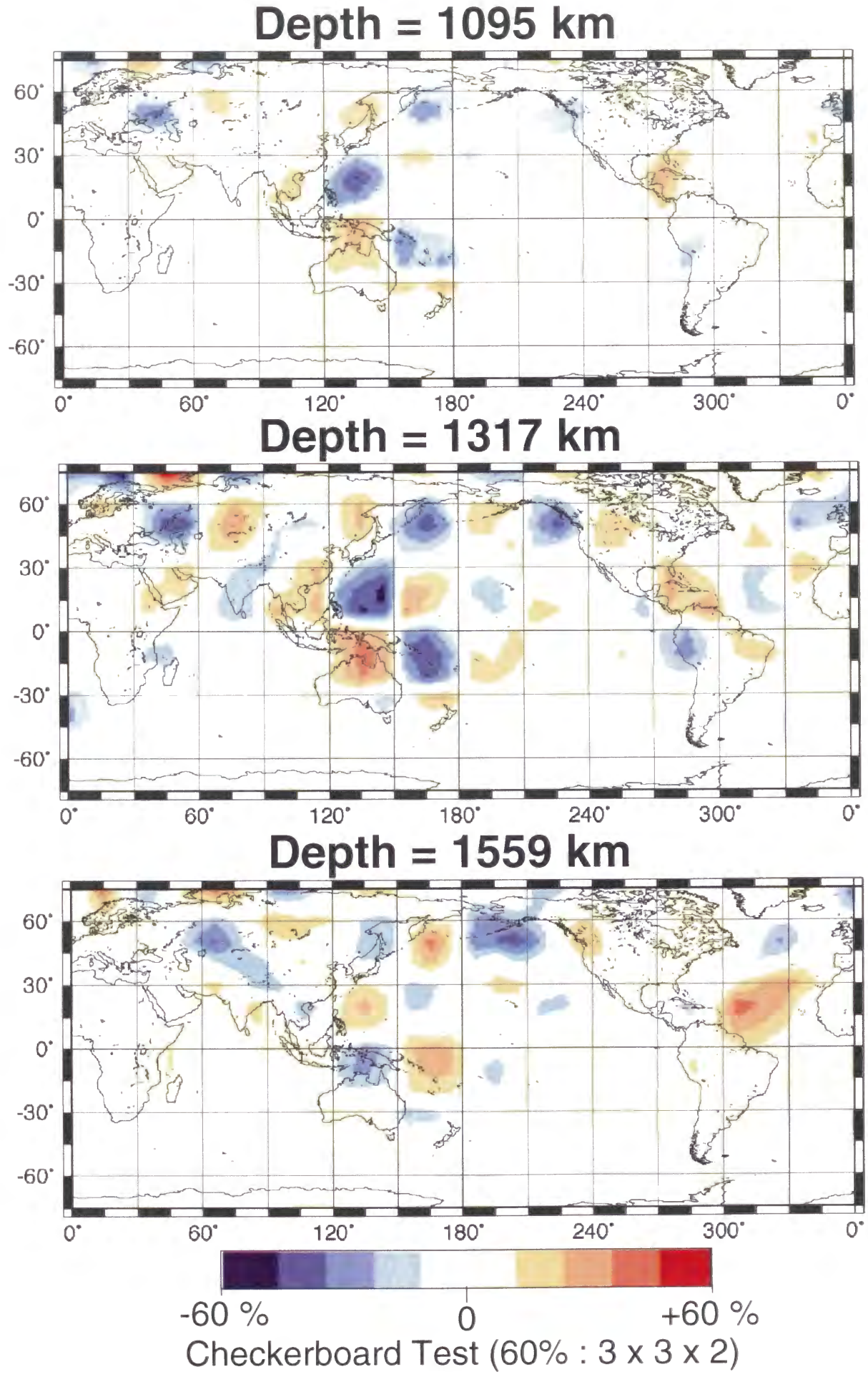

Figure 3.16 (4/5)

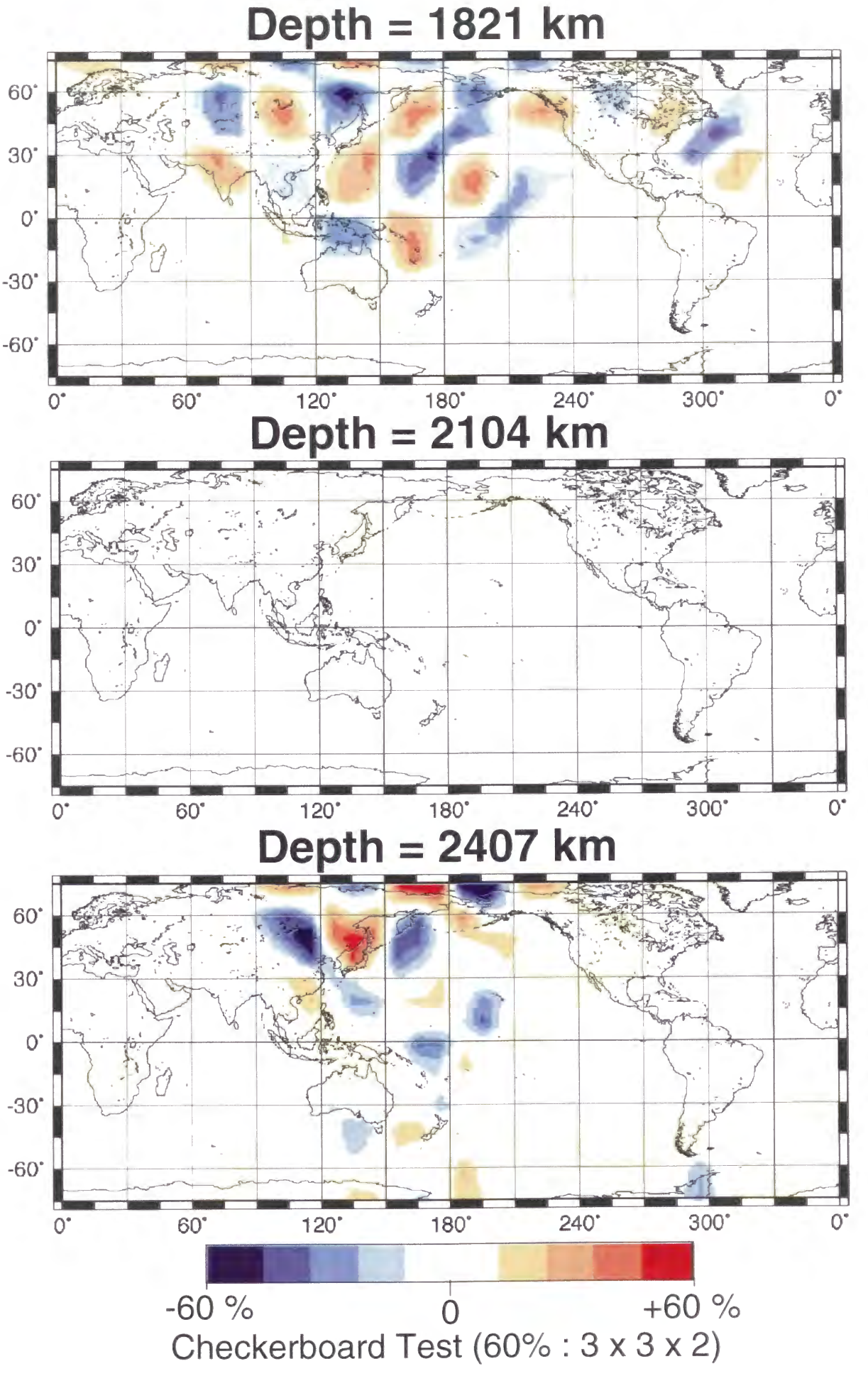

Figure 3.16 (5/5)

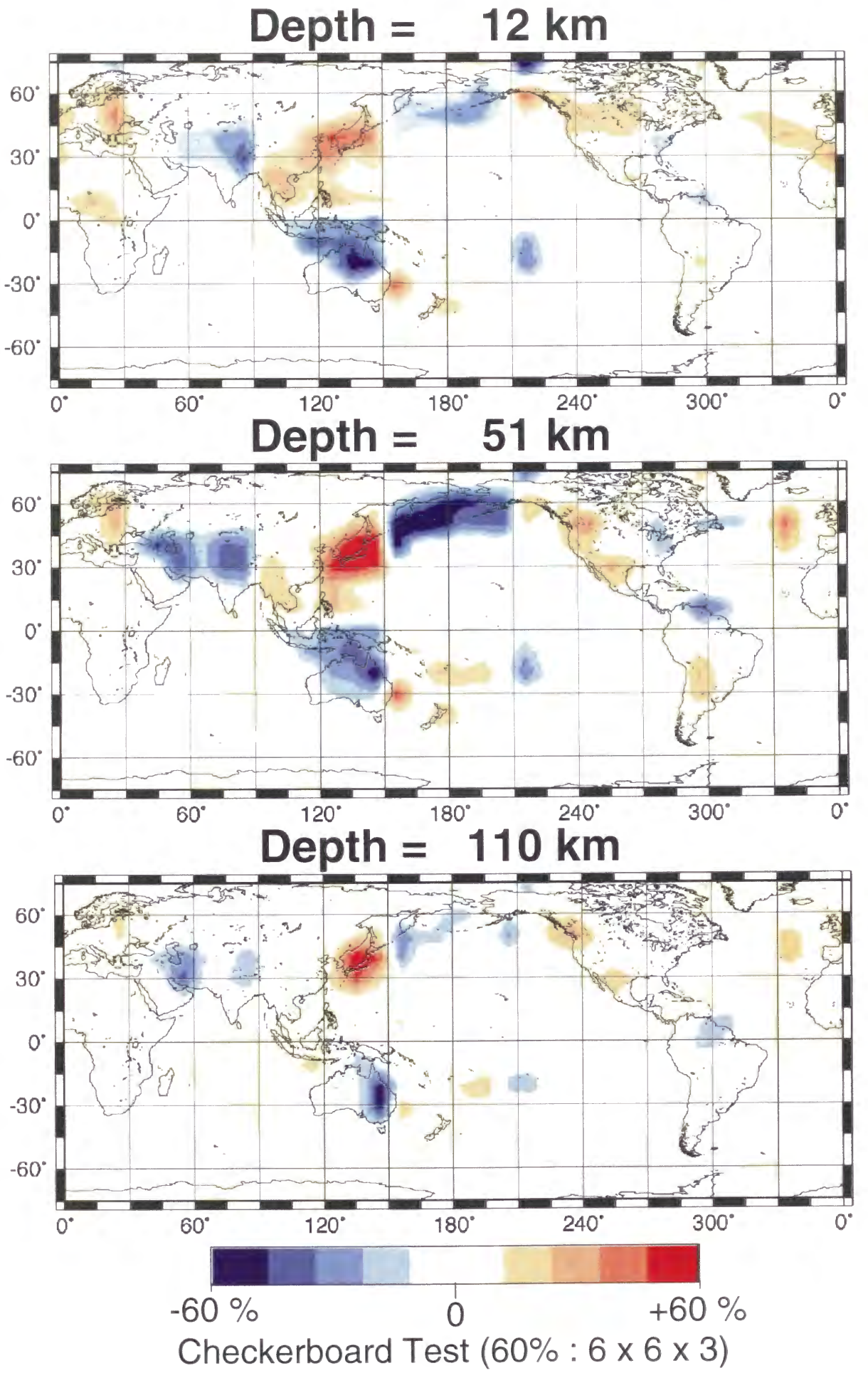

Figure 3.17 (1/5)

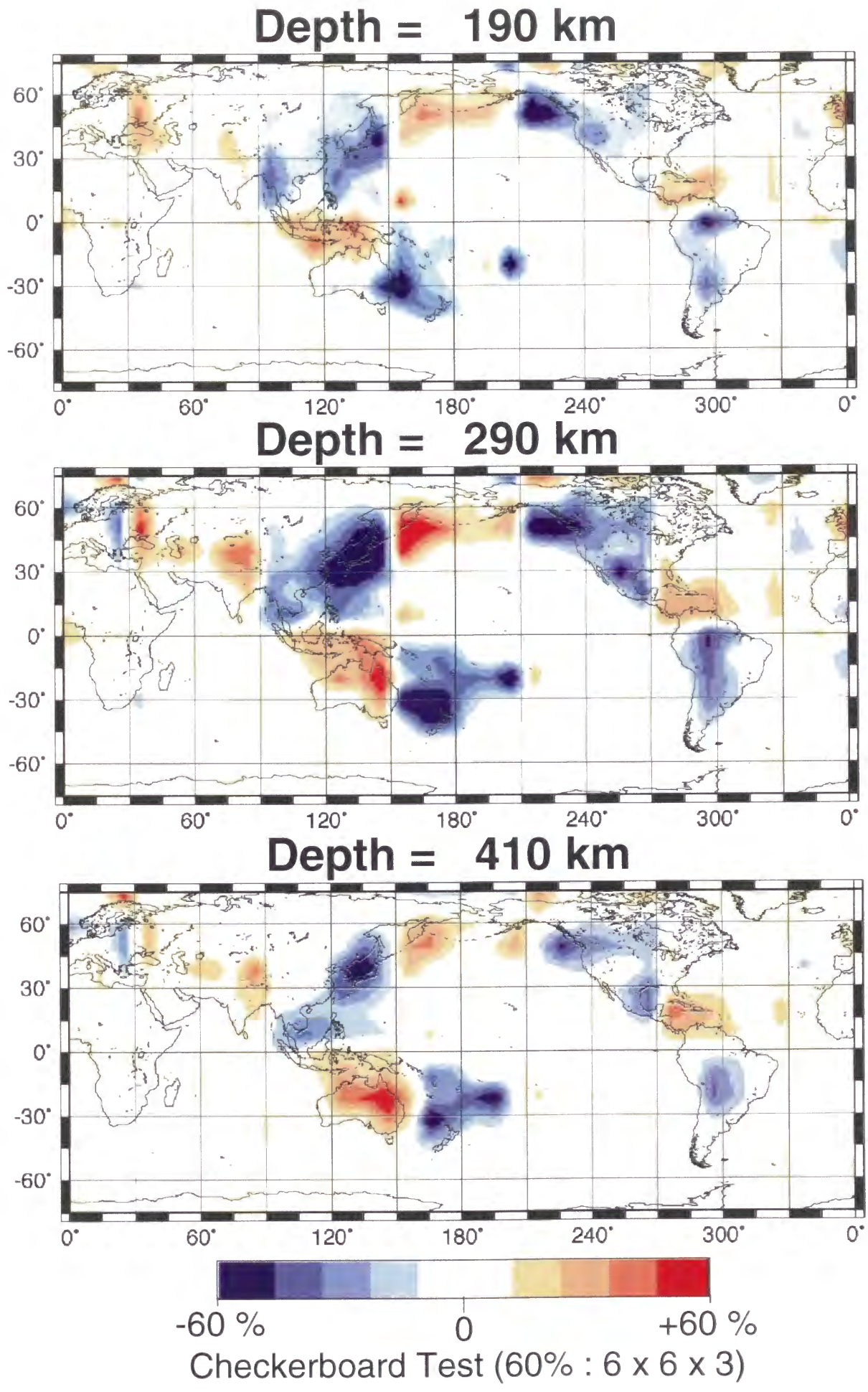

Figure 3.17 (2/5)

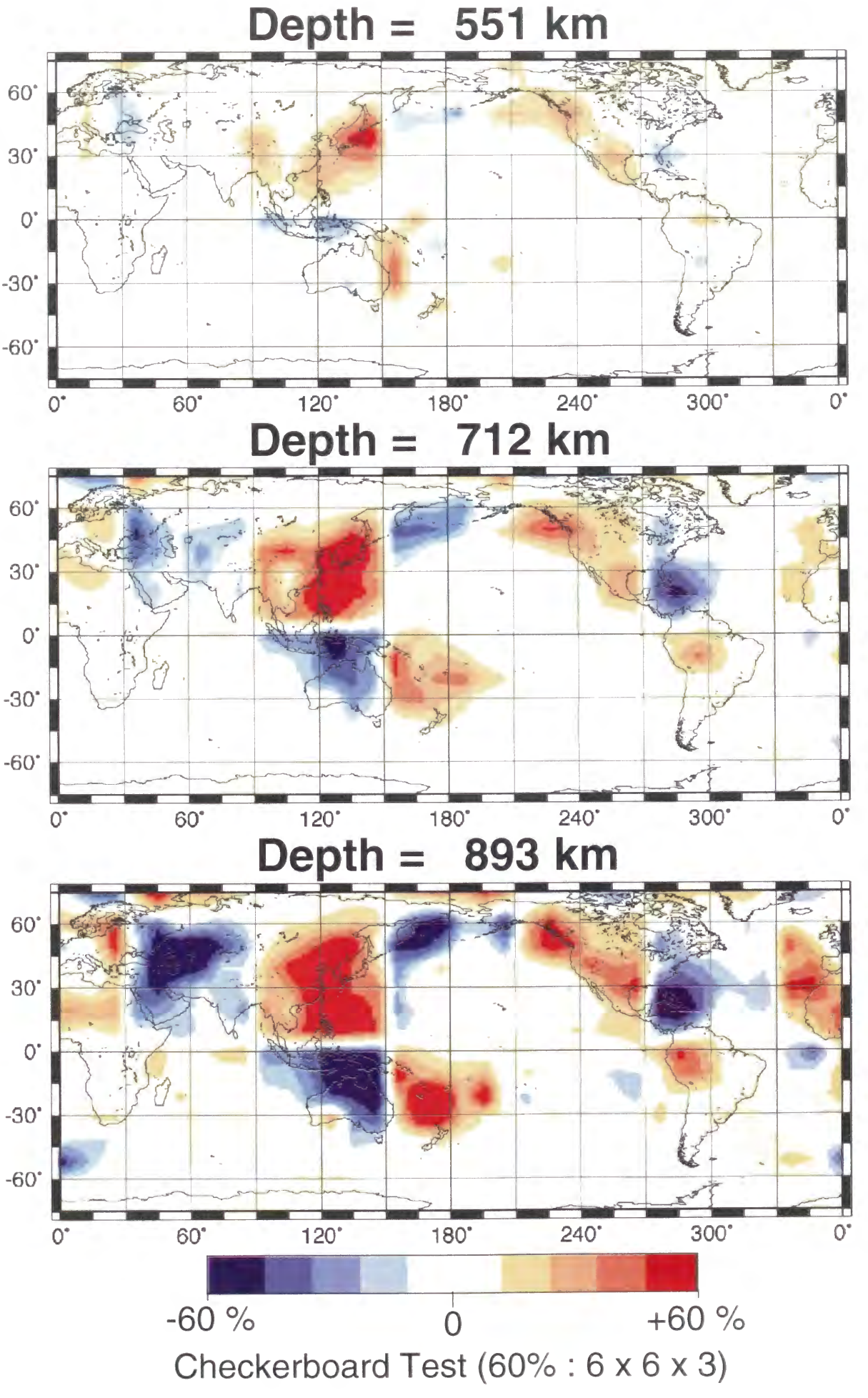

Figure 3.17 (3/5)

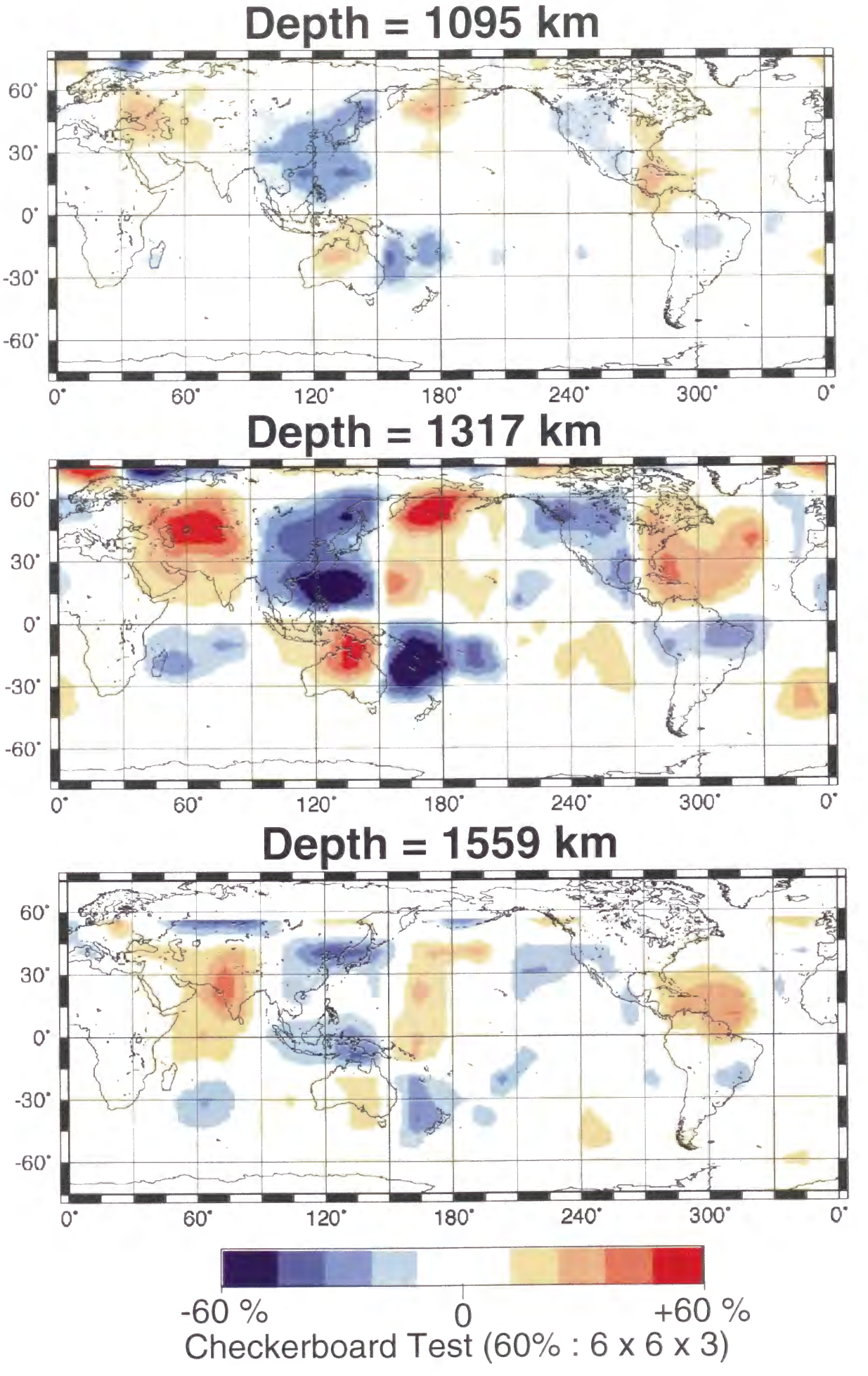

Figure 3.17 (4/5)

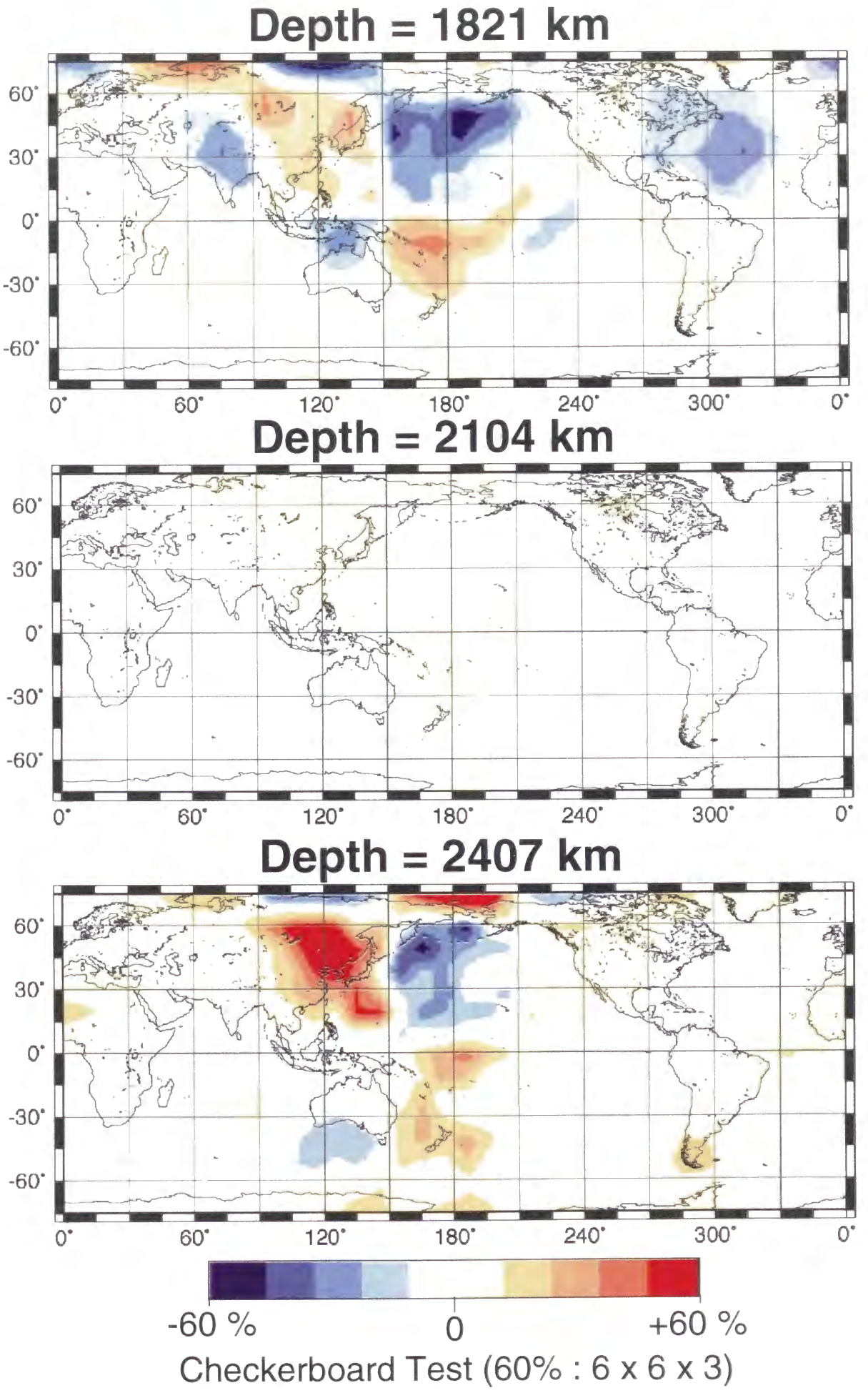

Figure 3.17 (5/5)

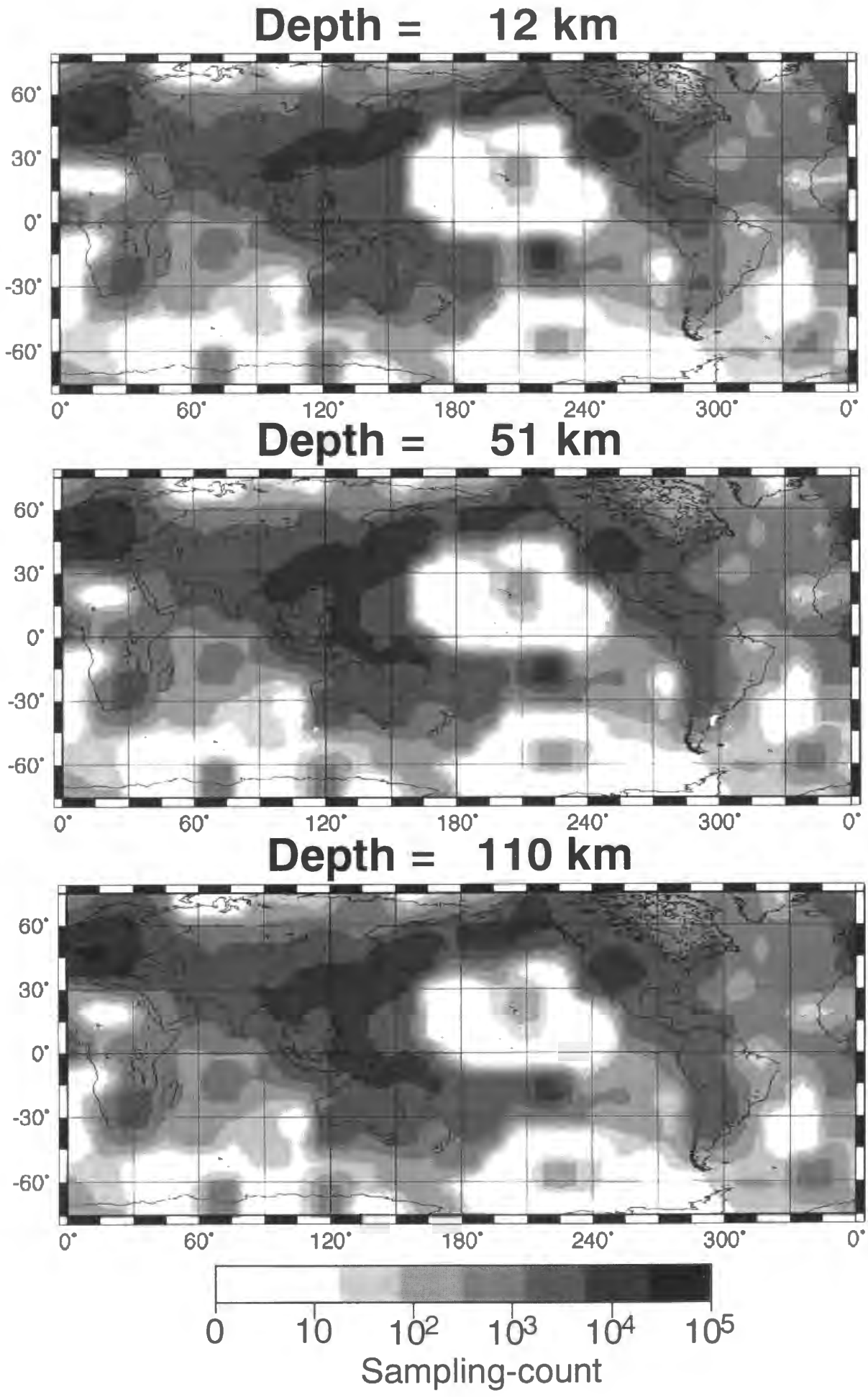

Figure 3.18(1/5)

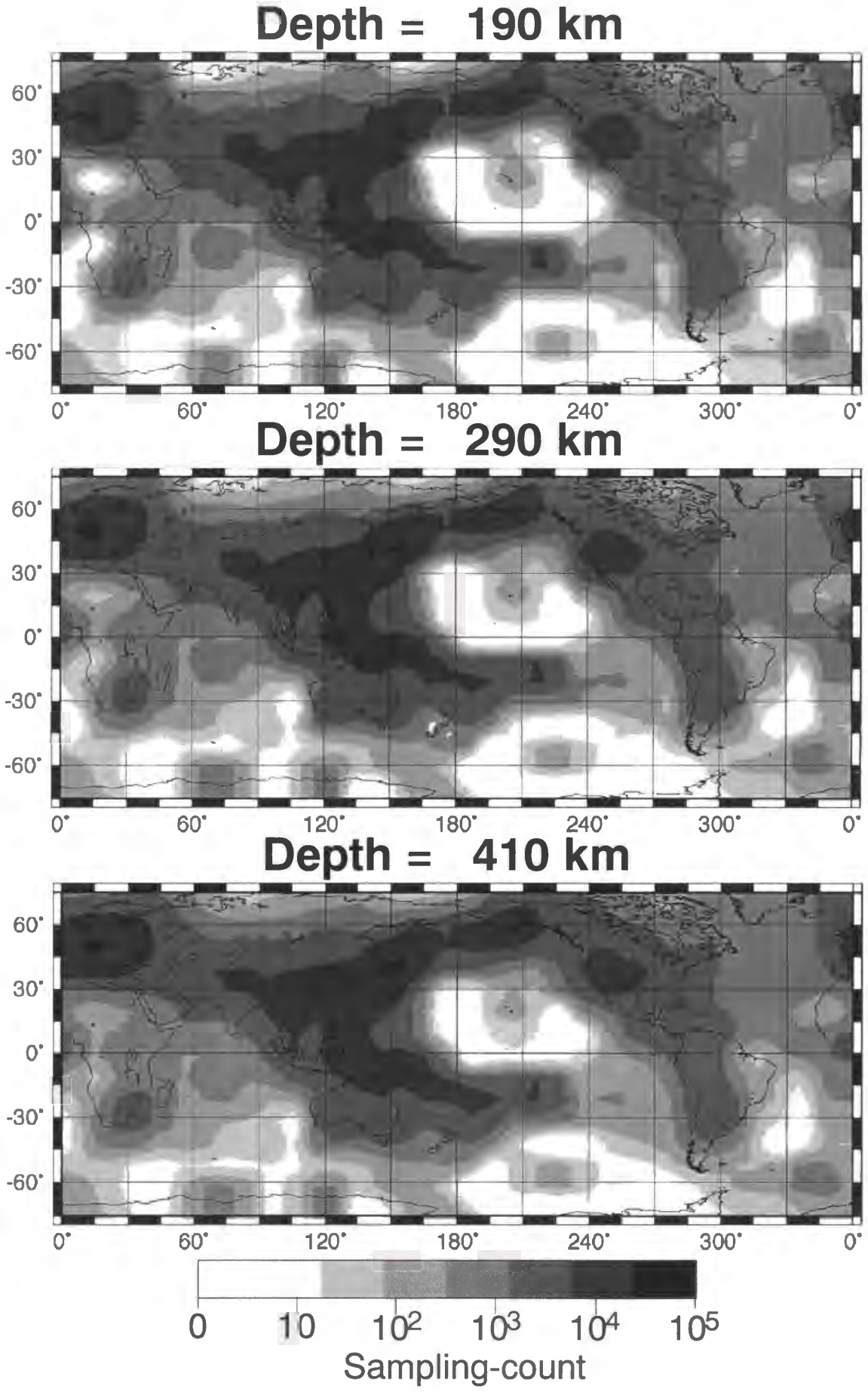

Figure 3.18(2/5)

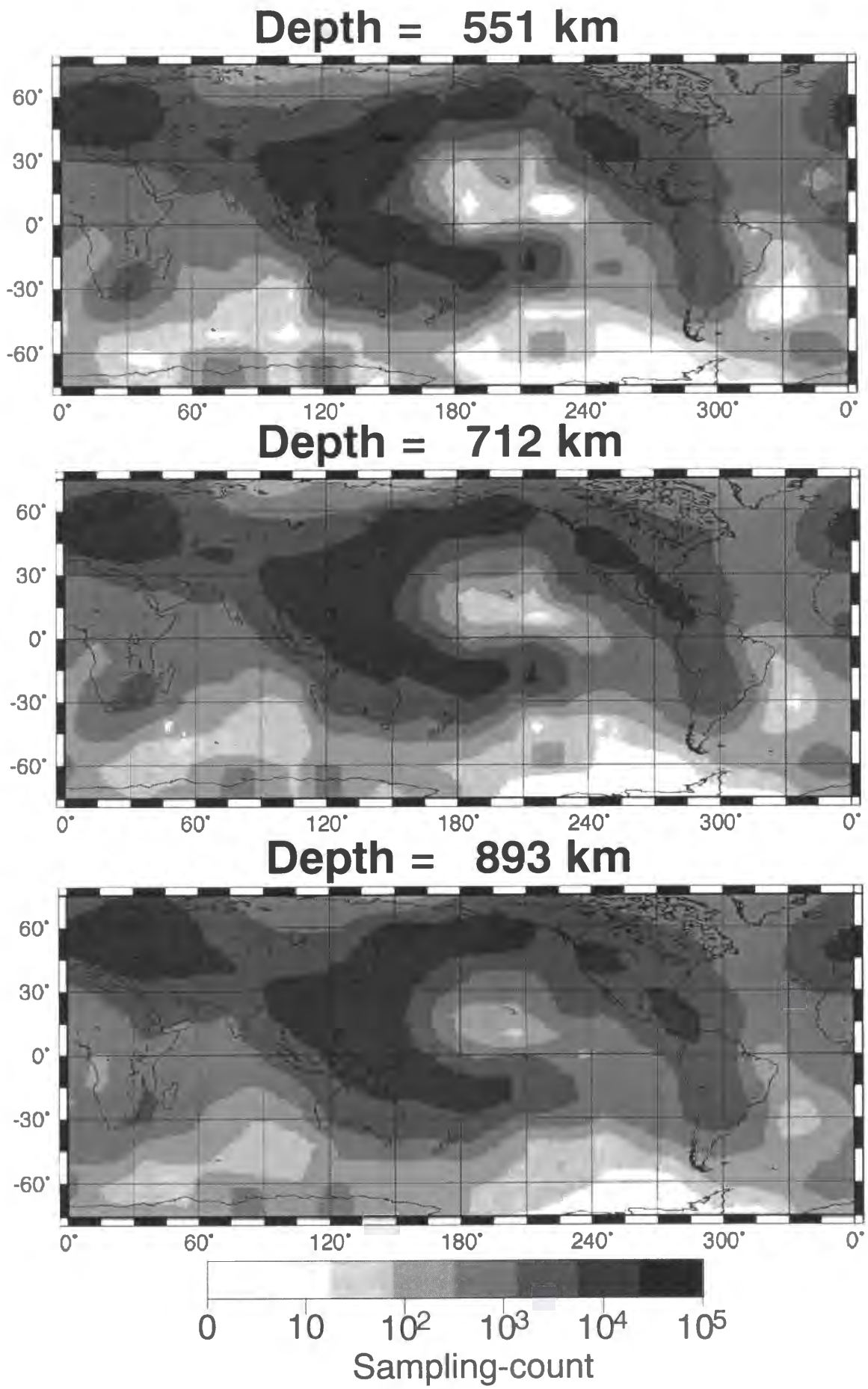

Figure 3.18(3/5)

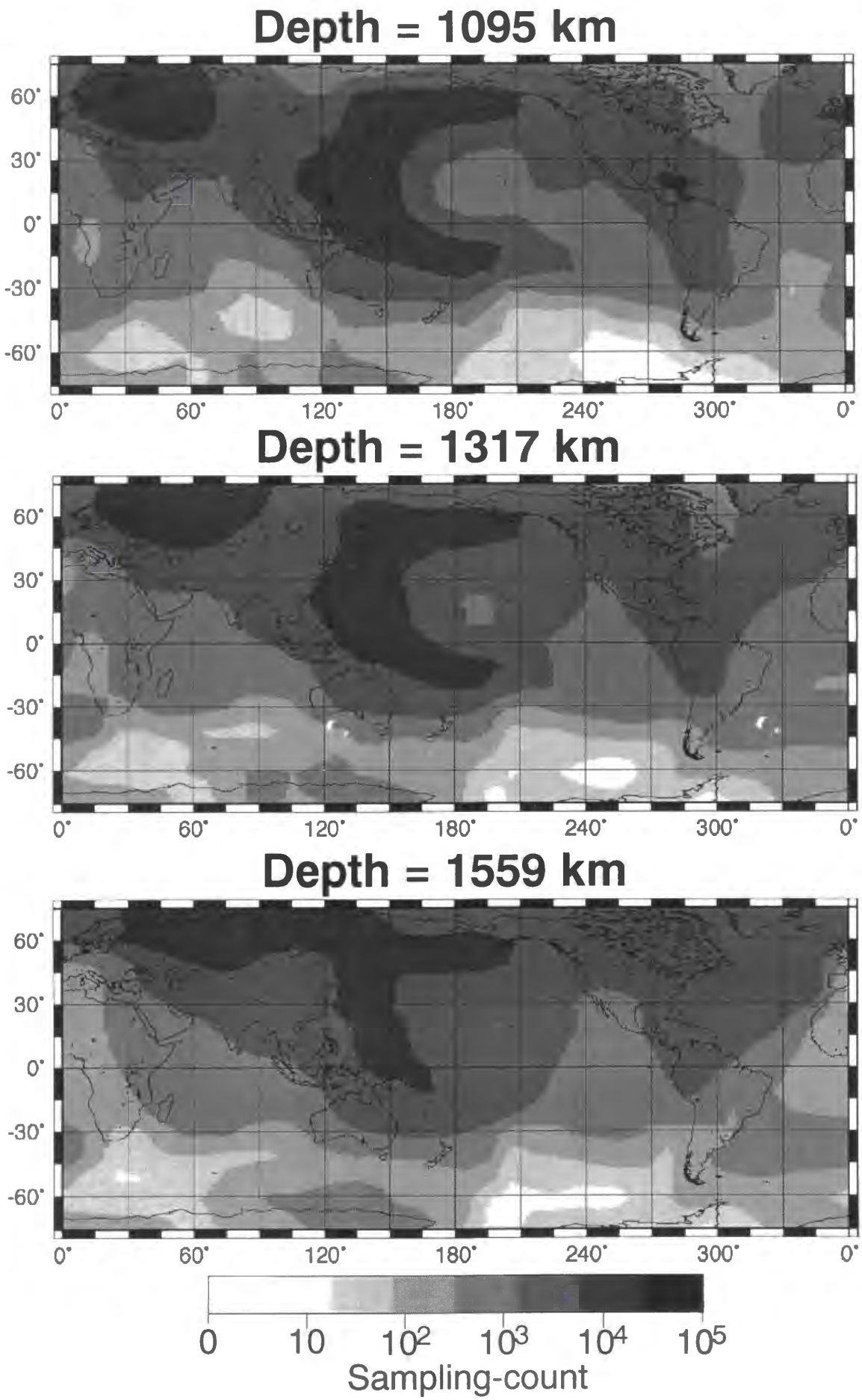

Figure 3.18(4/5)

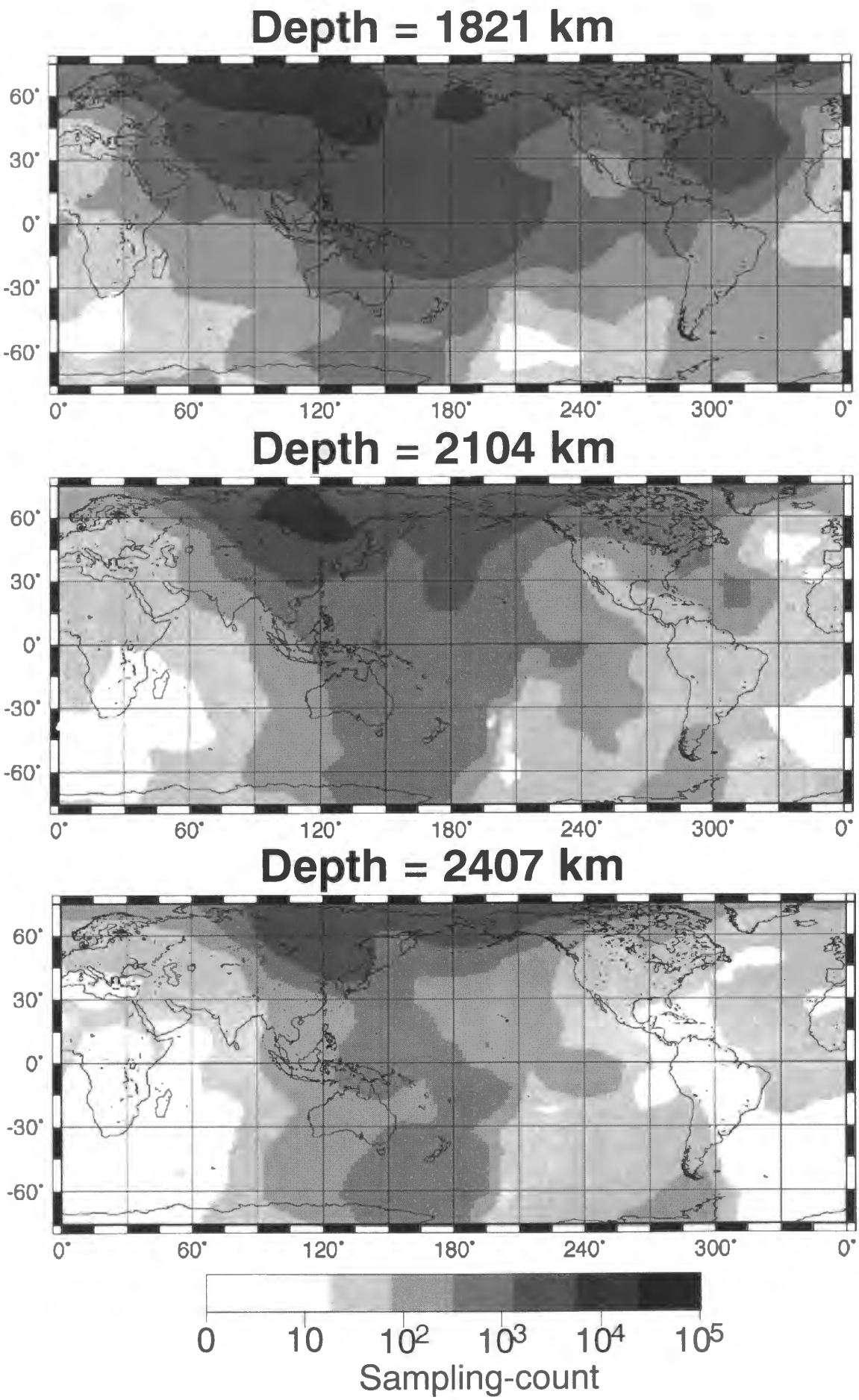

Figure 3.18(5/5)

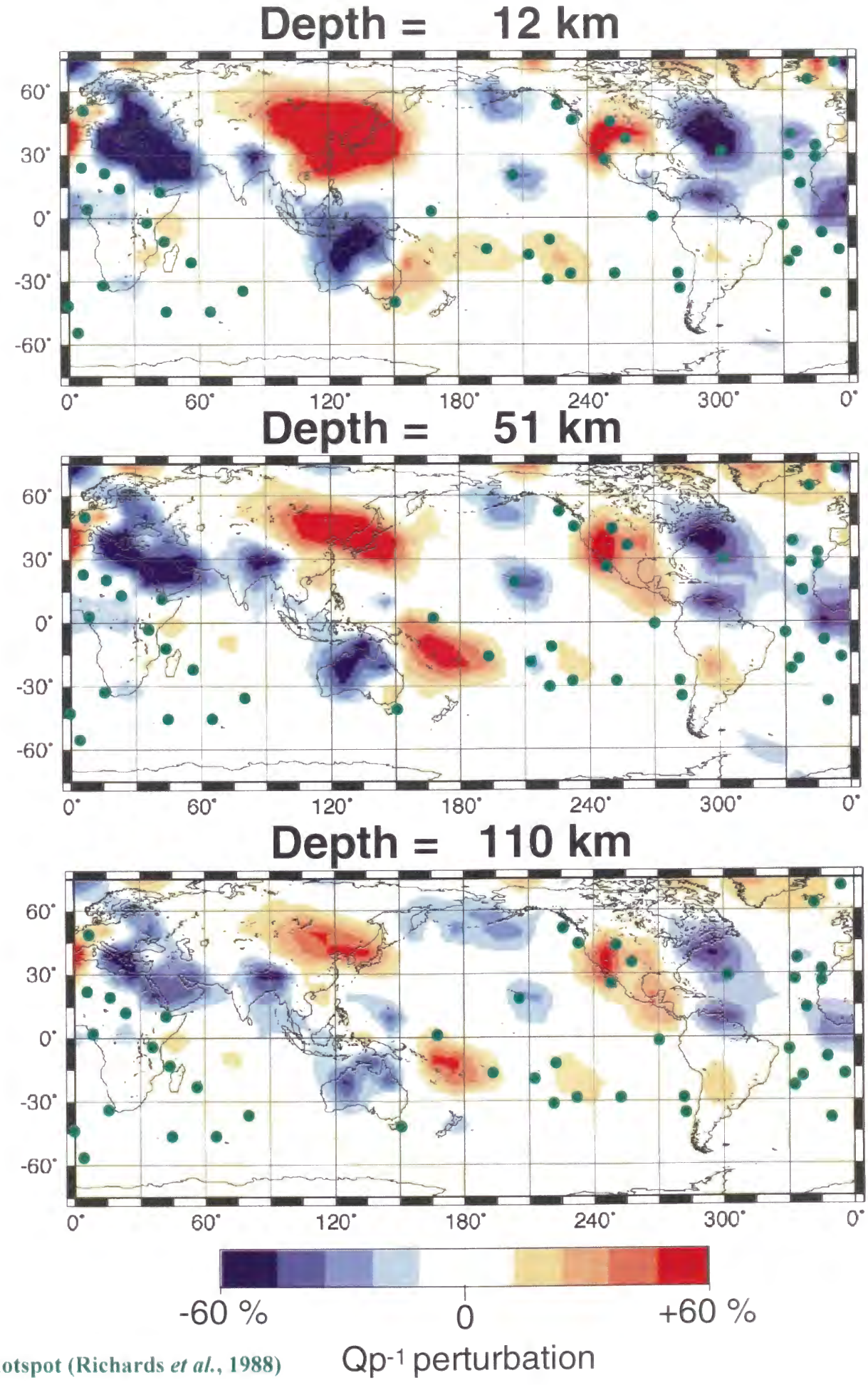

Figure 3.19(1/5)

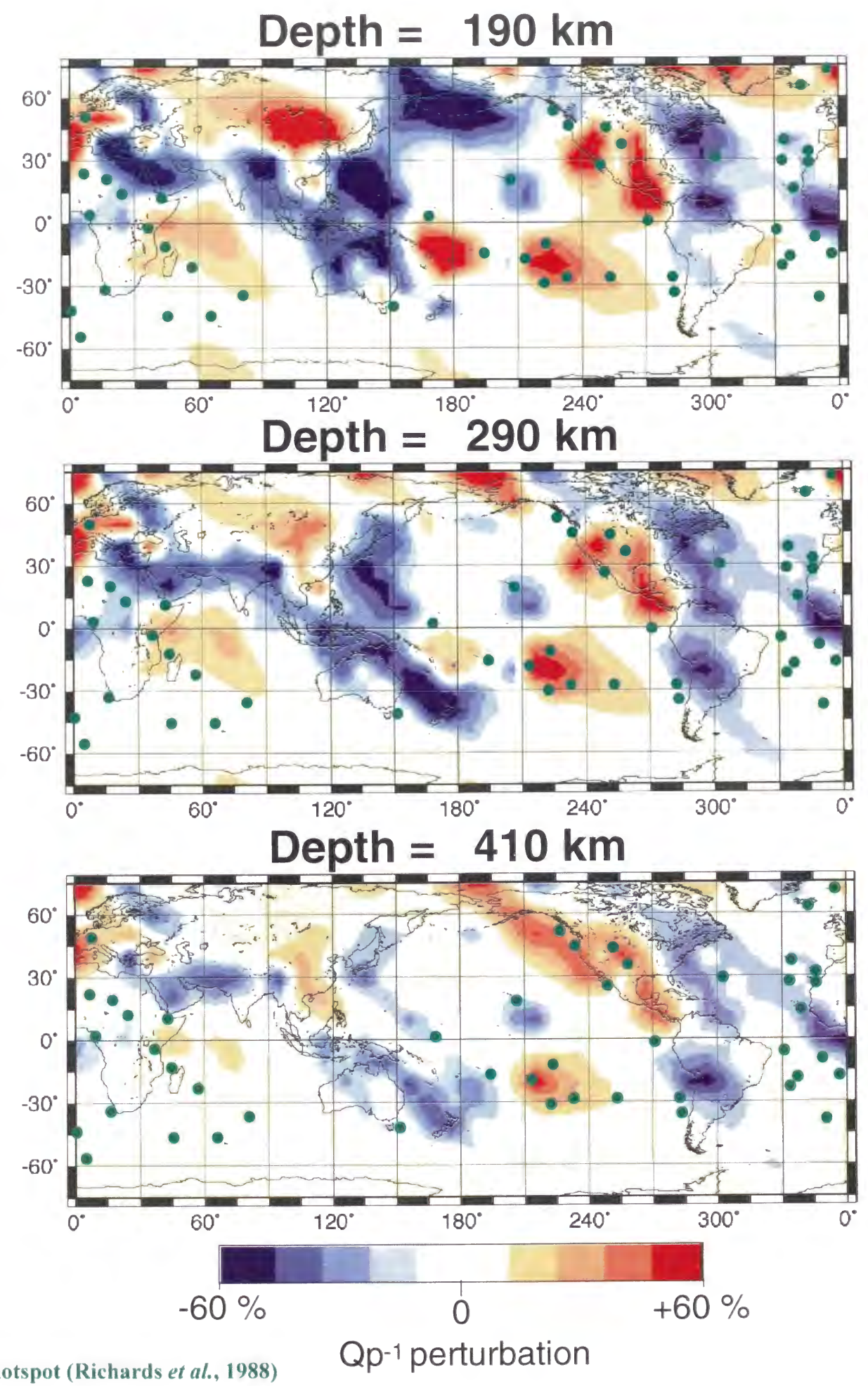

Figure 3.19(2/5)

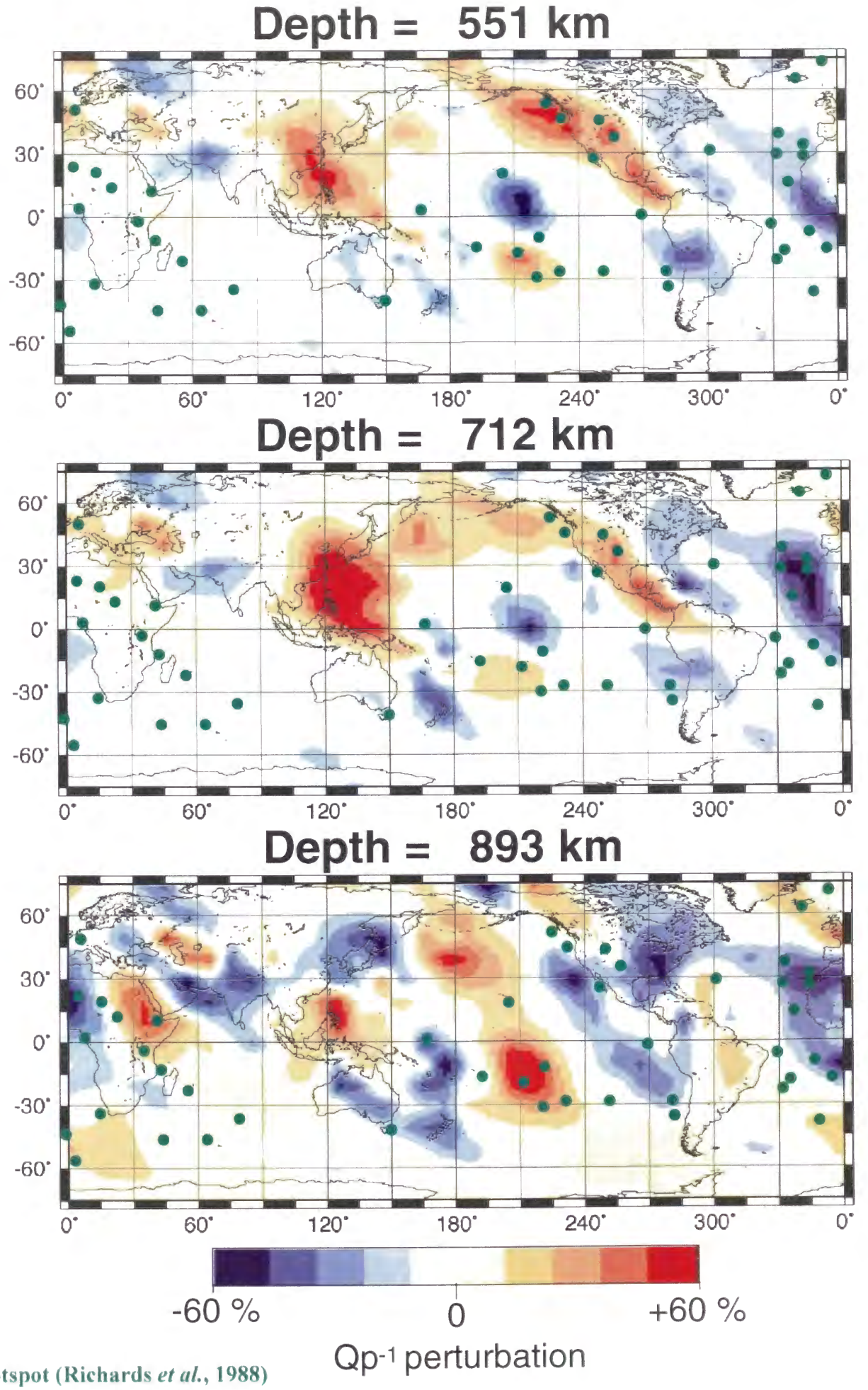

Figure 3.19(3/5)

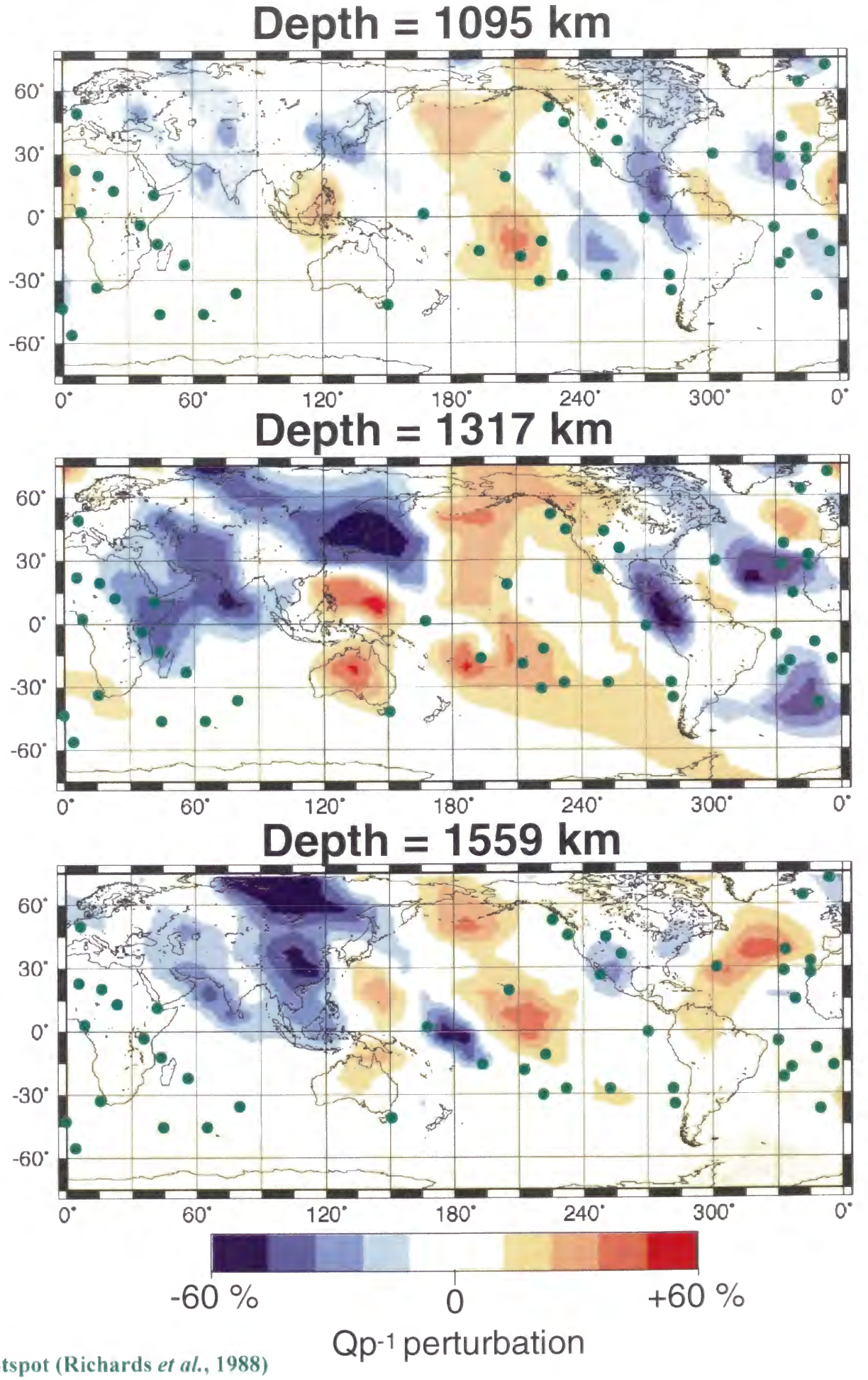

Figure 3.19(4/5)

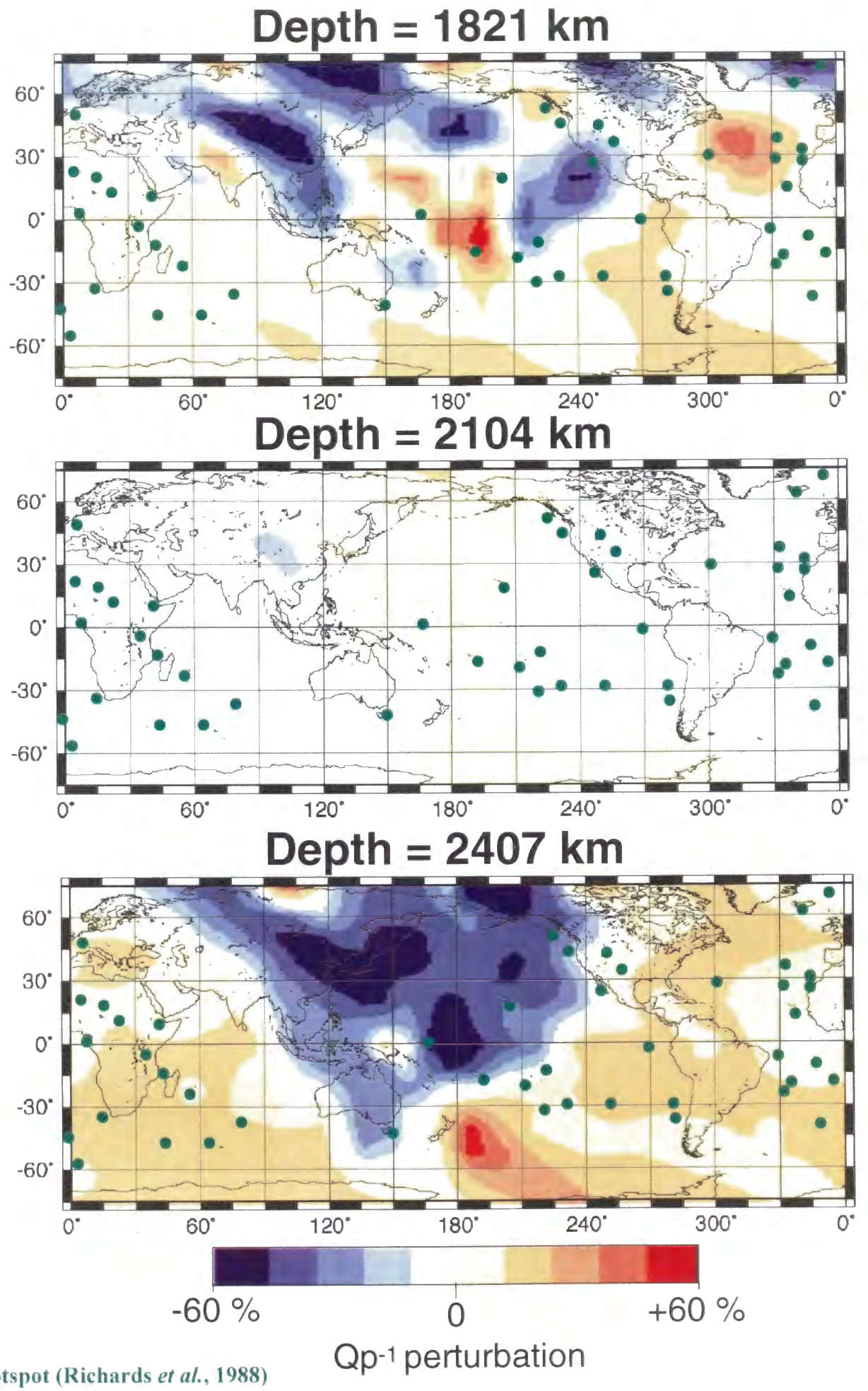

Figure 3.19(5/5)

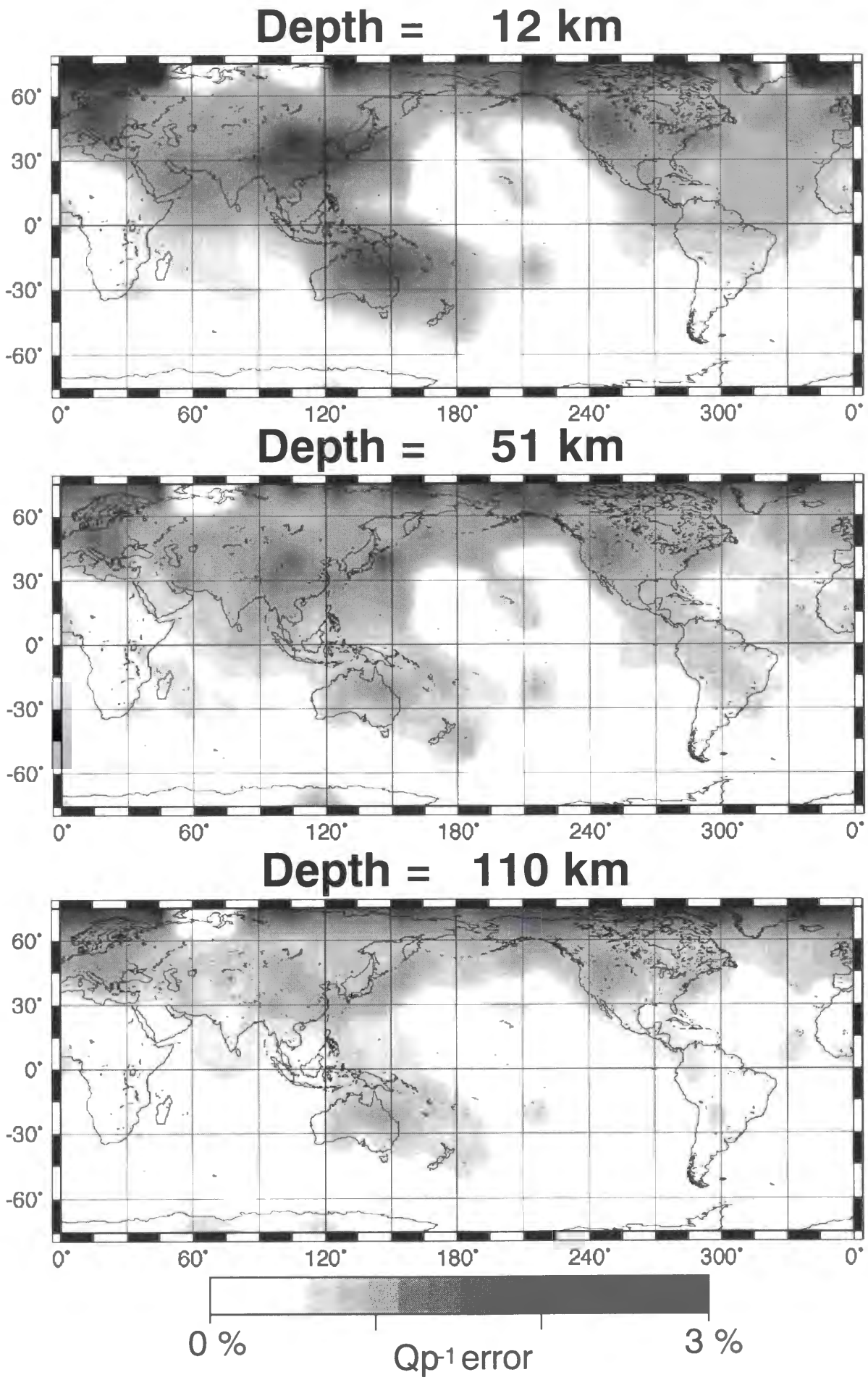

Figure 3.20 (1/5)

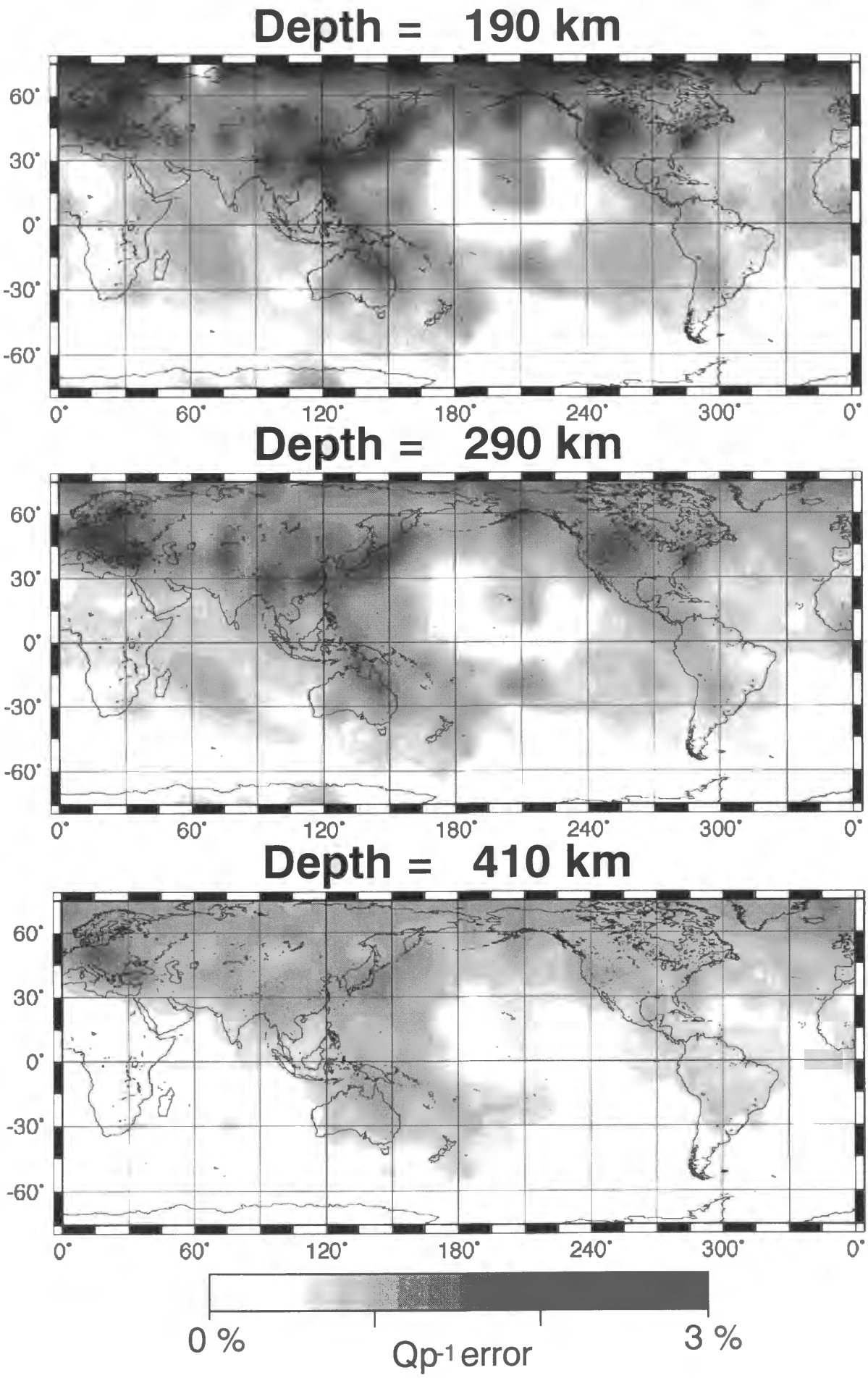

Figure 3.20 (2/5)

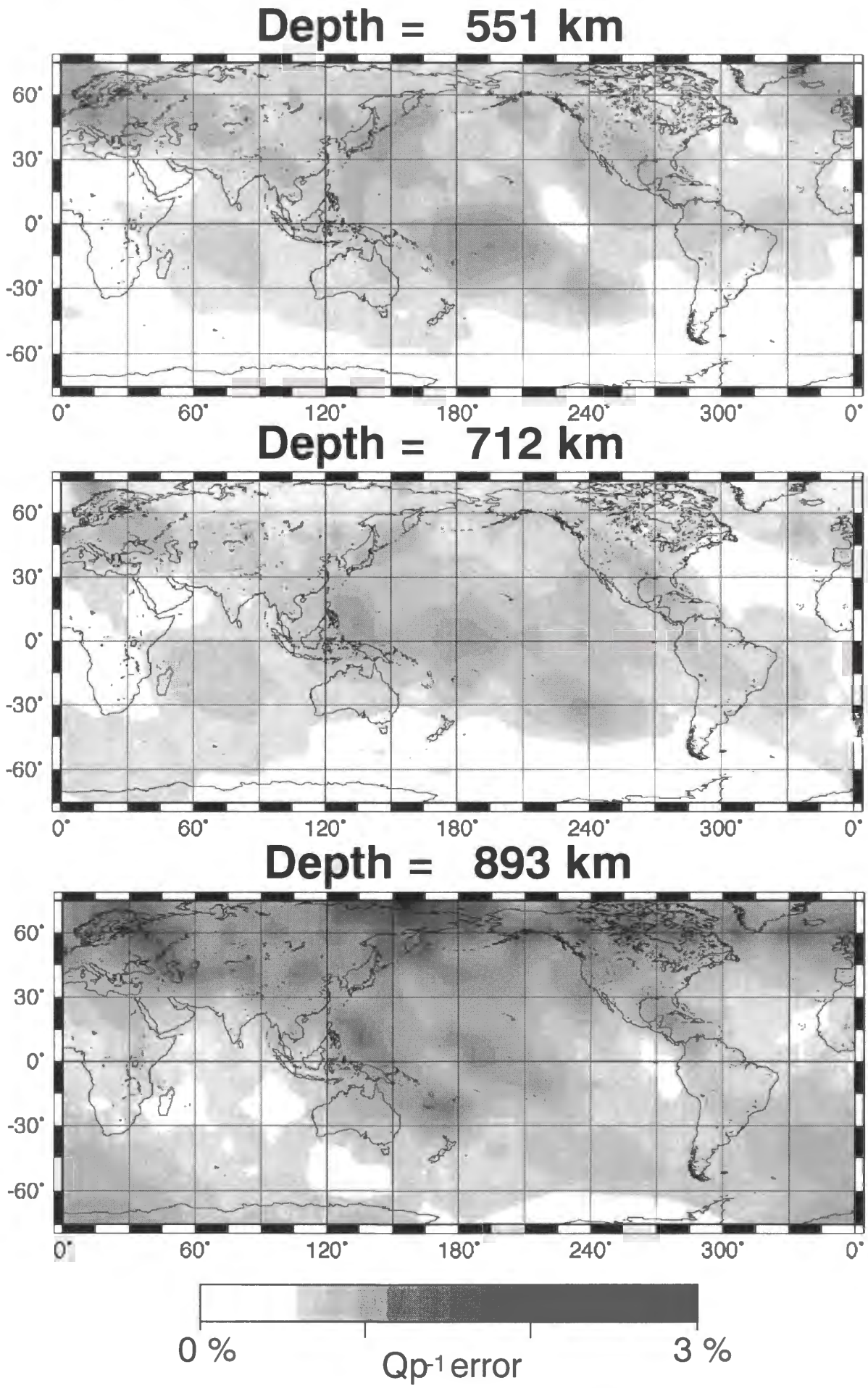

Figure 3.20 (3/5)

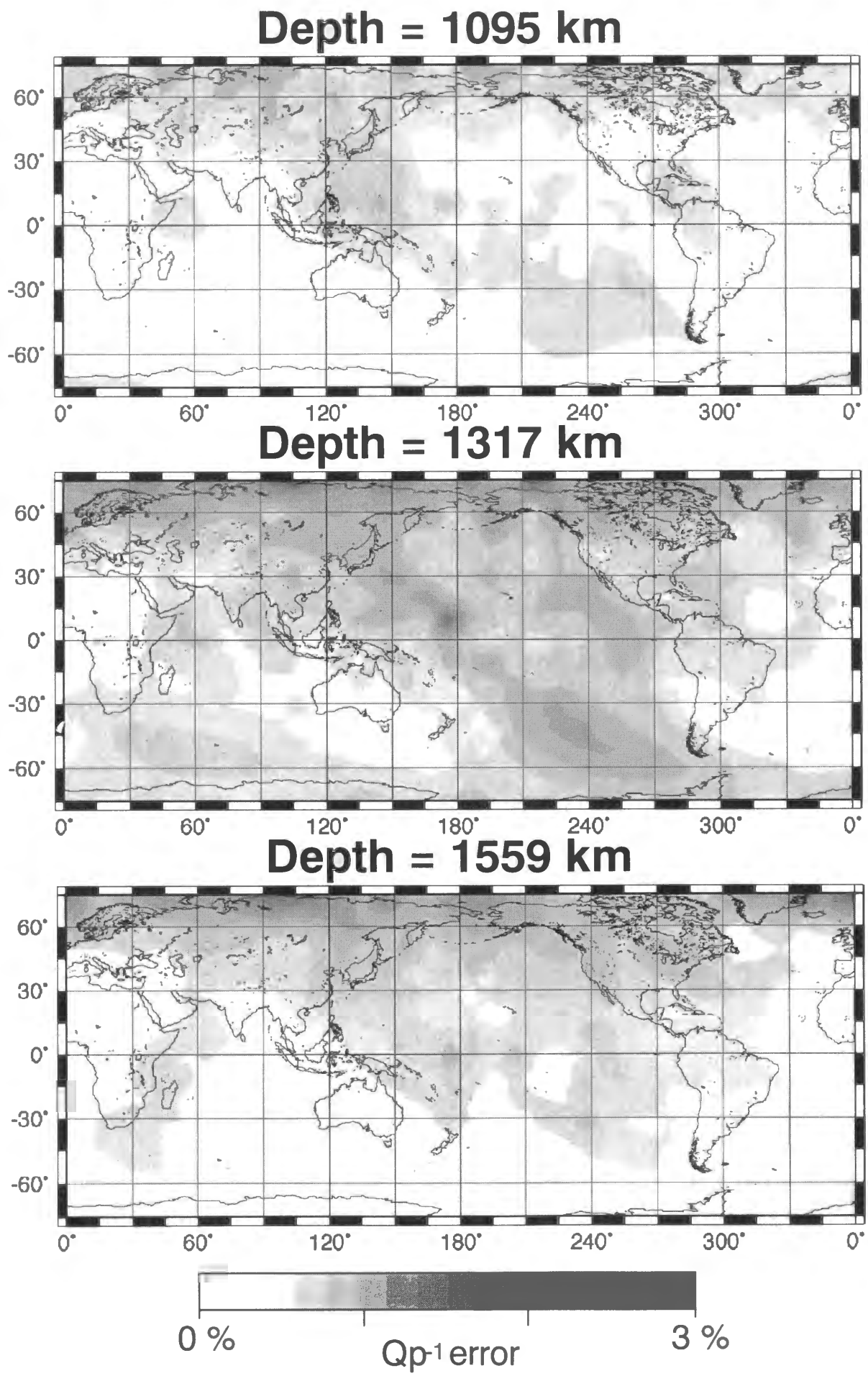

Figure 3.20 (4/5)

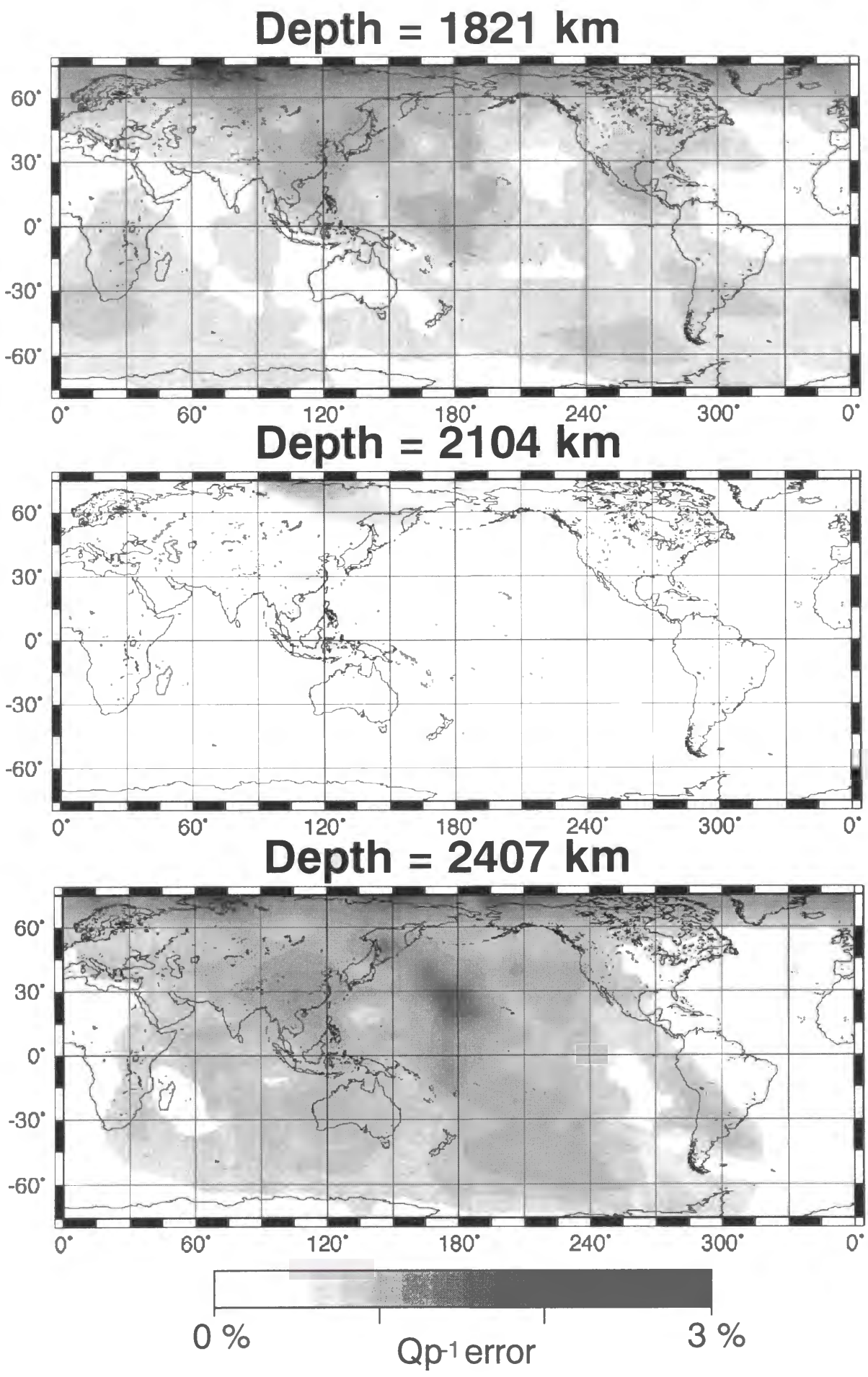

Figure 3.20 (5/5)

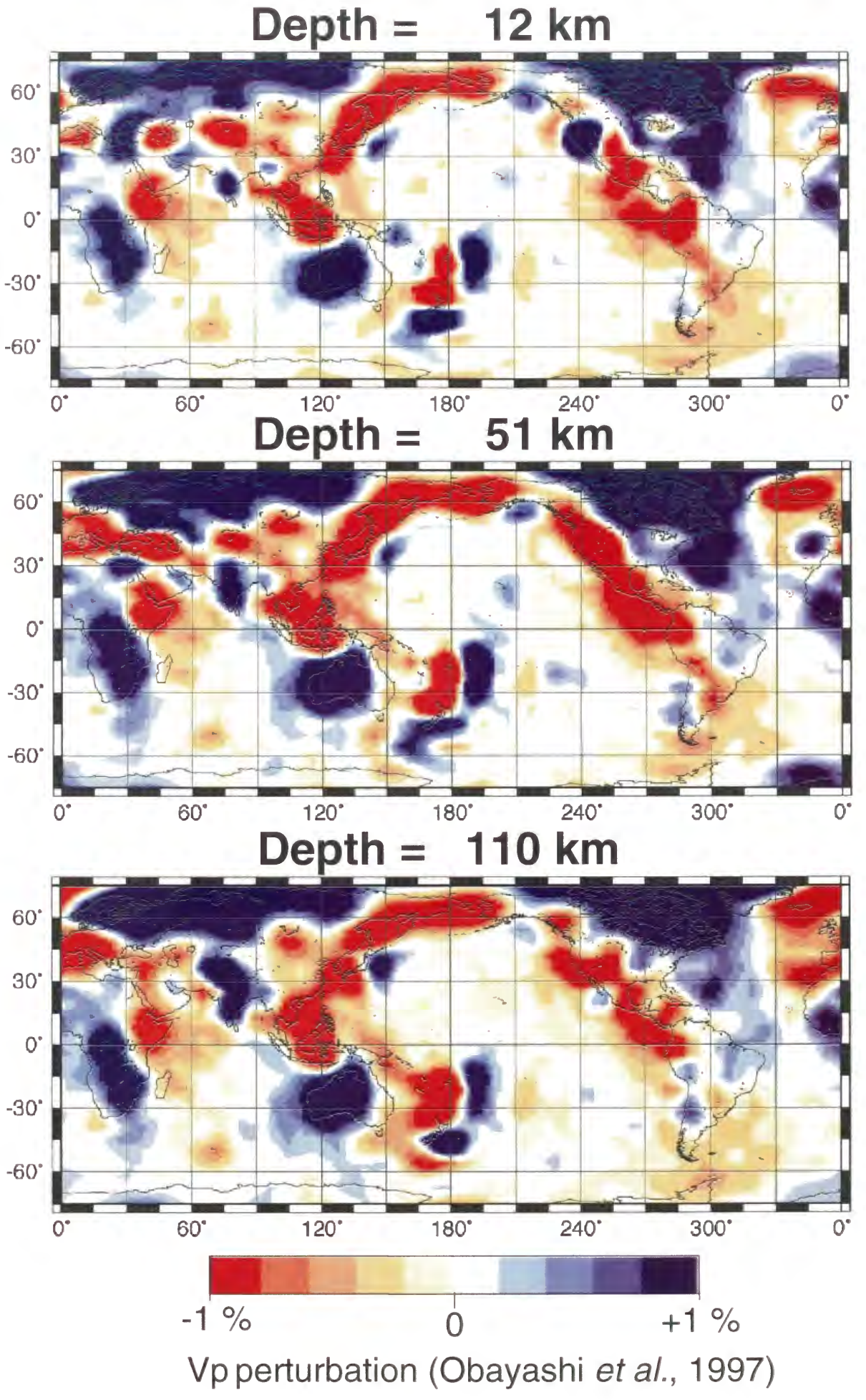

Figure 3.21 (1/5)

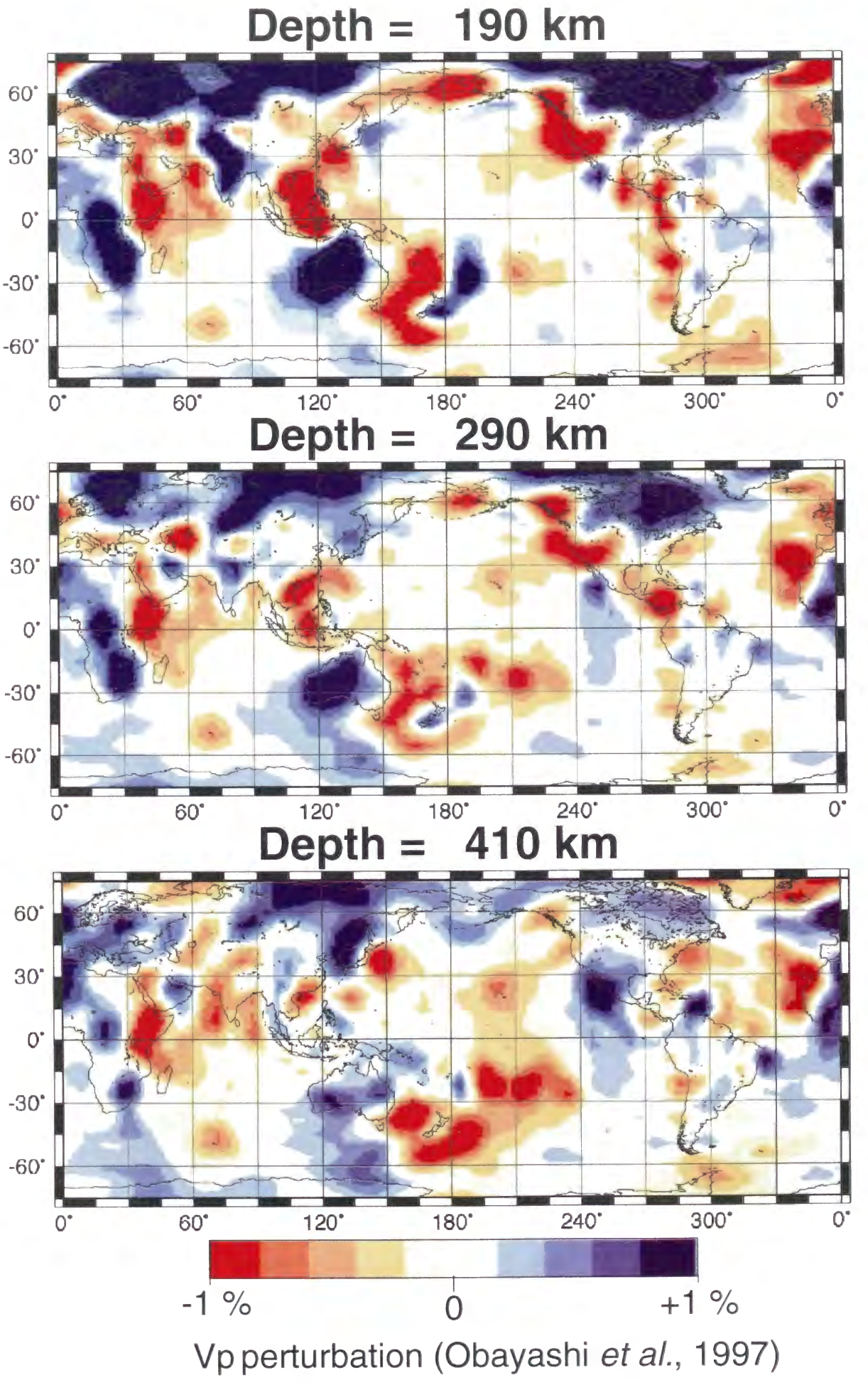

Figure 3.21 (2/5)

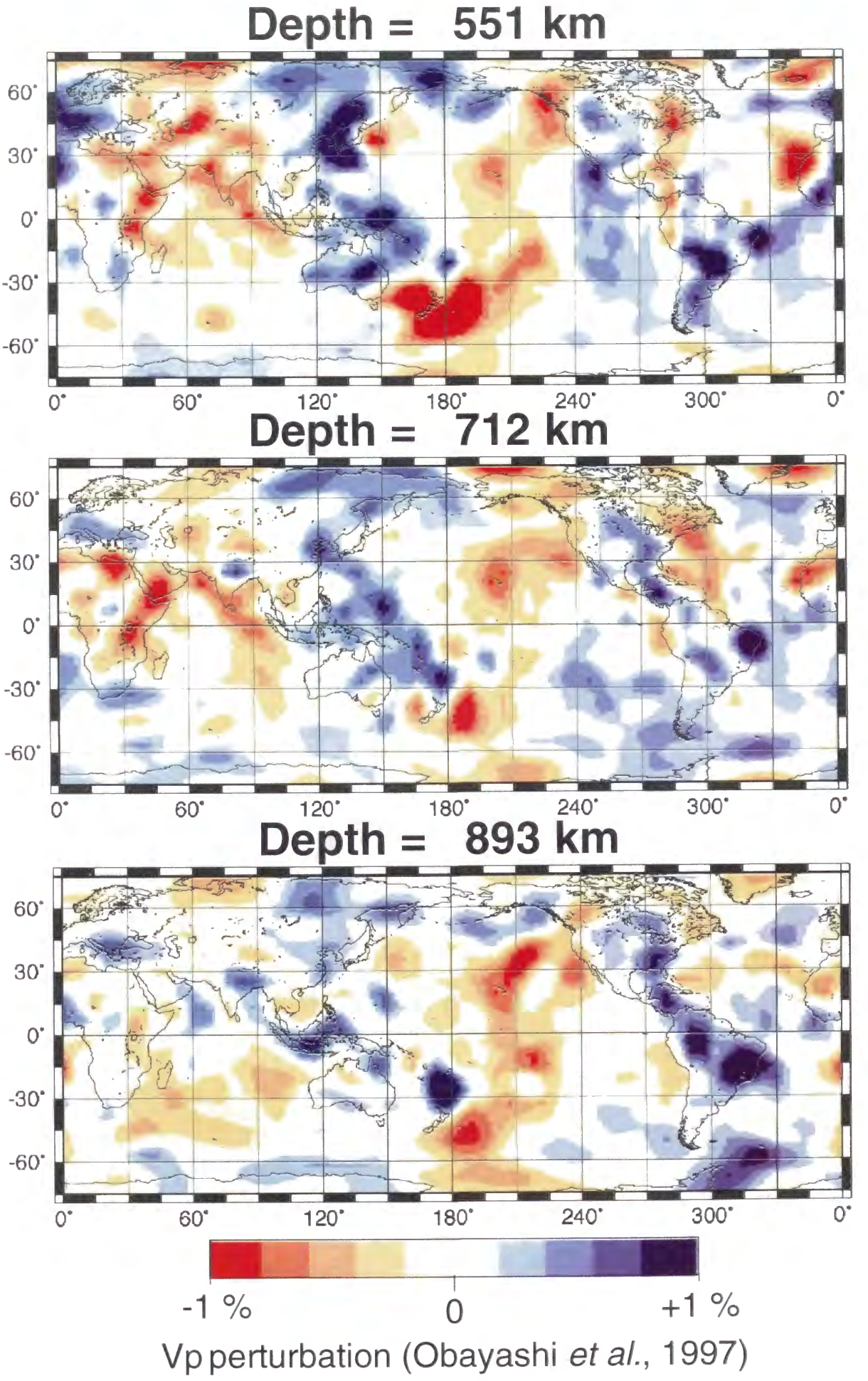

Figure 3.21 (3/5)

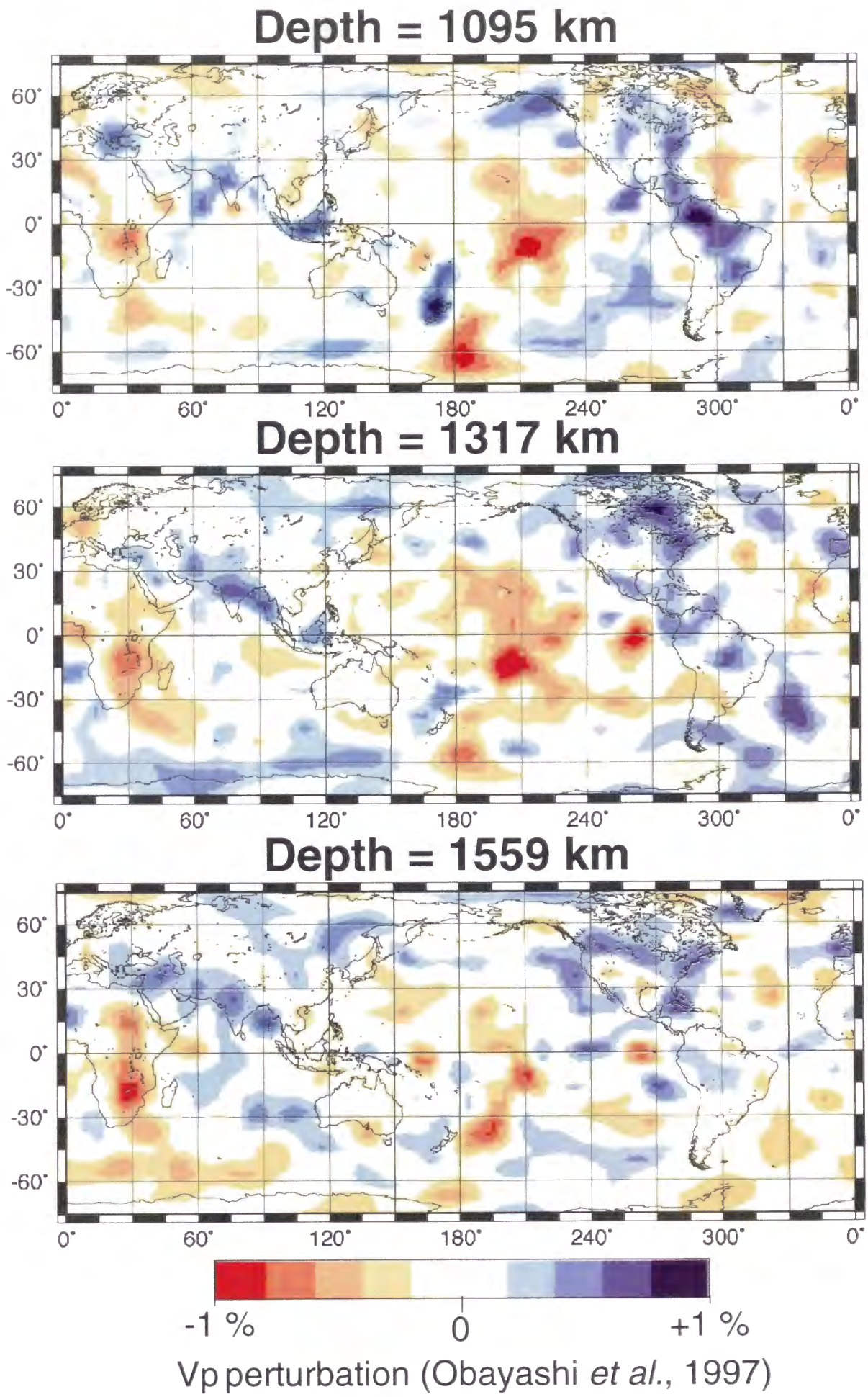

Figure 3.21 (4/5)

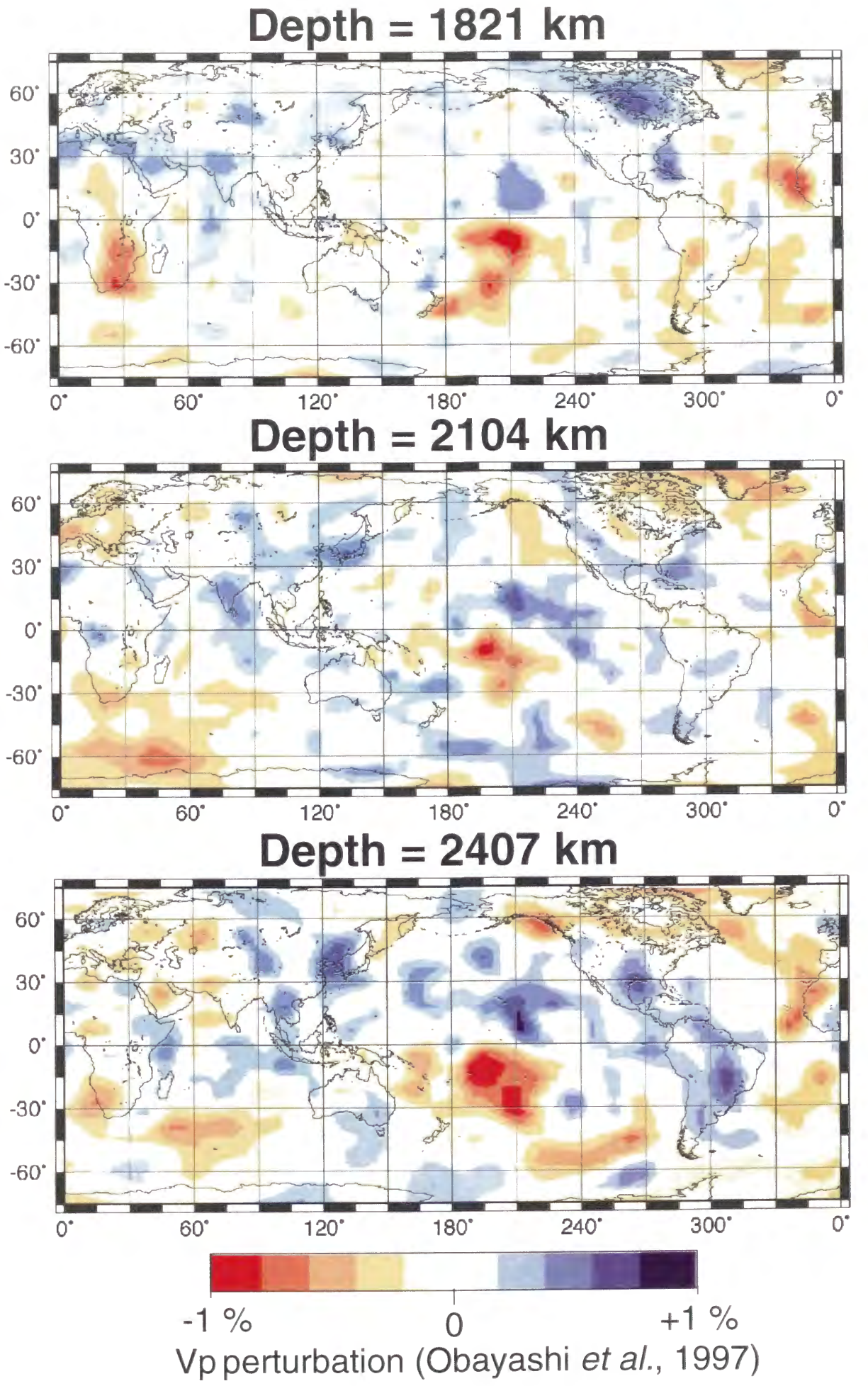

Figure 3.21 (5/5)

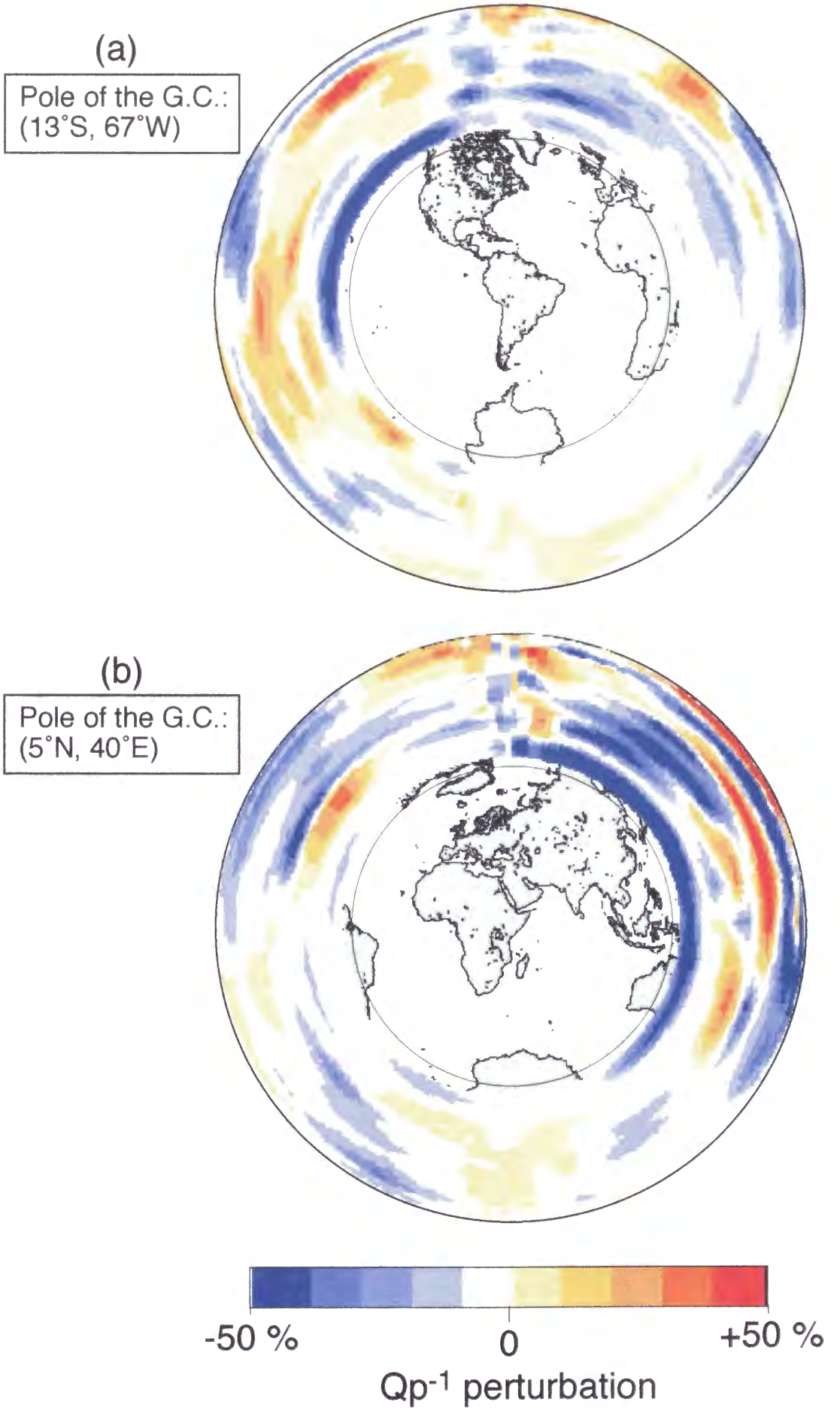

Figure 3.22 (1/4)

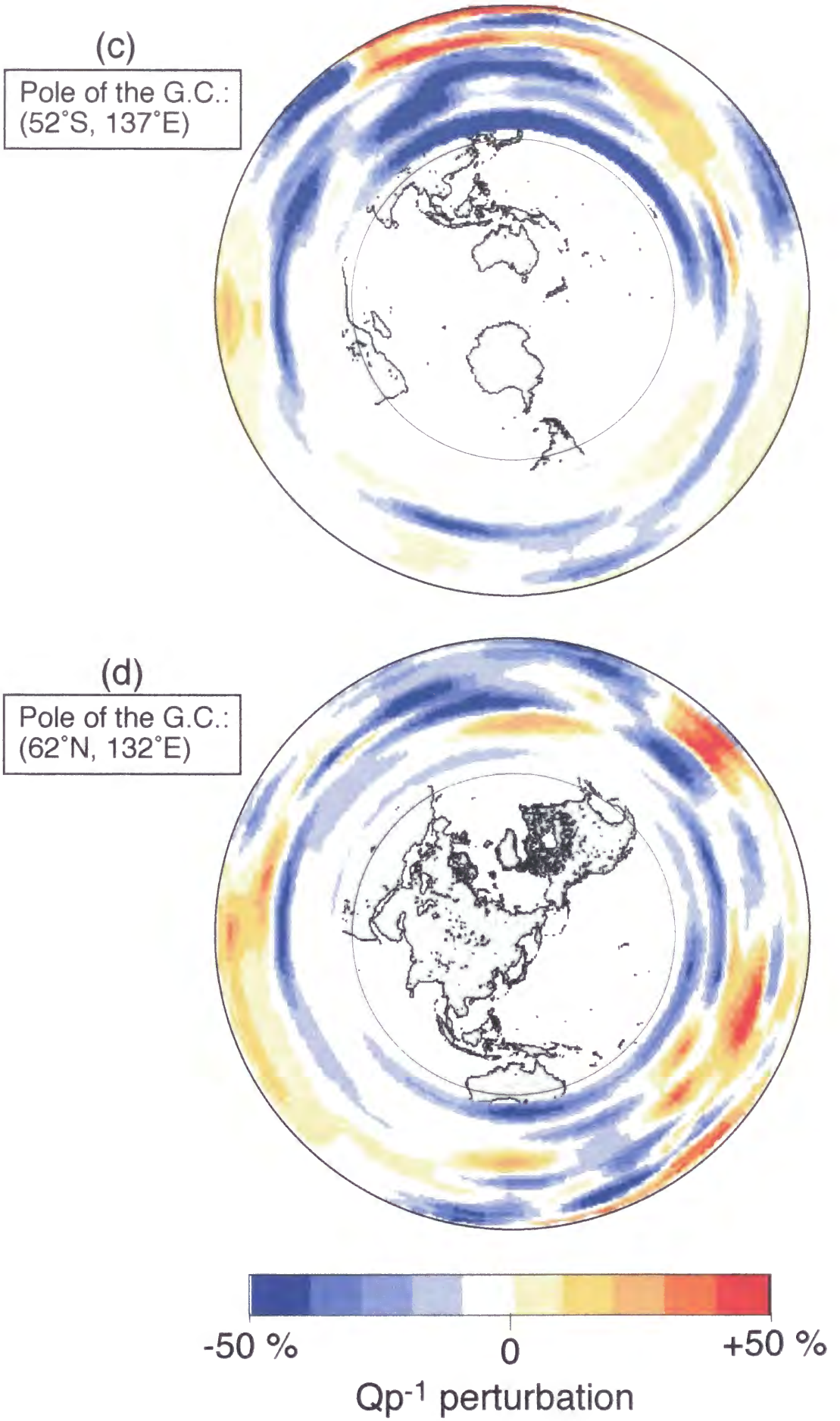

Figure 3.22 (2/4)

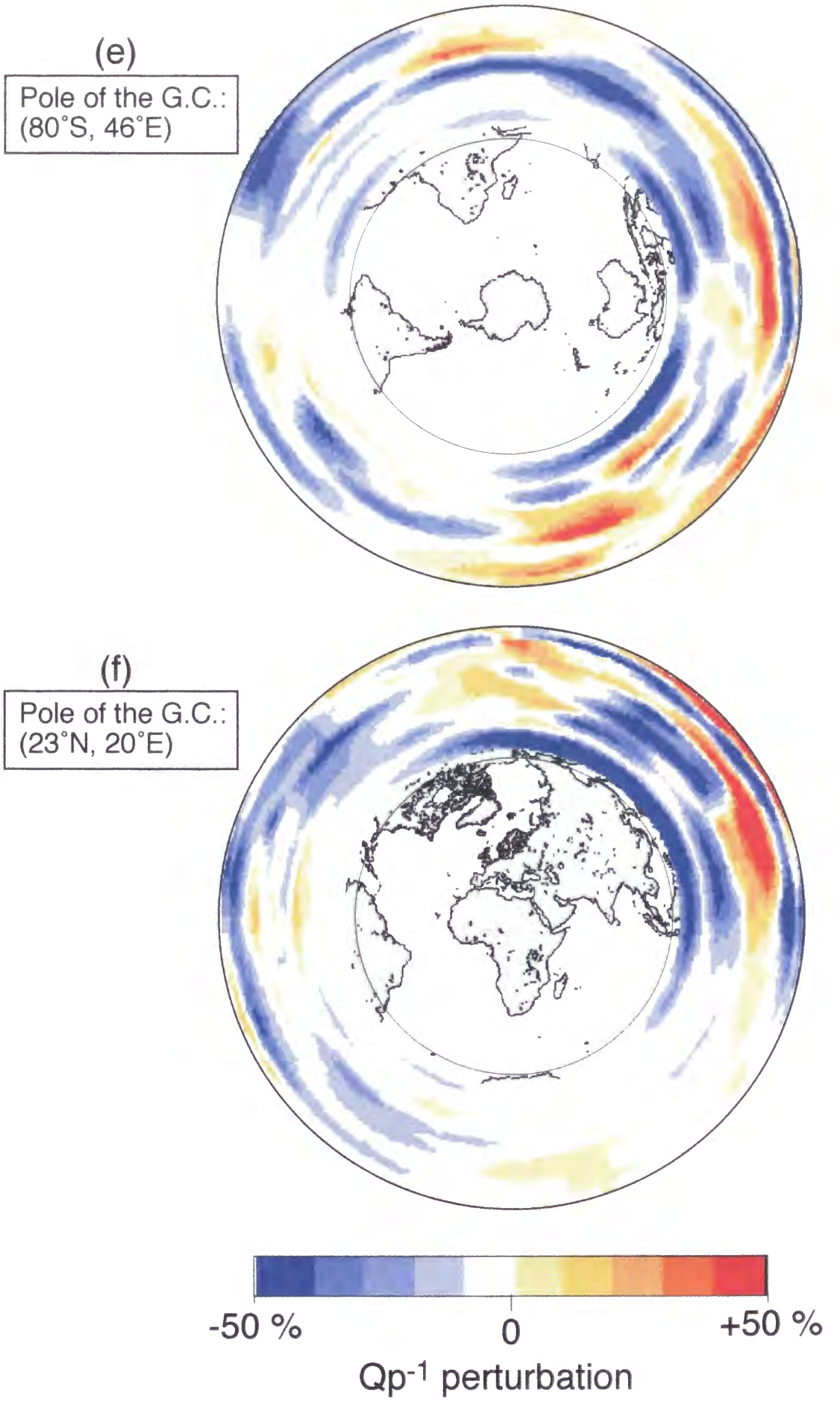

Figure 3.22 (3/4)

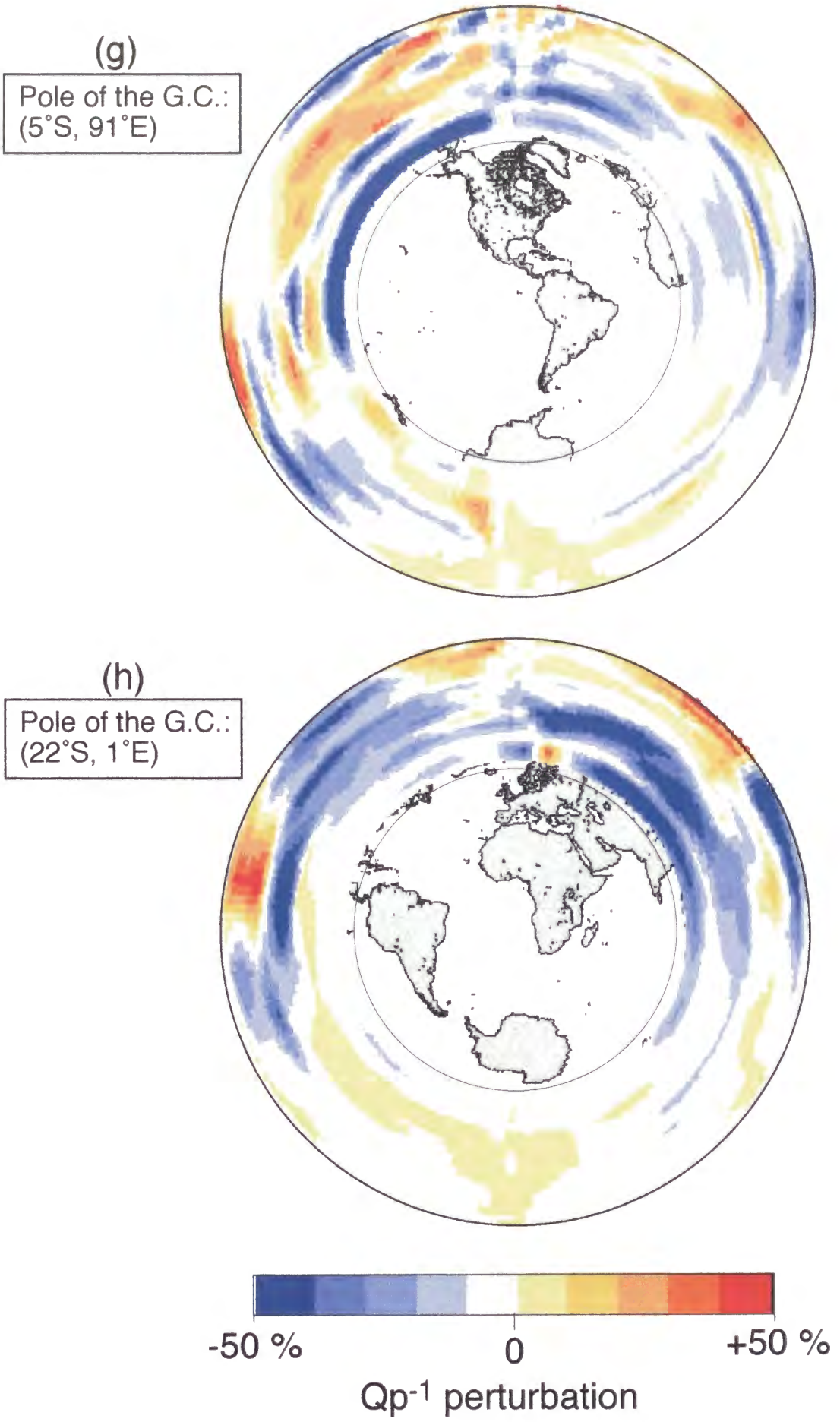

Figure 3.22 (4/4)

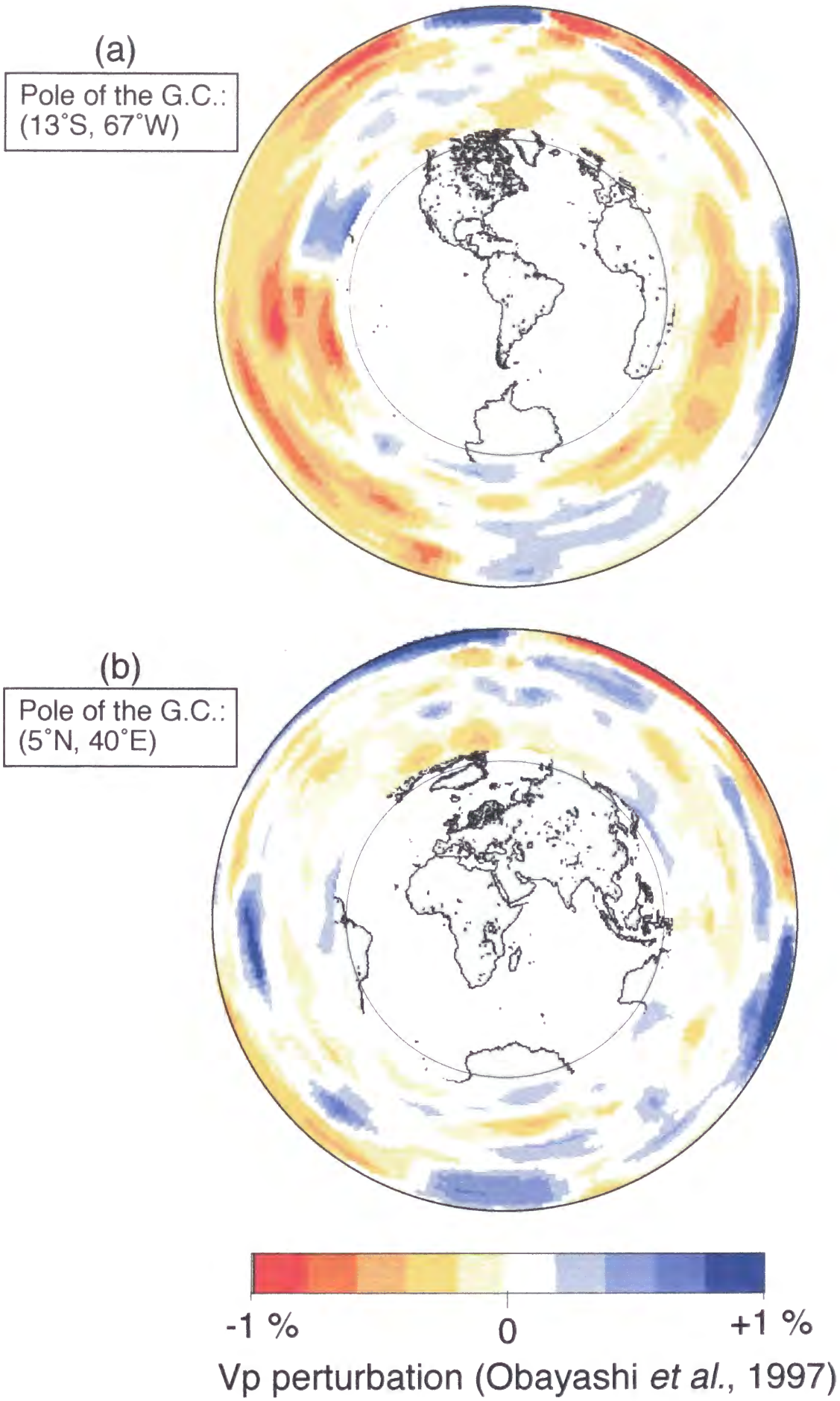

Figure 3.23 (1/4)

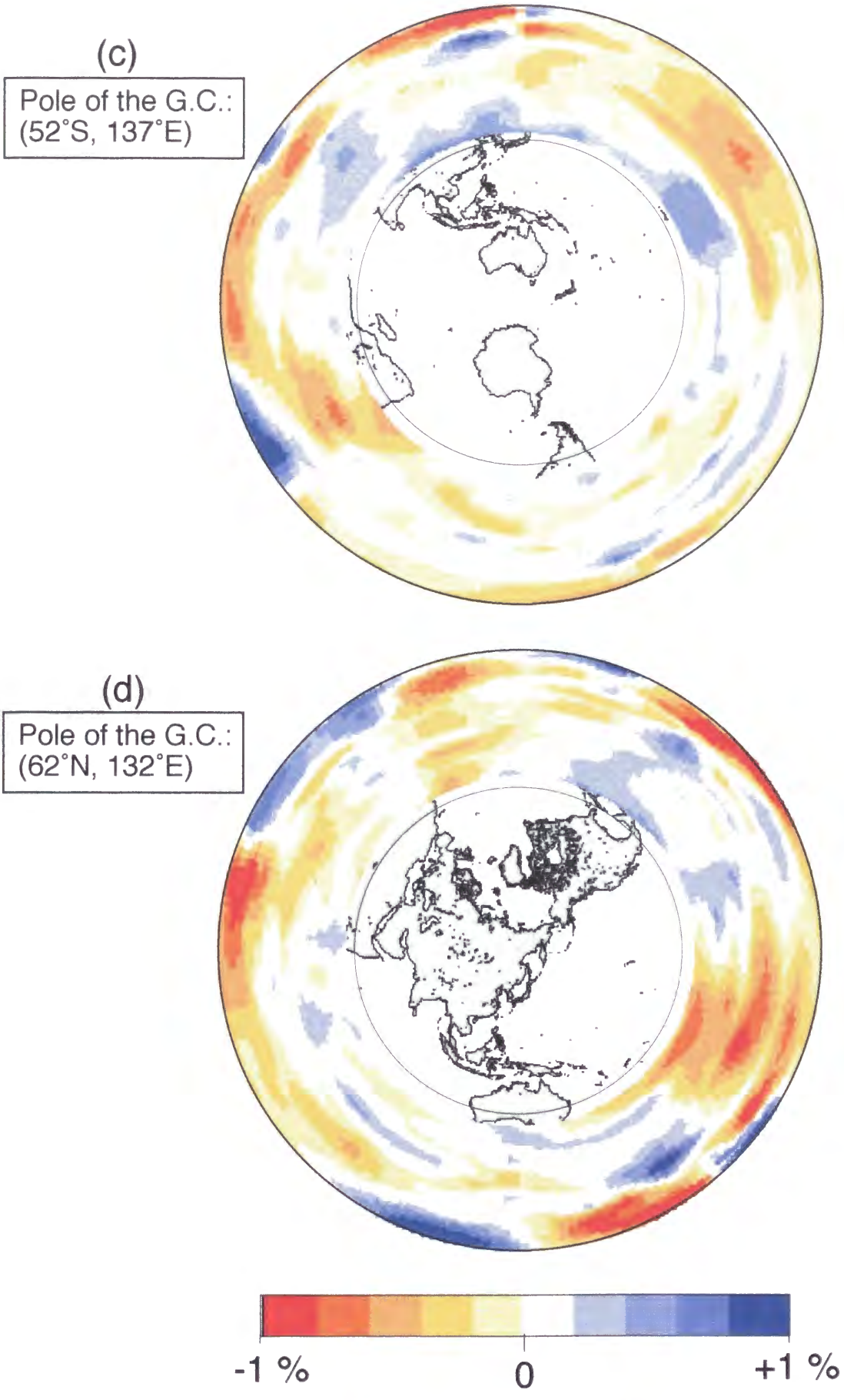

Figure 3.23 (2/4)

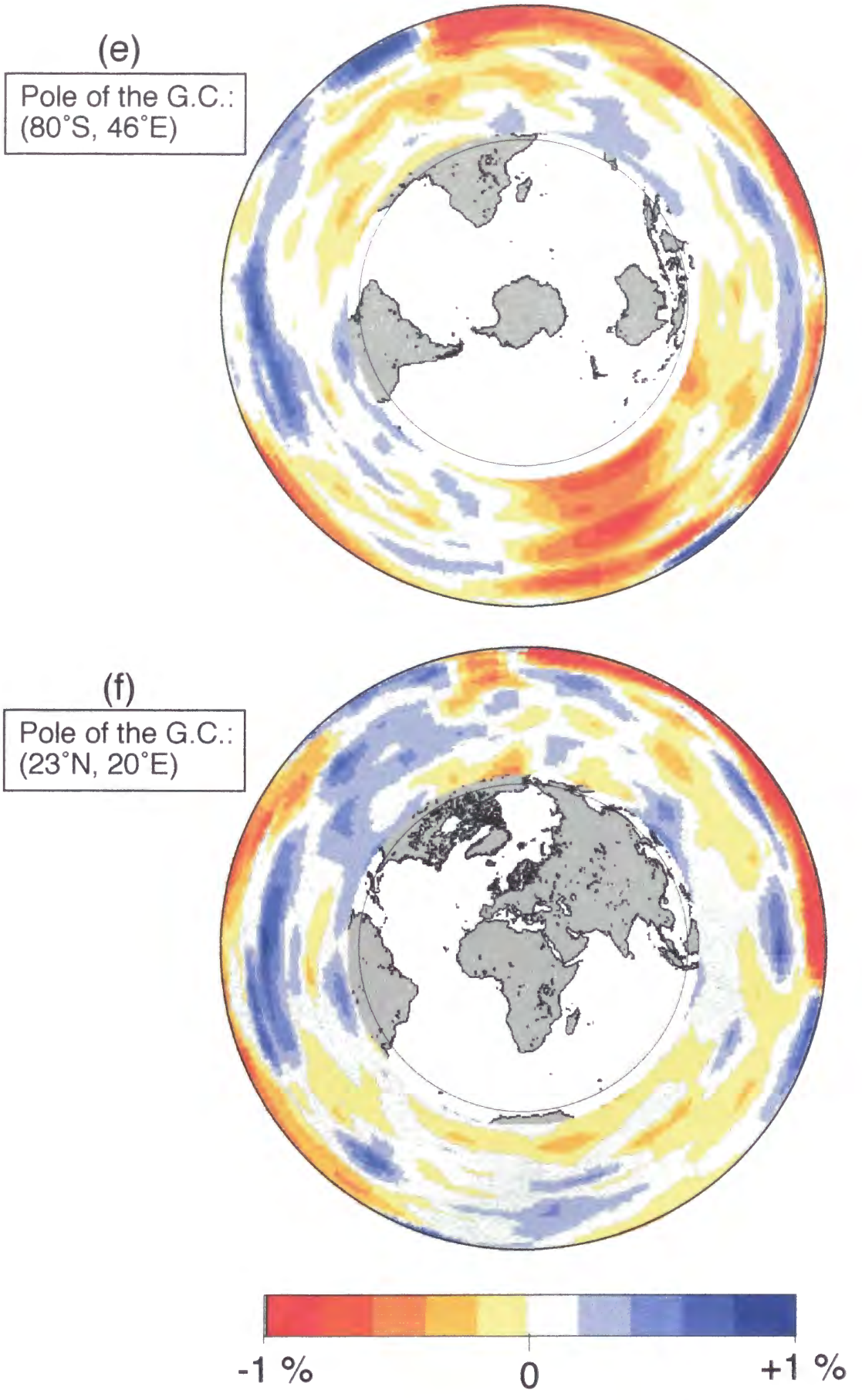

Figure 3.23 (3/4)

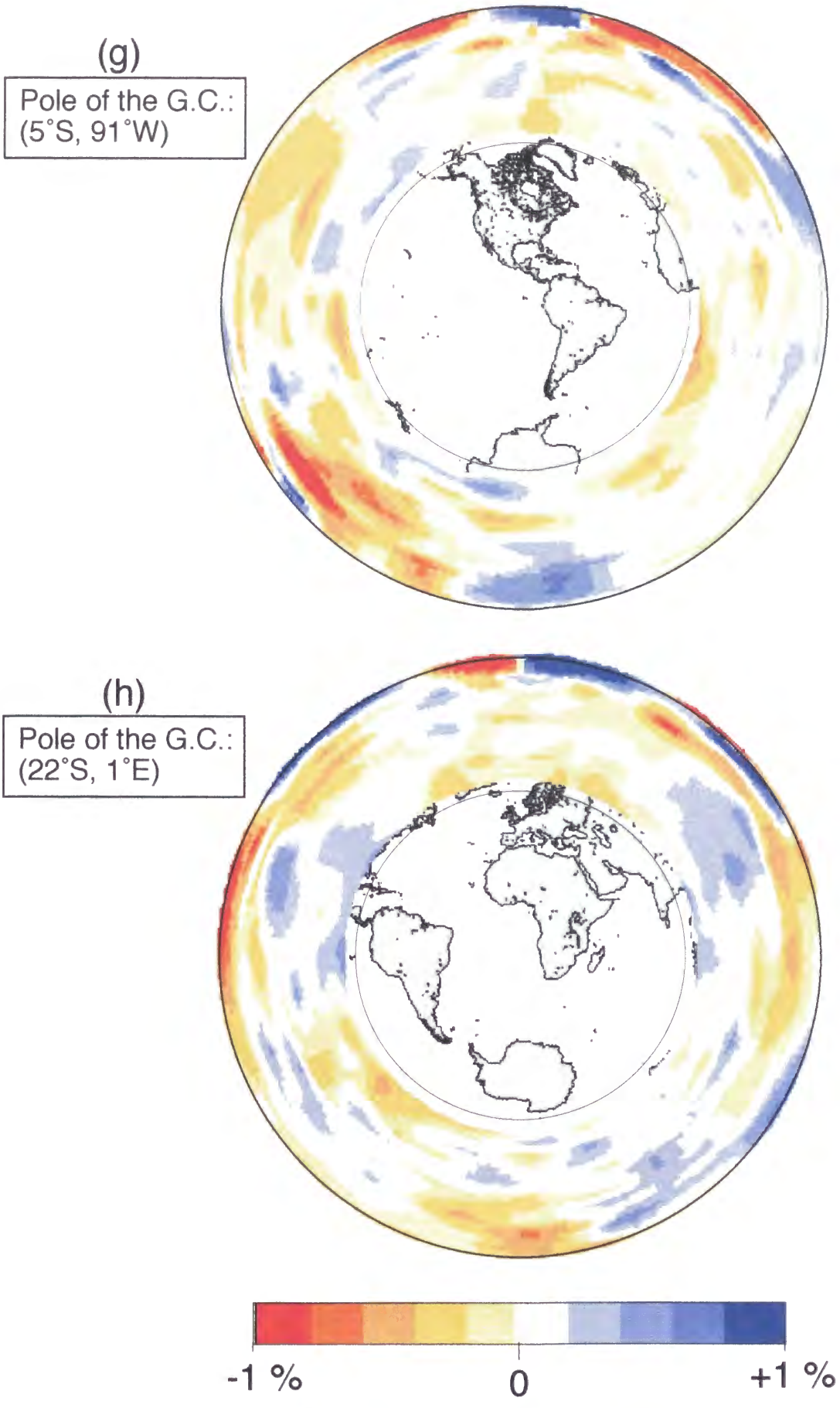

Figure 3.23 (4/4)

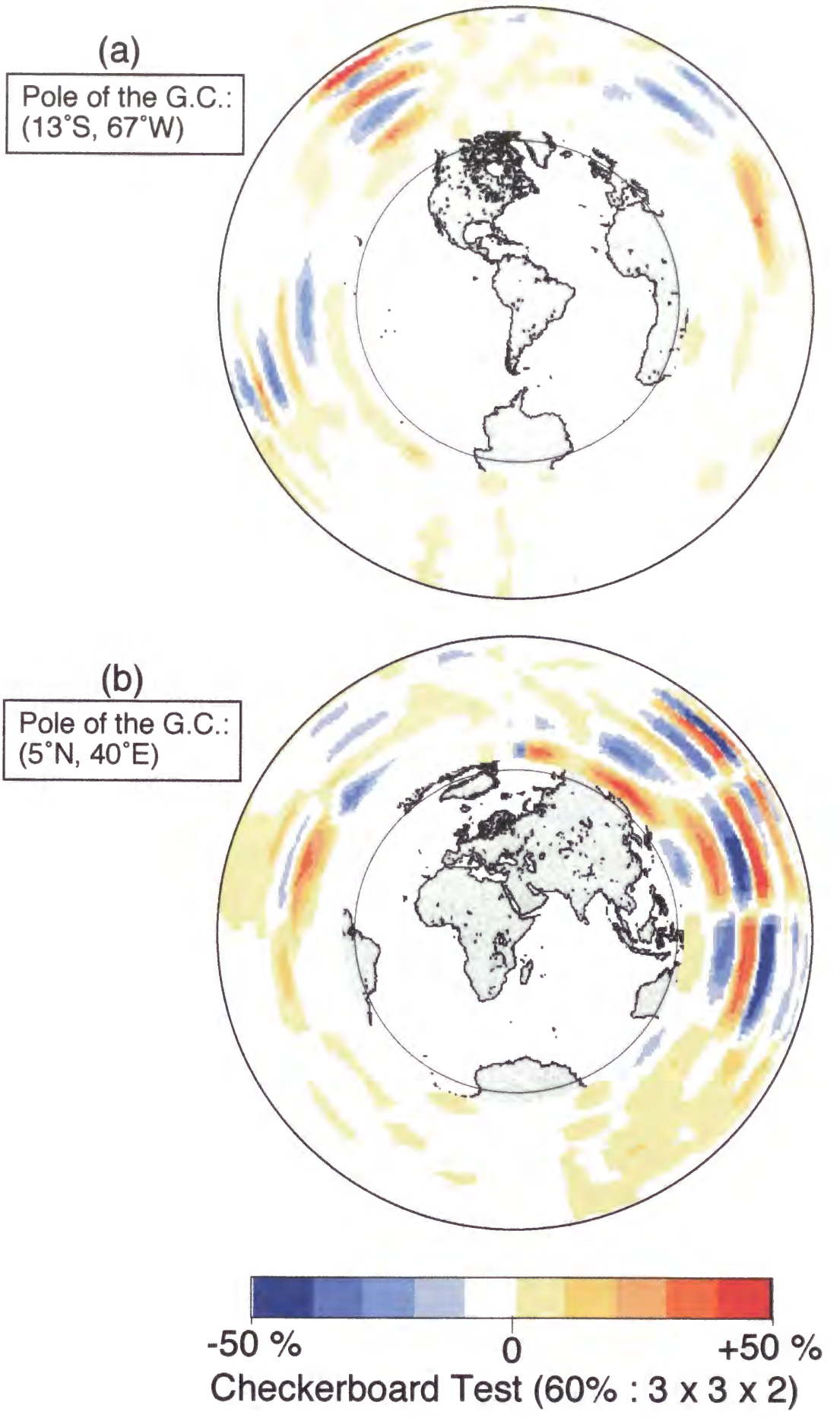

Figure 3.24 (1/4)

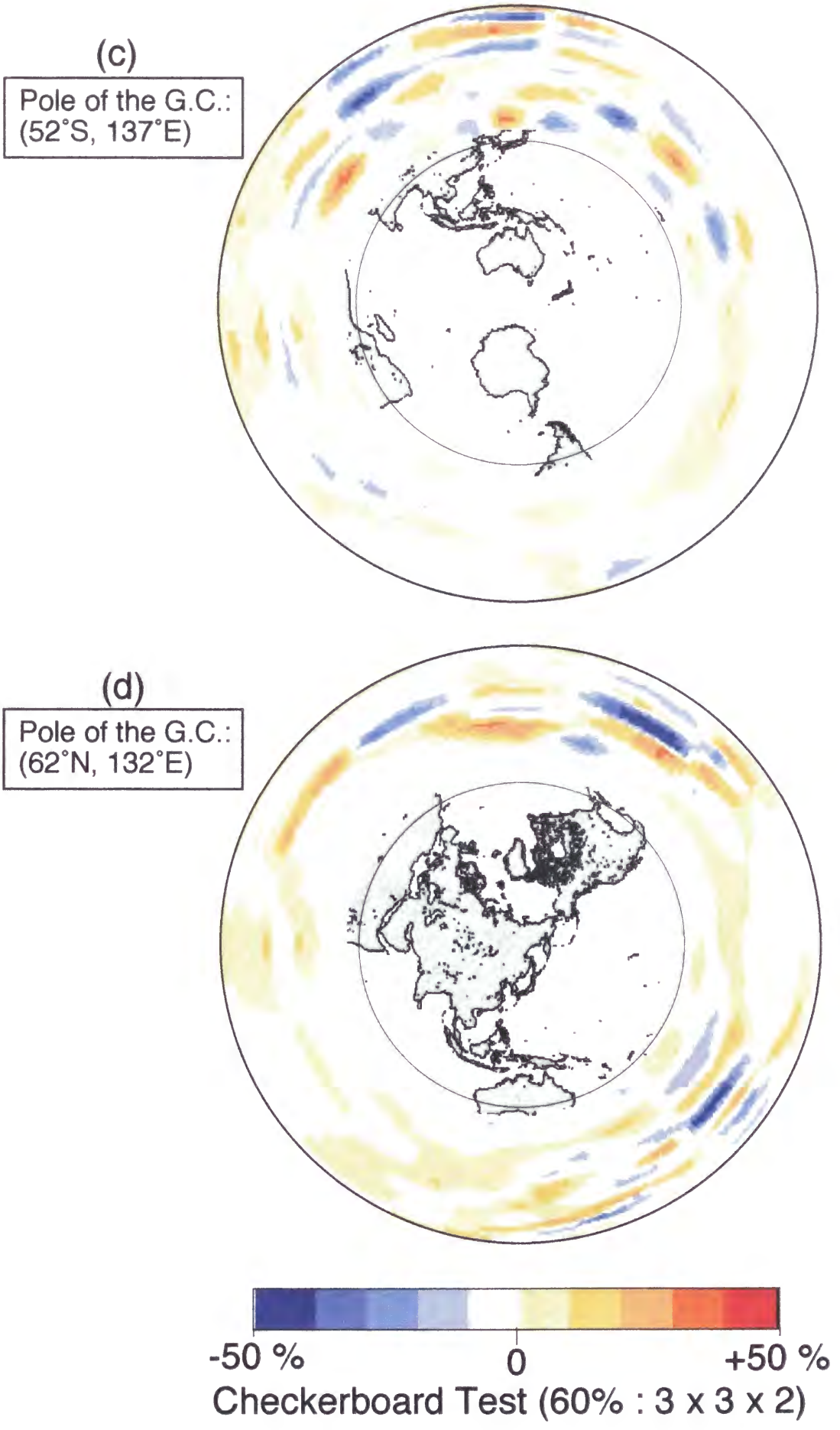

Figure 3.24 (2/4)

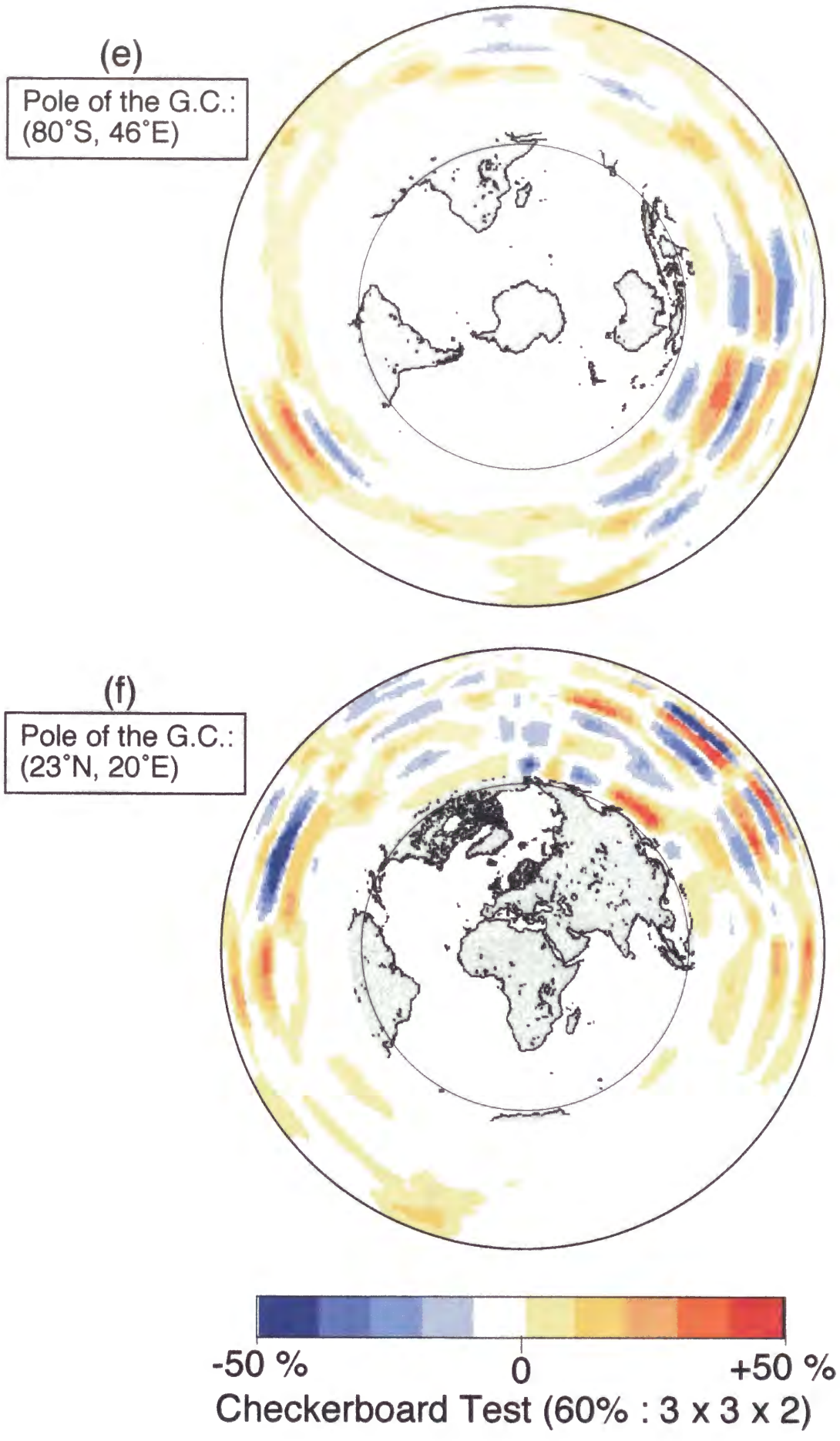

Figure 3.24 (3/4)

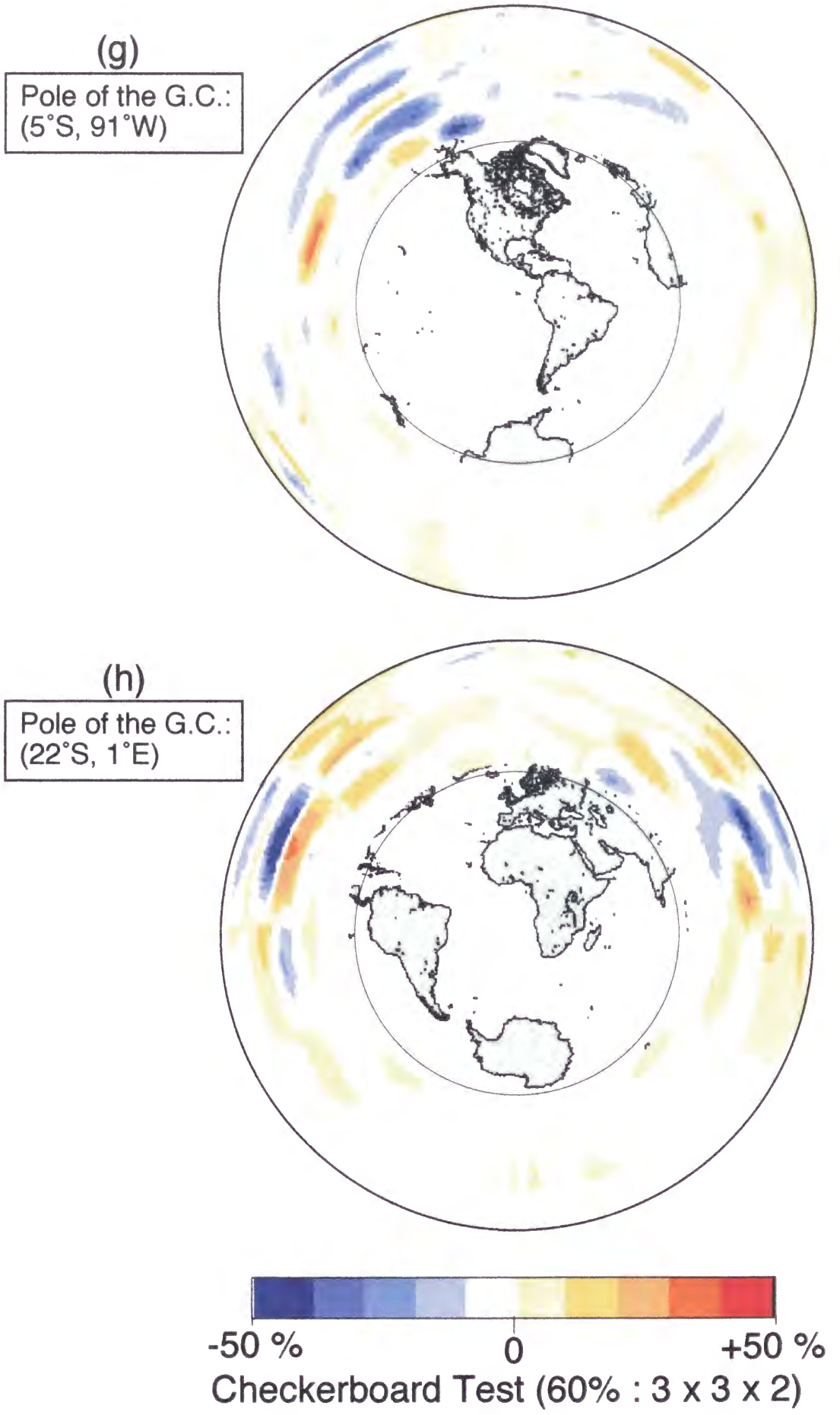

Figure 3.24 (4/4)

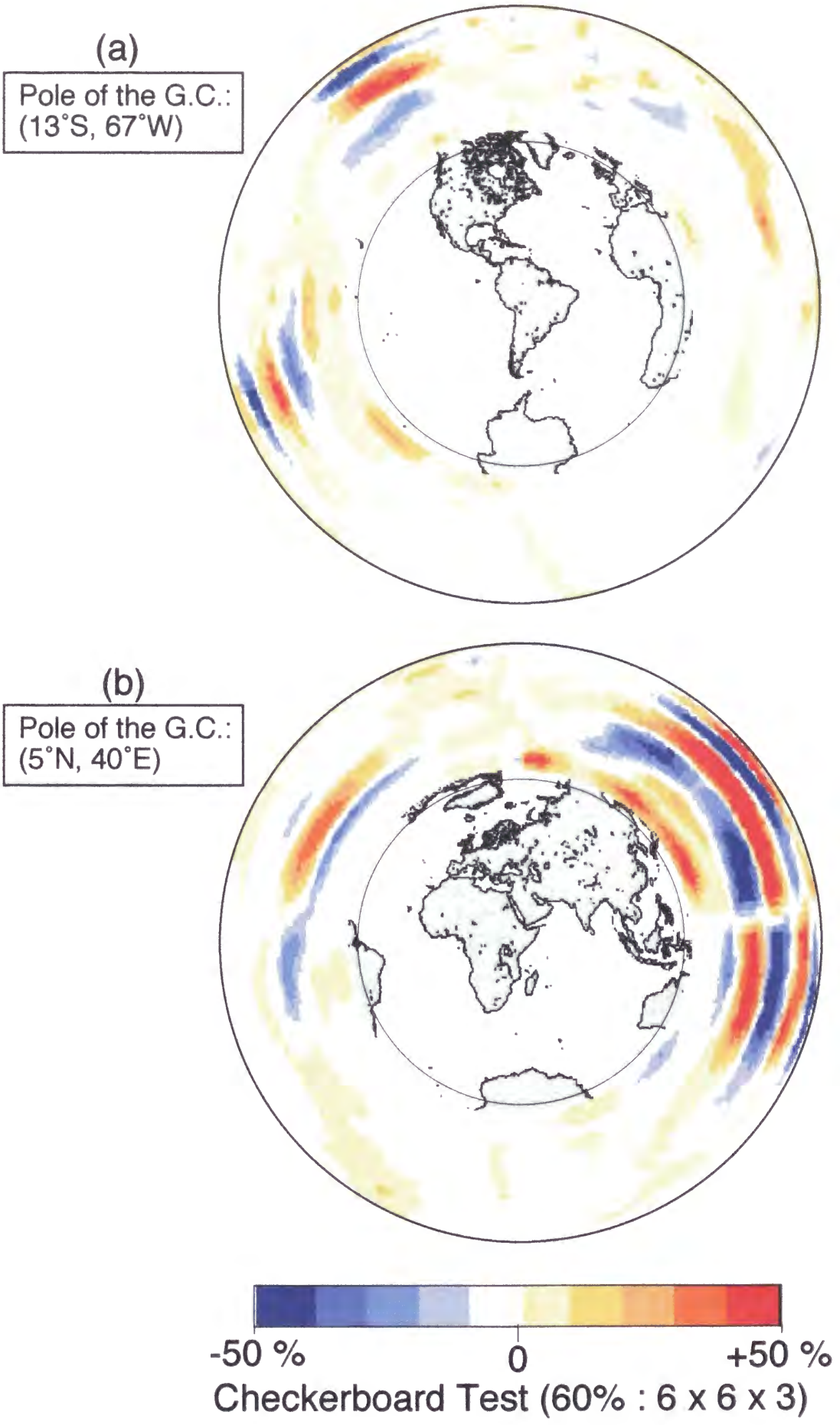

Figure 3.25 (1/4)

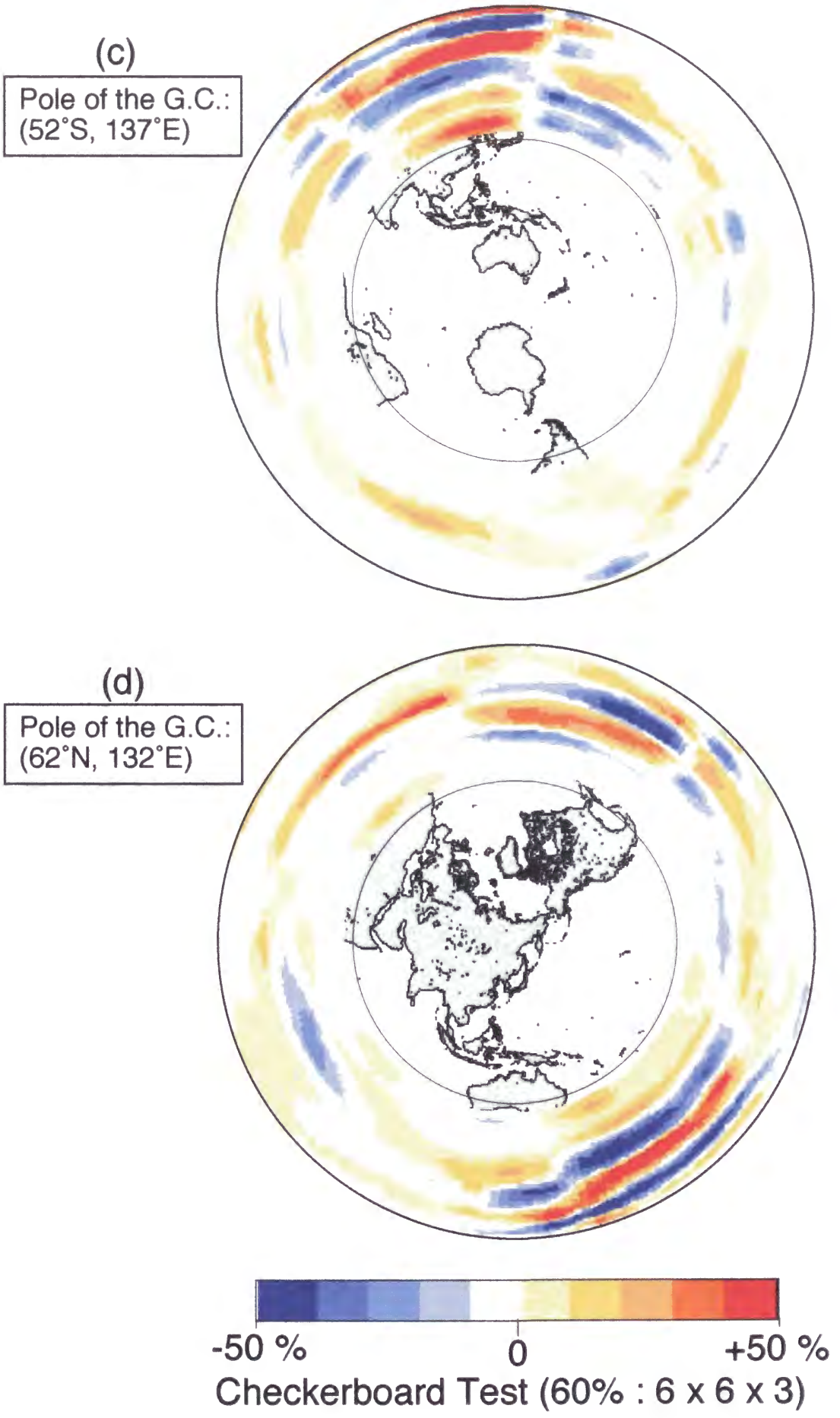

Figure 3.25 (2/4)

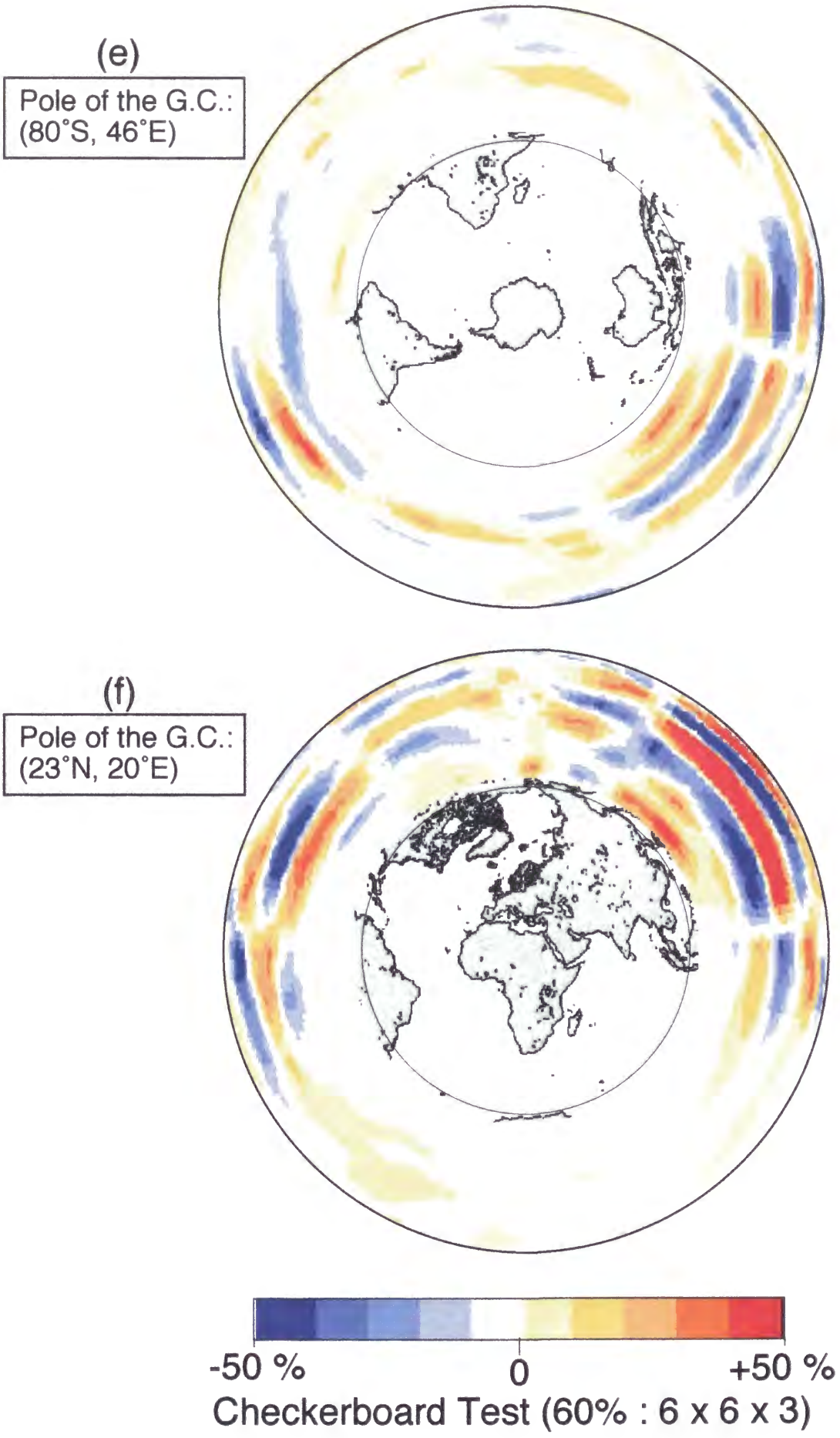

Figure 3.25 (3/4)

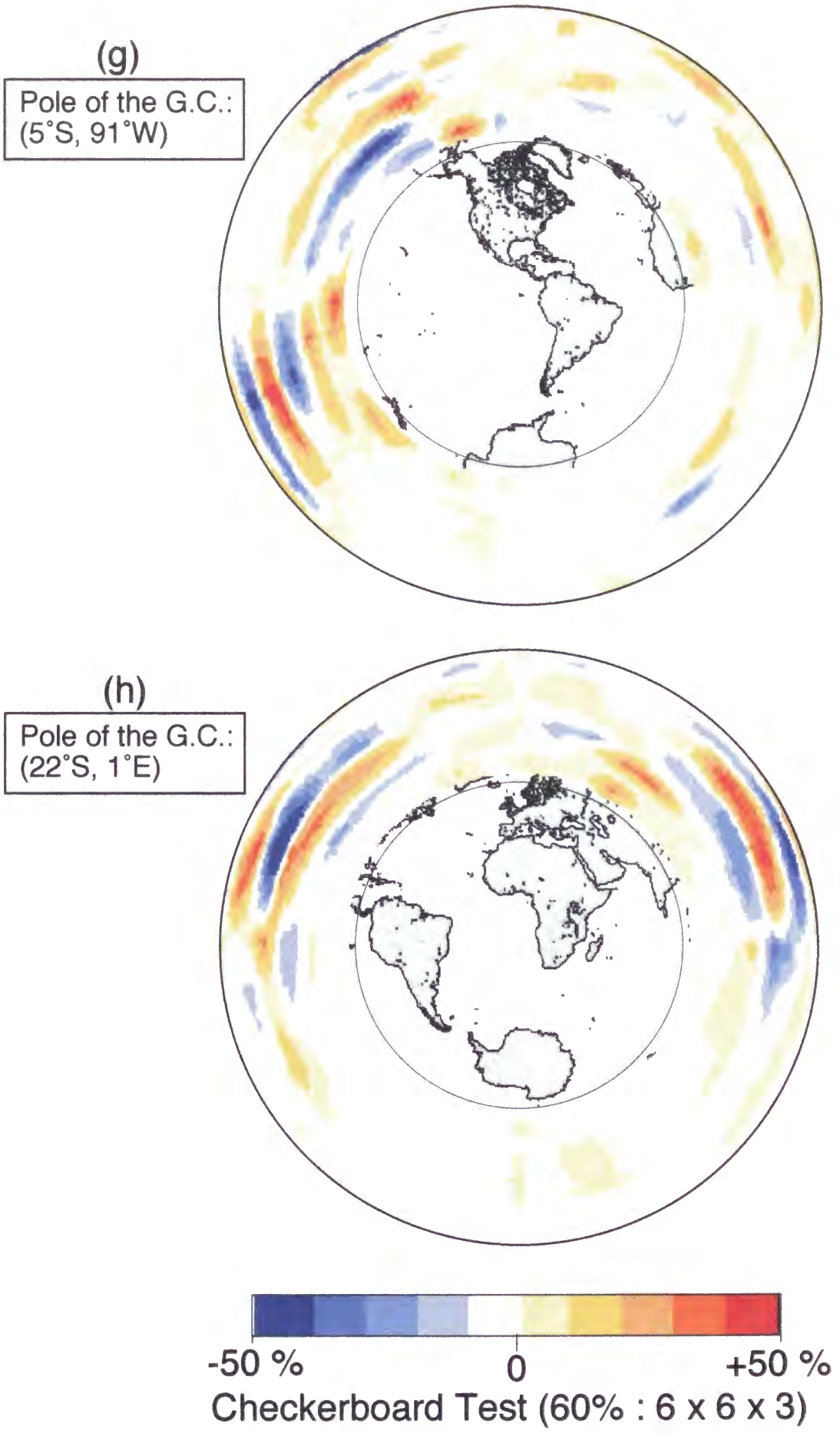

Figure 3.25 (4/4)

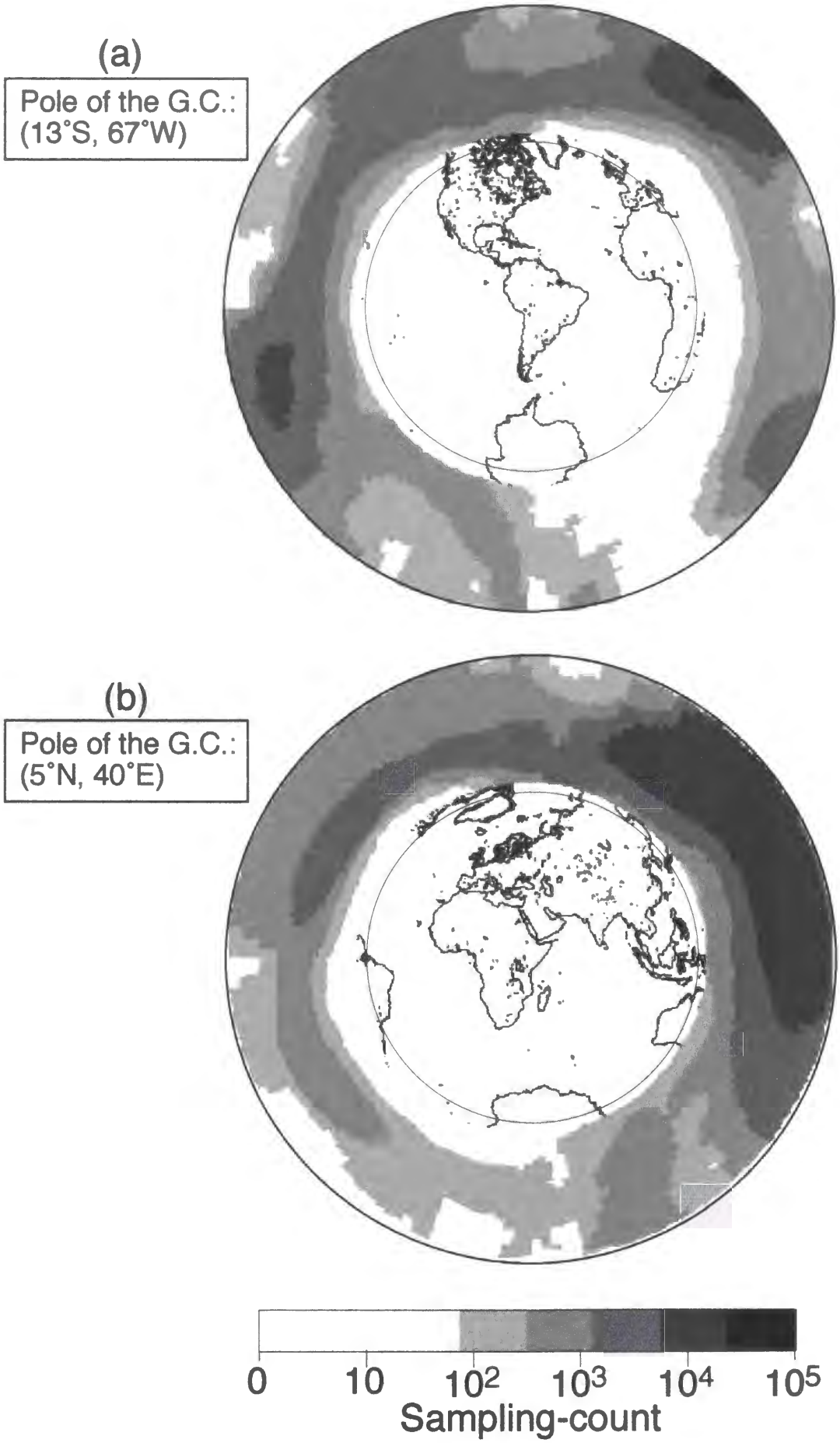

Figure 3.26 (1/4)

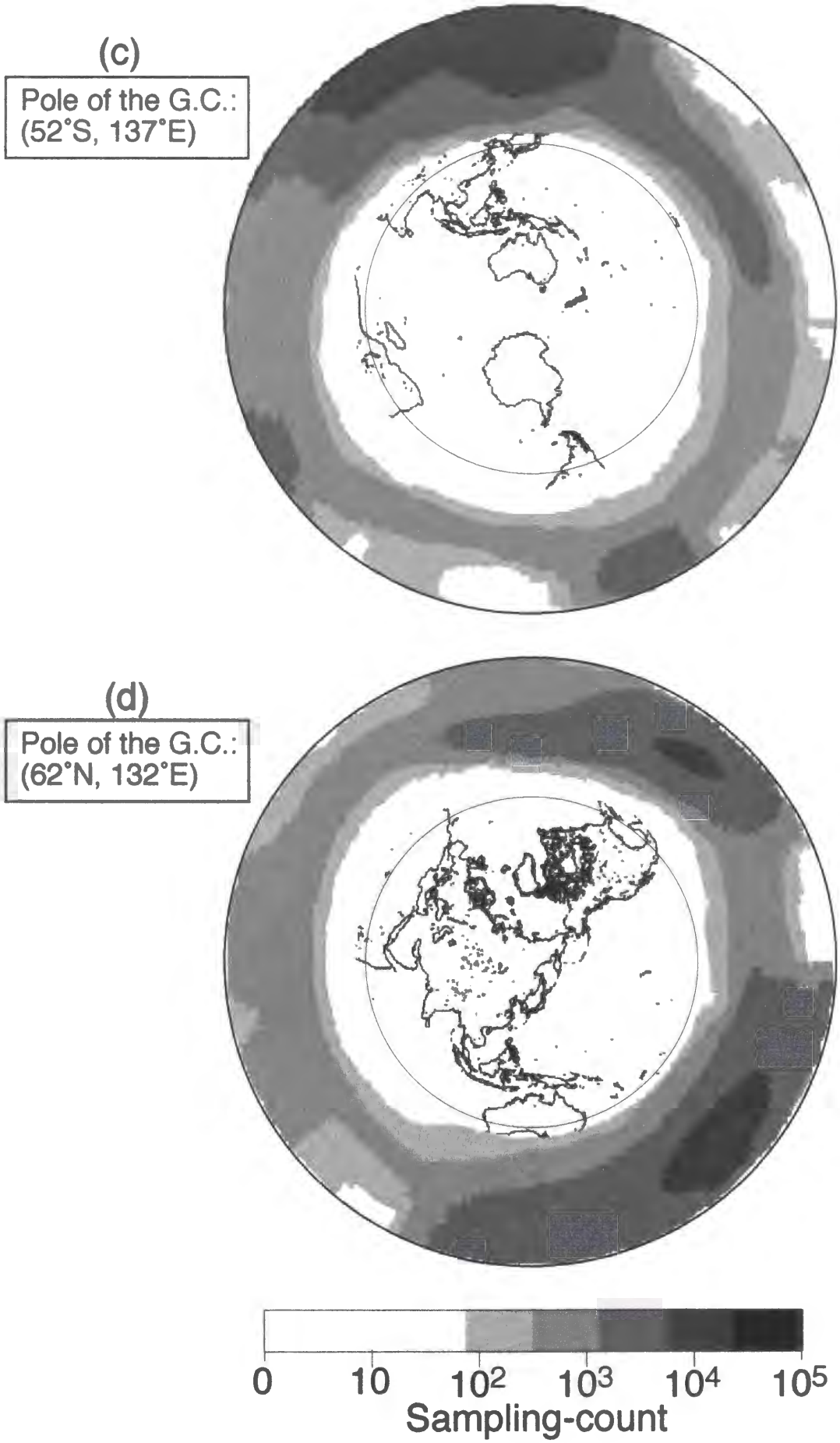

Figure 3.26 (2/4)

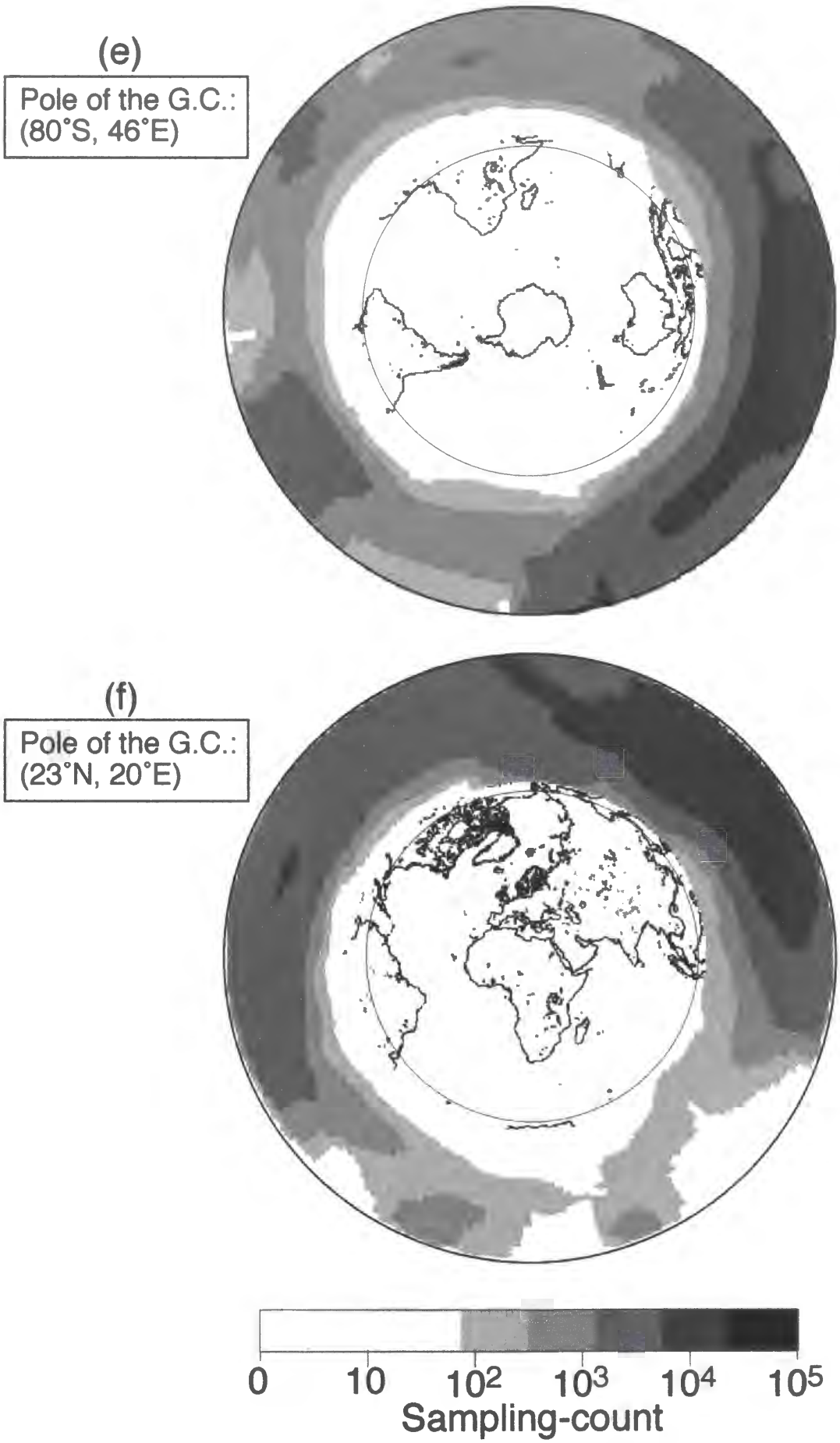

Figure 3.26 (3/4)

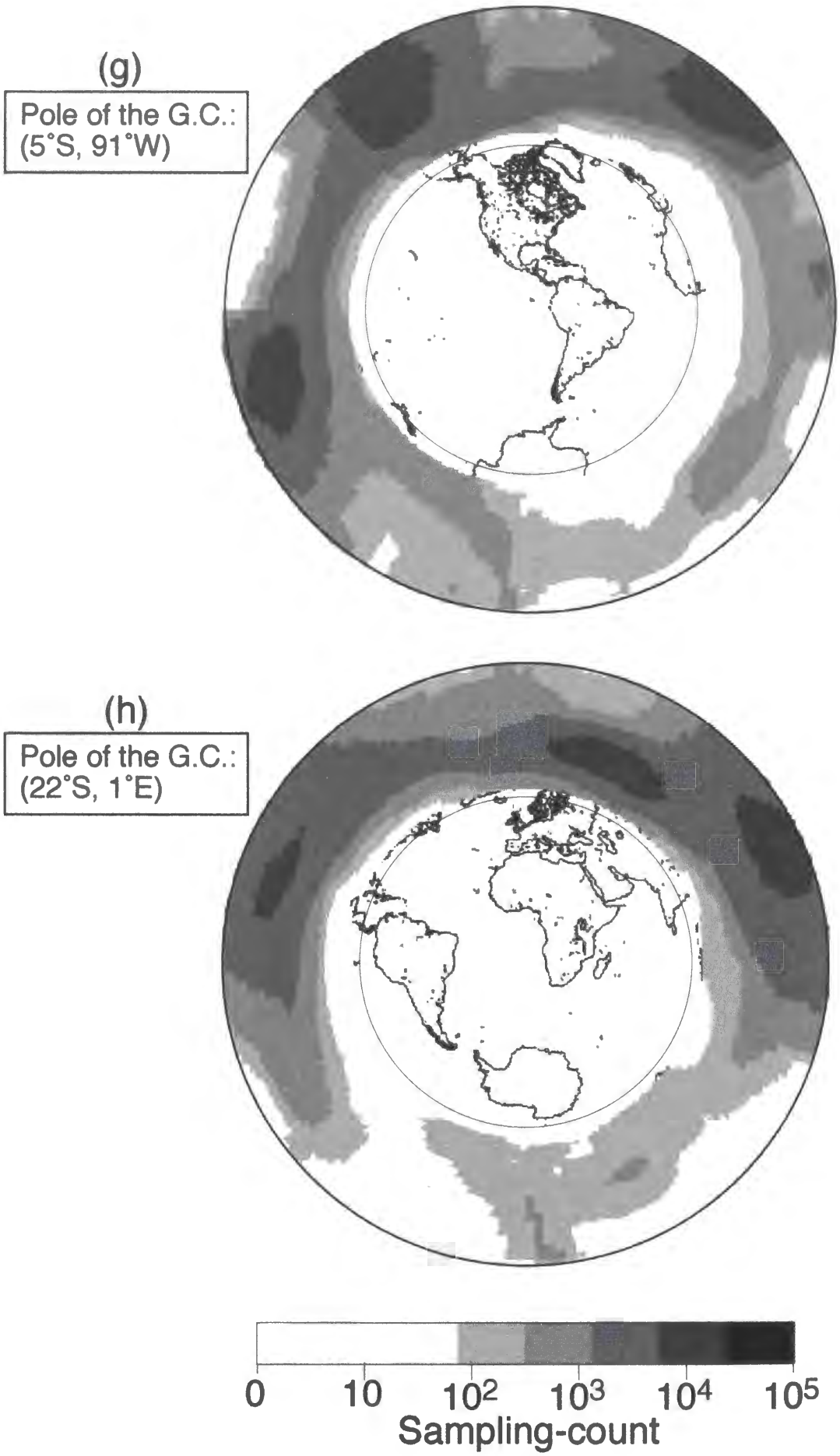

Figure 3.26 (4/4)

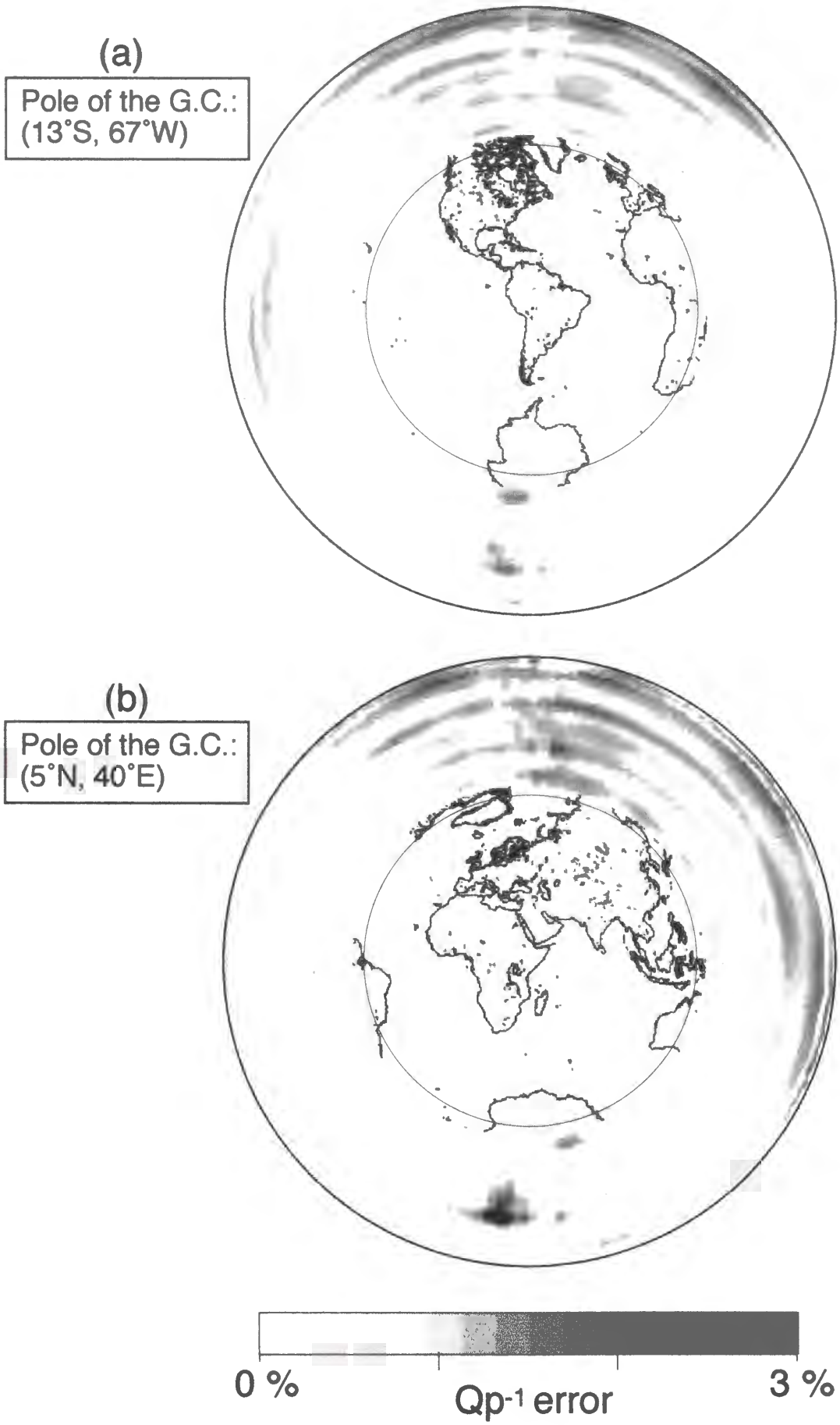

Figure 3.27 (1/4)

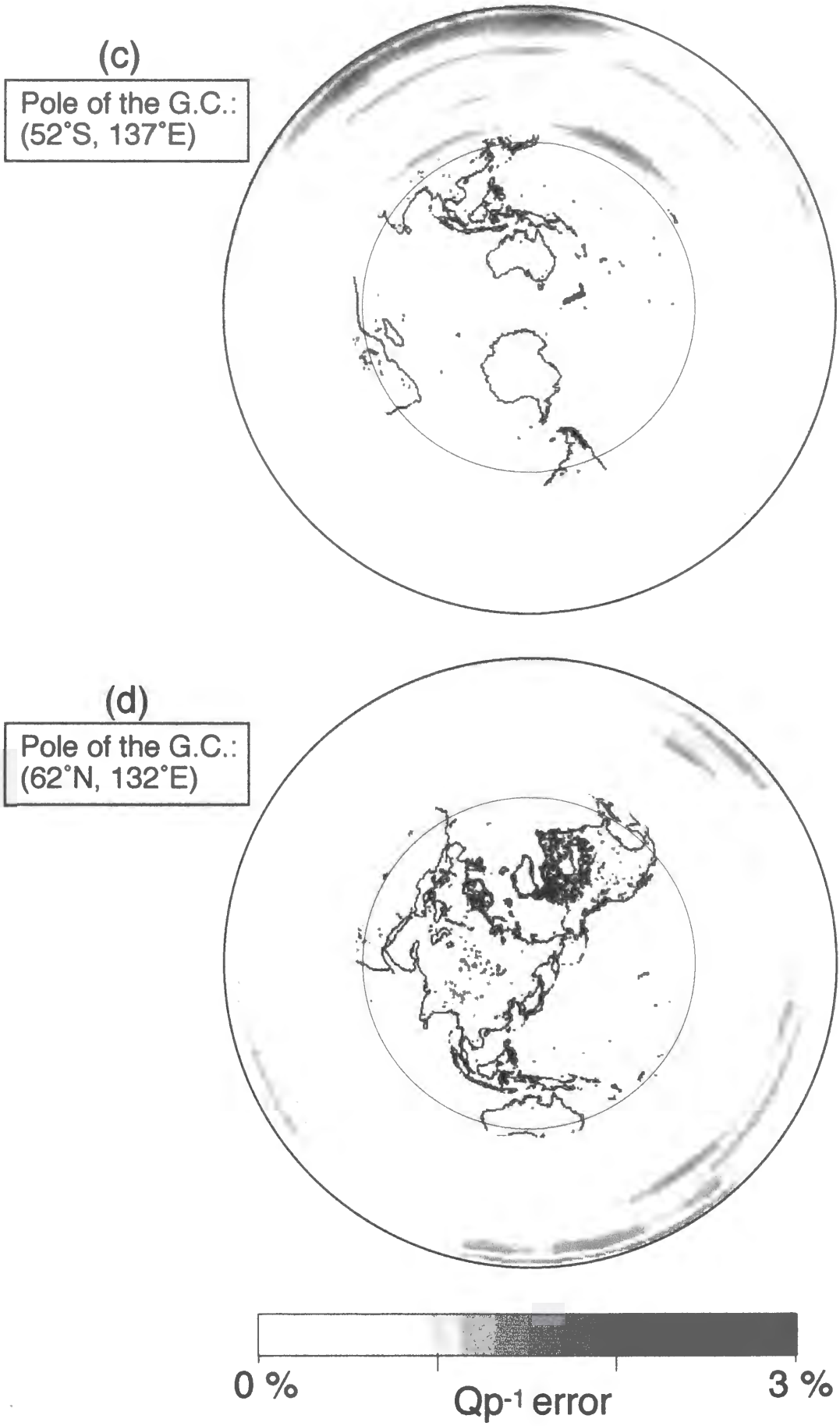

Figure 3.27 (2/4)

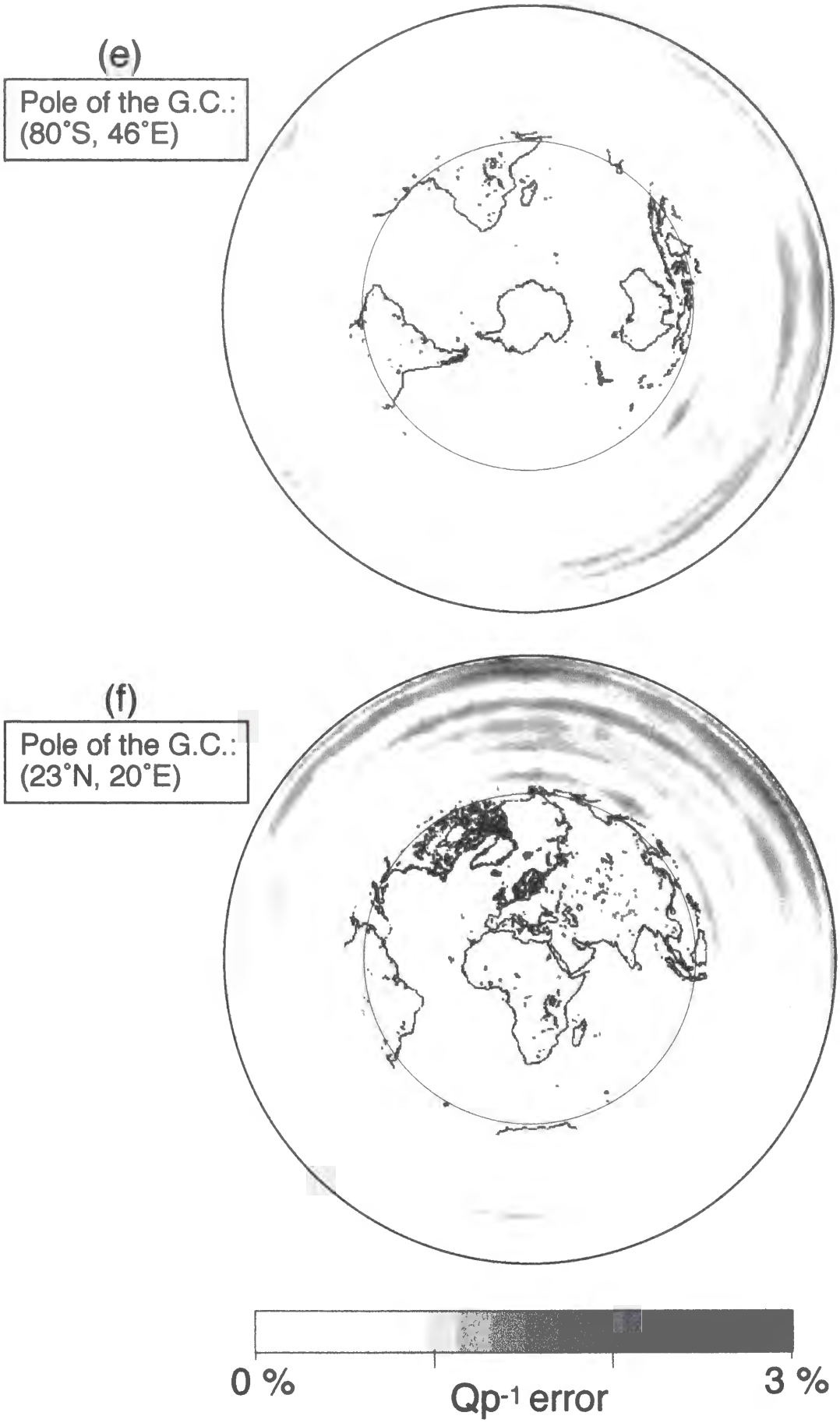

Figure 3.27 (3/4)

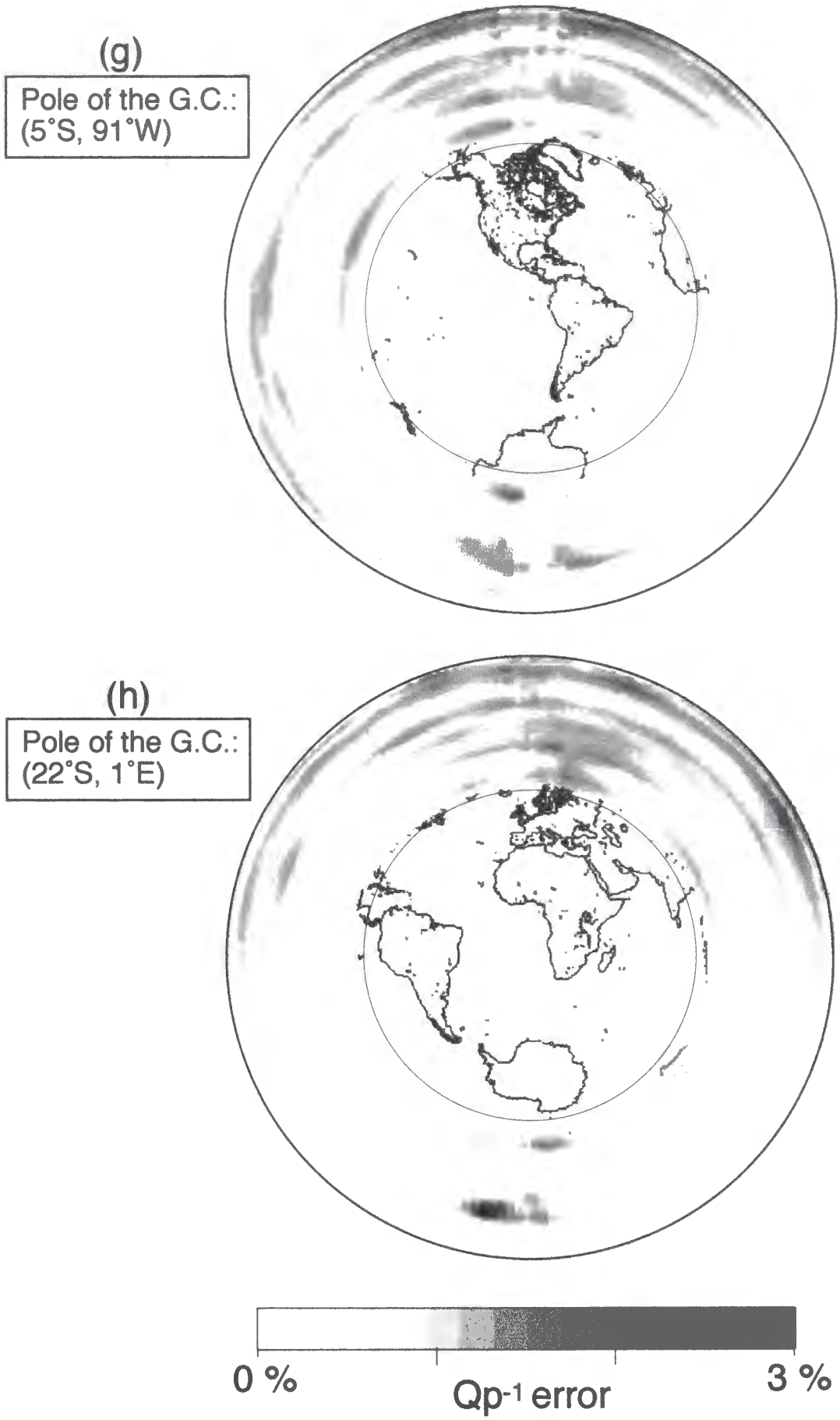

Figure 3.27 (4/4)

A)

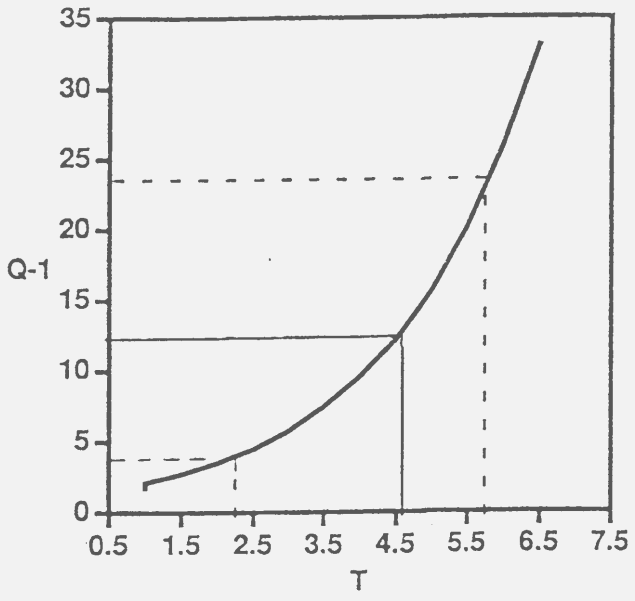

B)

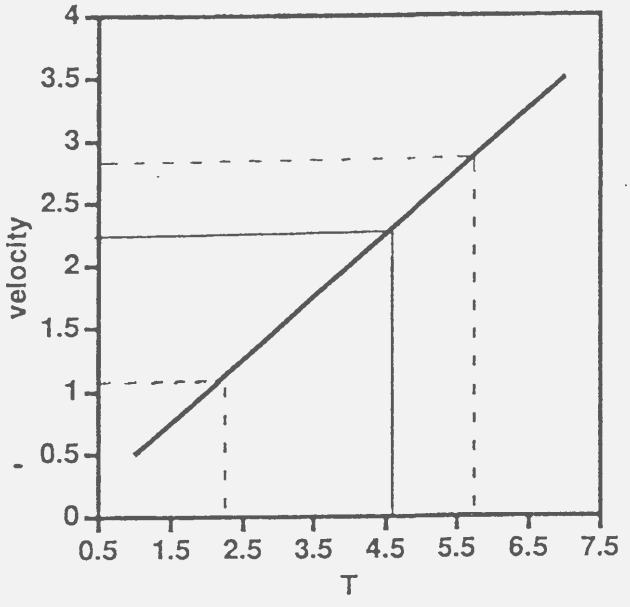

Figure 3.28

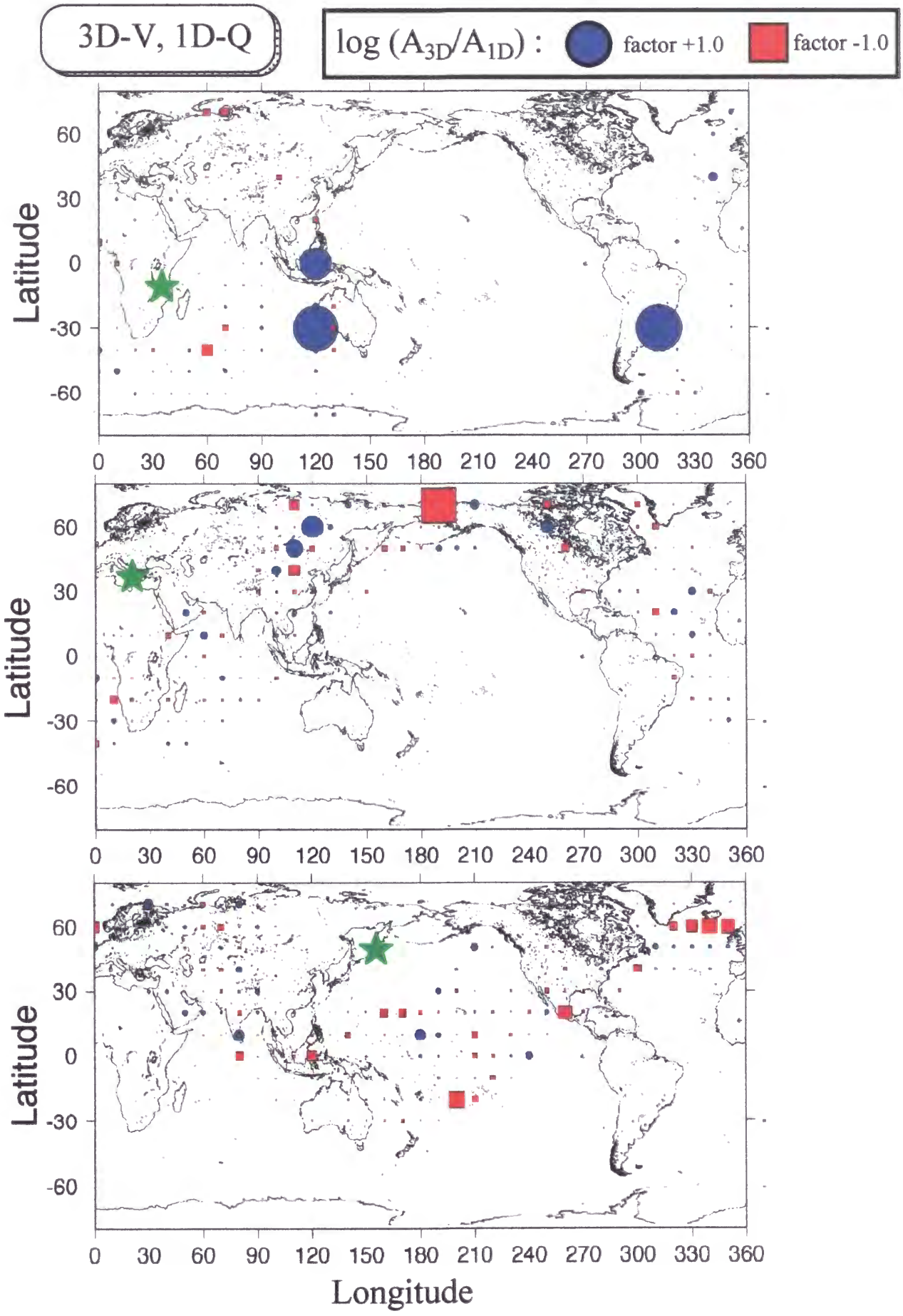
3D-V, 1D-Q
log (A3D/A1D) :
factor +1.0
factor -1.0
Latitude
Longitude
60
30
0
-30
-60
0
30
60
90
120
150
180
210
240
270
300
330
360

Fig. 3.29

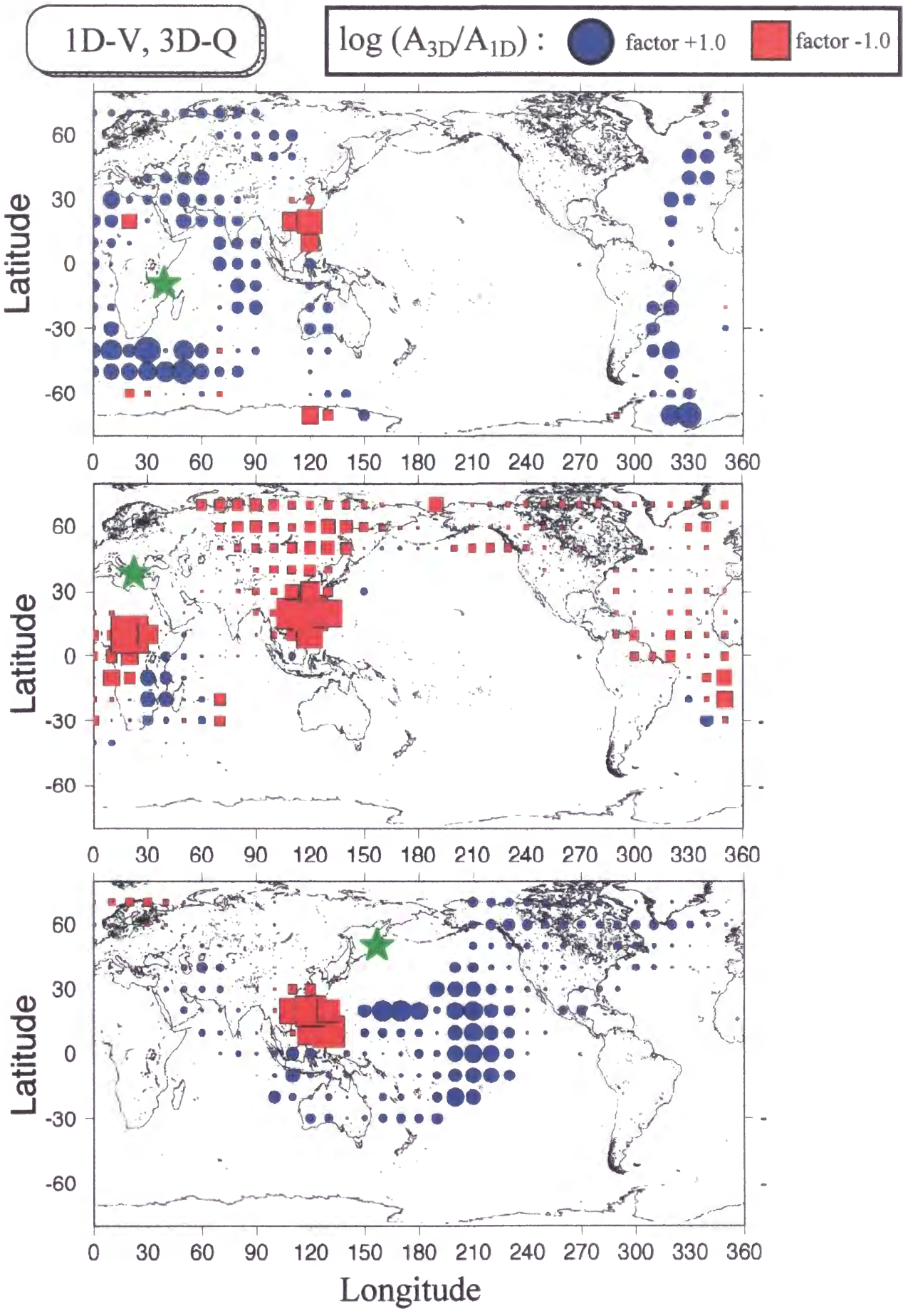
1D-V, 3D-Q
log (A3D/A1D) :
factor +1.0
factor -1.0
Latitude
Longitude
60
30
0
-30
-60
0
30
60
90
120
150
180
210
240
270
300
330
360

Fig. 3.30

Chapter 4.

General Conclusion

A whole mantle attenuation structure was obtained by applying a tomographic method to the P-wave amplitude data of the International Seismological Center Bulletin. This is the first result which delineates the whole mantle attenuation structure, not only in the upper mantle but including the lower mantle.

Before the tomographic inversion, I analyzed the ISC amplitude data based on the method of Negishi and Sato [1993]. Relative log-scaled amplitude was defined and the station correction term and azimuthal dependency were analyzed. 3,445 earthquakes and 718 seismic stations were investigated after the correction of radiation pattern and geometrical spreading effect. Averages and azimuthal dependency were obtained for relative log-scaled amplitudes. The azimuthal dependency of P-wave travel time residuals, which were recently compiled and re-determined with AK135 travel time table by Engdahl *et al.* [1998], were also analyzed by the same process, and the correlation between log-scaled amplitude anomalies and relative travel time residuals were investigated. Azimuth-independent terms for amplitudes at the central part of old continents, such as Eurasia and North America, are generally large, while there are small amplitudes around the Pacific Ocean and southern Europe. These station anomalies seems to have weak correlation with the type of crustal structure. The first azimuthal terms, which indicate the arrival direction with larger amplitude, have more complex distributions and do not show an obvious global tendency. The second-azimuthal terms show systematic distributions, east-west directions around the western Pacific Ocean, north-south directions in North America, and complex area in Europe. The results of the travel time residuals are similar to the result by Dziewonski and Anderson [1983]. The second azimuthal terms show good relations with the S-wave polarization anisotropy. There exist systematic clusters of negative correlation between amplitude and travel time for large amplitudes in southern Eurasia (western China and India) and for small amplitudes in the southern part of southeastern Asia (Malaysia, Singapore and Indonesia). This means that large amplitude observations are due to weak attenuation in the crust and the upper mantle in southern Eurasia, while there exists a strong attenuation area beneath Southeast Asia region.

The whole mantle three-dimensional structure of P-wave attenuation was obtained using the ISC data corrected above. I developed a attenuation tomography formula by using

grid model formulation. The simultaneous inversion technique determined source amplitude and one-dimensional attenuation structure down to 2700 km depth, then three-dimensional perturbations from the one-dimensional model were calculated. The attenuation in the upper mantle is relatively stronger than that in the lower mantle. The lateral variations in long-wavelength attenuation show similar patterns to the previous P-wave velocity studies. Two major high attenuation zones appear to be located in the central Pacific and beneath northern Africa in the middle to lower mantle, while low-attenuation region spread beneath the Eurasia continental shield in the upper to middle mantle. There exists some remarkable high attenuation zones in the upper and lower mantle. Hotspots are located close to those regions, therefore the high attenuation may be due to upwelling flow.

Bibliography

Adams, R.D., A.A. Hughes and D.M. McGregor, Analysis procedures at the International Seismological Center, *Phys. Earth Planet. Inter.*, **30**, 85 - 93, 1982.

Akaike, H., Likelihood and Bayes procedure. In: J.M. Bernardo, M.H. De Groot, D.V. Lindley and A.F.M. Smith (Editors), *Bayesian Statistics*, University Press, Valencia, Spain, pp. 143 - 166., 1980.

Aki, K. and W.H.K. Lee, Determination of three-dimensional velocity anomalies under a seismic array using first P-arrival times from local earthquakes, 1, A homogeneous initial model, *J. Geophys. Res.*, **81**, 4381 - 4399, 1976.

Aki, K., A. Cristoffersson and E.S. Husebye, Determination of the three-dimensional seismic structure of the lithosphere, *J. Geopys. Res.*, **82**, 277 - 296, 1977.

Aki, K. and P.G. Richards, *Quantitative Seismology: Theory and Method*, W.H. Freeman, New York, 932 pp., 1980.

Anderson, D.L., A. Ben-Menahem and C.B. Archambeau, Attenuation of seismic energy in the upper mantle, *J. Geophys. Res.*, **70**, 1441 - 1448, 1965.

Anderson, D.L. and R.S. Hart, Q of the Earth, *J. Geophys. Res.*, **83**, 5869 - 5882, 1978.

Ando, M., ScS polarization anisotropy around the Pacific ocean, *J. Geophys. Res.*, **88**, 5850 - 5864.

Aoike, K., T. Sato and O. Nishizawa, An optimum P-velocity tomographic model of Northern Tohoku region based on bootstrap statistics, *J. Seismol. Soc. Jpn.*, **51**, 19 - 30, 1998 (in Japanese with English abstract).

Besana, G.M., H. Negishi and M. Ando, The three-dimensional attenuation structure beneath the Philippine archipelago based on seismic intensity data inversion, *Earth Planet. Sci. Lett.*, **151**, 1 - 11, 1997.

Červený, V., 1985, The application of ray tracing to the numerical modeling of seismic wavefields in complex structures, in *Seismic Shear Waves, Handbook of Geophysical Exploration, Section I*, Seismic exploration (ed. G.P. Dohr), Geophysical Press, London, vol. 15, 1 - 124, 1985.

Cleary, J. and A.L. Hales, An analysis of the travel times of P waves to North American stations, in the distance range 32° to 100°, *Bull. Seismol. Soc. Am.*, **56**, 467 - 489, 1966.

Creager, K.C. and T.A. Jordan, Slab penetration into the lower mantle, *J. Goephys. Res.*, **89**, 3031 - 3049, 1984.

Davies, J.H., Lower bound estimate of average earthquake mislocation from variance of travel-time residuals, *Phys. Earth Planet. Inter.*, **75**, 89 - 101, 1992.

Dziewonski, A.M., Mapping the lower mantle: Determination of lateral heterogeneity in P velocity up to degree and order 6, *J. Geopys. Res.*, **89**, 5929 - 5952, 1984.

Dziewonski, A.M. and D.L. Anderson, Preliminary reference Earth model, *Phys. Earth Planet. Inter.*, **25**, 297 - 356, 1981.

Dziewonski, A.M. and D.L. Anderson, Travel times and station corrections for P waves at teleseismic distances, *J. Geophys. Res.*, **88**, 3295 - 3314, 1983.

Durek, J.J., M.H. Ritzwoller and J.H. Woodhouse, Constraining upper mantle anelasticity using surface wave amplitudes, *Geophys. J. Int.*, **114**, 249 - 272, 1993.

Engdahl, E.R., R. van der Hilst and R. Buland, Global teleseismic earthquake relocation with improved travel times and procedures for depth determination, *Bull. Seismol. Soc. Am.*, **88**, 772 - 743, 1998.

Flanaghan, M.P. and D.A. Wiens, Attenuation structure beneath the Lau back arc spreading center from teleseismic S phases, *Geophys. Res. Lett*, **17**, 2117 - 2120, 1990.

Fukao Y., M. Nenbai and M. Obayashi, Subducting slabs stagnant in the mantle transition zones, *J. Geophys. Res.*, **97**, 4809 - 4822, 1992.

Grand, S.P., Tomographic inversion for shear velocity beneath the North American Plate, *J. Geophys. Res.*, **92**, 14065 - 14090, 1987.

Gutenberg, B. and C.F. Richter, Advantages of using geocentric latitude in calculating distances, *Beitr. Geophys.*, **40**, 380, 1933.

Gutenberg, B. and C.F. Richter, Magnitude and energy of earthquakes, *Annali Geofis.*, **9**, 1, 1956.

Haddon, R.A. and E.S. Hysebye, Joint interpretation of P-wave travel time and amplitude anomalies in terms of lithospheric heterogeneities, *Geophys. J. R. astr. Soc.*, **55**, 19 - 43, 1978.

Hager, B.H. and R.W. Clayton, Constraints on the structure of mantle convection using seismic observations, flow models, and the geoid, in *Mantle Convection* (ed. W.R. Peltier), Gordon and Breach, New York, 657 - 763, 1989.

Herrin, E., W. Tucher, J. Taggart, D.W. Gordon and J.L. Lobdell, Estimation of surface focus P travel times, *Bull. Seismol. Soc. Am.*, **58**, 1273 - 1291, 1968.

Hirahara, K., Detection of three-dimensional velocity anisotropy, *Phys. Earth Planet. Inter.*, **51**, 71 - 85, 1988.

Hirahara, K., A. Ikami, M. Ishida and T. Mikumo, Three-dimensional P-wave velocity structure beneath Central Japan: Low-velocity bodies in the wedge portion of the upper mantle above high-velocity subducting plates, *Tectonophysics*, **163**, 63 - 73, 1989.

Ho-Liu, P., H. Kanamori and R.W. Clayton, Applications of attenuation tomography to Imperial Valley and Coso-Indian Wells region, Southern California, *J. Geophys. Res.*, **93**, 10501 - 10520, 1988.

Inoue, H., Teleseismic tomography: Global modeling, in *Seismic Tomography: Theory and Practice*, (ed. H.M. Iyer and K. Hirahara), Chapman and Hall, London, 133 - 162, 1993

Inoue, H., Y. Fukao, K. Tanabe and Y. Ogata, Whole mantle P-wave travel time tomography, *Phys. Earth Planet. Inter.*, **59**, 294 - 328, 1990.

Jackson, I., M.S. Paterson and J.D. FitzGerald, Seismic wave dispersion and attenuation in Aheim dunite: An experimental study, *Geophys. J. Int.*, **108**, 517 - 534, 1992.

Jeffreys, H., An alternative to the rejection of observations, *Proc. Roy. Soc. London*, A, **137**, 78 - 87, 1932.

Jeffreys, H., *Theory of Probability*, Oxford Univ. Press, Oxford, 1939.

Jeffreys, H. and K.E. Bullen, *Seismological Tables*, British Association for the Advancement of Science, London, 1940.

Kampfmann, W. and H. Berckhemer, High temperature experiments on the elastic and anelastic behavior of magmatic rocks, *Phys. Earth Planet. Inter.*, **40**, 223 - 247, 1985.

Kaneshima, S., Shear-wave splitting induced by seismic anisotropy in the Earth, *J. Seismol. Soc. Jpn.*, **44**, Special issue, 71 - 83, 1991 (in Japanese with English abstract).

Kennett, B.L.N., *Seismic Wave Propagation in Stratified Media*, Cambridge Univ. Press, pp. 342, 1983.

Kennett, B.L.N., *IASPEI 1991 Seismological Tables*, research School of Earth Sciences, Australian National University, pp. 167, 1991.

Kennett, B.L.N. and E.R. Engdahl, Travel times for global earthquake location and phase identification, *Geophys. J. Int.*, **105**, 429 - 465, 1991.

Kennett, B.L.N., E.R. Engdahl and R. Buland, Constraints on seismic velocities in the Earth from traveltimes, *Geophys. J. Int.*, **122**, 108 - 124, 1995.

Kennett, B.L.N. and O. Gudmundsson, Ellipticity corrections for seismic phases, *Geophys. J. Int.*, **127**, 40 - 48, 1996.

Kennett, B.L.N., S. Widiyantoro and R.D. van der Hilst, Joint seismic tomography for bulk and shear wave speed in the Earth's mantle, *J. Geophys. Res.*, **103**, 12469 - 12493, 1998.

Koketsu, K. and S. Sekine, Pseudo-bending method for three-dimensional seismic ray tracing in a spherical earth with discontinuities, *Geophys. J. Int.*, **132**, 339 - 346, 1998.

Lanczos, C., An iteration method for the solution of the eigenvalue problem of linear differential and integral operators, *J. Res. N. B. S.*, **45**, 255 -5282, 1950.

Lees, J.M. and R.S. Crosson, Tomographic inversion for three-dimensional velocity structure at Mount St. Helens using earthquake data, *J. Geophys. Res.*, **94**, 5716 - 5728, 1989.

Masters, G., T.H. Jordan and P.G. Silver, Aspherical Earth structure from fundamental spheroidal mode data, *Nature*, **298**, 609 - 613, 1982.

Menke, W., *Geophysical Data Analysis: Discrete Inverse Theory (Revised ed.)*, Academic Press, London, pp. 289, 1989.

Mikami, N. and K. Hirahara, Global distribution of long-period P-wave attenuation and its tectonic implications, *J. Phys. Earth*, **29**, 97 - 117, 1981.

Mikumo, T., Long-period P waveforms and the source mechanism of intermediate earthquakes, *J. Phys. Earth*, **17**, 169 - 192, 1969.

Minster, J.B. and T.H. Jordan, Present-day plate motions, *J. Geophys. Res.*, **83**, 5331 - 5354, 1978.

Minster, J.B. and D.L. Anderson, A model of dislocation-controlled rheology for the mantle, *Philos. Trans. R. Soc. London*, A, **299**, 319 - 356, 1981.

Montagner, J.P. and B.L.N. Kennett, How to reconcile body-wave and normal mode reference Earth models ?, *Geophys. J. Int.*, **125**, 229 - 248, 1996.

Mooney, W.D., G. Laske and T.G. Masters, CRUST 5.1: A global crustal model at 5° x 5°, *J. Geophys. Res.*, **103**, 727 - 747, 1998.

Morelli, A. and A.M. Dziewonski, Body wave traveltimes and a spherically symmetric P- and S-wave velocity model, *Geophys. J. Int.*, **112**, 178 - 194, 1993.

Nakagawa, T. and Y. Oyanagi, *Experimental Data Analysis by least squares method*, Tokyo Univ. Press, pp. 206, 1982 (in Japanese).

Nakanishi, I., Attenuation of multiple ScS waves beneath the Japanese Arc., *Phys. Earth Planet. Inter.*, **19**, 337 - 347, 1979.

Nakanishi, I., Three-dimensional structure beneath the Hokkaido-Tohoku region as derived from a tomographic inversion of P-arrival times, *J. Phys. Earth*, **33**, 241 - 256, 1985.

Nakanishi, I. and D. Suetsugu, Resolution matrix calculated by a tomographic inversion method, *J. Phys. Earth*, **34**, 95 - 99, 1986.

Nakanishi, I. and Y. Motoya, Teleseismic P-wave travel time and amplitude anomalies observed in Hokkaido region, Japan, *J. Phys. Earth*, **38**, 163 - 177, 1990.

Negishi, H., Velocity heterogeneity in the crust around Hida mountains range, *Chikyu monthly*, **18**, 85 - 91, 1996 (in Japanese).

Negishi, H., 3D Q-tomography by using grid model formulation and application to the source region of the 1995 Kobe earthquake, *Fall meet. Prog. Abstr. Seismol. Soc. Jpn.*, P99, 1998 (in Japanese).

Negishi, H. and T. Sato, Amplitude and arrival time fluctuations of teleseismic P waves observed in northern part of Tohoku region, Japan, *J. Seismol. Soc. Jpn.*, **46**, 297 - 308, 1993 (in Japanese with English abstract).

Nishizawa, O, H. Noro and K. Masuda, A new method of tomography by means of bootstrap statistics I (method) - Algorithm based on EIC (Extended Information Criterion)-, *Bull. Geol. Surv. Japan*, **45**, 1 - 14, 1994 (in Japanese with English abstract).

Nishizawa, O. and H. Noro, Bootstrap statistics for velocity tomography: Application of a new information criterion, *Geophys. Prospec.*, **43**, 157 - 176, 1995.

Nolet, G., Seismic wave propagation and seismic tomography, in *Seismic Tomography*, (ed. G. Nolet), Reidel, Dordrecht, 1-23, 1987.

Obayashi, M., T. Sakurai and Y. Fukao, Comparison of recent tomographic models, *Abstract of Ocean Hemisphere Project Internal Symposium*, 29, 1997.

Ødegaard, E. and D.J. Doornbos, Seismic diffraction tomography of array data, *J. Geophys. Res.*, **98**, 4377 - 4388, 1993.

Paige, CC. and M.A. Saunders, LSQR: An algorithm for sparse linear equations and sparse least squares, *ACM Trans. Math. Softw.*, **8**, 43 - 71, 1982.

Pulliam, R.J., D.W. Vasco and L.R. Johnson, Tomographic inversions for mantle P wave velocity structure based on the minimization of l^2 and l^1 norms of International Seismological Center travel time residuals, *J. Geophys. Res.*, **98**, 699 - 734, 1993.

Resovsky, J.S. and M.H. Ritzwoller, Characterizing long-period seismic effects of long-wavelength elastic and anelastic models, *Geophys. J. Int.*, **117**, 365 - 393, 1994.

Richards, M.A., B.H. Hager and N.H. Sleep, Dynamically supported geoid highs over hotspots: Observation and theory, *J. Geophys. Res.*, **93**, 7690 - 7708, 1988.

Ringdal, F., Maximum-likelihood estimation of seismic magnitude, *Bull. Seismol. Soc. Am.*, **66**, 789 - 802, 1976.

Ringdal, F., P-wave amplitudes and source of scattering in m_b-observations, *J. Geophysics*, **43**, 611 - 622, 1977.

Romanowicz, B., A global tomographic model of shear attenuation in the upper mantle, *J. Geophys. Res.*, **100**, 12375 - 12394, 1995.

Romanowicz, B., G. Roult and T. Kohl, The upper mantle degree two pattern: Constraints from GEOSCOPE fundamental spheroidal mode eigenfrequency and attenuation measurements, *Geophys. Res. Lett.*, **14**, 1219 - 1222, 1987.

Sanders, C.O., Local earthquake tomography: attenuation - theory and results in *Seismic Tomography: Theory and Practice*, (ed. H.M. Iyer and K. Hirahara), Chapman and Hall, London, 676 - 694, 1993

Scherbaum, F., Combined inversion for the three-dimensional Q structure and source parameters using microearthquake spectra, *J. Geophys. Res.*, **95**, 12,423 - 12,438, 1990.

Sato, H., Scattering of seismic waves in random inhomogeneities, *J. Seismol. Soc. Jpn.*, **44**, Special issue, 85 - 97, 1991 (in Japanese with English abstract).

Sipkin, S.A. and T.H. Jordan, Regional variations of Q_{ScS}, *Bull. Seismol. Soc. Am.*, **70**, 1071 - 1102, 1980.

Silver, P.G. and W.W. Chan, Implications for continental structure and evolution from seismic anisotropy, *Nature*, **335**, 34 - 39.

Sekiguchi, S., Amplitude distribution of seismic waves for laterally heterogeneous structures including a subductiing slab, *Geophys. J. Int.*, **111**, 448 - 464, 1992.

Solomon, S.C. and M.N. Toksöz, Lateral variation of attenuation of P and S waves beneath the United States, *Bull. Seismol. Soc. Am.*, **60**, 819 - 838, 1970.

Stewart, I.C.F, A procedure for detecting lateral variations of P-wave attenuation in the lower mantle, *Phys. Earth Planet. Inter.*, **26**, 198 - 207, 1981.

Suda, N., N. Shibata and Y. Fukao, Degree-2 pattern of attenuation structure in the upper mantle from apparent complex frequency measurements of fundamental spheroidal modes, *Geophys. Res. Lett.*, **18**, 1119 - 1122, 1991.

Suetsugu, D. and I. Nakanishi, Three-dimensional velocity map of the upper mantle beneath the Pacific Ocean as determined from Rayleigh wave dispersion, *Phys. Earth Planet. Inter.*, **47**, 205 - 229, 1987.

Tajima, F. and S.P. Grand, Variation of transition zone high-velocity anomalies and depression of 660 km discontinuity associated with subduction zones from the southern Kuriles to Izu-Bonin and Ryukyu, *J. Geophys. Res.*, **103**, 15015 - 15036, 1998.

Tarantora, A. and B. Valette, Generalized nonlinear inverse problems solved using the least squares criterion, R*ev. Geophys. Space Phys.*, **20**, 219 - 232, 1982.

Teng, T.L., Attenuation of body waves and the Q structure of the mantle, *J. Geophys. Res.*, **73**, 2195 - 2208, 1968.

Thomson, C.J. and D. Gubbins, Three-dimensional lithospheric modeling at NORSAR: Linearity of the method and amplitude variations fro the anomalies, *Geophys. J. R. astr. Soc.*, **71**, 1 - 36, 1982.

Thurber, C.H., Earthquake locations and three-dimensional crustal structure in the Coyote Lake area, Central California, *J. Geophys. Res.*, **88**, 8226 - 8236, 1983.

Turkey, J.W., *Exploratory Data Analysis*, Addison-Wesley, 1977

Um, J. and C.H. Thurber, A fast algorithm for two-point seismic ray tracing, *Bull. Seismol. Soc. Am.*, **77**, 972 - 986, 1987.

van der Hilst, R.D., S. Widiyantoro and E.R. Engdahl, Evidence for deep mantle circulation from global tomography, *Nature*, **386**, 578 - 584, 1997.

van der Sluis, A. and H.A. van der Vorst, Numerical solution of large, sparse linear systems arising from tomographic problems, in *Seismic Tomography*, (ed. G. Nolet), Reidel, Dordrecht, 53-87, 1987

Young, C.Y. and R.W. Ward, Three-dimensional Q (super-1) model of the Coso Hot Springs known geothermal resource area, *J. Geophys. Res.*, **85**, 2459 - 2470, 1980.

Zhao, D., A. Hasegawa and S. Horiuchi, Tomographic imaging of P and S wave velocity structure beneath northeastern Japan, *J. Geophys. Res.*, **97**, 19909 - 19928, 1992.

Zhao, D., D. Christensen and H. Pulpan, Tomographic imaging of the Alaska subduction zone, *J. Geophys. Res.*, **100**, 6487 - 6504, 1995.

Zhao, D., H. Kanamori, H. Negishi and D. Wiens, Tomography of the source area of the 1995 Kobe earthquake: Evidence for fluids at the hypocenter ?, *Science*, **274**, 1891 - 1894, 1996.

Zhao, D. and H. Negishi, The 1995 Kobe earthquake: Seismic image of the source zone and its implications for the rupture nucleation, *J. Geophys. Res.*, **103**, 9967 - 9986, 1998.

Zoback, M.L. and M. Zoback, State of stress in the conterminous United States, *J. Geophys. Res.*, **85**, 6113 - 6156, 1980.

Appendix A

Azimuthal variation of log-amplitude anomalies and relative travel time residuals.

A-1 Azimuthal variation of log-amplitudes

x-axis: azimuth viewed from each station to events

y-axis: relative log-amplitude anomaly

curve: the least-square fit of equation (2.4.1)

horiz. line: the constant term A_0 of equation (2.4.1)

A-2 Azimuthal variation of travel times

x-axis: azimuth viewed from each station to events

y-axis: relative travel time residuals

curve: the least-square fit of equation (2.4.1)

horiz. line: the constant term A_0 of equation (2.4.1)

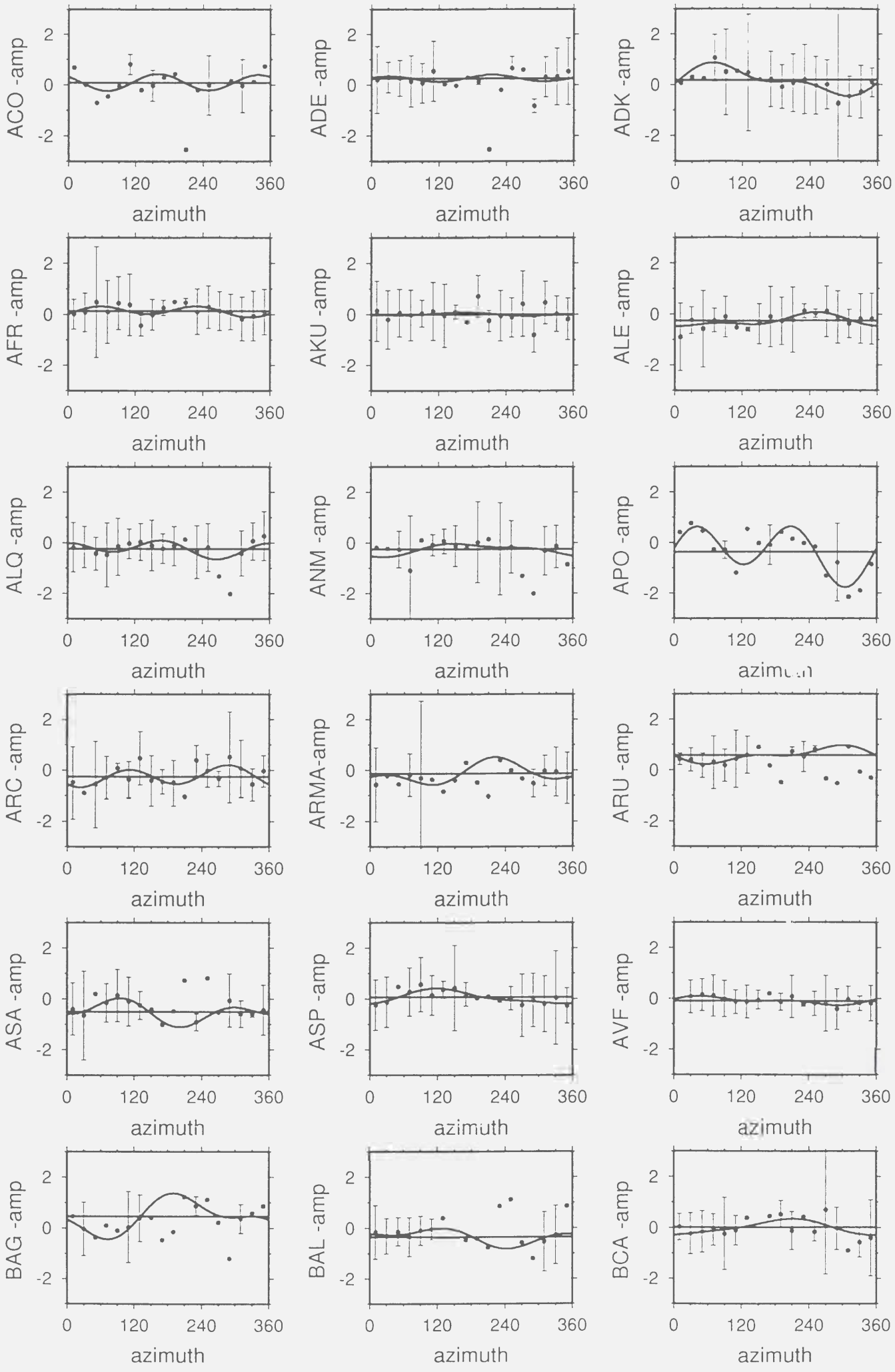
ACO -amp
ADE -amp
ADK -amp
AFR -amp
AKU -amp
ALE -amp
ALQ -amp
ANM -amp
APO -amp
ARC -amp
ARMA-amp
ARU -amp
ASA -amp
ASP -amp
AVF -amp
BAG -amp
BAL -amp
BCA -amp
2
0
-2
0
120
240
360
azimuth

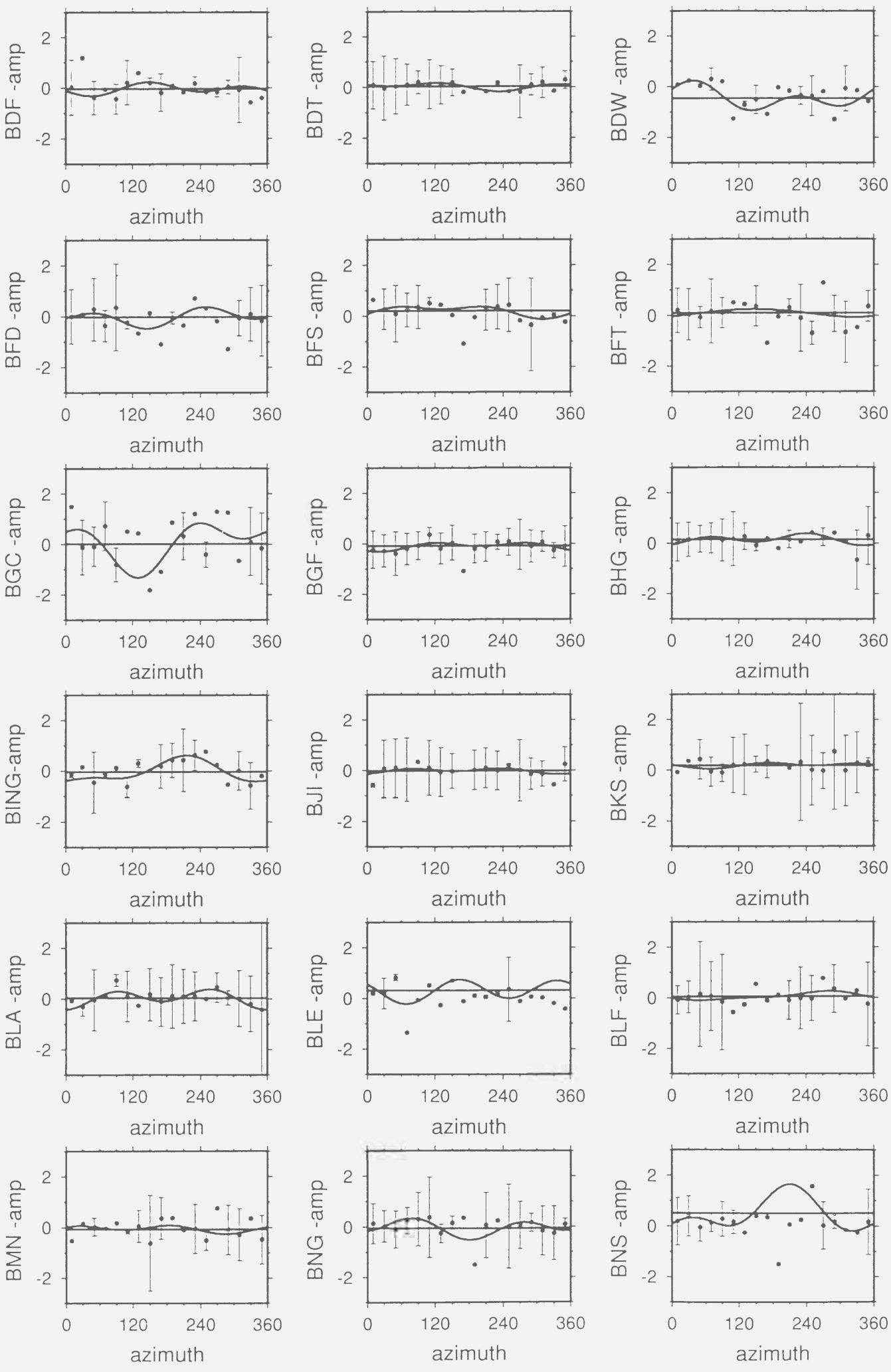
BDF -amp
BDT -amp
BDW -amp
BFD -amp
BFS -amp
BFT -amp
BGC -amp
BGF -amp
BHG -amp
BING-amp
BJI -amp
BKS -amp
BLA -amp
BLE -amp
BLF -amp
BMN -amp
BNG -amp
BNS -amp
2
0
-2
0
120
240
360
azimuth

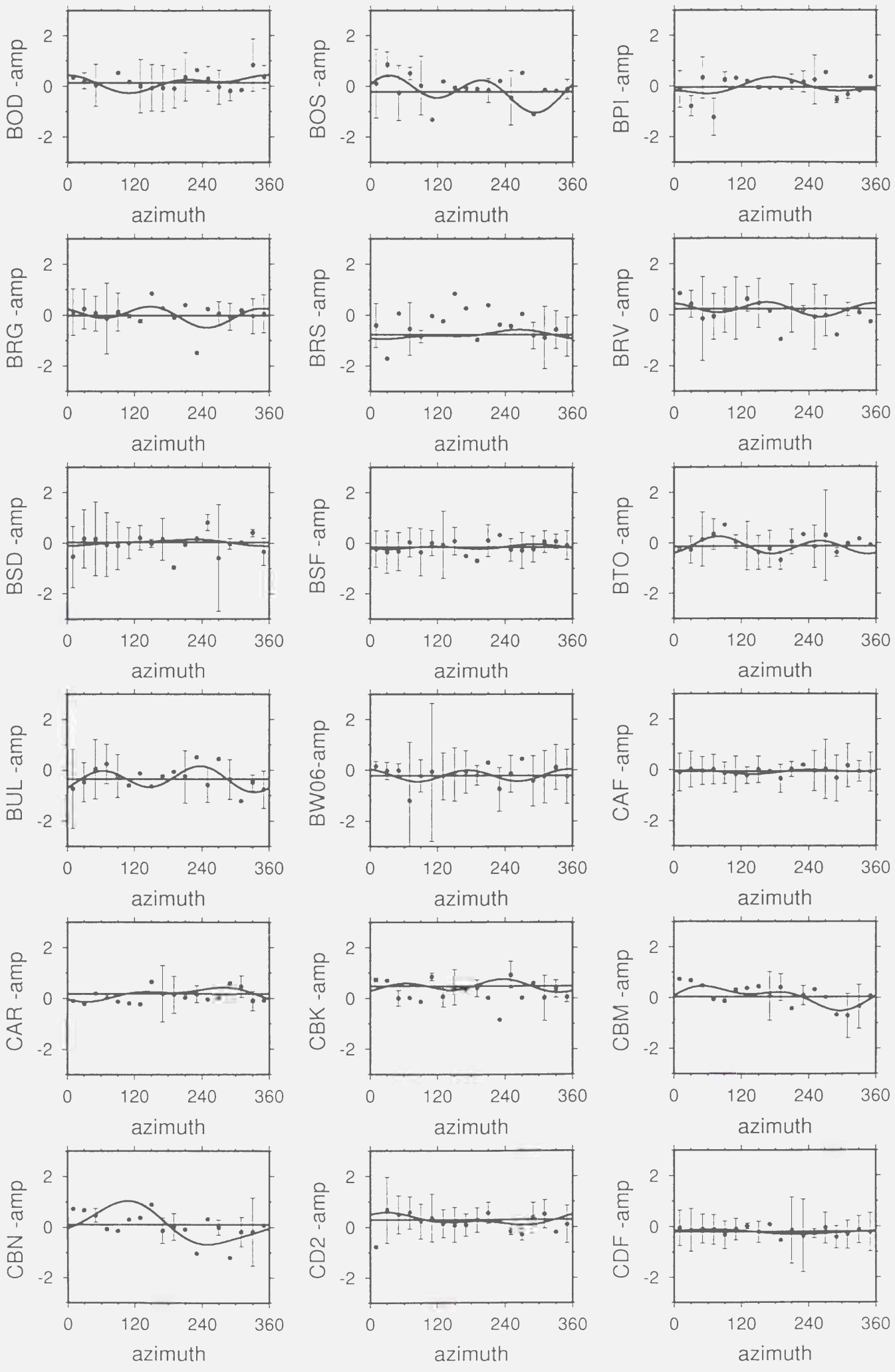
BOD -amp
BOS -amp
BPI -amp
BRG -amp
BRS -amp
BRV -amp
BSD -amp
BSF -amp
BTO -amp
BUL -amp
BW06-amp
CAF -amp
CAR -amp
CBK -amp
CBM -amp
CBN -amp
CD2 -amp
CDF -amp
2
0
-2
0
120
240
360
azimuth

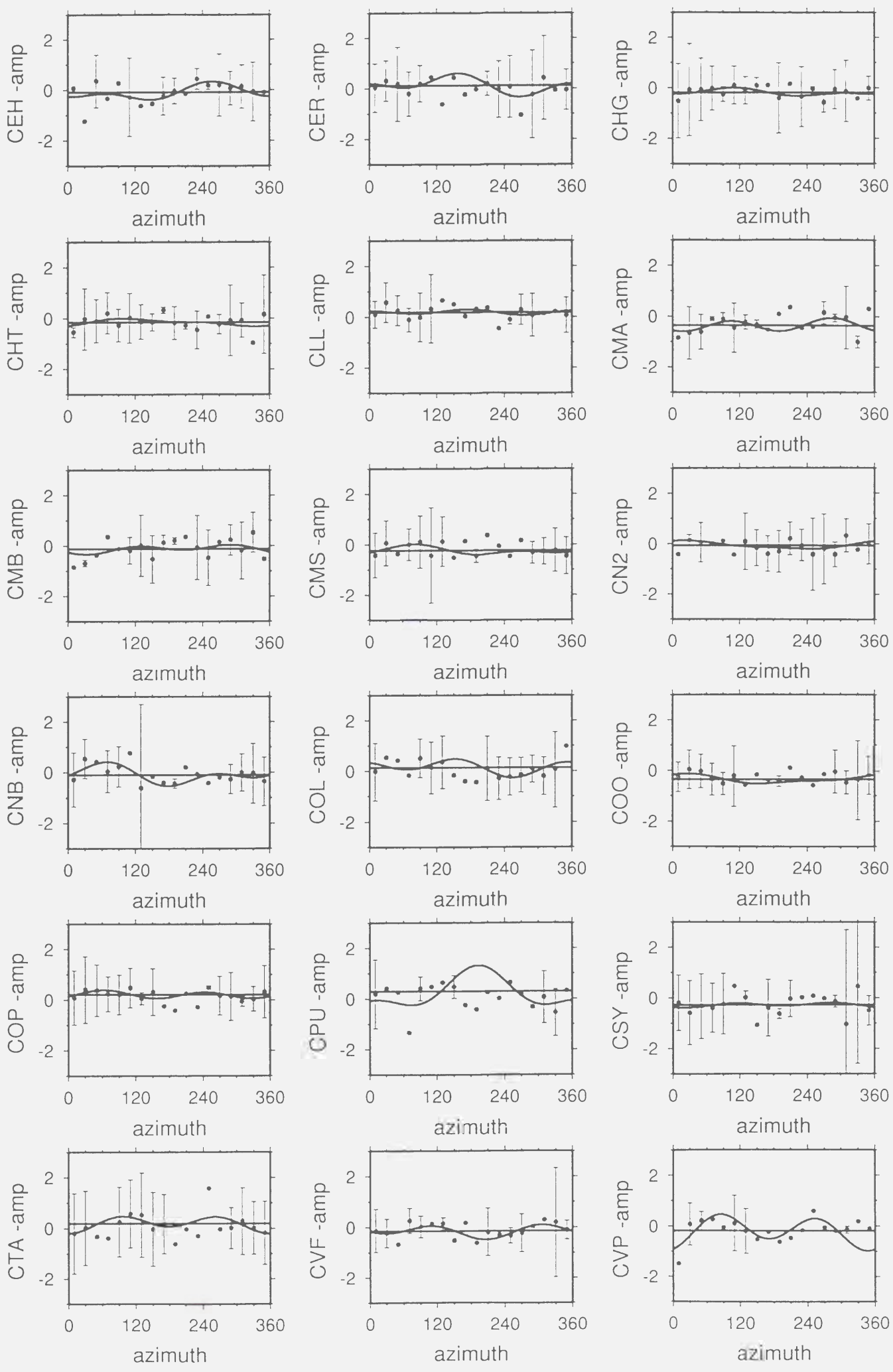
CEH -amp
CER -amp
CHG -amp
CHT -amp
CLL -amp
CMA -amp
CMB -amp
CMS -amp
CN2 -amp
CNB -amp
COL -amp
COO -amp
COP -amp
CPU -amp
CSY -amp
CTA -amp
CVF -amp
CVP -amp
azimuth
2
0
-2
0
120
240
360

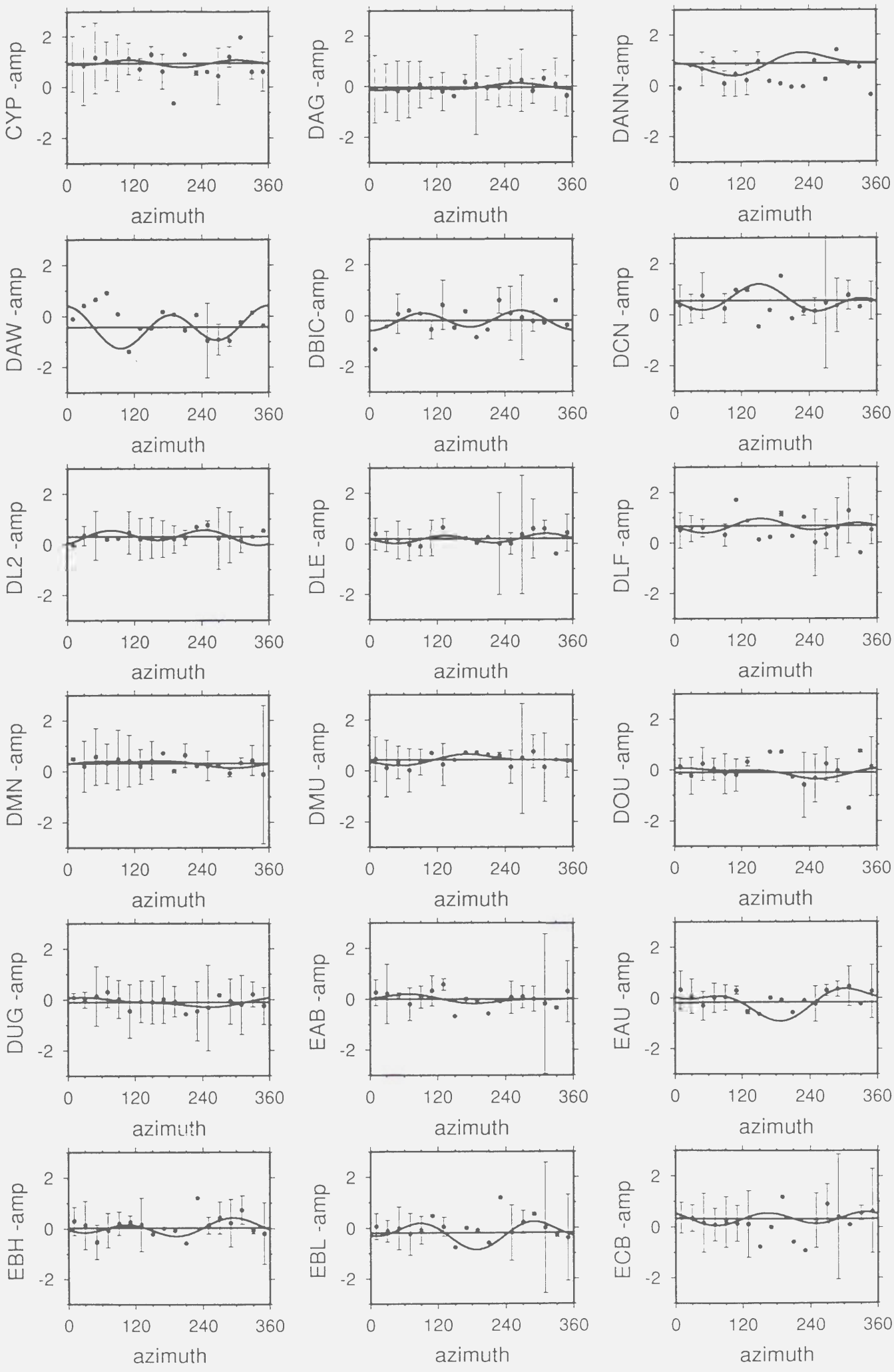
CYP -amp
DAG -amp
DANN-amp
DAW -amp
DBIC-amp
DCN -amp
DL2 -amp
DLE -amp
DLF -amp
DMN -amp
DMU -amp
DOU -amp
DUG -amp
EAB -amp
EAU -amp
EBH -amp
EBL -amp
ECB -amp
2
0
-2
0
120
240
360
azimuth

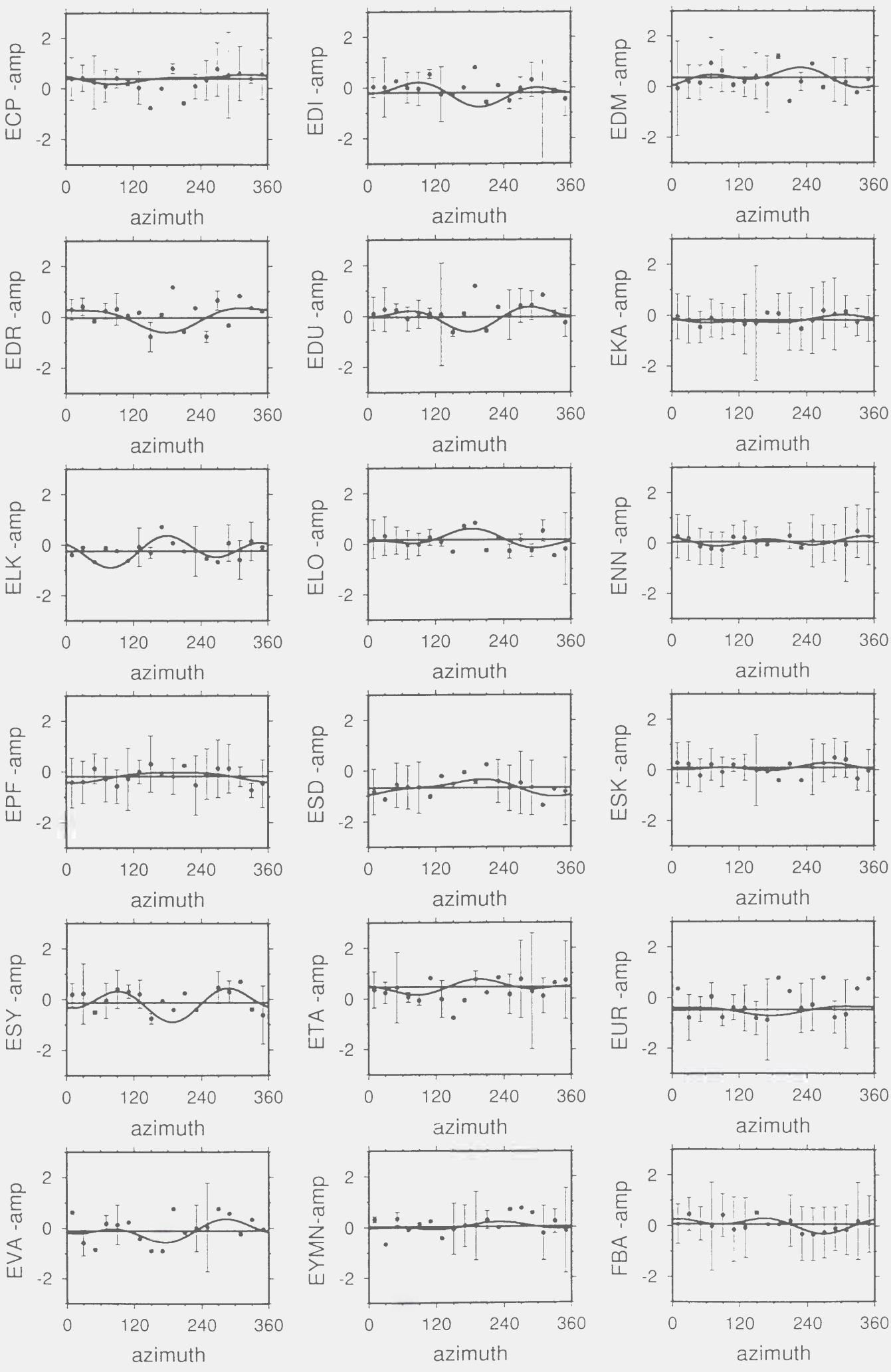
ECP -amp
EDI -amp
EDM -amp
EDR -amp
EDU -amp
EKA -amp
ELK -amp
ELO -amp
ENN -amp
EPF -amp
ESD -amp
ESK -amp
ESY -amp
ETA -amp
EUR -amp
EVA -amp
EYMN-amp
FBA -amp
azimuth
0
120
240
360
2
0
-2

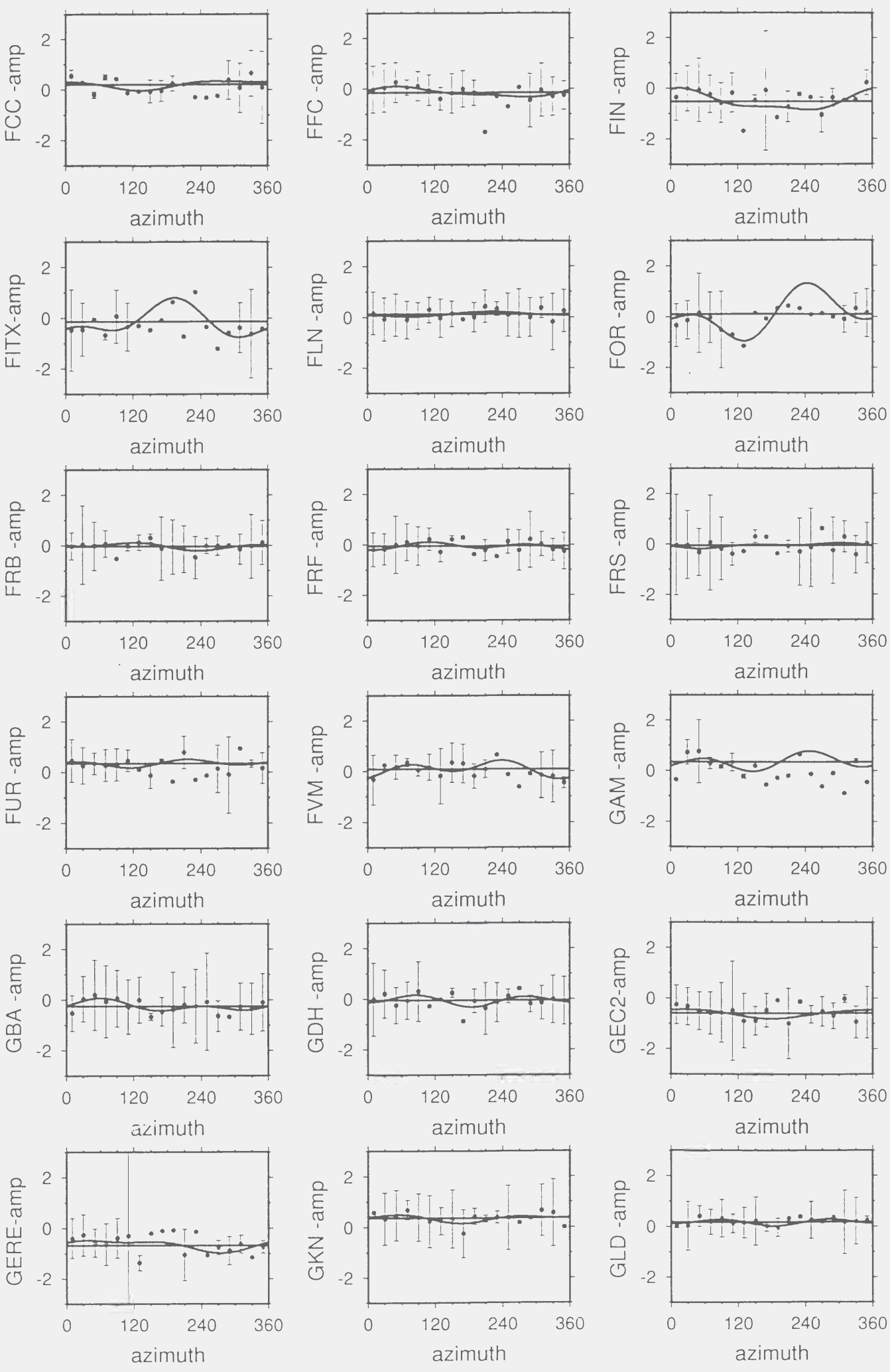
FCC -amp
FFC -amp
FIN -amp
FITX-amp
FLN -amp
FOR -amp
FRB -amp
FRF -amp
FRS -amp
FUR -amp
FVM -amp
GAM -amp
GBA -amp
GDH -amp
GEC2-amp
GERE-amp
GKN -amp
GLD -amp
2
0
-2
0
120
240
360
azimuth

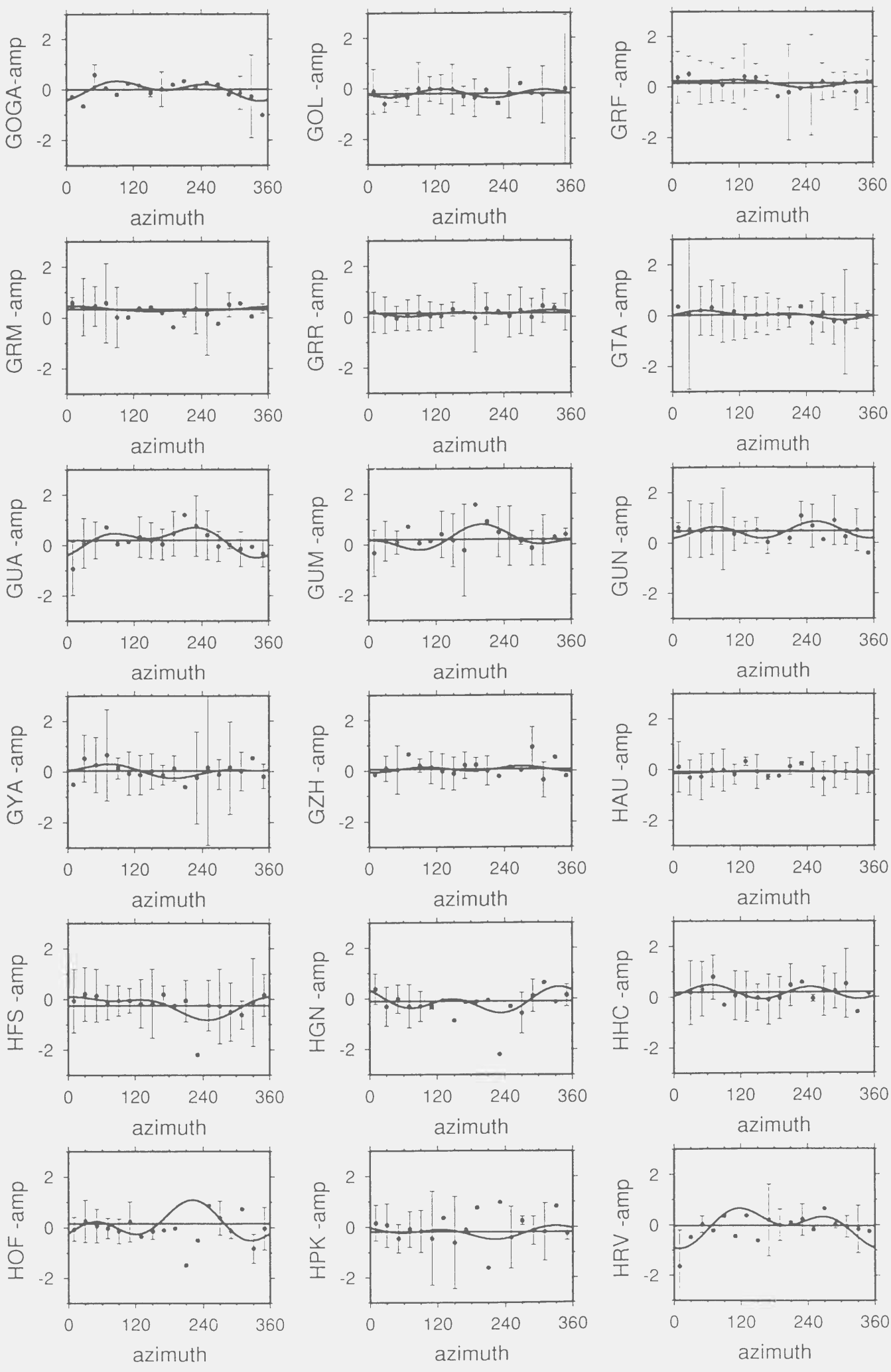
GOGA -amp
GOL -amp
GRF -amp
GRM -amp
GRR -amp
GTA -amp
GUA -amp
GUM -amp
GUN -amp
GYA -amp
GZH -amp
HAU -amp
HFS -amp
HGN -amp
HHC -amp
HOF -amp
HPK -amp
HRV -amp
2
0
-2
0
120
240
360
azimuth

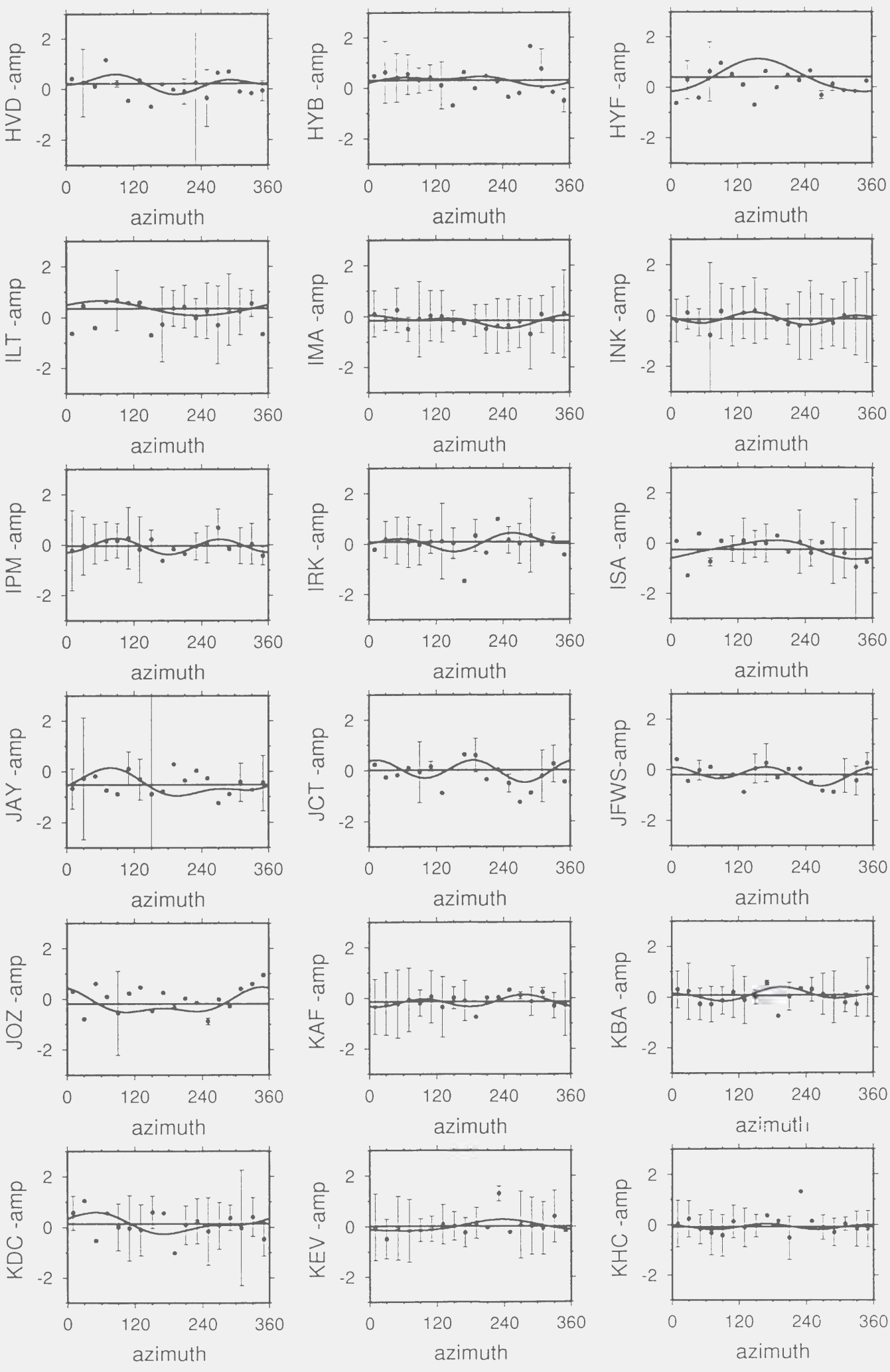
HVD -amp
HYB -amp
HYF -amp
ILT -amp
IMA -amp
INK -amp
IPM -amp
IRK -amp
ISA -amp
JAY -amp
JCT -amp
JFWS-amp
JOZ -amp
KAF -amp
KBA -amp
KDC -amp
KEV -amp
KHC -amp
2
0
-2
0
120
240
360
azimuth

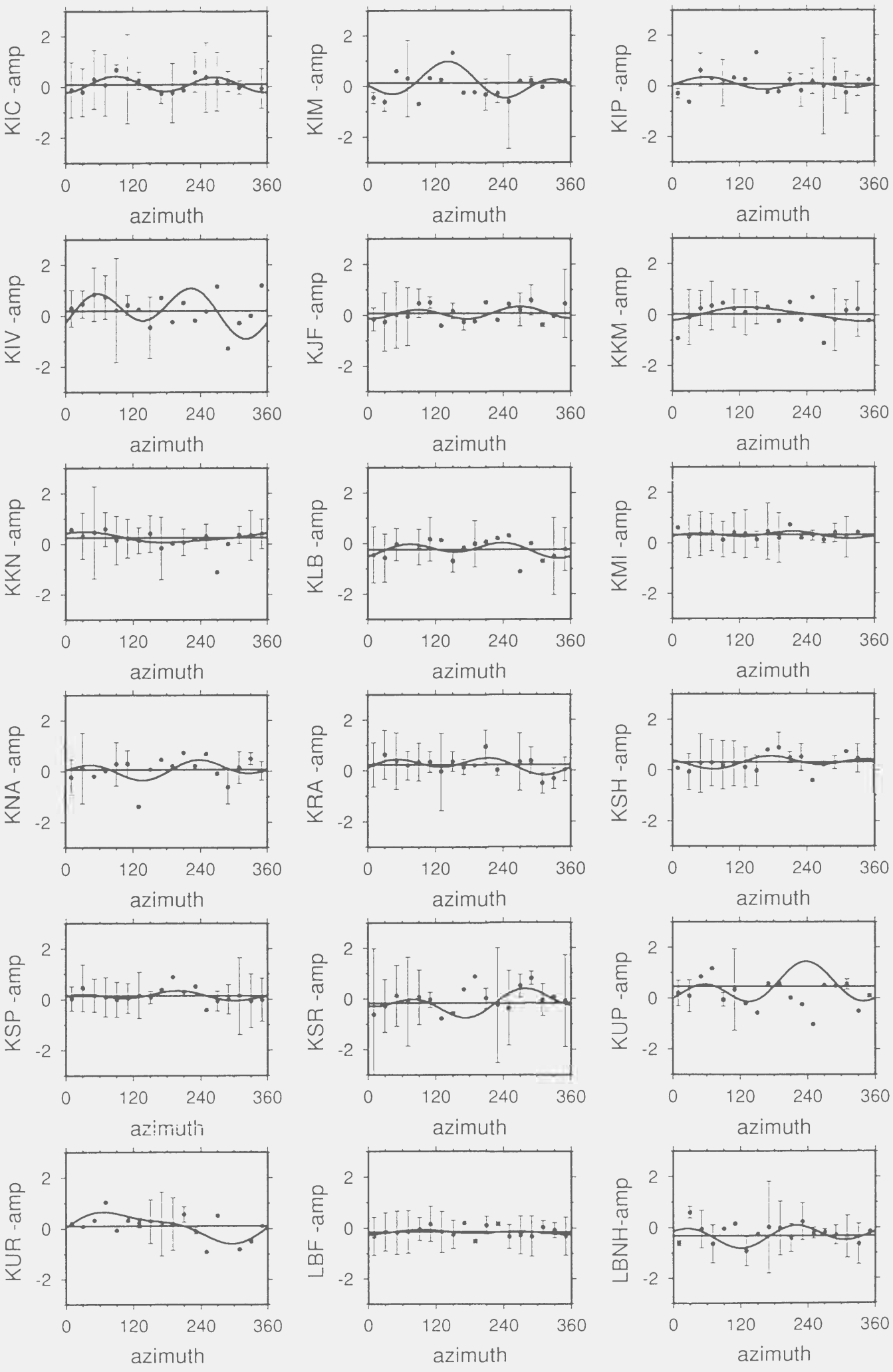
KIC -amp
KIM -amp
KIP -amp
KIV -amp
KJF -amp
KKM -amp
KKN -amp
KLB -amp
KMI -amp
KNA -amp
KRA -amp
KSH -amp
KSP -amp
KSR -amp
KUP -amp
KUR -amp
LBF -amp
LBNH-amp
2
0
-2
0
120
240
360
azimuth

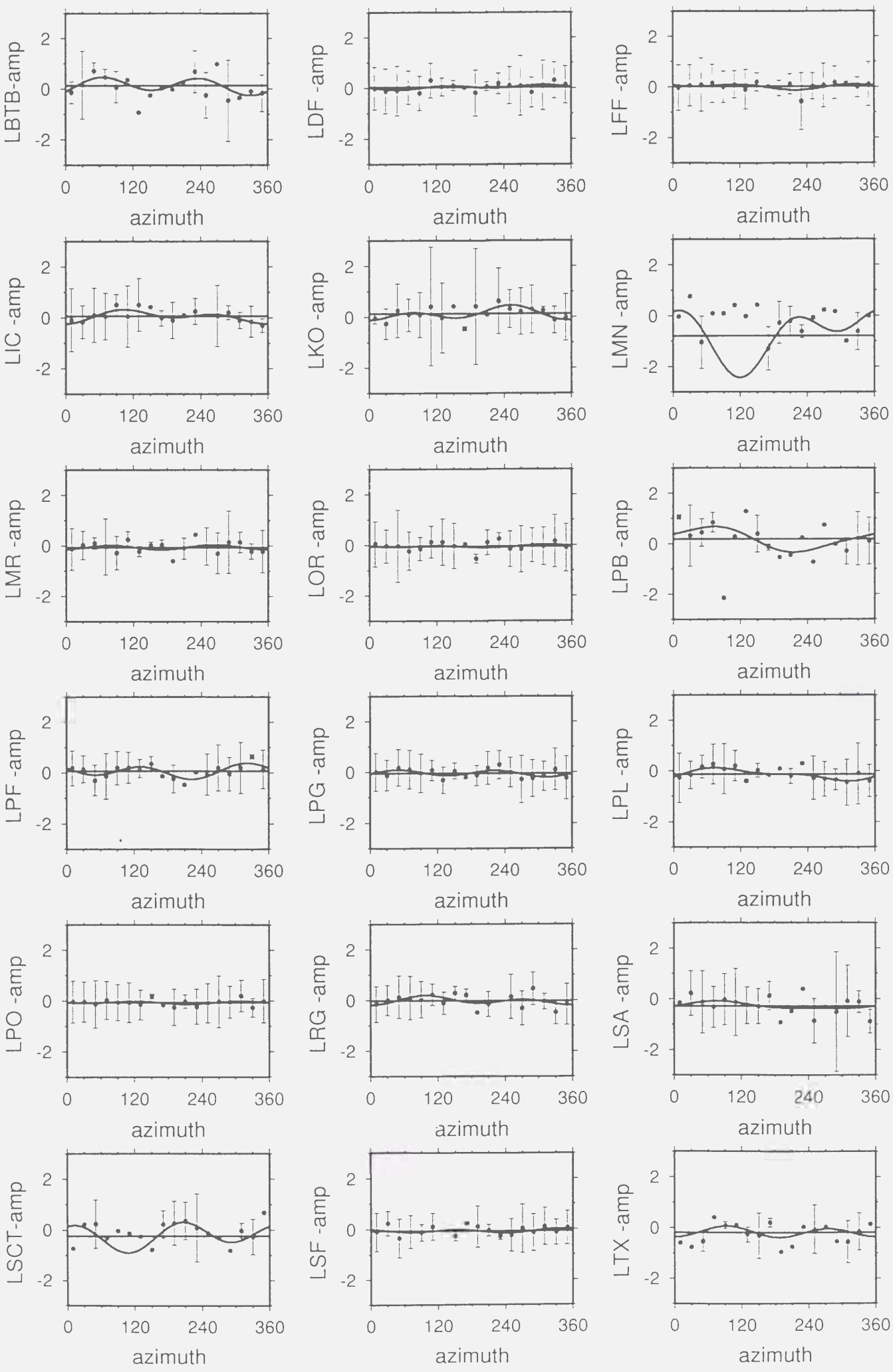
LBTB-amp
LDF -amp
LFF -amp
LIC -amp
LKO -amp
LMN -amp
LMR -amp
LOR -amp
LPB -amp
LPF -amp
LPG -amp
LPL -amp
LPO -amp
LRG -amp
LSA -amp
LSCT-amp
LSF -amp
LTX -amp
2
0
-2
0
120
240
360
azimuth

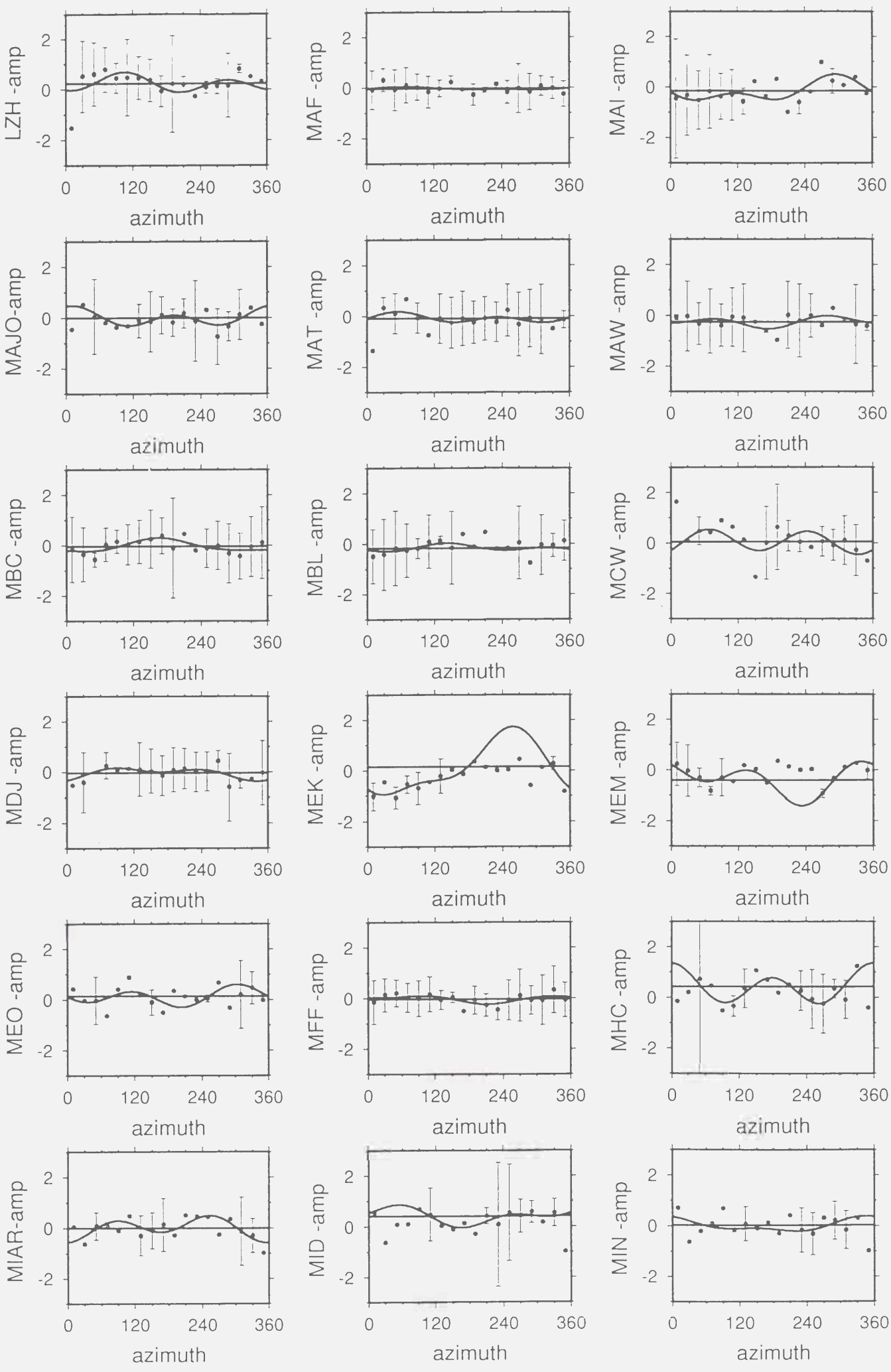
LZH -amp
MAF -amp
MAI -amp
MAJO-amp
MAT -amp
MAW -amp
MBC -amp
MBL -amp
MCW -amp
MDJ -amp
MEK -amp
MEM -amp
MEO -amp
MFF -amp
MHC -amp
MIAR-amp
MID -amp
MIN -amp
2
0
-2
0
120
240
360
azimuth

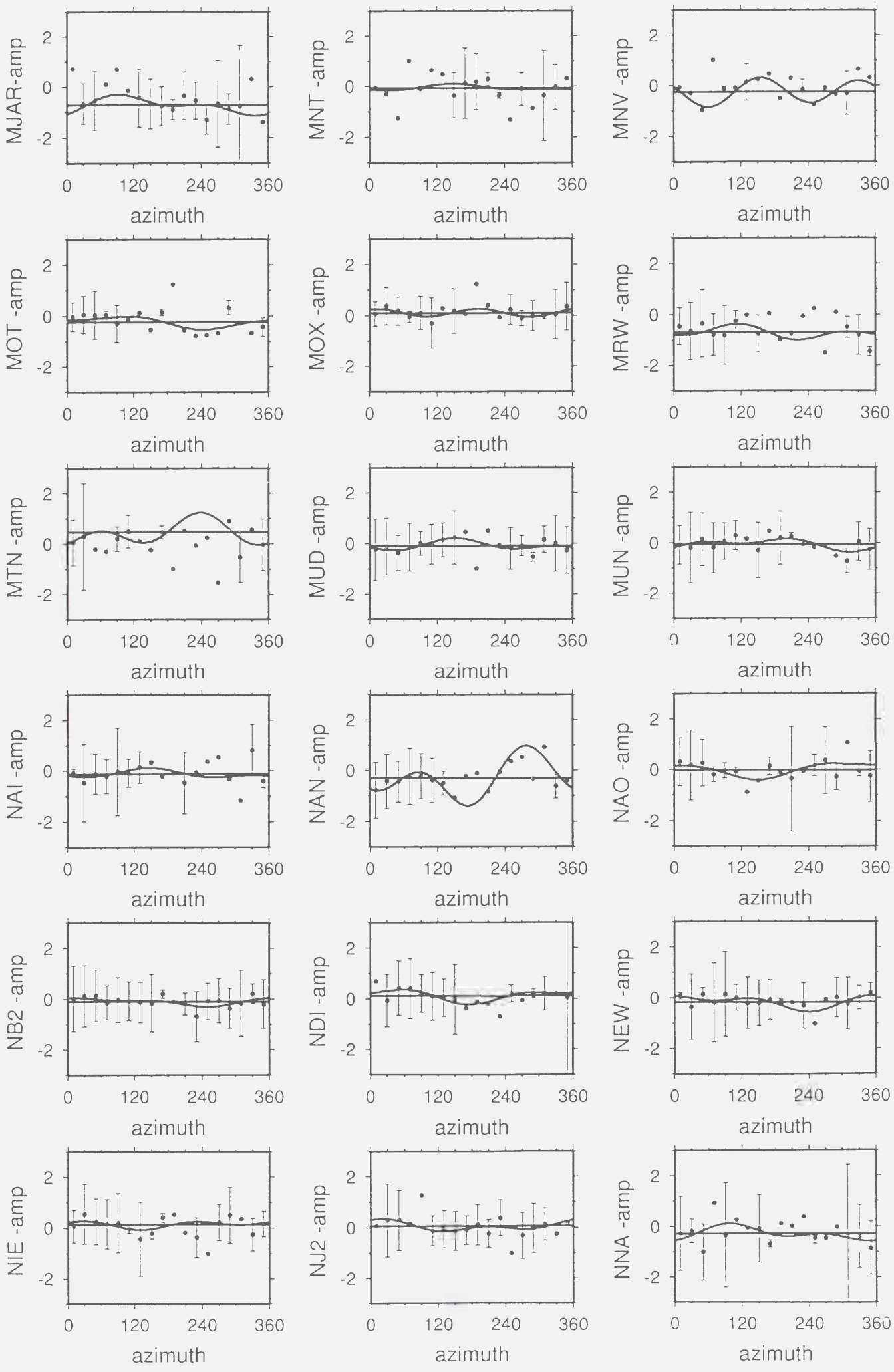
MJAR-amp
MNT -amp
MNV -amp
MOT -amp
MOX -amp
MRW -amp
MTN -amp
MUD -amp
MUN -amp
NAI -amp
NAN -amp
NAO -amp
NB2 -amp
NDI -amp
NEW -amp
NIE -amp
NJ2 -amp
NNA -amp
2
0
-2
0
120
240
360
azimuth

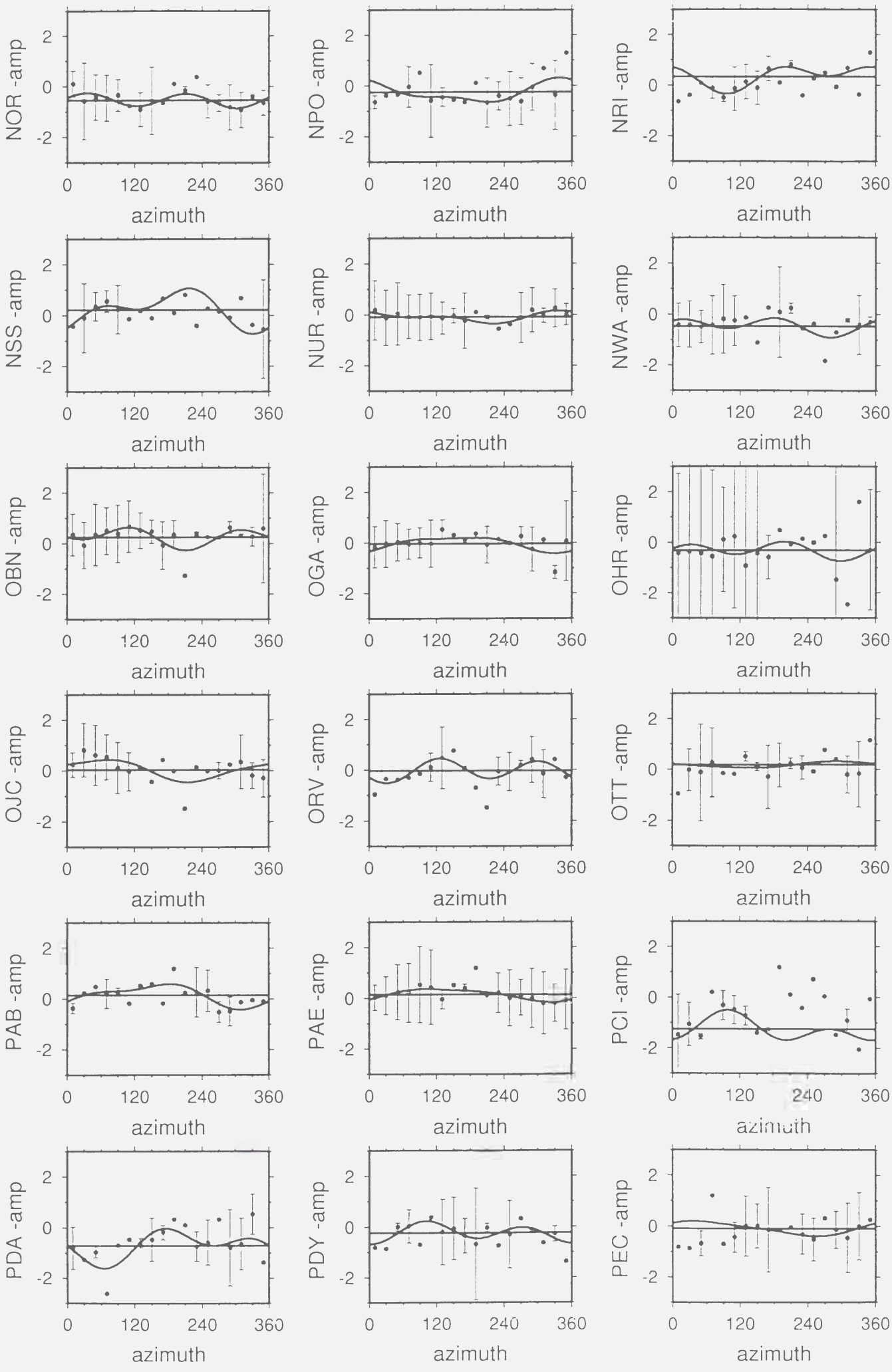
NOR -amp
NPO -amp
NRI -amp
NSS -amp
NUR -amp
NWA -amp
OBN -amp
OGA -amp
OHR -amp
OJC -amp
ORV -amp
OTT -amp
PAB -amp
PAE -amp
PCI -amp
PDA -amp
PDY -amp
PEC -amp
2
0
-2
0
120
240
360
azimuth

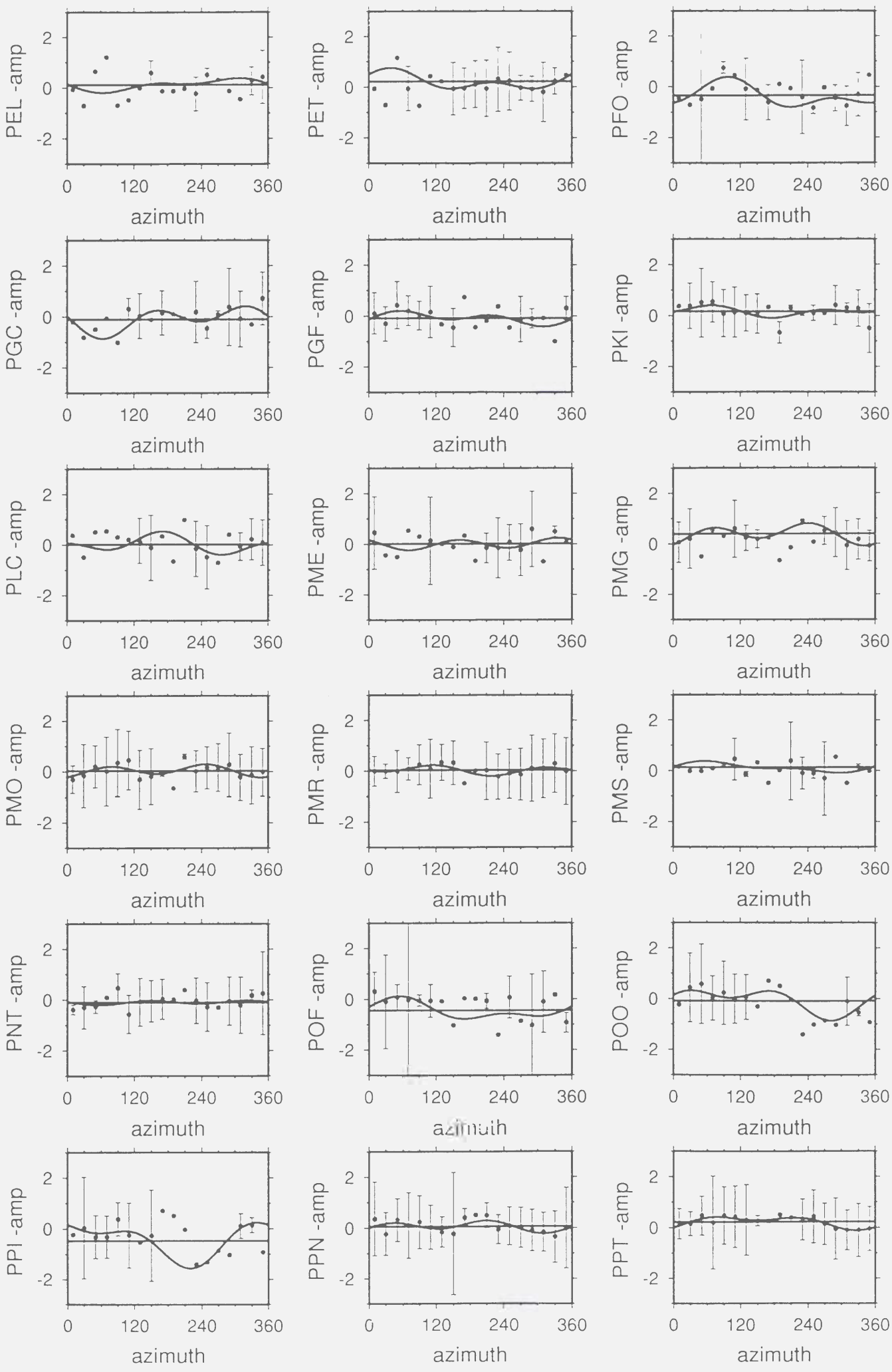
PEL -amp
PET -amp
PFO -amp
PGC -amp
PGF -amp
PKI -amp
PLC -amp
PME -amp
PMG -amp
PMO -amp
PMR -amp
PMS -amp
PNT -amp
POF -amp
POO -amp
PPI -amp
PPN -amp
PPT -amp
2
0
-2
0
120
240
360
azimuth

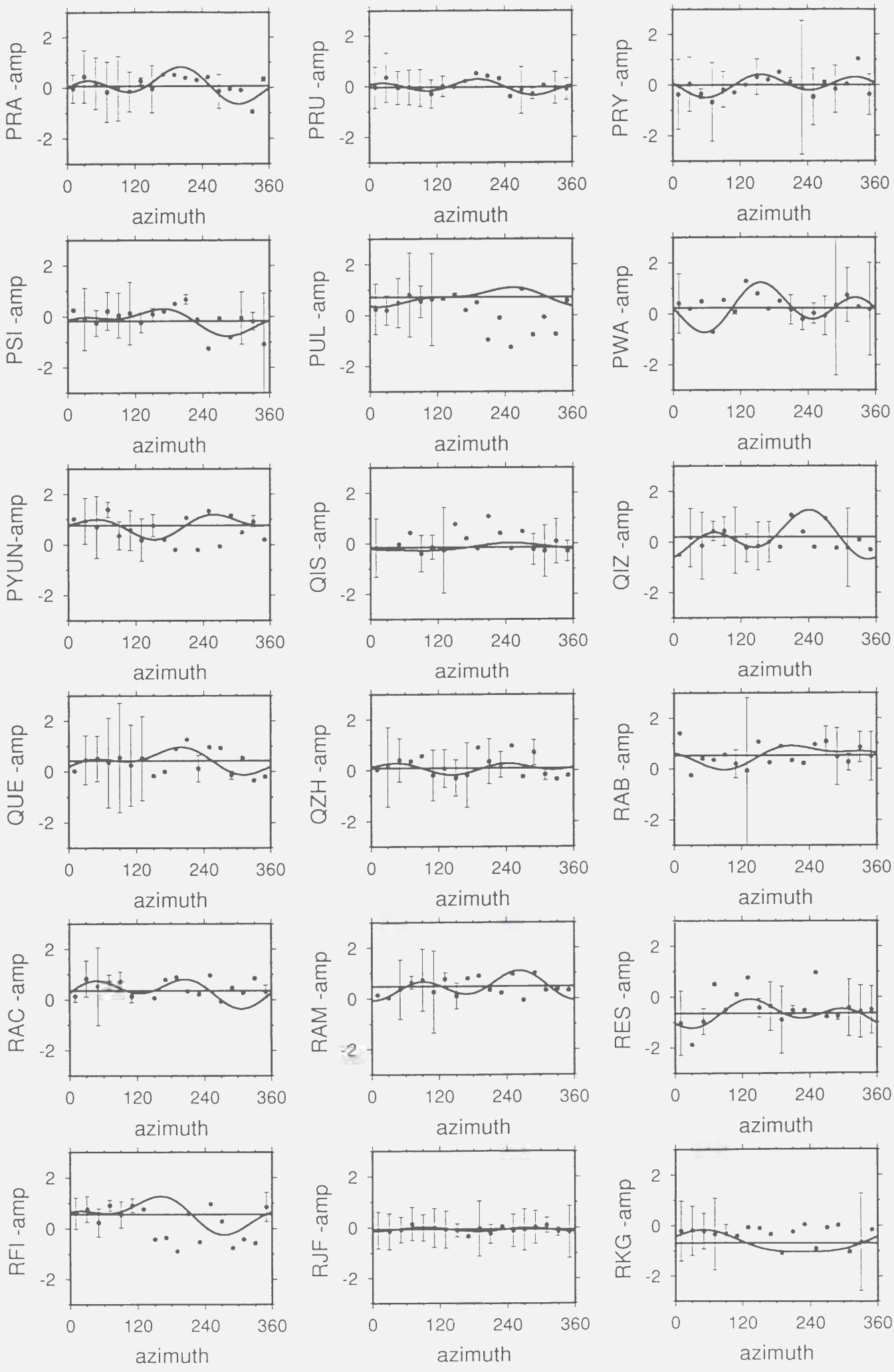
PRA -amp
PRU -amp
PRY -amp
PSI -amp
PUL -amp
PWA -amp
PYUN-amp
QIS -amp
QIZ -amp
QUE -amp
QZH -amp
RAB -amp
RAC -amp
RAM -amp
RES -amp
RFI -amp
RJF -amp
RKG -amp
azimuth
2
0
-2
0
120
240
360

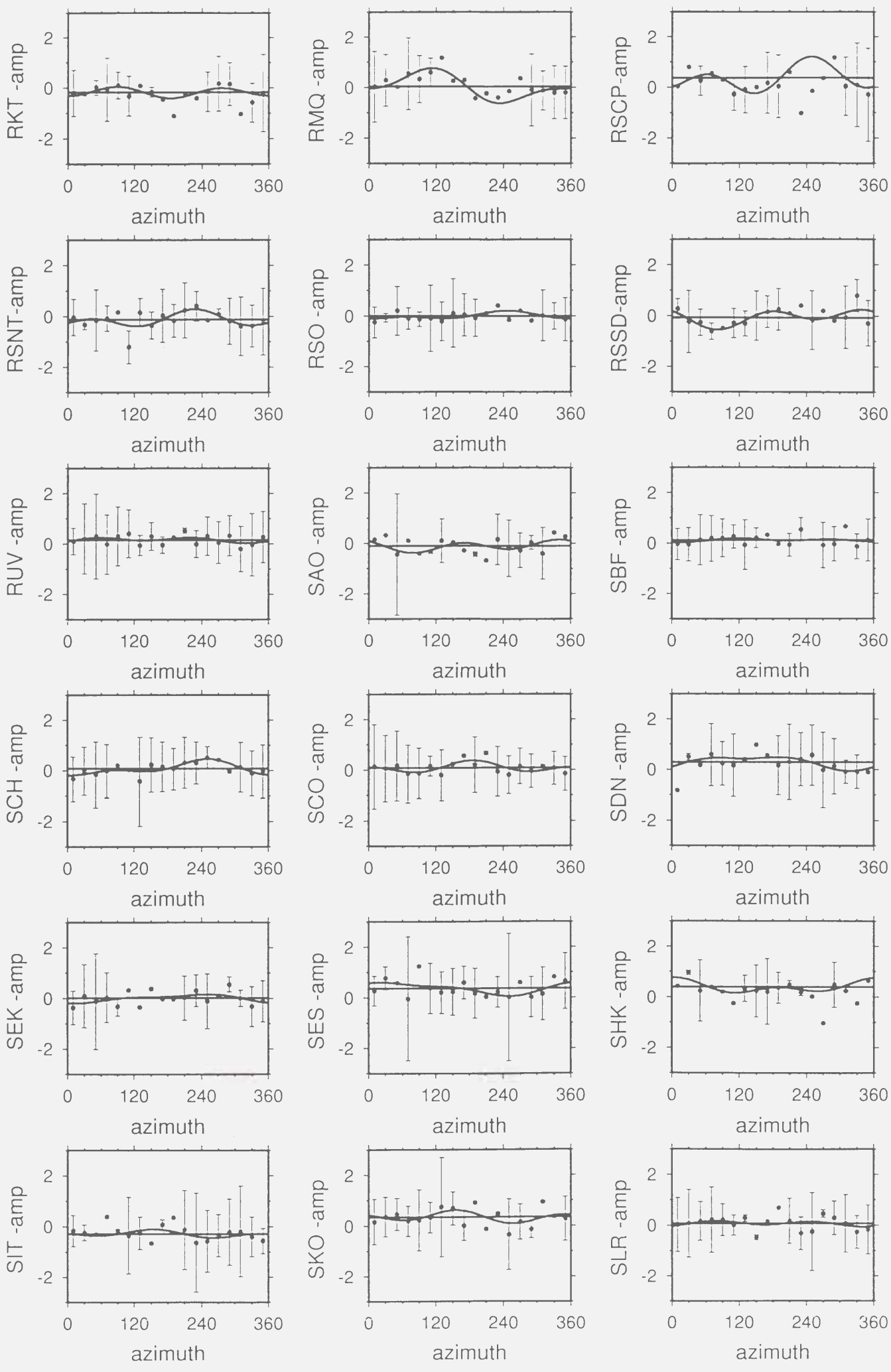
RKT -amp
RMQ -amp
RSCP-amp
RSNT-amp
RSO -amp
RSSD-amp
RUV -amp
SAO -amp
SBF -amp
SCH -amp
SCO -amp
SDN -amp
SEK -amp
SES -amp
SHK -amp
SIT -amp
SKO -amp
SLR -amp
2
0
-2
0
120
240
360
azimuth

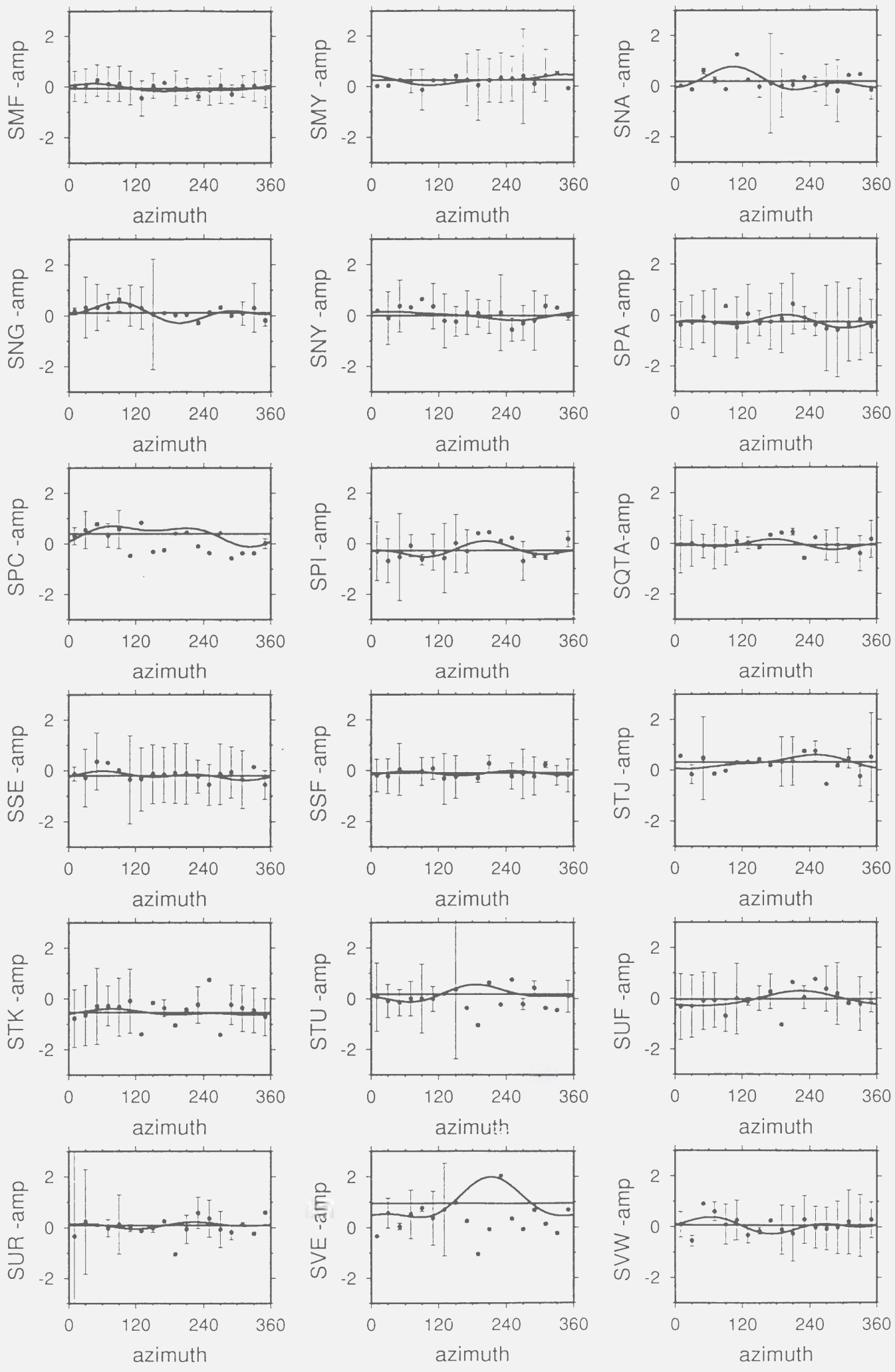
SMF -amp
SMY -amp
SNA -amp
SNG -amp
SNY -amp
SPA -amp
SPC -amp
SPI -amp
SQTA-amp
SSE -amp
SSF -amp
STJ -amp
STK -amp
STU -amp
SUF -amp
SUR -amp
SVE -amp
SVW -amp
2
0
-2
0
120
240
360
azimuth

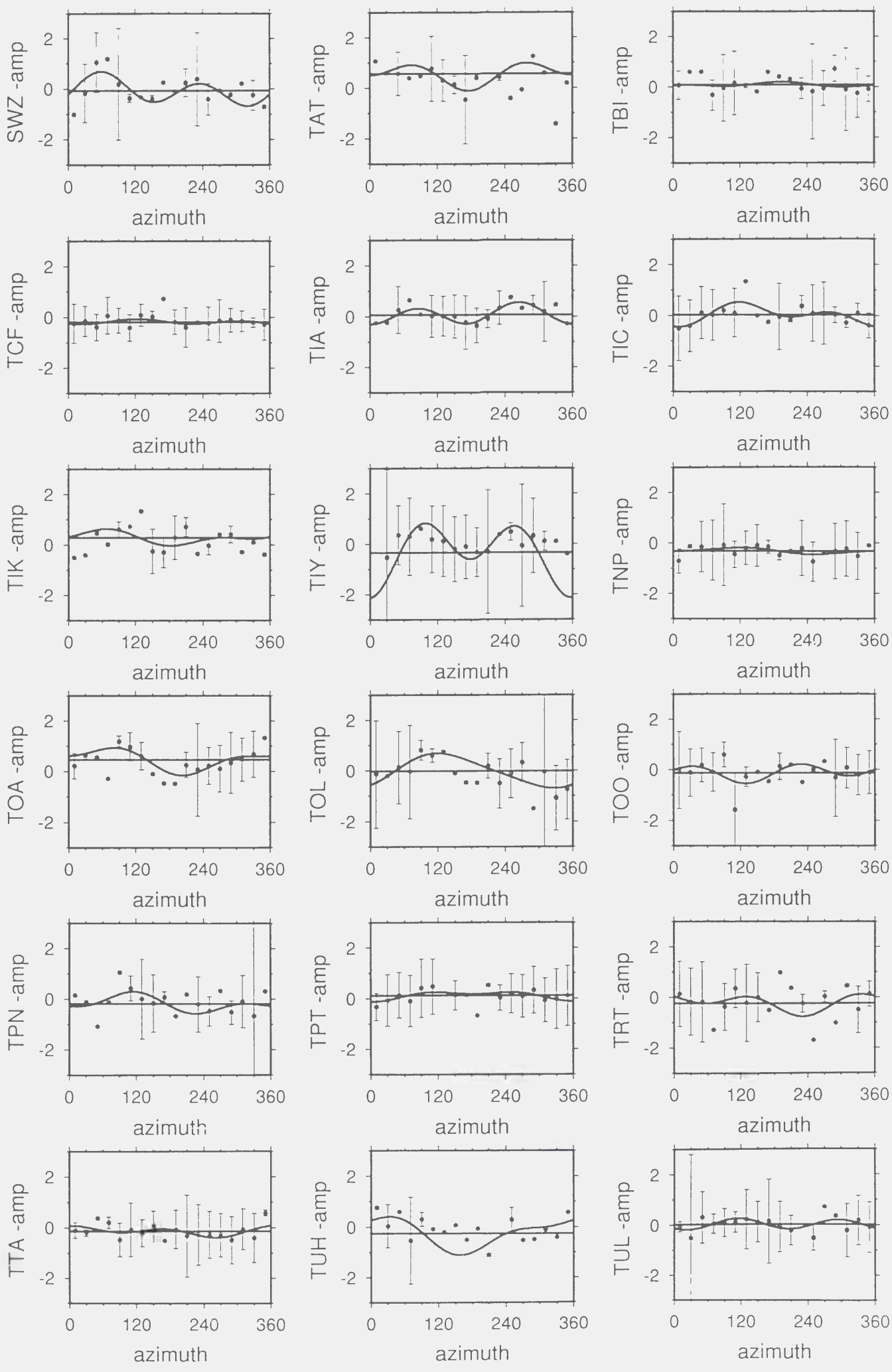
SWZ -amp
TAT -amp
TBI -amp
TCF -amp
TIA -amp
TIC -amp
TIK -amp
TIY -amp
TNP -amp
TOA -amp
TOL -amp
TOO -amp
TPN -amp
TPT -amp
TRT -amp
TTA -amp
TUH -amp
TUL -amp
azimuth
2
0
-2
0
120
240
360

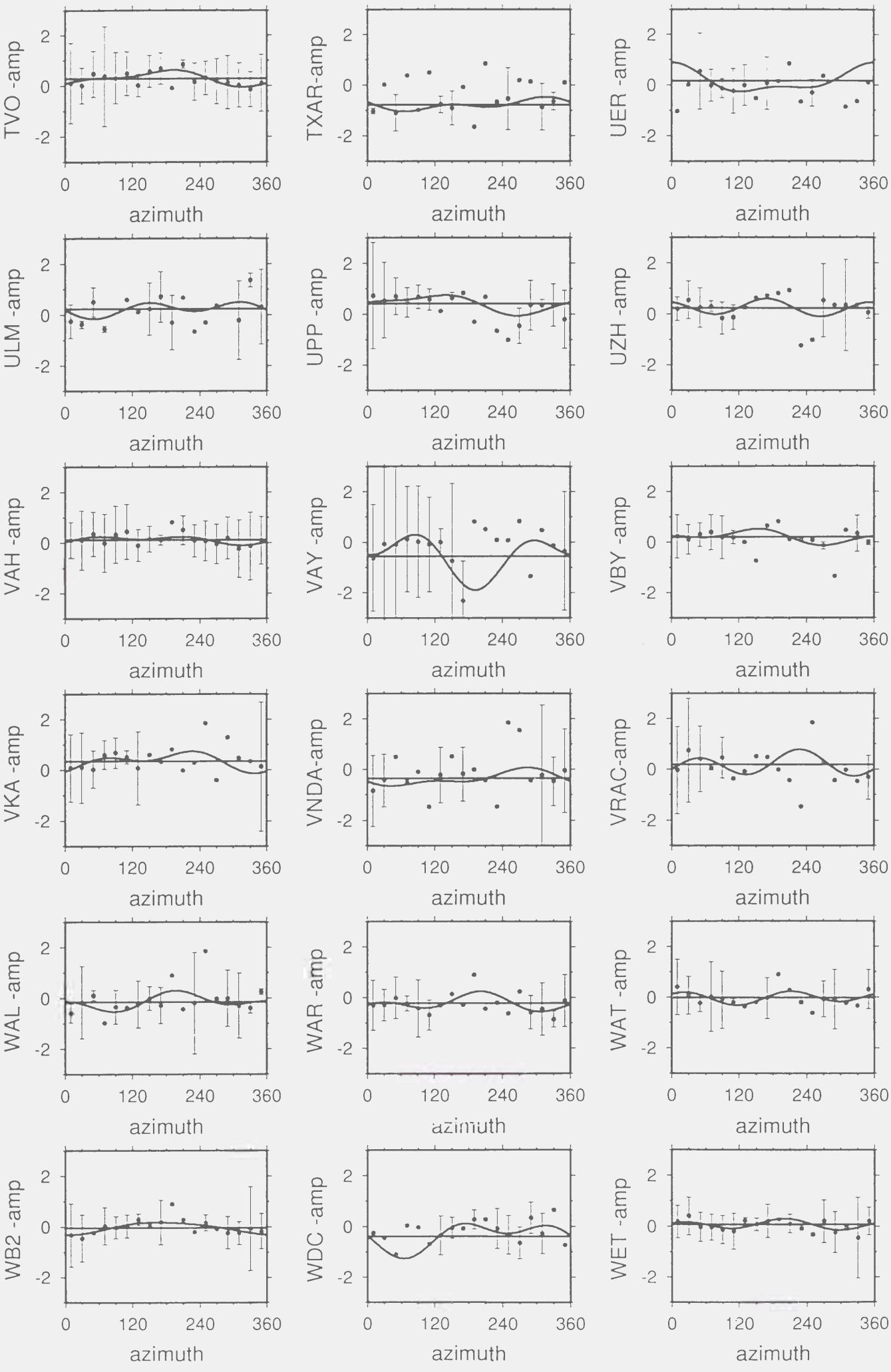
TVO -amp
TXAR-amp
UER -amp
ULM -amp
UPP -amp
UZH -amp
VAH -amp
VAY -amp
VBY -amp
VKA -amp
VNDA-amp
VRAC-amp
WAL -amp
WAR -amp
WAT -amp
WB2 -amp
WDC -amp
WET -amp
azimuth
0
120
240
360
2
0
-2

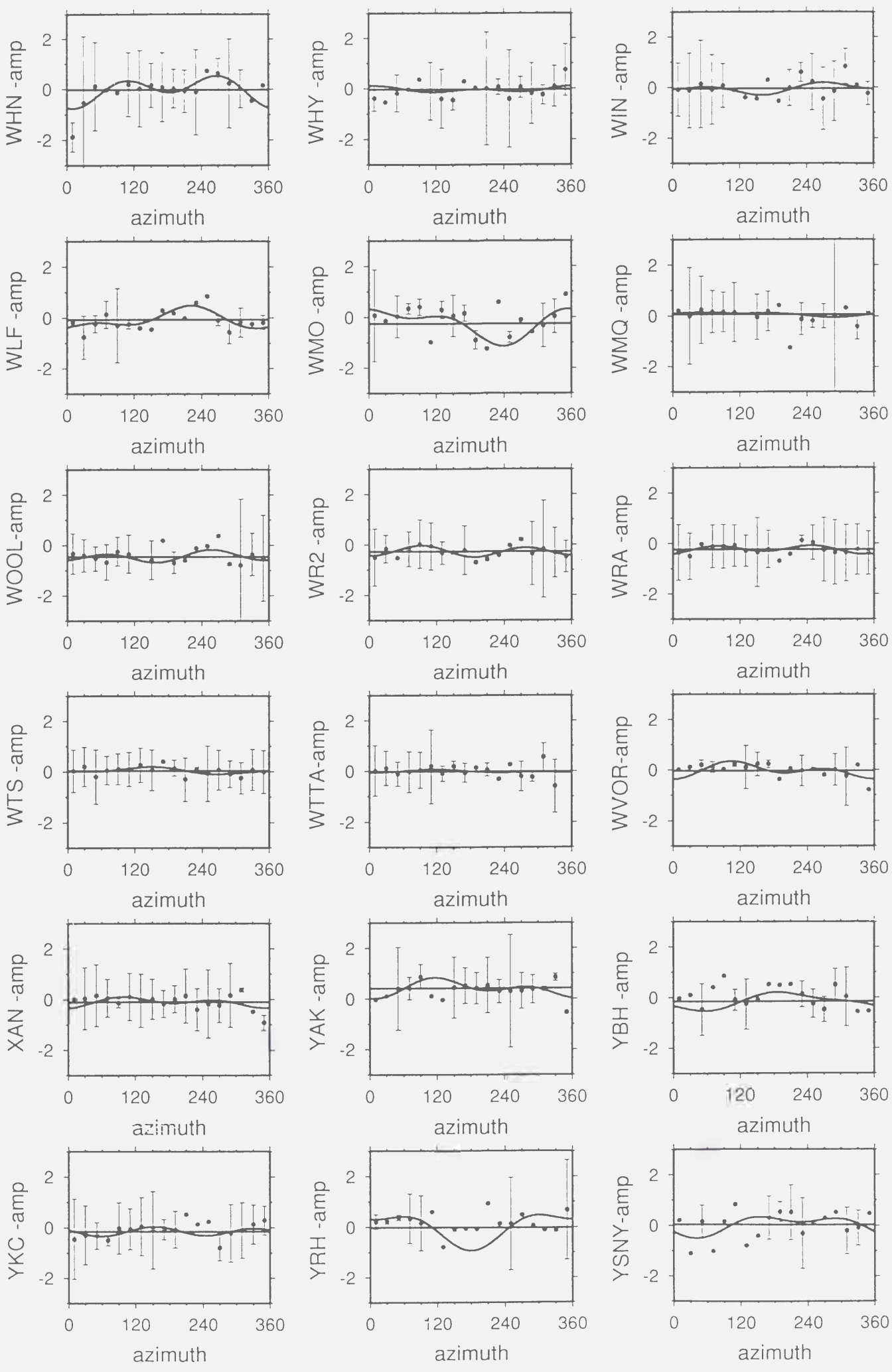
WHN -amp
WHY -amp
WIN -amp
WLF -amp
WMO -amp
WMQ -amp
WOOL-amp
WR2 -amp
WRA -amp
WTS -amp
WTTA-amp
WVOR-amp
XAN -amp
YAK -amp
YBH -amp
YKC -amp
YRH -amp
YSNY-amp
2
0
-2
0
120
240
360
azimuth

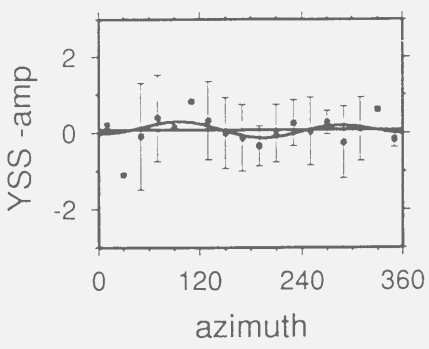
YSS -amp
2
0
-2
0
120
240
360
azimuth

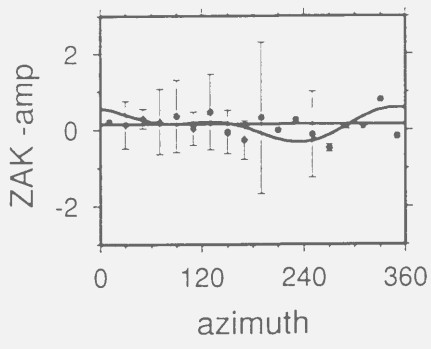
ZAK -amp
2
0
-2
0
120
240
360
azimuth

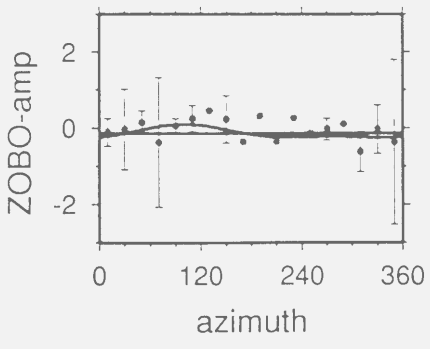
ZOBO-amp
2
0
-2
0
120
240
360
azimuth

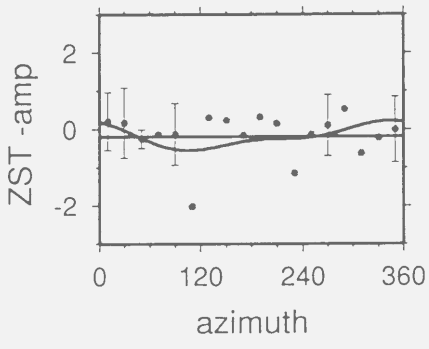
ZST -amp
2
0
-2
0
120
240
360
azimuth

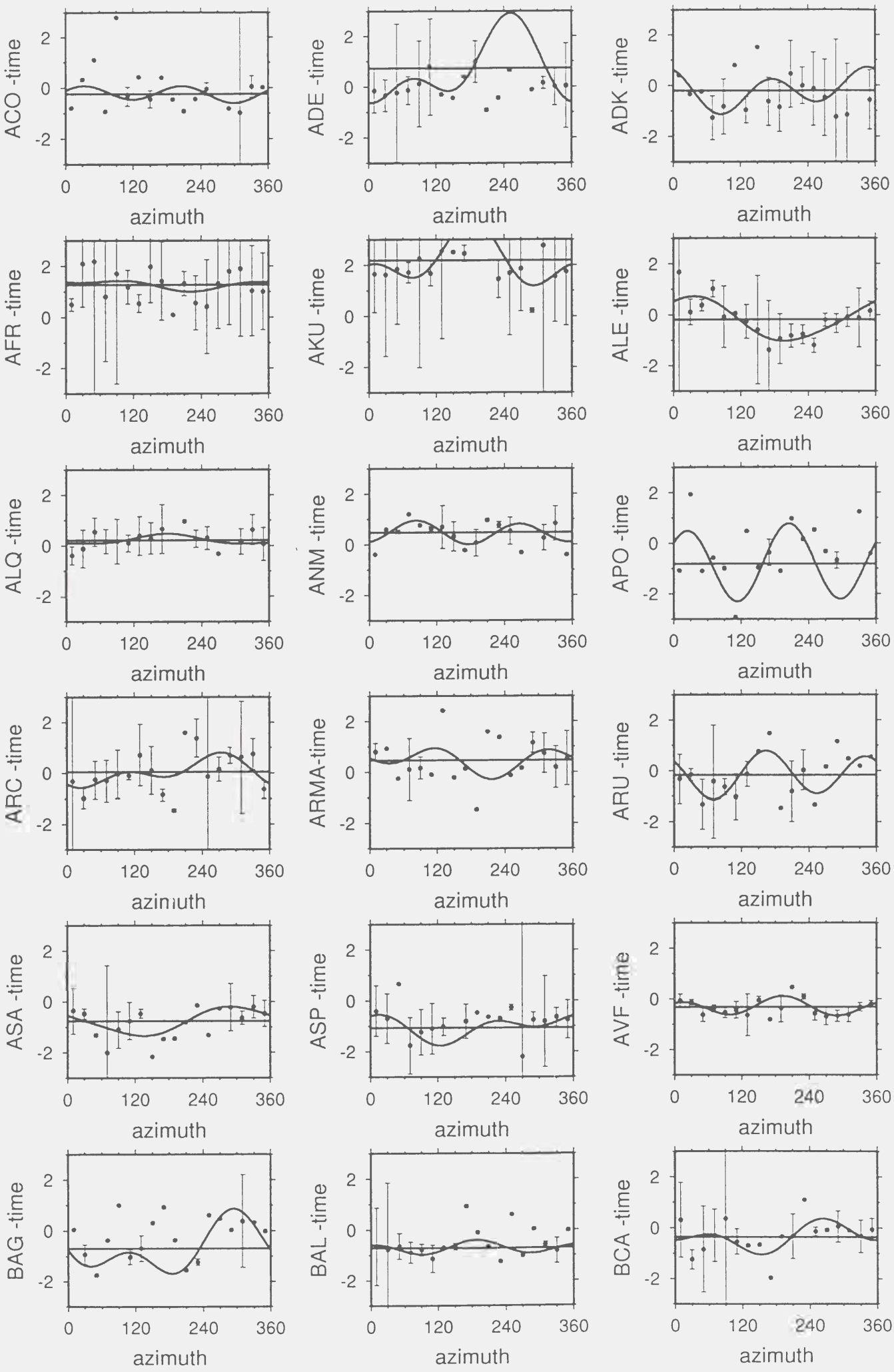
ACO -time
ADE -time
ADK -time
AFR -time
AKU -time
ALE -time
ALQ -time
ANM -time
APO -time
ARC -time
ARMA-time
ARU -time
ASA -time
ASP -time
AVF -time
BAG -time
BAL -time
BCA -time
azimuth
2
0
-2
0
120
240
360

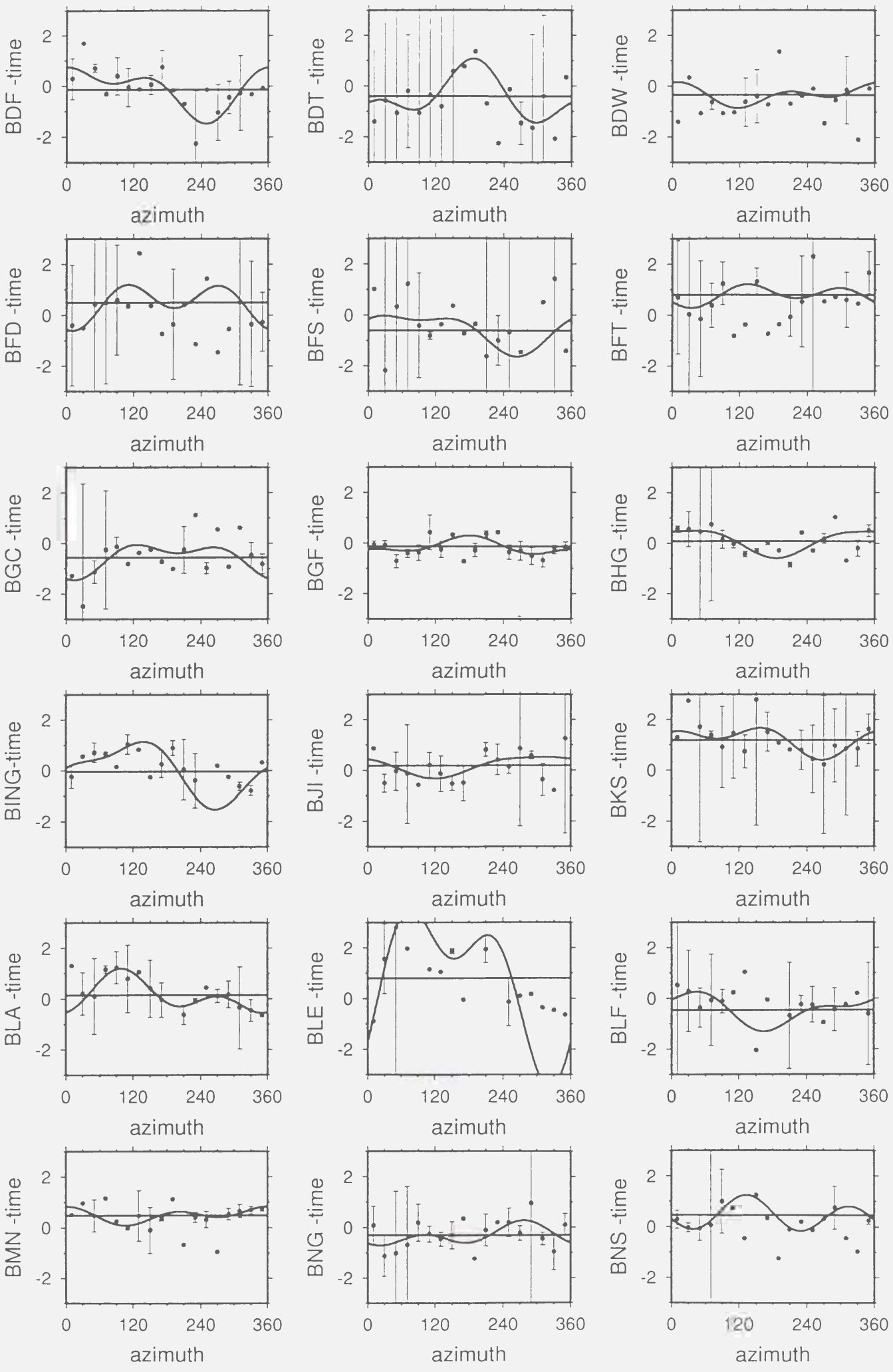
BDF -time
BDT -time
BDW -time
BFD -time
BFS -time
BFT -time
BGC -time
BGF -time
BHG -time
BING-time
BJI -time
BKS -time
BLA -time
BLE -time
BLF -time
BMN -time
BNG -time
BNS -time
azimuth
2
0
-2
0
120
240
360

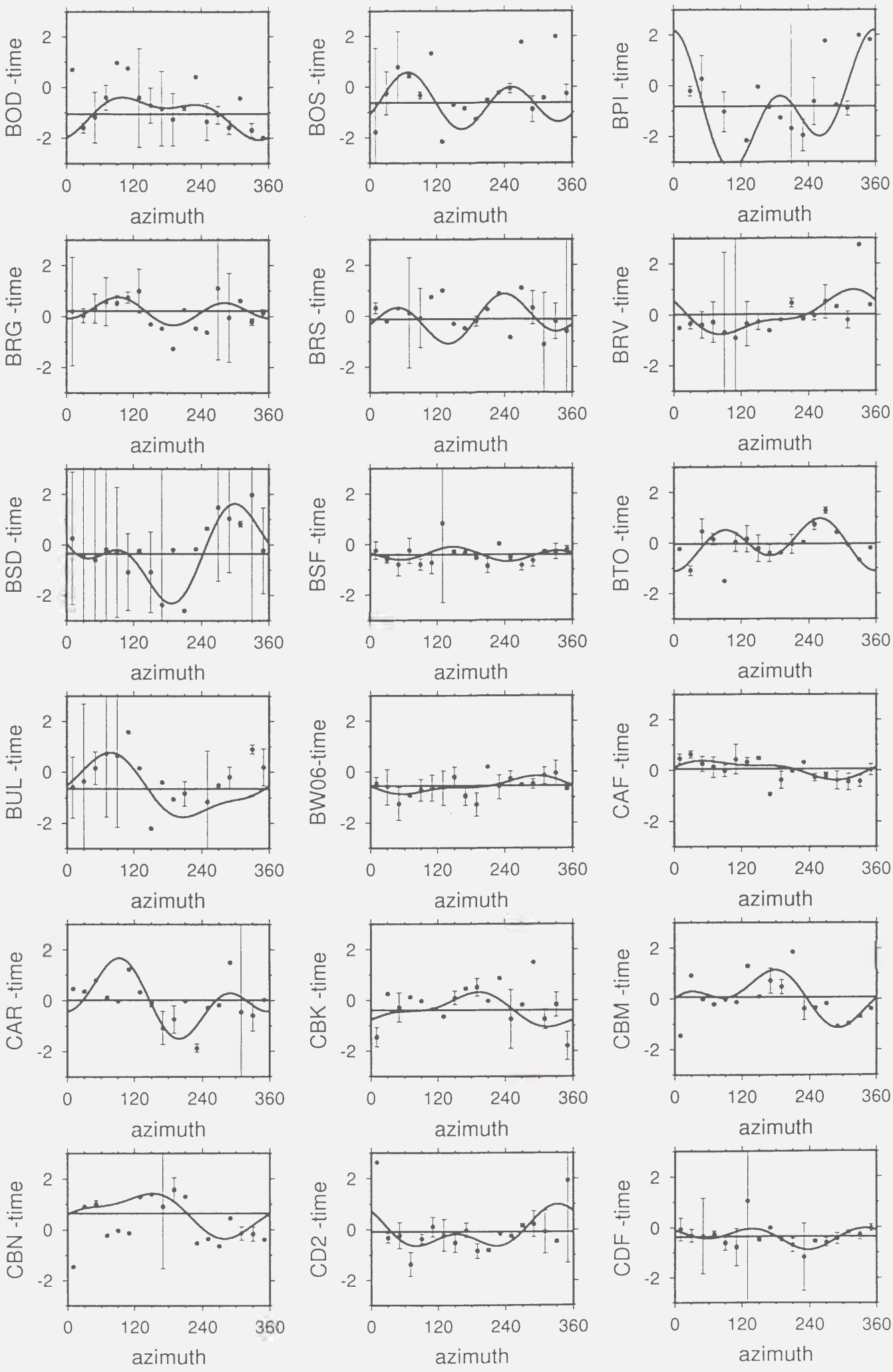
BOD -time
BOS -time
BPI -time
BRG -time
BRS -time
BRV -time
BSD -time
BSF -time
BTO -time
BUL -time
BW06-time
CAF -time
CAR -time
CBK -time
CBM -time
CBN -time
CD2 -time
CDF -time
azimuth
2
0
-2
0
120
240
360

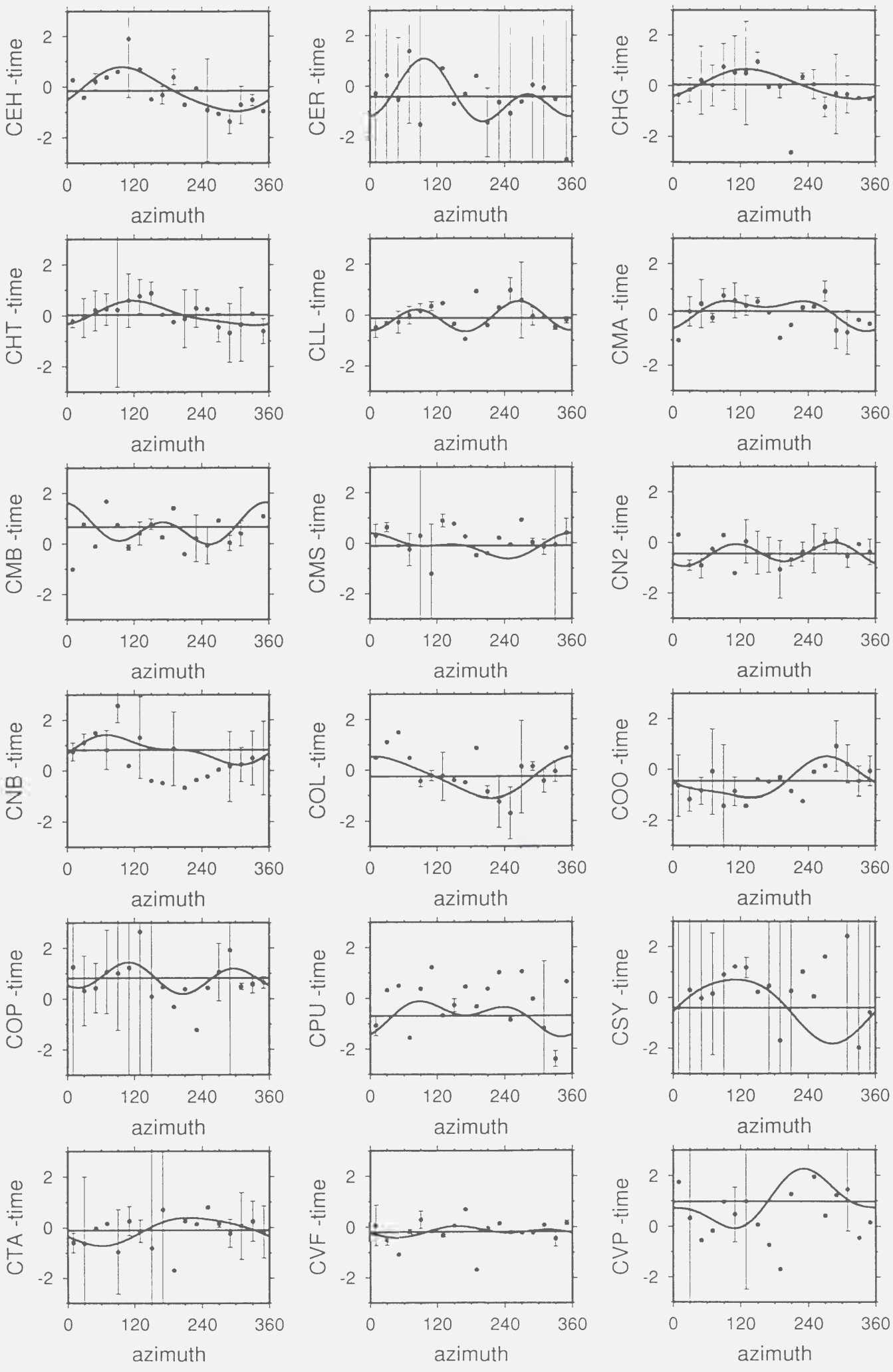
CEH -time
CER -time
CHG -time
CHT -time
CLL -time
CMA -time
CMB -time
CMS -time
CN2 -time
CNB -time
COL -time
COO -time
COP -time
CPU -time
CSY -time
CTA -time
CVF -time
CVP -time
azimuth
0
120
240
360
2
0
-2

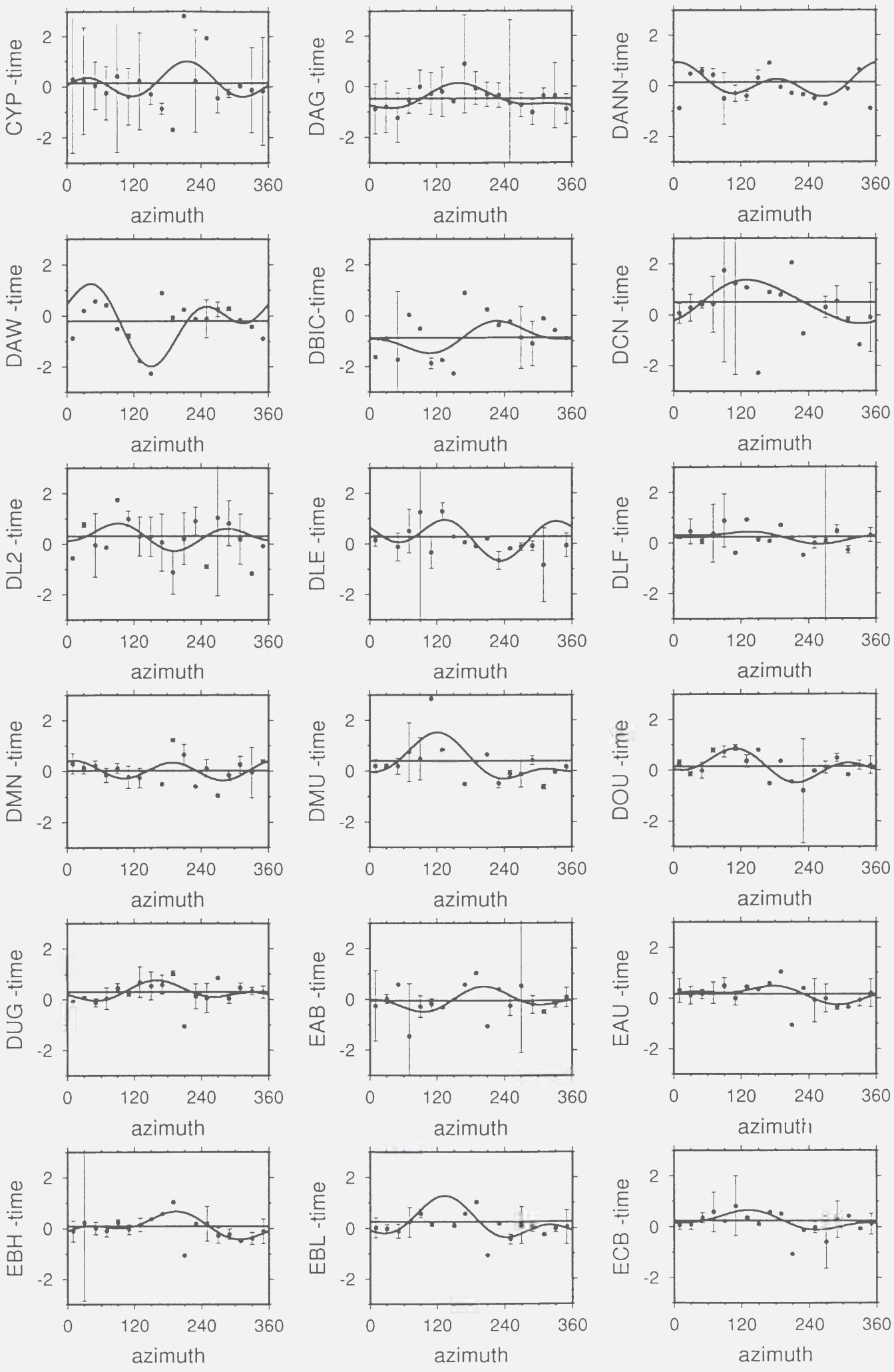
CYP -time
DAG -time
DANN-time
DAW -time
DBIC-time
DCN -time
DL2 -time
DLE -time
DLF -time
DMN -time
DMU -time
DOU -time
DUG -time
EAB -time
EAU -time
EBH -time
EBL -time
ECB -time
azimuth
0
120
240
360
2
0
-2

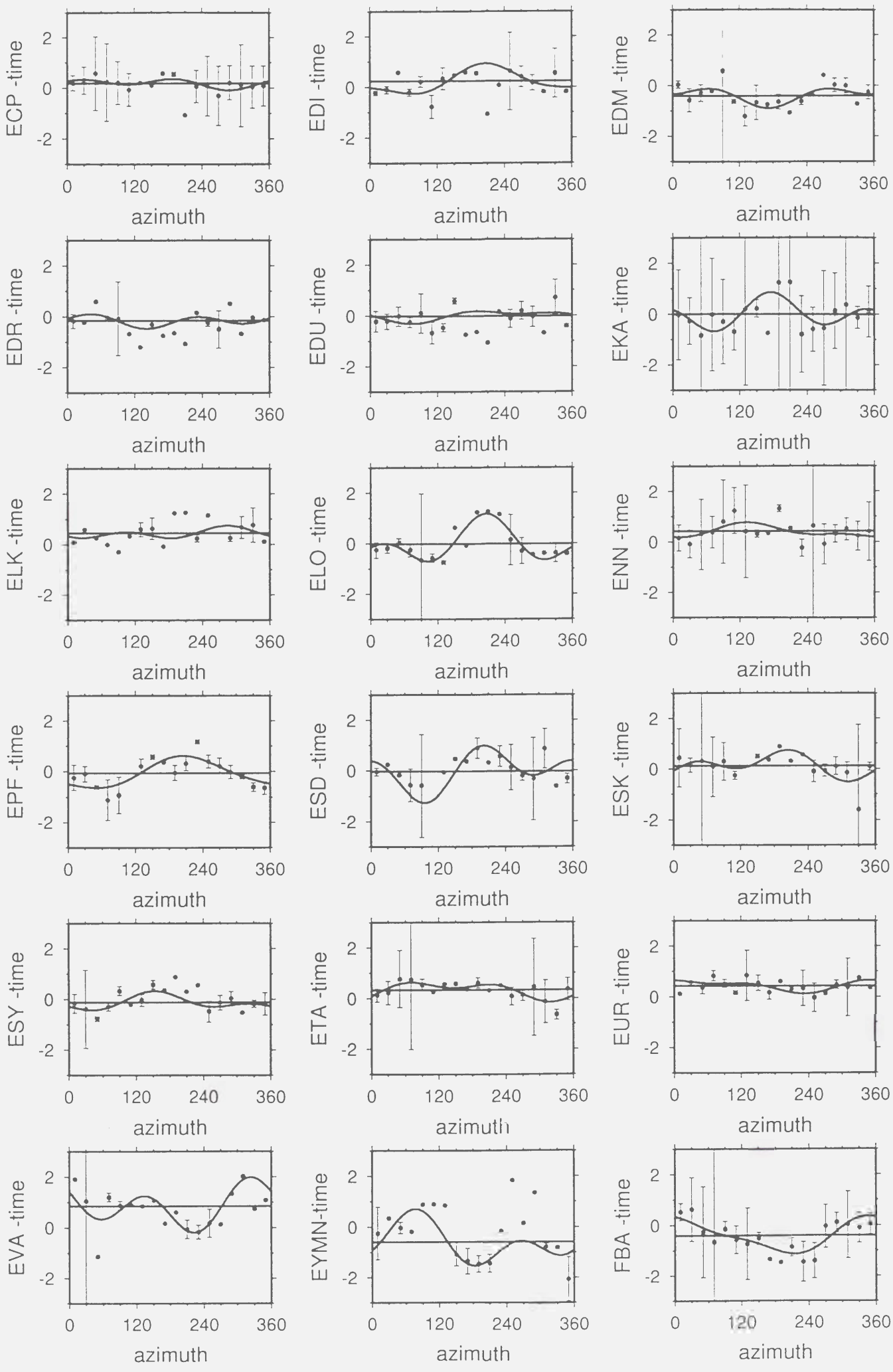
ECP -time
EDI -time
EDM -time
EDR -time
EDU -time
EKA -time
ELK -time
ELO -time
ENN -time
EPF -time
ESD -time
ESK -time
ESY -time
ETA -time
EUR -time
EVA -time
EYMN-time
FBA -time
azimuth
0
120
240
360
2
0
-2

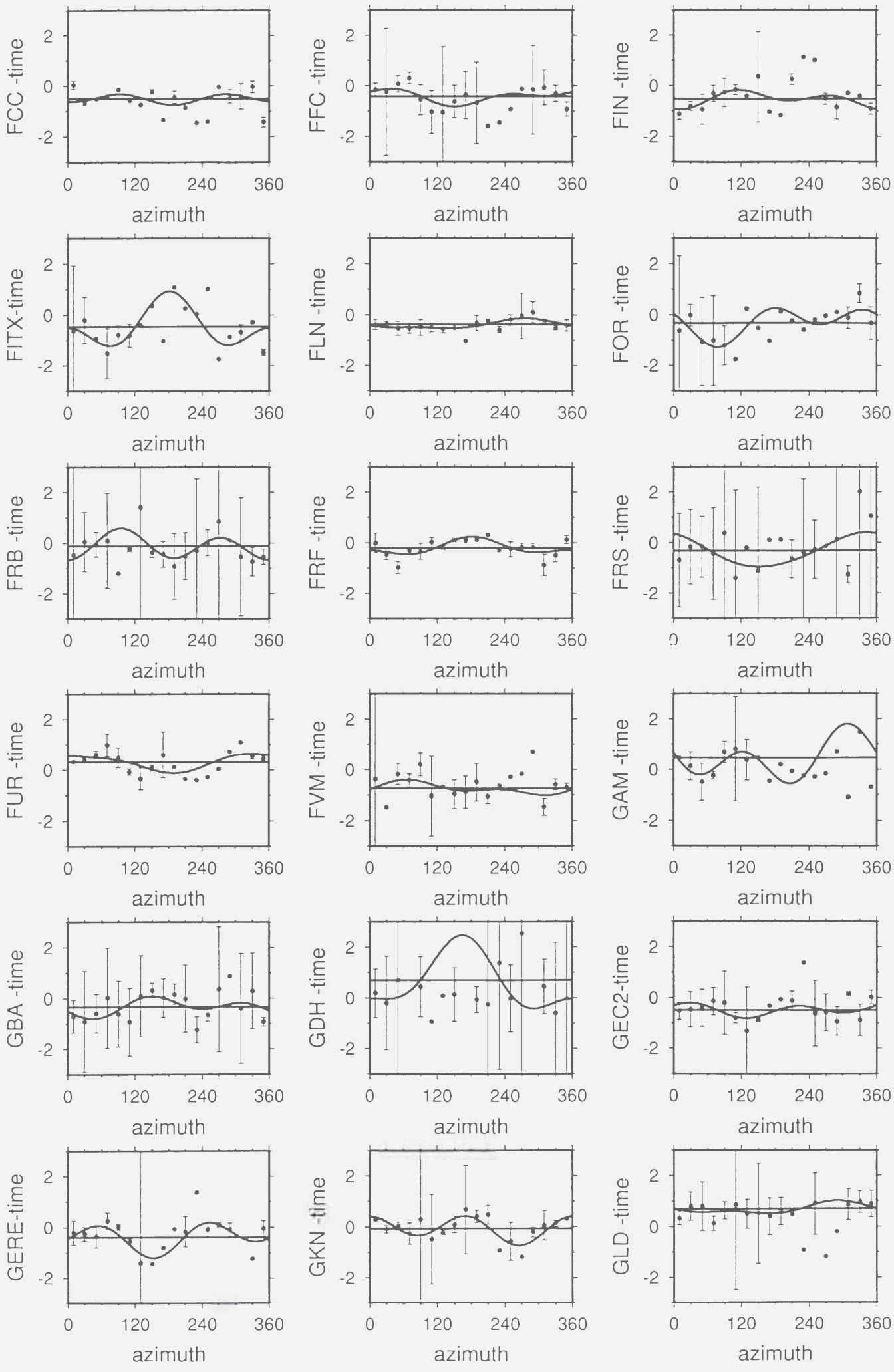
FCC -time
FFC -time
FIN -time
FITX-time
FLN -time
FOR -time
FRB -time
FRF -time
FRS -time
FUR -time
FVM -time
GAM -time
GBA -time
GDH -time
GEC2-time
GERE-time
GKN -time
GLD -time
azimuth
0
120
240
360
2
0
-2

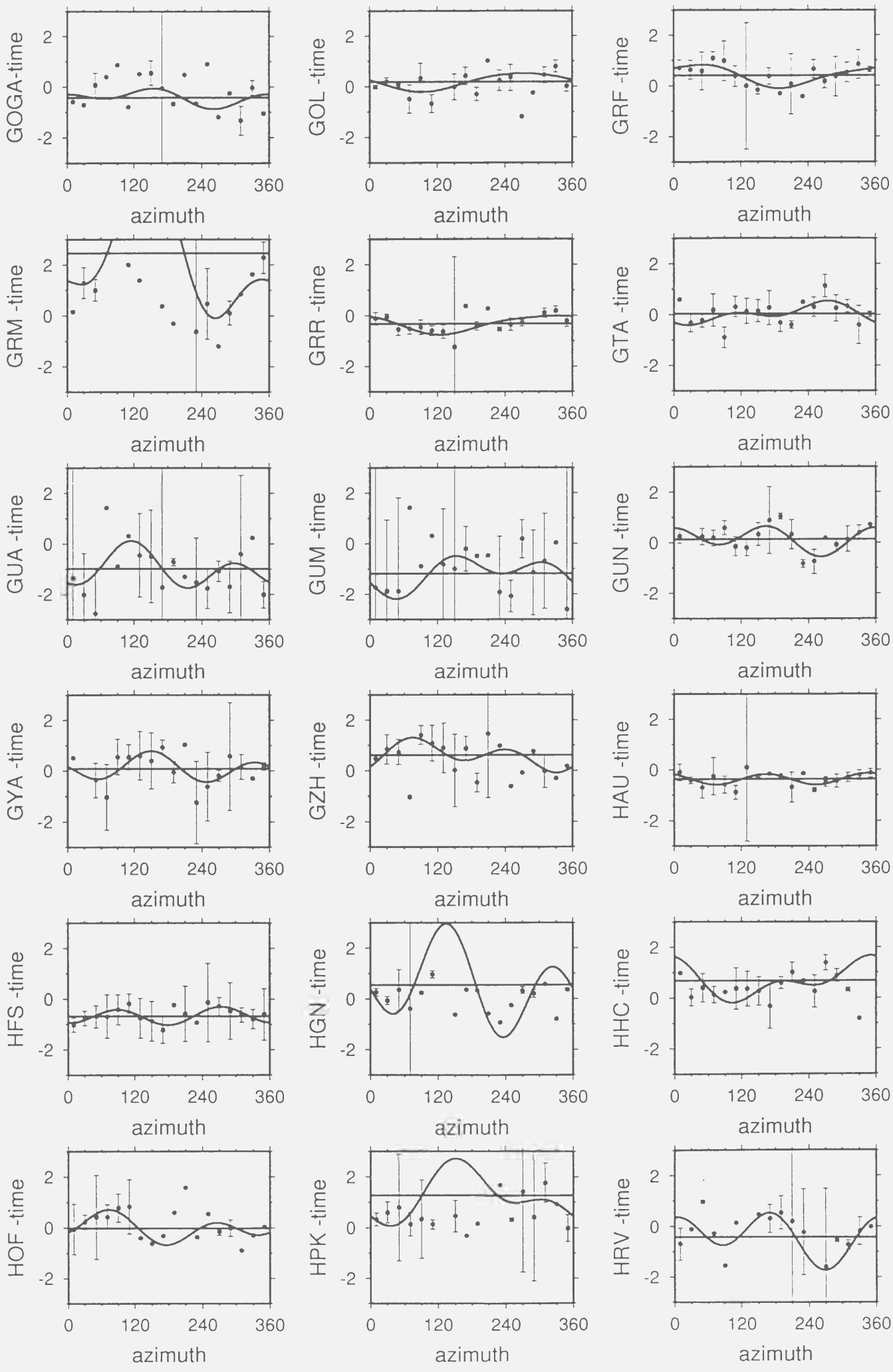
GOGA-time
GOL -time
GRF -time
GRM -time
GRR -time
GTA -time
GUA -time
GUM -time
GUN -time
GYA -time
GZH -time
HAU -time
HFS -time
HGN -time
HHC -time
HOF -time
HPK -time
HRV -time
azimuth
0
120
240
360
2
0
-2

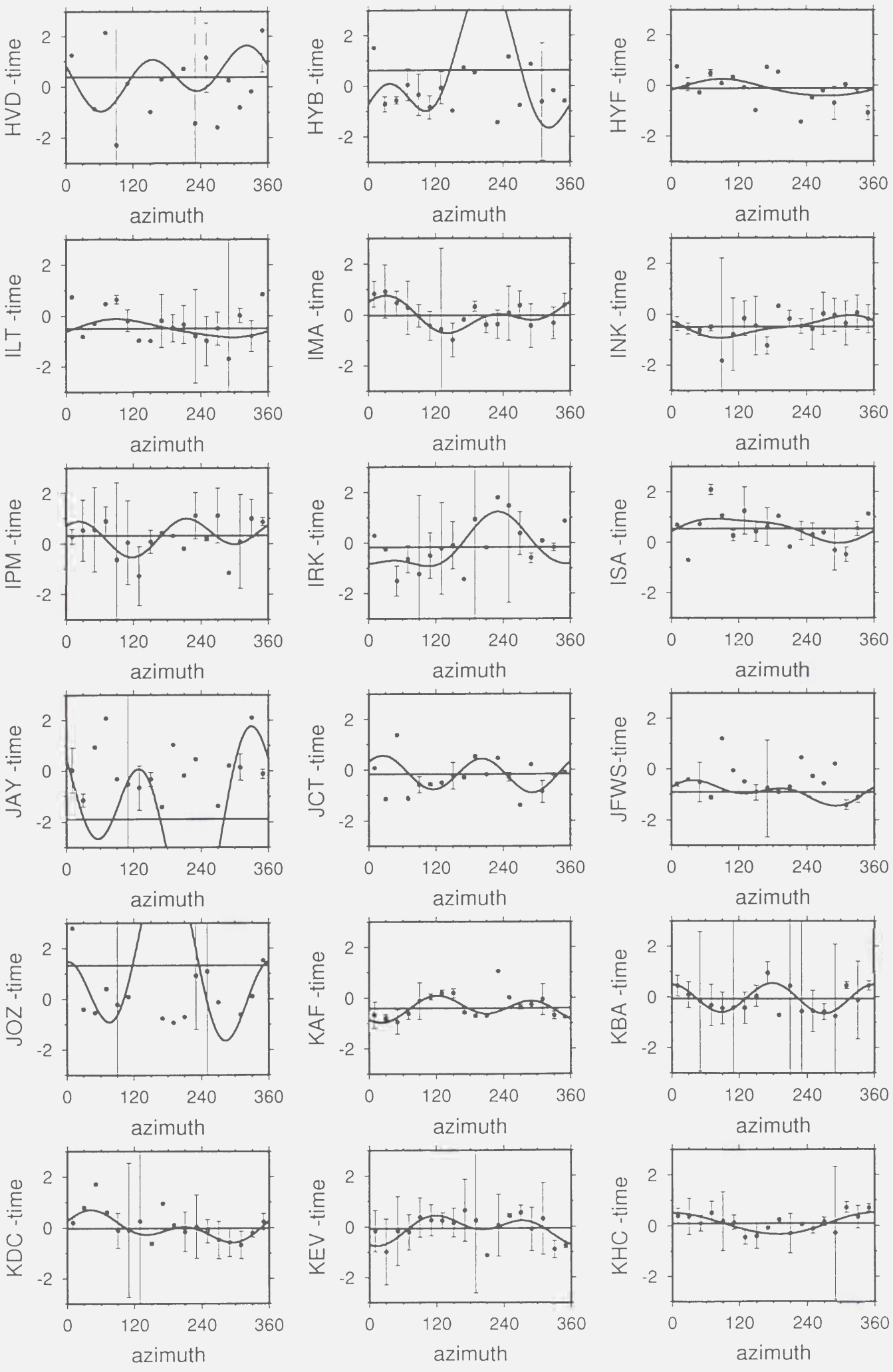
HVD -time
HYB -time
HYF -time
ILT -time
IMA -time
INK -time
IPM -time
IRK -time
ISA -time
JAY -time
JCT -time
JFWS-time
JOZ -time
KAF -time
KBA -time
KDC -time
KEV -time
KHC -time
azimuth
2
0
-2
0
120
240
360

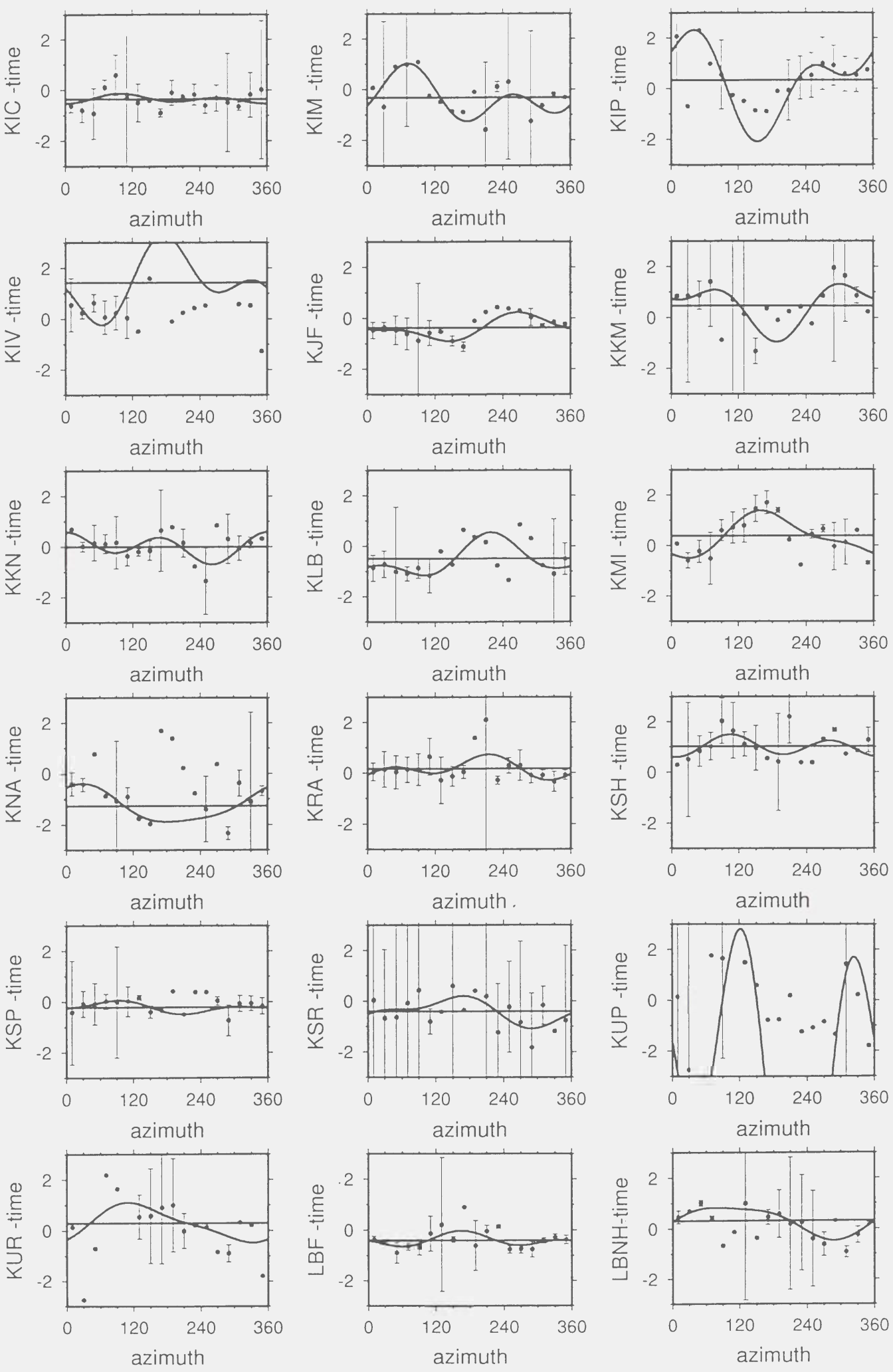
KIC -time
KIM -time
KIP -time
KIV -time
KJF -time
KKM -time
KKN -time
KLB -time
KMI -time
KNA -time
KRA -time
KSH -time
KSP -time
KSR -time
KUP -time
KUR -time
LBF -time
LBNH-time
azimuth
2
0
-2
0
120
240
360

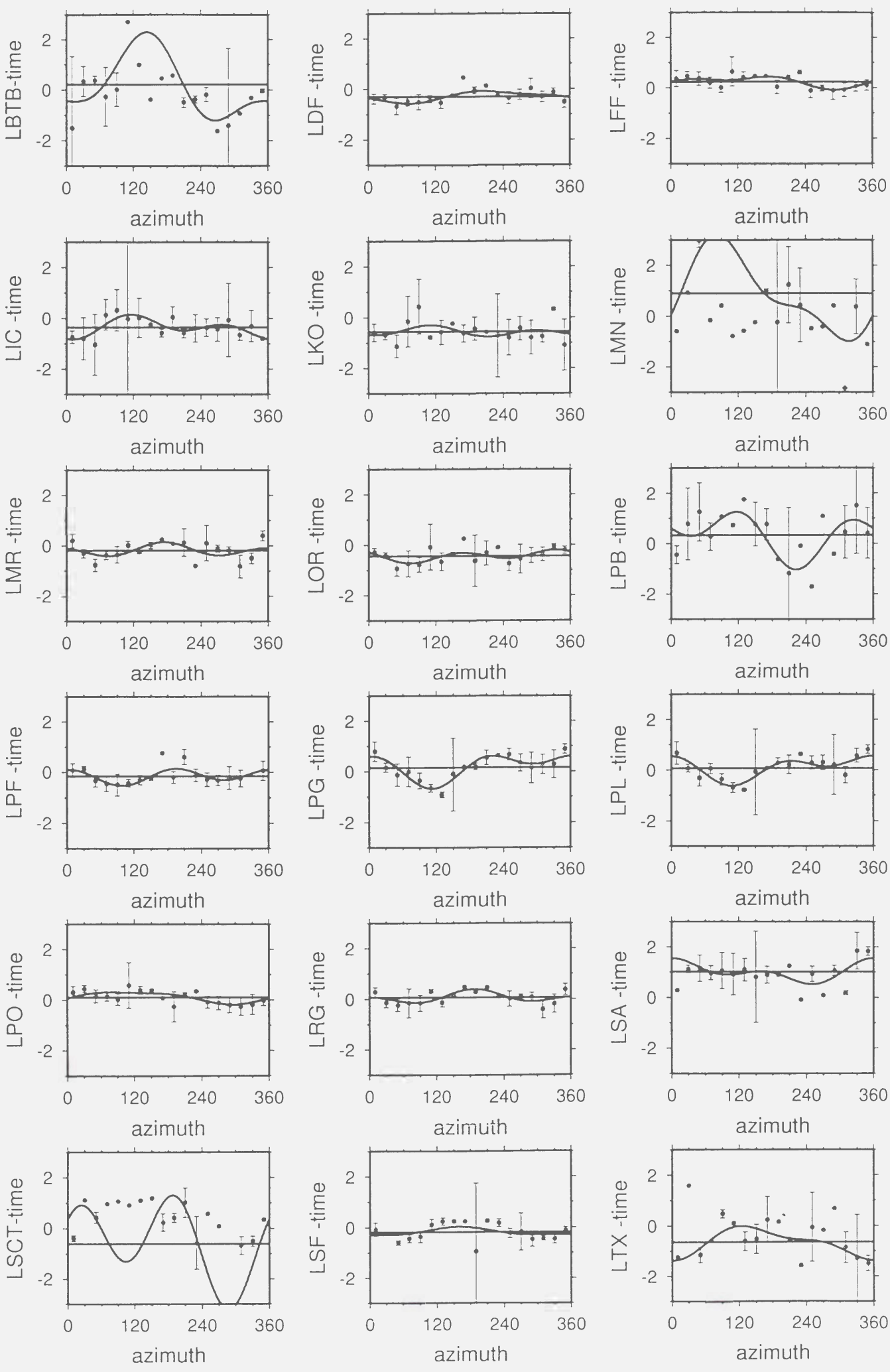
LBTB-time
LDF -time
LFF -time
LIC -time
LKO -time
LMN -time
LMR -time
LOR -time
LPB -time
LPF -time
LPG -time
LPL -time
LPO -time
LRG -time
LSA -time
LSCT-time
LSF -time
LTX -time
azimuth
2
0
-2
0
120
240
360

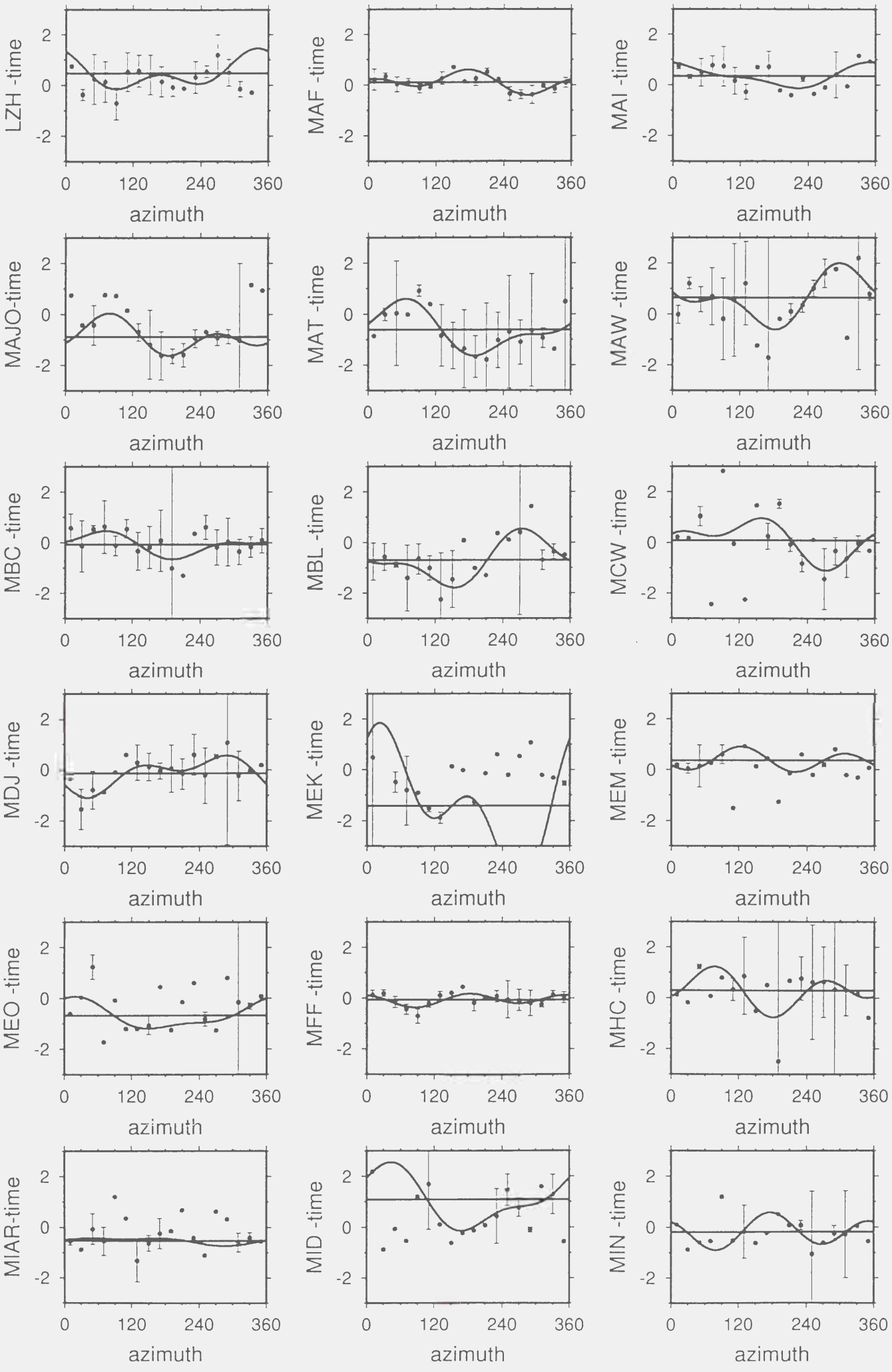
LZH -time
MAF -time
MAI -time
MAJO-time
MAT -time
MAW -time
MBC -time
MBL -time
MCW -time
MDJ -time
MEK -time
MEM -time
MEO -time
MFF -time
MHC -time
MIAR-time
MID -time
MIN -time
azimuth
0
120
240
360
2
0
-2

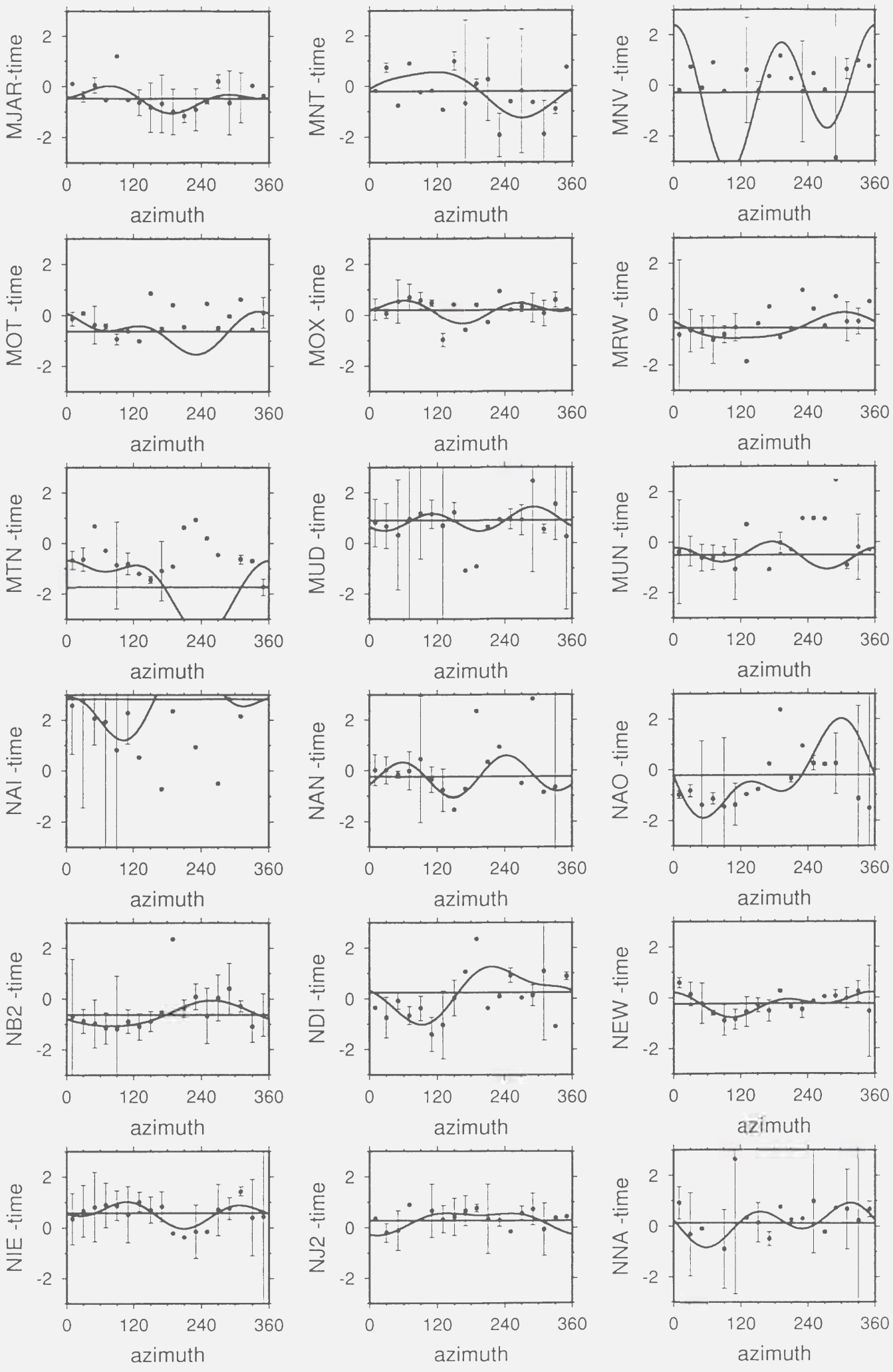
MJAR-time
MNT -time
MNV -time
MOT -time
MOX -time
MRW -time
MTN -time
MUD -time
MUN -time
NAI -time
NAN -time
NAO -time
NB2 -time
NDI -time
NEW -time
NIE -time
NJ2 -time
NNA -time
azimuth
0
120
240
360
2
0
-2

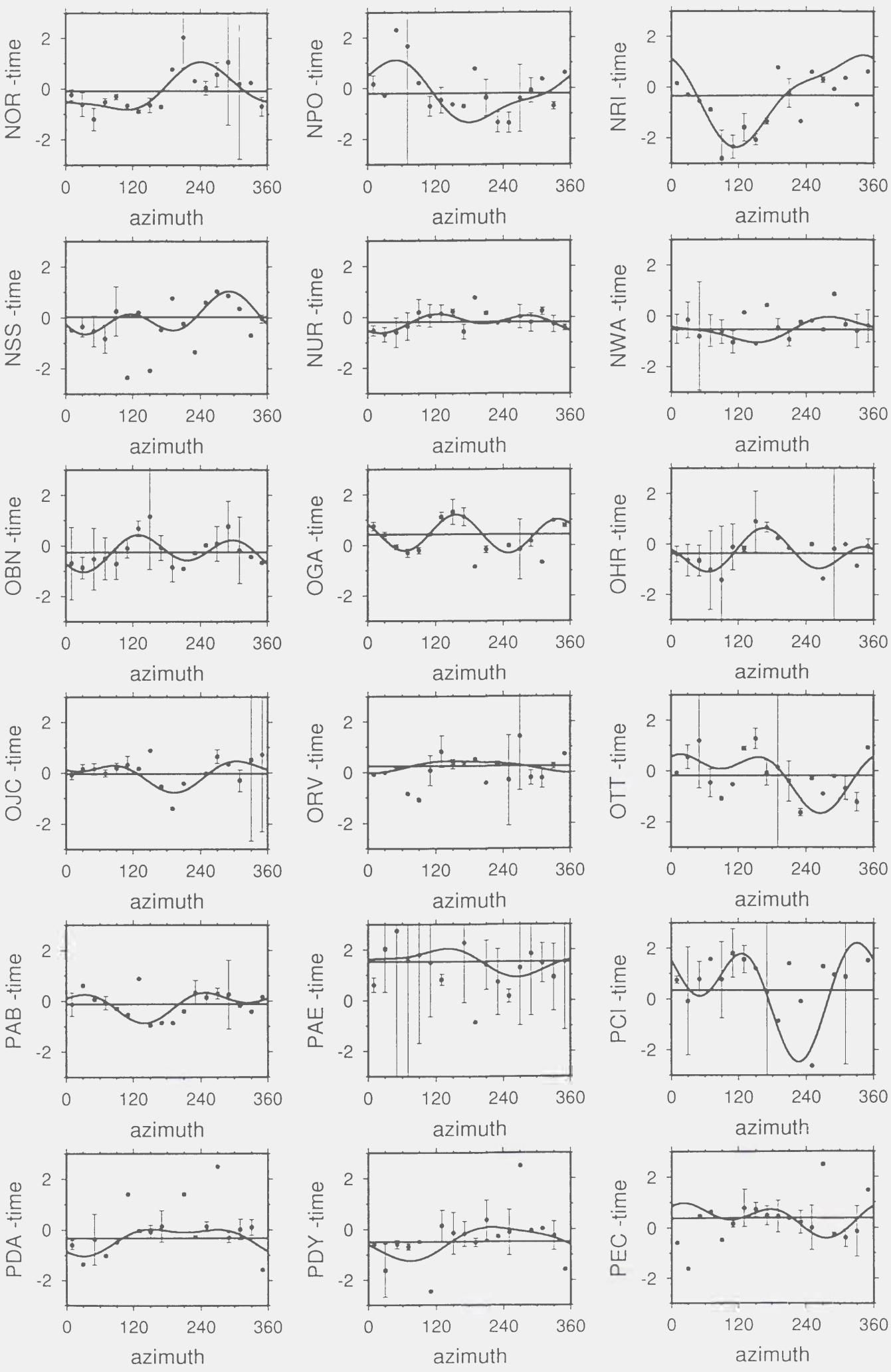
NOR -time
NPO -time
NRI -time
NSS -time
NUR -time
NWA -time
OBN -time
OGA -time
OHR -time
OJC -time
ORV -time
OTT -time
PAB -time
PAE -time
PCI -time
PDA -time
PDY -time
PEC -time
2
0
-2
0
120
240
360
azimuth

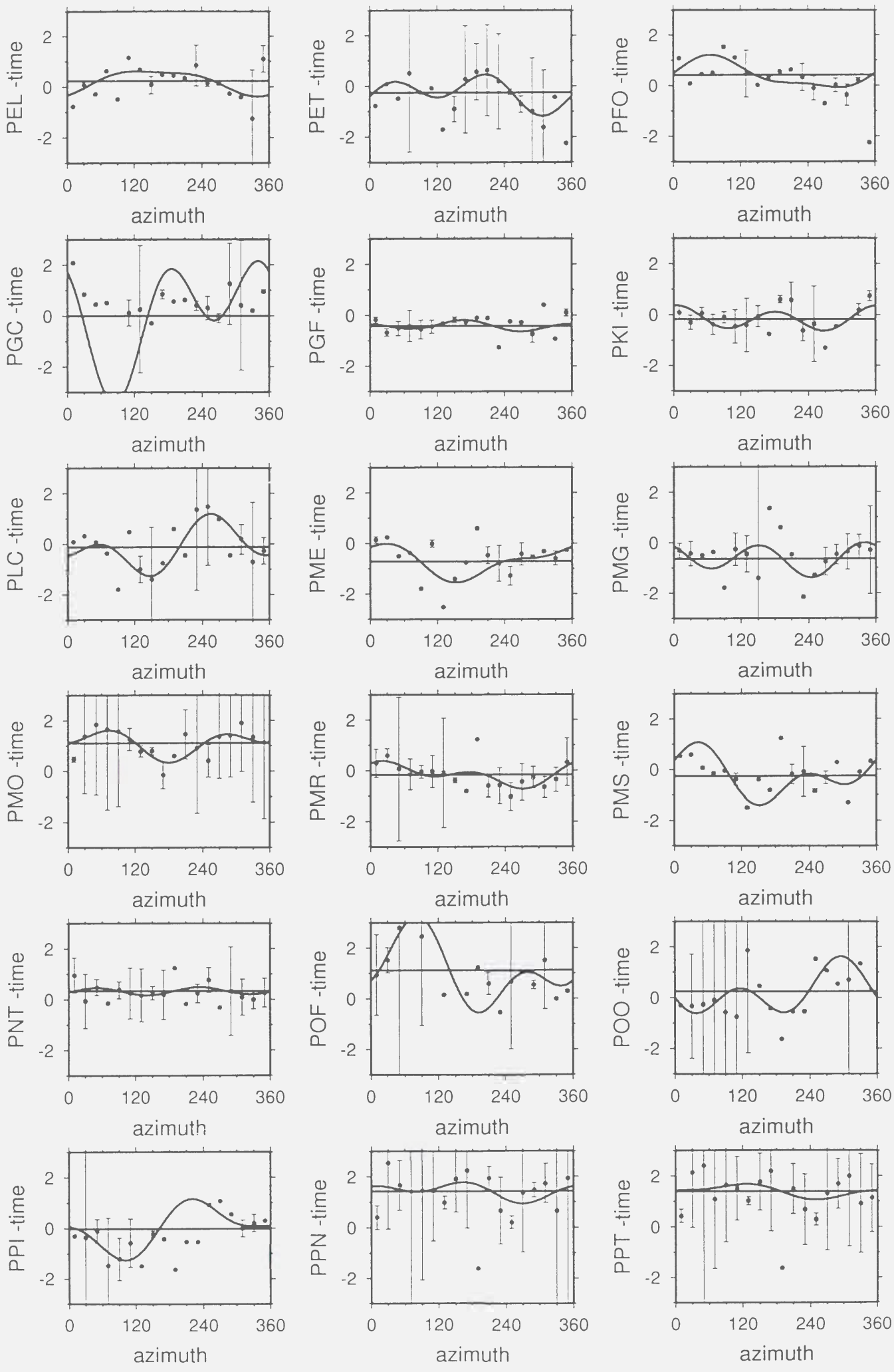
PEL -time
PET -time
PFO -time
PGC -time
PGF -time
PKI -time
PLC -time
PME -time
PMG -time
PMO -time
PMR -time
PMS -time
PNT -time
POF -time
POO -time
PPI -time
PPN -time
PPT -time
azimuth
2
0
-2
0
120
240
360

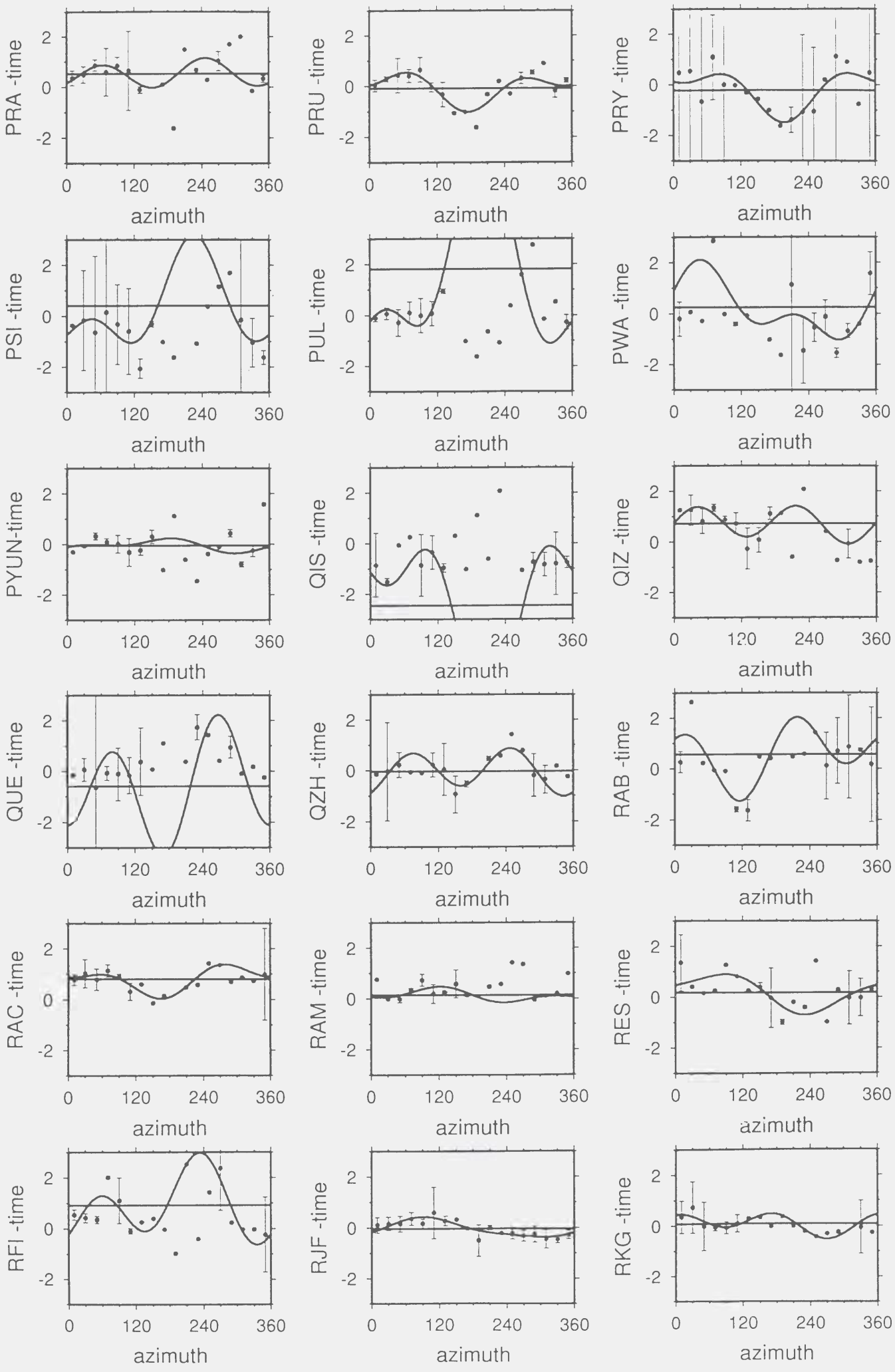
PRA -time
PRU -time
PRY -time
PSI -time
PUL -time
PWA -time
PYUN-time
QIS -time
QIZ -time
QUE -time
QZH -time
RAB -time
RAC -time
RAM -time
RES -time
RFI -time
RJF -time
RKG -time
azimuth
2
0
-2
0
120
240
360

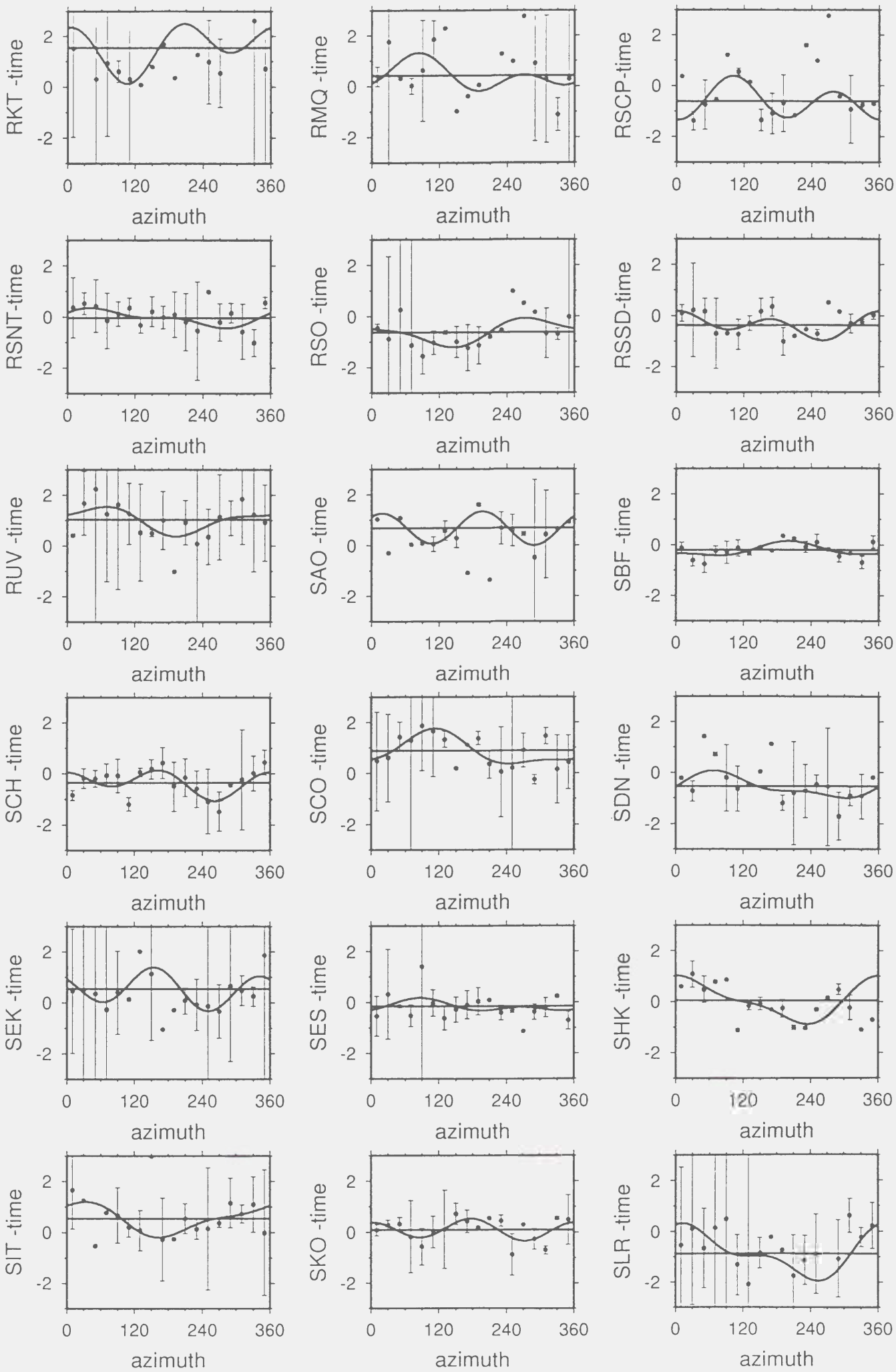
RKT -time
RMQ -time
RSCP-time
RSNT-time
RSO -time
RSSD-time
RUV -time
SAO -time
SBF -time
SCH -time
SCO -time
SDN -time
SEK -time
SES -time
SHK -time
SIT -time
SKO -time
SLR -time
azimuth
2
0
-2
0
120
240
360

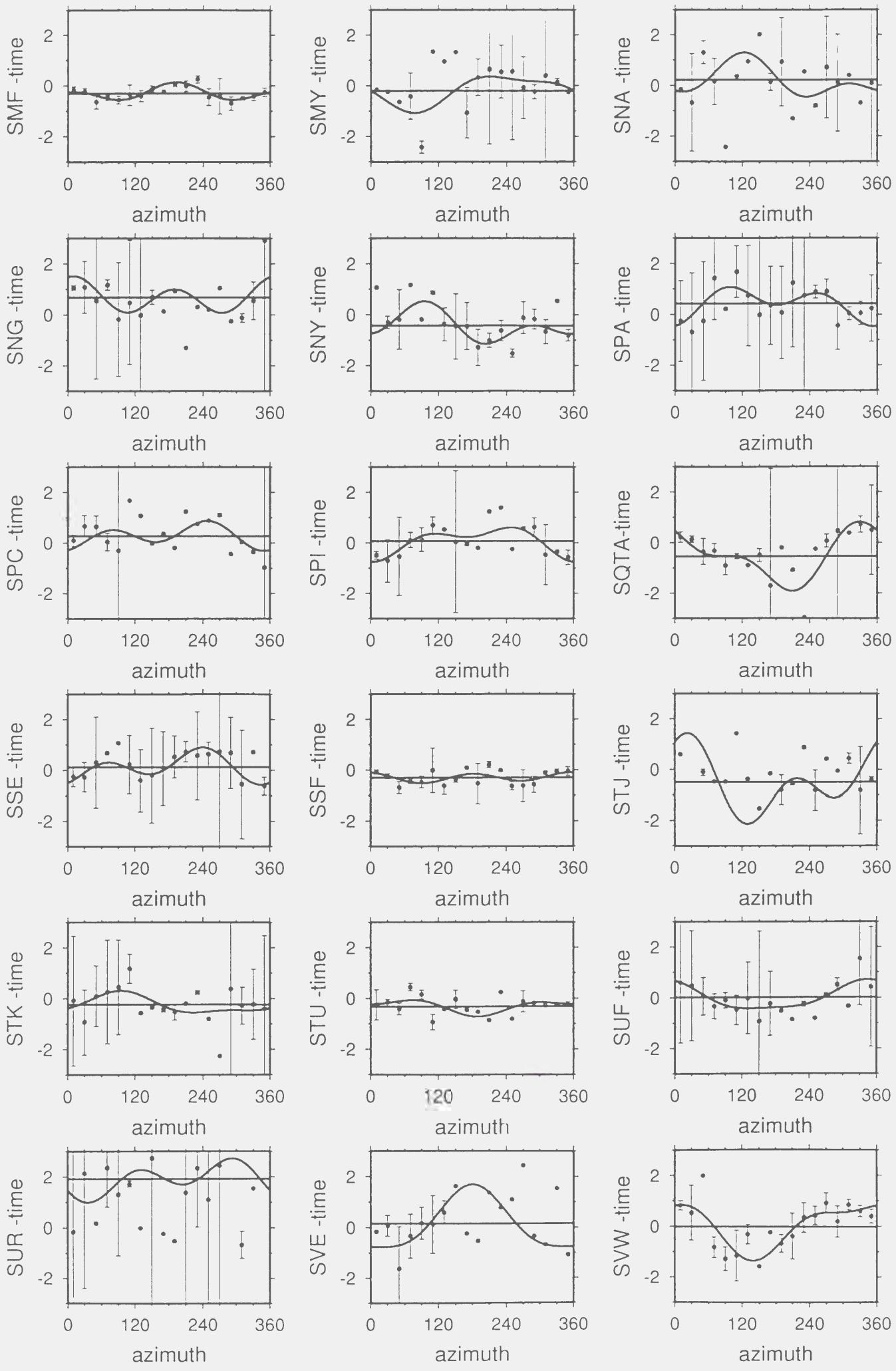
SMF -time
SMY -time
SNA -time
SNG -time
SNY -time
SPA -time
SPC -time
SPI -time
SQTA-time
SSE -time
SSF -time
STJ -time
STK -time
STU -time
SUF -time
SUR -time
SVE -time
SVW -time
azimuth
0
120
240
360
2
0
-2

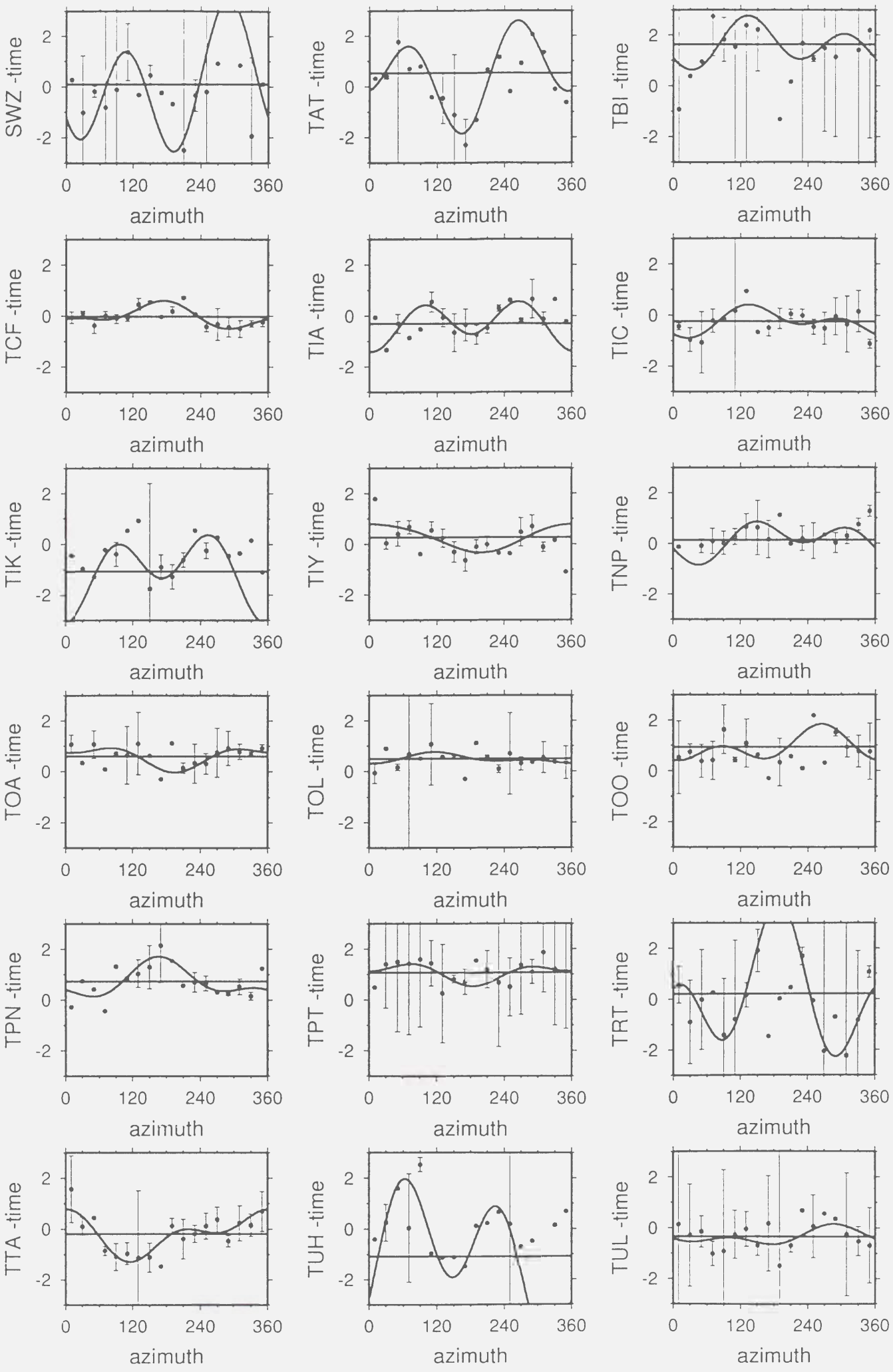
SWZ -time
TAT -time
TBI -time
TCF -time
TIA -time
TIC -time
TIK -time
TIY -time
TNP -time
TOA -time
TOL -time
TOO -time
TPN -time
TPT -time
TRT -time
TTA -time
TUH -time
TUL -time
azimuth
0
120
240
360
2
0
-2

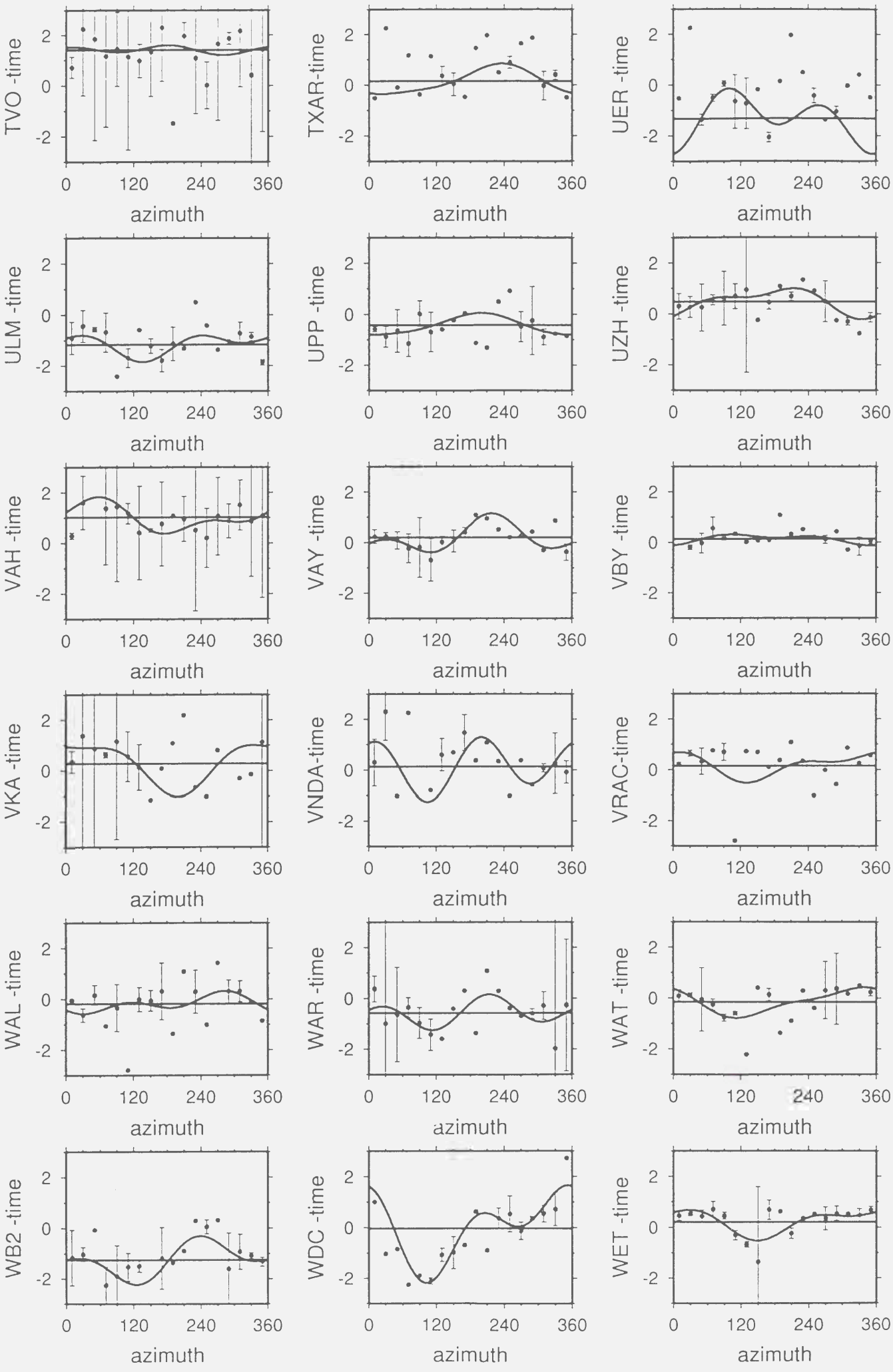
TVO -time
TXAR-time
UER -time
ULM -time
UPP -time
UZH -time
VAH -time
VAY -time
VBY -time
VKA -time
VNDA-time
VRAC-time
WAL -time
WAR -time
WAT -time
WB2 -time
WDC -time
WET -time
azimuth
0
120
240
360
2
0
-2

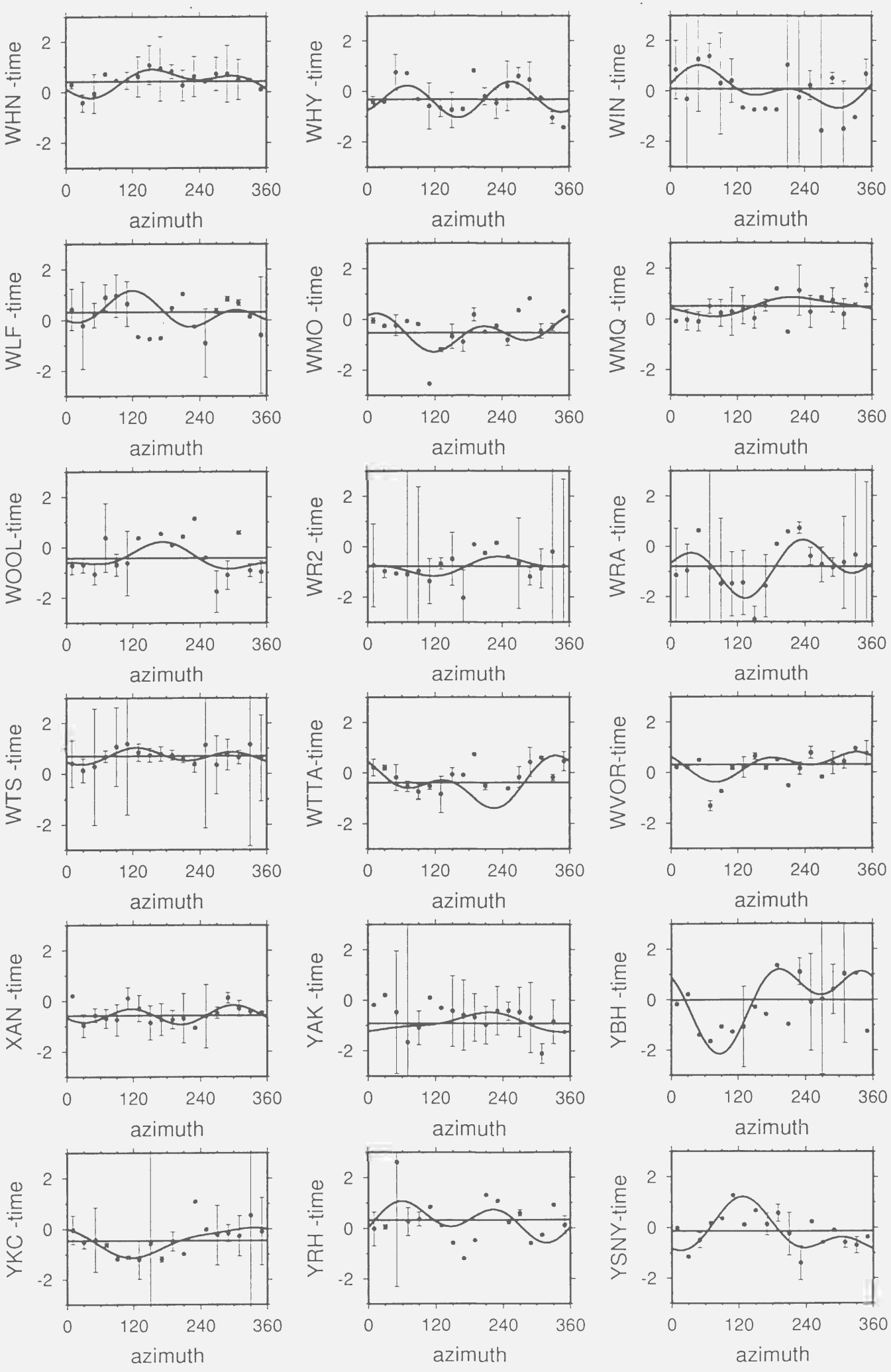
WHN -time
WHY -time
WIN -time
WLF -time
WMO -time
WMQ -time
WOOL-time
WR2 -time
WRA -time
WTS -time
WTTA-time
WVOR-time
XAN -time
YAK -time
YBH -time
YKC -time
YRH -time
YSNY-time
2
0
-2
0
120
240
360
azimuth

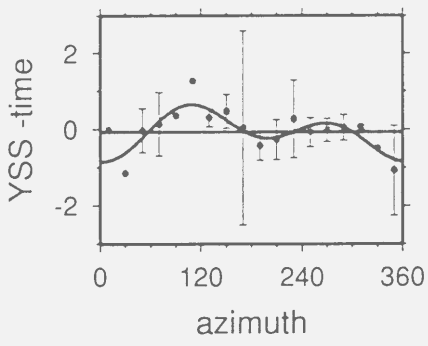
YSS -time
2
0
-2
0
120
240
360
azimuth

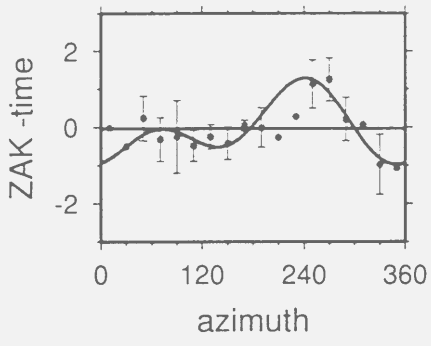
ZAK -time
2
0
-2
0
120
240
360
azimuth

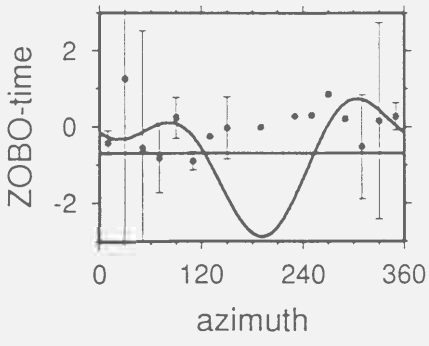
ZOBO-time
2
0
-2
0
120
240
360
azimuth

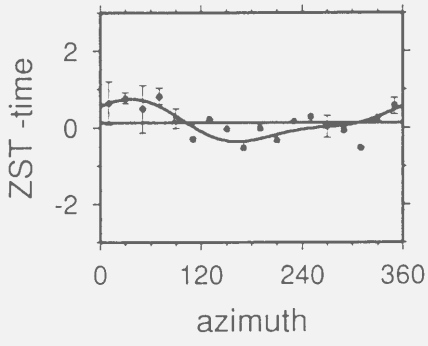
ZST -time
2
0
-2
0
120
240
360
azimuth

Appendix B

Amplitude and travel time station corrections for ISC stations

B-1 Amplitude station corrections

B-2 Travel time station corrections

ist	ID number of station
stc	station code
Neve	number of events used for calculation
Nw	number of windows used for fitting
lat.	latitude (degree)
lon.	longitude (degree)
elev	elevation (m)
ave	average term
a0	azimuth-independent term
a1, dir1	amplitude and direction of first azimuth-dependent term
a2, dir2	amplitude and direction of second azimuth-dependent term
rms0, rms1	RMS residuals before and after the fitting
vr	variance reduction
corr	correlation coefficient between amplitude and travel time

Appendix B-1: Station Correction for log-amplitude

ist	stc	Neve	Nw	lat.	lon.	elev	ave	a0	a1	dir1	a2	dir2	rms0	rms1	vr	corr
13	AAI	80	8	-3.700	128.167	79	-.205						.75			
18	AAS	21	4	-62.160	-58.463	14	-.555						3.20			
46	ACO	50	11	36.699	-99.146	521	.159	.094	.022	191.4	.322	159.3	1.12	.95	28.5	-.26
63	ADE	269	14	-34.967	138.709	654	.234	.252	.031	222.7	.121	33.3	.85	.82	5.3	.35
66	ADK	617	15	51.863	-176.655	0	.085	.180	.499	93.0	.272	54.3	.98	.41	82.1	-.18
82	AFR	522	17	-17.538	-149.778	50	.131	.134	.062	146.3	.184	53.5	.55	.44	37.0	.25
83	AGA	21	7	38.795	-27.232	79	.443						.49			
88	AGM	14	6	47.082	-69.023	238	.707						1.31			
90	AGR	11	6	27.133	78.017	163	.758						1.04			
116	AKRL	16	4	23.660	32.710	0	.260						1.07			
117	AKSR	19	6	23.672	33.021	0	.435						1.28			
118	AKU	543	18	65.687	-18.107	24	.001	.001	.048	151.4	.036	168.3	.76	.75	1.8	.62
121	ALE	382	18	82.483	-62.400	64	-.265	-.265	.209	244.2	.127	75.2	.60	.44	46.9	-.61
131	ALQ	961	17	34.942	-106.458	1853	-.215	-.234	.151	103.3	.270	173.3	.81	.63	38.6	.42
172	ANM	192	14	64.705	-165.417	330	-.258	-.264	.219	185.3	.096	121.8	.78	.66	28.0	.00
173	ANN	117	9	44.883	37.300	0	.237						1.33			
177	ANT	29	8	-23.699	-70.415	79	.101						1.07			
186	APA	12	5	67.550	33.333	0	-.098						1.23			
194	APO	18	11	60.590	14.030	340	-.446	-.366	.450	123.5	.960	33.4	2.20	1.01	78.9	.52
202	AQU	10	7	42.354	13.403	720	.537						1.18			
213	ARC	208	18	40.877	-124.075	59	-.248	-.248	.116	254.6	.358	109.1	1.01	.79	39.0	.30
214	ARE	12	5	-16.571	-71.563	2451	-.082						.77			
221	ARMA	172	11	-30.448	151.730	1129	-.292	-.131	.368	236.3	.280	37.2	.70	.60	24.9	-.65
227	ARU	184	13	56.100	58.600	250	.508	.584	.272	270.7	.164	131.5	.62	.39	59.7	.10
228	ARV	11	6	43.635	13.021	0	.232						1.55			
229	ASA	245	14	43.770	142.373	111	-.432	-.512	.317	49.4	.331	104.6	.75	.35	77.6	-.14
234	ASH	105	9	37.950	58.350	219	.365						.80			
241	ASP	978	16	-23.683	133.897	600	.055	.058	.269	129.8	.088	109.2	.59	.30	74.1	-.41
243	ASS	10	5	43.105	12.762	0	.017						1.32			
280	AVF	623	17	46.855	3.376	224	-.096	-.096	.121	75.1	.089	33.8	.34	.21	59.5	.28
301	BAG	128	10	16.411	120.580	1506	.438	.453	.660	220.1	.381	176.9	1.18	.42	87.6	.21
308	BAL	207	12	-30.665	116.772	300	-.312	-.354	.301	80.5	.182	146.5	.54	.23	82.4	-.21
332	BBU	33	5	26.215	50.457	0	.220						1.23			
333	BCA	134	15	41.550	41.673	500	.005	.007	.294	197.5	.064	48.1	.84	.64	41.1	.02
353	BDF	92	13	-15.788	-47.933	1254	-.007	-.043	.121	186.6	.186	142.4	.64	.52	33.2	-.29
356	BDI	17	7	44.173	10.720	0	-.352						1.14			
362	BDT	526	14	17.233	99.050	0	.070	.030	.117	65.7	.094	139.1	.31	.25	32.5	.38
365	BDW	77	11	42.862	-109.582	2190	-.522	-.448	.324	24.5	.376	40.8	1.26	.91	47.6	.65
371	BEE	59	9	26.017	50.522	0	.042						1.66			
384	BEW	15	6	-32.415	22.630	870	.149						.86			
386	BFD	166	12	-37.176	142.544	234	-.034	-.018	.223	298.1	.258	60.6	.69	.50	47.6	-.33
390	BFS	111	14	-26.898	26.785	1309	.216	.200	.198	129.9	.130	40.8	.65	.54	31.4	.34
391	BFT	101	14	-25.687	30.043	1868	.064	.100	.154	146.1	.009	55.3	1.14	1.12	4.1	-.17
395	BGC	53	13	37.962	-122.170	610	.198	.016	.781	302.3	.564	41.8	2.13	1.68	38.2	.04
397	BGF	592	17	46.558	2.846	389	-.097	-.095	.101	199.4	.115	111.9	.41	.31	41.3	.46
412	BHG	292	15	47.721	12.879	474	.140	.149	.097	199.8	.165	65.5	.59	.50	28.3	.25
418	BHO	13	7	31.508	-94.873	143	-.165						1.40			
432	BING	149	13	42.157	-76.067	407	.019	-.029	.446	209.6	.199	39.7	1.10	.64	65.8	-.37
440	BJA	24	6	25.992	50.608	0	.395						.71			
441	BJI	691	16	40.040	116.175	43	-.013	-.017	.069	160.3	.079	68.0	.43	.40	13.5	-.07
445	BKB	12	4	-1.283	116.833	0	.269						1.51			
456	BKS	693	16	37.877	-122.235	275	.186	.185	.069	237.5	.072	160.8	.52	.49	10.5	.24
460	BLA	390	16	37.211	-80.421	634	.035	.029	.170	191.6	.288	85.4	.66	.43	58.0	.42
462	BLE	32	11	-33.900	18.645	78	.129	.296	.113	237.2	.409	159.9	1.33	1.18	21.2	-.07
463	BLF	186	15	-29.109	26.188	1419	.061	.053	.150	265.5	.056	112.9	.75	.70	15.0	-.57
474	BLS	30	8	59.450	6.590	1169	-.358						1.06			
490	BMN	262	13	40.563	-117.267	1504	-.066	-.055	.082	111.1	.116	14.4	.78	.74	8.7	.43
501	BNG	160	17	4.367	18.567	0	-.019	-.045	.195	22.2	.287	87.9	.97	.80	31.1	.56
503	BNI	10	6	45.077	6.752	0	-.291						1.05			
507	BNS	131	11	50.964	7.175	200	.318	.509	.669	203.6	.480	33.0	1.02	.66	57.5	-.22
512	BOB	11	7	44.770	9.582	930	.317						1.32			
514	BOD	222	14	57.850	114.183	0	.158	.135	.241	307.6	.177	13.1	.69	.56	34.9	-.01
525	BOS	39	12	-31.598	-64.546	1200	-.133	-.220	.310	97.4	.529	25.6	1.42	1.03	46.7	-.31
532	BPI	55	13	-26.175	28.030	1700	-.104	-.050	.258	185.9	.142	172.9	1.13	1.05	13.9	.10
546	BRF	10	5	26.073	50.583	0	.430						.85			
547	BRG	282	16	50.874	13.946	296	.019	-.008	.195	78.1	.295	156.8	1.10	.95	25.5	.09
556	BRS	119	10	-27.392	152.775	524	-.792	-.775	.138	247.1	.083	93.0	.89	.85	9.0	.41
557	BRT	14	6	40.878	17.204	0	.236						.91			
559	BRV	208	15	71.274	-156.785	14	.224	.236	.091	92.0	.228	169.5	.63	.48	41.3	-.24
564	BSD	306	16	55.110	14.910	87	.012	.026	.113	196.0	.042	69.5	.78	.76	6.0	.01
566	BSF	496	18	47.832	6.792	1200	-.150	-.150	.045	289.8	.072	112.6	.58	.56	6.1	.33
567	BSI	76	9	5.500	95.317	0	.401						1.71			
586	BTO	228	13	40.598	110.018	1120	-.116	-.140	.096	80.0	.299	79.5	.68	.47	52.1	.51
598	BUL	88	16	-20.143	28.613	1340	-.328	-.356	.141	193.8	.417	60.3	1.07	.75	50.5	.15
618	BWO6	581	17	42.767	-109.632	2223	-.204	-.217	.016	339.5	.230	173.7	.79	.70	22.7	.34
641	CAF	575	17	44.926	2.065	629	-.069	-.074	.052	312.2	.059	51.2	.34	.32	14.3	.20
649	CAR	40	10	10.507	-66.927	1031	.185	.175	.203	233.2	.129	115.1	.71	.58	32.9	.03
671	CBK	141	12	48.947	-57.997	379	.411	.473	.097	205.3	.194	59.8	.77	.69	19.0	.13
672	CBM	54	14	46.932	-68.121	250	.040	.045	.354	101.2	.226	32.3	1.00	.69	52.5	.41
673	CBN	60	10	38.205	-77.373	70	-.145	.099	.803	94.9	.178	122.7	1.43	.92	58.4	.50
692	CCM	44	8	38.107	-91.346	223	-.014						.96			
702	CD2	566	16	30.910	103.758	628	.264	.281	.184	42.5	.117	24.2	.62	.50	33.1	-.35
707	CDF	463	17	48.394	7.271	1100	-.207	-.210	.101	55.8	.015	98.0	.35	.30	24.9	.45
722	CEH	159	17	35.891	-79.093	151	-.102	-.093	.254	267.2	.190	73.2	.96	.79	31.8	-.13
727	CER	103	14	-33.362	19.295	472	.048	.122	.279	124.0	.253	167.0	.89	.68	41.1	.17
744	CGL	11	5	39.362	9.297	1049	-.361						1.76			
747	CGP	95	9	8.455	124.694	50	-.024						.86			
752	CGY	16	7	-26.348	26.375	0	.129						.78			
761	CHG	609	16	18.790	98.977	416	-.177	-.185	.118	93.8	.079	114.8	.49	.43	23.7	.48
774	CHT	663	18	22.350	91.817	14	-.155	-.155	.130	128.4	.058	79.6	.68	.64	12.1	.00
797	CK1	15	8	44.499	8.399	0	.187						1.28			
813	CLL	277	15	51.309	13.004	230	.179	.187	.046	133.3	.083	178.1	.48	.45	11.3	-.24
827	CMA	140	15	64.290	-149.180	180	-.329	-.358	.068	278.3	.233	104.6	.84	.73	23.5	.15
828	CMB	301	14	38.035	-120.385	718	-.114	-.120	.093	226.9	.129	119.6	.86	.82	9.7	.50
841	CMS	152	11	-31.487	145.828	254	-.210	-.241	.153	71.3	.105	84.1	.55	.43	37.6	.54
847	CN2	764	13	43.801	125.448	230	-.093	-.063	.154	31.9	.046	12.5	.58	.51	22.0	-.30
848	CNB	239	12	-35.315	149.363	850	-.002	-.097	.288	41.0	.260	77.0	.97	.74	43.0	.11
880	COL	218	13	64.900	-147.783	182	.089	.144	.180	93.7	.245	161.5	.82	.65	38.5	.47
883	COO	138	13	-30.578	151.892	652	-.313	-.356	.168	12.2	.066	36.7	.49	.38	37.3	.13
884	COP	476	16	55.683	12.433	13	.200	.202	.045	61.1	.142	62.6	.46	.38	31.5	-.21
885	COR	19	7	44.585	-123.303	123	-.196						3.24			
909	CPU	39	10	40.673	-112.190	2227	.044	.278	.681	193.9	.355	13.5	1.43	1.15	35.7	.52
913	CPZ	12	6	50.210	-5.585	197	-.277						1.06			
960	CSY	360	14	-66.344	110.639	56	-.285	-.274	.043	212.4	.079	108.9	.82	.80	3.8	-.27
962	CTA	513	14	-20.088	146.255	356	.190	.191	.134	174.9	.256	89.0	1.09	.94	24.6	.49
990	CVF	103	13	42.568	8.870	529	-.134	-.156	.128	21.2	.213	117.9	.65	.55	28.3	.32

995	CYP	66	11	17.600	121.700	0	-.138	-.194	.249	119.7	.549	79.1	1.18	.82	51.8	-.15
1011	CYP	301	16	51.380	23.000	0	.954	.942	.050	32.2	.116	116.0	.89	.87	5.3	.25
1025	DAG	910	18	76.770	-18.770	16	-.044	-.044	.109	257.1	.066	86.0	.44	.39	23.2	.44
1029	DANN	82	11	28.350	83.760	2500	.732	.860	.350	260.8	.170	29.7	.86	.60	51.6	.36
1033	DAV	32	7	7.088	125.575	85	.725						.59			
1034	DAW	43	10	-5.550	150.467	250	-.579	-.433	.240	319.3	.662	1.6	1.12	.66	65.1	-.10
1037	DBIC	38	13	6.701	-4.913	25	-.136	-.178	.082	218.4	.330	90.7	1.29	1.17	19.0	.20
1048	DCN	258	16	53.343	-7.278	150	.474	.548	.276	147.2	.361	151.9	.97	.76	39.8	.08
1055	DDK	16	6	53.387	-6.339	85	.381						1.58			
1095	DL2	120	13	38.906	121.628	61	.341	.311	.103	161.1	.240	70.6	.44	.29	55.6	-.05
1098	DLE	184	15	53.287	-6.544	140	.196	.196	.038	296.4	.166	133.8	.69	.62	18.2	-.50
1099	DLF	158	15	53.296	-6.531	96	.632	.656	.102	182.5	.208	149.4	1.11	1.04	12.1	-.33
1110	DMN	371	18	27.690	85.160	2224	.306	.306	.126	117.8	.051	24.8	.53	.48	18.2	-.11
1113	DMU	257	14	53.899	-6.911	280	.381	.420	.164	203.6	.091	159.2	.56	.49	25.0	.29
1126	DOI	20	7	44.535	7.354	1014	-.439						1.40			
1133	DOL	116	16	50.210	4.692	221	-.098	-.098	.174	64.7	.090	169.8	1.12	1.06	9.7	.36
1137	DPC	26	6	50.133	16.511	759	.141						.56			
1151	DRLN	23	9	49.310	-57.542	238	-.655						1.35			
1175	DUG	440	16	10.195	-112.813	1476	-.082	-.101	.165	46.9	.056	4.8	.50	.42	31.0	-.09
1202	EAB	148	15	56.188	-1.340	250	.029	-.003	.135	41.8	.077	78.6	.70	.67	9.8	.13
1206	EAU	124	14	55.845	-3.455	349	.004	-.167	.478	353.9	.290	103.0	.80	.54	55.2	-.51
1210	EBH	142	14	56.248	-3.508	375	.104	.033	.158	318.5	.247	110.2	.72	.58	34.5	-.10
1212	EBL	100	14	55.773	-3.044	365	-.052	-.194	.273	2.8	.384	99.4	.78	.59	42.0	.10
1218	ECB	186	15	52.366	-6.781	125	.306	.332	.051	276.1	.238	161.4	1.06	.98	14.8	-.07
1227	ECP	337	15	52.180	-6.369	4	.389	.393	.142	280.7	.077	165.8	.53	.44	31.0	-.05
1231	EDI	78	13	55.923	-3.186	125	-.085	-.210	.293	34.0	.275	103.2	.66	.53	36.2	-.59
1236	EDM	280	16	53.222	-113.350	730	.336	.364	.223	186.2	.228	59.0	.89	.72	34.5	.16
1237	EDR	40	14	56.934	-2.604	388	.128	-.007	.450	354.5	.152	93.1	1.10	.93	27.4	-.31
1239	EDU	136	13	56.548	-3.011	275	.069	-.032	.310	347.7	.277	92.6	.64	.42	57.3	-.15
1258	EKA	878	17	55.333	-3.159	229	-.169	-.174	.131	304.5	.074	126.4	.47	.39	29.6	.35
1271	ELK	103	10	40.848	-115.288	2210	-.214	-.234	.251	228.8	.446	172.9	1.00	.67	54.5	-.45
1274	ELO	132	15	56.471	-3.712	495	.100	.168	.257	166.3	.195	9.6	.77	.63	32.5	.49
1279	ELT	23	9	53.250	86.267	0	-.025						1.48			
1299	ENN	831	18	50.767	5.923	119	.055	.055	.064	327.5	.155	165.9	.46	.37	36.8	.09
1306	EPF	571	17	13.031	.340	750	-.200	-.191	.202	192.6	.044	102.3	.72	.63	23.3	.36
1332	ESD	88	15	16.323	-122.150	1608	-.699	-.682	.289	175.9	.099	42.7	.68	.51	44.1	.18
1331	ESK	270	14	55.317	-3.200	241	.107	.092	.088	285.4	.093	94.8	.54	.49	16.3	.38
1342	ESY	140	14	55.918	-2.615	324	.030	-.132	.287	357.2	.182	99.4	1.02	.79	40.3	-.13
1345	ETA	176	15	52.696	-6.210	140	.407	.418	.181	227.2	.169	6.3	.74	.64	25.9	-.14
1359	EUR	204	13	39.483	-115.967	2177	-.494	-.500	.174	352.7	.059	89.0	.84	.78	12.2	.33
1361	EVA	55	13	-26.555	29.170	1621	-.076	-.109	.267	317.1	.255	94.9	1.09	.96	22.3	.44
1371	EYMN	116	10	48.062	-91.600	474	.020	.035	.114	234.9	.073	49.4	.71	.68	6.9	-.19
1381	FBA	826	16	64.860	-147.835	180	.044	.067	.180	93.9	.186	178.0	.61	.43	49.8	.43
1385	FCC	70	11	58.762	-94.087	39	.219	.202	.174	309.0	.060	45.2	.64	.57	18.9	.51
1399	FFC	770	16	54.725	-101.933	337	-.135	-.148	.187	65.9	.068	42.9	.57	.45	37.0	.54
1408	FHC	65	9	40.802	-123.985	610	.027						1.35			
1415	FIN	149	16	44.209	8.208	589	-.480	-.520	.382	22.7	.152	10.3	1.12	.89	36.4	-.19
1419	FITX	61	13	-18.192	125.728	109	-.293	-.141	.580	182.5	.369	17.8	1.32	.84	59.7	.74
1424	FKO	18	4	35.363	-97.386	351	.195						.80			
1431	FLN	785	17	48.763	-.482	0	.112	.116	.088	229.4	.027	15.5	.41	.38	14.3	.10
1455	FOR	91	11	40.863	-73.885	24	-.186	.102	.777	269.9	.538	54.5	1.07	.54	74.9	.30
1463	FRB	136	16	63.747	-68.547	17	-.030	-.027	.115	76.4	.078	138.1	.38	.30	39.2	.26
1466	FRF	508	17	43.657	6.768	310	-.050	-.053	.062	137.9	.112	105.9	.48	.42	21.0	-.07
1475	FRS	186	15	-29.750	25.322	0	-.055	-.049	.076	249.6	.058	137.3	.67	.64	6.9	-.30
1477	FRU	20	7	42.833	74.617	0	.227						.67			
1495	FUR	318	15	48.166	11.276	564	.317	.341	.073	259.6	.112	29.7	.66	.63	9.4	.14
1496	FVI	11	6	46.682	12.909	0	.029						.94			
1497	FVM	447	15	37.990	-90.510	310	.055	.087	.176	184.9	.240	67.7	.70	.49	50.3	-.11
1506	GAC	38	7	45.703	-75.470	112	-.358						.73			
1509	GAM	49	10	39.000	70.317	1299	.290	.343	.175	274.6	.275	63.5	.86	.69	36.3	-.37
1511	GAP	17	7	47.477	11.064	725	.139						1.06			
1518	GBA	868	17	13.604	77.436	25	-.241	-.248	.160	57.4	.152	61.5	.57	.44	42.6	-.46
1544	GDH	321	16	69.250	-53.533	23	-.063	-.053	.100	20.2	.169	93.1	.70	.61	23.4	-.48
1551	GEC2	370	16	48.951	13.715	1136	-.585	-.605	.182	4.8	.030	79.8	.60	.53	23.8	.50
1557	GERE	154	16	48.951	13.715	1136	-.660	-.666	.214	89.5	.101	8.4	.85	.75	23.2	.08
1596	GKN	248	18	28.030	81.670	1478	.347	.347	.116	358.9	.091	71.6	.52	.45	22.8	-.13
1601	GLD	495	14	39.750	-105.221	1761	.166	.170	.049	3.0	.103	95.0	.29	.23	39.7	.34
1613	GMB	20	6	38.167	15.863	1350	-.238						.95			
1636	GOGA	48	10	33.512	-83.616	150	-.034	.001	.226	149.8	.242	78.4	.77	.61	37.7	.12
1638	GOL	593	16	39.700	-105.371	2358	-.206	-.199	.021	81.5	.165	130.5	.47	.36	38.6	.09
1649	GRBI	11	8	49.472	11.687	493	-.061						1.11			
1653	GRF	658	17	49.692	11.222	499	.162	.158	.142	71.1	.049	149.7	.46	.38	30.7	.02
1656	GRI	60	9	38.821	16.451	479	.060						.54			
1658	GRM	97	13	-33.312	26.508	601	.358	.337	.088	9.0	.028	22.2	.46	.43	11.3	-.20
1660	GRO	61	8	43.317	45.700	123	.426						.72			
1663	GRR	636	17	48.388	-.851	0	.145	.147	.065	285.7	.077	153.4	.33	.28	27.1	.29
1664	GRS	20	6	39.500	46.333	0	.367						.66			
1679	GTA	822	17	39.400	99.800	1340	.015	.018	.108	93.6	.105	43.5	.41	.32	39.8	.03
1685	GUA	411	16	13.538	144.912	230	.179	.206	.404	172.5	.313	64.7	1.12	.69	62.6	.18
1689	GUM	221	15	20.680	-103.324	1567	.288	.212	.331	216.3	.262	15.2	1.08	.87	35.3	.14
1690	GUX	231	17	28.006	85.994	2900	.450	.470	.107	254.8	.273	76.3	.76	.60	36.9	-.63
1709	GYA	610	18	26.459	106.664	1161	.028	.028	.193	35.4	.125	88.9	.77	.67	24.8	-.49
1713	GZH	195	14	23.087	113.344	10	.072	.071	.032	219.3	.098	95.8	.70	.67	6.2	.17
1733	HAU	789	18	48.005	6.350	569	-.086	-.086	.050	187.1	.014	107.2	.44	.43	3.9	.33
1766	HFS	850	17	60.134	13.696	223	-.243	-.251	.390	61.4	.192	161.8	1.28	1.04	34.0	.09
1768	HGH	10	7	51.638	-2.806	209	-.221						1.03			
1769	HGN	88	13	50.890	6.067	135	-.073	-.113	.257	355.0	.332	152.6	.74	.46	61.3	.04
1774	HHC	534	17	40.849	111.564	1169	.174	.186	.044	67.6	.258	65.3	.73	.59	35.1	.15
1799	HKT	12	3	29.950	-95.833	-122	-.124						.90			
1836	HOF	288	13	50.314	11.877	565	.005	.159	.447	207.3	.497	44.4	.91	.48	72.6	.19
1852	HPK	162	15	54.004	-1.690	226	-.187	-.193	.149	16.3	.154	138.7	1.23	1.19	6.8	-.07
1867	HRV	118	14	42.506	-71.552	180	-.095	-.029	.485	173.6	.445	104.1	1.20	.74	62.6	-.03
1900	HVD	33	10	-30.604	25.496	1378	.255	.225	.220	37.2	.230	98.2	.99	.83	29.2	.11
1910	HYA	45	7	61.310	6.220	29	.199						1.83			
1911	HYB	235	11	17.417	78.553	509	.322	.306	.147	139.0	.106	41.5	.89	.84	10.9	.19
1914	HYF	32	11	47.285	2.694	428	.177	.407	.648	159.4	.068	150.2	1.15	.87	42.8	-.07
1955	ILT	184	13	67.833	-178.800	0	.297	.361	.285	59.0	.016	69.4	.73	.57	38.7	.08
1958	IMA	1013	17	66.085	-153.786	0	-.165	-.163	.177	51.0	.125	163.6	.58	.45	41.2	.33
1973	INGI	21	8	-8.818	115.145	202	.235						1.19			
1975	INK	721	17	68.237	-133.520	39	-.136	-.133	.079	114.0	.196	149.5	.56	.43	41.5	-.31
1984	IPM	837	16	4.581	101.027	246	-.011	-.043	.049	23.5	.285	90.7	.69	.51	44.9	.17
1993	IRK	188	14	52.267	104.317	467	.083	.083	.187	303.2	.224	67.9	1.18	1.05	21.9	.60
1996	ISA	249	16	35.643	-118.477	759	-.268	-.254	.361	166.6	.067	39.5	1.08	.89	33.0	.27
2045	JAY	64	12	-2.500	140.667	400	-.569	-.517	.442	66.1	.236	82.7	.84	.63	44.0	-.24
2059	JCT	87	12	30.479	-99.802	591	.012	.009	.088	95.6	.393	9.2	1.00	.79	38.0	.16
2080	JFWS	96	10	43.042	-90.381	335	-.051	-.212	.150	87.9	.297	176.6	.71	.63	21.5	.24
2112	JIRN	45	9	27.660	86.190	3063	.307						.52			
2188	JOZ	16	10	-27.445	32.078	244	-.131	-.180	.417	345.9	.231	168.2	1.38	1.12	35.1	.08
2196	JRS	67	9	49.192	-2.099	52	.316						1.36			

2258	KAF	365	16	62.113	26.306	201	-.140	-.142	.088	274.3	.192	96.0	.59	.46	39.3	.51
2263	KALI	13	6	-7.106	106.659	810	.526						1.47			
2276	KBA	682	17	17.184	13.447	1720	.070	.088	.144	213.8	.175	12.0	.61	.50	32.7	.31
2300	KDC	467	16	57.748	-152.492	0	.134	.138	.333	26.3	.161	62.1	1.11	.96	24.8	.16
2311	KED	35	6	12.926	-12.321	0	-.279						1.60			
2315	KELI	16	7	-8.217	114.491	591	-.256						1.09			
2321	KEV	437	18	67.755	27.007	79	.016	.016	.221	237.8	.039	54.0	.85	.76	19.5	.04
2331	KGM	284	9	2.015	103.317	103	.263						.48			
2337	KHC	569	16	49.131	13.579	699	-.092	-.089	.018	164.3	.104	168.7	.55	.52	10.3	.11
2351	KIC	418	17	6.360	-4.741	174	.113	.104	.035	136.1	.300	86.6	.65	.39	63.1	.37
2356	KIM	31	11	-28.752	24.780	1320	-.032	.136	.356	131.8	.488	144.0	1.44	1.13	38.8	-.13
2358	KIP	66	11	21.123	-158.014	72	.080	.068	.126	46.8	.164	63.2	.63	.56	21.5	.21
2360	KIS	82	7	47.017	28.867	0	.838						.48			
2362	KIV	109	11	13.950	42.683	1200	.329	.205	.377	156.5	.744	49.8	1.55	1.17	43.3	.31
2364	KJF	99	15	64.199	27.715	159	.090	.078	.061	274.8	.205	89.9	.79	.70	21.8	.29
2371	KKM	364	14	6.045	116.211	0	.011	.043	.260	145.4	.039	93.2	1.14	1.04	17.0	-.25
2372	KKN	319	17	27.790	85.280	1919	.257	.253	.191	21.0	.045	48.6	.48	.34	49.9	-.13
2380	KLB	232	11	-31.673	117.850	300	-.289	-.234	.126	167.6	.226	66.3	.70	.53	42.9	.01
2389	KLM	23	8	3.100	101.650	0	.271						.91			
2407	KMI	508	16	25.123	102.740	1945	.321	.321	.055	173.7	.095	39.7	.44	.40	14.7	-.04
2420	KMY	29	8	59.320	5.370	57	-.257						1.31			
2421	KMZ	11	6	-13.505	25.837	1223	-.393						.54			
2423	KNA	121	12	15.750	128.767	54	-.011	.058	.170	285.2	.275	51.2	1.24	1.13	17.3	.40
2436	KOD	39	7	10.233	77.467	2315	-.032						.61			
2442	KOL	91	9	41.493	35.911	144	.484						.70			
2444	KON	19	9	59.649	9.632	216	-.313						1.03			
2462	KRA	543	17	50.052	19.937	223	.204	.217	.164	140.3	.234	41.8	.78	.61	38.0	.68
2488	KSH	434	18	39.455	75.980	1286	.297	.297	.108	220.5	.174	168.7	.74	.66	21.4	.00
2489	KSI	10	7	-3.638	102.673	0	-1.419						1.80			
2493	KSP	566	15	50.843	16.293	379	.112	.133	.086	168.8	.129	23.7	.36	.26	47.3	-.10
2494	KSR	199	16	-25.850	26.897	1623	-.101	-.169	.311	318.8	.335	90.6	.92	.64	50.8	-.55
2512	KTK1	35	9	69.117	23.271	340	.298						.95			
2519	KUG	11	6	-10.163	123.653	52	-.723						2.81			
2525	KUP	33	10	-10.168	123.586	52	.180	.455	.451	238.9	.534	57.5	.91	.68	43.3	-.51
2526	KUR	64	11	45.233	147.867	0	.092	.097	.539	100.3	.189	38.2	1.28	.82	58.6	.40
2557	LAR	12	6	41.314	-105.583	0	.283						1.69			
2569	LBF	698	17	46.985	3.977	714	-.157	-.160	.035	125.3	.070	88.8	.45	.43	8.7	.57
2573	LBNH	114	15	44.301	-72.009	367	-.244	-.316	.177	281.5	.331	32.9	.89	.71	36.9	.08
2578	LBTB	74	13	-25.145	25.720	1027	.197	.139	.111	137.5	.295	60.9	.99	.82	30.7	.12
2604	LDF	661	17	48.594	-.122	289	.036	.038	.042	256.6	.070	137.3	.35	.32	15.6	.03
2619	LEM	49	9	-6.833	107.617	1241	-.051						1.48			
2633	LFF	603	17	14.937	.736	193	.017	.014	.075	37.4	.068	130.6	.40	.36	19.1	-.31
2648	LHC	43	9	48.417	-89.267	195	.073						.79			
2660	LIC	307	17	6.225	-5.028	100	.053	.058	.157	146.4	.162	93.7	.51	.33	58.0	.56
2672	LJC	66	9	46.043	14.533	395	.427						.75			
2678	LKO	155	16	9.644	-5.639	435	.127	.126	.150	237.1	.192	75.2	.64	.48	42.6	-.21
2699	LMN	54	10	45.870	-64.860	363	-.430	-.803	.916	306.4	.730	27.3	1.44	1.15	36.1	.02
2701	LMQ	23	6	47.548	-70.327	418	-.671						.82			
2702	LMR	482	18	43.333	6.509	200	-.058	-.058	.018	293.9	.087	81.9	.55	.53	7.4	-.42
2723	LOF	29	7	68.260	13.620	79	-.159						.61			
2730	LOR	881	17	47.267	3.850	529	-.045	-.046	.026	351.7	.040	129.5	.41	.41	3.9	.57
2731	LPA	49	6	-34.909	-57.932	14	-.382						2.90			
2735	LPB	74	13	-16.677	-68.234	3292	.211	.175	.472	52.6	.101	102.3	1.20	.91	41.9	.47
2738	LPF	668	17	48.165	-1.108	156	.068	.067	.111	7.5	.233	136.4	.61	.41	51.2	-.21
2739	LPG	696	18	45.627	6.765	2569	-.019	-.049	.033	116.4	.125	45.7	.41	.35	27.7	.15
2741	LPL	401	17	45.665	6.874	2069	-.139	-.140	.204	105.5	.104	57.6	.53	.35	55.7	-.31
2743	LPO	618	17	44.683	1.187	330	-.063	-.064	.021	30.6	.047	124.9	.29	.28	9.4	.08
2754	LRG	563	18	43.454	6.360	100	-.021	-.021	.085	119.0	.130	95.1	.58	.52	20.3	.00
2765	LSA	380	16	29.700	91.150	3657	-.272	-.276	.140	76.5	.048	75.0	.90	.86	8.2	-.42
2766	LSCT	84	12	41.784	-73.294	317	-.076	-.229	.218	273.2	.456	19.9	1.12	.94	29.8	.49
2768	LSF	518	17	46.250	1.530	430	-.068	-.066	.021	11.8	.070	156.5	.37	.35	11.1	.01
2777	LSZ	33	8	-15.366	28.232	1184	-.392						.59			
2798	LTX	143	13	29.334	-103.667	1013	-.198	-.180	.053	82.3	.193	93.4	.88	.82	14.3	.04
2825	LZH	630	18	36.050	103.833	1518	.235	.235	.160	90.7	.294	106.5	1.19	1.05	22.1	-.12
2832	MAF	567	17	46.265	2.714	469	-.032	-.033	.053	74.0	.023	58.7	.37	.36	7.2	.41
2835	MAI	267	15	35.472	135.387	30	-.206	-.161	.377	293.2	.284	115.1	1.14	.85	43.7	.07
2836	MAJO	154	12	36.542	138.209	421	-.033	.004	.189	8.0	.286	11.7	.75	.58	40.8	.18
2837	MAK	12	6	43.017	47.433	0	.679						.78			
2840	MAN	29	5	14.667	121.083	70	.564						.53			
2845	MAT	786	15	36.538	138.208	439	-.103	-.080	.113	60.9	.153	54.0	.49	.37	40.6	.46
2848	MAW	466	16	-67.604	62.870	12	-.241	-.246	.139	331.1	.158	88.7	.67	.58	25.6	.45
2852	MBC	997	17	76.242	-119.358	14	-.034	-.031	.242	169.1	.092	161.7	.65	.47	47.6	-.33
2857	MBL	202	14	-21.160	119.833	200	-.171	-.165	.097	148.7	.103	140.4	.58	.53	17.8	-.50
2878	MCQ	16	6	-54.499	158.956	14	-.434						.89			
2884	MCW	113	13	48.797	-122.973	693	-.010	.054	.088	127.1	.436	65.5	1.26	1.04	32.2	-.09
2897	MDJ	527	14	44.616	129.592	250	-.028	-.039	.190	151.8	.145	72.6	.62	.52	29.6	.02
2911	MEEK	50	8	-26.678	118.745	529	-.096						.71			
2914	MEK	30	10	-26.613	118.545	514	-.468	.156	1.184	247.6	.429	86.6	1.13	.56	75.5	-.14
2916	MEM	105	10	50.692	6.066	0	-.282	-.413	.500	36.7	.515	147.1	.90	.46	73.9	.12
2918	MEO	39	11	34.785	-98.596	465	.226	.134	.175	333.9	.322	119.5	.96	.84	23.3	.06
2923	MEU	10	4	37.101	14.930	985	-.624						.72			
2928	MFF	639	17	46.601	-.143	259	-.021	-.027	.132	37.5	.080	120.7	.42	.33	38.6	-.06
2938	MGD	61	9	60.100	150.700	219	.072						.53			
2947	MGR	16	6	40.176	15.598	259	.322						1.04			
2953	MHC	162	13	37.342	-121.642	1281	.278	.428	.288	2.1	.635	178.8	1.24	.78	60.1	-.11
2955	MHI	10	4	36.300	59.595	1100	-.007						.53			
2961	MIAR	209	14	34.657	-93.630	207	-.069	.005	.230	198.1	.365	80.8	.96	.62	57.5	.29
2963	MID	37	11	59.427	-146.338	0	.411	.414	.290	18.5	.226	65.2	.50	.37	45.6	.33
2969	MIN	92	11	40.345	-121.605	1495	.037	.026	.244	352.6	.117	159.8	.74	.58	39.4	.23
2978	MJAR	177	13	36.542	138.209	421	-.756	-.720	.291	124.3	.192	80.1	.71	.57	35.0	-.13
2990	MKS	44	8	-5.067	119.633	28	.082						1.40			
3013	MME	10	4	44.194	10.700	2160	.155						.74			
3033	MNI	24	6	1.450	124.800	128	-.061						1.95			
3034	MNK	66	9	53.900	27.567	0	.433						.84			
3038	MNO	13	5	37.931	14.695	1840	-.188						.53			
3042	MNS	15	8	42.396	12.800	600	.086						1.51			
3043	MNT	87	13	45.502	-73.623	112	-.070	-.058	.103	155.4	.062	144.8	1.20	1.19	2.8	.45
3045	MNV	65	11	38.572	-118.194	1506	-.152	-.260	.100	207.0	.505	152.9	1.14	.69	63.4	.06
3058	MOL	34	8	62.600	7.680	97	.166						.95			
3064	MOR	43	6	42.103	140.572	18	.212						.50			
3065	MOS	24	8	55.733	37.633	120	.495						.86			
3066	MOT	102	13	30.797	-104.082	2019	-.229	-.239	.234	77.1	.072	141.7	.84	.73	23.9	.53
3070	MOX	240	17	50.646	11.616	453	.102	.111	.011	141.0	.156	13.5	.44	.36	32.7	-.46
3071	MOY	42	9	51.683	100.983	0	.016						.94			
3101	MRW	226	15	-41.232	174.705	0	-.671	-.704	.183	86.5	.179	120.5	1.04	.95	15.7	-.20
3128	MTA	71	8	41.700	44.800	0	.110						.77			
3138	MTN	113	11	-12.847	131.130	79	.204	.457	.368	232.9	.410	60.1	.91	.81	21.5	-.44
3150	MUD	312	14	56.460	9.170	12	-.104	-.077	.159	157.5	.137	150.1	.49	.35	48.7	-.20
3153	MUN	340	12	-31.978	116.208	234	-.066	-.066	.179	149.5	.133	38.8	.67	.54	34.8	.09

3173	MYNC	33	7	35.139	-84.229	550	.024						.63					
3180	WZF	17	9	46.215	2.584	479	-.113						1.01					
3199	NAI	116	15	-1.339	36.837	1692	-.128	-.129	.150	142.8	.091	148.6	1.03	.99	7.6	-.06		
3203	NAN	88	11	32.063	118.783	7	-.422	-.302	.604	301.6	.737	92.8	1.21	.60	75.6	-.01		
3204	NAO	163	16	60.887	10.974	379	-.010	-.020	.300	323.4	.095	63.3	1.00	.84	29.6	.67		
3212	NB2	868	17	61.097	11.347	717	-.100	-.103	.138	52.4	.072	169.1	.51	.43	27.9	-.59		
3237	NDI	339	13	28.683	77.217	230	.159	.122	.225	6.8	.127	80.6	.61	.44	48.1	-.22		
3247	NEW	557	16	48.263	-117.120	759	-.133	-.168	.234	51.9	.158	153.9	.66	.50	43.5	-.10		
3268	NIE	430	16	49.424	20.322	555	.128	.139	.094	316.1	.111	39.2	.73	.69	11.5	.14		
3276	NJ2	423	12	32.052	118.854	45	.010	.050	.159	10.1	.136	24.1	.51	.38	43.3	-.59		
3305	NNA	101	14	-12.023	-76.922	574	-.284	-.285	.228	114.5	.174	91.3	1.11	.98	21.5	-.34		
3314	NOR	109	15	81.600	-16.683	35	-.558	-.545	.045	101.3	.270	33.2	.63	.43	53.0	.17		
3319	NPA	36	8	-15.087	39.253	374	.079						1.00					
3325	NPO	132	12	64.814	-146.915	418	-.200	-.260	.399	349.3	.177	151.1	1.39	1.13	34.2	.52		
3331	NRI	54	10	69.400	88.100	39	.154	.342	.348	275.7	.329	5.3	.92	.41	80.2	.67		
3340	NSS	42	10	64.650	11.970	101	.104	.224	.614	176.6	.421	51.5	.91	.27	91.2	-.23		
3350	NUR	673	17	60.509	24.651	101	-.079	-.090	.175	11.1	.121	143.0	.45	.29	59.7	-.09		
3360	NVL	37	7	-70.767	11.833	86	.068						.54					
3363	NWA	354	14	-33.020	117.240	264	-.465	-.466	.176	106.9	.272	8.9	1.17	1.02	23.2	-.07		
3365	NWL	18	8	-27.757	29.981	1332	-.026						1.88					
3387	OBN	355	17	55.167	36.600	0	.273	.259	.227	43.0	.303	119.3	1.03	.81	38.1	.39		
3397	OCO	22	6	35.590	-97.540	351	-.135						.91					
3400	ODAN	75	9	26.860	87.390	2045	.473						.75					
3402	ODD	18	8	59.950	6.670	629	.019						.70					
3410	OGA	285	16	46.868	11.025	934	-.025	-.033	.298	152.0	.095	57.0	.83	.66	36.0	-.02		
3418	OHR	315	15	41.214	20.939	739	-.358	-.328	.145	138.9	.285	25.1	2.10	2.03	6.6	-.31		
3426	OJC	235	15	50.245	19.934	391	.096	.036	.411	46.8	.099	111.4	1.22	1.02	30.6	.06		
3470	ORO	16	7	45.625	7.980	1161	-.403						.59					
3472	ORV	146	12	39.555	-121.500	360	.083	-.026	.103	178.6	.408	123.1	.93	.66	49.6	.13		
3491	OTT	141	14	45.394	-75.716	82	.164	.177	.126	301.1	.021	93.3	.95	.92	4.9	.22		
3506	OXF	76	8	34.512	-89.409	101	.314						1.11					
3511	PAB	36	11	39.546	-4.348	0	.009	.143	.422	144.0	.175	28.4	.81	.51	60.3	-.03		
3517	PAE	509	17	-17.662	-149.580	59	.132	.139	.241	131.6	.060	57.8	.52	.31	65.5	.56		
3530	PAS	14	6	34.148	-118.172	294	.088						1.15					
3555	PCI	133	11	-.933	119.883	0	-1.159	-1.259	.376	97.8	.379	98.0	1.18	.75	59.5	-.31		
3560	PCO	17	5	36.691	-96.978	331	-.214						.51					
3563	PCT	70	9	14.715	101.427	0	-.080						1.36					
3566	PDA	130	15	37.743	-25.662	35	-.727	-.719	.495	227.1	.429	161.3	1.67	1.20	48.5	.72		
3576	PDY	138	12	59.633	112.703	0	-.207	-.229	.165	137.8	.324	97.3	.76	.52	51.9	-.10		
3577	PEC	341	13	33.970	-117.257	615	-.098	-.082	.270	59.3	.061	8.1	1.08	1.00	15.1	.44		
3582	PEL	31	11	-33.144	-70.685	689	.110	.117	.208	265.8	.128	144.7	1.04	.98	12.1	-.27		
3584	PEN	11	5	30.467	-87.183	0	-.262						1.66					
3588	PET	207	13	53.017	158.650	0	.147	.220	.289	39.3	.243	38.8	.82	.60	45.9	.09		
3594	PFO	86	12	33.609	-116.455	1279	-.279	-.343	.432	89.6	.309	101.1	1.08	.58	70.6	.78		
3598	PGC	214	13	48.650	-123.451	4	-.065	-.115	.345	255.0	.409	150.9	1.09	.81	45.4	.58		
3599	PGD	10	5	43.875	11.721	1600	-.248						.97					
3601	PGF	193	17	42.548	9.141	1129	-.062	-.082	.171	102.3	.187	46.2	.97	.89	16.0	.05		
3604	PGP	35	5	13.480	120.960	0	-.309						.36					
3611	PHC	52	9	50.700	-127.433	32	-.081						1.14					
3631	PII	14	7	43.762	10.588	50	-.190						1.03					
3636	PIP	20	5	18.325	120.619	150	-.038						.63					
3651	PKI	348	18	27.610	85.490	2757	.165	.165	.136	27.1	.142	78.7	.72	.64	21.1	-.41		
3660	PLC	94	12	37.763	-122.012	462	-.011	.013	.258	150.7	.275	175.4	1.03	.88	27.8	-.55		
3669	PLP	19	5	11.165	124.979	133	-.572						1.00					
3678	PME	110	11	61.733	-149.167	231	-.002	.008	.053	289.4	.199	158.9	.94	.89	11.0	.05		
3679	PMG	245	12	-9.409	147.154	67	.282	.386	.179	187.7	.319	67.7	.66	.27	82.5	-.48		
3685	PMO	762	17	-15.004	-147.897	2	.046	.044	.084	191.9	.197	73.3	.61	.48	37.0	.36		
3687	PMR	1318	18	61.592	-149.131	0	.034	.034	.106	60.3	.139	123.8	.47	.37	38.4	.22		
3688	PMS	51	10	61.245	-149.561	716	.052	.126	.176	79.5	.093	45.0	.78	.73	11.5	.61		
3705	PNT	689	14	49.317	-119.617	550	-.095	-.103	.024	246.6	.078	146.4	.63	.61	5.1	-.25		
3711	POF	86	14	-29.382	19.950	0	-.376	-.441	.351	48.1	.216	57.7	1.26	1.04	31.6	.64		
3716	POO	244	14	18.533	73.850	555	.024	-.092	.451	100.3	.320	11.6	1.07	.76	50.1	-.64		
3727	PPI	122	10	-.452	100.384	0	-.238	-.475	.728	30.2	.378	134.8	1.08	.54	75.1	-.35		
3731	PPN	496	17	-17.531	-149.432	0	.042	.053	.108	149.8	.178	36.8	.57	.45	36.2	.07		
3733	PPR	66	9	9.750	118.733	14	-.178						.77					
3735	PPT	513	17	-17.569	-149.576	259	.217	.224	.200	142.7	.142	57.6	.46	.19	82.1	.03		
3741	PRA	155	12	50.070	14.430	202	.017	.073	.362	167.0	.457	28.3	.89	.62	51.3	.10		
3757	PRU	430	15	49.988	14.542	301	-.041	-.031	.114	148.1	.231	17.5	.51	.32	60.2	-.25		
3760	PRY	126	13	-26.928	27.473	0	-.083	.001	.152	221.2	.350	150.9	1.00	.78	39.7	-.38		
3761	PRZ	34	9	42.483	78.400	0	.228						.99					
3770	PSI	264	14	2.691	98.919	0	-.182	-.165	.391	124.4	.242	7.2	1.23	1.01	32.3	.32		
3798	PTZ	23	9	-14.390	31.390	1026	-.280						1.43					
3804	PUL	73	10	59.767	30.317	64	.595	.714	.294	225.8	.137	90.2	.59	.30	73.8	.54		
3825	PWA	49	12	61.651	-149.879	136	.214	.239	.397	193.7	.687	151.0	1.14	.58	74.0	-.38		
3832	PYA	126	9	44.033	43.050	497	.489						.42					
3838	PYUN	100	14	28.100	82.990	1866	.764	.774	.289	316.1	.289	66.5	1.03	.81	39.0	-.36		
3840	PZI	41	9	37.105	15.067	0	.079						.77					
3852	QIS	162	11	-20.627	139.652	330	-.155	-.153	.145	255.0	.028	63.7	.55	.49	22.1	.05		
3854	QIZ	163	11	19.029	109.843	230	.064	.197	.506	218.0	.605	65.8	.93	.36	85.2	.18		
3857	QLP	62	8	-26.587	144.248	209	.169						.91					
3870	QUE	114	11	30.188	66.950	1713	.528	.425	.366	163.8	.262	31.4	.92	.66	48.3	-.32		
3879	QZH	170	11	25.031	118.667	20	.069	.089	.105	326.3	.170	53.6	.76	.64	27.5	.25		
3882	RAB	41	11	-4.193	152.171	182	.525	.520	.375	256.3	.193	5.7	1.20	1.08	18.4	-.03		
3883	RAC	94	11	50.083	18.183	209	.409	.346	.304	132.0	.396	36.1	.74	.50	54.9	.12		
3888	RAM	70	10	37.766	41.292	850	.457	.469	.249	238.1	.400	86.5	.72	.46	59.1	.06		
3889	RAN	23	7	16.867	96.183	14	.149						.77					
3891	RAR	41	9	-21.212	-159.773	28	-.097						.93					
3892	RAT	24	7	51.941	178.451	225	.031						.86					
3917	RDP	10	6	41.758	12.717	759	.351						.42					
3930	RES	138	15	74.687	-94.900	14	-.672	-.653	.275	172.2	.365	126.3	1.01	.67	56.1	.04		
3937	RFI	38	10	41.305	13.998	0	.491	.559	.525	120.4	.348	174.9	1.15	.76	56.8	.06		
3961	RJF	624	17	45.305	1.516	409	-.070	-.075	.020	49.5	.079	94.9	.24	.19	32.1	.07		
3963	RKG	173	10	-34.098	117.104	300	-.551	-.704	.432	48.9	.099	49.7	.81	.24	91.0	.30		
3965	RKT	283	16	-23.118	-134.972	100	-.155	-.166	.053	32.6	.189	92.2	.51	.40	39.2	-.29		
3974	RMP	13	6	41.911	12.723	379	.263						.38					
3975	RMQ	172	13	-26.540	148.800	360	.185	.028	.543	88.3	.256	125.3	.99	.52	72.5	.57		
4013	RSCP	90	14	35.600	-85.589	580	.239	.377	.370	264.6	.472	66.4	.95	.63	56.0	-.19		
4017	RSNT	393	17	62.480	-114.592	50	-.143	-.124	.190	231.3	.223	46.1	.83	.68	31.9	-.26		
4018	RSO	289	15	60.572	-152.788	1921	-.030	.003	.123	245.8	.084	67.7	.32	.26	34.9	.42		
4020	RSSD	381	14	44.154	-104.062	2059	-.088	-.072	.216	269.9	.267	169.4	.84	.54	59.0	.20		
4041	RUV	791	17	-15.189	-147.384	3	.159	.163	.056	141.5	.081	48.7	.47	.44	12.9	.03		
4063	SAD	17	6	33.822	73.183	837	-.363						1.21					
4070	SAL	13	6	45.675	10.612	70	.876						1.56					
4073	SAO	187	13	36.765	-121.445	230	-.120	-.112	.100	294.6	.192	164.0	.66	.56	27.7	-.10		
4082	SBA	65	9	-77.850	166.756	37	-.311						1.06					
4086	SBF	371	18	43.981	7.452	817	.118	.118	.038	168.4	.050	110.2	.51	.50	4.1	.00		
4102	SCH	415	17	54.817	-66.783	540	.075	.086	.235	236.7	.144	77.2	.58	.35	63.7	-.33		
4107	SCO	332	17	70.483	-21.950	68	.077	.086	.130	189.9	.155	4.6	.57	.46	35.3	.06		
4124	SDI	11	6	41.758	13.954	0	.032						1.59					

4126	SDN	340	15	55.413	-160.622	23	.280	.291	.242	139.6	.103	45.9	.71	.53	43.1	.49
4129	SDV	23	9	8.886	-70.633	1580	.159						.87			
4136	SEK	186	16	-28.323	27.625	1485	.000	.007	.145	213.5	.065	95.3	.65	.59	18.4	-.19
4141	SES	408	16	50.396	-111.042	769	.386	.356	.237	55.4	.088	171.9	.81	.71	23.9	.75
4150	SFI	10	7	43.960	11.870	0	.118						1.11			
4170	SGO	10	6	40.633	15.384	0	-.438						1.09			
4181	SHE	46	7	40.633	18.633	0	.267						.65			
4187	SHK	96	10	34.530	132.678	284	.371	.387	.199	357.5	.171	7.1	.54	.42	37.7	.60
4188	SHL	58	7	25.567	91.883	1600	.152						.70			
4214	SIT	288	14	57.057	-135.324	18	-.304	-.293	.096	131.5	.097	159.1	.44	.39	24.3	.23
4221	SJG	41	8	18.112	-66.150	456	-.012						.51			
4238	SKO	379	17	42.021	21.496	345	.338	.337	.118	124.3	.182	160.8	.80	.71	21.7	.26
4239	SKR	24	9	50.667	156.100	0	.102						1.19			
4251	SLL	11	5	60.477	13.323	419	.426						.95			
4256	SLR	366	17	-25.753	28.420	1348	.071	.068	.042	140.1	.086	72.3	.69	.67	5.6	-.30
4265	SMF	593	17	46.645	3.841	458	-.057	-.064	.135	38.2	.056	46.4	.42	.34	33.8	-.29
4274	SMT	39	8	38.467	70.067	0	.289						.22			
4278	SMY	282	12	52.722	174.120	46	.246	.255	.158	314.7	.084	178.5	.40	.30	46.0	.57
4280	SNA	138	13	-70.309	-2.358	52	.169	.194	.321	96.6	.242	106.0	.90	.67	45.0	.12
4284	SNF	73	9	50.586	4.133	108	.051						.48			
4285	SNG	379	15	7.173	100.620	4	.196	.125	.245	52.8	.217	97.2	.55	.33	63.8	-.28
4297	SNY	512	14	41.828	123.578	54	-.024	.004	.160	60.7	.046	.9	.63	.57	19.6	.41
4298	SNZ	25	6	34.380	134.908	370	.116						1.15			
4301	SOC	11	7	43.583	39.717	192	.448						.84			
4307	SOI	11	6	38.121	16.099	0	-.270						1.57			
4317	SPA	1190	17	-90.104	115.000	2927	-.251	-.255	.134	167.0	.159	22.9	.57	.44	39.4	.19
4319	SPC	57	10	49.188	20.245	1771	.382	.393	.321	137.9	.192	55.7	.82	.49	64.3	.66
4323	SPI	107	15	57.160	-170.225	0	-.307	-.267	.190	214.6	.184	19.7	.73	.63	24.7	.06
4339	SQTA	334	16	47.255	11.287	1307	-.061	-.056	.111	141.6	.122	1.8	.57	.51	20.8	.05
4344	SRD	33	9	6.932	-72.853	1639	.186						1.14			
4352	SRO	69	9	47.813	18.313	0	.088						1.20			
4364	SSE	833	15	31.096	121.187	9	-.212	-.203	.098	98.2	.112	52.8	.51	.47	17.5	.35
4365	SSF	669	17	47.061	3.507	360	-.103	-.108	.009	322.4	.085	69.0	.42	.39	10.9	.48
4374	SSP	60	8	36.925	-116.219	2065	.281						.96			
4381	STA	23	7	17.695	74.000	665	.399						.83			
4382	STB	11	5	50.703	6.900	270	-.097						1.30			
4389	STJ	48	10	47.572	-52.733	61	.271	.298	.234	232.1	.083	85.7	.79	.67	28.1	-.39
4390	STK	599	17	-31.882	141.592	212	-.549	-.550	.092	78.7	.066	77.3	.94	.92	4.3	.76
4397	STU	102	12	48.771	9.193	375	.102	.173	.254	206.1	.143	177.5	.58	.38	57.3	-.29
4404	SUE	18	6	61.120	4.860	9	.252						.77			
4405	SUF	183	15	62.719	26.150	185	-.098	-.043	.279	224.1	.039	43.1	.60	.43	47.0	-.20
4412	SUR	80	14	-32.380	20.728	0	.100	.092	.064	271.1	.088	36.3	.62	.59	8.8	.04
4423	SVE	70	10	56.800	60.633	275	.735	.950	.732	215.3	.307	32.5	1.20	.53	80.3	.60
4436	SVW	586	17	61.182	-155.633	762	.079	.060	.187	27.5	.181	72.9	.79	.68	26.3	.27
4449	SWZ	18	12	-27.182	25.325	1342	.042	-.068	.252	76.3	.512	56.8	1.36	.89	57.6	-.24
4479	TAP	74	9	25.033	121.517	8	.260						1.48			
4482	TAT	96	13	34.983	139.867	0	.448	.555	.308	318.1	.359	86.6	1.03	.65	59.3	.67
4490	TBI	221	16	23.319	149.461	9	.073	.081	.068	180.3	.061	18.4	.74	.73	3.8	-.13
4503	TCF	622	17	46.288	2.210	592	-.179	-.177	.046	126.0	.076	123.1	.34	.31	19.9	.21
4519	THRI	19	6	-8.370	115.543	1000	.140						.68			
4555	TIA	256	13	36.211	117.124	300	.108	.073	.119	261.4	.358	85.6	.72	.35	76.7	.74
4556	TIC	277	17	6.550	-5.000	137	.024	.042	.282	154.2	.268	108.6	.96	.71	45.3	.72
4562	TIK	56	11	71.633	128.867	0	.241	.286	.225	40.5	.155	79.1	.95	.81	28.2	.18
4569	TIY	154	15	37.713	112.434	850	-.211	-.341	.773	172.4	1.028	87.3	2.42	1.62	55.3	-.65
4578	TKL	17	2	35.730	-83.840	349	-.555						.50			
4588	TLG	20	9	43.267	77.383	850	.086						1.19			
4621	TNP	585	16	38.220	-117.227	1932	-.308	-.320	.115	95.5	.039	142.2	.50	.46	15.7	-.12
4626	TOA	344	15	62.147	-146.223	908	.478	.460	.435	40.3	.209	104.2	1.06	.74	51.5	.54
4632	TOL	82	15	39.881	-4.049	479	-.105	-.017	.667	133.0	.095	89.6	1.49	.97	57.2	.34
4635	TOO	323	13	-37.571	145.490	603	-.140	-.125	.153	296.2	.285	41.2	1.12	1.00	20.8	.26
4640	TOV	16	5	9.820	-69.876	649	.033						1.24			
4651	TPX	168	15	-8.419	146.987	989	-.139	-.181	.282	90.0	.219	122.5	1.20	1.04	24.8	.27
4655	TPT	771	17	-14.984	-147.620	3	.114	.117	.145	180.1	.095	91.5	.51	.42	34.0	.23
4674	TRN	18	9	10.650	-61.400	24	-.219						1.52			
4675	TRO	47	8	69.632	18.928	14	-.103						1.40			
4680	TRT	218	13	-7.650	112.500	0	-.176	-.228	.262	42.2	.273	142.8	1.23	1.03	29.2	-.11
4689	TSI	10	4	3.508	98.695	0	.460						.96			
4692	TSM	90	9	4.223	118.072	0	.423						.70			
4700	TTA	690	16	62.930	-156.022	913	-.150	-.139	.119	58.7	.144	177.1	.63	.54	26.6	.19
4716	TUH	30	10	-33.297	19.150	189	-.029	-.259	.639	354.4	.256	58.6	1.31	1.06	35.1	.18
4718	TUL	528	17	35.910	-95.793	256	.026	.019	.025	131.5	.199	114.7	.71	.62	22.9	.33
4730	TVO	543	17	-17.782	-149.252	660	.276	.295	.270	162.4	.118	31.4	.62	.40	57.6	.30
4751	TXAR	133	12	29.338	-103.670	1013	-.762	-.782	.177	292.2	.156	143.0	1.06	.98	13.8	-.48
4772	UER	41	10	51.567	94.083	0	-.024	.173	.485	353.4	.234	4.2	.72	.52	47.8	-.67
4778	UKR	17	7	50.950	84.750	0	-.241						1.31			
4782	ULM	112	13	50.397	-95.950	280	.204	.229	.151	235.6	.236	140.9	1.27	1.16	16.9	-.26
4793	UPA	75	8	9.115	-79.540	41	.311						.84			
4795	UPP	126	13	59.858	17.627	14	.428	.397	.344	100.1	.132	166.8	.86	.62	48.4	.29
4819	UZH	121	14	48.633	22.300	0	.246	.239	.078	139.6	.287	171.4	1.24	1.15	14.8	-.30
4824	VAH	763	17	-15.237	-147.636	3	.117	.123	.122	134.0	.103	44.6	.46	.37	34.0	.27
4833	VAY	284	13	41.361	22.601	167	-.323	-.555	.709	19.4	.639	99.7	1.87	1.37	46.5	-.48
4838	VBY	90	11	45.545	15.316	259	.213	.197	.224	118.1	.149	167.4	.49	.35	49.8	.08
4878	VIR	15	6	-28.080	26.863	1340	.429						1.20			
4882	VKA	55	13	48.265	16.318	400	.373	.344	.286	179.2	.225	60.5	1.23	1.11	18.4	-.54
4884	VLA	32	9	43.117	131.900	74	.258						.76			
4903	VNDA	145	15	-77.640	161.956	97	-.354	-.362	.283	271.1	.154	110.2	1.59	1.50	11.2	-.02
4909	VOY	36	8	46.167	13.985	1072	-.176						1.41			
4918	VRAC	57	10	49.390	16.700	0	.106	.185	.176	219.4	.419	48.5	.82	.57	51.2	.43
4939	VVI	10	7	46.129	12.486	514	.229						.93			
4955	WAL	203	14	47.460	-115.965	0	-.163	-.150	.252	223.8	.224	9.4	.99	.83	30.6	-.26
4958	WAR	219	14	52.242	21.024	109	-.327	-.220	.224	186.3	.243	25.3	.72	.65	19.4	.43
4960	WAT	180	15	-30.317	115.883	0	-.055	-.024	.076	283.0	.225	27.7	.54	.37	52.7	.19
4962	WB2	169	13	-20.028	134.360	425	-.062	-.035	.233	179.5	.039	106.4	.49	.27	69.4	-.11
4985	WDC	257	13	40.580	-122.540	300	-.240	-.391	.496	241.6	.379	155.9	1.12	.74	55.7	.21
4997	WET	323	15	49.145	12.880	612	.032	.057	.077	177.2	.167	22.6	.51	.42	32.4	-.08
5017	WHN	575	15	30.544	114.350	26	-.015	-.017	.335	204.6	.422	97.5	1.37	.97	49.7	.32
5021	WHY	210	15	60.747	-135.007	1292	-.051	-.042	.074	2.1	.086	11.2	.77	.75	6.2	-.40
5029	WIN	161	14	-22.567	17.100	1728	.002	-.046	.157	312.9	.130	76.9	.84	.80	9.9	-.12
5047	WLF	90	13	49.796	6.174	0	-.148	-.066	.347	212.2	.204	45.8	.89	.67	42.6	-.37
5059	WME	16	6	53.516	-4.334	129	-.149						.42			
5061	WMO	201	15	34.718	-98.589	504	-.143	-.259	.582	47.8	.317	153.7	1.38	.96	50.9	.41
5062	WMQ	556	17	43.821	87.695	970	.072	.073	.082	101.3	.042	20.2	.46	.43	12.1	-.02
5082	WOOL	224	15	-31.073	121.678	0	-.436	-.448	.098	281.6	.182	74.4	.69	.61	22.2	-.63
5095	WR2	320	15	-20.068	134.472	414	-.261	-.268	.053	60.4	.192	95.5	.49	.35	47.4	-.37
5099	WRA	1110	17	-19.948	134.351	0	-.234	-.236	.060	170.7	.139	73.6	.40	.31	41.9	.32
5117	WTS	806	18	51.995	6.810	43	.034	.034	.114	128.6	.061	159.8	.40	.34	28.9	.13
5118	WTTA	313	17	47.388	11.663	1764	-.015	-.016	.050	114.6	.029	116.9	.59	.58	2.9	.33
5127	WVOR	237	13	42.439	-118.667	1343	-.010	-.026	.195	134.9	.209	97.1	.70	.54	41.1	-.23
5138	XAN	619	17	34.040	108.921	629	-.094	-.106	.119	143.5	.134	89.0	.70	.64	16.3	.21

5146	YAK	209	14	62.017	129.717	0	.398	.406	.237	146.6	.227	108.2	.74	.63	28.7	.09
5151	YBH	159	11	41.868	-122.805	968	-.091	-.151	.318	213.7	.106	163.3	.84	.70	29.6	.44
5160	YKA	46	9	62.579	-114.646	0	-.398						.91			
5162	YKC	257	16	62.478	-114.473	197	-.117	-.158	.036	173.4	.166	151.9	.64	.58	20.2	.02
5168	YKU	15	6	59.581	-139.836	19	.337						1.02			
5181	YOU	11	5	-34.278	148.382	503	.405						1.88			
5186	YRH	70	11	52.835	-4.740	300	.220	-.017	.616	357.7	.301	91.1	.90	.70	39.3	.27
5189	YSNY	101	14	42.558	-78.575	628	.041	.028	.325	216.6	.212	132.6	1.35	1.17	24.6	.42
5190	YSS	271	14	47.033	142.860	97	.073	.091	.077	51.0	.157	100.7	.62	.56	19.2	.22
5204	ZAK	202	13	50.383	103.283	0	.134	.146	.318	26.9	.206	154.9	.76	.57	42.5	-.69
5219	ZOBO	76	14	-16.294	-68.190	4396	-.124	-.131	.162	101.7	.073	99.5	.60	.51	25.8	.37
5224	ZST	137	14	48.196	17.103	250	-.187	-.188	.309	321.2	.140	175.7	1.51	1.38	16.0	.28

Appendix B-2: Station Correction for travel time

ist	stc	Neve	Nw	lat.	lon.	elev	ave	a0	a1	dir1	a2	dir2	rms0	rms1	vr	corr
13	AAI	80	8	-3.700	128.167	79	.009						1.73			
18	AAS	21	4	-62.160	-58.463	14	.523						1.58			
46	ACO	50	11	36.699	-99.146	521	-.540	-.227	.073	118.0	.300	29.3	.62	.59	10.6	-.16
63	ADE	269	14	-34.967	138.709	654	.015	.728	1.326	244.4	.884	75.0	1.93	1.55	35.2	.31
66	ADK	647	15	51.863	-176.655	0	-.365	-.203	.337	304.0	.673	170.6	1.30	1.17	18.6	-.16
82	AFR	522	17	-17.538	-149.778	50	1.263	1.270	.185	47.6	.086	127.3	.59	.57	6.0	.25
83	AGA	21	7	38.795	-27.232	79	1.709						.97			
88	AGM	14	6	47.082	-69.023	238	2.023						3.35			
90	AGR	11	6	27.133	78.017	163	1.922						1.73			
116	AKRL	16	4	23.660	32.710	0	1.378						1.77			
117	AKSR	19	6	23.672	33.021	0	1.771						.95			
118	AKU	543	18	65.687	-18.107	24	1.795	2.190	.872	175.0	.711	6.0	1.21	.89	46.0	.56
124	ALE	382	18	82.483	-62.400	64	-.118	-.192	.866	28.7	.089	60.2	.75	.40	71.1	-.59
134	ALQ	961	17	34.942	-106.458	1853	.248	.221	.184	176.8	.067	.7	.35	.32	16.7	.41
172	ANM	192	14	64.705	-165.417	330	.438	.469	.086	51.7	.409	85.0	.43	.29	53.1	-.01
173	ANN	117	9	44.883	37.300	0	-.143						.85			
177	ANT	29	8	-23.699	-70.415	79	.404						1.71			
186	APA	12	5	67.550	33.333	0	-.149						.77			
194	APO	18	11	60.590	14.030	340	-.815	-.814	.152	223.8	1.440	24.8	1.96	1.63	31.0	.51
202	AQU	10	7	42.354	13.403	720	.965						.77			
213	ARC	208	18	40.877	-124.075	59	.079	.051	.440	250.7	.359	100.9	.80	.69	26.5	.30
214	ARE	12	5	-16.571	-71.563	2451	.755						.80			
221	ARMA	172	11	-30.448	151.730	1129	.560	.451	.315	42.3	.422	126.1	.73	.70	8.1	-.66
227	ARU	184	13	56.400	58.600	250	-.621	-.172	.164	207.7	.839	162.1	.82	.52	59.2	.27
228	ARV	11	6	43.635	13.021	0	.327						.50			
229	ASA	245	14	43.770	142.373	111	-.687	-.770	.556	302.0	.078	76.3	.67	.50	44.1	-.06
234	ASH	105	9	37.950	58.350	219	.835						.82			
241	ASP	978	16	-23.683	133.897	600	-.893	-1.062	.394	320.1	.330	30.0	.79	.68	25.0	-.40
243	ASS	10	5	43.105	12.762	0	.496						1.16			
280	AVF	623	17	46.855	3.376	224	-.319	-.324	.122	183.4	.315	13.9	.32	.21	55.9	.29
304	BAG	128	10	16.411	120.580	1506	-.742	-.705	.869	301.9	.707	111.8	.90	.37	82.8	.28
308	BAL	207	12	-30.665	116.772	300	-.774	-.716	.101	201.0	.223	7.7	.26	.17	54.7	-.26
332	BBH	33	5	26.215	50.457	0	-.035						2.07			
333	BCA	134	15	41.550	41.673	500	-.261	-.355	.427	296.9	.373	73.8	.71	.60	28.1	.00
353	BDF	92	13	-15.788	-47.933	1254	-.080	-.139	.824	58.0	.529	163.3	.80	.45	68.6	-.33
356	BDI	17	7	44.173	10.720	0	-.060						.34			
362	BDT	526	14	17.233	99.050	0	-.642	-.411	.857	173.3	.656	11.0	.94	.64	53.9	.38
365	BDW	77	11	42.862	-109.582	2190	-.292	-.336	.295	328.9	.290	18.2	.38	.21	68.4	.68
371	BEE	59	9	26.017	50.522	0	-.484						2.31			
384	BEW	15	6	-32.415	22.630	870	.309						1.15			
386	BFD	166	12	-37.176	142.544	234	.018	.488	.447	188.1	.649	101.1	.87	.59	54.7	-.32
390	BFS	111	14	-26.898	26.785	1309	-.874	-.605	.720	79.7	.317	175.5	1.32	1.20	18.2	.24
391	BFT	101	14	-25.687	30.043	1868	.673	.801	.199	194.7	.324	126.8	.69	.63	15.6	-.18
395	BGC	53	13	37.962	-122.170	610	-.885	-.564	.533	189.5	.357	105.6	.83	.68	34.0	.09
397	BGF	592	17	46.558	2.846	389	-.190	-.145	.268	170.6	.176	4.0	.36	.29	35.0	.45
412	BHG	292	15	47.721	12.879	474	.415	.093	.523	7.6	.160	93.6	.51	.34	54.1	.24
418	BHO	13	7	34.508	-94.873	143	-.187						.39			
432	BING	149	13	42.157	-76.067	407	-.089	-.030	1.148	101.6	.421	165.4	1.15	.74	58.3	-.37
440	BJA	24	6	25.992	50.608	0	-.350						1.41			
441	BJI	691	16	40.040	116.175	13	-.107	.176	.413	300.8	.092	27.5	.56	.48	28.2	-.08
445	BKB	12	4	-1.283	116.833	0	3.372						2.44			

456	BKS	693	16	37.877	-122.235	275	.832	1.180	.430	93.2	.362	174.4	.61	.43	49.9	.21
460	BLA	390	16	37.211	-80.421	634	-.144	.142	.569	108.8	.495	94.9	.60	.21	87.9	.51
462	BLE	32	11	-33.900	18.645	78	1.582	.792	2.616	134.1	1.749	56.4	1.87	1.23	56.5	-.08
463	BLF	186	15	-29.109	26.188	1419	-.181	-.453	.598	5.2	.316	63.5	.62	.47	43.0	-.59
474	BLS	30	8	59.150	6.590	1169	1.130						.99			
490	BMN	262	13	40.563	-117.267	1504	.478	.484	.195	312.8	.231	10.7	.32	.23	46.8	.38
501	BNG	160	17	4.367	18.567	0	-.377	-.315	.291	267.5	.307	99.1	.58	.49	28.3	.54
503	BNI	10	6	45.077	6.752	0	.724						.73			
507	BNS	131	11	50.964	7.175	200	.242	.453	.222	126.0	.570	133.8	.46	.19	83.6	-.16
512	BOB	11	7	44.770	9.582	930	.593						.53			
514	BOD	222	14	57.850	114.183	0	-.806	-1.054	.652	153.0	.378	77.7	.64	.40	60.6	-.17
525	BOS	39	12	31.598	-64.546	1200	-.328	-.616	.322	44.2	.894	70.4	.97	.78	35.9	-.31
532	BPI	55	13	-26.175	28.030	1700	-.777	-.822	1.459	336.3	1.679	2.6	2.18	1.34	62.3	.10
546	BRF	10	5	26.073	50.583	0	.966						2.78			
547	BRG	282	16	50.874	13.946	296	.275	.217	.179	46.8	.419	96.6	.49	.37	42.7	.10
556	BRS	119	10	27.392	152.775	524	-.372	-.118	.363	278.1	.704	55.5	.54	.36	56.0	.35
557	BRT	11	6	10.878	17.201	0	.124						.43			
559	BRV	208	15	71.274	-156.785	11	-.482	.011	.716	301.8	.313	150.7	.86	.66	40.9	-.15
564	BSD	306	16	55.110	14.910	87	-.356	-.357	1.316	333.0	.915	108.6	1.25	.55	80.7	.01
566	BSF	196	18	47.832	6.792	1200	-.511	-.408	.088	125.9	.230	150.7	.40	.36	19.7	.38
567	BSI	76	9	5.500	95.317	0	-1.041						1.88			
586	BTO	228	13	40.598	110.018	1120	.115	-.044	.384	212.6	.758	85.7	.58	.28	77.1	.52
598	BUL	88	16	-20.143	28.613	1340	-.195	-.658	1.103	62.7	.385	87.9	1.53	1.26	32.7	.15
618	BWO6	581	17	42.767	-109.632	2223	-.362	-.557	.275	276.2	.142	128.1	.40	.33	29.9	.26
641	CAF	575	17	11.926	2.065	629	.190	.053	.318	95.1	.143	24.9	.36	.25	51.1	.21
649	CAR	40	10	10.507	-66.927	1031	-.621	.014	.890	61.3	.917	99.3	1.07	.61	66.8	.07
671	CBK	141	12	48.947	-57.997	379	-.375	-.392	.536	166.6	.249	27.2	.72	.56	39.2	.10
672	CBM	54	14	46.932	-68.121	250	-.010	.059	.746	138.3	.564	12.0	.86	.51	64.8	.41
673	CBN	60	10	38.205	-77.373	70	.430	.647	.758	114.9	.284	178.7	.83	.50	64.5	.50
692	CCM	11	8	38.107	-91.316	223	-.525						1.53			
702	CD2	566	16	30.910	103.758	628	-.282	-.076	.591	332.1	.478	152.5	.70	.50	48.2	-.37
707	CDF	163	17	18.394	7.271	1100	-.345	-.372	.225	55.1	.297	148.5	.46	.37	36.0	.45
722	CEH	159	17	35.891	-79.093	151	-.354	-.159	.849	106.8	.124	80.9	.81	.50	62.0	-.13
727	CER	103	14	-33.362	19.295	472	-.596	-.425	.714	89.8	.794	98.5	1.41	1.17	30.8	.14
744	CGL	11	5	39.362	9.297	1049	.933						.77			
747	CGP	95	9	8.455	124.694	50	-.934						1.77			
752	CGY	16	7	-26.348	26.375	0	-.624						3.40			
761	CHG	609	16	18.790	98.977	416	.279	.053	.582	137.0	.044	102.6	.50	.25	74.3	.62
774	CHT	663	18	22.350	91.817	14	.338	.043	.450	127.8	.110	105.7	.44	.28	59.2	.18
797	CK1	15	8	44.199	8.399	0	-.015						1.02			
813	CLL	277	15	51.309	13.004	230	-.185	-.123	.163	273.9	.199	85.0	.47	.26	70.5	-.29
827	CMA	140	15	64.290	-149.180	180	.345	.133	.459	163.4	.301	73.5	.56	.38	53.9	-.01
828	CMB	301	14	38.035	-120.385	718	.330	.662	.402	3.5	.577	173.2	.88	.73	30.0	.48
841	CMS	152	11	-31.487	115.828	254	.093	-.102	.345	36.0	.235	167.9	.58	.52	17.3	.54
847	CN2	764	13	43.801	125.448	230	-.336	-.436	.101	219.7	.402	108.6	.37	.21	68.3	-.28
848	CNB	239	12	-35.315	149.363	850	.652	.820	.469	99.5	.219	53.2	.68	.52	41.7	.19
880	COL	218	13	64.900	-147.783	182	-.385	-.263	.788	23.7	.119	151.9	.72	.44	62.5	.50
883	COO	138	13	-30.578	151.892	652	-.473	-.446	.739	282.4	.226	84.8	.68	.41	63.6	.13
884	COP	476	16	55.683	12.433	13	.738	.809	.180	65.3	.496	112.6	.66	.56	29.3	-.27
885	COR	19	7	44.585	-123.303	123	1.199						.61			
909	CPI	39	10	40.673	-112.190	2227	-.992	-.694	.446	149.1	.405	74.6	.90	.75	29.5	.50
913	CPZ	12	6	50.210	-5.585	197	.257						.48			
960	CSY	360	14	-66.344	110.639	56	.112	-.403	1.259	105.1	.167	8.8	2.57	2.41	12.4	-.27
962	CTA	513	14	-20.088	146.255	356	-.235	-.105	.533	234.1	.087	164.0	.53	.40	41.2	.52
990	CVF	103	13	42.568	8.870	529	-.193	-.177	.114	196.1	.133	147.2	.35	.33	13.6	.32
995	CVP	66	11	17.600	121.700	0	.772	.967	.945	251.4	.420	40.7	1.38	1.13	32.4	-.17
1011	CYP	301	16	51.380	23.000	0	.064	.159	.323	213.8	.519	35.5	.80	.68	28.2	.25
1025	DAG	910	18	76.770	-18.770	16	-.670	-.468	.415	168.3	.200	154.8	.48	.34	49.1	.46
1029	DANN	82	11	28.350	83.760	2500	-.003	.129	.340	17.1	.463	5.7	.45	.25	69.1	.37
1033	DAV	32	7	7.088	125.575	85	.328						1.49			
1034	DAW	43	10	-5.550	150.467	250	-.009	-.203	.974	352.8	.906	54.6	.88	.33	85.5	-.33
1037	DBIC	38	13	6.701	-4.913	25	-1.040	-.868	.482	253.5	.246	34.3	.71	.58	31.7	.11
1048	DCN	258	16	53.343	-7.278	150	.255	.515	.838	140.6	.089	97.9	.84	.59	49.5	.14
1055	DDK	16	6	53.387	-6.339	85	-.264						.40			
1095	DL2	420	13	38.906	121.628	61	.212	.314	.234	35.7	.376	98.8	.68	.59	23.5	-.01
1098	DLE	184	15	53.287	-6.544	140	.146	.291	.369	57.8	.597	143.0	1.10	.98	20.8	-.50
1099	DLF	158	15	53.296	-6.531	96	.273	.228	.198	92.0	.091	160.6	.43	.39	15.7	-.35
1110	DMN	371	18	27.690	85.160	2224	-.056	.023	.059	56.0	.349	10.8	.49	.41	27.9	-.16
1113	DMC	257	14	53.899	-6.911	280	.201	.391	.741	113.1	.396	124.9	.83	.54	57.6	.33
1126	DOI	20	7	44.535	7.354	1014	-.430						1.53			
1133	DOU	116	16	50.210	4.692	224	.199	.160	.384	76.2	.378	117.9	.48	.26	69.6	.36
1137	DPC	26	6	50.433	16.511	759	.855						1.20			
1151	DRLN	23	9	49.310	-57.542	238	-.373						.87			
1175	DUG	440	16	40.195	-112.813	1476	.433	.286	.251	173.7	.227	156.3	.31	.18	66.4	-.24
1202	EAB	148	15	56.188	-4.340	250	-.191	-.049	.294	225.5	.277	17.6	.48	.43	21.4	.08
1206	EAU	124	14	55.845	-3.455	349	.157	.151	.260	130.1	.171	14.4	.26	.15	68.2	-.39
1210	EBH	142	14	56.248	-3.508	375	-.021	.094	.370	166.7	.262	24.9	.25	.11	80.3	-.39
1212	EBL	100	14	55.773	-3.044	365	.157	.257	.579	127.4	.440	135.5	.90	.70	38.3	.10
1218	ECB	186	15	52.366	-6.781	125	.111	.230	.299	111.8	.148	143.5	.34	.25	46.7	-.12
1227	ECP	337	15	52.180	-6.369	4	.175	.186	.114	112.9	.157	17.7	.22	.17	42.8	-.05
1234	EDI	78	13	55.923	-3.186	125	.003	.230	.521	217.4	.192	18.3	.40	.30	43.0	-.59
1236	EDM	280	16	53.222	-113.350	730	-.296	-.396	.268	353.0	.227	81.7	.42	.33	36.8	.10
1237	EDR	40	14	56.934	-2.604	388	-.177	-.162	.111	347.2	.208	47.2	.37	.33	19.6	-.33
1239	EDU	136	13	56.548	-3.014	275	-.196	-.009	.193	247.6	.114	167.5	.39	.36	16.0	-.19
1258	EKA	878	17	55.333	-3.159	229	-.185	.004	.350	195.2	.524	171.9	.61	.45	47.0	.29
1271	ELK	103	10	40.848	-115.288	2210	.540	.439	.128	286.8	.171	105.0	.35	.31	19.4	-.47
1274	ELO	132	15	56.471	-3.712	495	-.284	-.012	.583	208.7	.597	26.0	.59	.20	87.9	.46
1279	ELT	23	9	53.250	86.267	0	-1.023						.95			
1299	ENX	831	18	50.767	5.923	119	.229	.420	.247	140.9	.115	127.6	.40	.35	24.1	.01
1306	EPF	571	17	43.031	.340	750	-.255	-.073	.614	213.3	.093	9.3	.58	.36	60.1	.10
1332	ESD	88	15	46.323	-122.150	1608	-.072	-.044	.616	251.2	.666	11.1	.96	.72	44.8	.19
1334	ESK	270	14	55.317	-3.200	241	.123	.125	.348	164.1	.362	33.8	.50	.42	30.0	.42
1342	ESY	140	14	55.918	-2.615	324	-.199	-.125	.258	164.6	.195	149.2	.34	.25	44.2	-.14
1345	ETA	176	15	52.696	-6.210	140	.290	.328	.285	132.2	.201	51.6	.37	.25	53.4	-.14
1359	EUR	204	13	39.483	-115.967	2177	.452	.433	.217	39.9	.109	149.1	.27	.21	35.0	.33
1361	EVA	55	13	-26.555	29.170	1621	.553	.849	.456	354.7	.754	139.2	.88	.58	55.8	.45
1371	EYMN	116	10	48.062	-91.600	474	-.972	-.596	.665	62.4	.661	80.8	.74	.45	63.5	-.18
1381	FBA	826	16	64.860	-147.835	180	-.530	-.413	.661	9.1	.196	149.2	.60	.34	66.9	.51
1385	FCC	70	11	58.762	-94.087	39	-.457	-.510	.065	8.7	.177	98.2	.47	.45	8.4	.46
1399	FFC	770	16	54.725	-101.933	337	-.310	-.433	.239	350.2	.174	53.8	.41	.34	30.5	.53
1408	FHC	65	9	40.802	-123.985	610	1.106						1.18			
1415	FIN	149	16	44.209	8.208	589	-.633	-.534	.206	162.6	.232	106.3	.47	.40	26.5	-.26
1419	FITX	61	13	-18.192	125.728	109	-.670	-.451	.720	182.6	.660	1.4	.74	.45	63.8	.74
1424	FKO	18	4	35.363	-97.386	351	-.018						1.78			
1431	FLN	785	17	48.763	-.482	0	-.348	-.383	.182	279.0	.062	94.8	.19	.13	53.3	.06
1455	FOR	91	11	40.863	-73.885	24	-.590	-.326	.440	255.0	.507	168.3	.76	.50	57.4	.26
1463	FRB	436	16	63.747	-68.547	17	-.524	-.115	.192	104.5	.506	94.0	.59	.46	39.3	.28
1466	FRF	508	17	43.657	6.768	310	-.250	-.199	.272	188.2	.166	179.5	.35	.26	44.7	-.03
1475	FRS	186	15	-29.750	25.322	0	-.221	-.328	.674	338.2	.057	174.9	.88	.75	26.9	-.29

1477 FRU	20	7	42.833	74.617	0	.635						.92								
1495 FLR	318	15	48.166	11.276	564	.430	.311	.350	.2	.096	108.7	.43	.35	33.1	.13					
1496 FVI	11	6	16.682	12.909	0	.025						.64								
1497 FVM	447	15	37.990	-90.510	310	-.812	-.749	.216	84.3	.151	58.9	.45	.40	18.9	-.09					
1506 GAC	38	7	15.703	-75.470	112	-.361						.88								
1509 GAM	49	10	39.000	70.317	1299	.240	.154	.580	323.4	.792	125.8	.59	.22	86.3	-.41					
1511 GAP	17	7	47.477	11.064	725	.585						.55								
1518 GBA	868	17	13.601	77.136	25	-.577	-.338	.231	195.9	.268	141.1	.52	.45	25.8	-.59					
1544 GDH	321	16	69.250	-53.533	23	.100	.688	1.282	157.7	.515	168.9	2.17	1.93	21.3	-.46					
1551 GEC2	370	16	48.951	13.715	1136	-.415	-.490	.120	334.5	.215	35.0	.39	.35	22.2	.53					
1557 GERE	154	16	48.951	13.715	1136	-.203	-.393	.326	323.5	.489	64.0	.54	.33	63.5	.22					
1596 GKN	248	18	28.030	84.670	1478	-.219	-.072	.198	86.9	.468	174.9	.49	.32	57.2	-.11					
1601 GLD	195	14	39.750	-105.221	1761	.718	.691	.211	296.5	.110	108.2	.25	.20	37.2	.37					
1613 GMB	20	6	38.167	15.863	1350	-.169						.86								
1636 GOGA	48	10	33.512	-83.616	150	-.236	-.427	.235	104.6	.234	165.6	.54	.49	18.2	.07					
1638 GOL	593	16	39.700	-105.371	2358	.214	.190	.360	273.4	.044	2.2	.43	.35	34.2	.12					
1649 GRB1	11	8	49.472	11.687	493	.785						1.31								
1653 GRF	658	17	49.692	11.222	499	.618	.405	.425	22.2	.111	84.9	.41	.27	55.4	.26					
1656 GRI	60	9	38.821	16.451	479	.386						.85								
1658 GRM	97	13	-33.312	26.508	601	1.396	2.457	2.548	133.3	1.297	150.5	1.83	.88	77.0	-.11					
1660 GRO	61	8	43.317	15.700	123	.985						1.06								
1663 GRR	636	17	48.388	-.851	0	-.234	-.330	.362	312.5	.073	23.7	.37	.26	52.5	.25					
1664 GRS	20	6	39.500	46.333	0	.275						.80								
1679 GTA	822	17	39.100	99.800	1340	.092	.035	.295	216.1	.248	103.4	.46	.37	34.8	.05					
1685 GUA	111	16	13.538	144.912	230	-.879	-.981	.451	106.9	.658	115.9	1.02	.89	23.2	.20					
1689 GUM	221	15	20.680	-103.324	1567	-1.215	-1.187	.515	214.6	.503	139.5	.86	.69	36.6	.16					
1690 GUN	231	17	28.006	85.991	2900	.055	.139	.244	87.9	.457	171.5	.50	.36	48.0	-.60					
1709 GYA	610	18	26.459	106.664	1161	.180	.091	.235	137.2	.462	151.4	.63	.51	35.4	-.46					
1713 GZH	195	14	23.087	113.344	10	.786	.609	.341	113.9	.438	68.4	.58	.48	32.4	.15					
1733 HAU	789	18	48.005	6.350	569	-.388	-.380	.016	356.2	.220	164.4	.27	.22	35.3	.32					
1766 HFS	850	17	60.134	13.696	223	-.650	-.671	.074	309.4	.308	91.6	.29	.19	58.2	.08					
1768 HGH	10	7	51.638	-2.806	209	.243						.64								
1769 HGN	88	13	50.890	6.067	135	.174	.547	.975	109.8	1.541	138.4	1.64	1.21	45.6	.12					
1774 HHC	534	17	40.849	111.564	1169	.366	.680	.622	324.6	.450	179.3	1.40	1.30	14.6	.18					
1799 HKT	12	3	29.950	-95.833	-122	.093						.66								
1836 HOF	288	13	50.314	11.877	565	.263	-.010	.327	41.2	.449	78.5	.45	.27	64.0	.53					
1852 HPK	162	15	54.004	-1.690	226	.561	1.269	.963	173.5	.584	142.1	1.97	1.79	17.6	-.13					
1867 HRV	118	14	42.506	-71.552	180	-.012	-.421	.198	97.4	.819	177.8	1.12	.84	43.0	.03					
1900 HVD	33	10	-30.604	25.196	1378	-.554	.392	.489	273.6	.942	148.2	1.86	1.72	15.3	.21					
1910 HYA	45	7	61.310	6.220	29	.427						.92								
1911 HYB	235	11	17.417	78.553	509	-.466	.609	2.148	204.1	1.581	33.6	2.07	1.11	71.2	.11					
1914 HYF	32	11	47.285	2.694	128	-.019	-.120	.332	91.8	.041	86.6	.53	.45	27.4	-.05					
1955 ILT	184	13	67.833	-178.800	0	-.627	-.499	.351	100.3	.054	70.1	.57	.51	21.6	.14					
1958 IMA	1013	17	66.085	-153.786	0	.073	-.023	.457	3.5	.392	39.2	.52	.29	69.1	.28					
1973 INGI	21	8	-8.818	115.145	202	-.520						1.82								
1975 INK	721	17	68.237	-133.520	39	-.168	-.493	.379	293.9	.136	156.1	.47	.37	40.4	-.31					
1984 IPM	837	16	1.581	101.027	246	.234	.329	.263	286.6	.600	28.4	.74	.58	38.4	.14					
1993 IRK	188	14	52.267	104.317	467	-.341	-.170	.968	232.9	.132	49.5	1.00	.64	59.2	.60					
1996 ISA	249	16	35.643	-118.477	759	.270	.534	.456	109.6	.127	33.2	.70	.61	24.4	.18					
2045 JAY	64	12	-2.500	140.667	100	-.519	-1.878	2.069	25.8	2.627	140.3	2.32	1.13	76.3	-.05					
2059 JCT	87	12	30.479	-99.802	591	-.433	-.173	.090	69.4	.668	23.3	.66	.48	45.9	.21					
2080 JFWS	96	10	43.042	-90.381	335	-.962	-.917	.285	81.8	.279	27.9	.29	.07	93.7	.21					
2112 JIRN	45	9	27.660	86.190	3063	.227						.53								
2188 JOZ	16	10	-27.445	32.078	244	.456	1.324	2.232	169.9	2.347	179.7	2.17	1.12	73.0	.09					
2196 JRS	67	9	49.192	-2.099	52	.147						1.35								

2258 KAF	365	16	62.113	26.306	204	-.598	-.409	.200	174.5	.381	115.6	.38	.20	73.1	.48					
2263 KALI	13	6	-7.106	106.659	810	-.661						1.77								
2276 KBA	682	17	47.184	13.447	1720	-.052	-.057	.040	127.7	.570	179.0	.49	.28	68.4	.31					
2300 KDC	467	16	57.748	-152.492	0	-.275	-.016	.371	62.0	.370	36.6	.42	.21	73.9	.20					
2311 KED	35	6	12.926	-12.321	0	-.220						2.62								
2315 KELI	16	7	-8.217	114.491	591	-.779						2.61								
2321 KEV	437	18	67.755	27.007	79	-.062	-.067	.334	178.0	.362	106.5	.54	.41	43.4	.04					
2331 KGM	284	9	2.015	103.317	103	.476						.89								
2337 KHC	569	16	49.131	13.579	699	.259	.077	.419	5.3	.018	150.8	.37	.23	61.5	.15					
2351 KIC	448	17	6.360	-4.741	174	-.469	-.354	.095	118.9	.138	95.8	.39	.37	10.3	.23					
2356 KIM	31	11	-28.752	24.780	1320	-.216	-.317	.635	61.0	.723	75.3	.91	.56	62.9	-.09					
2358 KIP	66	11	21.423	-158.014	72	.634	.340	1.509	355.8	1.062	56.4	.71	.23	89.5	.25					
2360 KIS	82	7	47.017	28.867	0	-.376						.81								
2362 KIV	109	11	43.950	42.683	1200	.443	1.426	1.118	202.8	.909	166.5	1.98	1.56	37.3	.14					
2364 KJF	99	15	64.199	27.715	159	-.496	-.376	.438	289.1	.217	74.6	.42	.19	80.0	.31					
2371 KKM	364	14	6.045	116.211	0	.801	.461	.835	1.6	.585	99.9	.81	.55	54.5	-.18					
2372 KKN	319	17	27.790	85.280	1919	-.126	-.004	.258	59.3	.456	174.3	.53	.39	44.8	-.17					
2380 KLB	232	11	-31.673	117.850	300	-.880	-.499	.669	227.9	.379	34.6	.42	.18	82.6	.02					
2389 KLM	23	8	3.100	101.650	0	.479						.96								
2407 KMI	508	16	25.123	102.740	1945	.435	.366	.800	178.7	.288	145.5	.73	.33	78.9	-.02					
2420 KMY	29	8	59.320	5.370	57	1.643						1.81								
2421 KMZ	11	6	-13.505	25.837	1223	.860						.62								
2423 KNA	121	12	-15.750	128.767	54	-.841	-1.264	.727	23.6	.154	35.7	.64	.42	57.7	.43					
2436 KOD	39	7	10.233	77.467	2315	.272						.94								
2442 KOL	94	9	41.493	35.911	144	.045						.55								
2444 KON	19	9	59.649	9.632	216	-.861						2.05								
2462 KRA	543	17	50.052	19.937	223	.103	.172	.289	190.3	.298	40.5	.56	.48	26.7	.59					
2488 KSH	434	18	39.455	75.980	1286	1.316	1.006	.137	123.7	.358	103.3	.58	.51	22.8	-.12					
2489 KSI	10	7	-3.638	102.673	0	.043						1.93								
2493 KSP	566	15	50.843	16.293	379	-.099	-.224	.194	61.0	.129	106.3	.25	.20	36.3	.07					
2494 KSR	199	16	-25.850	26.897	1623	-.310	-.407	.496	133.3	.248	7.2	.65	.53	32.8	-.55					
2512 KTK1	35	9	69.117	23.271	340	-.203						.94								
2519 KUG	11	6	-10.163	123.653	52	2.735						2.65								
2525 KUP	33	10	-10.168	123.586	52	.768	-3.729	4.204	50.0	5.598	132.3	3.56	2.20	62.0	-.38					
2526 KUR	64	11	45.233	147.867	0	.474	.293	.712	129.1	.186	88.6	.84	.71	28.7	.41					
2557 LAR	12	6	41.314	-105.583	0	-.811						.81								
2569 LBF	698	17	46.985	3.977	714	-.498	-.403	.183	169.1	.195	163.6	.32	.27	29.8	.59					
2573 LBNH	144	15	44.301	-72.009	367	.080	.313	.633	104.1	.155	22.1	.56	.31	68.8	.10					
2578 LBTB	74	13	-25.145	25.720	1027	-.144	.217	1.469	131.9	.657	149.9	1.10	.72	57.4	.10					
2604 LDF	661	17	48.594	-.122	289	-.369	-.301	.209	237.6	.072	173.8	.21	.14	57.5	.11					
2619 LEM	49	9	-6.833	107.617	1241	.427						1.73								
2633 LFF	603	17	44.937	.736	193	.223	.237	.205	120.5	.120	17.8	.26	.19	43.8	-.31					
2648 LHC	43	9	48.417	-89.267	195	-.325						2.18								
2660 LIC	307	17	6.225	-5.028	100	-.429	-.348	.269	149.3	.289	108.0	.39	.26	54.4	.55					
2672 LJU	66	9	46.043	14.533	395	-.036						.64								
2678 LKO	155	16	9.644	-5.639	435	-.616	-.558	.110	92.0	.153	114.2	.43	.41	9.5	-.24					
2699 LMN	54	10	45.870	-64.860	363	.304	.898	1.752	100.2	.714	70.5	1.48	.98	56.3	.03					
2701 LMQ	23	6	47.548	-70.327	418	-.076						1.00								
2702 LMR	482	18	43.333	6.509	200	-.130	-.179	.130	179.1	.202	173.2	.37	.32	22.6	-.43					
2723 LOF	29	7	68.260	13.620	79	-.181						1.13								
2730 LOR	881	17	47.267	3.850	529	-.458	-.443	.103	282.1	.185	160.6	.26	.21	34.4	.56					
2734 LPA	49	6	-34.909	-57.932	14	.573						1.05								
2735 LPB	74	13	-16.677	-68.234	3292	.630	.320	.688	53.8	.687	129.9	.94	.69	45.5	.46					
2738 LPF	668	17	48.165	-1.108	156	-.117	-.152	.115	267.7	.270	9.4	.27	.17	61.5	-.19					
2739 LPG	696	18	45.627	6.765	2569	.207	.161	.478	292.1	.364	22.3	.48	.20	82.9	.13					

2741	LPL	101	17	15.665	6.874	2069	.143	.072	.397	299.5	.314	14.2	.44	.23	72.5	-.30
2743	LPO	618	17	44.683	1.187	330	.150	.113	.233	110.0	.066	28.9	.27	.20	44.0	.11
2754	LRG	563	18	43.454	6.360	100	.013	.065	.162	194.8	.165	5.5	.26	.20	42.3	.02
2765	LSA	380	16	29.700	91.150	3657	1.025	1.008	.324	28.2	.268	172.4	.48	.39	33.5	-.39
2766	LSCT	84	12	41.784	-73.294	317	.041	-.606	.967	117.2	1.646	15.7	2.25	1.68	43.8	.52
2768	LSF	518	17	46.250	1.530	430	-.177	-.184	.152	158.6	.059	160.2	.34	.32	10.5	.03
2777	LSZ	33	8	-15.366	28.232	1184	.799						2.20			
2798	LTX	143	13	29.334	-103.667	1013	-.588	-.651	.558	157.3	.233	103.5	.69	.50	46.0	.01
2825	LZH	630	18	36.050	103.833	1518	.304	.476	.535	332.3	.449	163.5	1.23	1.13	17.0	-.17
2832	MAF	567	17	46.265	2.714	469	.054	.097	.251	139.1	.309	3.9	.31	.14	77.9	.38
2835	MAI	267	15	35.472	135.387	30	.105	.360	.428	12.2	.162	153.6	.48	.33	50.8	.05
2836	MAJO	154	12	36.542	138.209	421	-1.131	-.876	.455	56.6	.504	83.3	.43	.14	89.3	.24
2837	MAK	12	6	13.017	47.433	0	.678						1.44			
2840	MAN	29	5	14.667	121.083	70	.123						2.37			
2845	MAT	786	15	36.538	138.208	139	-1.075	-.607	.875	15.2	.425	78.3	.79	.42	72.2	.47
2848	MAW	166	16	-67.604	62.870	12	.613	.645	.899	324.8	.604	106.0	.94	.58	62.0	.44
2852	MBC	997	17	76.242	-119.358	14	.001	-.066	.411	35.6	.235	89.3	.54	.42	39.8	-.34
2857	MBL	202	14	-21.160	119.833	200	-.801	-.697	.885	297.6	.160	81.4	.88	.47	71.4	-.42
2878	MCQ	16	6	54.199	158.956	14	1.413						1.05			
2881	MCW	113	13	48.797	-122.973	693	-.044	.080	.741	108.3	.492	176.7	.86	.53	61.8	-.08
2897	MDJ	527	14	44.616	129.592	250	.080	-.129	.569	235.6	.415	125.4	.67	.38	66.5	.08
2911	MEEK	50	8	-26.678	118.745	529	-.650						.74			
2914	MEK	30	10	-26.613	118.545	514	-.507	-1.407	2.025	55.5	1.654	12.7	1.96	1.37	51.1	-.10
2916	MEM	105	10	50.692	6.066	0	.178	.355	.143	108.4	.406	125.0	.31	.13	81.3	-.16
2918	MEO	39	11	34.785	-98.596	465	-.562	-.682	.562	10.2	.203	26.3	.81	.70	26.6	.02
2923	MEU	10	4	37.101	14.930	985	.815						.81			
2928	MFF	639	17	46.601	-.143	259	-.059	-.073	.085	252.4	.214	177.7	.24	.18	46.0	-.04
2938	MGD	61	9	60.100	150.700	219	-.133						.97			
2947	MGR	16	6	40.176	15.598	259	-.141						.49			
2953	MHC	162	13	37.342	-121.642	1281	.566	.280	.476	30.9	.643	85.0	.93	.71	41.0	-.18
2955	MHI	10	4	36.300	59.595	1100	.403						.92			
2961	MIAR	209	14	34.657	-93.630	207	-.500	-.527	.139	106.1	.068	17.0	.43	.42	5.3	.28
2963	MID	37	11	59.427	-146.338	0	.858	1.082	1.110	23.4	.465	55.0	.76	.52	54.2	.32
2969	MIN	92	11	40.345	-121.605	1495	-.222	-.192	.205	204.8	.590	173.4	.43	.21	76.4	.19
2978	MJAR	177	13	36.542	138.209	421	-.737	-.468	.350	31.1	.278	90.4	.39	.24	61.8	-.26
2990	MKS	14	8	-5.067	119.633	28	.360						1.64			
3013	MME	10	4	14.194	10.700	2160	.714						.20			
3033	MNI	24	6	1.450	124.800	128	-.088						.95			
3034	MNK	66	9	53.900	27.567	0	.154						.80			
3038	MNO	13	5	37.931	14.695	1840	.290						1.83			
3042	MNS	15	8	12.396	12.800	600	-.223						.46			
3043	MNT	87	13	45.502	-73.623	112	-.686	-.198	.879	96.0	.181	173.4	.98	.81	32.9	.34
3045	MNV	65	11	38.572	-118.194	1506	.159	-.287	.937	298.6	2.275	6.4	2.01	1.38	53.1	.07
3058	MOL	34	8	62.600	7.680	97	.051						.85			
3061	MOR	13	6	42.103	110.572	18	-1.482						1.12			
3065	MOS	24	8	55.733	37.633	120	-.005						.71			
3066	MOT	102	13	30.797	-104.082	2019	-.254	-.621	.560	26.5	.427	149.1	.84	.65	39.1	.60
3070	MOX	210	17	50.646	11.616	453	.268	.202	.239	355.5	.292	72.6	.47	.39	31.3	-.37
3071	MOY	42	9	51.683	100.983	0	.655						.71			
3101	MRW	226	15	-41.232	174.705	0	-.684	-.537	510	303.0	.107	129.3	.60	.45	44.6	-.20
3128	MTA	71	8	41.700	44.800	0	.273						1.33			
3138	MTN	113	11	-12.847	131.130	79	-.862	-1.734	1.273	60.7	.649	155.6	.84	.62	45.1	-.45
3150	MUD	312	14	56.160	9.170	12	.847	.892	.131	294.3	.105	111.4	.55	.46	28.8	-.12
3153	MUN	310	12	-31.978	116.208	234	-.467	-.515	.179	130.2	.403	.1	.33	.20	61.3	.08
3173	MYNC	33	7	35.139	-84.229	550	-.462						.96			
3180	MZF	17	9	46.215	2.584	479	.096						.54			
3199	NAI	116	15	-1.339	36.837	1692	2.042	2.831	1.120	243.4	.832	24.8	1.34	.90	54.8	.00
3203	NAN	88	11	32.063	118.783	7	-.111	-.236	.180	283.3	.687	61.1	.59	.33	68.2	-.01
3204	NAO	163	16	60.887	10.974	379	-.860	-.218	1.377	282.4	.939	125.7	2.31	1.93	30.6	.57
3212	NB2	868	17	61.097	11.347	717	-.798	-.634	.508	259.5	.070	78.4	.47	.28	65.7	-.63
3237	NDI	339	13	28.683	77.217	230	-.724	.233	.941	253.8	.393	13.7	.83	.49	65.3	-.24
3247	NEW	557	16	48.263	-117.120	759	-.236	-.232	.305	306.3	.271	8.2	.43	.29	54.3	-.10
3268	NIE	430	16	49.424	20.322	555	.704	.572	.256	42.9	.354	117.3	.41	.30	48.6	.20
3276	NJ2	423	12	32.052	118.854	45	.358	.272	.390	193.5	.182	103.8	.34	.20	64.0	-.58
3305	NNA	101	14	-12.023	-76.922	574	.182	.125	.412	260.2	.585	141.6	1.32	1.19	18.2	-.35
3314	NOR	109	15	81.600	-16.683	35	-.197	-.083	.859	248.3	.291	55.5	.85	.55	58.2	.17
3319	NPA	36	8	-15.087	39.253	374	.984						2.88			
3325	NPO	132	12	64.814	-146.915	418	-.582	-.209	1.064	30.7	.360	64.5	.85	.57	55.0	.61
3331	NRI	54	10	69.400	88.100	39	-1.594	-.338	1.626	308.9	.496	13.5	1.14	.41	87.1	.66
3340	NSS	42	10	64.650	11.970	101	-.229	.034	.452	283.4	.556	113.4	.62	.24	85.0	-.16
3350	NUR	673	17	60.509	24.651	101	-.355	-.182	.181	193.5	.255	114.3	.31	.21	56.5	-.21
3360	NVL	37	7	-70.767	11.833	86	.094						1.24			
3363	NWA	354	14	-33.020	117.240	264	-.508	-.532	.427	306.7	.152	81.0	.47	.36	43.1	-.07
3365	NWL	18	8	-27.757	29.981	1332	.827						2.16			
3387	OBN	355	17	55.167	36.600	0	-.461	-.248	.254	190.4	.559	123.8	.61	.40	56.9	.26
3397	OCO	22	6	35.590	-97.540	351	.253						1.95			
3400	ODAS	75	9	26.860	87.390	2045	.129						.61			
3402	ODD	18	8	59.950	6.670	629	.799						.68			
3410	OGA	285	16	46.868	11.025	934	.255	.425	.106	132.2	.685	157.2	.55	.18	89.0	-.02
3418	OHR	315	15	41.214	20.939	739	-.679	-.383	.371	174.2	.629	164.0	.67	.37	69.9	-.28
3426	OJC	235	15	50.245	19.934	391	.144	-.029	.436	4.4	.325	106.2	.54	.35	57.3	.17
3470	ORO	16	7	45.625	7.980	1161	-.199						1.02			
3472	ORV	146	12	39.555	-121.500	360	.124	.243	.220	175.8	.052	101.8	.48	.46	8.6	.15
3491	OTT	141	14	45.394	-75.716	82	-.319	-.179	.870	82.5	.612	176.8	.92	.62	54.8	.33
3506	OXF	76	8	34.512	-89.409	101	-.766						.60			
3514	PAB	36	11	39.546	-4.348	0	.120	-.122	.408	315.5	.345	50.7	.27	.19	49.8	-.03
3517	PAE	509	17	-17.662	-149.580	59	1.317	1.534	.453	103.2	.205	163.7	.78	.69	22.6	.57
3530	PAS	14	6	34.148	-118.172	294	.009						1.46			
3555	PCI	133	11	-.933	119.883	0	1.050	.340	1.313	38.5	1.519	138.3	.90	.56	60.9	-.29
3560	PCO	17	5	36.691	-96.978	331	-.176						.62			
3563	PCT	70	9	14.715	101.427	0	.815						1.98			
3566	PDA	130	15	37.743	-25.662	35	-.077	-.332	.469	210.1	.231	121.2	.54	.37	54.4	.70
3576	PDY	138	12	59.633	112.703	0	-.150	-.488	.620	245.7	.147	173.5	.79	.63	37.2	.14
3577	PEC	341	13	33.970	-117.257	615	.105	.376	.389	79.5	.426	10.0	.51	.34	55.3	.53
3582	PEL	31	11	-33.144	-70.685	689	.237	.228	.482	155.9	.133	72.9	.75	.65	25.8	-.26
3584	PEN	11	5	30.467	-87.183	0	-.824						1.15			
3588	PET	207	13	53.017	158.650	0	.125	-.260	.394	146.4	.547	35.0	.69	.40	66.9	-.04
3594	PFO	86	12	33.609	-116.455	1279	.164	.433	.583	73.8	.207	60.6	.56	.34	62.6	.81
3598	PGC	214	13	48.650	-123.451	4	.477	.005	1.630	268.8	1.807	173.2	2.22	1.56	50.8	.60
3599	PGD	10	5	43.875	11.721	1600	.909						.78			
3601	PGF	193	17	42.548	9.144	1129	-.412	-.425	.095	137.5	.154	171.9	.34	.31	15.8	.06
3604	PGP	35	5	13.480	120.960	0	-.683						1.91			
3611	PHC	52	9	50.700	-127.433	32	.560						.92			
3631	PII	14	7	43.762	10.588	50	-.432						.64			
3636	PIP	20	5	18.325	120.619	150	-.462						1.22			
3651	PKI	348	18	27.610	85.490	2757	-.269	-.166	.137	23.6	.409	2.5	.51	.40	37.5	-.43
3660	PLC	94	12	37.763	-122.012	162	.063	-.116	.737	283.1	.670	68.2	1.06	.68	58.9	-.54
3669	PLP	19	5	11.165	124.979	133	-.228						1.45			
3678	PME	110	11	61.733	-149.167	231	-.622	-.721	.623	353.4	.275	49.7	.72	.59	33.0	.04

3679	PMG	245	12	-9.409	147.154	67	-.354	-.639	.186	49.4	.569	155.7	.82	.70	26.4	-.46
3685	PMO	762	17	-15.004	-147.897	2	1.260	1.103	.405	9.7	.372	88.0	.55	.41	43.9	.39
3687	PMR	1318	18	61.592	-149.131	0	-.459	-.167	.340	59.5	.296	10.8	.55	.44	35.9	.35
3688	PMS	51	10	61.245	-149.561	716	-.324	-.250	.753	16.8	.671	49.8	.65	.46	49.1	.58
3705	PNT	689	14	49.317	-119.617	550	.210	.319	.024	287.7	.141	52.2	.28	.25	16.2	-.22
3711	POF	86	14	-29.382	19.950	0	1.385	1.120	1.235	61.8	.993	87.8	1.26	.55	80.8	.58
3716	POO	244	14	18.533	73.850	555	-.283	.229	.630	294.2	.763	115.8	.98	.74	42.8	-.69
3727	PPI	122	10	-.452	100.384	0	-.559	-.007	.917	254.7	.471	24.1	.78	.38	75.9	-.38
3731	PPN	496	17	-17.531	149.432	0	1.301	1.428	.250	104.6	.249	176.4	.65	.60	15.7	.11
3733	PPR	66	9	9.750	118.733	14	1.248						1.58			
3735	PPT	513	17	-17.569	-149.576	259	1.265	1.389	.250	91.5	.106	148.6	.62	.58	10.8	.07
3741	PRA	155	12	50.070	14.430	202	.550	.516	.143	258.6	.495	65.6	.40	.17	80.8	.22
3757	PRC	430	15	49.988	14.542	301	.289	-.078	.523	5.3	.424	81.9	.52	.21	84.0	.09
3760	PRY	126	13	-26.928	27.473	0	-.129	-.218	.789	15.7	.491	107.0	.85	.59	51.8	-.35
3761	PRZ	34	9	42.483	78.400	0	.950						.70			
3770	PSI	264	14	2.691	98.919	0	-.463	.405	1.640	226.2	1.123	45.1	1.60	.98	62.3	.22
3798	PTZ	23	9	-14.390	31.390	1026	.302						2.14			
3804	PUL	73	10	59.767	30.317	64	.098	1.822	3.400	197.5	1.769	24.2	1.34	.37	92.3	.58
3825	PWA	49	12	61.651	-149.879	136	-.186	.249	1.132	59.5	.769	42.4	1.26	.92	46.8	-.32
3832	PYA	126	9	41.033	43.050	497	-.156						.89			
3838	PYUN	100	11	28.100	82.990	1866	-.085	-.050	.208	145.5	.140	17.6	.49	.45	13.7	-.32
3840	PZI	41	9	37.105	15.067	0	.451						1.09			
3852	QIS	162	11	20.627	139.652	330	-.848	-2.461	2.619	27.2	1.812	118.6	1.53	.76	75.1	.01
3851	QIZ	163	11	19.029	109.843	230	.514	.717	.141	134.4	.666	39.2	.57	.33	67.7	.23
3857	QLP	62	8	-26.587	144.248	209	-.021						.66			
3870	QUE	114	11	30.188	66.950	1713	-.123	-.599	.940	303.6	2.069	84.4	2.06	1.50	46.5	-.31
3879	QZH	170	11	25.031	118.667	20	-.034	-.025	.228	186.9	.788	71.4	.51	.21	82.6	.24
3882	RAB	41	11	-4.193	152.171	182	-.188	.556	.802	273.9	1.076	29.4	1.16	.77	56.1	.04
3883	RAC	94	11	50.083	18.183	209	.914	.789	.481	325.3	.318	82.0	.45	.18	83.9	.33
3888	RAM	70	10	37.766	41.292	850	.214	.128	.215	100.6	.147	129.8	.26	.20	43.0	.08
3889	RAN	23	7	16.867	96.183	14	-.480						1.41			
3891	RAR	41	9	-21.212	-159.773	28	.439						1.68			
3892	RAT	24	7	51.941	178.451	225	-.717						1.63			
3917	RDP	10	6	41.758	12.717	759	.200						.53			
3930	RES	138	15	74.687	-94.900	14	.045	.175	.742	63.0	.177	126.1	.68	.42	61.4	-.01
3937	RFI	38	10	41.305	13.998	0	.635	.916	.887	218.5	1.207	56.0	1.03	.53	73.0	-.01
3961	RJF	624	17	45.305	1.516	109	.033	-.032	.372	98.6	.089	84.2	.33	.16	75.7	.04
3963	RKG	173	10	-34.098	117.104	300	.170	.072	.231	91.1	.366	179.4	.32	.17	71.6	.39
3965	RKT	283	16	23.118	-134.972	100	.726	1.555	.615	279.8	.812	16.8	1.37	1.14	30.8	-.52
3974	RMP	13	6	41.911	12.723	379	1.178						1.88			
3975	RMQ	172	13	-26.540	148.800	360	.451	.432	.446	71.8	.419	86.5	1.04	.91	22.9	.55
4013	RSCP	90	14	35.600	-85.589	580	-.833	-.606	.313	107.3	.676	99.7	.74	.47	60.2	-.09
4017	RSNT	393	17	62.180	-114.592	50	-.235	-.030	.300	71.1	.157	24.3	.43	.36	31.3	-.24
4018	RSO	289	15	60.572	-152.788	1921	-.790	-.616	.481	303.0	.175	69.7	.57	.44	38.3	.34
4020	RSSD	381	14	41.151	-104.062	2059	-.165	-.370	.273	48.6	.379	175.1	.44	.33	44.9	.22
4041	RUV	791	17	-15.189	-147.384	3	1.077	1.026	.476	30.4	.212	92.8	.57	.45	37.6	.02
4063	SAD	17	6	33.822	73.183	837	-1.136						.66			
4070	SAL	13	6	45.675	10.612	70	.605						.92			
4073	SAO	187	13	36.765	-121.145	230	.196	.667	.058	151.4	.632	17.7	.53	.27	73.1	-.10
4082	SBA	65	9	-77.850	166.756	37	1.293						1.06			
4086	SBF	371	18	43.981	7.452	847	-.289	-.213	.247	205.5	.114	17.5	.30	.23	42.8	.08
4102	SCH	415	17	54.817	-66.783	540	-.226	-.353	.280	89.8	.127	170.6	.55	.42	43.0	-.34
4107	SCO	332	17	70.183	-21.950	68	.649	.884	.642	108.2	.236	117.0	.64	.41	58.6	.11
4124	SDI	11	6	41.758	13.954	0	.031						.67			
4126	SDN	340	15	55.413	-160.622	23	-.703	-.553	.452	80.9	.196	59.3	.56	.43	41.0	.48
4129	SDV	23	9	8.886	-70.633	1580	-.300						.94			
4136	SEK	186	16	-28.323	27.625	1485	.282	.535	.250	112.6	.677	157.5	.68	.45	56.3	-.15
4141	SES	408	16	50.396	-111.042	769	-.273	-.153	.183	87.8	.146	86.8	.51	.47	12.1	.76
4150	SFI	10	7	43.960	11.870	0	.931						.47			
4170	SGO	10	6	40.633	15.384	0	-.214						1.21			
4181	SHE	46	7	40.633	48.633	0	.833						.62			
4187	SHK	96	10	34.530	132.678	284	-.042	.047	.807	26.5	.285	165.2	.65	.33	74.9	.57
4188	SHL	58	7	25.567	91.883	1600	-.346						1.11			
4214	SIT	288	14	57.057	-135.324	18	.789	.538	.594	4.5	.204	56.5	.56	.39	51.7	.20
.721	SJG	41	8	18.112	-66.150	456	-1.535						1.31			
4238	SKO	379	17	42.021	21.496	345	.103	.088	.103	136.4	.362	179.8	.45	.36	37.4	.26
4239	SKR	24	9	50.667	156.100	0	-.414						1.61			
4251	SLL	11	5	60.477	13.323	419	-.534						.83			
4256	SLR	366	17	-25.753	28.420	1348	-.475	-.876	.862	38.4	.453	.7	1.29	1.06	32.0	-.34
4265	SMF	593	17	46.645	3.841	458	-.332	-.298	.193	192.3	.245	12.2	.25	.13	72.1	-.29
4274	SMT	39	8	38.467	70.067	0	.733						1.44			
4278	SMY	282	12	52.722	174.120	46	.118	-.205	.659	250.7	.221	173.3	.93	.77	31.4	.59
4280	SNA	138	13	-70.309	-2.358	52	.385	.217	.629	115.3	.457	125.4	.92	.77	30.3	-.02
4284	SNF	73	9	50.586	4.433	108	.256						.60			
4285	SNG	379	15	7.173	100.620	4	.577	.678	.259	11.3	.577	9.8	.79	.62	38.4	-.27
4297	SNY	512	14	41.828	123.578	51	-.486	-.424	.514	76.6	.464	100.0	.58	.36	61.7	.41
4298	SNZ	25	6	34.380	134.908	370	-.287						1.32			
4301	SOC	41	7	43.583	39.717	192	-.279						1.31			
4307	SOI	11	6	38.121	16.099	0	-.323						.69			
4317	SPA	1190	17	-90.104	115.000	2927	.357	.429	.439	158.9	.472	86.0	.68	.51	44.7	.18
4319	SPC	57	10	49.188	20.245	1771	.308	.274	.252	209.3	.399	73.7	.68	.58	26.1	.68
4323	SPI	107	15	57.160	-170.225	0	-.204	.065	.509	193.6	.321	88.9	.60	.39	56.5	.16
4339	SQTA	334	16	47.255	11.287	1307	-.168	-.546	1.042	359.5	.533	133.6	.95	.48	74.6	.07
4344	SRD	33	9	6.932	-72.853	1639	-1.304						1.39			
4352	SRO	69	9	47.813	18.313	0	.777						.81			
4364	SSE	833	15	31.096	121.187	9	-.028	.121	.365	210.5	.460	65.6	.49	.23	78.0	.25
4365	SSF	669	17	47.061	3.507	360	-.309	-.306	.048	298.0	.178	178.6	.28	.25	22.3	.45
4374	SSP	60	8	36.925	-116.219	2065	-.670						1.15			
4381	STA	23	7	17.695	74.000	665	.292						1.50			
4382	STB	11	5	50.703	6.900	270	.283						.54			
4389	STJ	48	10	47.572	-52.733	61	-.449	-.503	1.040	357.9	1.012	28.5	1.40	1.02	46.7	-.39
4390	STK	599	17	-31.882	141.592	212	-.064	-.239	.387	89.6	.152	98.3	.72	.65	17.6	.76
4397	STU	102	12	48.771	9.193	375	-.154	-.317	.251	17.8	.153	96.3	.39	.34	21.8	-.38
4404	SUE	18	6	61.120	4.860	9	.656						.60			
4405	SUF	183	15	62.719	26.150	185	.020	.010	.556	341.7	.150	166.7	.59	.40	54.5	-.20
4412	SUR	80	14	-32.380	20.728	0	1.669	1.912	.420	243.3	.555	121.0	1.66	1.56	11.4	.01
4423	SVE	70	10	56.800	60.633	275	-.064	.150	1.227	181.0	.312	.5	.93	.47	73.9	.58
4436	SVW	586	17	61.182	-155.633	762	.273	-.013	.983	326.5	.372	44.6	.94	.57	62.8	.21
4449	SWZ	48	12	-27.182	25.325	1342	-.391	.102	1.093	301.0	2.346	108.2	2.31	1.63	50.4	-.23
4479	TAP	74	9	25.033	121.517	8	.302						.58			
4482	TAT	96	13	34.983	139.867	0	-.212	.522	.983	315.7	1.517	77.4	1.29	.43	88.8	.69
4490	TBI	221	16	-23.349	-149.461	9	1.635	1.627	.423	159.1	.774	129.3	1.17	.98	29.1	-.11
4503	TCF	622	17	46.288	2.210	592	-.081	-.008	.396	153.6	.246	2.8	.36	.18	75.1	.20
4549	THRI	19	6	-8.370	115.543	1000	-.245						1.63			
4555	TIA	256	13	36.211	117.124	300	-.184	-.296	.349	193.6	.764	92.4	.59	.30	73.2	.72
4556	TIC	277	17	6.550	-5.000	137	-.441	-.239	.388	170.2	.356	125.3	.50	.35	52.1	.66
4562	TIK	56	11	71.633	128.867	0	-.935	-1.060	.912	185.9	1.162	84.1	.77	.44	67.2	.35
4569	TIY	454	15	37.713	112.434	850	.138	.268	.558	14.4	.057	123.3	.61	.45	44.4	-.65
4578	TKL	17	2	35.730	-83.840	349	-1.087						.55			

4588	TLG	20	9	43.267	77.383	850	.370						.78				
4621	TNP	585	16	38.220	-117.227	1932	.304	.139	.457	212.0	.549	138.1	.99	.83	30.7	-.06	
4626	TOA	341	15	62.147	-146.223	908	.608	.588	.385	17.0	.237	104.0	.40	.26	56.9	.51	
4632	TOL	82	15	39.881	-4.049	179	.498	.488	.169	127.3	.110	111.8	.30	.26	25.9	.34	
4635	TOO	323	13	-37.571	145.190	603	.699	.941	.440	261.3	.460	85.8	.57	.38	55.3	.19	
4640	TOV	16	5	9.820	-69.876	649	.339						1.37				
4651	TPN	168	15	-8.419	146.987	989	.717	.732	.633	174.0	.353	163.4	.70	.44	59.5	.27	
4655	TPT	771	17	-14.984	-147.620	3	1.217	1.064	.301	13.1	.238	91.5	.45	.37	31.6	.23	
4671	TRN	18	9	10.650	-61.400	24	-.394						1.56				
4675	TRO	47	8	69.632	18.928	14	-.537						.94				
4680	TRT	218	13	-7.650	112.500	0	-.660	.211	1.663	177.7	1.989	9.3	1.32	.50	85.3	-.19	
4689	TSI	10	4	3.508	98.695	0	.632						1.77				
4692	TSM	90	9	4.223	118.072	0	.426						.86				
4700	TTA	690	16	62.930	-156.022	913	-.003	-.187	.717	320.7	.483	15.8	.75	.36	77.5	.09	
4716	TUH	30	10	-33.297	19.150	189	.237	-1.086	1.673	125.2	2.386	54.1	2.33	1.09	78.0	.17	
4718	TUL	528	17	35.910	-95.793	256	-.455	-.338	.276	295.0	.216	103.9	.54	.47	24.0	.35	
4730	TVO	543	17	-17.782	-149.252	660	1.420	1.410	.070	128.2	.150	6.2	.65	.64	3.1	.28	
4751	TXAR	133	12	29.338	-103.670	1013	.192	.150	.570	228.4	.129	65.5	.61	.45	46.5	-.49	
4772	UER	41	10	51.567	94.083	0	-.818	-1.329	.672	149.2	.800	89.6	.64	.46	48.0	-.67	
4778	UKR	17	7	50.950	84.750	0	-.505						.80				
4782	ULM	112	13	50.397	-95.950	280	-1.012	-1.173	.372	316.2	.307	45.3	.60	.50	30.8	-.32	
4793	UPA	75	8	9.115	-79.540	41	.179						1.24				
4795	UPP	126	13	59.858	17.627	14	-.651	-.434	.422	195.1	.069	25.7	.37	.27	46.0	.20	
4819	UZH	121	14	48.633	22.300	0	.363	.482	.480	170.7	.241	56.6	.44	.23	74.0	-.31	
4824	VAH	763	17	-15.237	-147.636	3	1.000	1.013	.544	38.7	.319	65.9	.71	.55	40.2	.27	
4833	VAY	284	13	41.361	22.601	167	.030	.202	.519	225.2	.432	35.9	.33	.20	62.1	-.43	
4838	VBY	90	11	45.545	15.316	259	.067	.137	.164	157.4	.108	83.2	.23	.16	52.1	.08	
4878	VIR	15	6	-28.080	26.863	1340	1.506						3.11				
4882	VKA	55	13	48.265	16.318	400	.769	.266	.964	16.9	.326	111.4	.82	.51	62.1	-.57	
4884	VLA	32	9	43.117	131.900	74	.459						1.01				
4903	VNDA	145	15	-77.640	161.956	97	.741	.144	.361	272.5	1.043	15.6	1.84	1.62	22.9	-.04	
4909	VOY	36	8	46.167	13.985	1072	-.443						.50				
4918	VRAC	57	10	49.390	16.700	0	.505	.159	.463	328.2	.248	32.5	1.09	1.00	16.3	.49	
4939	VVI	10	7	46.129	12.486	514	.188						.72				
4955	WAL	203	14	47.460	-115.965	0	.122	-.178	.251	261.3	.262	109.2	.55	.49	21.2	-.25	
4958	WAR	219	14	52.242	21.024	109	-.389	-.582	.287	243.8	.493	29.6	.62	.53	26.7	.37	
4960	WAT	180	15	-30.317	115.883	0	-.058	-.162	.529	312.7	.162	3.6	.71	.56	38.4	.23	
4962	WB2	169	13	-20.028	134.360	425	-1.414	-1.265	.665	273.0	.439	46.8	.81	.60	44.0	-.12	
4985	WDC	257	13	40.580	-122.540	300	.072	-.043	1.257	303.3	.991	6.4	1.19	.49	83.0	.21	
4997	WET	323	15	49.145	12.880	612	.446	.211	.494	338.3	.248	54.8	.59	.42	50.7	.15	
5017	WHN	575	15	30.544	114.350	26	.536	.420	.381	208.2	.287	138.8	.39	.18	79.8	.34	
5021	WHY	210	15	60.747	-135.007	1292	.065	-.317	.132	306.8	.616	73.4	.61	.39	59.1	-.52	
5029	WIN	161	14	-22.567	17.100	1728	.385	.083	.547	73.5	.438	44.1	.94	.76	34.8	-.07	
5047	WLF	90	13	19.796	6.174	0	.411	.326	.391	107.7	.454	122.2	.58	.44	41.2	-.39	
5059	WME	16	6	53.516	-4.334	129	-.466						1.13				
5061	WMO	201	15	31.718	-98.589	504	-.528	-.534	.342	339.5	.502	21.2	.69	.51	46.8	.41	
5062	WMQ	556	17	43.821	87.695	970	.334	.504	.349	242.3	.086	7.9	.45	.37	31.6	-.06	
5082	WOOL	224	15	31.073	121.678	0	-.691	-.428	.130	162.9	.231	178.1	.67	.58	24.3	-.65	
5095	WR2	320	15	-20.068	134.472	414	-.874	-.781	.278	265.3	.172	40.3	.53	.47	20.6	-.33	
5099	WRA	1110	17	-19.948	134.351	0	-1.122	-.800	.566	290.3	.752	47.8	.91	.57	60.3	.37	
5117	WTS	806	18	51.995	6.810	43	.481	.690	.116	161.3	.247	122.0	.31	.24	40.7	.02	
5118	WTTA	313	17	47.388	11.663	1764	-.079	-.394	.633	5.8	.544	146.5	.92	.69	43.5	.36	
5127	WVOR	237	13	42.439	-118.667	1343	.318	.302	.354	274.1	.342	165.7	.55	.41	45.0	-.22	
5138	XAN	619	17	34.040	108.921	629	-.478	-.566	.089	329.0	.320	118.4	.33	.22	55.6	.27	
5146	YAK	209	14	62.017	129.717	0	-.649	-.907	.329	199.7	.120	47.5	.51	.43	27.7	.14	
5151	YBH	159	11	41.868	-122.805	968	.327	-.009	1.173	265.4	.985	176.9	1.01	.30	91.2	.47	
5160	YKA	46	9	62.579	-114.646	0	-1.029						1.94				
5162	YKC	257	16	62.478	-114.473	197	-.337	-.461	.553	307.3	.143	14.8	.50	.24	76.6	.02	
5168	YKU	15	6	59.581	-139.836	19	2.089						1.06				
5181	YOU	11	5	-34.278	148.382	503	.675						.89				
5186	YRH	70	11	52.835	-4.740	300	.224	.317	.369	114.3	.565	51.5	.81	.67	32.1	.21	
5189	YSNY	101	14	42.558	-78.575	628	-.276	-.142	.797	130.4	.563	126.3	.72	.35	76.7	.40	
5190	YSS	271	14	47.033	142.860	97	.065	-.073	.393	151.5	.448	99.9	.39	.20	72.7	.07	
5204	ZAK	202	13	50.383	103.283	0	-.234	-.026	.710	226.2	.631	65.6	.63	.24	85.8	-.71	
5219	ZOBO	76	14	-16.294	-68.190	4396	-.009	-.701	1.320	.6	.888	105.0	1.47	1.03	51.4	.31	
5224	ZST	137	14	48.196	17.103	250	.588	.141	.467	17.6	.178	48.9	.42	.21	75.5	.44	

Appendix C

The whole-mantle P-wave attenuation structure :QPB3DV2

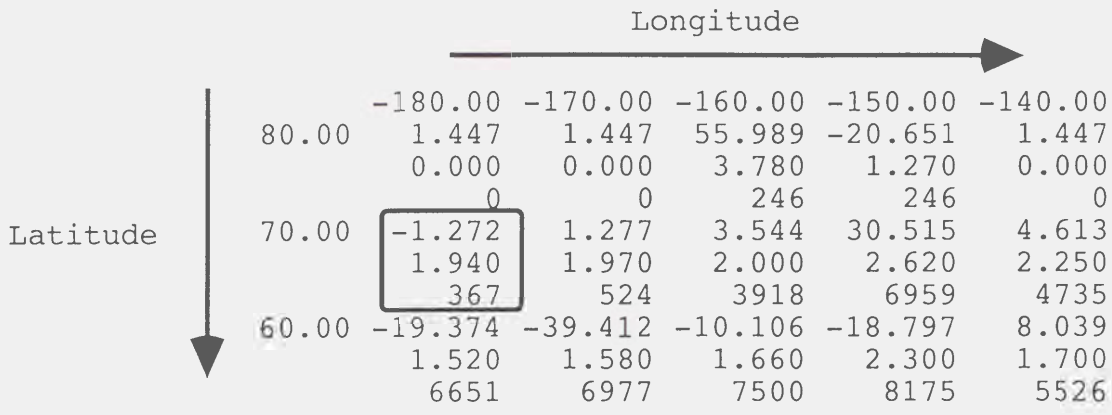

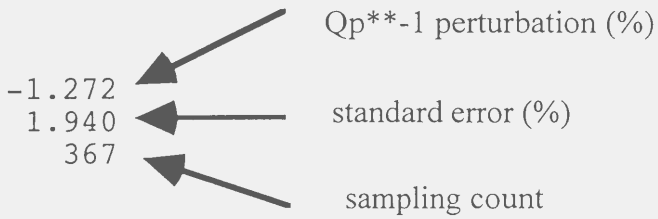

Depth = 12 km

	-180.00	-170.00	-160.00	-150.00	-140.00	-130.00	-120.00	-110.00	-100.00	-90.00	-80.00	-70.00	-60.00	-50.00	-40.00	-30.00	-20.00	-10.00
80.00	1.447	1.447	55.989	-20.651	1.447	2.436	-12.664	1.823	52.016	33.680	1.447	30.269	55.890	-34.098	1.447	64.013	-68.626	-54.510
	0.000	0.000	3.780	1.270	0.000	1.660	1.490	2.190	1.530	1.310	0.000	1.190	2.140	1.350	0.000	3.630	1.650	2.050
	0	0	246	246	0	672	1071	1071	139	139	0	393	393	32	0	561	1595	1329
70.00	-1.272	1.277	3.544	30.515	4.613	2.320	3.072	-3.260	-0.753	23.090	25.545	12.287	19.705	37.245	1.447	4.295	44.659	-28.931
	1.940	1.970	2.000	2.620	2.250	2.260	1.890	1.880	2.020	2.020	2.410	1.750	1.850	2.370	0.000	3.430	3.180	2.720
	367	524	3918	6959	4735	1844	1981	1811	139	139	11	476	821	360	0	591	2172	1855
60.00	-19.374	-39.412	-10.106	-18.797	8.039	14.351	8.608	9.557	1.554	-10.502	-1.312	6.432	4.115	7.401	17.152	9.482	10.302	17.780
	1.520	1.580	1.660	2.300	1.700	1.440	1.560	1.550	1.440	0.940	1.150	0.920	1.410	0.950	1.480	0.970	1.410	1.580
	6651	6977	7500	8175	5526	1668	1713	2316	1039	209	58	969	1271	360	410	456	799	5078
50.00	-7.893	-35.457	-33.851	-12.385	-3.957	-18.736	19.547	20.440	15.483	-16.843	-33.484	-50.195	-20.122	-9.549	-10.611	-2.135	1.194	-5.705
	1.000	0.890	0.900	1.000	1.220	1.410	2.010	1.700	1.310	1.390	1.310	1.350	1.010	1.390	1.470	1.220	1.550	1.500
	6447	6679	3651	1494	823	3099	6056	5476	2400	490	1357	1895	818	221	410	587	177	8247
40.00	-4.484	-5.432	1.447	1.447	1.447	8.647	-75.817	-60.206	50.294	-9.033	-56.036	-69.993	-50.503	-21.692	-17.857	-41.756	-15.316	16.993
	0.950	0.800	0.000	0.000	0.000	1.420	1.810	1.740	1.350	1.400	1.870	1.560	1.070	1.020	1.020	1.370	0.930	1.160
	23	21	0	0	1	4580	10080	9270	5688	2835	2267	1631	368	313	293	727	529	4156
30.00	1.447	-10.004	-11.506	-0.040	1.447	26.118	61.675	-1.146	17.818	13.038	-3.176	-49.289	-50.321	-24.184	-11.633	-17.265	-19.678	-1.483
	0.000	0.770	0.660	0.390	0.000	0.520	1.220	1.270	1.180	1.080	1.060	0.880	1.030	1.120	1.090	0.960	0.930	0.830
	0	19	91	72	0	2167	5134	6043	4867	2520	962	310	69	515	710	551	362	267
20.00	1.447	-7.262	-37.703	-34.489	1.447	1.447	17.988	4.050	-28.885	-0.163	-13.764	-18.150	-17.846	-18.683	-12.562	-9.965	-20.568	-19.513
	0.000	0.740	0.920	0.690	0.000	0.000	0.710	0.950	1.190	1.020	0.910	0.860	1.050	1.080	1.110	1.100	0.880	0.580
	0	19	123	104	0	0	34	1192	2272	1627	832	592	664	725	704	13	58	47
10.00	1.447	1.447	-11.982	-17.727	1.447	1.447	1.447	3.527	-0.802	-4.266	-32.190	-51.843	-29.196	-6.986	-2.662	-13.139	-28.036	-45.552
	0.000	0.000	0.820	0.760	0.000	0.000	0.000	0.790	1.130	1.060	0.910	0.900	1.030	1.100	1.050	0.940	0.710	0.900
	0	0	32	32	0	0	0	701	1872	2590	3340	2481	669	368	506	293	224	1423
0.00	1.447	1.447	1.447	1.447	1.447	1.447	1.295	1.782	1.716	-4.361	0.673	-12.848	-15.335	-4.309	2.127	1.463	-39.467	-35.269
	0.000	0.000	0.000	0.000	0.000	0.000	0.480	0.760	0.930	1.050	0.980	1.000	0.980	1.070	1.070	0.740	0.620	0.490
	0	0	0	0	0	0	20	233	343	1117	3299	2405	98	19	234	328	593	1769
-10.00	21.058	15.591	7.175	20.877	20.638	7.927	1.576	0.960	1.290	-3.131	-9.219	11.925	6.035	5.880	5.772	2.580	-3.004	-9.346
	0.890	0.490	0.460	0.730	0.450	0.400	0.420	0.620	0.720	0.650	0.820	0.850	0.910	0.860	0.750	0.740	0.480	0.420
	1728	1635	77	6357	6357	58	249	265	125	200	1115	1113	207	120	123	45	660	578
-20.00	22.944	24.098	14.870	9.078	30.275	21.454	7.345	4.258	2.230	1.447	-2.286	16.833	12.631	9.119	5.349	1.447	1.170	0.781
	1.130	0.830	0.690	1.240	0.530	0.580	0.520	0.490	0.570	0.000	0.390	0.560	0.650	0.640	0.530	0.000	0.340	0.570
	3930	3288	165	6663	6915	392	361	371	90	0	1088	1313	208	118	117	0	356	356
-30.00	1.039	5.941	9.105	8.200	10.357	15.493	9.935	7.452	4.588	1.360	-1.677	-5.975	2.652	4.756	1.447	1.447	1.453	1.744
	1.080	0.620	0.540	0.590	0.480	0.470	0.510	0.510	0.410	0.380	0.330	0.380	0.420	0.730	0.000	0.000	0.160	0.250
	2746	2050	66	306	558	334	132	226	147	31	1355	1454	124	50	0	0	171	171
-40.00	-6.864	-1.447	1.447	1.447	1.447	1.447	4.220	4.250	4.440	1.963	-1.319	-5.279	-4.292	0.719	1.447	1.447	2.599	2.108
	1.090	0.580	0.000	0.000	0.000	0.000	0.320	0.410	0.400	0.290	0.320	0.260	0.330	0.340	0.000	0.000	0.140	0.130
	1086	348	0	0	0	0	13	39	69	83	582	627	123	49	0	0	64	64
-50.00	-1.226	1.447	1.447	-0.463	-3.801	-3.583	-0.407	1.024	1.760	1.764	-0.622	-4.319	-9.877	-9.073	-1.315	1.740	2.538	2.713
	0.980	0.000	0.000	0.170	0.160	0.110	0.150	0.210	0.220	0.200	0.180	0.240	0.220	0.230	0.250	0.150	0.130	0.140
	553	0	0	65	115	50	13	13	12	52	62	50	56	40	12	280	331	67
-60.00	1.447	1.447	1.447	1.337	0.108	-0.543	1.447	1.447	1.447	1.447	1.447	-0.757	-4.375	-13.030	-14.663	-4.413	0.308	1.945
	0.000	0.000	0.000	0.030	0.060	0.060	0.000	0.000	0.000	0.000	0.000	0.200	0.220	0.220	0.240	0.230	0.230	0.180
	0	0	0	65	115	50	0	0	0	0	0	28	81	87	61	342	326	27
-70.00	1.447	1.447	1.447	1.447	1.447	1.447	1.447	1.447	1.447	1.447	1.447	1.447	0.350	-1.879	-6.572	-9.004	-5.303	-1.503
	0.000	0.000	0.000	0.000	0.000	0.000	0.000	0.000	0.000	0.000	0.000	0.000	0.330	0.340	0.220	0.320	0.340	0.300
	0	0	0	0	0	0	0	0	0	0	0	0	25	47	49	45	27	153
-80.00	1.447	1.447	1.447	1.447	1.447	1.447	1.447	1.447	1.447	1.447	1.447	1.447	1.447	1.447	1.447	1.447	1.447	3.823
	0.000	0.000	0.000	0.000	0.000	0.000	0.000	0.000	0.000	0.000	0.000	0.000	0.000	0.000	0.000	0.000	0.000	0.380
	0	0	0	0	0	0	0	0	0	0	0	0	0	0	0	0	0	153

Depth = 12 km

	0.00	10.00	20.00	30.00	40.00	50.00	60.00	70.00	80.00	90.00	100.00	110.00	120.00	130.00	140.00	150.00	160.00	170.00
80.00	20.538	55.092	17.138	1.447	1.447	-1.239	-1.964	17.760	1.447	-13.710	-5.467	-5.063	17.960	3.786	-14.049	1.447	1.447	1.447
	2.610	1.400	2.150	0.000	0.000	1.150	0.970	1.580	0.000	1.190	1.310	3.820	1.650	1.140	1.260	0.000	0.000	0.000
	504	398	15	0	0	38	60	57	0	15	102	108	309	397	99	0	0	0
70.00	-41.556	-14.179	17.899	15.503	6.942	1.447	1.447	1.447	12.022	10.199	1.447	1.447	0.794	10.706	7.408	-2.985	-1.991	-0.566
	3.030	3.090	2.610	3.030	3.460	0.000	0.000	0.000	1.070	0.820	0.000	0.000	2.680	2.270	1.910	2.180	1.850	1.810
	710	2985	4358	2052	15	0	0	0	95	95	0	0	483	574	167	75	177	218
60.00	1.126	-25.847	-53.285	-19.416	5.378	8.528	12.663	15.236	20.959	33.030	37.347	30.867	28.253	20.719	15.944	11.692	0.681	-8.494
	1.940	2.220	2.300	1.680	1.360	1.210	0.930	1.350	1.090	1.250	1.360	1.060	1.410	1.330	1.330	1.420	1.310	1.250
	7440	10059	10284	4088	848	286	588	314	288	536	1040	1600	1120	426	385	1302	2172	3390
50.00	19.180	40.317	-55.249	-54.821	-12.338	4.080	11.820	20.816	37.201	56.948	67.361	68.566	66.152	64.331	46.970	23.755	13.282	-8.562
	2.010	2.500	2.060	1.330	1.060	1.230	1.460	1.210	1.340	1.550	1.490	1.370	1.510	1.380	1.320	1.060	1.050	1.030
	26357	30583	14782	4923	2444	1691	796	1483	2409	1643	1204	2716	4081	2722	8691	13332	6106	3290
40.00	56.518	-75.633	-64.366	-48.380	-52.866	-8.748	4.196	-9.193	5.700	51.860	68.416	76.163	78.075	76.858	71.487	43.634	13.852	1.447
	1.580	1.840	1.900	1.080	1.340	1.340	1.270	1.470	1.410	1.830	2.610	2.200	2.080	1.930	1.950	1.160	0.780	0.000
	19525	23265	9806	3547	2282	2454	1770	3587	3770	2995	4680	7827	7545	6699	13850	14851	4100	0
30.00	9.681	-45.155	-71.565	-63.429	-55.472	-56.908	-4.592	-14.382	-58.632	-20.043	42.877	62.808	72.618	70.052	66.354	42.409	1.447	1.447
	0.630	0.830	1.210	1.480	1.480	1.690	1.620	1.520	1.830	2.160	2.080	2.290	2.350	1.900	1.760	1.220	0.000	0.000
	359	443	980	1123	972	2123	3323	3496	4097	6311	8586	8659	6801	6901	6330	2838	0	0
20.00	1.447	1.447	1.447	-61.722	-53.163	-52.275	-23.578	-0.839	-32.301	-13.016	34.331	49.336	47.001	33.039	21.199	14.585	1.447	1.447
	0.000	0.000	0.000	0.990	1.530	1.680	1.640	1.610	1.580	1.680	1.830	1.860	1.650	1.310	1.160	1.150	0.000	0.000
	0	0	0	313	727	2026	2242	2814	4171	5983	5795	2527	4348	4438	2164	1368	0	0
10.00	-24.162	-14.894	-16.021	2.774	-6.117	-5.325	-2.811	-1.418	-10.059	-15.424	-24.837	-12.069	-15.388	-15.346	-18.385	-9.381	1.447	1.447
	0.840	0.360	0.420	0.650	1.180	1.450	1.500	1.350	1.350	1.430	1.340	1.370	1.540	0.880	0.630	0.740	0.000	0.000
	1292	273	273	432	836	1011	666	1804	1730	2713	4621	2669	4451	3705	1469	1364	0	0
0.00	-23.305	-14.133	-25.838	7.193	23.612	10.754	10.865	9.675	-0.649	-4.786	-18.807	-38.873	-30.440	-40.472	-28.605	3.697	1.046	4.024
	0.750	0.450	0.480	0.720	0.810	1.020	1.020	1.080	0.820	0.970	1.280	1.270	1.520	1.450	1.280	1.120	1.030	0.360
	1292	273	492	1016	806	58	256	269	219	1849	3931	3512	4485	4485	3147	4212	2430	12
-10.00	1.447	1.447	4.640	7.825	13.532	11.923	10.446	12.501	4.673	-0.983	-6.024	-37.182	-49.309	-70.513	-33.217	5.138	18.593	12.084
	0.000	0.000	0.350	0.560	0.700	0.700	0.700	0.640	0.480	0.700	0.780	1.330	1.630	2.020	1.890	1.780	1.580	1.490
	0	0	329	932	777	186	453	613	309	692	1123	1680	2665	3934	4188	4347	4500	2228
-20.00	1.447	-3.661	2.772	23.549	9.133	5.196	5.507	6.026	4.958	0.971	-8.424	-30.146	-63.177	-27.146	-33.511	44.038	23.863	18.334
	0.000	0.250	0.350	0.510	0.450	0.700	0.690	0.730	0.480	0.430	0.530	1.170	1.710	2.130	2.360	2.080	1.780	1.600
	0	215	2311	2386	540	224	359	463	104	61	61	779	1161	3966	4332	1063	2738	3278
-30.00	1.447	-5.626	-26.768	-12.153	6.122	3.644	2.332	3.022	3.079	2.581	1.447	-17.574	-35.440	-5.678	48.862	28.311	30.477	10.086
	0.000	0.250	0.630	0.940	0.430	0.460	0.530	0.710	0.650	0.530	0.000	0.770	1.480	1.370	1.740	1.620	1.550	1.520
	0	430	2613	2322	198	185	132	53	44	18	0	2287	2558	2481	4568	3062	909	1206
-40.00	1.447	-0.503	-6.508	-10.441	-4.060	1.558	1.639	1.717	2.605	1.264	2.759	2.996	0.790	-0.008	21.192	20.944	11.499	-4.524
	0.000	0.200	0.260	0.300	0.340	0.290	0.310	0.380	0.460	0.490	0.420	0.490	0.650	0.790	0.970	0.940	0.960	1.240
	0	183	421	242	41	146	105	13	53	51	11	1841	2122	570	1925	2051	490	794
-50.00	1.641	1.004	1.013	1.447	1.447	1.447	1.447	1.447	1.534	1.550	-1.389	2.534	2.955	3.489	3.727	7.404	5.082	2.801
	0.160	0.130	0.110	0.000	0.000	0.000	0.000	0.000	0.190	0.220	0.390	0.320	0.330	0.340	0.590	0.450	0.580	0.850
	45	40	11	0	0	0	0	0	22	33	11	15	30	56	109	177	199	646
-60.00	2.749	1.902	1.200	1.447	1.447	1.447	2.922	1.632	1.447	1.447	1.447	-4.467	1.551	1.801	2.098	2.107	3.068	1.454
	0.170	0.190	0.090	0.000	0.000	0.000	0.220	0.070	0.000	0.000	0.000	0.370	0.240	0.210	0.260	0.320	0.300	0.390
	45	40	11	0	0	0	484	484	0	0	0	378	378	41	109	209	155	17
-70.00	1.086	2.752	2.295	1.447	1.447	1.447	2.550	2.753	1.447	1.447	1.447	-2.118	-2.591	1.447	1.447	2.247	4.123	3.173
	0.210	0.310	0.310	0.000	0.000	0.000	0.310	0.350	0.000	0.000	0.000	0.500	0.590	0.000	0.000	0.170	0.230	0.210
	153	70	70	0	0	0	484	484	0	0	0	378	378	0	0	34	269	237
-80.00	3.418	6.712	3.408	1.447	1.447	1.447	1.447	1.447	1.447	-0.098	1.447	-5.954	-5.404	1.447	1.447	1.447	13.511	31.310
	0.700	0.280	0.450	0.000	0.000	0.000	0.000	0.000	0.000	0.060	0.000	0.630	0.350	0.000	0.000	0.000	0.710	3.320
	153	70	70	0	0	0	0	0	1	6	2	231	311	0	0	3	237	237

Depth = 51 km

	-180.00	-170.00	-160.00	-150.00	-140.00	-130.00	-120.00	-110.00	-100.00	-90.00	-80.00	-70.00	-60.00	-50.00	-40.00	-30.00	-20.00	-10.00
80.00	-0.277	52.205	27.581	-34.454	-0.277	6.412	-17.247	-6.734	49.993	28.174	-7.144	36.373	51.707	5.201	-0.277	51.867	-66.287	-53.313
	0.000	3.170	1.940	2.400	0.000	1.510	1.460	1.840	1.440	1.210	1.420	1.150	1.820	2.350	0.000	1.760	1.380	1.730
	0	12	246	246	0	727	1071	514	139	139	5	393	394	84	1	730	1602	1429
70.00	-1.574	0.028	25.618	24.246	-5.159	-3.001	1.775	-6.481	-6.120	19.548	21.749	6.883	20.260	34.922	20.161	11.872	14.106	-25.593
	1.980	2.180	2.500	2.050	2.480	2.100	1.880	1.960	1.900	1.810	1.810	2.220	1.990	1.780	2.280	2.060	2.050	1.900
	378	541	5114	7055	4765	1903	2000	1248	139	139	110	512	821	360	8	855	2184	1979
60.00	-17.576	-28.753	-7.884	-13.215	6.237	9.014	2.468	4.559	-2.505	-12.038	-1.224	7.703	3.904	9.317	18.894	18.097	16.236	16.473
	1.440	1.460	1.610	2.160	1.550	1.160	1.300	1.120	1.210	0.950	0.950	0.880	1.290	0.880	1.330	0.860	1.180	1.260
	8155	8837	9154	8567	5611	1681	1598	2316	1044	221	117	969	1274	362	413	641	868	5078
50.00	-4.738	-27.830	-31.067	-11.534	1.798	-2.330	26.872	13.510	8.817	-17.675	-25.192	-41.543	-13.384	-3.861	-0.448	8.982	7.648	-1.934
	1.250	1.170	1.440	1.090	1.140	1.210	1.800	1.510	1.030	0.960	1.110	1.180	0.700	0.890	1.160	0.940	1.230	1.250
	7824	8375	4291	1810	925	3379	6135	5796	2954	507	1375	1882	819	221	446	597	193	7955
40.00	-0.396	-4.450	-0.277	-0.277	-0.277	31.304	-64.295	-36.126	42.309	-13.562	-52.754	-63.247	-38.603	-13.549	-6.650	-19.580	-4.656	17.427
	1.440	1.010	0.000	0.000	0.000	1.290	1.720	1.510	1.030	1.050	1.590	1.140	0.650	0.650	0.610	0.980	0.620	0.760
	108	64	0	0	4	5050	10528	9025	5724	2796	2411	1693	369	327	341	745	533	3694
30.00	-0.277	-11.649	-14.792	-3.250	-0.277	30.166	64.352	33.465	32.871	10.784	-5.364	-42.054	-40.027	-21.147	-5.294	-7.512	-10.790	-0.469
	0.000	0.990	0.920	0.540	0.000	0.490	1.210	0.940	0.970	0.850	0.720	0.400	0.550	0.560	0.600	0.520	0.540	0.590
	0	22	91	72	0	2509	5642	6382	4880	2493	1113	407	69	524	718	576	350	199
20.00	-0.277	-10.613	-42.574	-39.705	-0.277	-0.277	23.421	28.917	32.507	21.077	-8.505	-17.938	-18.121	-23.361	-16.976	-8.848	-15.102	-13.997
	0.000	0.740	0.870	0.760	0.000	0.000	0.610	1.010	0.910	0.960	0.510	0.480	0.410	0.590	0.690	0.730	0.590	0.570
	0	31	123	104	0	0	35	1570	3487	3427	1759	1226	1035	756	706	13	58	95
10.00	-0.277	-0.277	-17.134	-24.219	-0.277	-0.277	-0.277	13.429	33.138	28.972	-31.181	-55.659	-38.558	-12.038	-5.967	-18.581	-31.192	-34.025
	0.000	0.000	0.760	1.010	0.000	0.000	0.000	0.660	0.950	0.960	0.910	0.590	0.680	0.620	0.790	0.870	0.690	0.820
	0	0	39	38	0	0	0	1159	3144	4318	4410	3071	1041	365	510	293	334	1533
0.00	-0.277	-0.277	-0.277	-0.277	-0.277	-0.277	0.151	1.974	6.182	2.859	-3.174	-16.621	-20.884	-9.380	-0.913	-0.629	-51.760	-40.252
	0.000	0.000	0.000	0.000	0.000	0.000	0.430	0.650	0.770	0.680	0.940	0.970	0.610	0.610	0.780	0.810	0.800	0.600
	0	0	0	0	0	0	20	235	345	1279	4074	3096	116	20	240	333	606	1787
-10.00	37.071	17.663	-7.929	-5.116	16.618	8.084	1.841	0.311	-0.416	-5.084	-9.732	11.589	3.028	3.054	3.005	0.845	-4.694	-12.794
	0.680	0.430	0.400	0.680	0.540	0.320	0.400	0.590	0.590	0.550	0.800	0.780	0.800	0.730	0.380	0.560	0.480	0.390
	2155	1996	1012	6357	6134	58	249	265	125	265	2032	2112	284	120	123	55	643	592
-20.00	47.317	31.521	2.885	-26.562	17.432	19.023	9.548	6.182	1.708	-0.277	5.639	39.334	13.386	7.397	3.380	-0.277	0.270	-0.240
	0.650	0.790	0.490	1.220	0.530	0.580	0.440	0.410	0.450	0.000	0.430	0.780	0.810	0.790	0.780	0.000	0.350	0.400
	4919	4061	1221	6635	6711	392	361	371	90	0	1881	2438	506	119	118	0	356	356
-30.00	9.617	7.988	6.145	-0.666	-1.289	11.341	9.668	9.887	5.358	1.628	1.898	16.438	16.565	5.212	-0.277	-0.277	0.054	0.650
	0.690	0.530	0.570	0.560	0.520	0.490	0.450	0.500	0.350	0.260	0.280	0.510	0.590	1.010	0.000	0.000	0.110	0.250
	3507	2605	138	270	556	334	132	226	150	35	2194	2529	260	50	0	0	171	171
-40.00	-0.962	-1.346	-0.277	-0.277	-0.277	-0.277	2.775	3.429	4.316	1.897	-1.350	-3.859	2.120	4.367	-0.277	-0.277	0.984	0.458
	1.000	0.600	0.000	0.000	0.000	0.000	0.370	0.410	0.390	0.300	0.290	0.250	0.360	0.380	0.000	0.000	0.180	0.110
	1340	495	0	0	0	0	14	40	69	83	1029	1078	124	49	0	0	64	64
-50.00	-3.000	-0.277	-0.277	-2.398	-6.099	-5.435	-1.860	-0.474	0.263	0.433	-2.044	-6.169	-12.024	-9.323	-0.003	2.380	1.953	1.204
	1.050	0.000	0.000	0.190	0.240	0.150	0.180	0.260	0.250	0.230	0.310	0.340	0.270	0.250	0.250	0.190	0.160	0.140
	596	0	0	65	115	50	13	13	12	52	67	56	56	41	14	416	467	68
-60.00	-0.277	-0.277	-0.277	-0.381	-1.852	-2.610	-0.277	-0.277	-0.277	-0.277	-0.277	-2.690	-6.834	-16.416	-17.099	-3.662	1.516	1.555
	0.000	0.000	0.000	0.030	0.070	0.090	0.000	0.000	0.000	0.000	0.000	0.280	0.330	0.340	0.250	0.290	0.190	0.290
	0	0	0	65	115	50	3	3	0	0	0	33	81	87	61	464	451	30
-70.00	-0.277	-0.277	-0.277	-0.277	-0.277	-0.277	-0.277	-0.277	-0.277	-0.277	-0.277	-0.386	-1.542	-4.005	-9.180	-11.375	-6.183	-1.665
	0.000	0.000	0.000	0.000	0.000	0.000	0.000	0.000	0.000	0.000	0.000	0.390	0.300	0.400	0.410	0.360	0.400	0.310
	0	0	0	0	0	0	0	0	0	0	0	5	25	47	44	68	47	155
-80.00	-0.277	-0.277	-0.277	-0.277	-0.277	-0.277	-0.277	-0.277	-0.277	-0.277	-0.277	-0.277	-0.277	-0.277	-0.277	-0.277	-0.277	1.894
	0.000	0.000	0.000	0.000	0.000	0.000	0.000	0.000	0.000	0.000	0.000	0.000	0.000	0.000	0.000	0.000	0.000	0.310
	0	0	0	0	0	0	0	0	0	0	0	0	0	0	0	0	0	153

Depth = 51 km

	0.00	10.00	20.00	30.00	40.00	50.00	60.00	70.00	80.00	90.00	100.00	110.00	120.00	130.00	140.00	150.00	160.00	170.00
80.00	20.770	53.542	23.881	-1.967	-10.517	-2.680	-2.773	14.448	9.459	-24.741	-28.512	-16.884	19.316	11.071	-8.664	-0.277	-0.277	-0.277
	1.240	1.010	1.150	1.840	1.110	0.750	0.970	1.240	0.990	2.370	1.760	2.420	0.860	1.400	2.710	0.000	0.000	0.000
	530	405	107	40	30	42	60	60	17	66	106	191	348	397	114	2	0	0
70.00	-37.329	-12.151	17.841	18.832	8.375	-0.277	-0.277	-0.277	8.780	11.160	-4.400	-13.764	-13.683	2.327	5.224	-1.874	-2.100	-1.606
	2.060	1.940	2.050	1.970	2.290	0.000	0.000	0.000	2.210	1.550	2.100	1.600	2.210	1.610	1.880	2.250	2.260	1.640
	949	2973	4313	2140	246	0	1	1	95	95	51	10	460	581	241	18	171	399
60.00	0.967	-18.847	-51.076	-20.242	7.271	9.734	10.747	10.977	13.734	23.051	26.822	17.043	8.761	-1.117	-4.626	0.135	0.837	-7.461
	1.550	1.810	1.820	1.520	1.230	0.910	0.830	1.210	1.120	1.090	0.880	1.020	1.280	1.240	1.300	1.180	1.310	1.220
	7676	10546	11303	4457	950	335	588	515	338	541	1133	1597	1083	437	468	2692	4411	4847
50.00	21.052	45.480	-30.896	-50.738	-7.617	5.797	8.806	12.360	22.032	37.204	55.894	57.329	54.652	52.179	17.078	0.313	25.065	-2.601
	1.670	2.040	1.710	1.050	1.130	1.300	1.460	1.380	1.250	1.500	1.360	1.160	1.200	1.230	0.960	1.240	1.640	1.290
	26581	31003	15421	5070	2489	2034	1087	1757	2550	1738	1348	2763	4005	2735	13982	21123	10175	4501
40.00	52.488	-70.243	-58.419	-12.039	-39.424	-6.219	2.779	-17.012	-13.325	23.218	47.549	58.775	64.003	68.517	63.640	33.601	10.816	14.788
	1.180	1.520	1.800	0.850	1.230	1.280	1.020	1.350	1.370	1.620	2.010	1.410	1.250	1.210	2.220	1.560	1.030	0.930
	19637	24104	10183	3715	2475	3058	2310	4257	4433	2679	5230	8077	7797	7183	20921	22821	5957	34
30.00	8.849	-33.603	-67.006	-53.897	-46.348	-59.837	-13.253	-18.786	-58.767	-52.290	14.285	14.512	22.454	45.543	56.674	32.725	-0.277	-0.277
	0.470	0.590	0.920	0.840	0.610	1.700	1.160	1.080	1.390	1.850	1.620	1.690	1.670	1.370	1.550	1.200	0.000	0.000
	329	450	1108	1239	1122	2379	3459	4089	4790	6139	9081	9291	8486	8492	8811	4921	0	0
20.00	-4.652	-0.277	-0.277	-58.194	-50.036	-48.455	-29.409	-9.481	-32.537	-14.950	21.143	34.706	-2.333	-10.438	9.188	15.222	-0.277	-0.277
	0.430	0.000	0.000	0.670	0.630	0.580	0.840	0.970	1.260	1.360	1.410	1.170	1.210	1.080	1.170	1.210	0.000	0.000
	50	0	0	308	733	2054	2324	2879	4294	6581	6371	3673	6583	6257	3203	2201	1	0
10.00	-14.443	-15.269	-14.782	3.456	-4.130	-0.829	0.758	-6.344	-14.439	-11.140	-16.988	-0.941	11.242	-9.465	-31.479	6.903	-0.277	-0.277
	0.800	0.370	0.370	0.420	0.520	0.630	0.850	0.890	1.140	1.090	1.040	0.660	1.080	0.860	0.920	1.050	0.000	0.000
	1292	274	295	460	831	1029	666	1808	1730	3483	5209	3294	6600	5857	2056	1927	1	0
0.00	-19.222	-12.434	-26.004	6.690	21.397	10.326	12.682	8.852	-12.199	-2.599	-4.737	-22.680	5.863	18.284	4.127	46.327	35.398	6.533
	0.610	0.370	0.500	0.610	0.520	0.530	0.650	0.980	0.970	0.840	0.920	0.740	0.780	0.730	0.710	0.800	0.830	0.400
	1292	274	528	1059	809	74	267	284	225	2592	5506	4762	6975	7495	4708	6667	4005	13
-10.00	-0.277	-0.277	1.296	2.637	8.490	9.539	11.855	16.244	0.092	-2.940	1.053	-20.444	-24.593	-63.624	-5.950	35.622	63.274	50.375
	0.000	0.000	0.400	0.560	0.590	0.600	0.490	0.650	0.690	0.690	0.620	0.610	0.760	0.930	0.770	0.770	1.080	0.930
	0	1	369	969	781	204	453	613	309	765	2028	2727	3513	5577	6364	6965	7315	3537
-20.00	-1.232	-3.187	1.733	17.924	4.171	0.956	4.755	7.588	5.622	-0.856	-6.810	-27.601	-63.154	-36.018	-52.353	29.968	42.097	55.775
	0.330	0.260	0.310	0.480	0.590	0.630	0.590	0.540	0.460	0.390	0.460	0.590	0.950	1.250	1.590	1.160	0.860	1.060
	5	212	2308	2390	527	242	354	458	106	63	61	850	1324	4028	4417	1201	4054	4569
-30.00	-0.817	-5.804	-20.566	-9.744	3.305	0.492	0.017	2.351	3.908	2.195	-0.277	-16.706	-45.164	-20.539	23.209	9.272	20.560	17.456
	0.350	0.400	0.540	0.770	0.440	0.670	0.650	0.640	0.520	0.420	0.000	0.510	1.120	0.630	0.910	0.950	0.840	0.820
	5	436	2572	2297	189	185	135	54	46	18	0	2110	2558	2584	4257	2743	1097	1450
-40.00	-0.277	-1.992	-6.710	-9.339	-4.449	-0.745	-0.520	-0.276	0.561	0.402	1.264	0.438	-3.485	-7.115	12.494	11.099	3.689	-6.956
	0.000	0.380	0.370	0.260	0.240	0.310	0.450	0.500	0.430	0.410	0.360	0.360	0.480	0.500	0.540	0.640	0.730	1.030
	0	218	458	289	41	146	110	13	53	51	11	1833	2115	573	1925	2073	573	936
-50.00	-0.214	-0.835	-0.730	-0.277	-0.277	-0.277	-0.277	-0.277	-0.731	-4.121	-3.669	0.554	0.533	0.892	0.834	4.349	1.133	-0.085
	0.120	0.120	0.180	0.000	0.000	0.000	0.000	0.000	0.240	0.260	0.270	0.290	0.270	0.350	0.490	0.340	0.480	0.850
	45	40	15	0	0	0	0	0	22	33	11	15	30	56	109	181	223	707
-60.00	1.412	0.197	-0.584	-0.277	-0.277	-0.277	0.970	-0.114	-0.277	-0.277	-6.954	-7.711	-0.719	-0.301	0.344	0.650	1.756	-0.544
	0.150	0.280	0.120	0.000	0.000	0.000	0.180	0.060	0.000	0.000	0.440	0.420	0.180	0.150	0.280	0.290	0.250	0.380
	50	40	15	0	0	1	484	484	0	0	14	378	378	41	109	211	155	14
-70.00	0.354	1.409	0.665	-0.277	-0.277	-0.277	0.902	1.008	-0.277	-0.277	-1.993	-6.966	-5.710	-0.277	-0.277	0.479	2.157	1.573
	0.460	0.210	0.500	0.000	0.000	0.000	0.240	0.270	0.000	0.000	0.630	1.030	0.770	0.000	0.000	0.180	0.210	0.220
	159	70	70	0	0	1	484	484	0	0	14	378	378	0	0	42	269	237
-80.00	0.362	3.650	0.999	-0.277	-0.277	-0.277	2.083	2.782	-1.552	-1.295	-2.926	-9.934	-4.287	7.742	4.959	-1.055	10.646	22.880
	0.660	0.190	0.580	0.000	0.000	0.000	0.180	0.370	0.120	0.240	0.190	1.020	0.600	0.590	0.460	0.170	1.410	0.830
	154	70	70	0	0	4	13	40	45	45	48	982	1116	200	17	10	237	237

Depth = 110 km

	-180.00	-170.00	-160.00	-150.00	-140.00	-130.00	-120.00	-110.00	-100.00	-90.00	-80.00	-70.00	-60.00	-50.00	-40.00	-30.00	-20.00	-10.00
80.00	2.428	39.653	5.734	-29.689	2.428	16.710	-15.735	-11.579	46.286	23.365	-2.893	39.307	27.171	4.547	11.429	14.230	-24.816	-49.976
	0.000	2.080	1.250	1.690	0.000	1.280	1.170	1.380	1.330	1.090	1.040	1.380	1.000	0.860	2.110	1.410	1.330	1.190
	0	174	246	249	0	737	1071	414	179	139	196	334	594	296	48	656	1588	1221
70.00	-1.109	1.235	18.780	10.097	-10.085	-3.849	5.542	-4.643	-7.411	17.023	18.555	7.442	21.772	23.365	13.924	13.025	15.647	-2.398
	1.590	1.900	1.940	2.120	2.070	2.050	1.760	2.160	2.020	1.940	1.850	2.210	1.960	1.790	1.920	2.150	2.130	2.030
	384	986	5950	7375	3773	1925	2101	1156	193	142	281	514	779	361	65	948	2219	1815
60.00	-25.869	-23.685	-4.842	-13.256	-2.277	1.174	-2.463	2.224	-3.628	-10.957	-1.923	7.603	4.701	10.254	14.112	12.753	12.115	7.718
	1.040	1.110	1.160	1.500	1.210	0.990	0.890	0.730	0.910	0.730	0.630	0.710	0.870	0.770	0.970	0.690	0.890	1.070
	8374	9241	10347	9062	4856	1829	1775	2130	1060	298	306	972	1316	405	456	722	993	5223
50.00	-17.022	-31.268	-27.038	-7.707	0.778	-8.346	17.284	5.936	5.059	-15.188	-18.934	-35.518	-9.458	-1.969	0.452	5.930	4.220	-4.501
	0.920	0.820	1.240	0.830	0.920	0.760	1.410	1.230	0.760	0.670	0.780	0.950	0.560	0.600	0.790	0.650	0.870	1.000
	8059	8561	4666	2287	1114	3373	5833	5451	2741	662	1384	1859	846	222	489	635	343	7961
40.00	-8.330	-8.538	-10.327	2.428	9.117	21.386	-60.750	-25.701	29.728	-11.651	-44.901	-48.982	-26.559	-8.321	-4.410	-16.140	-6.133	12.522
	0.770	0.490	0.390	0.000	0.580	0.810	1.310	1.060	0.850	0.730	1.310	0.770	0.530	0.480	0.480	0.690	0.480	0.520
	568	400	17	1	13	5396	10424	9533	5459	2737	2533	1762	383	333	418	762	510	3559
30.00	2.428	-6.022	-9.099	-2.037	2.428	28.210	54.267	17.342	27.971	6.691	-6.833	-31.591	-23.648	-13.440	-2.018	-4.883	-8.008	1.092
	0.000	0.600	0.630	0.540	0.000	0.620	0.980	0.640	0.540	0.690	0.610	0.380	0.430	0.460	0.460	0.490	0.450	0.440
	0	44	91	70	0	2818	5819	6176	4246	2442	1489	705	72	507	721	584	353	181
20.00	2.428	-4.372	-24.505	-24.223	2.428	2.428	17.814	17.375	40.975	25.468	-3.470	-15.303	-10.004	-14.499	-11.265	-5.378	-9.195	-6.737
	0.000	0.450	0.510	0.560	0.000	0.000	0.490	0.710	0.610	0.650	0.380	0.450	0.390	0.480	0.540	0.580	0.470	0.390
	0	50	123	103	0	0	41	1592	3889	3980	2012	1419	1206	742	700	18	58	105
10.00	2.428	2.428	-13.076	-18.145	2.428	2.428	2.428	12.144	34.382	33.724	-15.845	-47.887	-35.691	-6.655	-1.642	-11.289	-24.054	-22.268
	0.000	0.000	0.490	0.570	0.000	0.000	0.000	0.370	0.660	0.740	0.770	0.400	0.620	0.420	0.570	0.610	0.500	0.660
	0	3	46	42	0	0	0	1226	3629	4834	5029	3756	1237	360	530	323	387	1561
0.00	2.428	2.428	2.428	2.428	2.428	2.428	2.882	4.421	8.391	8.816	-1.749	-10.597	-15.898	-7.043	1.991	3.046	-35.830	-29.738
	0.000	0.000	0.000	0.000	0.000	0.000	0.350	0.490	0.430	0.380	0.680	0.530	0.310	0.380	0.570	0.540	0.560	0.520
	0	0	0	0	0	0	20	235	345	1287	5198	4259	122	24	259	333	620	1755
-10.00	32.191	11.666	-3.638	7.485	18.728	9.965	4.611	3.227	2.936	-0.627	-1.675	10.905	3.849	4.755	4.683	3.657	0.303	-6.339
	0.450	0.320	0.280	0.530	0.330	0.340	0.320	0.470	0.530	0.450	0.500	0.510	0.470	0.590	0.430	0.460	0.350	0.260
	2423	2237	1775	6357	5181	58	249	267	128	364	2881	3258	589	120	125	58	533	441
-20.00	37.519	21.006	-3.900	-0.054	23.734	19.614	11.320	7.919	4.531	3.388	5.169	26.107	10.640	7.868	5.234	2.428	3.068	2.528
	0.640	0.520	0.420	0.900	0.450	0.420	0.370	0.380	0.440	0.520	0.340	0.680	0.530	0.480	0.470	0.000	0.300	0.270
	5606	4649	2024	6624	5844	394	364	369	90	14	2152	3686	1719	120	120	1	327	329
-30.00	-6.150	2.605	1.759	2.068	7.427	13.778	11.039	10.883	7.374	4.791	5.532	14.874	11.189	5.629	2.428	2.428	2.769	3.208
	0.740	0.460	0.280	0.370	0.430	0.460	0.390	0.410	0.410	0.360	0.360	0.530	0.430	0.520	0.000	0.000	0.140	0.170
	3965	2976	223	301	461	334	142	226	158	42	2283	3499	1346	50	0	0	167	171
-40.00	-5.495	-3.794	2.428	2.428	2.428	2.428	5.028	5.307	6.187	4.584	2.733	0.250	3.412	4.631	2.428	2.428	3.430	3.017
	0.800	0.590	0.000	0.000	0.000	0.000	0.320	0.330	0.300	0.300	0.270	0.260	0.320	0.270	0.000	0.000	0.160	0.190
	1399	543	0	0	0	0	12	38	69	83	1114	1258	280	49	0	0	65	65
-50.00	-5.245	2.428	2.428	1.173	-2.106	-2.193	0.615	2.158	2.428	2.949	1.229	-1.869	-6.801	-5.426	1.742	4.507	4.295	3.627
	0.600	0.000	0.000	0.150	0.210	0.180	0.200	0.240	0.000	0.220	0.290	0.260	0.240	0.320	0.260	0.180	0.160	0.140
	587	0	0	65	115	51	15	13	1	41	75	63	56	49	37	496	539	71
-60.00	2.428	2.428	2.428	2.384	1.217	0.375	0.993	1.773	2.428	2.428	2.428	0.624	-2.583	-10.347	-11.428	-1.011	3.747	3.795
	0.000	0.000	0.000	0.020	0.060	0.080	0.070	0.050	0.000	0.000	0.000	0.230	0.240	0.270	0.220	0.270	0.190	0.220
	0	0	0	65	115	51	12	10	0	0	1	34	81	86	70	557	547	80
-70.00	3.484	2.428	2.428	2.428	2.428	2.428	2.428	2.428	2.428	2.428	2.428	2.346	1.480	-0.398	-4.537	-6.534	-2.616	1.136
	0.240	0.000	0.000	0.000	0.000	0.000	0.000	0.000	0.000	0.000	0.000	0.280	0.230	0.290	0.300	0.270	0.300	0.250
	7	0	0	0	0	0	0	0	0	0	0	7	25	36	31	69	57	155
-80.00	1.733	2.428	2.428	2.428	2.428	2.428	2.428	2.428	2.428	2.428	2.428	2.428	2.428	2.428	2.428	2.428	2.428	4.253
	1.160	0.000	0.000	0.000	0.000	0.000	0.000	0.000	0.000	0.000	0.000	0.000	0.000	0.000	0.000	0.000	0.000	0.240
	10	0	0	0	0	0	0	0	0	0	0	0	0	0	0	0	0	101

Depth = 110 km

	0.00	10.00	20.00	30.00	40.00	50.00	60.00	70.00	80.00	90.00	100.00	110.00	120.00	130.00	140.00	150.00	160.00	170.00
80.00	-2.119	40.317	27.293	2.661	-4.776	0.728	0.504	13.717	3.390	-21.456	-14.238	-8.409	12.267	-0.003	-10.020	-9.345	2.428	2.428
	1.270	0.840	1.270	1.310	0.900	0.670	0.670	1.020	0.900	1.920	1.080	1.050	1.180	0.740	1.270	0.770	0.000	0.000
	679	376	169	109	35	36	68	47	79	80	146	196	347	356	145	6	0	0
70.00	-24.758	-16.052	7.714	15.278	8.663	2.428	2.428	2.428	9.314	8.162	-4.664	-7.981	-7.588	1.318	-1.785	-7.441	-9.798	-3.124
	2.100	2.090	2.020	2.020	2.230	0.000	0.000	0.000	1.870	1.790	1.940	1.590	1.620	1.590	1.600	1.930	1.720	1.660
	1087	2759	4045	2163	847	0	1	1	93	95	76	51	405	584	282	22	152	438
60.00	2.688	-10.026	-43.390	-25.115	3.807	8.195	10.052	11.018	12.742	19.676	20.778	11.391	4.440	-3.074	-9.834	-15.819	-16.487	-18.510
	1.230	1.200	1.390	1.270	0.870	0.710	0.630	0.860	0.780	0.780	0.620	0.850	0.850	0.860	0.890	0.820	0.790	0.950
	8413	12054	12317	4783	1635	618	588	541	303	525	988	1394	1008	496	481	3068	4727	5191
50.00	16.804	33.744	-9.316	-43.986	-8.556	5.559	8.857	12.062	19.638	29.315	47.988	50.489	38.213	25.688	-0.099	-26.800	-3.630	-27.529
	1.300	1.510	1.320	0.860	0.860	0.770	0.830	0.920	0.870	1.060	1.080	0.680	0.910	0.770	0.670	1.240	1.080	0.630
	26588	31717	16389	5317	2562	2415	1079	1894	2680	1746	1860	2724	3370	2834	15571	23190	10976	4920
40.00	42.694	-57.436	-53.296	6.910	-25.666	-2.702	7.837	-9.420	-7.899	22.098	35.610	46.638	54.532	53.907	23.131	-0.409	-6.207	1.659
	0.870	1.070	1.190	0.760	0.930	0.990	0.630	1.020	0.800	0.980	1.250	1.050	0.950	0.820	1.380	1.170	0.640	0.700
	19676	23675	10239	3767	2625	3411	2451	4849	5245	2851	5639	7556	7316	8005	23068	25050	6485	203
30.00	9.178	-18.967	-55.207	-41.212	-31.943	-44.790	-7.670	-12.604	-49.400	-53.015	15.546	3.555	0.769	20.698	16.728	6.499	2.428	2.428
	0.340	0.380	0.580	0.530	0.400	0.980	0.770	0.700	0.800	1.270	0.970	1.250	1.320	1.120	1.180	0.540	0.000	0.000
	299	476	1096	1336	1231	2588	3463	4890	5699	6549	9330	9460	9832	10078	9723	5636	4	0
20.00	-0.070	2.428	2.428	-48.486	-44.171	-31.735	-18.415	-7.021	-27.988	-23.518	8.542	27.892	-15.341	-18.602	-6.724	2.400	2.315	2.428
	0.320	0.000	0.000	0.450	0.450	0.460	0.660	0.690	0.850	0.690	0.930	0.780	1.010	0.630	0.610	0.540	0.490	0.000
	59	0	3	308	745	1950	2128	2858	4366	6749	6421	4343	7785	7158	3866	3033	20	0
10.00	-5.413	-9.250	-9.933	5.487	-2.781	-0.077	4.107	-2.572	-15.216	-15.969	-14.111	-0.113	10.424	-6.976	-41.091	-7.011	4.381	2.428
	0.590	0.280	0.260	0.380	0.490	0.520	0.650	0.640	0.760	0.550	0.520	0.310	0.860	0.770	0.570	0.790	0.400	0.000
	1293	268	320	487	839	1065	666	1804	1730	3819	5634	3725	7588	6887	2707	2522	20	0
0.00	-13.688	-7.245	-19.805	8.256	20.938	10.261	12.210	9.083	-11.160	-7.536	-7.594	-21.890	5.903	26.872	-14.544	8.872	25.522	9.745
	0.520	0.290	0.370	0.480	0.450	0.490	0.540	0.660	0.520	0.450	0.650	0.380	0.610	0.840	0.740	0.730	0.580	0.340
	1248	273	542	1085	810	131	293	279	232	2849	5836	4975	8792	9676	5513	7684	4631	85
-10.00	2.428	2.428	2.891	3.646	8.010	10.339	11.840	15.405	1.137	-2.636	-4.661	-20.301	-12.717	-47.235	-21.086	-1.358	54.269	53.449
	0.000	0.000	0.320	0.430	0.490	0.540	0.480	0.470	0.370	0.370	0.430	0.520	0.610	0.830	0.770	0.800	0.940	0.780
	0	1	353	960	795	212	453	613	312	737	2076	2787	4568	6942	7250	7954	8816	4515
-20.00	1.900	0.857	3.668	15.155	5.673	2.498	6.485	8.525	6.739	1.110	-2.771	-18.978	-50.892	-14.341	-45.145	4.064	20.204	46.188
	0.230	0.210	0.240	0.360	0.460	0.530	0.570	0.510	0.330	0.210	0.360	0.420	0.790	1.050	1.370	1.050	0.730	0.850
	13	208	2216	2296	591	249	328	431	107	68	64	878	1449	4070	4446	1436	5213	5607
-30.00	2.002	-1.690	-11.429	-6.094	4.523	2.742	2.338	4.543	5.730	4.362	2.428	-6.501	-30.422	-12.988	13.416	0.420	2.187	2.162
	0.300	0.260	0.430	0.630	0.330	0.510	0.500	0.490	0.390	0.300	0.000	0.390	0.970	0.480	0.730	0.820	0.730	0.550
	10	432	2564	2320	228	186	145	61	47	18	0	2033	2558	2723	4278	2787	1243	1615
-40.00	2.428	1.121	-2.474	-4.448	-1.177	1.828	2.044	2.347	3.203	3.028	3.742	3.371	0.573	-3.457	9.199	7.053	-5.582	-24.015
	0.000	0.260	0.240	0.190	0.230	0.230	0.350	0.400	0.320	0.320	0.340	0.340	0.440	0.470	0.480	0.580	0.500	0.720
	0	220	534	362	40	146	113	17	53	51	11	1664	1953	641	1912	2078	528	978
-50.00	2.444	2.009	2.065	2.428	2.428	2.428	2.428	2.428	2.047	-0.566	-0.239	3.058	3.085	3.530	3.338	5.690	3.048	-1.352
	0.140	0.110	0.140	0.000	0.000	0.000	0.000	0.000	0.220	0.240	0.220	0.320	0.270	0.480	0.500	0.410	0.490	0.460
	42	40	15	0	1	4	3	3	22	33	11	15	30	55	109	181	232	704
-60.00	3.734	2.774	2.201	2.428	2.428	4.188	4.029	2.581	2.428	2.428	-2.810	-3.423	1.990	2.395	3.146	3.633	4.850	3.602
	0.120	0.210	0.090	0.000	0.000	0.360	0.350	0.140	0.000	0.000	0.340	0.320	0.170	0.200	0.350	0.250	0.320	0.440
	93	40	15	0	0	6	484	484	0	0	15	378	366	40	109	211	155	22
-70.00	2.713	3.630	3.106	2.428	2.428	3.011	4.498	4.077	2.428	2.428	1.104	-2.741	-1.853	2.428	2.428	2.690	3.818	4.166
	0.340	0.180	0.360	0.000	0.000	0.600	0.730	0.660	0.000	0.000	0.470	0.760	0.570	0.000	0.000	0.230	0.220	0.220
	177	76	70	0	0	6	484	484	0	0	15	378	366	0	0	46	269	231
-80.00	2.392	5.277	3.443	2.428	2.428	3.402	5.769	4.641	0.496	1.069	0.496	-4.826	0.305	8.626	6.735	2.336	1.486	18.393
	0.630	0.170	0.580	0.000	0.000	0.070	0.300	0.280	0.140	0.220	0.180	0.780	0.450	0.540	0.340	0.140	0.880	0.840
	127	73	65	0	4	16	28	43	51	36	58	987	1115	381	199	133	246	233

Depth = 190 km

	-180.00	-170.00	-160.00	-150.00	-140.00	-130.00	-120.00	-110.00	-100.00	-90.00	-80.00	-70.00	-60.00	-50.00	-40.00	-30.00	-20.00	-10.00
80.00	9.915	64.306	-38.678	-46.086	17.846	54.788	-41.452	-9.725	67.481	47.097	19.339	68.391	25.074	18.163	3.775	-18.507	70.546	-47.758
	0.000	2.210	1.800	2.450	2.130	2.130	1.890	1.890	2.170	1.260	1.250	2.670	1.620	1.090	2.460	2.330	3.090	1.810
	0	197	251	107	461	743	1071	421	211	220	242	343	567	331	270	659	1555	1244
70.00	-6.615	3.930	33.728	-6.609	-31.400	-7.490	19.604	-11.890	-10.532	29.004	34.975	25.575	49.623	36.492	26.869	15.938	5.523	44.391
	2.300	2.340	2.550	2.520	2.590	2.370	2.530	2.380	2.420	2.560	1.880	2.440	2.610	2.220	2.220	2.720	2.500	2.550
	430	1680	5993	7654	3187	2255	2135	1171	308	201	331	593	712	398	274	933	2260	1739
60.00	-56.146	-44.327	-3.632	-23.551	-20.227	-16.781	-15.799	-0.286	-14.020	-22.094	-8.378	14.140	14.546	25.371	25.601	24.259	18.044	6.005
	1.930	1.940	2.360	2.470	1.840	1.780	1.190	1.570	1.520	1.560	1.100	1.350	1.370	1.480	1.340	1.490	1.360	1.720
	8343	9997	10472	9901	3960	2506	2039	2047	1251	438	402	993	1005	392	485	773	1345	5374
50.00	-57.184	-55.226	-46.705	-23.338	-5.637	-34.347	19.937	5.050	7.461	-33.273	-36.413	-52.986	-19.348	-1.198	3.498	9.440	6.675	-8.000
	1.810	1.720	2.570	1.330	1.690	1.290	2.600	2.590	1.430	1.050	1.510	1.810	1.270	1.050	1.120	1.230	1.370	1.640
	8192	8661	5258	3291	1391	3733	5921	5554	2979	890	1411	1816	863	328	505	694	689	8384
40.00	-38.184	-29.156	-27.392	-15.941	10.412	25.985	-69.589	-16.317	55.575	-17.326	-56.965	-45.980	-41.465	-12.704	-6.770	-32.338	-15.611	23.246
	1.590	1.260	1.350	1.240	1.460	1.610	2.540	2.160	1.710	1.390	2.680	1.250	1.040	0.780	1.030	1.180	0.920	0.820
	1092	705	53	11	64	5879	10644	9824	5566	2789	2538	1758	375	285	480	746	464	4012
30.00	9.915	-4.302	-9.704	-1.865	9.915	61.515	60.736	6.873	58.342	6.803	-20.046	-47.211	-26.574	-20.919	-2.489	-7.125	-15.489	5.214
	0.000	1.300	1.510	1.160	0.000	1.030	2.050	1.400	1.290	1.180	1.400	0.930	0.620	0.860	0.800	1.000	0.870	0.750
	0	53	88	45	1	3206	6170	6563	4440	2477	1739	949	125	514	757	569	325	195
20.00	9.915	-1.525	-32.830	-34.077	9.915	21.905	33.146	11.178	68.422	42.618	-6.979	-33.591	-10.300	-20.805	-20.018	-8.946	-13.113	-6.830
	0.000	1.140	1.300	1.550	0.000	0.530	0.590	1.270	1.520	1.330	0.710	0.840	0.750	0.710	0.860	0.980	0.920	0.710
	0	63	123	84	0	23	111	1550	3860	4244	2200	1446	1230	725	689	32	58	123
10.00	9.915	3.605	-27.476	-38.329	9.915	9.915	16.219	21.469	62.732	63.599	-26.459	-56.394	-48.039	-3.922	2.494	-17.675	-45.042	-36.665
	0.000	0.940	1.200	1.370	0.000	0.000	0.590	0.620	1.170	1.520	1.430	0.750	1.180	0.770	0.990	1.000	0.860	1.380
	0	14	51	43	0	0	6	1286	3712	4986	5102	3756	1260	370	545	331	438	1638
0.00	9.915	9.915	9.915	9.915	9.915	16.327	12.240	14.179	17.020	15.980	-14.412	-23.960	-29.150	-7.049	9.759	11.289	-50.300	-50.988
	0.000	0.000	0.000	0.000	0.000	0.760	0.750	0.950	0.960	0.910	1.320	1.030	0.650	0.780	0.930	1.030	1.040	1.150
	0	0	0	0	0	14	34	235	358	1366	5193	4258	139	35	270	338	605	1743
-10.00	47.010	8.754	-2.918	38.399	43.409	27.513	16.424	11.150	8.144	-7.589	-19.708	-2.540	1.717	12.174	13.827	12.376	6.307	-12.509
	0.860	0.740	0.640	1.020	0.510	0.860	0.990	1.040	1.130	1.000	1.090	0.890	0.700	0.850	0.780	0.820	0.760	0.650
	3083	2822	2597	6352	4475	64	246	271	97	443	3077	3459	755	121	126	44	473	436
-20.00	44.489	16.829	-21.089	50.879	60.948	45.469	29.096	20.286	11.728	2.021	-20.402	-22.768	-1.499	13.915	14.193	9.915	10.767	7.618
	0.770	0.840	1.430	1.720	0.900	0.760	1.030	1.040	1.150	1.040	0.810	1.530	0.700	0.550	0.670	0.000	0.590	0.600
	6633	5595	2823	6684	4935	405	360	369	88	39	2371	4364	2326	120	119	1	320	329
-30.00	-13.531	-8.316	1.464	10.774	33.871	34.970	27.651	26.529	18.689	9.845	-0.881	-11.472	-11.279	6.158	9.915	9.915	10.834	11.030
	1.300	0.600	0.440	0.830	1.020	0.890	0.880	1.020	0.980	0.850	0.700	1.260	0.800	0.530	0.000	0.000	0.190	0.350
	4508	3283	301	408	410	341	150	234	158	45	2333	3905	2009	52	1	0	163	172
-40.00	-0.608	-2.744	9.915	9.915	9.915	9.915	15.046	15.613	17.052	12.828	6.307	-8.509	-6.917	1.567	9.915	9.915	12.037	11.283
	1.420	0.900	0.000	0.000	0.000	0.000	0.570	0.790	0.670	0.730	0.590	0.620	0.700	0.470	0.000	0.000	0.250	0.220
	1520	587	0	1	1	0	6	32	69	84	1125	1267	392	49	0	0	66	66
-50.00	-7.518	9.915	9.915	7.971	1.154	1.050	5.802	9.324	9.915	10.765	6.900	-0.599	-13.480	-13.972	0.137	11.106	12.805	12.102
	1.200	0.000	0.000	0.300	0.340	0.250	0.340	0.450	0.000	0.640	0.560	0.490	0.520	0.720	0.450	0.310	0.290	0.290
	518	0	4	69	115	55	15	13	1	41	75	66	63	50	52	497	540	72
-60.00	9.915	9.915	9.915	9.746	7.463	5.869	7.134	8.508	9.915	9.915	9.915	6.235	-0.738	-17.564	-22.996	-4.479	8.240	10.596
	0.000	0.000	0.000	0.040	0.110	0.130	0.100	0.090	0.000	0.000	0.000	0.410	0.430	0.510	0.430	0.480	0.340	0.360
	0	0	4	69	115	55	12	10	0	0	1	34	84	83	79	557	550	119
-70.00	11.932	9.915	9.915	9.915	9.915	9.915	9.915	9.915	9.915	9.915	9.915	9.776	8.015	4.034	-4.904	-10.604	-4.411	3.844
	0.470	0.000	0.000	0.000	0.000	0.000	0.000	0.000	0.000	0.000	0.000	0.440	0.400	0.480	0.500	0.480	0.510	0.440
	12	0	0	0	0	0	0	0	0	0	1	8	26	32	30	82	73	167
-80.00	9.757	9.915	9.915	9.915	9.915	9.915	9.915	9.915	9.915	9.915	9.915	9.915	9.915	9.915	9.915	9.915	9.915	14.715
	1.740	0.000	0.000	0.000	0.000	0.000	0.000	0.000	0.000	0.000	0.000	0.000	0.000	0.000	0.000	0.000	0.000	0.510
	38	3	0	0	0	0	0	0	0	0	0	0	0	0	0	0	0	70

Depth = 190 km

	0.00	10.00	20.00	30.00	40.00	50.00	60.00	70.00	80.00	90.00	100.00	110.00	120.00	130.00	140.00	150.00	160.00	170.00
80.00	-44.497	47.243	66.081	15.929	16.879	-3.471	23.452	6.047	-2.461	-17.994	-17.487	2.345	30.376	-41.464	-56.627	-32.991	9.915	9.915
	2.150	1.350	2.290	2.520	2.390	2.250	1.240	1.590	1.500	2.440	1.820	1.320	1.100	1.750	2.420	2.540	0.000	0.000
	790	420	249	167	66	47	75	90	111	133	162	174	341	324	157	35	4	0
70.00	-4.638	-30.262	0.974	32.248	23.016	20.532	9.915	18.669	15.596	10.477	-0.965	-7.821	-3.352	10.133	-21.368	-48.809	-46.644	-20.634
	2.370	2.440	2.510	2.460	2.540	2.820	0.000	2.560	2.310	2.200	2.630	2.460	2.480	2.310	2.130	2.730	2.670	2.080
	1367	2652	3617	2300	1355	8	2	9	41	102	88	91	403	571	287	34	131	415
60.00	17.515	13.204	-50.691	-47.140	5.579	19.409	27.193	27.544	31.793	38.361	35.797	20.030	3.475	-9.081	-18.508	-43.261	-59.131	-61.615
	1.850	1.840	2.580	2.510	1.530	1.730	1.620	1.540	1.630	1.440	1.440	1.720	1.570	1.760	1.480	1.630	1.540	2.240
	10215	14831	13266	5661	2247	607	588	553	268	533	1007	1384	1107	583	553	3030	4799	5434
50.00	40.687	64.692	35.115	-53.630	-12.539	18.013	21.990	28.715	42.114	55.256	68.711	70.000	43.897	6.323	-25.456	-47.278	-48.209	-64.105
	2.540	2.710	2.490	1.780	1.910	1.160	1.540	1.640	1.810	1.900	2.500	1.870	1.800	1.510	1.760	2.430	2.160	1.400
	26766	31775	17969	6299	2741	2509	1247	2001	2640	1942	2126	2425	3200	3100	16240	23484	11234	5357
40.00	68.900	-57.752	-66.482	45.177	-25.572	14.377	27.747	-12.463	-6.179	50.095	60.469	55.129	54.798	16.488	-31.754	-28.803	-24.083	-21.186
	1.550	1.980	2.210	2.170	1.730	2.120	1.270	2.230	1.480	1.840	2.010	1.940	2.000	1.580	2.800	2.350	1.150	1.280
	19697	22306	10212	4071	2871	3489	2959	6399	7035	3548	5512	7272	6821	8490	23627	25548	6968	584
30.00	22.884	-33.581	-59.925	-52.101	-40.935	-47.384	-10.994	-27.792	-52.736	-64.218	32.123	-27.322	-43.145	-55.729	-42.426	-18.848	-3.551	9.915
	0.570	0.560	0.950	1.120	1.040	1.430	1.210	1.380	1.300	2.550	1.860	2.740	2.420	2.460	2.130	1.310	1.340	0.000
	357	658	1248	1394	1345	2505	3787	6416	7579	6918	9249	9237	10775	11388	10144	6211	7	0
20.00	6.436	9.915	-31.971	-53.212	-55.176	-37.288	-24.059	-8.358	-43.971	-44.845	1.514	37.173	-51.620	-54.083	-54.821	-22.717	0.822	9.915
	0.500	0.000	0.600	0.740	0.970	0.880	1.000	0.980	1.570	1.530	1.790	1.720	2.170	1.200	0.950	1.230	0.850	0.000
	79	1	28	287	722	1827	2120	2787	4505	6898	6751	4749	8555	7752	4340	3416	57	0
10.00	-2.442	-12.736	-20.209	6.947	3.013	7.050	19.541	4.403	-25.804	-43.121	-41.894	-25.346	-34.215	-46.511	-59.890	-47.646	2.559	9.915
	1.030	0.530	0.590	1.000	0.990	1.150	1.060	0.890	1.390	1.130	1.150	0.920	1.920	1.560	1.370	1.670	0.810	0.000
	1298	252	324	603	884	1063	671	1659	1737	3977	5823	3989	7964	7375	3216	2774	212	0
0.00	-29.743	-10.509	-35.119	20.542	47.233	26.408	30.037	24.791	-18.949	-20.576	-19.371	-53.121	-40.431	-11.055	-45.793	-12.608	29.212	21.171
	0.820	0.600	0.660	0.950	0.930	1.120	1.150	1.100	0.800	1.020	1.400	0.950	1.310	2.030	1.470	1.310	0.930	0.800
	1248	256	542	1143	861	242	314	286	257	2805	5861	5152	9448	10057	6306	8014	5006	204
-10.00	-12.472	9.915	9.479	12.119	17.570	25.615	28.259	36.269	7.779	-1.340	-4.153	-40.668	-40.697	-56.256	-54.866	-19.933	65.161	67.348
	0.540	0.000	0.570	0.840	0.890	1.080	1.300	1.200	0.850	0.770	0.900	0.940	1.120	2.040	1.660	1.410	1.820	1.050
	13	1	349	934	817	247	456	607	331	704	2095	2916	4972	7302	7685	8208	9736	5318
-20.00	4.398	1.965	11.589	30.320	15.288	7.776	17.964	21.230	18.268	7.036	2.032	-24.798	-55.101	-8.845	-55.492	-31.279	11.722	70.038
	0.640	0.510	0.560	0.690	0.720	0.960	1.290	1.380	0.960	0.690	0.870	0.590	1.200	1.770	2.420	1.700	0.980	1.630
	13	203	2137	2242	730	252	332	426	124	66	64	954	1671	4228	4553	1823	6176	6287
-30.00	7.997	0.727	-14.631	-10.191	11.790	9.233	8.754	13.998	16.112	13.669	9.915	-1.428	-39.195	-21.915	20.299	-42.754	-5.388	10.008
	0.540	0.420	0.850	1.230	0.580	0.720	0.930	1.010	0.950	0.670	0.000	0.770	1.780	0.610	1.410	1.520	0.890	0.940
	13	415	2529	2302	377	191	153	65	55	24	0	1973	2557	2948	4146	2924	1364	1856
-40.00	9.915	7.269	0.558	-3.586	1.824	8.683	7.633	9.122	11.343	10.878	12.129	10.641	5.974	-2.888	12.309	11.717	-16.850	-45.021
	0.000	0.400	0.390	0.360	0.540	0.530	0.620	0.690	0.560	0.660	0.790	0.590	0.830	0.750	0.780	0.940	0.610	1.420
	0	207	592	430	56	146	115	19	54	50	11	1507	1808	857	1857	1910	398	1089
-50.00	10.036	9.369	9.232	9.915	9.915	10.032	9.882	8.638	8.735	3.802	4.300	10.661	10.186	10.735	9.917	12.168	9.366	-0.149
	0.200	0.230	0.300	0.000	0.000	0.440	0.330	0.440	0.450	0.380	0.400	0.730	0.570	0.890	0.860	0.710	0.830	0.790
	41	43	19	1	3	10	6	6	23	28	11	15	30	55	114	184	253	652
-60.00	11.592	10.403	9.660	9.915	9.915	14.061	14.525	12.281	9.778	9.915	-0.522	-1.928	8.711	9.366	10.758	11.962	13.531	11.895
	0.230	0.360	0.160	0.000	0.000	0.450	0.250	0.490	0.230	0.000	0.640	0.580	0.370	0.430	0.730	0.440	0.600	0.860
	120	49	21	0	0	44	484	483	27	0	21	378	363	36	107	208	150	30
-70.00	8.118	10.860	10.669	9.915	9.915	11.236	14.673	14.844	12.661	9.915	7.218	-0.181	1.288	9.915	9.915	10.775	13.256	13.227
	0.540	0.310	0.580	0.000	0.000	0.800	0.740	0.470	0.870	0.000	0.900	1.360	1.060	0.000	0.000	0.480	0.420	0.390
	181	82	53	0	0	54	484	483	32	0	22	378	363	0	0	56	267	226
-80.00	10.411	15.484	12.497	9.915	9.915	12.165	17.455	16.060	10.097	6.955	3.385	-3.544	8.113	22.969	18.697	12.956	15.434	44.252
	1.350	0.360	1.210	0.000	0.000	0.100	0.600	0.590	0.230	0.670	0.240	1.390	1.060	1.400	0.560	0.330	0.920	1.210
	99	78	46	0	4	16	30	54	47	40	56	802	1039	630	215	220	370	333

Depth = 290 km

	-180.00	-170.00	-160.00	-150.00	-140.00	-130.00	-120.00	-110.00	-100.00	-90.00	-80.00	-70.00	-60.00	-50.00	-40.00	-30.00	-20.00	-10.00
80.00	68.384	16.138	-55.297	-29.041	20.207	22.212	-42.761	14.318	45.343	29.919	43.060	31.655	4.326	2.117	-21.739	-26.193	71.867	69.241
	1.570	2.370	1.790	2.250	1.400	1.710	1.580	1.150	1.390	1.330	1.250	1.370	1.190	1.480	2.360	2.060	2.610	2.160
	13	191	238	107	737	778	1060	416	283	315	304	371	347	362	453	626	1424	1265
70.00	50.980	62.344	40.950	-20.321	-24.794	-4.048	6.053	-19.755	-4.393	16.775	20.968	29.844	29.269	16.633	9.020	-4.863	-9.894	38.903
	1.720	2.060	2.030	1.800	1.910	1.890	1.550	1.780	1.550	1.930	1.300	1.820	1.710	1.590	1.660	1.820	1.740	1.830
	451	2253	5485	6336	2920	2039	1825	852	362	173	358	661	588	435	532	943	2143	1882
60.00	-4.498	23.259	51.331	17.294	-6.492	-17.442	-16.459	-6.592	-22.429	-21.397	-13.943	5.255	14.911	17.150	12.804	11.055	1.619	-5.208
	1.390	1.360	2.070	1.960	1.630	1.700	1.380	1.540	1.320	1.320	1.230	1.340	1.210	1.490	1.190	1.520	1.420	1.400
	7830	10161	10525	9398	3686	2511	2236	1862	1387	573	524	1072	827	432	535	768	1821	4987
50.00	-21.210	-21.557	1.808	4.017	3.698	-17.455	16.125	11.357	1.894	-35.700	-36.010	-52.480	-22.056	-0.797	2.396	4.020	-2.068	-5.758
	1.320	1.090	1.860	1.580	1.200	1.480	1.830	2.000	1.720	1.360	1.450	1.710	1.180	1.030	1.020	0.850	1.010	1.230
	8213	8768	5818	3803	1808	4028	6018	5154	3182	1179	1376	1752	916	381	465	711	1225	8439
40.00	3.819	-4.541	-7.310	-2.621	7.426	27.482	-64.823	20.331	44.468	-16.536	-55.940	-10.040	-33.728	-11.998	-5.752	-23.545	-14.502	13.817
	0.880	0.860	1.200	0.910	1.000	1.640	2.030	2.020	1.480	1.330	2.350	1.040	1.090	0.750	1.120	1.060	0.750	0.770
	1349	774	150	78	278	5891	10622	9376	5874	3149	2542	1861	458	298	533	736	539	4324
30.00	8.604	1.099	-3.586	1.000	15.412	58.830	28.165	-32.701	45.456	-7.029	-31.967	-43.778	-10.088	-17.818	-6.024	-6.880	-15.899	3.440
	0.000	0.690	0.830	0.990	0.700	0.970	1.620	1.450	1.360	1.100	1.610	0.740	0.660	0.990	0.640	1.050	0.830	0.610
	2	50	92	41	82	3122	6316	6462	4688	2674	1983	1199	254	542	777	516	331	299
20.00	8.604	-4.974	-23.634	-21.233	8.604	19.289	19.628	-14.260	54.117	31.177	-8.845	-38.674	-9.937	-16.064	-20.165	-11.740	-10.014	-4.195
	0.000	0.830	0.750	1.250	0.000	0.610	0.510	1.190	1.600	1.210	0.800	0.790	0.740	0.620	0.610	0.640	0.820	0.690
	2	67	123	62	0	112	378	1926	4340	4668	2605	1543	1247	792	766	115	49	131
10.00	8.604	1.885	-30.841	-41.979	8.604	8.604	10.421	6.473	50.552	60.733	-10.075	-50.420	-43.775	-0.485	1.896	-17.410	-46.852	-22.767
	0.000	0.520	0.790	1.030	0.000	0.000	0.610	0.660	1.180	1.370	1.310	0.790	0.960	0.760	0.580	0.510	0.680	1.290
	0	21	48	31	0	0	74	1311	3736	5019	5080	3645	1273	489	544	342	679	1687
0.00	8.604	8.604	8.604	8.604	8.604	14.286	9.811	9.030	7.801	9.527	-20.305	-13.499	-23.285	-4.524	8.785	8.167	-49.540	-53.501
	0.000	0.000	0.000	0.000	0.000	0.650	0.710	0.860	0.840	1.050	1.200	0.940	0.720	0.640	0.640	0.650	0.770	1.220
	0	0	0	0	0	44	64	234	381	1463	5122	4230	200	43	276	349	801	1756
-10.00	26.813	0.673	-2.500	43.440	36.815	25.228	14.124	8.626	3.326	-18.962	-29.845	-31.152	-7.903	8.427	11.197	10.555	5.511	-14.277
	1.110	0.760	0.570	1.010	0.480	0.770	0.850	0.880	1.020	0.820	1.010	0.990	0.620	0.470	0.590	0.450	0.540	0.560
	3752	3350	3410	6299	3933	74	244	264	88	517	3182	3462	773	120	111	27	427	430
-20.00	8.393	1.444	-31.524	66.804	57.742	40.287	25.877	17.209	8.174	-6.873	-43.933	-52.398	-31.779	4.126	10.718	8.604	9.068	4.488
	0.920	0.800	1.730	1.500	0.760	0.630	0.760	0.810	1.010	0.980	0.770	1.390	0.950	0.780	0.630	0.000	0.430	0.460
	7145	6078	3670	6741	4347	384	345	365	83	98	2554	4370	2277	120	103	2	316	334
-30.00	-36.704	-12.530	-0.657	10.044	39.717	31.355	24.472	22.519	15.648	4.705	-13.014	-31.375	-34.630	-4.888	7.136	8.604	9.696	9.131
	1.360	0.940	0.350	0.750	0.930	0.810	0.830	0.840	0.880	0.780	0.700	1.130	0.840	0.850	0.680	0.000	0.330	0.380
	4726	3447	467	630	401	319	151	231	151	54	2311	3964	2032	70	15	0	159	173
-40.00	-31.110	-16.068	-2.786	8.604	8.604	8.604	12.920	13.498	14.400	10.061	1.706	-14.751	-15.871	-6.665	8.604	8.604	10.604	9.983
	0.940	0.590	0.630	0.000	0.000	0.000	0.590	0.800	0.580	0.700	0.560	0.620	0.700	0.590	0.000	0.000	0.170	0.290
	1530	565	12	2	2	0	8	35	69	87	1043	1270	462	49	0	4	68	69
-50.00	-23.367	8.604	2.603	2.221	0.488	1.218	4.648	8.092	8.604	9.208	5.770	-1.429	-13.589	-16.213	-5.120	9.005	11.712	10.614
	1.110	0.000	0.560	0.580	0.580	0.510	0.380	0.450	0.000	0.600	0.510	0.480	0.540	0.720	0.440	0.310	0.270	0.250
	376	0	6	71	113	59	15	12	1	41	89	79	61	54	69	499	538	100
-60.00	8.604	8.604	9.878	7.482	5.240	4.765	6.185	7.292	8.604	8.604	8.604	5.613	-0.476	-15.029	-21.602	-7.117	5.701	8.983
	0.000	0.000	0.060	0.200	0.220	0.180	0.180	0.130	0.000	0.000	0.000	0.340	0.370	0.450	0.490	0.480	0.370	0.310
	0	0	6	71	113	55	12	7	0	0	3	38	81	90	93	564	551	171
-70.00	10.503	8.604	8.604	8.604	8.604	8.604	8.604	8.604	8.604	8.604	8.604	8.528	7.105	3.714	-3.980	-9.701	-5.287	2.237
	0.430	0.000	0.000	0.000	0.000	0.000	0.000	0.000	0.000	0.000	0.000	0.310	0.310	0.360	0.400	0.420	0.440	0.400
	17	0	0	0	0	0	0	0	0	0	2	10	26	34	25	93	96	167
-80.00	11.602	6.472	6.900	8.604	8.604	8.604	8.604	8.604	8.604	8.604	8.604	8.604	8.604	8.604	8.604	8.604	8.604	13.391
	0.710	0.480	0.440	0.000	0.000	0.000	0.000	0.000	0.000	0.000	0.000	0.000	0.000	0.000	0.000	0.000	0.000	0.530
	133	81	12	0	0	0	0	0	0	0	0	0	0	0	0	0	0	60

Depth = 290 km

	0.00	10.00	20.00	30.00	40.00	50.00	60.00	70.00	80.00	90.00	100.00	110.00	120.00	130.00	140.00	150.00	160.00	170.00
80.00	-59.761	-15.170	63.633	17.061	23.092	10.006	-23.286	2.047	11.824	-0.533	3.875	24.273	64.826	22.564	-5.893	-2.006	38.638	68.622
	2.280	1.410	1.610	1.510	2.330	1.670	1.090	1.160	1.720	2.200	0.960	2.390	2.790	1.510	2.130	1.530	2.140	1.370
	1005	591	341	353	240	79	94	139	159	131	123	161	200	222	142	87	37	11
70.00	56.717	-22.108	-23.341	18.273	15.568	19.326	15.886	-0.741	2.960	8.918	5.033	4.146	12.607	39.420	28.853	10.916	3.980	21.606
	1.860	2.000	1.580	1.730	1.670	1.970	1.750	1.790	1.650	2.010	1.490	1.830	1.820	1.800	1.690	1.860	1.670	1.950
	1873	2914	2946	2905	1553	209	29	47	50	116	110	135	289	380	198	82	138	436
60.00	3.986	33.401	-38.394	-49.895	-9.725	9.544	18.691	22.532	15.165	17.379	18.773	9.046	-0.500	-6.529	7.913	17.987	8.431	-4.732
	1.390	1.630	2.370	2.000	1.570	1.520	1.320	1.460	1.780	1.430	1.720	1.420	1.370	1.410	1.350	1.410	0.970	1.090
	11955	18290	14306	7350	2736	783	605	560	369	524	869	1292	1151	668	654	3039	4906	5400
50.00	41.482	48.583	60.179	-48.071	-19.677	7.477	10.519	17.093	26.482	25.756	40.244	46.102	6.914	-26.849	-42.844	-22.192	28.784	-8.348
	2.170	2.570	2.370	1.680	1.710	1.370	0.900	1.970	1.490	1.570	1.890	1.690	1.750	1.450	1.550	2.220	1.640	1.150
	25338	31358	20117	8349	3345	2563	1740	2285	2536	2176	2270	2554	3174	3418	17350	24087	11526	5625
40.00	63.591	-32.422	-67.354	57.287	-16.270	-2.344	12.879	-20.764	-3.104	36.788	40.439	18.521	-1.076	-27.698	-46.534	-34.035	-0.747	16.123
	1.340	1.760	2.300	2.710	1.610	1.870	1.560	2.270	1.410	1.690	1.910	1.660	1.850	1.890	2.500	1.890	0.980	0.790
	17158	19982	11008	4871	3354	3619	4580	6415	6878	4227	5607	7248	7037	9570	25310	26098	7462	1116
30.00	14.448	-21.102	-49.952	-47.208	-35.804	-47.942	-34.723	-45.133	-42.756	-62.343	37.533	-18.915	-32.899	-56.769	-33.184	-19.769	-3.333	8.604
	0.550	0.620	0.760	1.200	1.150	1.260	0.970	1.660	1.490	2.420	1.730	2.540	1.920	2.210	1.890	0.850	0.780	0.000
	611	834	1308	1434	1579	2470	4656	6147	7399	7279	9668	9208	11885	13018	11597	6405	58	0
20.00	3.469	-9.698	-21.568	-39.351	-54.196	-21.100	-26.601	-12.157	-31.107	-38.366	8.274	41.509	-28.805	-42.537	-53.007	-13.855	-0.335	8.604
	0.570	0.590	0.510	0.560	0.760	0.730	0.750	0.920	1.500	1.810	1.560	1.420	1.930	1.190	1.100	1.230	0.770	0.000
	133	29	102	296	713	1800	1983	2080	4328	6952	7273	5359	9246	8427	4625	3338	138	0
10.00	1.955	-13.204	-20.321	11.765	7.564	5.840	19.540	5.019	-11.574	-25.644	-34.490	-15.128	-12.327	-28.304	-45.678	-49.556	-6.674	8.604
	0.820	0.620	0.600	0.740	0.790	0.920	0.760	0.850	1.290	1.220	1.140	0.860	1.640	1.500	1.170	1.330	0.820	0.000
	1309	205	339	683	938	1064	672	1123	1710	4147	6018	4245	8247	7780	3422	2814	348	0
0.00	-34.017	-13.181	-29.541	18.504	43.795	22.527	25.489	23.154	-14.505	-15.001	-9.233	-55.589	-39.287	-35.519	-26.284	-13.726	0.007	13.710
	0.650	0.580	0.620	0.790	0.830	0.870	0.790	0.820	0.890	1.020	1.330	0.990	1.180	1.910	1.130	1.190	0.780	0.800
	1253	208	545	1162	870	276	320	298	313	2761	5830	5188	9494	10282	6657	8386	5487	428
-10.00	-18.198	-5.082	4.113	12.119	13.739	22.134	23.399	31.283	8.744	1.684	6.639	-38.441	-36.949	-47.556	-56.416	-22.843	33.203	16.239
	0.610	0.590	0.570	0.760	0.830	1.090	1.130	0.930	0.720	0.880	0.850	0.980	1.140	2.020	1.600	1.330	1.690	1.030
	66	12	356	887	810	274	451	606	345	667	2159	3030	5121	7657	7924	8452	10085	5488
-20.00	1.862	-0.106	5.448	20.446	11.610	5.325	15.193	17.462	15.666	6.690	4.953	-11.629	-47.820	-1.956	-40.805	-49.781	-42.422	38.895
	0.450	0.510	0.560	0.610	0.730	1.000	1.250	1.230	0.780	0.710	0.940	0.640	1.030	1.550	2.090	1.400	0.870	1.480
	42	191	1971	2220	862	219	341	419	139	65	79	1050	1925	4472	4969	2547	6317	6348
-30.00	6.146	-0.071	-8.122	-11.586	7.931	6.649	6.606	11.912	13.688	11.836	8.604	2.646	-13.408	-21.799	19.999	-53.869	-59.133	-47.880
	0.400	0.360	0.780	1.030	0.500	0.620	0.910	1.110	1.020	0.590	0.000	0.660	1.590	0.840	1.500	1.410	1.160	1.080
	16	392	2448	2329	546	184	156	68	60	33	1	1786	2509	3070	4130	3285	1585	2038
-40.00	8.604	6.007	0.351	-2.573	0.765	7.591	5.501	7.356	9.592	9.124	10.017	7.891	5.411	-3.578	-2.583	-2.105	-48.202	-63.980
	0.000	0.380	0.410	0.310	0.470	0.390	0.480	0.690	0.700	0.840	0.770	0.450	0.740	0.780	0.800	0.820	0.690	1.400
	1	203	688	532	86	145	120	25	54	47	11	1235	1650	946	1838	1790	440	1124
-50.00	8.689	8.128	7.525	6.679	8.604	8.644	8.613	7.174	7.368	3.258	3.353	8.653	7.780	7.958	6.218	4.824	3.835	-8.786
	0.210	0.260	0.320	0.280	0.000	0.390	0.330	0.340	0.440	0.420	0.470	0.580	0.450	0.780	0.860	0.670	0.750	0.870
	44	45	24	7	4	13	10	8	18	21	11	19	30	57	116	199	283	516
-60.00	9.816	9.002	8.476	8.604	8.604	12.088	12.430	10.835	8.450	8.604	-0.176	-1.817	7.200	7.688	8.794	9.933	10.474	10.200
	0.230	0.270	0.140	0.000	0.000	0.370	0.190	0.410	0.190	0.000	0.490	0.450	0.310	0.370	0.610	0.370	0.540	0.790
	134	59	23	0	1	74	484	466	87	0	28	378	361	35	104	192	146	30
-70.00	6.433	8.924	9.089	8.604	8.604	9.822	12.580	12.678	11.015	8.604	6.524	0.598	1.232	8.604	8.604	9.294	11.737	11.330
	0.410	0.260	0.410	0.000	0.000	0.630	0.570	0.360	0.700	0.000	0.730	0.900	0.810	0.000	0.000	0.410	0.340	0.350
	183	88	48	1	1	75	484	468	92	0	28	378	359	0	1	60	255	213
-80.00	9.224	12.750	11.032	8.604	7.960	10.920	15.210	13.471	8.695	6.262	3.538	-0.329	10.457	21.329	16.561	13.345	13.312	45.206
	1.320	0.180	0.650	0.000	0.650	0.820	0.370	0.650	0.170	0.750	0.150	1.050	1.350	1.460	0.510	0.510	0.620	1.230
	89	70	40	1	7	26	55	63	43	32	35	520	1013	646	112	203	411	353

Depth = 410 km

	-180.00	-170.00	-160.00	-150.00	-140.00	-130.00	-120.00	-110.00	-100.00	-90.00	-80.00	-70.00	-60.00	-50.00	-40.00	-30.00	-20.00	-10.00
80.00	44.220	-11.019	-50.016	-1.552	13.360	-17.517	-22.318	13.126	15.133	26.016	22.007	-4.388	-6.751	-19.906	-30.053	11.872	29.638	70.837
	1.010	1.040	0.980	1.020	1.570	0.580	0.760	1.150	1.450	0.830	0.780	2.100	0.720	1.020	1.070	2.620	1.470	1.940
	58	150	175	600	839	833	514	475	540	339	365	317	315	485	576	744	1291	1472
70.00	39.489	43.316	17.995	-16.035	-7.256	2.521	-7.632	-15.487	-2.832	4.167	12.952	16.387	6.037	-0.215	-9.787	-17.525	-1.717	11.804
	1.340	1.300	1.350	1.310	1.240	1.300	1.030	1.130	1.100	1.330	1.090	1.110	1.420	1.230	1.160	1.240	1.650	1.390
	788	3392	5507	5357	2905	1980	1272	654	452	199	437	666	496	616	684	953	1623	2195
60.00	4.887	33.689	47.048	30.722	13.538	2.398	-0.298	-3.707	-15.107	-13.790	-11.776	-0.129	9.452	5.903	1.827	-2.466	-9.144	-4.755
	1.240	0.940	1.420	1.130	1.110	1.060	0.980	1.030	1.030	0.780	1.040	0.920	1.030	1.090	1.100	1.210	1.340	1.370
	7902	11277	10947	8330	3861	3000	2620	1678	1364	584	667	1140	798	490	562	667	1826	5172
50.00	-23.727	0.014	33.393	51.237	42.047	22.472	30.607	22.802	0.531	-20.472	-21.988	-38.354	-14.957	-0.835	0.134	-1.508	-8.433	1.793
	0.920	0.850	1.240	0.950	0.830	1.160	0.950	1.070	0.970	1.130	0.900	0.880	0.570	0.680	0.900	0.590	0.870	0.930
	8339	8959	6303	3924	2395	4687	6328	4579	3349	1493	1455	1599	839	433	474	712	1927	8770
40.00	3.399	-1.222	8.705	23.189	36.204	48.142	-16.875	54.325	25.546	-18.633	-36.543	3.857	-23.138	-11.990	-7.276	-12.161	-9.740	4.283
	0.850	0.900	0.750	0.800	0.830	1.250	1.250	1.150	0.920	0.910	1.220	0.750	0.920	0.510	0.780	0.880	0.570	0.700
	1431	825	357	275	1164	5946	10618	8654	5860	3395	2569	1756	516	388	622	721	1084	5100
30.00	3.563	2.753	3.077	7.090	17.567	43.306	41.965	3.211	40.530	-4.953	-35.427	-22.687	-4.486	-14.076	-12.922	-8.547	-13.128	1.725
	0.000	0.650	0.750	0.720	0.640	0.950	1.010	0.830	1.060	0.910	1.180	0.590	0.550	0.830	0.560	0.760	0.700	0.520
	4	48	87	42	629	3087	6512	6370	4981	3194	2176	1388	524	666	827	506	309	514
20.00	3.563	-6.164	-13.098	-7.026	3.563	10.187	10.159	4.643	47.919	23.606	-4.140	-29.585	-8.895	-11.145	-18.235	-13.898	-7.209	-0.778
	0.000	0.520	0.720	0.650	0.000	0.490	0.620	0.690	1.250	0.890	0.710	0.490	0.530	0.490	0.580	0.520	0.590	0.580
	4	71	123	60	0	253	743	2227	4738	5334	3181	1649	1266	936	757	221	76	264
10.00	3.563	-3.124	-30.327	-40.326	3.563	3.563	1.345	0.437	32.552	47.884	4.413	-27.483	-30.432	-0.166	-0.747	-14.487	-43.023	-6.523
	0.000	0.440	0.740	0.700	0.000	0.000	0.400	0.610	0.810	0.980	0.930	0.630	0.720	0.680	0.560	0.450	0.410	0.820
	1	23	40	21	0	0	132	1220	3727	5277	5330	3536	1297	618	527	364	1065	1685
0.00	3.563	0.179	-0.950	-6.278	3.563	7.450	3.792	1.893	-1.131	2.447	-12.380	-4.052	-11.539	-3.751	4.105	2.089	-41.872	-52.061
	0.000	0.400	0.460	0.550	0.000	0.300	0.440	0.600	0.650	0.750	0.820	0.780	0.740	0.790	0.680	0.490	0.440	0.890
	0	5	11	6	4	49	91	237	490	1601	5031	4126	244	40	259	335	1151	1741
-10.00	-2.955	5.122	10.634	26.970	18.541	15.187	6.898	2.936	-2.401	-22.957	-24.110	-31.063	-9.536	3.460	4.866	4.800	1.231	-13.128
	0.790	0.710	0.530	0.760	0.410	0.410	0.430	0.480	0.580	0.510	0.760	0.660	0.620	0.710	0.630	0.470	0.410	0.360
	4613	3860	3831	6148	3096	89	242	251	129	584	3377	3637	763	116	70	33	336	476
-20.00	-30.573	-13.890	22.503	61.268	35.507	24.394	14.361	9.251	2.323	-10.911	-47.279	-54.348	-30.959	-1.668	4.318	3.563	3.668	-0.256
	0.920	1.010	0.970	0.860	0.540	0.580	0.500	0.510	0.440	0.390	0.430	0.880	0.620	0.590	0.450	0.000	0.340	0.350
	8415	6827	4192	6732	3477	285	327	347	92	239	2749	4475	2135	126	62	4	285	321
-30.00	-26.668	-17.157	2.998	21.193	30.231	18.549	13.851	11.676	7.917	-0.587	-13.782	-21.116	-28.831	-7.559	2.565	3.563	4.572	3.496
	1.080	0.780	0.580	0.470	0.460	0.450	0.560	0.500	0.470	0.380	0.440	0.650	0.480	0.650	0.330	0.000	0.330	0.320
	5165	3565	559	761	403	245	162	234	153	174	2180	3964	1953	69	16	0	150	168
-40.00	-4.309	-9.083	-3.971	3.563	3.563	3.563	6.241	6.654	6.615	3.708	-2.225	-10.326	-12.154	-7.664	3.563	5.438	5.430	4.799
	0.650	0.590	0.550	0.000	0.000	0.000	0.430	0.500	0.390	0.400	0.440	0.440	0.360	0.460	0.000	0.290	0.320	0.230
	1475	517	29	4	1	1	13	40	78	123	864	1267	487	34	0	5	69	67
-50.00	-13.199	3.563	0.266	-1.104	-2.148	-1.296	0.810	3.291	3.855	3.581	1.744	-2.207	-8.713	-11.365	-6.777	3.428	6.623	5.473
	0.890	0.000	0.520	0.520	0.440	0.490	0.310	0.360	0.290	0.320	0.340	0.470	0.400	0.380	0.350	0.300	0.270	0.280
	201	4	31	75	111	55	15	9	11	44	104	98	71	67	111	488	501	196
-60.00	3.563	3.563	4.062	2.632	1.035	0.941	1.941	2.661	3.563	3.563	3.137	1.853	-1.259	-8.949	-13.401	-6.169	1.228	4.478
	0.000	0.000	0.060	0.200	0.210	0.140	0.170	0.100	0.000	0.000	0.280	0.290	0.420	0.350	0.360	0.380	0.370	0.280
	1	0	32	75	111	54	12	6	0	1	9	43	80	98	134	550	563	290
-70.00	4.194	3.563	3.563	3.563	3.563	3.563	3.563	3.563	3.563	3.563	3.563	3.366	2.674	0.970	-3.045	-6.255	-4.120	-0.090
	0.260	0.000	0.000	0.000	0.000	0.000	0.000	0.000	0.000	0.000	0.000	0.390	0.280	0.420	0.340	0.380	0.420	0.360
	31	0	0	0	0	0	0	0	0	1	4	11	24	24	23	88	138	188
-80.00	8.320	3.726	2.987	3.563	3.563	3.563	3.563	3.563	3.563	3.563	3.563	3.563	3.563	3.563	3.563	3.563	7.381	6.568
	0.390	0.370	0.280	0.000	0.000	0.000	0.000	0.000	0.000	0.000	0.000	0.000	0.000	0.000	0.000	0.000	0.240	0.550
	153	98	27	0	0	0	0	0	0	0	0	0	0	0	1	2	5	59

Depth = 410 km

	0.00	10.00	20.00	30.00	40.00	50.00	60.00	70.00	80.00	90.00	100.00	110.00	120.00	130.00	140.00	150.00	160.00	170.00
80.00	-37.382	-51.553	22.205	10.043	3.796	-23.155	-4.116	8.996	10.650	6.576	-1.828	14.943	33.865	5.822	3.149	10.129	35.332	55.281
	1.240	1.450	1.460	1.670	1.900	1.370	0.710	0.780	1.040	0.640	1.190	0.990	2.400	1.130	1.320	0.840	0.840	1.050
	1128	697	527	469	383	256	147	150	126	144	129	143	153	149	101	94	77	53
70.00	52.698	6.193	-27.526	-5.026	0.644	2.449	-8.397	-5.225	2.130	6.481	6.708	2.338	7.543	18.680	11.260	6.770	7.929	21.819
	1.540	1.420	1.410	1.430	1.300	1.370	1.360	1.230	1.070	1.250	1.040	1.190	1.180	1.470	1.230	1.290	1.190	1.210
	2532	3195	3011	3337	1869	1005	208	130	76	132	155	198	289	342	168	112	193	467
60.00	-7.972	19.626	-3.078	-42.171	-20.514	-2.378	3.329	1.929	-0.115	3.850	8.027	6.465	-0.405	-3.488	1.141	6.142	4.198	-0.394
	1.440	1.510	1.540	1.150	1.400	1.160	1.130	1.140	1.330	1.150	1.550	1.080	1.210	1.170	1.290	0.980	1.060	0.850
	13156	19655	15045	9549	3738	1619	834	562	631	589	619	1185	1185	896	792	3513	5288	5185
50.00	37.361	17.856	34.937	-1.660	-14.663	-3.145	2.941	7.186	7.529	3.506	13.134	20.312	2.080	-17.560	-22.336	-10.807	14.356	-5.080
	1.490	2.100	1.720	1.270	0.930	1.080	0.860	1.360	1.140	0.800	0.840	1.190	1.310	0.850	1.030	1.660	1.330	0.870
	23195	29252	22498	11224	4656	2668	2320	2253	2586	2261	2235	2825	3040	4237	18471	24191	12063	5931
40.00	45.185	10.184	-58.123	37.939	7.003	-11.398	-3.148	-3.387	7.654	20.002	29.111	10.293	-14.737	-18.124	-19.514	5.616	10.394	11.243
	0.940	1.240	1.640	1.980	0.980	1.090	1.250	1.310	1.000	1.060	1.340	1.070	1.310	1.630	1.650	1.340	1.130	0.820
	14632	16465	11471	5687	3904	3808	5425	6227	6094	4910	5775	7156	7654	11099	27080	25937	7798	1463
30.00	9.970	-2.981	-16.815	-22.614	-24.164	-36.248	-45.619	-40.179	-4.725	-48.538	33.702	12.855	-19.883	-43.409	3.176	-5.288	6.479	8.167
	0.470	0.580	0.530	0.770	0.810	0.880	0.760	1.170	1.130	1.610	1.120	1.570	1.260	1.480	1.560	1.080	0.950	1.000
	988	1151	1474	1455	1748	2462	4888	5736	6067	7773	9730	9042	12691	15064	13535	6614	400	7
20.00	5.536	-2.161	-3.632	-6.128	-46.035	-8.989	-22.823	-8.441	-8.799	-13.544	21.361	30.727	14.286	-8.146	-25.178	5.373	-1.573	3.563
	0.490	0.500	0.470	0.340	0.490	0.520	0.510	0.760	0.960	1.290	1.150	0.790	1.200	1.050	1.050	1.330	1.190	0.000
	275	67	176	404	659	1585	1825	1786	3498	6835	7860	6545	10367	9829	6178	3827	214	1
10.00	5.809	-6.098	-10.794	10.785	8.081	2.872	10.471	2.122	2.806	-1.747	-2.061	15.816	13.859	5.757	-4.343	-30.260	-9.628	1.023
	0.560	0.500	0.490	0.450	0.470	0.560	0.540	0.580	0.770	0.820	0.650	0.710	1.070	1.070	0.940	1.150	1.010	0.890
	1273	253	429	891	1060	1090	722	703	1738	4333	6213	4663	8766	8210	3758	3080	468	8
0.00	-22.216	-8.776	-16.130	11.008	26.657	11.707	13.330	13.571	-9.156	-8.236	-7.605	-35.599	-8.356	-27.323	10.560	-8.611	-15.345	0.929
	0.510	0.560	0.510	0.540	0.460	0.420	0.440	0.480	0.680	0.500	0.590	0.670	0.820	1.230	1.060	1.240	0.930	0.550
	1212	248	605	1129	872	283	325	344	398	2683	5810	5203	9667	10537	7079	8658	5936	797
-10.00	-17.270	-5.885	-0.250	7.990	7.182	11.959	11.850	16.910	5.271	1.116	8.775	-24.475	-14.038	-31.571	-49.209	-3.322	17.117	-22.740
	0.520	0.490	0.480	0.580	0.480	0.440	0.500	0.480	0.470	0.390	0.460	0.790	0.910	1.330	1.160	1.150	1.200	0.950
	141	48	370	819	799	283	422	598	375	630	2182	3215	5334	7941	8434	8799	10273	5825
-20.00	-1.687	-1.301	1.576	7.643	4.293	1.721	7.463	8.699	7.737	2.705	2.510	-5.014	-28.768	-12.193	-1.042	-48.104	-19.115	-20.815
	0.370	0.470	0.520	0.480	0.440	0.510	0.540	0.550	0.450	0.460	0.490	0.510	0.770	0.950	1.280	0.970	0.810	1.100
	60	177	1791	2187	1045	230	314	394	165	76	136	1304	2314	4546	5391	3320	6158	6488
-30.00	1.789	-1.420	-1.781	-8.899	2.171	1.842	1.555	5.634	6.741	5.690	3.563	1.237	0.289	-24.957	13.533	-24.194	-45.150	-18.542
	0.370	0.330	0.580	0.630	0.310	0.410	0.390	0.620	0.550	0.330	0.000	0.460	1.050	0.670	1.000	0.940	0.840	0.810
	21	493	2305	2321	752	187	149	74	65	39	4	1512	2433	2994	4176	3534	1800	2389
-40.00	3.491	2.093	-0.272	-2.231	-1.753	2.309	0.029	0.900	3.547	3.673	4.391	2.541	1.082	-6.846	-15.361	-5.303	-33.032	-53.676
	0.300	0.320	0.250	0.230	0.340	0.270	0.250	0.330	0.480	0.530	0.460	0.380	0.470	0.580	0.530	0.440	0.540	0.950
	15	308	786	622	122	144	119	29	54	48	12	813	1395	972	1589	1504	618	1160
-50.00	4.086	3.476	2.708	2.151	2.768	2.872	2.250	0.061	-1.146	-1.403	-0.549	3.518	2.717	2.111	-0.099	-2.490	-1.828	-6.676
	0.240	0.230	0.260	0.220	0.240	0.260	0.180	0.220	0.230	0.350	0.340	0.400	0.560	0.360	0.610	0.580	0.430	0.740
	44	51	27	10	7	15	14	12	12	17	11	24	30	59	122	208	280	334
-60.00	4.810	4.392	4.008	3.563	3.563	5.063	5.065	3.725	0.750	-2.098	-4.519	-4.489	2.571	3.140	3.394	3.735	3.281	3.234
	0.280	0.340	0.290	0.000	0.000	0.230	0.260	0.230	0.250	0.280	0.260	0.310	0.300	0.410	0.320	0.240	0.420	0.460
	145	70	23	3	4	77	430	410	199	8	31	379	353	24	110	181	143	30
-70.00	2.631	4.093	4.401	4.328	4.328	4.731	5.726	5.548	4.280	2.047	-0.617	-3.239	-2.423	3.563	4.056	4.099	5.096	4.615
	0.370	0.270	0.430	0.340	0.430	0.420	0.290	0.400	0.340	0.330	0.410	0.270	0.430	0.000	0.260	0.260	0.140	0.300
	187	94	47	8	6	77	433	411	202	8	30	378	350	3	8	66	246	208
-80.00	4.162	5.674	5.326	4.244	4.806	6.131	7.262	6.339	3.595	2.621	0.907	1.389	8.139	15.420	10.551	8.622	4.292	24.694
	0.930	0.190	0.070	0.680	0.710	0.200	0.560	0.780	0.390	0.160	0.390	0.400	1.140	1.260	1.390	1.330	0.440	0.610
	82	68	43	22	29	58	74	56	31	23	42	428	1003	710	80	132	316	348

Depth = 551 km

	-180.00	-170.00	-160.00	-150.00	-140.00	-130.00	-120.00	-110.00	-100.00	-90.00	-80.00	-70.00	-60.00	-50.00	-40.00	-30.00	-20.00	-10.00
80.00	6.268	-26.751	-17.553	-8.084	-4.054	-19.529	-5.753	-2.693	1.364	16.178	15.300	-3.332	-14.749	-28.551	-6.222	17.461	8.064	34.515
	0.710	0.430	0.860	1.940	0.920	1.050	0.620	0.500	1.480	0.410	0.560	0.570	1.290	0.940	2.330	1.000	1.210	1.470
	146	199	356	786	897	949	534	623	489	397	277	350	431	593	663	739	984	1245
70.00	25.546	17.743	-1.874	-6.804	-5.366	-4.003	-11.527	-9.631	-7.198	-4.039	4.745	9.318	3.295	-5.494	-16.059	-9.956	3.102	4.271
	0.860	0.750	0.700	0.780	1.030	0.970	0.650	0.680	0.650	0.900	0.690	0.620	0.620	0.900	0.920	1.540	1.080	1.100
	1785	3548	5183	3978	2853	1948	1160	794	451	335	542	782	608	826	856	863	1153	2061
60.00	13.580	29.827	30.400	26.075	19.818	9.826	0.438	-6.391	-10.735	-11.548	-12.341	-5.042	5.001	4.152	-0.564	-6.940	-7.736	-1.935
	1.020	0.910	0.990	0.750	0.830	0.710	0.750	0.700	0.720	0.550	0.740	0.670	0.870	0.690	0.800	0.960	1.270	1.190
	9338	11479	10865	6792	4088	3316	2926	1897	1361	617	820	1037	748	618	664	783	1802	5498
50.00	-19.257	9.916	34.550	51.392	54.454	42.526	27.311	14.135	-6.605	-14.079	-17.124	-22.959	-11.392	-1.849	-1.057	-5.097	-10.482	7.295
	0.710	0.880	1.100	0.960	0.710	0.780	0.820	0.680	0.710	0.630	0.630	0.530	0.560	0.640	0.950	0.840	0.910	1.090
	9007	9237	6841	4074	3293	5675	6975	4628	3441	1815	1527	1374	790	466	484	1019	3309	8900
40.00	1.479	0.879	13.597	28.936	43.666	51.566	27.644	53.871	7.661	-24.124	-16.293	-1.476	-21.614	-12.459	-10.440	-10.161	-12.206	4.018
	0.920	0.800	0.620	0.790	0.720	1.060	0.930	1.010	0.890	0.740	0.720	0.530	0.680	0.480	0.560	0.760	0.670	0.760
	1429	840	590	498	2144	6056	10096	7783	5539	3393	2355	1511	588	448	663	872	2464	5512
30.00	4.419	2.190	2.969	7.354	16.091	15.208	38.860	28.853	30.792	-1.892	-26.539	-1.205	-4.390	-12.948	-19.742	-18.972	-17.787	-2.211
	0.770	0.760	0.740	0.720	0.730	1.080	0.760	0.940	1.220	0.820	0.870	0.610	0.540	0.630	0.570	0.580	0.620	0.550
	62	170	139	44	1150	3075	6149	6211	5545	3721	2406	1617	828	775	753	595	421	823
20.00	-2.323	-9.943	-15.783	-6.365	0.512	1.305	-1.562	16.842	51.364	20.958	-17.849	-27.456	-8.584	-5.955	-16.660	-21.909	-14.709	-3.905
	0.720	0.760	0.890	0.670	0.650	0.840	0.820	0.730	1.010	1.110	0.760	0.550	0.640	0.680	0.710	0.640	0.580	0.550
	20	75	121	53	295	700	1219	2891	5359	6090	4283	2147	1273	982	697	415	133	379
10.00	-5.575	-13.372	-44.454	-52.479	-1.613	-2.631	-8.514	-1.205	25.999	48.554	21.145	-13.916	-28.025	-3.301	-3.015	-17.529	-46.152	-7.634
	0.920	0.970	0.940	0.820	0.000	0.620	0.840	0.860	0.760	0.840	1.020	0.760	0.670	0.770	0.820	0.750	0.660	0.630
	10	26	35	12	0	15	227	1051	3695	5686	5956	3647	1213	658	486	390	1136	1629
0.00	-3.441	-6.438	-28.352	-53.197	-19.671	-1.170	-2.809	-4.191	-4.278	3.977	9.432	5.793	-3.251	-5.685	-1.068	-5.544	-35.765	-48.751
	1.430	1.420	1.210	0.850	0.550	0.330	0.700	0.820	0.800	0.740	0.940	0.860	0.760	0.790	0.780	0.710	0.670	0.720
	24	76	104	197	115	53	116	282	771	1754	5091	4238	326	49	153	283	1266	1685
-10.00	-8.793	10.684	6.459	-6.313	-7.957	1.711	-0.087	-2.435	-7.297	-22.106	-15.663	-24.195	-2.638	1.701	0.280	-0.696	-5.615	-19.263
	1.420	1.540	1.360	1.210	0.930	0.610	0.570	0.620	0.690	0.660	0.800	0.750	0.750	0.720	0.820	0.690	0.610	0.450
	6351	5444	4482	5996	2599	124	256	257	352	690	3814	4243	1108	110	53	47	365	558
-20.00	-24.796	-1.840	36.594	44.444	13.173	11.188	5.415	3.800	-2.560	-14.142	-40.619	-43.105	-13.964	-1.032	0.648	0.059	-1.769	-5.863
	1.290	1.160	1.040	0.980	0.890	0.990	0.740	0.700	0.520	0.490	0.630	0.770	0.590	0.560	0.610	0.690	0.700	0.490
	10700	9172	4863	6572	2954	214	345	354	168	480	3183	5215	2556	134	51	17	234	307
-30.00	-1.788	1.906	16.596	22.224	19.186	9.436	6.067	4.243	2.178	-5.004	-13.542	-11.496	-18.563	-5.228	-0.745	-0.029	0.088	-1.719
	0.900	0.870	0.730	0.780	0.910	1.060	1.030	0.820	0.590	0.390	0.500	0.500	0.530	0.460	0.460	0.500	0.470	0.490
	6144	4370	601	772	450	173	191	232	146	481	2148	4067	2011	66	15	6	102	171
-40.00	0.431	0.118	1.524	3.854	4.405	3.929	1.991	1.028	0.203	-1.863	-3.805	-8.106	-10.219	-8.618	-1.613	0.196	0.537	0.062
	0.540	0.530	0.630	0.680	0.690	0.770	0.870	0.810	0.660	0.520	0.370	0.430	0.360	0.520	0.000	0.370	0.490	0.530
	1396	452	58	7	13	14	18	47	86	241	780	1201	493	28	2	9	68	66
-50.00	-14.290	-3.146	-2.371	-3.347	-4.054	-2.476	-1.214	-1.077	-1.300	-2.119	-2.957	-4.488	-8.489	-11.051	-9.927	-2.489	0.842	0.750
	0.620	0.460	0.440	0.480	0.490	0.540	0.400	0.410	0.340	0.400	0.400	0.370	0.320	0.310	0.390	0.350	0.390	0.490
	137	13	43	77	102	53	16	7	17	35	96	109	107	81	135	396	446	263
-60.00	-0.958	-4.655	-2.888	-2.699	-3.831	-3.326	-2.299	-1.613	-1.613	-1.613	-2.054	-2.771	-4.326	-8.962	-11.858	-8.069	-3.868	-0.442
	0.460	0.370	0.250	0.190	0.180	0.180	0.180	0.000	0.000	0.000	0.220	0.310	0.350	0.290	0.310	0.390	0.410	0.390
	5	9	42	77	103	53	13	3	0	1	13	45	78	94	154	471	579	394
-70.00	-0.669	-0.302	-1.613	-1.613	-1.613	-1.613	-1.613	-1.613	-1.613	-1.613	-1.598	-1.786	-2.225	-3.107	-5.352	-7.236	-6.246	-3.985
	0.390	0.280	0.000	0.000	0.000	0.000	0.000	0.000	0.000	0.000	0.160	0.180	0.230	0.270	0.250	0.260	0.310	0.330
	33	11	0	0	0	0	0	0	0	2	8	11	21	19	21	76	203	222
-80.00	4.164	1.563	1.346	0.978	0.528	-1.613	-1.613	-1.613	-1.613	-1.613	-1.613	-1.613	-1.613	-1.613	-1.613	0.192	1.433	0.349
	0.560	1.310	2.360	1.120	0.810	0.000	0.000	0.000	0.000	0.000	0.000	0.000	0.000	0.000	0.000	0.660	0.580	0.900
	185	139	103	29	14	0	0	0	0	1	1	1	0	1	3	17	22	54

Depth = 551 km

	0.00	10.00	20.00	30.00	40.00	50.00	60.00	70.00	80.00	90.00	100.00	110.00	120.00	130.00	140.00	150.00	160.00	170.00
80.00	25.699	-54.273	-28.751	-13.288	-11.823	2.934	1.800	0.106	2.641	4.195	1.198	6.873	3.441	-9.681	-0.119	18.208	33.040	28.591
	1.520	1.250	0.900	1.050	1.880	0.590	0.670	0.860	0.890	0.980	0.610	1.140	0.960	0.960	1.270	0.650	1.140	0.690
	1185	978	791	690	638	471	272	148	133	140	134	135	126	80	54	78	107	126
70.00	16.571	18.281	-20.513	-25.722	-20.098	-15.654	-6.152	-2.117	-0.782	1.370	3.446	2.655	4.602	3.759	-2.944	-1.525	8.069	20.819
	1.240	1.270	0.830	0.790	0.940	0.900	0.800	0.730	0.750	0.850	0.890	0.800	0.720	0.830	0.740	0.950	0.740	0.850
	3275	3367	3099	3607	2885	1659	747	190	111	168	208	240	326	305	194	129	354	606
60.00	-8.005	0.850	8.182	-24.087	-29.791	-16.629	-10.302	-4.135	-0.570	2.073	6.477	8.758	5.281	4.007	2.145	-1.070	-2.645	1.882
	1.380	1.500	1.420	1.180	1.200	0.970	0.960	0.950	0.860	0.830	0.990	0.900	0.890	0.800	0.920	0.800	1.010	0.840
	13523	19533	17493	11546	6114	2437	1223	707	797	782	651	1085	1196	1034	1596	4984	6316	5326
50.00	27.884	7.077	2.016	39.553	-4.537	-7.160	-2.394	2.737	6.403	8.726	15.125	23.622	22.452	5.000	2.865	11.460	13.163	-15.266
	1.210	1.620	1.260	1.270	1.010	1.150	1.130	0.800	1.040	0.670	0.950	0.940	1.040	0.840	1.000	1.390	1.300	0.740
	19471	25056	24079	14713	7297	3211	2744	2818	2746	2408	2350	2828	3150	4604	18795	23755	12327	6411
40.00	16.880	11.691	-16.091	15.969	32.080	-4.302	-4.990	5.089	15.726	20.056	42.062	36.937	23.809	24.994	4.688	36.441	26.683	13.581
	0.720	0.900	1.060	1.150	0.870	0.860	1.040	1.000	0.920	0.780	0.780	0.820	0.920	1.200	1.310	1.090	0.890	0.760
	9841	11341	11124	7361	4865	4062	5994	6376	5133	5291	5580	6976	8510	12387	27252	25006	7752	1857
30.00	3.863	-0.809	6.541	-3.265	-16.848	-15.222	-43.611	-30.322	1.621	-9.819	38.730	53.016	25.635	12.136	26.800	-0.098	14.557	10.686
	0.560	0.580	0.480	0.550	0.560	0.730	0.830	0.840	0.840	1.150	0.960	0.900	0.950	1.080	1.180	0.990	0.980	0.860
	1170	1439	1822	1588	1802	2534	4836	5637	4938	8390	9300	9338	13498	15797	13976	6582	706	100
20.00	5.183	1.404	5.203	5.696	-23.274	-10.609	-21.195	-12.197	-6.227	-2.694	28.755	49.314	53.888	30.382	16.833	13.387	-3.302	0.936
	0.470	0.560	0.480	0.400	0.470	0.410	0.600	0.740	0.570	0.900	1.050	0.790	0.920	1.050	0.800	1.040	0.950	0.980
	485	286	441	776	836	1544	1869	1869	3186	6643	8267	8184	12127	10794	7099	4363	312	59
10.00	1.382	-5.161	-7.983	8.292	8.759	1.223	1.611	-3.313	5.355	7.608	18.630	42.103	45.416	37.779	18.403	-9.636	-9.732	-6.034
	0.550	0.450	0.600	0.560	0.560	0.560	0.630	0.690	0.700	0.750	0.680	0.780	0.950	1.000	0.790	0.800	0.720	0.930
	930	511	566	1076	1101	1144	843	581	1807	4369	6476	5309	9635	8963	4921	3799	642	130
0.00	-14.166	-9.346	-11.747	5.436	14.569	4.714	5.121	6.192	-10.870	-7.525	-3.370	1.954	15.003	12.174	48.265	0.937	-14.395	-7.375
	0.550	0.540	0.540	0.630	0.710	0.720	0.780	0.800	0.760	0.700	0.760	0.810	0.820	1.040	0.760	0.970	1.040	1.290
	866	311	652	1201	903	309	380	420	572	2502	5489	5479	10252	10877	7807	9173	6424	1620
-10.00	-18.511	-8.105	-5.947	2.567	2.670	4.519	4.017	7.275	1.165	-2.062	7.110	-8.183	1.477	-18.588	-20.663	22.530	31.008	-17.171
	0.460	0.450	0.410	0.530	0.740	0.770	0.830	0.810	0.880	0.660	0.710	0.780	0.670	0.860	0.830	0.800	1.120	1.320
	234	89	408	861	772	353	467	586	400	585	2182	3676	5982	8300	9242	9525	10248	6485
-20.00	-8.520	-5.219	-3.170	-2.942	-2.086	-2.843	1.354	1.700	1.218	-1.135	0.025	-1.874	-14.140	-14.196	6.118	-29.490	-8.273	18.028
	0.420	0.450	0.430	0.430	0.630	0.700	0.750	0.790	0.840	0.750	0.660	0.600	0.610	0.670	0.940	0.820	0.750	1.120
	147	291	1483	2140	1170	287	289	349	171	78	218	1464	2644	4582	5724	3974	6111	7565
-30.00	-2.908	-4.666	-1.612	-10.974	-4.322	-3.250	-3.916	-0.462	0.107	-0.205	-1.005	0.514	4.629	-18.091	-2.991	16.282	-24.122	-3.559
	0.490	0.470	0.580	0.530	0.510	0.650	0.630	0.720	0.750	0.740	0.640	0.610	0.770	0.680	0.670	0.700	0.610	0.730
	142	865	2048	2308	880	203	157	79	68	49	15	1284	2446	2947	4054	3601	2202	3237
-40.00	-0.677	-1.569	-1.375	-3.512	-5.422	-3.060	-5.083	-4.950	-3.167	-3.219	-2.235	-2.126	-0.924	-5.259	-14.450	-3.728	-5.237	-42.830
	0.600	0.560	0.480	0.470	0.440	0.550	0.590	0.570	0.580	0.570	0.660	0.600	0.580	0.590	0.600	0.550	0.600	0.720
	118	600	842	634	143	141	110	40	64	48	18	416	1083	968	1284	1328	854	1223
-50.00	-0.197	-0.402	-0.649	-0.855	-1.244	-1.696	-2.562	-5.067	-6.725	-7.898	-8.589	-5.332	-3.469	-2.326	-2.452	-4.127	-3.620	-3.788
	0.510	0.530	0.510	0.470	0.450	0.460	0.470	0.500	0.470	0.480	0.520	0.560	0.570	0.570	0.620	0.640	0.590	0.570
	74	82	57	35	35	19	16	12	22	17	12	24	34	62	142	212	232	239
-60.00	-0.011	-0.097	0.003	0.215	0.462	0.370	-0.020	-1.223	-4.090	-7.162	-10.316	-12.937	-8.632	-5.338	-3.402	-1.663	-1.481	-1.468
	0.430	0.480	0.490	0.490	0.460	0.440	0.440	0.450	0.470	0.450	0.440	0.450	0.520	0.560	0.550	0.520	0.560	0.600
	164	78	21	10	15	79	315	406	285	59	38	380	350	65	109	178	139	35
-70.00	-1.817	-0.777	-0.318	-0.061	0.301	0.711	0.785	0.466	-0.722	-2.787	-5.379	-8.348	-10.572	-8.231	-5.773	-3.888	-1.785	-1.094
	0.350	0.370	0.410	0.400	0.430	0.440	0.430	0.410	0.420	0.460	0.460	0.460	0.450	0.460	0.410	0.380	0.420	0.430
	196	100	53	40	19	83	329	408	289	66	34	378	347	38	13	83	237	196
-80.00	-0.355	-0.243	-0.062	-0.418	-0.282	0.355	0.483	0.487	-1.489	-1.913	-4.150	-2.494	-1.444	4.430	0.393	2.008	-0.511	11.990
	0.940	0.600	0.780	0.310	0.300	0.520	0.500	0.260	0.310	0.380	0.570	0.490	1.160	0.580	0.380	0.840	0.300	0.400
	75	78	67	62	71	109	94	37	27	32	58	327	989	811	118	127	300	300

Depth = 712 km

	-180.00	-170.00	-160.00	-150.00	-140.00	-130.00	-120.00	-110.00	-100.00	-90.00	-80.00	-70.00	-60.00	-50.00	-40.00	-30.00	-20.00	-10.00
80.00	-23.368	-33.221	3.887	-0.697	-14.072	-12.001	-7.036	-7.107	-5.465	9.832	7.637	-5.417	-9.599	1.411	14.096	4.718	1.321	9.163
	1.160	1.030	0.540	0.640	0.500	0.660	0.730	0.610	0.440	0.650	1.170	0.660	0.480	0.830	0.830	0.740	0.680	1.310
	313	501	961	1081	1198	599	487	463	435	463	584	544	619	677	706	500	669	926
70.00	12.910	-2.958	-16.023	-4.155	-1.565	-7.218	-10.180	-9.380	-8.840	-7.776	0.238	3.435	-0.567	-4.673	-0.816	6.835	5.445	3.099
	0.670	0.800	0.930	0.800	0.800	0.640	0.670	0.740	0.670	0.640	0.670	0.880	0.550	0.570	0.670	0.830	0.710	0.700
	2731	4014	4458	3435	2533	1483	1100	960	527	562	719	855	817	923	922	792	1324	2058
60.00	31.186	28.605	17.087	6.788	6.520	5.945	-2.171	-8.015	-9.801	-10.891	-13.177	-6.260	1.502	3.363	2.411	2.526	6.487	5.831
	0.800	0.910	0.890	0.820	0.890	0.860	0.670	0.880	0.580	0.700	0.750	0.640	0.900	0.590	0.690	0.950	0.770	0.650
	10430	11956	9773	6334	4065	3738	3023	2009	1236	846	1003	1104	893	860	725	1005	2298	5456
50.00	12.478	23.122	36.491	34.245	23.391	20.679	15.441	3.139	-9.558	-12.287	-15.634	-16.193	-8.043	-3.237	-2.618	-7.296	-1.043	22.149
	0.660	0.820	0.680	0.720	0.610	0.660	0.810	0.580	0.560	0.560	0.660	0.510	0.490	0.700	0.790	1.020	0.720	0.940
	9917	10085	7041	4333	4200	6206	7022	4746	3060	2085	1505	1312	877	573	548	1622	5455	8736
40.00	18.566	12.265	16.965	21.066	12.138	25.119	26.373	39.040	-5.243	-24.515	-10.345	-8.231	-18.182	-16.810	-19.242	-22.819	-24.309	0.464
	0.780	0.720	0.590	0.640	0.610	0.820	0.800	1.050	0.790	0.690	0.530	0.420	0.390	0.320	0.490	0.590	0.720	0.730
	1421	907	834	852	3125	6186	8274	6867	4950	3309	2254	1464	679	453	701	1412	4292	5477
30.00	9.279	7.215	4.100	3.879	3.786	-32.873	21.814	39.399	16.335	-20.197	-11.217	10.404	-2.257	-9.028	-23.725	-54.247	-42.678	-16.333
	0.920	0.800	0.740	0.610	0.760	1.040	0.780	0.720	1.290	0.760	0.670	0.520	0.400	0.280	0.370	0.530	0.430	0.480
	472	443	332	134	1720	3144	4802	5446	6239	5140	2873	1925	984	720	686	771	928	1210
20.00	-2.233	-4.550	-5.508	-5.082	-4.170	-7.373	-12.276	20.989	50.992	29.843	-55.377	-24.708	-6.285	-1.055	-9.820	-37.258	-53.494	-12.927
	0.970	0.890	0.900	0.770	0.770	0.850	0.780	0.710	0.820	1.080	0.810	0.590	0.510	0.560	0.500	0.490	0.470	0.330
	28	68	94	48	838	1356	1435	3142	5781	6779	5414	2988	1420	914	631	506	456	714
10.00	-5.799	-10.071	-24.735	-21.505	-9.167	-8.472	-14.683	0.679	24.981	49.288	33.527	-13.001	-25.986	-4.214	-2.278	-19.434	-53.629	-19.609
	1.140	0.990	0.930	0.940	0.940	0.940	0.910	0.800	0.640	0.780	0.920	0.670	0.560	0.660	0.730	0.580	0.590	0.420
	45	29	31	11	17	140	370	790	3509	6272	6807	3929	1154	604	409	482	1183	1464
0.00	-3.507	-2.303	-24.415	-54.827	-15.223	-5.819	-5.895	-8.643	-3.877	11.182	19.889	21.091	4.224	-5.125	-2.959	-9.778	-27.903	-38.424
	1.390	1.210	0.960	0.980	0.910	0.970	0.930	0.880	0.760	0.710	1.010	0.770	0.660	0.660	0.760	0.660	0.650	0.500
	266	415	729	937	339	104	218	430	842	1867	4849	4148	586	89	147	387	1288	1388
-10.00	-1.968	11.863	8.455	-7.001	-13.285	-1.458	-3.468	-5.506	-15.039	-15.927	-9.905	-15.598	6.791	2.454	-1.726	-3.468	-9.439	-24.168
	0.990	1.040	0.850	0.940	0.920	0.820	0.900	0.750	0.800	0.720	0.770	0.850	0.770	0.720	0.810	0.760	0.640	0.460
	7159	6671	4798	5794	2172	573	333	455	533	823	3719	4201	1383	128	53	129	458	642
-20.00	9.073	16.830	21.502	27.377	4.342	5.702	1.793	1.498	-7.643	-23.687	-27.071	-33.676	-10.358	-1.012	-1.169	-2.525	-4.104	-7.771
	1.070	0.680	0.770	0.950	1.030	0.990	0.840	0.780	0.650	0.760	0.730	0.790	0.780	0.770	0.820	0.780	0.730	0.540
	10418	9461	5196	6355	2489	726	378	391	517	622	3398	5046	2391	440	53	32	177	303
-30.00	12.255	15.648	17.988	12.830	10.573	4.308	1.831	0.282	-1.658	-11.932	-14.792	-5.317	-15.988	-6.358	-2.368	-1.210	-1.876	-3.302
	0.670	0.730	0.730	0.830	1.000	1.290	1.060	0.940	0.770	0.530	0.670	0.660	0.700	0.750	0.780	0.780	0.700	0.650
	5596	3764	625	740	579	191	212	240	316	589	2024	3549	1804	409	18	12	93	118
-40.00	-13.651	2.363	3.212	3.094	1.372	0.753	-0.757	-1.856	-2.875	-3.764	-5.661	-7.217	-9.402	-10.051	-5.235	-1.439	0.429	-0.451
	0.350	0.410	0.600	0.730	0.760	0.870	0.950	0.870	0.750	0.670	0.390	0.510	0.590	0.700	0.720	0.750	0.750	0.740
	1193	398	133	8	35	32	21	39	86	294	591	969	553	95	29	50	117	149
-50.00	-15.490	-8.450	-4.813	-4.913	-4.248	-3.270	-2.793	-2.997	-3.651	-4.173	-4.159	-5.219	-8.467	-11.788	-12.433	-6.114	-0.601	2.547
	0.460	0.370	0.330	0.360	0.440	0.420	0.460	0.370	0.360	0.420	0.440	0.310	0.370	0.480	0.550	0.620	0.690	0.740
	156	62	53	79	87	49	14	14	24	34	88	166	137	81	153	255	380	274
-60.00	-2.476	-6.194	-5.717	-5.207	-6.708	-4.766	-3.695	-3.331	-3.254	-3.254	-3.759	-4.129	-5.302	-9.403	-11.018	-9.452	-5.876	-1.623
	0.500	0.420	0.290	0.210	0.170	0.150	0.120	0.120	0.000	0.000	0.210	0.300	0.260	0.270	0.380	0.470	0.550	0.620
	40	40	50	79	83	43	10	6	4	4	15	57	81	89	167	320	550	436
-70.00	-2.145	-1.818	-3.177	-3.254	-3.254	-3.254	-3.254	-3.254	-3.254	-3.254	-3.232	-3.454	-3.755	-4.373	-6.239	-7.446	-7.191	-5.498
	0.440	0.360	0.250	0.000	0.000	0.000	0.000	0.000	0.000	0.000	0.090	0.140	0.200	0.220	0.260	0.350	0.460	0.550
	38	30	8	2	1	0	0	1	2	3	8	12	18	18	22	84	212	237
-80.00	-0.008	0.484	0.161	0.955	0.578	1.543	1.447	-3.254	-3.254	-3.254	-3.254	-3.254	-3.254	-3.254	-2.609	-0.824	0.473	-1.701
	0.170	0.570	1.130	2.000	1.340	0.490	0.940	0.000	0.000	0.000	0.000	0.000	0.000	0.000	0.640	0.770	0.690	1.230
	152	201	153	122	99	32	13	3	4	4	3	3	2	4	9	27	41	85

Depth = 712 km

	0.00	10.00	20.00	30.00	40.00	50.00	60.00	70.00	80.00	90.00	100.00	110.00	120.00	130.00	140.00	150.00	160.00	170.00
80.00	-5.578	-18.077	-44.368	-5.409	-11.440	-0.261	0.165	-2.366	-0.373	2.512	2.628	4.079	4.164	-3.153	6.252	23.090	22.037	1.301
	2.530	1.270	0.830	0.580	0.470	0.770	0.620	0.660	0.530	0.530	0.750	0.640	0.740	0.990	1.340	0.960	1.360	0.780
	1187	1193	1295	1392	1182	822	537	385	148	120	114	108	82	43	35	95	165	224
70.00	5.019	-1.171	-10.656	-28.932	-18.397	-15.525	-7.976	-3.837	-3.002	-1.576	0.665	1.907	3.198	3.961	1.194	4.882	15.498	20.000
	0.930	1.570	0.940	0.790	0.730	0.610	0.700	0.740	0.760	0.710	0.610	0.680	0.600	0.660	0.730	1.020	0.750	0.930
	3723	4191	4907	4856	4665	2872	1510	713	206	164	284	406	461	312	270	264	570	1118
60.00	-0.520	2.565	2.844	-7.191	-29.052	-20.103	-11.876	-6.040	-2.500	-0.650	1.235	3.313	3.267	3.369	7.059	9.139	13.054	23.806
	0.710	0.910	0.960	1.200	0.930	0.740	0.680	0.770	0.640	0.810	0.600	0.680	0.600	0.640	0.640	0.770	0.890	0.770
	12215	17653	19780	14369	9460	4670	2193	1410	1024	944	782	884	1202	1271	5223	8672	7558	6512
50.00	25.220	20.073	-2.132	44.881	23.353	-1.907	-3.089	0.264	3.863	3.353	10.768	17.132	17.527	7.307	0.313	26.688	40.898	12.322
	0.970	0.910	1.130	1.100	1.130	0.860	0.950	0.740	1.050	0.630	0.810	0.750	1.050	0.730	0.930	1.170	0.870	0.590
	14581	20108	24068	18223	10982	5635	4643	4578	2840	2579	2514	2955	3424	5217	18677	23046	12278	7926
40.00	-0.944	13.411	21.620	11.494	42.767	13.288	3.897	-1.761	9.634	8.514	15.077	42.812	46.815	38.839	12.096	36.534	36.544	29.352
	0.840	0.850	0.780	0.930	0.990	0.780	0.920	0.900	0.770	0.920	0.630	0.920	0.750	1.010	1.010	0.910	0.750	0.770
	5916	7789	9961	8984	6488	5399	6195	6168	4912	5303	5348	6200	8929	13424	25663	23086	7091	2414
30.00	-1.607	0.776	21.892	7.397	-11.667	-9.320	-28.242	-23.554	-14.233	1.678	17.422	53.424	54.806	48.609	44.215	5.047	14.591	13.023
	0.810	0.710	0.720	0.540	0.580	0.530	0.750	0.700	0.780	0.760	0.820	0.840	0.980	0.840	0.870	0.740	0.880	0.800
	1136	1506	2155	2261	2371	2987	4621	4980	4575	8150	8826	9520	13673	15561	13911	6828	1433	613
20.00	7.981	15.036	13.672	4.226	-11.751	-17.577	-19.500	-14.309	-5.818	0.216	23.857	57.166	63.469	53.855	48.117	27.789	0.164	0.021
	0.430	0.700	0.610	0.420	0.390	0.390	0.540	0.640	0.510	0.830	0.800	0.880	1.200	1.140	0.770	0.900	0.860	0.880
	859	657	871	1070	1017	1339	1647	1624	3322	6537	8290	9399	13446	12001	8262	4539	756	143
10.00	-1.779	0.666	0.865	9.661	9.961	4.643	-1.823	-5.627	4.544	16.139	18.873	49.137	63.068	53.724	30.137	6.206	-5.926	-9.632
	0.420	0.470	0.620	0.530	0.470	0.490	0.580	0.650	0.680	0.660	0.780	0.790	1.170	1.440	0.890	0.900	1.040	1.160
	729	571	877	1310	1137	1068	911	519	1962	4273	6509	6493	10477	10326	6910	4793	1006	221
0.00	-10.005	-8.071	-5.817	7.154	9.630	3.399	4.004	3.465	-11.299	-3.802	5.115	12.398	40.006	51.611	53.807	7.264	-19.142	-10.814
	0.430	0.520	0.550	0.580	0.700	0.750	0.810	0.760	0.800	0.650	0.780	1.010	1.080	1.210	1.160	1.070	1.090	1.220
	544	318	649	1099	852	330	486	553	711	2572	4947	5692	10047	10894	8626	9113	6580	2506
-10.00	-14.234	-10.998	-8.600	-0.598	2.931	4.009	3.122	4.255	1.735	-2.503	5.313	-8.910	-3.033	12.716	15.854	30.522	22.819	-38.611
	0.420	0.430	0.420	0.540	0.740	0.890	0.900	0.910	0.790	0.740	0.640	0.840	0.910	0.910	0.850	0.920	0.900	1.170
	315	159	505	1057	850	354	491	551	453	616	2009	3810	6147	8217	9759	10014	9893	7798
-20.00	-9.885	-3.173	-6.621	-9.667	-3.680	-0.441	0.840	0.037	-0.795	-0.848	-0.729	-1.492	-12.270	-7.062	11.310	-7.207	-29.353	20.634
	0.500	0.450	0.460	0.470	0.670	0.850	0.890	0.920	0.800	0.790	0.730	0.670	0.710	0.730	0.750	0.770	0.760	0.890
	238	474	1278	1979	1231	378	308	312	136	101	267	1553	2904	4611	5974	4496	6223	8999
-30.00	-4.306	-3.939	1.817	-10.915	-7.880	-3.865	-3.440	-2.074	-1.654	-1.921	-2.229	-0.118	3.956	-11.470	-13.757	13.535	-43.630	-39.837
	0.590	0.520	0.570	0.520	0.570	0.750	0.770	0.880	0.840	0.700	0.700	0.630	0.710	0.630	0.620	0.560	0.650	0.770
	272	1118	1775	2036	966	270	165	97	66	57	57	1104	2397	2811	3936	3470	2453	3828
-40.00	-1.353	-1.153	0.146	-2.422	-6.241	-4.587	-5.689	-6.071	-4.819	-5.006	-4.484	-4.025	-1.541	-2.861	-11.402	-9.162	-13.732	-47.205
	0.720	0.630	0.610	0.600	0.580	0.680	0.730	0.680	0.740	0.660	0.610	0.550	0.510	0.510	0.440	0.470	0.430	0.630
	340	824	883	379	150	159	116	52	49	38	24	172	809	920	1250	1159	938	1257
-50.00	0.701	-0.925	-1.274	-1.629	-2.516	-2.951	-3.504	-5.742	-7.353	-8.734	-10.030	-7.962	-5.187	-3.004	-1.853	-3.525	-5.552	-5.664
	0.730	0.710	0.670	0.640	0.600	0.570	0.620	0.610	0.580	0.580	0.610	0.550	0.520	0.570	0.580	0.550	0.570	0.500
	256	234	187	39	42	45	27	23	24	20	18	97	114	87	172	235	215	209
-60.00	0.323	0.241	-0.404	-0.895	-1.206	-1.593	-1.874	-2.581	-4.844	-7.398	-10.276	-13.550	-11.304	-7.271	-4.862	-2.521	-2.110	-2.797
	0.680	0.690	0.680	0.660	0.640	0.600	0.570	0.580	0.590	0.560	0.520	0.510	0.510	0.480	0.530	0.540	0.560	0.600
	299	76	34	24	31	53	184	367	360	117	52	369	355	176	147	176	123	49
-70.00	-2.928	-1.178	-0.398	-0.423	-0.678	-0.966	-1.281	-1.473	-2.318	-3.855	-5.783	-8.145	-10.590	-10.257	-7.832	-5.740	-3.351	-2.374
	0.580	0.620	0.640	0.630	0.630	0.590	0.540	0.510	0.520	0.540	0.510	0.480	0.460	0.440	0.390	0.380	0.410	0.460
	168	97	69	45	79	83	228	385	362	156	55	368	349	142	50	89	221	174
-80.00	-0.044	-1.044	-0.830	-1.826	-1.916	-1.952	-2.504	-1.532	-1.930	-3.648	-4.867	-1.862	-2.304	4.351	-1.039	-1.710	-2.031	6.927
	0.690	0.530	0.570	0.470	0.370	0.470	0.110	0.060	0.250	0.470	0.480	0.400	1.190	1.050	0.220	0.260	0.280	0.130
	98	77	108	97	119	98	83	23	45	69	70	230	966	859	379	102	281	262

Depth = 893 km

	-180.00	-170.00	-160.00	-150.00	-140.00	-130.00	-120.00	-110.00	-100.00	-90.00	-80.00	-70.00	-60.00	-50.00	-40.00	-30.00	-20.00	-10.00
80.00	-54.279	4.825	60.900	24.045	-11.950	-25.260	-22.026	-9.094	-7.494	9.726	-11.169	9.558	9.838	34.452	29.654	-13.072	1.784	23.822
	1.870	1.170	1.280	1.840	1.880	1.680	2.140	1.300	1.240	0.840	1.500	2.110	0.710	1.160	1.770	1.110	1.510	1.400
	718	1105	1197	1322	974	639	512	344	427	649	783	694	764	638	548	447	531	784
70.00	-9.680	-38.809	-15.031	25.550	24.394	5.781	-10.700	-17.201	-14.275	-12.789	-2.709	-6.954	-0.255	4.213	18.619	22.900	3.484	1.080
	1.990	1.800	1.300	1.250	1.730	1.580	1.620	1.720	1.640	1.380	1.320	1.400	1.450	1.240	1.110	1.520	1.430	1.460
	3108	3801	3087	3080	2307	1579	1074	968	862	954	958	921	973	876	884	898	1578	2677
60.00	31.176	8.938	-9.988	-3.660	18.967	22.793	8.648	-8.282	-15.199	-19.274	-27.604	-9.988	-4.789	-0.462	5.126	13.787	20.046	-1.677
	1.930	1.700	1.850	1.990	1.570	2.040	1.420	2.040	1.730	1.890	1.950	1.520	1.960	1.360	1.870	1.940	1.710	1.910
	11079	11741	8392	5927	4316	3879	2921	2171	1414	1299	1205	1082	1015	960	921	1807	3202	5110
50.00	26.237	19.162	8.535	3.141	6.135	6.228	14.066	-8.025	-26.570	-29.058	-27.352	-20.283	-7.552	-4.353	-2.999	-5.430	15.548	41.012
	1.280	1.050	1.610	1.190	1.080	1.360	1.360	1.290	1.080	1.230	1.210	1.140	1.100	0.980	1.000	1.220	1.270	1.490
	10676	10015	6731	4591	4724	6521	6571	4951	2991	2288	1461	1243	871	729	1010	3341	6310	7754
40.00	48.719	28.399	21.016	-1.263	-29.639	-7.146	-13.359	-0.316	-45.544	-49.044	-30.103	-12.518	-13.056	-27.217	-17.275	-27.233	-20.918	-21.226
	1.540	1.500	1.300	0.970	1.250	1.290	1.250	1.210	0.910	0.970	0.850	0.850	0.660	0.760	0.930	0.850	0.990	0.820
	1413	1295	1351	1522	3676	6206	6621	5850	4242	3100	1887	1301	810	525	1082	2734	5044	5068
30.00	35.134	28.824	20.444	4.463	-33.545	-59.727	-10.328	-25.370	-31.475	-50.841	-1.689	21.689	4.753	-7.927	-13.554	-45.024	-49.725	-44.380
	1.280	1.370	1.240	1.060	1.110	1.510	0.890	0.890	1.400	1.040	0.820	0.830	0.590	0.720	0.650	0.770	0.550	0.700
	890	697	490	807	2330	3254	3275	4430	6030	6288	4056	2080	1196	748	841	1215	1485	1502
20.00	11.717	15.494	14.923	9.421	-7.721	-24.774	-23.380	11.690	-39.180	-1.406	-0.481	23.017	-11.158	3.389	-1.538	-23.514	-35.325	-19.440
	1.100	1.120	1.130	0.940	0.790	1.080	0.930	0.790	1.220	1.750	1.130	1.030	0.710	0.600	0.650	0.470	0.500	0.810
	117	180	212	496	1588	2004	1499	2857	5461	7360	6529	3858	1811	894	598	542	687	919
10.00	5.899	14.862	16.794	11.894	2.678	-17.571	-24.804	-2.469	4.300	11.515	-45.995	19.189	-14.631	-4.546	6.349	-29.490	-21.453	-23.381
	1.700	1.480	1.220	1.070	0.840	0.720	0.920	0.660	0.530	0.940	1.370	0.980	0.720	0.690	0.550	0.570	0.680	0.890
	185	77	42	110	349	409	492	884	3144	6151	7133	4474	1715	575	387	737	1224	1286
0.00	-1.673	27.301	44.099	32.452	11.437	-0.370	-14.961	-23.982	-15.235	1.371	-15.871	1.557	22.396	3.438	0.183	-15.712	-31.940	-14.738
	1.720	1.540	1.340	1.120	1.010	0.690	0.700	0.780	0.480	0.470	1.100	0.790	0.830	0.750	0.770	0.560	0.970	0.570
	967	1335	1800	1447	544	257	456	700	888	2072	4422	4033	1232	173	221	620	1244	1363
-10.00	-13.214	15.797	64.526	67.860	28.042	4.522	-12.279	-28.189	-37.918	-15.186	-20.247	2.257	21.282	13.012	3.345	-6.343	-24.109	-48.113
	0.900	1.100	1.140	1.420	1.030	0.780	0.770	0.680	0.730	0.390	0.740	0.820	0.550	0.640	0.660	0.920	0.740	0.670
	8066	7350	5351	5129	1977	1004	591	694	629	951	3476	4039	1577	314	133	247	543	671
-20.00	3.055	7.395	51.424	64.729	35.871	9.162	1.532	-3.999	-27.080	-35.676	-11.054	-5.781	15.153	10.000	8.275	4.744	-2.161	-13.377
	1.210	0.910	0.850	0.890	0.970	0.750	0.680	0.680	0.610	0.630	0.620	0.840	0.870	0.860	0.840	0.830	0.940	0.950
	10263	8456	5138	5259	1996	1259	547	726	689	788	3222	4432	2114	823	86	62	143	308
-30.00	14.113	20.496	20.578	31.374	30.996	15.244	6.729	4.579	-3.561	-15.150	-9.566	3.874	-1.460	5.640	9.419	11.217	10.729	6.791
	0.930	0.610	0.690	0.740	0.890	0.730	0.780	0.740	0.600	0.690	0.730	0.610	0.750	0.810	0.940	1.000	0.910	0.960
	4667	2340	597	667	658	487	220	411	599	696	1880	2802	1594	940	51	24	92	212
-40.00	-5.762	7.716	10.879	11.331	12.458	11.195	7.263	5.635	5.139	4.865	1.884	1.345	-7.871	-5.058	1.668	8.729	15.533	18.103
	0.650	0.840	0.720	0.950	0.880	0.830	0.910	0.900	0.700	0.690	0.790	0.690	0.710	0.820	0.970	0.990	1.050	1.090
	1005	381	142	38	55	41	23	48	234	296	476	756	621	441	78	109	171	382
-50.00	-21.205	-7.345	-0.139	2.754	5.214	6.219	6.026	4.525	4.420	5.431	5.108	2.926	-3.872	-13.206	-12.420	-6.948	5.084	16.308
	0.710	0.710	0.670	0.710	0.870	0.920	0.840	0.850	0.820	0.750	0.680	0.740	0.740	0.760	0.850	0.980	1.010	1.050
	203	117	62	69	74	48	20	22	25	31	120	232	174	138	154	226	360	335
-60.00	-5.856	-8.475	-4.817	-2.240	-0.161	4.020	5.588	5.909	5.443	5.325	5.444	4.922	2.321	-4.020	-6.502	-6.276	-2.698	3.459
	0.640	0.620	0.620	0.610	0.540	0.550	0.610	0.620	0.670	0.690	0.710	0.650	0.650	0.690	0.740	0.820	0.930	1.010
	72	53	52	70	52	21	12	5	5	9	23	65	75	84	166	312	521	449
-70.00	4.541	1.216	-1.351	-0.597	2.255	6.598	6.598	6.598	6.598	6.188	5.954	5.828	5.519	4.334	1.601	-0.135	-1.035	-0.227
	0.590	0.570	0.530	0.440	0.330	0.000	0.000	0.000	0.000	0.330	0.480	0.570	0.590	0.700	0.840	0.980	1.150	1.190
	52	32	20	18	9	2	2	2	2	7	7	18	16	16	28	122	224	239
-80.00	8.880	12.197	13.200	12.685	16.592	24.178	19.259	8.792	8.143	7.349	6.957	6.870	6.498	7.407	7.875	15.079	15.420	8.627
	0.710	0.890	0.100	0.720	1.360	3.250	2.670	1.950	3.440	1.820	0.160	0.230	0.420	0.850	2.560	2.040	4.180	3.520
	134	140	201	181	139	122	86	24	6	6	5	5	6	10	14	44	81	113

Depth = 893 km

	0.00	10.00	20.00	30.00	40.00	50.00	60.00	70.00	80.00	90.00	100.00	110.00	120.00	130.00	140.00	150.00	160.00	170.00
80.00	-12.519	13.484	-31.941	-37.577	18.921	5.608	3.256	-2.109	-6.108	-0.558	6.534	13.569	8.112	-4.390	6.642	27.048	2.911	-34.339
	2.020	2.370	1.800	1.280	1.240	1.200	1.070	1.480	1.180	1.130	1.640	3.070	2.060	2.760	3.360	2.220	2.330	2.010
	1073	1528	1681	1850	1900	1741	1287	679	423	257	154	149	136	165	202	247	363	490
70.00	9.143	-5.358	2.343	-17.244	-31.224	-10.256	-4.628	-0.879	-0.866	-2.941	-2.057	0.879	5.044	4.396	-1.020	3.024	16.653	10.906
	1.520	1.740	1.920	1.850	1.630	1.230	1.260	1.310	1.400	1.360	1.360	1.440	1.970	1.990	1.890	2.430	2.090	1.990
	4265	6002	8980	9141	7379	5169	3096	1535	833	514	509	566	602	601	527	575	992	1953
60.00	-7.528	-2.828	-7.135	2.678	-16.947	-36.531	-16.714	-4.467	1.041	1.718	-2.066	-8.046	-14.346	-16.846	-12.103	-3.852	7.236	31.762
	1.480	1.850	1.600	2.120	1.810	1.830	1.120	1.700	1.230	1.720	1.430	1.510	1.600	1.420	1.810	1.600	1.990	1.800
	9710	14938	18791	17544	13183	8769	4384	2538	1864	1240	1073	1002	1311	2945	8263	11518	8560	8562
50.00	2.990	2.297	-32.755	-13.272	59.410	23.190	-10.801	-4.028	7.528	3.542	1.905	-12.004	-29.541	-45.052	-51.967	-11.771	33.906	13.521
	1.490	1.060	1.570	1.580	2.020	1.480	1.290	1.410	1.500	1.100	1.360	1.460	1.460	1.470	1.840	1.810	1.920	1.250
	9437	14488	20376	19175	13719	9243	6037	5337	3174	2777	2726	3031	3425	8710	18542	22188	12135	9801
40.00	-23.068	-3.585	-0.673	-31.060	-18.423	44.024	43.345	-36.225	-4.752	21.746	-12.616	-22.345	-35.037	-17.465	-48.897	-13.990	27.066	57.772
	1.040	1.090	0.920	1.350	1.680	1.970	1.620	1.570	1.690	1.180	1.790	1.590	1.240	1.450	1.460	1.010	1.290	1.740
	3004	3670	7070	8512	7687	6903	6131	6019	4377	5301	5061	5337	7766	14290	22027	19137	6999	3002
30.00	-28.624	-5.092	33.367	31.041	-21.396	-57.678	-16.149	-40.723	-50.222	-12.698	-14.055	2.006	-34.970	-20.506	36.364	-26.905	-4.085	24.939
	0.880	0.990	1.060	1.070	0.980	0.930	1.180	0.710	1.250	1.500	1.280	1.090	1.210	0.990	1.460	1.070	1.080	1.280
	1000	1434	2117	2642	2805	3333	4044	3906	4359	7032	7650	8855	12736	14620	13142	7118	2336	1159
20.00	-48.612	-8.620	39.398	50.889	12.048	-37.170	-49.220	-25.816	-20.959	-10.205	7.438	36.861	60.551	4.197	8.097	20.226	4.394	5.218
	0.800	0.920	1.000	0.960	0.820	0.950	0.770	0.870	0.740	1.090	1.140	1.160	1.770	1.740	1.270	1.270	1.030	1.330
	1101	947	1314	1472	1394	1375	1485	1361	3750	6497	7926	9437	13235	12154	9323	5293	1468	340
10.00	-36.903	-27.392	23.786	52.573	40.408	27.272	-6.352	-23.076	-8.791	17.501	8.936	25.055	64.754	20.400	15.855	1.084	-6.651	-4.363
	0.590	0.670	0.890	0.960	0.890	0.640	0.710	0.800	0.720	1.020	1.170	0.850	1.360	1.970	1.510	1.140	1.170	1.660
	935	685	1139	1443	1287	1223	1142	708	2259	4000	6260	7359	11107	11575	9125	6522	2077	422
0.00	-16.345	-15.338	4.748	33.110	27.331	12.626	13.287	-4.841	-28.440	-6.388	21.524	24.257	28.634	28.415	13.953	11.615	-50.871	-17.746
	0.650	0.640	0.890	1.030	0.660	0.630	0.600	0.880	0.680	0.650	0.670	0.700	1.260	1.400	1.660	1.390	0.960	0.890
	529	220	678	1017	936	593	605	667	824	2562	4098	5328	9296	10493	9034	8890	6734	3337
-10.00	-12.824	-19.487	-5.677	4.956	11.406	8.872	11.122	10.028	5.596	3.443	19.344	11.760	-22.627	20.963	11.312	-4.082	1.060	-62.465
	0.610	0.680	0.580	0.710	0.790	0.550	0.580	0.630	0.630	0.480	0.680	0.650	1.020	0.970	1.280	1.180	1.270	1.060
	365	193	600	1225	997	466	488	512	447	622	1565	3377	6258	7981	9365	10231	9609	9045
-20.00	-14.585	-10.042	-10.705	-20.886	-11.066	3.410	5.741	8.395	7.129	9.872	11.493	10.513	-49.670	-34.606	14.232	-10.247	-44.300	-34.483
	0.700	0.460	0.640	0.530	0.440	0.360	0.580	0.620	0.520	0.490	0.430	0.760	0.850	1.080	1.090	1.270	1.700	1.880
	319	450	986	1598	1288	655	336	259	118	214	443	1458	2981	4904	5966	5284	6562	9320
-30.00	0.259	12.345	11.574	-9.243	-12.353	-2.551	4.460	4.531	7.765	7.128	5.461	7.558	6.975	-29.091	-38.678	-0.548	-12.000	-23.523
	0.840	0.890	0.490	0.710	0.500	0.630	0.560	0.580	0.640	0.530	0.650	0.600	0.820	0.890	0.800	0.680	1.370	1.360
	699	1110	1408	1441	957	503	177	124	68	72	128	931	2269	2476	3151	3335	2773	3828
-40.00	13.502	13.820	16.652	8.510	-1.176	1.321	2.438	1.603	2.529	1.582	0.112	-1.173	4.121	6.194	-11.925	-24.062	-37.364	-40.464
	0.970	1.020	0.860	0.800	0.770	0.680	0.670	0.540	0.670	0.580	0.650	0.550	0.510	0.650	0.600	0.650	0.660	0.670
	790	943	792	194	171	162	115	70	45	40	39	78	550	831	1121	983	949	1198
-50.00	25.120	19.589	14.101	12.105	8.637	7.678	7.510	4.392	1.161	-2.402	-6.591	-7.758	-3.906	2.647	7.270	2.518	-9.528	-22.782
	1.070	1.020	1.020	0.860	0.870	0.760	0.710	0.660	0.530	0.630	0.600	0.540	0.510	0.530	0.550	0.610	0.560	0.710
	283	268	186	42	64	68	61	36	24	21	34	170	233	190	200	217	176	186
-60.00	9.698	15.064	15.043	13.089	11.616	10.380	10.210	9.772	6.310	2.212	-3.183	-10.221	-12.089	-6.962	-0.681	5.253	6.218	1.304
	1.070	1.110	1.070	1.050	0.960	0.880	0.790	0.720	0.700	0.630	0.590	0.570	0.540	0.510	0.560	0.570	0.590	0.630
	300	74	32	31	44	58	119	308	369	205	92	301	360	252	146	144	126	95
-70.00	2.527	5.996	10.116	12.070	12.101	11.395	10.766	10.797	9.828	7.342	5.123	2.092	-2.871	-6.983	-6.485	-2.482	3.029	5.521
	1.210	1.290	1.240	1.150	1.080	0.950	0.820	0.750	0.770	0.790	0.660	0.610	0.750	0.810	0.720	0.620	0.530	0.570
	164	94	86	111	82	73	126	318	394	241	131	312	371	269	202	110	206	149
-80.00	10.132	5.119	8.145	8.128	8.445	7.548	7.419	11.116	12.613	4.902	6.011	18.633	20.582	13.468	10.950	1.050	7.613	20.838
	2.190	2.870	2.650	1.220	1.160	0.670	0.090	0.180	0.460	1.870	0.910	1.170	2.680	3.280	2.130	1.650	0.550	0.620
	130	111	111	133	104	73	16	24	74	86	99	216	773	926	612	173	234	240

Depth = 1095 km

	-180.00	-170.00	-160.00	-150.00	-140.00	-130.00	-120.00	-110.00	-100.00	-90.00	-80.00	-70.00	-60.00	-50.00	-40.00	-30.00	-20.00	-10.00
80.00	-1.839	38.777	39.066	18.688	-15.759	-23.036	-24.190	-17.196	-14.248	4.104	12.533	6.869	6.170	-4.502	-24.750	-27.351	6.856	17.527
	0.900	0.980	1.370	1.070	1.690	1.050	0.900	1.340	0.490	0.460	0.980	0.710	0.380	0.420	0.620	0.700	0.920	0.610
	1114	1151	1158	1063	742	548	524	738	880	951	926	744	617	631	623	725	802	949
70.00	-17.716	-7.646	15.910	27.003	22.675	3.924	-8.671	-16.222	-16.926	-16.068	-6.619	1.781	3.439	4.489	-0.077	-12.393	-19.922	-7.250
	1.040	1.050	0.990	0.710	0.880	1.030	1.010	0.860	0.950	0.750	0.700	0.800	0.860	0.720	0.690	0.720	0.740	0.730
	2909	2726	2984	2950	2190	1529	1273	1089	1156	1262	1239	951	888	929	1045	1532	2521	3752
60.00	9.520	6.651	6.994	14.382	21.781	20.870	10.485	-0.220	-9.633	-15.940	-18.857	-10.572	-5.328	-0.352	4.640	6.008	-1.744	-10.944
	0.720	0.860	0.820	0.810	0.770	0.710	0.690	0.790	0.710	0.650	0.830	0.670	0.720	0.640	0.890	0.780	0.650	0.690
	10617	9945	7144	5297	4150	3413	2720	1878	1712	1531	1303	992	956	865	1513	2630	4051	4731
50.00	27.991	29.261	25.328	17.512	9.718	8.423	15.415	0.993	-8.624	-14.771	-13.208	-11.283	-7.557	-4.025	0.977	13.560	19.876	6.892
	0.680	0.570	0.680	0.520	0.630	0.650	0.590	0.440	0.550	0.510	0.500	0.450	0.540	0.620	0.510	0.480	0.790	0.630
	10385	8724	6342	4772	4595	5755	5271	4515	3110	2223	1413	1000	902	893	2366	5069	5775	6372
40.00	30.603	24.967	21.263	9.044	5.519	3.545	11.043	3.053	-22.269	-14.737	-15.607	-4.333	-3.430	-11.711	-10.178	5.956	19.240	6.573
	0.630	0.610	0.490	0.390	0.620	0.490	0.510	0.460	0.470	0.530	0.490	0.500	0.320	0.470	0.490	0.430	0.570	0.310
	1678	2045	1946	2323	3502	5263	5051	4577	3579	2426	1514	1117	934	943	2175	4654	4714	3681
30.00	27.466	20.534	17.905	-1.712	-11.712	-11.719	5.538	-2.839	-27.772	-20.960	-7.181	-4.161	-5.391	-10.391	-33.364	-13.483	-1.498	6.721
	0.340	0.530	0.460	0.390	0.450	0.480	0.550	0.450	0.580	0.550	0.600	0.450	0.450	0.420	0.420	0.390	0.350	0.430
	1218	987	803	1513	2603	2949	2179	2886	4527	5036	4126	2546	1521	1099	1367	1743	1565	1092
20.00	16.941	17.419	13.581	3.709	-30.260	-6.851	-0.356	-2.341	-29.709	-36.968	10.232	22.778	-7.150	-16.691	-24.537	-33.188	5.678	24.667
	0.440	0.470	0.510	0.590	0.690	0.580	0.470	0.510	0.540	0.860	0.600	0.600	0.330	0.380	0.350	0.400	0.280	0.330
	706	653	606	1232	2129	2199	1216	1954	4408	6226	6341	4053	2430	1047	767	579	615	780
10.00	12.481	17.672	18.166	11.380	0.384	-14.959	-8.485	-1.718	-18.094	-44.723	0.217	23.167	14.550	0.798	-2.199	-8.215	3.544	26.376
	0.550	0.640	0.560	0.550	0.620	0.400	0.600	0.580	0.540	0.790	0.650	0.650	0.400	0.320	0.230	0.330	0.360	0.360
	585	510	655	834	889	636	613	1010	2173	4120	6016	4393	2490	792	486	557	876	918
0.00	7.793	23.042	32.805	23.526	5.974	-8.194	-12.766	-6.697	-8.516	-23.517	-32.414	17.045	18.059	9.493	0.665	-5.331	-3.763	14.429
	0.490	0.600	0.520	0.690	0.510	0.490	0.430	0.600	0.530	0.450	0.640	0.620	0.470	0.420	0.320	0.400	0.300	0.380
	2245	2478	2456	1543	605	487	628	890	903	2247	4034	3911	1484	428	473	649	884	807
-10.00	8.221	17.728	41.769	37.447	12.337	-15.458	-26.168	-16.507	-7.047	-8.048	-32.360	-16.457	8.872	4.269	-1.534	-9.205	-15.841	-9.000
	0.500	0.720	0.650	0.530	0.580	0.360	0.620	0.530	0.540	0.470	0.550	0.690	0.400	0.420	0.440	0.370	0.290	0.390
	7786	6938	5548	3474	1654	1187	782	832	710	1184	3115	3785	1397	579	332	382	544	527
-20.00	24.975	14.844	35.297	33.421	15.352	-13.529	-25.781	-25.737	-14.288	-5.401	-8.607	-5.613	0.335	3.140	-1.523	-5.014	-19.447	-20.861
	0.600	0.580	0.640	0.590	0.570	0.500	0.660	0.820	0.510	0.470	0.330	0.420	0.450	0.490	0.300	0.300	0.320	0.260
	8900	6642	4221	2605	1656	1351	997	860	783	885	2527	3191	1556	868	468	155	198	361
-30.00	9.230	14.094	13.552	18.419	14.300	4.368	-8.188	-12.981	-9.411	0.764	-1.412	-13.023	-3.730	-0.988	0.515	-0.318	-5.612	-12.219
	0.530	0.590	0.530	0.590	0.620	0.640	0.580	0.800	0.790	0.440	0.440	0.350	0.450	0.370	0.420	0.250	0.260	0.300
	3193	1365	408	348	587	566	507	523	616	732	1281	1643	1385	975	568	56	232	585
-40.00	1.695	2.696	5.947	7.277	8.157	6.202	3.684	0.990	0.552	2.912	2.950	-2.072	-7.988	-6.852	-6.194	-2.861	0.106	-8.017
	0.380	0.450	0.550	0.620	0.640	0.680	0.670	0.600	0.700	0.670	0.480	0.390	0.450	0.520	0.440	0.300	0.340	0.360
	728	298	62	51	67	47	55	187	235	258	359	576	711	728	390	119	303	664
-50.00	-5.457	-3.209	-2.158	1.386	4.067	5.155	4.547	4.654	4.595	4.464	4.356	2.373	-4.669	-6.677	-6.798	-10.469	-3.432	-1.406
	0.400	0.470	0.530	0.650	0.690	0.650	0.650	0.640	0.580	0.580	0.610	0.540	0.390	0.400	0.390	0.430	0.370	0.380
	210	126	54	49	67	48	13	21	30	24	132	290	259	209	164	217	196	303
-60.00	-1.207	-4.016	-5.039	-5.278	-1.276	2.630	4.930	4.857	5.089	5.173	5.014	4.839	3.486	0.550	-0.465	-0.899	-2.683	-0.845
	0.360	0.390	0.450	0.520	0.600	0.590	0.540	0.500	0.500	0.490	0.470	0.500	0.500	0.430	0.420	0.400	0.410	0.410
	81	42	31	29	23	15	9	5	7	17	59	75	73	77	148	216	245	231
-70.00	1.580	0.144	-2.073	-3.263	-2.876	-0.460	2.468	4.953	5.080	5.128	5.187	5.133	5.088	4.698	3.448	2.354	1.508	0.297
	0.380	0.380	0.410	0.400	0.380	0.320	0.210	0.000	0.180	0.290	0.350	0.370	0.400	0.430	0.420	0.500	0.630	0.630
	37	20	26	34	31	22	13	1	5	6	7	15	19	27	49	138	208	217
-80.00	5.578	3.351	2.487	3.141	5.281	9.423	10.592	9.325	7.448	5.173	4.953	5.114	5.223	5.785	8.335	7.848	4.884	4.742
	0.040	0.290	0.770	0.600	0.190	0.870	1.940	3.600	2.330	0.070	0.000	0.100	0.180	0.450	0.630	0.350	2.770	2.230
	86	109	113	138	190	175	135	72	11	6	4	6	7	14	15	57	96	132

Depth = 1095 km

	0.00	10.00	20.00	30.00	40.00	50.00	60.00	70.00	80.00	90.00	100.00	110.00	120.00	130.00	140.00	150.00	160.00	170.00
80.00	-10.039	6.161	7.701	-26.390	-28.842	7.317	11.100	10.377	7.485	-0.035	-4.806	-6.199	-2.846	7.521	3.887	2.532	-18.168	-32.100
	1.180	0.780	0.730	1.660	0.760	0.790	1.440	0.980	0.740	0.920	0.510	0.690	0.590	0.540	1.660	0.580	0.640	1.290
	984	1488	2287	2873	2812	2306	2153	1803	1288	807	495	305	350	406	444	544	595	797
70.00	3.704	-5.103	-1.162	2.514	-12.515	-22.233	-9.798	-1.438	3.132	4.604	2.214	-0.926	-3.190	-3.058	2.103	3.367	3.767	-7.414
	0.780	0.840	0.760	0.690	1.080	0.990	0.810	1.070	1.030	0.960	0.970	0.780	0.750	0.760	0.790	1.080	0.820	0.750
	4249	6871	11435	13334	11863	8873	6356	3815	2428	1553	1142	799	770	910	1220	1698	1912	2300
60.00	-10.364	-1.787	-8.560	-3.661	1.898	-12.675	-21.397	-14.201	-7.544	-3.608	-1.012	0.335	-1.017	-5.259	-6.814	2.511	8.902	12.179
	0.770	0.750	0.890	0.690	0.940	0.830	0.870	1.030	0.830	1.010	0.840	0.940	0.990	0.730	0.900	0.740	1.020	0.830
	5647	10554	14867	17009	15433	12093	8424	4663	3056	2185	1585	1300	1472	7621	10774	12076	9203	9138
50.00	-6.323	-7.134	-9.139	-32.492	-5.861	1.446	-22.133	-18.983	-9.563	-6.482	-9.892	-10.946	-11.222	-15.137	-23.567	-2.894	30.738	32.697
	0.510	0.490	0.500	0.710	0.700	1.000	0.700	0.650	0.740	1.030	0.700	0.770	0.890	0.680	0.970	0.620	0.700	0.650
	4320	8226	12185	13704	11822	9772	7610	4813	3304	2878	2554	2347	3112	13350	17909	18860	11384	9865
40.00	6.090	-1.245	-5.066	-13.945	-16.943	5.754	-0.617	-34.046	-14.718	9.311	-9.784	-30.851	-27.751	-17.021	-19.172	-9.431	15.389	29.632
	0.440	0.520	0.440	0.550	0.610	0.710	0.660	0.530	0.760	0.700	0.790	0.750	0.780	0.850	0.680	0.600	0.470	0.490
	887	1379	3354	5758	6384	6230	5645	4492	4276	4644	4036	3961	6291	13107	16471	12412	6216	3235
30.00	8.564	3.440	0.954	2.132	-6.090	-22.585	-12.390	-17.782	-21.568	6.404	3.473	-13.553	-29.497	-36.846	-9.557	-1.296	-2.773	26.516
	0.450	0.450	0.450	0.490	0.600	0.560	0.410	0.520	0.460	0.520	0.690	0.640	0.830	0.860	0.890	0.730	0.460	0.390
	674	1077	1931	2395	2451	2565	2378	2016	3883	5491	5006	6526	9289	11519	11075	6304	3080	1523
20.00	19.292	-2.521	-1.128	-0.124	-5.901	-9.030	-32.385	-13.148	-11.192	-9.037	10.444	19.331	18.572	-10.145	-17.748	-20.052	5.808	7.953
	0.440	0.440	0.440	0.390	0.550	0.510	0.450	0.400	0.520	0.420	0.550	0.640	0.840	0.860	0.850	0.860	0.520	0.490
	904	879	1460	1708	1448	1257	1285	1013	3402	5293	5454	7572	9895	9745	8943	5842	2315	894
10.00	17.614	3.401	10.441	7.994	-3.858	-4.136	-18.073	-21.612	-10.286	7.035	12.568	24.587	36.777	-2.862	7.928	-14.881	2.187	13.048
	0.250	0.350	0.380	0.510	0.620	0.700	0.510	0.380	0.390	0.580	0.570	0.800	0.740	0.850	1.020	0.740	0.690	0.940
	796	613	1249	1340	1000	1096	1088	805	2252	3363	4627	5691	8096	9861	9139	6672	2775	1095
0.00	11.378	5.099	4.468	7.232	9.480	0.849	-2.504	-10.357	-14.067	2.985	18.576	28.240	27.712	-12.131	-9.633	17.447	-20.386	0.482
	0.390	0.300	0.400	0.540	0.630	0.660	0.580	0.440	0.390	0.520	0.510	0.600	0.760	0.650	0.820	0.830	0.710	0.470
	466	184	654	1136	991	916	749	888	957	2146	2961	3910	6821	8630	8743	9094	6498	4249
-10.00	4.671	3.069	-0.818	-1.713	2.990	4.624	4.455	3.241	-0.596	4.893	8.483	18.547	13.088	-5.120	-10.018	-0.470	-3.023	-6.588
	0.340	0.270	0.210	0.400	0.510	0.550	0.510	0.400	0.350	0.450	0.460	0.470	0.580	0.630	0.730	0.630	0.680	0.680
	338	194	560	1238	1111	832	528	607	514	601	1127	2283	4696	6436	7255	8729	8428	8818
-20.00	-1.641	2.637	-0.293	-11.796	-9.126	0.803	3.854	5.118	5.047	4.354	5.449	11.273	1.710	7.230	5.050	-5.902	-7.505	-3.881
	0.320	0.230	0.430	0.390	0.330	0.440	0.400	0.330	0.260	0.430	0.450	0.410	0.430	0.550	0.600	0.490	0.630	0.640
	353	337	673	1229	1172	775	473	202	243	311	537	1257	2650	4422	5207	5059	6029	8016
-30.00	-10.439	7.762	5.619	-1.240	-6.501	-3.261	1.412	2.458	3.870	4.482	3.282	4.471	12.778	10.218	1.953	-6.731	-11.951	7.435
	0.260	0.340	0.240	0.320	0.310	0.300	0.450	0.330	0.340	0.370	0.490	0.440	0.330	0.430	0.510	0.380	0.490	0.680
	847	910	822	748	774	547	345	133	80	97	199	763	1745	2178	2455	2497	2588	2982
-40.00	-11.292	-0.091	6.098	4.442	0.845	0.202	1.701	1.958	1.625	1.238	0.322	-0.105	2.900	6.987	5.911	0.061	-10.126	-10.773
	0.410	0.310	0.340	0.400	0.400	0.270	0.320	0.350	0.380	0.300	0.350	0.370	0.360	0.310	0.390	0.460	0.380	0.390
	938	879	483	112	137	112	84	67	44	50	74	114	286	685	784	698	771	866
-50.00	0.139	-0.446	2.301	4.553	4.323	3.547	3.979	3.683	2.434	0.694	-1.925	-4.555	-3.428	0.272	3.348	4.311	1.207	-3.978
	0.420	0.440	0.410	0.430	0.460	0.430	0.350	0.330	0.330	0.380	0.350	0.310	0.310	0.310	0.320	0.370	0.400	0.370
	273	200	41	24	67	81	81	75	57	30	65	218	304	230	211	153	120	161
-60.00	0.495	1.811	2.100	3.117	4.267	4.898	5.254	5.772	5.049	3.418	1.376	-2.123	-5.300	-3.973	-1.922	0.500	2.342	1.854
	0.420	0.440	0.460	0.450	0.450	0.450	0.430	0.390	0.360	0.320	0.340	0.350	0.350	0.340	0.350	0.370	0.380	0.370
	140	54	20	26	48	66	77	239	348	260	203	264	367	274	180	150	155	120
-70.00	0.587	1.370	2.284	2.924	3.605	4.385	5.064	5.547	5.878	5.523	4.857	4.022	1.126	-1.103	-1.801	-3.048	-1.596	0.815
	0.580	0.570	0.590	0.570	0.490	0.430	0.400	0.400	0.380	0.350	0.310	0.330	0.430	0.510	0.510	0.550	0.510	0.420
	148	126	125	120	102	95	48	229	365	304	259	235	504	704	582	337	177	142
-80.00	5.789	6.385	6.857	7.549	7.333	6.838	7.493	7.653	7.121	7.604	7.880	10.819	14.819	-6.604	25.187	-7.596	-8.093	4.525
	1.390	1.280	1.620	1.670	0.870	0.330	0.390	0.440	0.550	0.480	0.120	0.350	1.120	2.050	1.460	1.960	2.060	0.200
	129	134	147	130	99	79	31	36	56	79	109	153	543	923	694	455	201	170

Depth = 1317 km

	-180.00	-170.00	-160.00	-150.00	-140.00	-130.00	-120.00	-110.00	-100.00	-90.00	-80.00	-70.00	-60.00	-50.00	-40.00	-30.00	-20.00	-10.00
80.00	41.789	33.335	21.714	13.948	4.881	1.282	-17.251	-41.912	-28.571	8.448	4.314	3.618	-8.495	-29.035	-24.154	10.525	44.540	28.279
	1.740	1.460	1.260	1.180	0.840	1.020	0.970	1.460	1.050	0.810	0.940	0.730	0.780	1.040	1.010	1.080	1.270	0.920
	1113	1117	862	646	894	1161	1185	1251	1242	1172	992	957	1023	1184	1406	1718	1849	1505
70.00	24.916	33.706	33.086	27.496	21.555	13.910	8.187	-4.126	-25.268	-27.984	-11.139	-4.618	-0.850	-4.054	-15.058	-18.849	-5.274	17.073
	1.490	1.380	1.300	1.700	1.460	1.130	1.330	1.140	1.300	1.450	1.320	1.160	1.210	1.110	1.060	1.400	1.270	1.180
	2489	2682	3173	2948	2176	1950	1489	1406	1496	1461	1177	1130	1317	1570	2023	2716	3650	3723
60.00	25.007	30.150	31.190	29.903	29.029	25.895	21.072	15.543	3.830	-13.786	-19.958	-18.361	-9.831	3.519	11.967	7.180	-7.262	-13.154
	0.990	1.510	1.110	0.830	1.380	1.100	1.220	1.120	0.970	1.110	1.050	0.980	1.090	0.880	1.090	1.090	0.770	1.070
	10313	8374	6390	5343	4331	3285	2520	2075	2017	1726	1400	1050	1156	1670	2245	3010	4192	3876
50.00	38.656	40.909	29.795	18.042	17.175	24.328	22.441	11.451	9.172	-5.504	-9.818	-16.521	-16.938	-1.876	22.837	36.931	21.344	-6.153
	0.770	1.180	0.910	0.910	0.970	0.780	1.070	0.860	0.780	0.750	0.590	0.840	0.550	0.600	0.850	1.080	0.730	0.730
	10170	8436	6465	4851	4569	4392	4051	3566	2959	1958	1376	1015	1234	2679	4007	4740	4618	2595
40.00	29.164	28.846	23.868	10.817	17.759	12.236	11.658	1.383	-5.026	-8.085	-11.883	-7.022	-17.449	-24.724	-6.055	26.955	19.679	10.600
	0.950	0.790	0.800	0.660	1.000	0.720	0.510	0.670	0.640	0.730	0.650	0.790	0.610	0.570	0.640	0.920	0.690	0.590
	2961	2754	2578	2958	3260	3679	3459	3311	3093	2721	1896	1257	1494	2859	4612	4708	3900	1480
30.00	30.078	30.326	20.653	11.597	7.650	14.945	14.091	-15.549	-21.076	-18.250	-8.922	4.755	-23.329	-43.208	-46.181	-45.774	-29.406	-2.095
	0.890	1.070	0.810	0.790	0.950	0.980	0.950	0.540	0.700	0.820	0.860	0.880	0.810	0.620	0.730	0.560	0.510	0.460
	1464	1660	1695	1963	2564	2043	1061	1754	3116	3927	3765	2899	2634	2140	2411	2306	1411	453
20.00	35.073	27.242	15.957	-1.664	-1.798	22.476	26.342	6.182	-43.424	-35.995	-2.797	21.434	-7.386	-49.671	-45.126	-34.194	-24.519	-14.878
	0.880	0.790	0.930	0.930	1.050	1.100	0.990	0.860	0.630	0.530	0.680	0.840	0.610	0.530	0.500	0.630	0.600	0.560
	1243	1220	1670	2645	2814	1849	820	1183	3126	4919	5126	4459	3652	1911	1297	641	338	361
10.00	28.532	26.659	18.259	-16.561	6.213	6.196	10.910	17.394	-29.745	-57.908	-33.140	11.441	22.879	3.185	-3.551	-1.333	-3.871	-6.514
	0.990	0.880	0.700	0.960	0.890	0.840	1.080	1.100	0.770	0.840	0.540	0.910	0.650	0.480	0.490	0.580	0.570	0.540
	1277	1225	2001	2370	2071	1043	674	977	1764	2690	3996	3847	2756	1251	656	501	421	346
0.00	0.555	16.556	33.491	23.310	-2.159	2.224	2.217	14.193	-1.293	-49.327	-52.610	-2.257	7.835	12.199	5.661	4.805	3.493	2.049
	0.790	0.600	0.840	0.620	0.760	0.740	0.920	1.090	0.960	0.710	0.810	0.660	0.680	0.650	0.620	0.650	0.560	0.450
	4091	4101	3267	2556	848	610	722	847	1100	2099	2998	3260	1502	710	527	574	546	381
-10.00	39.538	-2.718	39.623	30.560	24.314	2.833	0.484	14.442	12.234	-6.776	-24.583	-1.352	9.572	7.935	0.686	-11.109	-6.794	1.158
	0.920	1.200	0.760	0.820	0.790	0.760	0.910	1.050	0.900	0.610	0.620	0.660	0.570	0.620	0.650	0.600	0.520	0.500
	7439	6586	5215	3180	1260	1010	796	752	558	1439	2551	2931	1081	634	423	390	357	342
-20.00	54.306	37.137	35.934	34.882	26.142	15.096	0.266	7.884	14.697	5.369	-2.428	9.456	9.741	3.712	-9.703	-19.782	-28.511	-0.461
	0.840	0.860	1.050	0.870	0.910	0.900	0.790	0.900	0.750	0.560	0.550	0.540	0.600	0.670	0.430	0.510	0.480	0.490
	7136	5142	3083	1522	1292	1274	997	865	689	755	1912	2064	1016	819	591	355	289	280
-30.00	22.685	26.008	23.295	25.743	24.691	24.645	20.979	18.679	22.433	15.553	2.241	-8.547	0.297	-2.581	-11.249	-26.181	-41.322	-7.606
	0.630	0.860	1.000	1.110	1.150	0.970	0.930	0.860	0.910	0.700	0.450	0.420	0.530	0.570	0.560	0.500	0.500	0.510
	1845	889	271	239	460	556	542	554	594	481	771	866	1105	990	838	597	772	891
-40.00	5.709	11.894	13.930	15.568	17.451	16.697	17.145	17.798	18.474	16.300	7.680	-12.658	-22.736	-14.347	-27.913	-42.210	-40.406	-30.966
	0.620	0.760	0.970	1.070	1.190	1.210	1.060	0.980	0.860	0.810	0.720	0.470	0.380	0.570	0.540	0.430	0.450	0.550
	597	324	48	68	68	85	169	237	241	204	196	396	715	835	793	669	810	880
-50.00	0.982	3.711	6.635	8.930	10.775	12.161	12.931	13.902	14.638	15.007	13.920	7.795	-7.459	-3.958	-5.194	-19.334	-20.634	-15.687
	0.570	0.690	0.820	0.950	1.060	1.130	1.160	1.120	1.040	0.940	0.840	0.720	0.580	0.520	0.510	0.560	0.500	0.520
	205	110	28	47	61	42	23	26	21	50	142	290	321	338	291	239	235	251
-60.00	-2.287	-1.361	0.993	4.077	6.844	8.908	10.518	11.640	12.555	13.299	14.061	14.222	12.347	6.971	7.099	5.690	-0.527	-3.249
	0.610	0.640	0.700	0.770	0.860	0.960	1.030	1.050	1.050	1.020	0.950	0.860	0.760	0.660	0.620	0.550	0.550	0.560
	77	22	16	18	19	10	8	6	25	47	103	121	85	108	121	125	134	96
-70.00	-3.769	-4.018	-2.456	0.632	3.874	6.815	9.257	10.698	11.453	12.100	12.631	13.273	13.816	13.470	11.107	10.185	9.224	5.952
	0.780	0.740	0.700	0.680	0.680	0.730	0.810	0.840	0.840	0.850	0.850	0.830	0.770	0.700	0.640	0.680	0.770	0.780
	62	14	18	39	37	29	23	24	27	27	36	14	27	32	82	132	205	198
-80.00	-10.404	-1.722	4.387	8.621	13.736	15.101	20.296	20.191	13.706	12.744	11.912	11.847	12.711	13.477	14.344	14.462	14.374	15.768
	3.220	1.910	1.090	0.850	0.330	0.370	0.730	0.490	0.140	0.120	0.190	0.250	0.210	0.300	0.180	0.670	2.130	2.610
	50	41	82	109	117	191	193	147	92	24	7	5	8	14	23	60	120	156

Depth = 1317 km

	0.00	10.00	20.00	30.00	40.00	50.00	60.00	70.00	80.00	90.00	100.00	110.00	120.00	130.00	140.00	150.00	160.00	170.00
80.00	-10.246	-18.438	23.207	16.883	-41.365	-55.196	-41.286	-10.159	3.839	2.149	-7.222	-5.091	-13.729	-31.375	-5.069	-0.392	18.479	37.250
	1.330	1.450	1.350	1.400	0.920	1.170	1.080	1.920	1.500	2.000	1.260	0.940	2.100	2.070	1.410	1.310	1.230	1.400
	1183	1428	2963	4596	5419	5739	5793	4959	3747	2631	1676	1368	1058	785	669	670	803	953
70.00	20.568	4.209	-8.478	5.918	11.247	-15.624	-44.344	-43.463	-33.354	-18.767	-11.663	-11.942	-11.011	-14.082	-22.546	-12.969	-4.864	9.342
	1.320	1.360	1.300	1.600	1.440	1.230	1.560	1.360	1.370	1.560	1.680	1.520	1.470	1.380	1.640	1.520	1.370	1.260
	3123	5312	10022	13692	15149	14826	13707	10941	8226	5845	3912	3020	2727	4303	4232	3498	2673	2559
60.00	-5.521	8.613	1.478	-12.184	-0.843	15.271	-3.594	-32.821	-40.181	-39.326	-31.574	-25.464	-26.363	-33.049	-27.910	-22.107	-3.782	8.148
	1.130	1.120	1.110	1.130	1.250	1.240	1.080	0.990	1.050	0.840	1.020	1.120	1.180	1.060	1.210	1.110	1.250	0.900
	3265	5531	10603	13968	15745	15258	13091	10179	6696	4877	3867	3391	5455	10797	12337	9859	8669	8995
50.00	-7.982	-8.180	-2.006	-17.036	-43.582	-27.058	-11.248	-6.737	-27.321	-27.993	-35.844	-40.401	-44.285	-51.145	-52.218	-39.671	3.595	38.467
	1.020	0.660	0.810	0.870	0.850	1.120	0.840	0.800	0.890	1.050	1.020	0.990	1.000	1.020	1.050	0.930	0.900	0.900
	1356	1955	4358	6053	7258	7744	7054	6076	4048	2886	2385	2289	4669	14975	17668	12983	10054	9505
40.00	-0.326	-5.860	-9.739	-14.622	-25.674	-43.316	-44.522	-34.287	2.707	-4.439	-22.473	-45.165	-49.679	-50.585	-55.015	-52.364	-39.624	7.936
	0.630	0.680	0.480	0.710	0.690	0.650	0.840	0.640	0.990	0.880	0.920	0.960	1.000	1.140	1.110	0.910	0.770	0.740
	306	536	1487	2803	4082	4274	4274	4154	4288	3971	2920	3943	6064	11587	12432	7160	5417	3751
30.00	0.347	-11.665	-16.324	-16.594	-18.247	-39.970	-46.260	-34.735	-2.432	13.200	2.993	-31.812	-38.956	-36.498	-42.210	-44.977	-28.044	19.085
	0.550	0.570	0.430	0.490	0.620	0.530	0.510	0.660	0.740	0.940	1.000	0.820	0.740	1.040	1.150	1.160	0.910	0.830
	289	573	993	1364	1782	2072	1984	2592	3763	4326	3480	5506	7410	9390	9126	5867	3372	1775
20.00	-2.035	-9.337	-33.692	-28.740	-20.508	-23.968	-45.865	-43.573	-6.840	-10.603	-20.749	27.464	47.210	47.530	7.914	-26.538	-25.548	10.775
	0.550	0.520	0.390	0.430	0.640	0.730	0.650	0.820	0.830	0.740	0.920	0.790	0.860	0.730	1.070	1.070	1.270	0.980
	401	545	860	1181	1043	983	1008	1315	2945	4052	3727	6455	7935	8344	8937	6882	3739	1790
10.00	-5.160	-0.470	-19.141	-38.618	-39.235	-36.940	-35.218	-54.043	-44.809	-12.890	-11.185	18.076	40.413	44.967	67.278	18.019	-4.189	24.651
	0.470	0.540	0.550	0.570	0.680	0.850	0.610	0.610	0.860	0.750	0.650	0.760	0.700	1.040	0.990	0.960	0.850	1.900
	383	429	824	925	889	982	998	850	2155	2836	3388	4861	6861	8644	8720	7243	4441	2309
0.00	1.570	3.415	-0.664	-36.755	-39.177	-31.419	-14.336	-21.553	-29.620	-14.358	-4.393	-4.811	10.168	-12.096	29.750	13.167	10.808	-17.340
	0.510	0.580	0.550	0.550	0.680	0.770	0.810	0.480	0.630	0.810	0.570	0.490	0.530	0.630	0.900	0.680	0.890	1.070
	322	163	518	972	899	1034	929	803	886	1384	1926	3263	5584	7587	8315	8635	6834	5457
-10.00	6.818	4.835	6.320	-24.741	-41.163	-20.121	-4.673	-6.189	-5.119	0.267	-6.981	8.036	12.167	29.602	20.272	8.803	3.633	30.002
	0.540	0.500	0.500	0.580	0.560	0.690	0.720	0.610	0.490	0.690	0.590	0.470	0.640	0.530	0.770	0.800	0.650	1.040
	269	168	445	993	965	970	746	602	546	599	752	1545	3292	5175	5447	6880	7841	7706
-20.00	11.932	11.419	7.995	-6.203	-20.452	-17.611	-3.210	2.650	2.363	1.949	3.151	15.735	44.798	52.222	24.478	5.747	4.563	23.949
	0.530	0.600	0.530	0.580	0.570	0.500	0.660	0.620	0.530	0.500	0.530	0.460	0.470	0.660	0.460	0.890	0.590	0.660
	223	192	421	884	1051	741	643	466	394	423	592	1023	2351	3752	4109	4214	5276	6186
-30.00	18.677	18.532	12.703	5.954	-2.579	-4.793	-2.362	1.851	1.967	1.355	0.519	3.972	22.181	38.635	29.558	-1.284	-12.410	3.092
	0.650	0.690	0.670	0.640	0.640	0.660	0.550	0.580	0.530	0.470	0.640	0.520	0.440	0.440	0.550	0.530	0.650	0.540
	834	689	169	243	551	505	434	312	183	171	233	588	1284	1685	1925	1974	2241	2077
-40.00	-0.958	15.116	14.974	11.433	7.435	4.111	2.979	3.375	2.162	0.555	-0.172	-0.562	1.813	11.704	16.127	10.043	-2.914	-5.429
	0.680	0.720	0.790	0.800	0.770	0.750	0.740	0.710	0.740	0.660	0.520	0.570	0.430	0.470	0.550	0.480	0.470	0.640
	786	623	69	64	93	85	70	55	40	58	110	195	245	407	600	595	595	628
-50.00	-7.720	3.325	9.705	11.214	10.714	8.336	6.359	6.202	5.130	2.650	-1.000	-3.457	-1.798	1.935	3.793	4.653	3.239	1.199
	0.560	0.680	0.780	0.830	0.840	0.840	0.830	0.790	0.760	0.740	0.640	0.550	0.550	0.500	0.500	0.530	0.560	0.570
	144	60	19	24	42	64	86	107	164	140	88	216	297	244	224	113	76	150
-60.00	-2.948	-0.600	3.616	7.481	9.767	10.623	10.090	9.401	9.406	7.346	4.844	1.253	-2.884	0.391	1.707	0.647	-0.595	-1.920
	0.610	0.640	0.650	0.700	0.760	0.790	0.810	0.820	0.790	0.750	0.720	0.670	0.630	0.620	0.590	0.580	0.550	0.560
	61	41	36	21	30	71	85	205	337	382	301	394	448	299	244	140	150	140
-70.00	3.185	2.202	2.760	4.626	7.246	9.534	10.748	10.974	10.900	10.836	9.744	8.422	5.567	3.356	5.434	4.580	0.704	-1.688
	0.730	0.700	0.710	0.680	0.630	0.650	0.670	0.680	0.680	0.650	0.650	0.680	0.710	0.790	0.750	0.670	0.740	0.730
	143	130	147	126	100	46	47	187	330	340	296	320	484	651	787	524	276	127
-80.00	13.317	15.262	15.840	14.608	14.603	16.366	16.346	14.064	14.204	16.189	17.647	16.116	18.009	1.320	37.089	34.212	-2.009	-10.040
	1.810	1.220	1.120	1.510	0.520	0.340	0.680	0.330	0.570	0.240	0.100	0.830	0.860	1.460	2.570	0.560	2.450	2.840
	137	126	139	120	99	46	39	56	52	60	89	137	385	763	765	567	254	89

Depth = 1559 km

	-180.00	-170.00	-160.00	-150.00	-140.00	-130.00	-120.00	-110.00	-100.00	-90.00	-80.00	-70.00	-60.00	-50.00	-40.00	-30.00	-20.00	-10.00
80.00	0.810	-9.790	-14.392	-1.029	14.252	5.864	-4.081	-16.193	17.983	25.016	14.133	7.394	-0.277	-3.803	-7.918	-12.611	-23.732	9.100
	1.020	0.870	0.800	0.720	0.780	1.070	1.330	0.760	0.520	0.600	0.750	0.880	0.750	1.310	1.770	0.890	2.030	0.950
	904	820	796	973	1460	1654	1818	1830	1757	1619	1658	1688	1813	2249	2814	3182	2950	1954
70.00	20.620	11.424	1.467	-5.497	-2.540	6.094	5.562	-0.384	-9.625	2.615	11.990	11.854	9.429	4.953	0.762	-3.934	-9.260	-18.106
	1.220	1.170	1.020	1.000	0.860	0.830	1.040	0.860	0.870	0.940	0.750	0.890	0.970	1.000	1.040	1.350	1.150	1.500
	2981	3325	3316	2862	2291	1986	2037	1929	1859	1742	1755	1891	1998	2606	3234	3684	3507	2997
60.00	34.328	26.462	16.752	9.881	7.344	6.134	6.607	5.608	-0.193	-7.594	-6.014	1.196	8.863	13.918	11.797	4.467	-2.818	-10.219
	1.030	1.000	0.920	0.960	0.930	0.960	0.780	0.770	0.710	0.740	0.760	0.670	0.450	0.680	0.700	0.580	0.650	0.750
	8753	7106	5807	4956	3655	2465	2331	2019	2026	1878	1488	1521	1693	1865	1968	2302	2621	2575
50.00	41.641	34.809	16.532	5.269	6.771	9.609	-1.649	-2.401	-1.339	-9.328	-16.377	-7.990	8.239	25.992	28.418	18.749	7.859	-0.820
	0.780	0.810	0.670	0.820	0.830	0.750	0.850	0.710	0.860	0.770	0.780	0.660	0.470	0.480	0.580	0.480	0.440	0.390
	9308	7866	5620	4090	3649	2779	2505	2458	2262	1840	1366	1842	2570	3194	3624	3671	1825	426
40.00	13.354	14.441	5.611	7.495	3.948	-2.606	-16.259	-14.827	-7.278	-14.238	-18.117	-0.748	24.895	45.152	46.809	31.125	13.590	3.483
	0.880	0.670	0.620	0.620	0.650	0.770	0.810	0.720	0.770	0.970	0.820	0.770	0.620	0.650	0.690	0.530	0.410	0.340
	3169	2977	2776	2287	2388	1864	1663	1902	1920	2231	2303	2835	3324	4238	4409	3811	2054	130
30.00	8.186	16.149	18.688	7.981	5.107	-1.467	-23.424	-30.428	-3.936	-4.265	-2.588	26.220	39.331	25.672	10.734	0.150	5.354	0.263
	0.530	0.820	0.710	0.710	0.660	0.650	0.840	0.730	0.620	0.640	0.810	0.890	0.760	0.680	0.510	0.480	0.370	0.400
	1998	2088	1910	1670	1977	1230	564	783	1570	2562	2896	3448	3872	3797	3058	2031	927	110
20.00	23.011	27.578	21.708	29.995	7.895	15.393	-11.005	-17.151	2.371	11.586	9.773	17.999	20.951	11.890	-14.941	-11.377	-7.877	-4.842
	0.600	0.400	0.610	0.740	0.780	0.690	0.740	0.760	0.620	0.560	0.570	0.600	0.680	0.590	0.420	0.320	0.360	0.420
	1697	2018	2577	2847	2376	1390	609	650	1546	2846	3110	3724	3187	2543	1824	620	207	142
10.00	1.072	26.366	42.670	45.283	34.621	12.491	5.357	3.745	2.390	9.230	14.989	15.751	15.799	6.362	-1.791	-9.119	-8.850	-5.864
	0.830	0.650	0.670	0.710	0.620	0.820	0.800	0.740	0.600	0.590	0.650	0.710	0.670	0.540	0.510	0.500	0.430	0.420
	2349	2413	3673	3118	1915	925	653	779	1177	1611	1824	2312	2186	1233	619	341	120	153
0.00	-53.963	13.790	24.001	47.731	21.178	6.741	3.436	11.279	1.394	-2.088	11.167	21.167	7.791	3.746	1.264	0.256	-0.221	-0.441
	0.810	0.680	0.890	0.530	0.510	0.570	0.820	0.730	0.600	0.580	0.630	0.680	0.690	0.570	0.460	0.530	0.520	0.490
	4142	4170	3622	2901	1339	602	693	714	931	1448	1790	1590	1096	569	435	243	150	119
-10.00	-38.331	-22.662	9.431	12.052	18.840	10.056	3.518	6.855	4.525	-8.801	0.716	12.243	7.515	1.027	1.505	2.160	4.082	3.554
	0.620	0.510	0.610	0.490	0.500	0.690	0.750	0.770	0.640	0.580	0.590	0.550	0.610	0.620	0.610	0.420	0.460	0.480
	5545	5576	4124	2443	716	761	586	570	485	1123	1577	1191	496	417	309	206	213	153
-20.00	5.172	-1.566	2.647	3.415	5.648	11.990	12.423	10.240	8.282	1.994	1.109	4.384	2.227	-0.955	4.150	5.615	8.873	7.966
	0.560	0.390	0.670	0.590	0.560	0.590	0.580	0.730	0.690	0.540	0.550	0.580	0.550	0.460	0.470	0.490	0.450	0.480
	3954	3456	1836	847	598	852	628	518	304	637	969	737	292	409	375	307	275	233
-30.00	9.293	5.212	1.930	3.570	3.976	6.774	13.504	15.439	11.803	8.928	6.733	4.994	2.398	-2.293	2.492	6.356	1.407	14.291
	0.510	0.450	0.440	0.590	0.660	0.840	0.750	0.560	0.540	0.530	0.500	0.500	0.600	0.550	0.440	0.500	0.430	0.480
	1139	643	175	139	185	397	381	399	322	197	174	196	284	770	800	689	788	826
-40.00	0.553	5.400	3.816	3.179	3.384	3.220	4.531	7.615	8.871	8.482	8.521	8.723	5.777	0.358	-4.979	-9.075	-7.050	2.959
	0.480	0.440	0.510	0.510	0.530	0.610	0.740	0.730	0.580	0.570	0.520	0.440	0.370	0.420	0.420	0.410	0.430	0.460
	619	387	37	66	74	100	157	203	170	49	148	313	417	697	774	747	828	825
-50.00	-2.216	1.218	3.284	3.509	3.601	3.756	3.877	4.410	5.396	6.534	7.647	9.332	8.799	8.086	4.401	0.170	-2.418	-1.458
	0.400	0.430	0.430	0.500	0.510	0.510	0.530	0.570	0.590	0.540	0.500	0.480	0.450	0.390	0.400	0.370	0.400	0.410
	239	123	19	24	41	29	28	35	37	50	178	284	296	331	321	235	217	172
-60.00	0.479	0.663	1.704	2.827	3.320	3.632	3.947	4.227	4.481	4.955	5.814	6.567	7.466	7.771	7.939	6.448	3.972	1.821
	0.440	0.430	0.440	0.440	0.450	0.470	0.500	0.530	0.540	0.550	0.520	0.470	0.440	0.430	0.410	0.400	0.410	0.440
	103	18	11	13	13	10	8	11	46	61	142	178	126	137	139	137	98	54
-70.00	3.031	2.255	1.976	2.178	2.607	2.960	3.705	4.672	4.996	4.831	4.802	5.157	5.657	6.263	6.645	7.016	6.487	5.035
	0.340	0.340	0.330	0.340	0.360	0.370	0.400	0.440	0.470	0.460	0.460	0.450	0.430	0.420	0.450	0.470	0.510	0.520
	68	12	11	21	21	31	32	32	29	39	40	29	29	73	99	116	129	124
-80.00	4.124	4.816	5.352	4.604	3.254	2.292	2.605	11.105	11.896	6.304	4.438	3.913	4.208	4.142	3.952	3.471	5.834	3.258
	0.320	0.190	0.200	0.160	0.280	0.390	0.390	0.530	0.640	0.170	0.150	0.150	0.190	0.280	0.590	1.190	1.060	1.860
	47	41	35	51	81	110	219	200	147	88	7	10	19	36	54	81	122	125

Depth = 1559 km

	0.00	10.00	20.00	30.00	40.00	50.00	60.00	70.00	80.00	90.00	100.00	110.00	120.00	130.00	140.00	150.00	160.00	170.00
80.00	9.663	-6.521	-16.577	4.514	23.257	-16.148	-60.794	-63.407	-57.322	-52.493	-44.556	3.372	33.354	5.210	-11.933	34.117	34.280	12.703
	0.730	1.370	0.900	1.570	0.900	1.090	1.190	1.250	1.270	1.630	1.280	1.520	1.230	1.960	0.710	1.070	1.660	1.250
	951	900	2703	5017	6325	7185	7679	7975	7722	7367	6527	5329	3736	2022	1084	819	759	906
70.00	-5.973	0.849	-3.539	-10.723	-3.851	8.952	-3.427	-44.867	-56.012	-56.579	-55.024	-51.598	-30.806	-1.501	1.208	-2.638	17.511	26.317
	1.280	0.920	0.930	1.060	1.220	1.160	1.150	1.220	1.360	1.500	1.460	1.370	1.310	1.040	1.360	1.000	0.960	1.210
	1828	2229	5145	9821	12841	14877	16043	16144	15089	13631	12600	11723	10805	9696	6273	4150	3298	2972
60.00	-20.159	-13.251	-6.080	-6.933	-13.485	-8.008	5.572	-2.843	-31.240	-48.216	-50.563	-51.136	-51.388	-42.834	-17.229	-5.095	14.631	29.454
	0.990	1.010	0.650	0.750	0.730	0.880	0.940	0.880	0.810	0.860	0.790	0.900	1.110	1.150	0.780	0.970	0.930	0.870
	1610	2039	4514	8222	10171	12531	13504	12937	11692	10079	9479	10249	11381	12882	13419	6881	6784	7999
50.00	-7.569	-11.185	-9.942	-9.777	-14.903	-30.297	-19.304	-7.493	-15.654	-28.062	-33.216	-27.477	-22.225	-29.870	-22.481	-6.327	9.196	33.736
	0.550	0.550	0.610	0.590	0.550	0.790	0.770	0.770	0.750	0.560	0.690	0.790	0.990	0.880	0.880	1.010	0.720	0.770
	320	342	826	1958	3217	5319	6194	6507	5755	3758	2214	2570	7541	14623	15899	6972	7350	8962
40.00	-2.381	-4.938	-5.771	-10.603	-17.438	-13.791	-20.853	-10.664	-14.813	-42.441	-51.283	-37.627	-0.456	8.719	-19.072	-14.039	-8.527	-4.542
	0.270	0.350	0.430	0.450	0.540	0.560	0.720	0.690	0.700	0.660	0.680	0.830	0.900	0.930	0.910	0.690	0.710	0.590
	104	177	576	1359	2315	3358	4345	4809	4294	3236	2614	3662	5219	9341	9215	4890	4645	3898
30.00	-5.812	-8.658	-5.371	-4.201	-20.648	-30.645	-22.285	-9.212	-8.959	-29.033	-47.410	-51.984	-10.827	21.123	22.579	-14.569	-3.857	8.506
	0.270	0.220	0.360	0.440	0.510	0.580	0.560	0.540	0.490	0.550	0.700	0.900	0.930	0.800	0.820	0.850	0.690	0.580
	108	213	534	803	1124	1677	2320	3265	3811	3252	3153	4660	5968	6680	6421	5105	3521	2258
20.00	-8.154	-9.950	-8.944	0.217	1.703	-14.585	-44.467	-25.199	2.537	-18.209	-34.933	-22.378	-9.037	22.225	37.042	20.302	-16.763	8.635
	0.400	0.260	0.300	0.450	0.510	0.570	0.600	0.480	0.490	0.400	0.660	0.740	0.810	0.820	0.790	0.900	0.600	0.610
	164	238	442	662	639	724	1180	1837	2407	2812	2606	4100	5214	5852	6720	6261	4129	2645
10.00	-5.634	-4.244	-5.694	0.415	2.333	1.590	-14.038	-38.822	-23.264	-15.100	-28.007	-32.370	-19.207	-5.477	24.824	18.587	-20.680	-37.010
	0.410	0.320	0.370	0.550	0.580	0.640	0.690	0.580	0.410	0.330	0.430	0.570	0.590	0.720	0.750	0.940	0.930	0.890
	156	198	395	486	697	678	760	945	1772	2159	2200	3448	4950	6042	7115	6495	4672	3079
0.00	-0.574	0.235	2.307	2.729	-1.287	-4.331	-1.240	-8.021	-13.504	-11.573	-12.489	-27.283	-25.710	4.590	10.165	-0.375	-13.664	-59.571
	0.490	0.520	0.490	0.580	0.630	0.550	0.590	0.490	0.370	0.320	0.340	0.380	0.520	0.640	0.730	0.760	0.820	1.070
	126	142	287	532	631	730	735	622	539	680	1038	2106	3760	5394	6690	6417	6212	4505
-10.00	2.754	2.334	3.103	3.037	-3.604	-5.362	-9.892	-11.070	-5.108	-5.186	-7.617	-4.936	1.523	24.819	31.037	17.191	4.844	1.706
	0.480	0.500	0.510	0.640	0.630	0.610	0.500	0.370	0.370	0.370	0.260	0.420	0.360	0.500	0.640	0.680	0.570	0.880
	145	143	205	410	536	691	608	497	497	451	446	1024	2060	3594	4200	4930	6078	5358
-20.00	4.768	3.369	1.798	2.025	0.398	-6.615	-10.594	-8.161	-6.202	-3.195	-2.236	1.493	13.356	19.728	8.730	7.414	1.494	6.752
	0.520	0.530	0.560	0.560	0.650	0.530	0.480	0.480	0.460	0.390	0.350	0.460	0.420	0.420	0.380	0.560	0.620	0.630
	134	110	120	241	489	615	582	514	422	400	406	680	1473	2438	2532	2826	3504	4079
-30.00	9.356	4.214	2.828	2.159	0.324	-2.683	-4.015	-5.192	-3.555	-1.528	-0.607	2.322	2.997	11.018	5.987	-6.923	-13.423	-2.408
	0.520	0.580	0.610	0.620	0.570	0.570	0.540	0.530	0.500	0.360	0.390	0.420	0.460	0.440	0.360	0.330	0.520	0.730
	566	174	43	46	168	351	386	326	234	195	220	388	785	1142	1306	1515	1679	1507
-40.00	8.803	6.089	4.045	3.368	3.126	2.204	0.468	-0.467	-0.646	-0.966	-1.276	-1.363	-0.601	2.598	3.546	-0.837	-7.194	-12.243
	0.520	0.600	0.630	0.600	0.560	0.530	0.520	0.500	0.510	0.510	0.300	0.300	0.290	0.340	0.410	0.350	0.360	0.420
	549	162	22	27	60	66	62	52	49	55	132	234	249	313	314	362	450	525
-50.00	2.116	4.432	4.343	3.983	4.115	4.520	4.071	3.261	2.551	0.915	-1.154	-1.593	-2.661	0.891	2.461	2.370	-0.481	-4.275
	0.430	0.500	0.580	0.610	0.570	0.550	0.560	0.540	0.460	0.390	0.350	0.340	0.350	0.350	0.370	0.410	0.420	0.420
	83	25	15	16	26	38	52	87	167	223	192	241	272	281	248	126	101	192
-60.00	1.056	1.702	2.853	3.486	3.988	4.470	4.858	4.885	5.004	3.848	2.066	1.268	-1.165	0.173	2.276	3.203	2.862	1.315
	0.460	0.440	0.450	0.510	0.550	0.540	0.510	0.520	0.510	0.470	0.410	0.390	0.400	0.410	0.420	0.420	0.420	0.440
	41	35	31	27	43	62	76	167	248	347	363	414	513	507	409	233	199	147
-70.00	3.432	2.243	1.949	2.421	3.075	3.821	4.348	4.672	4.826	4.953	4.494	3.527	2.791	1.469	2.983	5.183	4.947	4.163
	0.460	0.420	0.410	0.430	0.470	0.470	0.460	0.460	0.450	0.440	0.440	0.410	0.380	0.420	0.430	0.380	0.340	0.360
	114	111	103	91	77	63	63	100	191	243	299	348	462	651	805	616	452	126
-80.00	3.655	2.779	2.616	2.905	3.681	5.414	6.028	5.222	5.085	5.296	5.558	6.602	5.960	2.993	7.885	34.570	13.350	6.961
	0.520	0.170	0.070	0.410	0.680	0.420	0.050	0.330	0.420	0.110	0.360	0.540	0.380	0.440	1.190	0.430	0.390	0.210
	103	98	103	84	84	65	64	43	35	34	78	118	263	528	772	623	405	64

Depth = 1821 km

	-180.00	-170.00	-160.00	-150.00	-140.00	-130.00	-120.00	-110.00	-100.00	-90.00	-80.00	-70.00	-60.00	-50.00	-40.00	-30.00	-20.00	-10.00
80.00	10.088	-7.319	-4.783	3.358	-22.909	-51.055	-51.343	-4.644	10.214	-4.635	-10.679	-12.446	-18.815	-33.422	-46.181	-48.004	-33.199	-1.760
	1.000	2.470	2.400	1.430	1.290	1.080	0.920	1.250	1.020	1.350	1.440	1.070	1.020	0.980	1.420	1.970	1.760	0.790
	839	867	1046	1924	2267	2354	2186	2244	2459	2750	3102	3161	3139	3011	2828	2551	2250	1308
70.00	15.255	11.674	2.411	-0.556	2.645	-9.026	-37.482	-45.173	-27.944	-9.243	-6.962	-8.349	-9.662	-13.155	-21.460	-35.395	-42.080	-37.686
	1.370	1.470	1.740	1.410	1.460	1.290	1.460	1.360	1.150	1.220	1.270	1.470	1.440	1.230	1.270	1.220	1.540	1.420
	4762	3751	3493	2882	2814	2582	2208	2051	2121	1945	2066	2269	2427	2828	2876	2590	2329	1543
60.00	-4.084	0.073	12.915	16.150	16.736	14.330	2.446	-18.782	-32.223	-25.361	-12.348	-4.233	-2.875	-2.809	-4.125	-7.080	-13.291	-20.316
	1.180	0.990	0.830	1.100	0.970	0.880	0.840	0.920	0.770	0.760	0.940	0.790	0.860	0.880	1.040	0.900	0.830	1.130
	6970	5758	5095	3854	2728	1635	1401	1509	1636	1405	1347	1388	1362	1318	897	568	725	652
50.00	-46.697	-41.998	-13.968	17.678	21.261	5.473	3.336	-3.070	-7.575	-9.632	-6.914	10.622	16.850	15.059	11.601	8.658	6.217	3.274
	1.020	0.750	0.840	0.830	0.670	0.880	0.640	0.860	0.840	0.890	0.820	0.710	0.500	0.430	0.470	0.530	0.690	0.680
	7474	5829	3390	2614	1882	1190	1203	1303	1420	1299	1320	1761	2122	2500	2030	582	123	112
40.00	-47.966	-41.054	-17.074	1.706	-1.208	-13.922	-15.500	-7.490	-1.956	-4.032	-0.520	12.551	41.179	44.825	29.344	17.069	10.089	6.920
	1.170	0.660	0.610	0.640	0.570	0.640	0.700	0.810	0.940	0.890	0.880	0.940	0.770	0.540	0.520	0.510	0.530	0.520
	2965	2731	1911	1340	860	385	520	646	779	1242	1822	2308	2816	3338	2944	1423	122	40
30.00	-9.986	-0.436	-3.987	-11.498	-14.220	-32.576	-38.486	-20.356	-10.115	-0.358	3.486	14.779	33.429	39.643	34.363	19.039	6.507	1.094
	1.030	0.780	0.560	0.460	0.550	0.550	0.830	0.910	0.970	0.880	0.660	0.610	0.590	0.650	0.530	0.530	0.550	0.550
	2308	2135	1493	811	604	308	212	231	481	1209	1896	2497	3290	2753	1980	1020	126	39
20.00	-16.453	37.749	-2.875	-19.333	-24.470	-47.010	-47.143	-23.579	-5.682	1.194	6.945	8.293	9.378	26.191	25.447	13.723	2.459	-6.704
	0.860	1.100	0.780	0.460	0.530	0.740	0.850	1.060	1.010	0.840	0.650	0.490	0.550	0.470	0.370	0.440	0.510	0.490
	2130	2247	2164	1893	1346	523	184	196	338	450	565	1447	1892	1628	1094	290	74	60
10.00	9.030	18.036	6.673	-34.928	-33.250	-43.146	-38.788	-15.343	4.788	12.954	11.464	12.282	9.459	10.979	12.280	7.018	-1.218	-1.989
	0.950	0.970	0.880	0.660	0.550	0.650	0.690	0.840	0.970	0.820	0.640	0.500	0.420	0.360	0.320	0.250	0.340	0.430
	2496	2600	3035	2234	1359	610	400	330	511	619	519	883	1139	790	293	147	65	74
0.00	35.735	53.125	-12.147	-39.996	-27.282	-20.788	-7.473	2.904	9.593	18.910	14.076	11.902	6.189	3.305	0.397	-1.218	1.491	2.894
	1.010	0.860	0.750	0.590	0.710	0.690	0.520	0.560	0.650	0.700	0.650	0.530	0.480	0.450	0.430	0.380	0.330	0.450
	3366	2837	2753	1906	1138	577	485	389	408	644	648	258	218	186	144	52	43	64
-10.00	44.458	58.221	0.494	-30.302	-15.047	6.403	7.284	10.860	12.399	13.785	13.215	6.316	3.126	-2.171	-6.999	0.038	3.332	4.918
	1.050	0.760	0.660	0.740	0.550	0.700	0.670	0.470	0.690	0.730	0.640	0.610	0.580	0.530	0.530	0.540	0.510	0.520
	3522	3002	2320	1085	550	546	427	316	194	475	526	215	108	101	77	46	39	56
-20.00	20.209	40.693	24.290	-8.762	-7.276	6.531	16.970	16.572	14.178	12.560	8.920	2.278	-1.034	-2.473	1.910	6.213	7.510	6.631
	0.680	0.640	0.490	0.530	0.530	0.510	0.670	0.580	0.650	0.810	0.810	0.730	0.680	0.670	0.600	0.680	0.740	0.710
	1852	1404	1038	350	288	386	284	211	173	201	206	125	97	109	110	74	75	64
-30.00	13.151	13.787	11.250	5.461	1.328	5.837	12.351	17.714	17.620	15.817	11.037	4.331	-3.345	-0.535	4.353	11.154	12.883	9.675
	0.590	0.600	0.680	0.750	0.730	0.640	0.670	0.760	0.650	0.720	0.850	0.880	0.840	0.760	0.690	0.670	0.760	0.830
	750	523	80	73	107	190	202	185	157	104	95	100	88	148	259	243	251	226
-40.00	10.677	13.246	7.472	6.282	6.360	6.682	7.958	11.737	14.533	15.840	14.810	11.610	6.834	2.855	5.457	9.533	12.105	11.157
	0.670	0.750	0.720	0.700	0.730	0.720	0.740	0.730	0.750	0.720	0.780	0.760	0.780	0.810	0.800	0.710	0.700	0.730
	690	461	33	45	68	75	86	92	59	30	101	179	161	168	300	290	300	280
-50.00	10.910	12.131	11.718	9.625	9.134	9.556	10.193	11.246	13.037	15.447	17.642	19.017	14.928	12.063	10.427	9.960	10.276	10.513
	0.590	0.650	0.710	0.760	0.780	0.780	0.770	0.810	0.830	0.770	0.710	0.660	0.620	0.620	0.650	0.670	0.680	0.700
	351	172	11	12	18	38	56	65	53	51	185	232	186	128	181	133	113	78
-60.00	14.018	12.859	12.593	12.233	11.307	10.761	10.750	11.156	12.203	14.090	16.249	18.581	18.609	17.118	15.929	13.777	11.916	10.915
	0.550	0.550	0.580	0.650	0.710	0.750	0.770	0.780	0.800	0.810	0.780	0.730	0.660	0.600	0.570	0.590	0.630	0.660
	142	47	8	11	13	12	21	37	45	52	176	206	140	104	100	92	75	38
-70.00	15.831	14.375	13.388	12.895	12.476	11.667	10.848	11.090	12.585	13.973	14.729	15.531	16.628	17.014	16.622	15.920	14.330	12.641
	0.460	0.430	0.420	0.440	0.460	0.510	0.570	0.630	0.680	0.680	0.630	0.650	0.680	0.680	0.620	0.540	0.540	0.550
	88	20	20	22	28	21	21	19	26	82	144	136	67	69	97	81	88	72
-80.00	8.260	9.264	10.993	11.160	11.600	11.144	7.298	7.328	20.094	31.108	23.689	14.494	12.658	12.589	12.447	13.735	11.741	9.220
	0.870	0.570	0.290	0.240	0.300	0.210	0.470	0.450	0.860	0.770	0.500	0.250	0.490	0.760	0.800	0.300	0.200	0.720
	41	40	42	40	34	78	98	207	190	125	90	76	58	60	61	67	89	76

Depth = 1821 km

	0.00	10.00	20.00	30.00	40.00	50.00	60.00	70.00	80.00	90.00	100.00	110.00	120.00	130.00	140.00	150.00	160.00	170.00
80.00	1.204	-1.589	-5.021	-8.627	-30.692	26.573	43.816	-12.386	-47.637	-49.236	-52.805	-52.347	-51.171	-42.853	-19.202	45.923	51.794	9.253
	0.700	0.750	0.970	1.390	2.090	2.780	2.150	2.800	1.430	2.570	2.070	1.890	1.880	1.500	2.420	1.900	2.710	1.160
	541	356	1313	2376	3482	4663	6137	7463	8205	8307	7787	6841	5502	3999	3013	1961	1292	899
70.00	-20.521	-11.459	-8.348	-8.645	-10.844	-21.980	0.784	20.661	2.378	-29.105	-42.873	-48.396	-50.477	-51.288	-48.405	-39.503	2.123	26.017
	1.320	1.390	1.220	1.180	1.340	1.690	2.120	2.000	2.060	1.640	1.780	1.540	1.690	1.720	1.590	1.550	1.670	1.650
	653	516	1539	3319	5552	7694	10363	12749	14261	14893	14090	13288	12168	10625	5841	4041	3508	3867
60.00	-24.236	-23.624	-19.947	-16.459	-17.134	-22.993	-29.669	-13.518	-0.927	-11.173	-27.239	-39.706	-43.988	-44.998	-46.838	-44.510	-30.952	-18.456
	1.080	1.190	0.800	0.840	0.950	1.030	1.130	1.300	1.410	1.340	1.200	1.170	1.150	1.080	1.230	1.210	1.190	0.970
	386	323	706	1680	2890	4808	7790	9498	10738	11563	11720	11830	12883	13178	9036	4610	4883	5852
50.00	-1.329	-6.705	-10.012	-11.241	-11.440	-20.669	-44.653	-54.194	-51.720	-43.907	-29.470	-17.236	-19.147	-34.813	-27.202	-23.843	-27.939	-43.298
	0.740	0.780	0.770	0.700	0.710	0.800	0.630	0.980	1.120	0.930	0.770	1.050	0.930	1.450	1.070	0.840	1.060	1.050
	76	78	102	321	975	1829	3267	4450	4767	4797	5062	5727	9243	10151	8045	3463	4211	6294
40.00	5.883	2.842	-0.271	-2.907	-4.949	9.035	9.145	-31.648	-54.553	-59.146	-58.061	-40.227	-0.399	-2.913	-21.896	-14.791	-22.627	-47.121
	0.470	0.540	0.570	0.590	0.640	0.770	0.780	0.710	0.760	1.020	1.060	1.280	1.240	1.030	1.150	1.040	0.540	0.820
	36	42	63	317	964	1814	2498	3359	3327	3200	3283	4029	5360	7070	6435	2887	3351	3270
30.00	0.826	0.543	-1.943	-2.006	-9.137	-16.574	28.476	33.688	-8.179	-37.022	-51.740	-48.778	-12.570	8.918	18.295	-2.192	-11.600	-15.145
	0.480	0.540	0.570	0.520	0.550	0.580	0.660	0.660	0.770	0.910	1.080	1.090	1.190	0.940	0.960	0.900	0.970	0.860
	52	55	73	322	671	1192	1594	2212	2472	1901	2796	3602	4131	3648	3834	3361	2777	2474
20.00	-4.603	-2.615	-4.790	0.988	3.169	-11.228	-18.862	19.419	12.580	-14.249	-26.113	-42.451	-32.000	-10.952	26.966	39.851	38.432	13.682
	0.500	0.540	0.560	0.580	0.540	0.500	0.390	0.430	0.520	0.860	1.120	1.110	1.000	0.740	0.730	0.790	0.890	0.860
	68	60	84	282	444	548	1051	1447	1685	1195	1647	2157	2580	3023	3914	3900	3161	2639
10.00	-1.202	0.338	1.993	3.871	8.849	8.888	0.012	2.007	6.212	-9.909	-27.262	-42.908	-31.879	-15.538	-1.114	3.772	32.890	13.897
	0.410	0.560	0.670	0.580	0.560	0.570	0.560	0.540	0.550	0.690	0.860	0.940	0.950	0.800	0.710	1.080	1.020	1.120
	68	80	87	160	367	421	500	536	915	952	1059	1497	2050	3216	4130	4045	3467	2802
0.00	4.383	4.196	4.652	7.996	9.913	10.671	9.027	7.462	5.185	-1.911	-11.113	-29.084	-30.635	18.386	18.587	-12.513	2.538	39.246
	0.520	0.620	0.760	0.740	0.600	0.560	0.560	0.630	0.670	0.590	0.550	0.710	0.780	0.820	0.720	0.780	1.020	1.200
	74	58	53	77	187	286	312	158	178	281	352	837	1723	2784	3320	3379	3516	2913
-10.00	5.814	4.788	5.939	8.596	11.302	9.572	6.744	7.611	7.499	3.945	-1.497	-5.714	-7.831	1.797	16.999	-5.192	-4.742	42.934
	0.590	0.680	0.860	0.850	0.710	0.590	0.500	0.620	0.710	0.690	0.460	0.350	0.520	0.640	0.700	0.470	0.550	0.970
	71	56	58	38	63	128	125	154	169	217	249	511	1157	2135	2550	2483	2920	3066
-20.00	5.282	5.386	6.646	8.590	9.280	7.372	4.696	3.441	3.277	3.946	3.675	6.248	5.558	0.319	-17.172	-19.674	-26.719	-9.752
	0.650	0.740	0.810	0.810	0.730	0.620	0.590	0.550	0.620	0.600	0.500	0.400	0.400	0.580	0.550	0.610	0.710	0.510
	41	50	48	23	30	134	181	217	200	219	270	407	866	1325	1402	1551	1816	2078
-30.00	5.651	6.531	7.579	7.866	8.745	6.236	2.625	2.388	3.272	4.802	5.606	13.979	9.714	6.466	-6.794	-17.877	-23.708	-12.552
	0.830	0.790	0.770	0.750	0.650	0.610	0.570	0.560	0.520	0.580	0.530	0.490	0.530	0.510	0.500	0.530	0.570	0.640
	29	23	17	18	29	84	113	162	176	161	157	287	469	735	763	875	1019	915
-40.00	8.797	7.086	7.564	8.128	7.958	8.198	7.981	7.212	8.665	8.682	6.567	8.734	12.248	11.628	10.276	4.677	0.557	-1.763
	0.790	0.810	0.830	0.840	0.760	0.680	0.690	0.620	0.570	0.570	0.590	0.570	0.580	0.610	0.680	0.620	0.480	0.610
	29	14	12	22	28	40	39	44	54	78	121	192	270	343	376	451	587	572
-50.00	9.696	8.228	6.896	6.980	7.536	8.141	8.803	9.638	11.485	14.584	12.511	11.756	6.784	10.133	14.446	15.001	12.882	9.220
	0.750	0.780	0.760	0.730	0.710	0.690	0.720	0.750	0.710	0.640	0.570	0.550	0.580	0.590	0.610	0.610	0.580	0.570
	10	8	12	18	21	22	33	37	146	197	238	242	295	361	292	237	217	302
-60.00	10.285	9.302	7.987	6.650	6.238	6.723	7.427	8.475	9.889	12.003	14.102	13.661	11.348	9.996	12.246	15.680	16.365	16.363
	0.660	0.690	0.720	0.730	0.710	0.700	0.680	0.680	0.700	0.690	0.640	0.590	0.560	0.550	0.560	0.600	0.600	0.590
	18	14	18	21	43	56	68	67	179	235	290	365	443	654	617	693	551	403
-70.00	11.480	10.525	9.397	8.195	7.058	6.416	6.634	7.315	8.277	9.562	11.138	12.359	12.050	11.496	12.791	16.144	18.104	16.967
	0.530	0.520	0.550	0.610	0.680	0.720	0.720	0.680	0.620	0.600	0.590	0.570	0.570	0.530	0.480	0.450	0.450	0.480
	39	40	59	60	72	71	79	69	65	92	161	267	384	561	645	765	624	434
-80.00	9.334	9.749	7.377	6.372	7.122	8.046	8.819	10.025	10.714	11.955	13.072	13.358	9.064	2.601	16.147	47.254	40.428	19.796
	0.100	0.340	0.090	0.220	0.840	1.050	1.010	1.000	0.430	0.330	0.480	0.590	0.590	1.620	0.930	1.040	0.480	0.350
	35	38	52	74	80	77	79	68	56	35	62	84	200	351	601	620	416	97

Depth = 2104 km

	-180.00	-170.00	-160.00	-150.00	-140.00	-130.00	-120.00	-110.00	-100.00	-90.00	-80.00	-70.00	-60.00	-50.00	-40.00	-30.00	-20.00	-10.00
80.00	5.647	3.132	-6.897	-13.569	-13.127	-8.614	-4.477	-4.072	-4.631	-3.227	-3.238	-4.272	-5.470	-4.109	-0.841	0.767	0.644	-0.212
	0.340	0.250	0.200	0.410	0.730	0.530	0.360	0.420	0.330	0.120	0.080	0.080	0.080	0.080	0.170	0.140	0.160	0.240
	956	1475	2067	2659	2665	2619	2514	2427	2362	2273	2246	2142	2054	1934	1583	1099	440	178
70.00	10.374	8.376	6.040	-0.195	-6.485	-9.173	-8.296	-5.964	-4.700	-4.340	-3.492	-3.110	-3.437	-4.197	-3.949	-2.326	-0.819	-0.160
	0.500	0.410	0.330	0.270	0.140	0.370	0.420	0.380	0.390	0.360	0.250	0.160	0.130	0.130	0.130	0.120	0.130	0.150
	3875	3160	3057	3141	2900	2388	1913	1336	1041	974	1026	1060	1067	1192	1100	740	329	161
60.00	12.694	11.909	10.110	6.922	2.606	-1.601	-4.080	-4.527	-3.972	-3.270	-2.644	-2.040	-1.775	-1.879	-2.187	-2.229	-1.684	-0.972
	0.200	0.270	0.280	0.270	0.240	0.120	0.110	0.200	0.250	0.270	0.280	0.240	0.180	0.140	0.110	0.090	0.060	0.060
	4578	3867	3265	2278	1230	686	580	558	529	558	519	410	286	134	44	34	44	75
50.00	10.427	11.396	9.252	5.204	1.984	0.909	0.123	-0.645	-0.982	-0.545	0.110	0.295	0.117	-0.033	-0.135	-0.304	-0.478	-0.496
	0.300	0.160	0.100	0.150	0.180	0.190	0.160	0.080	0.060	0.100	0.140	0.170	0.170	0.160	0.140	0.120	0.100	0.070
	2695	1809	1371	907	509	333	293	379	429	403	383	311	189	54	12	16	16	18
40.00	5.048	5.474	3.339	-1.001	-3.009	-1.867	-0.460	0.378	0.393	0.516	1.300	1.212	0.967	0.685	0.501	0.413	0.327	0.183
	0.340	0.250	0.180	0.110	0.120	0.140	0.160	0.160	0.110	0.070	0.040	0.050	0.080	0.110	0.110	0.110	0.100	0.080
	1806	1265	786	419	156	99	41	83	144	263	428	401	209	28	16	16	18	18
30.00	5.549	3.092	-0.024	-2.274	-4.510	-4.618	-2.272	-0.465	0.365	0.577	0.690	0.864	0.808	0.538	0.201	-0.004	-0.007	0.070
	0.220	0.180	0.130	0.130	0.130	0.140	0.150	0.150	0.130	0.100	0.070	0.040	0.040	0.060	0.070	0.070	0.080	0.070
	1615	1117	519	242	138	100	57	61	103	216	313	207	375	359	129	19	15	17
20.00	8.394	7.187	-0.301	-3.457	-5.301	-5.097	-2.771	-1.028	-0.084	0.414	0.533	0.431	0.576	0.504	0.074	-0.524	-0.860	-0.718
	0.260	0.170	0.110	0.130	0.170	0.170	0.160	0.130	0.110	0.090	0.070	0.060	0.060	0.060	0.060	0.060	0.070	0.070
	1313	1159	714	295	197	134	80	39	39	44	37	108	374	366	122	22	29	43
10.00	9.486	7.210	-0.344	-5.892	-8.486	-4.763	-1.879	-0.851	-0.520	-0.045	0.345	0.342	0.178	0.246	-0.261	-0.796	-1.415	-1.155
	0.210	0.200	0.130	0.150	0.190	0.200	0.170	0.140	0.100	0.080	0.070	0.070	0.070	0.070	0.070	0.070	0.070	0.070
	1279	1257	838	366	220	210	199	119	68	70	36	45	249	157	37	37	43	50
0.00	3.578	4.825	-1.026	-7.338	-7.306	-2.065	1.318	0.507	-0.333	-0.563	-0.194	0.155	0.003	-0.261	-0.756	-1.673	-1.217	-0.586
	0.120	0.160	0.160	0.170	0.190	0.200	0.180	0.160	0.120	0.100	0.090	0.090	0.090	0.090	0.090	0.080	0.070	0.070
	1135	1193	705	367	352	363	287	186	80	63	54	23	25	41	46	45	43	34
-10.00	6.164	7.535	1.300	-3.541	-3.810	-0.642	1.194	1.223	0.502	-0.209	-0.655	-0.350	-0.185	-0.696	-1.391	-1.284	-0.748	-0.214
	0.110	0.100	0.140	0.150	0.170	0.170	0.170	0.160	0.130	0.110	0.100	0.090	0.100	0.100	0.100	0.100	0.090	0.080
	1166	1137	852	111	309	308	270	145	31	44	45	31	28	34	38	35	21	18
-20.00	2.992	5.806	2.665	-0.718	-1.317	-0.299	0.684	0.792	0.573	0.081	-0.570	-0.854	-0.349	-0.532	-0.640	-0.679	-0.230	0.160
	0.110	0.080	0.090	0.110	0.150	0.180	0.170	0.160	0.130	0.100	0.100	0.090	0.090	0.080	0.090	0.100	0.100	0.090
	884	782	678	38	40	115	97	99	87	36	29	30	37	38	35	23	17	16
-30.00	1.831	1.717	1.235	-0.220	-0.551	0.189	0.781	0.952	0.746	0.100	-0.416	-0.753	-0.539	-0.217	-0.126	0.049	0.225	0.460
	0.100	0.070	0.080	0.090	0.120	0.150	0.170	0.140	0.100	0.090	0.100	0.110	0.100	0.080	0.070	0.070	0.070	0.080
	493	338	46	41	56	131	118	106	92	32	48	42	36	22	15	16	14	15
-40.00	2.885	1.933	0.623	0.044	-0.135	0.206	0.544	0.922	0.910	0.491	-0.178	-0.557	-0.432	-0.101	0.070	0.268	0.442	0.594
	0.100	0.090	0.080	0.050	0.060	0.070	0.080	0.090	0.070	0.080	0.090	0.100	0.100	0.080	0.070	0.060	0.050	0.040
	638	408	37	38	65	67	82	71	47	23	74	92	51	45	18	9	9	10
-50.00	2.117	2.158	1.506	0.913	0.699	0.737	0.876	1.235	1.515	1.456	1.036	0.571	0.106	-0.122	0.144	0.313	0.494	0.653
	0.070	0.070	0.070	0.080	0.070	0.070	0.070	0.070	0.070	0.080	0.090	0.090	0.080	0.070	0.060	0.060	0.050	0.030
	540	335	16	19	29	44	70	77	60	50	166	201	77	42	38	19	10	12
-60.00	2.091	1.912	1.788	1.530	1.282	1.165	1.160	1.231	1.528	1.879	1.987	1.783	1.165	0.625	0.439	0.478	0.507	0.577
	0.070	0.060	0.060	0.070	0.070	0.080	0.080	0.080	0.080	0.090	0.100	0.100	0.100	0.090	0.070	0.060	0.050	0.040
	273	100	10	21	18	21	41	49	53	73	215	223	76	42	37	28	19	18
-70.00	1.710	1.755	1.696	1.623	1.494	1.348	1.212	1.132	1.230	1.671	2.097	2.121	1.831	1.403	0.994	0.738	0.635	0.598
	0.060	0.070	0.070	0.060	0.070	0.070	0.070	0.080	0.080	0.090	0.100	0.100	0.100	0.090	0.080	0.070	0.060	0.040
	153	27	24	34	36	42	38	36	94	151	174	177	59	20	26	20	18	21
-80.00	1.639	0.709	0.720	0.782	0.742	0.859	0.973	0.359	0.582	2.219	5.256	2.580	1.059	0.787	0.816	0.846	0.752	0.739
	0.070	0.070	0.050	0.040	0.050	0.020	0.030	0.060	0.070	0.190	0.270	0.150	0.050	0.030	0.070	0.110	0.100	0.120
	50	38	34	43	40	50	110	150	218	223	172	142	61	51	36	24	15	15

Depth = 2104 km

	0.00	10.00	20.00	30.00	40.00	50.00	60.00	70.00	80.00	90.00	100.00	110.00	120.00	130.00	140.00	150.00	160.00	170.00
80.00	-0.697	-1.905	-2.999	-2.497	-0.299	-0.187	1.281	-1.291	-5.117	-7.494	-5.853	-0.940	5.203	7.404	10.512	16.035	13.879	6.936
	0.240	0.090	0.080	0.090	0.140	0.280	0.290	0.700	1.630	1.790	1.240	1.020	0.930	0.510	0.160	1.470	0.920	0.460
	131	130	163	521	1164	1715	2303	2887	3280	3677	4066	4345	4673	4688	4150	3434	2688	1645
70.00	-0.241	-0.538	-1.321	-2.291	-2.584	-1.701	-1.103	0.056	-0.375	-2.364	-4.500	-4.833	-2.661	1.302	4.161	7.153	11.366	13.314
	0.200	0.220	0.170	0.120	0.110	0.120	0.190	0.230	0.290	0.870	1.240	1.190	1.070	0.980	0.750	0.390	0.490	0.600
	133	123	143	415	1019	1703	2530	3532	4778	5648	6101	6170	5236	4031	3951	3934	3235	3664
60.00	-0.536	-0.539	-0.881	-1.557	-2.316	-2.763	-2.726	-2.530	-0.941	0.673	0.674	-0.747	-2.294	-1.478	0.876	2.970	5.848	9.652
	0.060	0.100	0.140	0.130	0.110	0.080	0.090	0.120	0.150	0.110	0.350	0.660	0.790	0.820	0.810	0.720	0.540	0.140
	84	71	72	62	140	444	1265	2911	5255	6302	6807	6650	6160	5443	3110	2337	3078	4189
50.00	-0.458	-0.512	-0.692	-0.908	-1.223	-1.813	-2.843	-5.201	-8.456	-6.155	-0.520	4.137	4.095	-0.321	-2.078	0.229	2.556	7.940
	0.060	0.050	0.060	0.090	0.110	0.110	0.110	0.120	0.150	0.170	0.160	0.120	0.250	0.380	0.440	0.500	0.530	0.500
	23	34	47	42	41	59	135	966	2644	3894	4901	6220	6666	5953	3633	1304	1668	2172
40.00	0.026	-0.244	-0.501	-0.666	-0.680	-0.895	-1.557	-3.504	-9.641	-18.088	-12.205	-1.658	4.630	2.743	-2.921	-1.278	0.245	2.519
	0.070	0.050	0.040	0.040	0.070	0.100	0.120	0.140	0.150	0.180	0.190	0.180	0.140	0.110	0.140	0.190	0.280	0.360
	20	23	31	34	33	80	194	420	1309	2154	2752	3480	3705	3540	2242	840	1265	1857
30.00	-0.091	-0.401	-0.792	-0.869	-0.679	-0.371	-0.370	-1.106	-4.278	-9.511	-14.530	-8.084	-0.780	1.321	1.666	0.497	0.517	2.861
	0.070	0.060	0.060	0.050	0.050	0.070	0.100	0.120	0.150	0.180	0.200	0.200	0.190	0.170	0.150	0.120	0.190	0.250
	19	25	37	39	30	71	232	276	324	692	1698	2043	1108	936	1056	957	1279	1581
20.00	-0.548	-0.994	-1.263	-1.348	-0.770	-0.049	0.370	0.035	-1.778	-5.919	-8.233	-8.870	-3.258	-0.896	1.923	2.698	2.689	6.128
	0.070	0.070	0.070	0.070	0.080	0.080	0.100	0.120	0.160	0.200	0.240	0.260	0.250	0.220	0.180	0.160	0.170	0.280
	34	30	42	43	24	32	123	172	204	322	526	658	346	517	1184	1323	1273	1545
10.00	-0.613	-0.567	-0.739	-0.650	-0.370	0.154	0.531	0.549	-0.392	-3.214	-5.444	-6.750	-3.235	0.258	2.228	1.995	-1.069	2.354
	0.070	0.080	0.090	0.080	0.070	0.080	0.090	0.120	0.150	0.190	0.240	0.260	0.270	0.230	0.210	0.160	0.170	0.170
	41	29	21	27	23	19	24	41	72	220	355	467	399	826	1313	1316	932	1050
0.00	-0.234	-0.072	0.081	0.087	0.211	0.304	0.473	0.503	0.112	-1.229	-2.613	-5.586	-4.748	0.167	3.901	1.202	-2.702	1.442
	0.090	0.090	0.100	0.100	0.090	0.070	0.080	0.120	0.150	0.180	0.220	0.230	0.230	0.210	0.190	0.150	0.150	0.180
	35	25	16	18	19	25	28	36	63	144	193	346	541	1157	1396	1149	741	841
-10.00	0.141	0.265	0.429	0.506	0.507	0.497	0.329	0.229	-0.138	-0.573	-1.160	-2.542	-3.564	-3.472	-1.241	-0.664	-1.962	0.072
	0.090	0.110	0.120	0.120	0.110	0.090	0.080	0.090	0.130	0.160	0.190	0.200	0.200	0.180	0.150	0.120	0.110	0.170
	29	30	15	11	13	23	22	28	64	83	118	262	490	1041	1190	752	677	1084
-20.00	0.302	0.343	0.455	0.563	0.514	0.371	0.299	-0.022	-0.383	-0.275	-0.375	-0.633	-1.535	-3.094	-3.644	-3.302	-2.891	-0.848
	0.090	0.090	0.110	0.110	0.110	0.110	0.100	0.100	0.110	0.130	0.160	0.180	0.170	0.150	0.130	0.100	0.120	0.110
	20	19	8	11	11	9	20	51	66	74	107	218	347	508	625	697	591	906
-30.00	0.479	0.489	0.452	0.497	0.511	0.411	0.244	0.193	0.019	0.118	0.223	1.065	0.437	-1.394	-2.946	-1.911	-2.034	-0.254
	0.080	0.080	0.090	0.090	0.100	0.100	0.100	0.100	0.090	0.100	0.110	0.130	0.150	0.140	0.110	0.090	0.070	0.120
	17	17	9	14	10	10	15	49	74	63	110	195	321	455	471	553	626	506
-40.00	0.594	0.554	0.603	0.600	0.580	0.398	0.402	0.448	0.612	0.843	0.963	0.830	0.754	0.868	0.568	0.456	0.346	0.356
	0.040	0.060	0.080	0.090	0.090	0.100	0.110	0.110	0.090	0.080	0.080	0.080	0.090	0.110	0.110	0.090	0.070	0.110
	10	6	11	14	13	12	8	22	37	90	139	214	318	390	394	424	615	534
-50.00	0.679	0.644	0.612	0.614	0.608	0.559	0.479	0.515	0.597	0.921	1.189	1.203	0.244	-0.037	0.871	1.321	1.565	1.749
	0.030	0.030	0.040	0.060	0.080	0.070	0.090	0.100	0.110	0.110	0.100	0.080	0.070	0.070	0.070	0.070	0.070	0.070
	7	6	10	14	19	17	21	30	64	160	193	208	241	372	521	492	485	483
-60.00	0.686	0.682	0.659	0.627	0.598	0.558	0.505	0.455	0.508	0.683	0.948	0.975	0.856	0.558	0.342	0.768	1.423	2.017
	0.000	0.020	0.030	0.040	0.050	0.050	0.060	0.070	0.080	0.100	0.100	0.090	0.090	0.080	0.070	0.060	0.070	0.070
	4	5	10	13	17	21	45	56	76	168	181	250	388	593	751	703	705	482
-70.00	0.606	0.653	0.663	0.639	0.606	0.572	0.519	0.483	0.484	0.534	0.641	0.756	0.699	0.617	0.640	0.789	1.426	1.511
	0.040	0.030	0.030	0.030	0.040	0.040	0.050	0.060	0.070	0.070	0.080	0.090	0.100	0.090	0.080	0.070	0.060	0.060
	14	15	12	14	27	50	64	65	63	58	67	136	305	453	544	690	623	466
-80.00	0.756	0.655	0.719	0.511	0.357	0.396	0.404	0.269	0.425	0.646	0.794	0.788	0.381	-0.884	0.692	1.711	4.439	6.521
	0.120	0.100	0.050	0.010	0.020	0.010	0.040	0.080	0.100	0.100	0.060	0.060	0.100	0.390	0.080	0.060	0.080	0.720
	18	22	25	36	46	63	59	60	52	54	75	74	110	110	82	195	215	141

Depth = 2407 km

	-180.00	-170.00	-160.00	-150.00	-140.00	-130.00	-120.00	-110.00	-100.00	-90.00	-80.00	-70.00	-60.00	-50.00	-40.00	-30.00	-20.00	-10.00
80.00	-54.012	-46.049	-39.921	5.017	45.996	29.098	10.525	2.252	8.562	17.387	18.659	17.219	11.340	4.957	0.560	-5.996	-9.179	-8.302
	2.370	1.860	1.910	1.890	1.200	0.880	1.500	1.050	0.760	0.910	0.760	0.590	0.740	0.890	0.870	0.930	0.970	0.880
	1418	1391	1578	1666	1697	1668	1589	1470	1310	1053	779	408	155	78	56	48	49	50
70.00	-52.370	-53.053	-49.919	-45.450	-32.873	1.131	13.156	11.155	6.766	7.735	12.302	15.076	15.784	13.387	9.176	5.215	0.496	-3.060
	1.440	1.980	1.710	1.660	1.610	1.530	1.400	1.480	1.450	1.370	1.370	1.310	1.180	1.160	1.270	1.330	1.330	1.460
	2890	2285	2000	1949	1819	1386	918	575	346	281	191	132	63	58	57	57	59	60
60.00	-29.407	-43.180	-46.979	-45.771	-41.556	-32.862	-13.096	1.493	7.460	8.362	9.651	12.235	14.384	15.357	14.651	12.666	10.524	8.202
	1.050	0.930	1.020	0.810	0.800	0.830	0.780	0.700	0.660	0.710	0.700	0.590	0.540	0.620	0.580	0.610	0.540	0.700
	2973	2240	1689	842	326	143	49	59	78	83	64	42	21	19	20	20	21	23
50.00	-35.468	-36.676	-41.524	-39.316	-32.375	-22.363	-10.915	-1.110	6.636	11.168	13.240	14.302	15.354	15.783	15.401	14.271	13.114	12.861
	0.900	0.850	0.870	0.890	0.860	0.780	0.620	0.550	0.530	0.470	0.460	0.420	0.400	0.380	0.430	0.390	0.380	0.430
	609	458	267	158	99	45	28	39	69	58	45	18	17	15	14	18	18	21
40.00	-40.957	-44.093	-48.527	-44.607	-29.978	-7.296	3.736	7.629	11.063	15.089	16.119	15.812	15.559	14.139	12.530	11.834	11.713	11.788
	1.350	0.930	1.240	1.010	1.030	1.040	0.850	0.570	0.450	0.380	0.380	0.420	0.410	0.410	0.420	0.410	0.360	0.420
	261	249	191	96	69	18	27	21	42	51	26	17	16	21	22	23	21	20
30.00	-43.634	-46.257	-46.387	-43.025	-38.480	-21.526	0.616	9.656	16.646	19.254	18.572	15.682	13.407	9.774	7.407	7.860	10.395	11.862
	1.720	0.940	0.900	1.100	1.020	0.940	0.860	0.820	0.650	0.430	0.350	0.400	0.420	0.410	0.440	0.410	0.320	0.290
	193	231	188	113	72	54	40	26	21	23	15	16	25	29	24	20	13	13
20.00	-45.585	-35.142	-33.766	-37.356	-32.934	-22.510	-4.948	8.038	15.400	21.845	21.323	18.032	11.632	8.492	6.182	6.582	6.512	8.416
	1.940	1.430	0.790	0.920	1.060	0.840	0.620	0.750	0.750	0.000	0.330	0.340	0.360	0.380	0.390	0.420	0.340	0.290
	199	289	212	91	81	62	45	26	11	2	5	13	25	34	24	18	18	23
10.00	-46.908	-38.689	-30.612	-28.521	-13.469	1.548	5.695	7.802	12.314	18.094	21.845	20.315	14.875	9.715	6.597	3.292	0.384	-0.206
	1.200	1.110	1.070	0.920	0.900	0.980	0.760	0.670	0.710	0.590	0.000	0.290	0.340	0.360	0.330	0.350	0.340	0.260
	294	313	227	95	84	51	46	34	20	11	2	9	19	18	17	28	31	29
0.00	-53.209	-43.667	-35.327	-30.890	-5.644	16.150	22.402	18.284	14.943	14.167	18.344	21.845	18.655	13.024	6.344	-2.438	-4.576	1.504
	1.280	0.970	0.800	0.850	0.800	0.680	0.620	0.490	0.640	0.770	0.590	0.000	0.300	0.330	0.300	0.300	0.420	0.280
	312	282	170	83	117	197	175	103	26	14	6	2	8	16	26	31	33	30
-10.00	-43.857	-29.566	-15.152	-9.966	-2.334	10.430	18.329	21.939	20.113	16.051	13.927	17.027	19.114	15.729	8.305	4.055	3.526	4.995
	0.960	1.040	0.990	0.880	0.870	0.740	0.580	0.530	0.520	0.910	0.940	0.560	0.320	0.260	0.270	0.210	0.270	0.310
	617	523	327	44	99	190	172	81	8	10	18	14	5	11	24	30	25	20
-20.00	-5.938	4.142	9.754	10.350	10.698	13.075	17.989	20.321	19.600	18.071	14.672	14.245	17.010	18.637	16.953	13.381	11.989	13.513
	1.000	1.010	1.150	0.980	1.040	0.740	0.690	0.620	0.480	0.500	0.930	0.740	0.480	0.340	0.290	0.370	0.290	0.230
	531	406	255	17	13	27	26	25	17	19	21	16	5	11	21	21	14	14
-30.00	29.940	22.436	15.490	12.454	11.118	11.965	14.163	16.109	14.289	13.749	14.764	13.672	16.303	19.390	20.336	19.742	18.073	17.194
	0.810	0.910	0.960	1.050	0.900	1.000	0.700	0.560	0.520	0.720	0.650	0.840	0.730	0.510	0.360	0.310	0.370	0.380
	341	207	31	31	37	42	40	31	19	20	25	21	6	6	9	10	13	12
-40.00	57.192	37.735	22.199	10.626	6.776	8.383	10.907	10.378	10.061	8.744	9.159	11.603	12.368	16.251	21.845	20.929	21.218	20.208
	1.000	1.010	1.030	1.010	0.990	0.990	0.820	0.860	0.630	0.500	0.580	0.710	0.850	0.820	0.000	0.290	0.270	0.330
	582	367	34	38	47	41	48	41	24	20	41	34	8	5	4	6	9	8
-50.00	53.657	46.697	33.459	23.215	15.275	12.021	10.829	12.479	11.206	10.256	8.707	8.179	7.770	6.179	10.391	15.497	18.389	21.664
	0.940	1.020	1.040	1.110	1.120	1.070	0.990	0.840	0.750	0.700	0.570	0.500	0.460	0.530	0.550	0.200	0.290	0.210
	583	383	20	20	21	45	57	58	44	37	86	78	8	8	10	6	8	11
-60.00	26.140	35.524	34.865	30.741	26.057	21.069	17.844	16.575	16.584	14.795	12.760	11.513	9.573	6.128	2.300	5.883	11.351	16.191
	0.820	0.810	0.880	0.910	0.970	0.980	0.990	0.960	0.930	0.840	0.750	0.670	0.660	0.570	0.400	0.320	0.240	0.260
	485	297	16	23	24	35	47	52	42	95	194	185	30	10	11	7	8	8
-70.00	15.276	20.758	26.299	28.463	27.923	25.893	23.113	20.401	18.260	17.396	16.604	15.919	14.557	12.527	9.624	6.948	7.897	10.923
	0.610	0.620	0.580	0.610	0.620	0.680	0.720	0.810	0.900	0.920	0.810	0.680	0.600	0.540	0.480	0.430	0.360	0.320
	408	39	40	47	41	44	47	70	121	198	210	178	31	6	5	5	6	9
-80.00	41.303	25.270	16.149	14.896	16.926	16.444	17.506	20.197	14.191	11.088	15.647	25.008	22.984	20.771	17.240	16.040	21.845	20.132
	0.460	0.480	1.290	1.820	1.730	1.990	1.090	0.480	1.010	2.030	1.580	1.010	0.210	0.210	0.530	0.310	0.000	0.720
	58	50	71	84	91	89	99	153	188	223	226	140	17	12	10	5	4	8

Depth = 2407 km

	0.00	10.00	20.00	30.00	40.00	50.00	60.00	70.00	80.00	90.00	100.00	110.00	120.00	130.00	140.00	150.00	160.00	170.00
80.00	-6.878	-8.106	-13.998	-25.868	-35.001	-39.684	-33.215	21.127	62.105	36.417	-10.844	-33.513	-38.501	-43.822	-46.528	-10.666	0.822	-61.319
	0.850	0.780	0.970	1.450	1.750	1.910	2.360	1.030	1.920	1.480	1.200	1.450	1.760	1.520	1.490	1.590	2.060	2.050
	74	82	92	102	124	170	363	617	960	1402	1799	2149	2456	2676	2755	2766	2623	2479
70.00	-4.332	-4.407	-5.352	-9.259	-17.969	-30.257	-36.561	-36.766	-20.802	14.148	20.374	1.201	-22.675	-33.843	-39.991	-43.711	-34.959	-20.546
	1.260	1.560	1.430	1.160	1.460	1.640	1.780	1.940	1.610	1.390	1.420	1.420	1.440	1.690	1.810	1.810	1.670	1.740
	85	94	95	101	103	116	272	555	1230	2206	2920	3115	2863	2181	2445	2752	2863	2999
60.00	6.214	4.941	3.825	1.369	-4.504	-15.800	-30.276	-38.910	-44.312	-43.736	-33.871	-17.289	-25.060	-36.973	-40.339	-42.482	-42.064	-35.852
	0.760	0.680	0.730	0.670	0.710	0.760	0.900	0.990	0.960	0.860	0.720	0.960	1.080	1.130	1.100	1.010	1.010	0.960
	30	32	24	26	53	54	101	270	899	2354	3454	3832	3753	2717	1015	925	1852	2811
50.00	12.898	12.952	12.637	11.078	6.629	-2.321	-12.843	-25.238	-36.873	-47.120	-54.208	-50.497	-40.497	-44.011	-55.246	-52.101	-45.995	-39.847
	0.550	0.670	0.670	0.750	0.780	0.810	0.870	0.910	0.960	1.020	1.150	1.090	1.020	1.310	1.940	1.500	1.280	1.040
	20	18	19	25	23	42	48	37	120	742	1758	3279	3700	3045	1096	540	446	614
40.00	12.656	13.979	14.819	13.891	10.846	5.365	-1.025	-5.119	-18.868	-35.069	-48.444	-56.969	-53.445	-48.071	-52.270	-51.507	-46.805	-43.009
	0.550	0.620	0.650	0.720	0.840	0.950	1.010	1.040	1.090	1.300	1.300	1.320	1.120	0.830	0.990	1.230	1.860	1.350
	15	15	16	16	21	24	33	32	74	246	411	859	1571	1655	857	373	274	276
30.00	12.843	13.369	12.640	10.324	6.445	4.013	5.225	4.978	-4.513	-29.974	-35.324	-46.438	-52.325	-50.784	-48.896	-44.135	-44.602	-43.046
	0.410	0.490	0.450	0.520	0.640	0.820	0.960	1.140	1.220	1.370	1.570	1.390	1.410	1.230	1.140	1.200	1.790	2.230
	17	16	17	17	20	27	37	34	56	75	98	137	175	361	458	370	266	193
20.00	9.414	11.381	11.379	8.444	1.191	-2.593	4.020	10.368	4.201	-19.862	-27.976	-35.507	-41.292	-47.351	-47.008	-34.270	-44.173	-49.517
	0.350	0.420	0.460	0.630	0.800	0.870	0.880	0.960	1.050	1.170	1.440	1.490	1.110	0.760	0.910	1.060	1.270	2.050
	17	19	17	19	16	16	18	17	35	79	156	177	148	300	732	785	456	238
10.00	6.340	12.097	12.668	8.289	8.167	8.851	11.392	15.336	10.825	-12.115	-29.459	-26.825	-32.083	-26.856	-23.435	-24.057	-45.019	-54.741
	0.420	0.500	0.590	0.670	0.840	0.950	1.000	0.950	0.920	0.990	0.990	1.230	1.240	1.030	1.190	1.160	1.230	1.630
	20	13	11	15	18	14	14	20	33	119	184	240	250	556	915	908	544	332
0.00	7.031	13.689	16.368	15.624	14.722	15.195	16.954	16.237	14.046	-4.214	-32.943	-31.225	-28.249	-27.656	21.534	-2.605	-48.104	-52.101
	0.370	0.480	0.600	0.620	0.640	0.760	0.830	0.880	0.830	0.840	0.840	1.030	1.060	1.020	0.940	0.950	1.360	1.600
	16	11	10	15	17	13	18	22	44	106	183	259	319	614	864	753	403	354
-10.00	10.670	15.591	18.451	18.697	18.837	19.183	17.142	13.340	9.378	6.851	-13.519	-25.733	-28.938	-36.968	-30.220	-10.272	-34.147	-50.548
	0.340	0.450	0.550	0.630	0.420	0.520	0.760	0.700	0.600	0.520	0.580	0.750	0.930	0.830	0.920	0.630	0.890	1.630
	14	13	7	11	14	10	17	19	35	50	109	197	285	397	482	303	261	521
-20.00	13.863	15.011	17.511	18.755	19.407	21.845	16.874	10.741	6.400	3.072	2.943	-5.054	-20.573	-30.879	-30.939	-29.366	-18.927	-3.116
	0.380	0.480	0.630	0.740	0.450	0.000	0.680	0.740	0.700	0.720	0.830	0.930	0.850	0.650	0.570	0.760	0.650	0.820
	14	13	8	8	7	3	6	9	17	32	63	94	140	152	239	239	150	444
-30.00	17.241	17.123	17.262	17.866	18.416	18.345	15.831	11.449	9.974	3.170	-4.388	8.179	-9.762	-34.147	-32.451	-10.181	0.735	20.157
	0.370	0.540	0.690	0.830	0.660	0.460	0.500	0.620	0.620	0.650	0.730	0.830	0.870	0.820	0.760	0.590	0.610	0.700
	12	9	7	7	5	7	5	7	33	43	104	136	219	273	303	375	418	318
-40.00	19.208	18.794	19.165	19.349	18.769	18.178	16.394	15.393	15.116	14.062	15.466	14.943	-2.340	-33.245	-27.660	-8.458	4.198	25.551
	0.390	0.490	0.660	0.750	0.750	0.640	0.650	0.650	0.670	0.710	0.670	0.750	0.740	0.770	0.780	0.730	0.710	0.880
	8	5	8	10	11	12	9	16	33	96	137	201	261	273	356	412	616	504
-50.00	20.721	20.195	20.097	20.614	20.295	19.147	17.956	17.070	16.951	15.905	18.507	19.331	1.543	-19.951	-12.272	-7.799	-4.005	19.457
	0.330	0.420	0.530	0.610	0.650	0.660	0.660	0.690	0.680	0.730	0.800	0.780	0.830	0.800	0.660	0.750	0.770	0.870
	9	7	10	11	12	18	13	15	30	109	168	203	250	356	574	666	662	749
-60.00	21.845	20.871	20.715	20.998	21.446	21.100	20.171	18.735	16.975	16.785	16.405	16.064	13.415	4.133	-4.311	-3.733	0.163	14.441
	0.000	0.260	0.330	0.430	0.480	0.550	0.600	0.590	0.610	0.600	0.580	0.640	0.650	0.610	0.610	0.630	0.700	0.820
	4	7	7	9	7	12	13	18	29	92	141	143	289	428	641	739	855	769
-70.00	14.604	18.726	20.067	20.641	21.091	21.410	21.082	20.291	19.261	17.903	16.958	16.087	15.055	13.564	10.373	7.372	8.186	9.163
	0.370	0.310	0.240	0.300	0.330	0.360	0.430	0.470	0.470	0.500	0.490	0.450	0.530	0.600	0.530	0.490	0.510	0.520
	13	14	9	8	8	8	18	34	44	48	71	84	172	323	427	508	632	485
-80.00	21.024	21.698	21.617	21.606	21.834	22.034	20.423	17.987	16.565	16.763	12.956	12.524	14.182	12.112	18.229	27.148	41.641	43.323
	1.050	0.660	0.210	0.500	0.310	0.110	0.260	0.420	0.520	0.520	1.620	2.540	2.720	3.100	2.490	1.720	1.410	0.990
	14	15	22	23	26	33	43	48	66	71	86	90	93	89	84	80	135	133